THE UNIVERSITY OF CHICAGO

1. TUNGSTEN PHOTOREDOX CHROMOPHORES CONTAINING AMINE-FUNCTIONALIZED DIPHOSPHINE AND N-HETEROCYCLIC CARBENE LIGANDS. 2. THE CHEMISTRY OF LOW-COORDINATE COBALT COMPOUNDS SUPPORTED BY N-HETEROCYCLIC CARBENES AND BULKY AMINES.

A DISSERTATION SUBMITTED TO

THE FACULTY OF THE DIVISION OF THE PHYSICAL SCIENCES

IN CANDIDACY FOR THE DEGREE OF

DOCTOR OF PHILOSOPHY

DEPARTMENT OF CHEMISTRY

BY

CHRISTOPHER BRIAN HANSEN

CHICAGO, ILLINOIS

DECEMBER 2017

To my family with love.

Mom, Dad, Grandpa, Jason, and Greg.

None of this would have been possible without you

TABLE OF CONTENTS

LIST OF FIGURES

Figure **Page**

LIST OF SCHEMES

Scheme **Page**

LIST OF TABLES

Table **Page**

LIST OF CHARTS

Chart **Page**

LIST OF EQUATIONS

ACKNOWLEDGEMENTS

This journey would not have been possible without a multitude of people. First and foremost I would like to thank my family for the never ending support and love. This would have been an impossible task without all of you. Mom and Dad, I cannot put into words the impact you've both had on me in terms of both growth as a person and a scientist, as well as personal rocks to lean on during recovery, transition into new aspects of my life, and completion of this work. I also must thank Grandpa, Rob, Jason, Anthony, Cathy, Vanessa, Kris, Jeremy, Will, and Lydia for always being there for me to talk, unwind, and for unwavering support through the good times and the bad.

Equally, I must also thank the two research advisors I was fortunate enough to work with at Chicago. Greg Hillhouse provided an extremely supportive and nurturing environment to blossom as a scientist. He instilled the deep virtues of scientific curiosity and a dedication to deep fundamental understanding of chemistry I hold dear today. A truer understanding of the work hard play hard philosophy has never been clearer. I also have to thank the extended Hillhouse scientific family tree for exceptional support and camaraderie. I cannot thank Mike Hopkins enough for accepting me into his group, and providing an equally enlightening environment in which to prosper. You provided invaluable scientific insight, and taught me to think critically and deliberately about every step and every result. Under his tutelage I became a better writer and a better and more complete scientist. It was an honor and a privilege to work in both groups. I must also thank professors John Anderson and Rich Jordan for serving on my thesis committee and being incredibly supportive and advocates for me throughout my time at Chicago. I would also like to thank Dr. Ian Steele and Dr. Alex Filatov for help with a lot of the crystallography presented in this work, and for being willing and enthusiastic teachers.

None of this would have been possible without building upon the beautiful work and scientific accomplishments of others. I need to extend a special thank you to Nicole and Steve from the Hillhouse group for making me feel welcome at Chicago, and for all you taught me. My undergraduate Nik was privilege to mentor, despite the almost unfathomable number of J-Young tubes, filter flasks, and schlenk lines that paid the price in the process. To the rest of the Hillhouse group, thank you for the wonderful years. From the Hopkins group, I must especially thank Hunter for his guidance and assistance in transition into the group, and with all matters tungsten and spectroscopy. I'd also like to thank Mark for being a willing lunch partner, and always being there to talk through scientific problems and ideas. To the rest of the Hopkins group, thank you for welcoming me, and always being willing to get coffee. It was an honor to work and grow in both research groups. I would also like to thank the Jordan, Lewis, Yu, Talapin, and Anderson groups for always being available to lend supplies, discuss problems, and hangout.

There are a lot of other people who made this journey possible. I cannot thank my friends enough for all their support, both from home and Chicago. Will and Connlann for being great roommates and willing partners to get weird with. Dan and Cam for convincing me to come to Chicago and furthering my passion for old man beers. Kim for sharing the burden of running softball, and being an amazing friend. The UW Burn Center for wonderful care, compassion, and tough love. My fireworks family, especially Jim, Steve, Gary, and Lee for thoughts, prayers, and substantial support. Matt, Landon, Wayne, Mike, Pat, Zach, Tim, and Nathan for making Chicago feel like home and welcoming me with open arms. My undergraduate advisor, John, for always being available to talk and for advice. Team Beer for an uncountable number of enjoyable Friday evenings, an even more uncountable number of Old Styles, and one championship (so far). Last, but not least, I want to thank the Chemistry

department for their flexibility and continued support from the very beginning to the very end. It's been a long, unique journey, but I'm glad I've had all of you with me.

ABSTRACT

The development of renewable and sustainable energy sources is a major challenge facing the world population. Our growing energy demand is primarily driven by a growing global population, increasing global industrialization, and overall enhancement of the quality of life in developing regions. Among alternative sources of energy, solar is perceived as one of the most promising and utilizable resources. Solar energy is disadvantaged by difficulty in storing the energy once captured. Artificial photosynthesis involves the conversion of solar energy into chemical potential via solar fuel generation from a renewable feedstock. Our group views tungsten alkylidyne chromophores as promising candidates due to their visible light absorption profile, long-lived excited states, and strong photoreduction properties. The work presented in the first half of this thesis describes design and characterization of tungsten alkylidyne chromophores for improved catalytic turnover, as well as enhanced photoreduction properties. The work presented in the second half of this thesis describes work done on low-coordinate cobalt amines and bulky N-heterocyclic carbene stabilized iron carbonyls for hydrosilylation.

Chapter 2 describes the incorporation of chelating phosphine ligands with with pendant Brønsted basic groups for improved catalytic turnover utilizing hydrogen. We report the synthesis and characterization of both a model tungsten hydride compound utilizing conventional ligands, as well a second compound bearing ligands with Brønsted basic sites. Using ligands with Brønsted basic sites, we are able to change the preferred location of protonation. Chapter 3 describes our design and synthetic efforts toward using strongly sigma donating N-heterocyclic carbene ligands to increase photoredox potentials. Chapters 4 and 5 describe work done in a previous research group on the synthesis, structure, characterization, and reactivity of low-coordinate cobalt amide compounds. A detailed study of the protonolysis and aminolysis of a three-coordinate cobalt amide chloride is discussed. Chapter 6 describes work on an iron

tetracarbonyl supported by an extremely bulky N-heterocyclic carbene. The synthesis, structure, and catalytic hydrosilylation chemistry are discussed. Appendix I reports the structure of a cobalt bis(anilide) discovered during work described in Chapter 4. Appendix II collects data of the structural studies reported in this thesis.

CHAPTER 1

Introduction.

One of the major challenges facing the world population is the development of renewable and sustainable energy practices. As of 2001, the global energy usage was estimated at 13.5 TW.[1] As of 2007, our energy usage had increased 20% to 16.2 TW.[2] The 2001 value is projected to double by the middle of the 21st century, and quadruple by 2100.[1] An increasing global population, steady industrialization of the world, and overall increases in quality of life in these developing regions are the primary drivers of our growing energy demand. Currently a majority of our energy generation comes from oil, coal, and natural gas.[3] This energy source is sufficient to satisfy our demands for the current time, but ultimately other energy sources will need to be developed. With continued use of fossil fuels comes a continued rise in atmospheric CO_2 concentrations and continued tensions in the geopolitical climate.

Various energy sources have been explored as alternatives to meet our growing energy requirements.[4] The energy density of wind power generation is too low, and the source is intermittent. Energy generation derived from biomass is hampered by low efficiency of photosynthesis. Nuclear power is the second largest energy producer behind fossil fuels, but meeting demand would require construction of nuclear power plants at a very rapid rate.[3] Among alternative sources of energy, solar is perceived as the most promising and most utilizable resource. Solar insolation provides 120,000 TW, or more energy in one hour than the global human population consumes in one year.[5] The utilization of solar energy will require technological improvements in both solar capture/conversion and resultant energy storage. Direct usage of solar energy is limited by variable availability due to weather and the diurnal cycle. If solar energy is to be a major energy source, it must be stored and dispatched on demand

to the end user. An especially attractive approach is to store solar converted energy in the form of chemical bonds, i.e., in an artificial photosynthetic process.

Utilizing artificial photosynthetic processes to generate a renewable carbon-based feedstock provides the most direct way to integrate into our existing energy infrastructure. Carbon dioxide is the most obvious and attractive carbon source for a renewable carbon-based feedstocks.[6] Reduction of carbon dioxide provides routes to produce formate, methanol, and methane as well as higher hydrocarbons via the Fischer-Tropsch process.[7] The direct reduction of CO_2 is difficult due to thermodynamically unfavorable energetics, largely due to the large reorganization energy of the CO_2 radical.[8] None the less, effective catalysts for the reduction of CO_2 have been developed based on cobalt, rhenium, and ruthenium systems.[7]

Photosynthesis in nature relies on excited-state electron-transfer reactions of chromophores.[9] Drawing inspiration from nature, synthetically designed transition metal chromophores for artificial photosynthesis offer a wide breadth of reactivity. Chromophore photoredox chemistry has been fundamental to development of water splitting,[10,11] CO_2 reduction processes,[12-14] and photovoltaic materials,[15] as well as finding applications for the mediation of organic transformations.[16,17] Chromophores have established a versatile role in organic syntheses by activating substrates and enabling novel and unprecedented reactivity patterns.[16] Visible light is abundant in the solar spectrum, but many organic substrates are unable to absorb this lower energy radiation making visible light chromophores attractive catalysts. Visible light chromophores offer a controlled way to harness energy from light to generate high energy species under relatively mild conditions, without inducing undesired reactivity by direct absorption of the organic substrate. The field of visible light photoredox chemistry is typified by catalysts such as tris(2,2'-bipyridine) ruthenium(II) ($Ru(bpy)_3^{2+}$) and tris[2-phenylpyridinato-

C^2,*N*]iridium(III) ($Ir(ppy)_3$).[18-20] $Ru(bpy)_3^{2+}$ has found applications in energy related transformations including areas such as water splitting, photovoltaic cells, and energy storage.[21] $Ru(bpy)_3^{2+}$ has been known to mediate organic transformations for almost 40 years.[22] However, only recently has photoredox catalysis garnered widespread utilization within the synthetic community.[18,19,23]

A general description by which photoredox chromophores function is shown in Figure 1.1. The generalized Jablonski diagram shown in Figure 1.1a describes the generation of the excited state. The chromophore absorbs a quantum of light, resulting in the promotion of an electron to generate a singlet excited electronic state of the molecule. In order to provide a sufficient lifetime for the excited state to do productive chemistry, most effective chromophores are often found to undergo intersystem crossing to form a longer-lived triplet excited state. [18,19] The excited electronic state can simultaneously make the catalyst a better reductant and a better oxidant (Figure 1.1b). The promoted electron is more easily transferred to an acceptor, resulting in net oxidation of the chromophore and reduction of the acceptor. Alternatively, the excitation of an electron generates a low energy hole. This vacant site can more easily accept an electron from a donor, resulting in net reduction of the chromophore and oxidation of the donor. These phenomena for instance make the excited state of $Ru(bpy)_3^{2+}$ simultaneously both a stronger excited state reductant and oxidant than its ground state. [18,19]

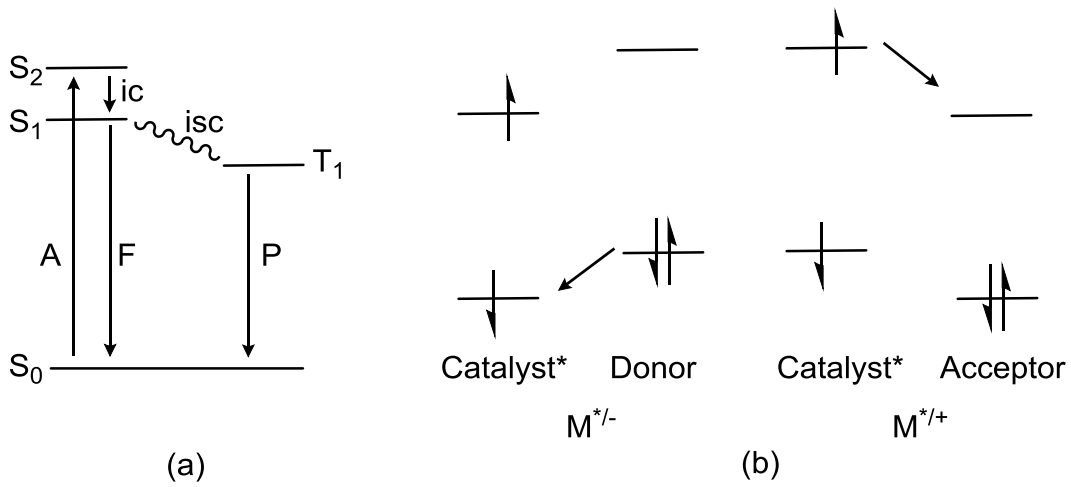

Figure 1.1. Electronic transitions in chromophores, and depiction of excited state quenching. (a) Generalized Jablonski diagram. A = photon absorbance, ic = internal conversion, isc = inter system crossing, F = fluorescence, P = phosphorescence. (b) Orbital diagram depicting excited state oxidation and reduction.

Another class of compounds that bear promise as photoredox catalysts are tungsten alkylidyne compounds (Figure 1.2a). Luminescent tungsten alkylidyne complexes are strong ground state reductants and low energy visible light absorbers, giving rise to strong excited-state photoreductive activity.[24] The electronic structure of tungsten alkylidynes lend themselves to systematic tuning of the photophysical and redox properties.[25-27] The HOMO consists of primarily d_{xy} parentage, while the LUMO consists of primarily W≡C π^* parentage (Figure 1.2b). These two orbitals are orthogonal, allowing for independent control by synthetic manipulation.[25] The energy of the HOMO is influenced most strongly by the equatorial ligands. Stronger donors raise the energy of the HOMO. The LUMO is primarily influenced by the nature of the alkylidyne and axial X group.[26] Computational methods have been developed for predictive modeling and screening of electronic and electrochemical properties.[27] The energy of the HOMO was found to scale linearly with the oxidation potential $E_{1/2}$. The HOMO-LUMO gap is correlated with the energy of the emissive excited state, E_{00}.

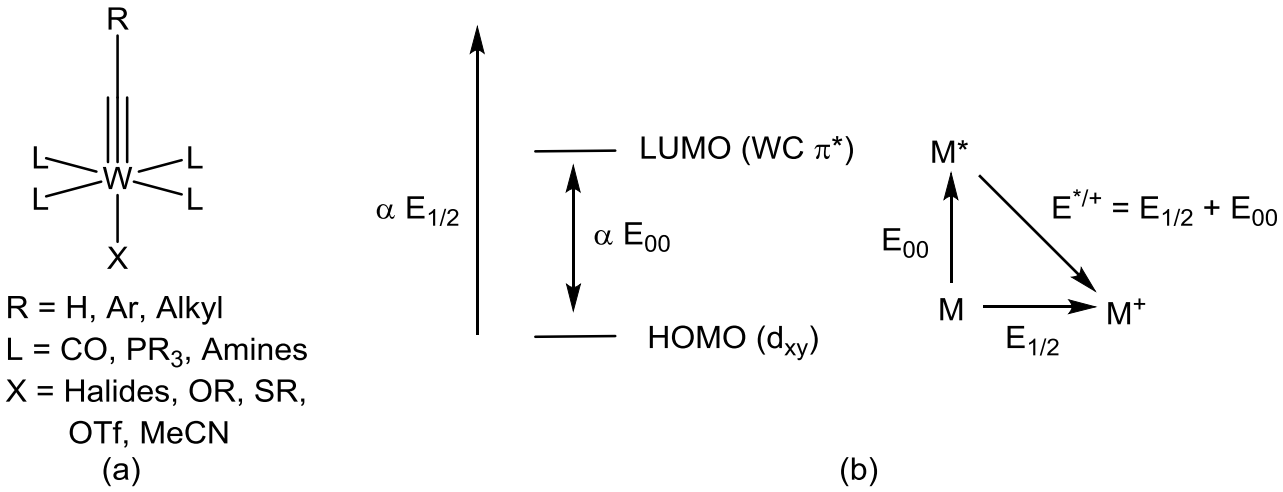

Figure 1.2. Generalized tungsten alkylidyne geometric and electronic structure. (a) Tungsten alkylidyne structure with common substitutions. (b) Electronic structure, and general photoreductive pathway.

One of the largest complications of the current state of photoredox chemistry is the incorporation of non-renewable sacrificial redox equivalents such as trialkylamines, ascorbate, BNAH, and dithionite often used in the catalytic process.[28] These sacrificial reagents quickly decomposes upon oxidation, which suppresses charge-recombination. By preventing this unproductive pathway, sacrificial donors largely eliminate the problem of matching the different time scales of photochemical and substrate reaction rates. The use of such sacrificial reagents reduces or negates the value of the stored photochemical energy. It would be preferable to utilize renewable redox equivalents to carry out this chemistry. Ideally, H_2 could be used to regenerate the catalyst, which may be obtained by coupling with water splitting chemistry. Our group has previously shown that the oxidized d^1 state of a tungsten benzylidyne photoredox chromophore, $[W(CPh)(dppe)_2Cl]OTf$, is capable of activating H_2 to form a d^0 cationic tungsten hydride species, $[HW(CPh)(dppe)_2Cl]OTf$, which may be regenerated to the photoactive d^2 compound by reaction with an equivalent of base (Scheme 1.1).[29] The H_2 activation in this system, however proceeds slowly and inefficiently.

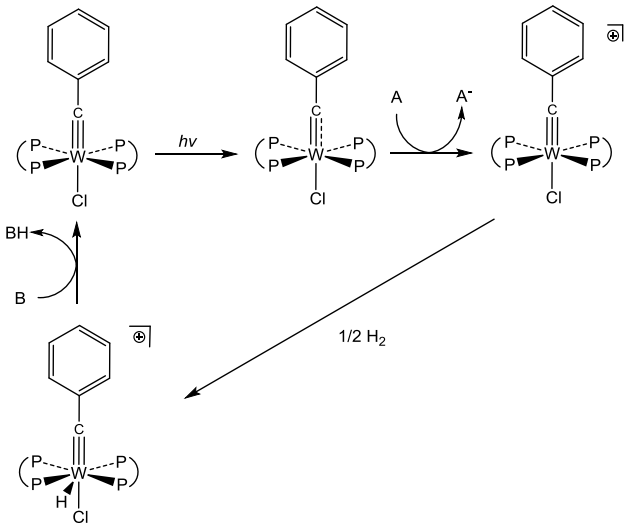

Scheme 1.1. Example cycle of photoactivation of acceptor, and regeneration of active species with hydrogen and base for tungsten alkylidyne system.

Pioneering work by DuBois, Bullock *et al.* lead to the development of biomimetic ligands that incorporate the coordination properties of chelating phosphines with Brønsted basicity of pendant amines in the second-coordination sphere in a highly tunable configuration.[30-33] These ligands have been drawing attention in molecular catalysis as proton shuttles for H_2 production[30,34,35] and activation,[33] as well as the activation of other small molecules.[36-40] The pendant amine moieties are posited to function much like enzyme catalytic sites by pre-organizing substrates near the active site and facilitating the shuttling of protons. Incorporation of ligands of this type into tungsten alkylidyne chromophores is envisioned as a way to enable catalytic regeneration in a more facile manner, or aid in the regeneration of a catalytically active species by shuttling protons to the molecular periphery for deprotonation. Work in this thesis explores this direction for the more efficient regeneration of active chromophores.

The archetypal photoredox chromophores, $[Ru(bpy)_3]_2^+$ and *fac*-$Ir(ppy)_3$, have excited-state oxidation potentials of −1.2 V and −2.1 V respectively (vs $Fc^{0/+}$ in ACN).[20,41,42] These values put the reducing strength of $[Ru(bpy)_3]^{2+}$* on the same order of magnitude as

conventional moderate reductants like cobaltocene ($E_{1/2}$ = −1.3 V vs. $Fc^{0/+}$ in THF).[43] By contrast, photoreduced *fac*-$Ir(ppy)_3^-$ has a significantly less positive oxidation potential, approaching conventional strong reductants such as Na(Hg) ($E_{1/2}$ = −2.36 V vs. $Fc^{0/+}$ in THF).[43] These two catalysts possess rich chemistry, but are limited in the substrates they can activate. By developing visible light photoreductants with even more negative oxidation potentials, a substrate scope with more breadth including less conventional and more difficult to access substrates may become accessible. The strongest photoreductants to date in the literature, $W(CNDIPP)_6$, have potentials as high as −2.8 V.[44] Continuing this trend may allow for reactions typically preformed with reactive alkali metals to be carried out with homogeneous photoredox catalysts.

We propose the use of tungsten alkylidynes to push the limit of conventional photoreductant capabilities. The ground state oxidation potential of a prototypical tungsten benzylidyne compound, $W(CPh)(dmpe)_2Cl$, is −0.82 V vs. $Fc^{0/+}$.[27] The excited state reduction potential of −2.76 V falls between those of *fac*-$Ir(ppy)_3$ and $W(CNDIPP)_6$.[44,45] The tunable structure provides a means by which the electronic properties of the resulting compounds can be modulated.[27] It has been previously shown the highest occupied molecular orbital (HOMO) and primary redox orbital of tungsten–alkylidyne complexes of type $W(CR)L_4X$ is primarily of d_{xy} parentage. Consistent with this, the ligands located around the equatorial plane have been shown to exhibit the strongest influence on the energy of the HOMO, which tracks close to linearly with the ground state oxidation potential.[26,27] Stronger sigma donating equatorial ligands will increase the electron density and thus raise the energy of the HOMO, resulting in stronger reductants. N-heterocyclic carbenes (NHCs) are an attractive alternative to phosphines for this purpose.[46] Both phosphines and NHC ligands are known to be good sigma donors. In comparison, NHC ligands

are often stronger donors than their phosphine counterparts as evidenced by their respective Tolman parameters.[47] Work in this thesis explores this direction for the generation of more strongly reducing tungsten alkylidyne complexes.

In Chapter 2 we report efforts to create a tungsten benzylidyne system which more efficiently oxidizes hydrogen. A photocatalytically relevant d^0 tungsten hydride is prepared and characterized, including a measurement of the pK_a. Using this compound as a model, we design a new compound containing a Dubois-type chelating phosphine with pendant Brønsted basic groups. This compound is prepared, and its protonation chemistry is probed.

Chapter 3 reports our efforts to prepare and characterize tungsten benzylidyne compounds containing N-heterocylic carbene ligands. A computational study is preformed to screen potential ligands, substitution patterns, and electronic effects. Synthetic trials were carried out to prepare promising candidates from the computational screen. Two crystallographically characterized derivatives are reported

Chapters 4–6 describe research conducted under the direction of Professor Greg Hillhouse, who was my research advisor until his death in 2014. Chapter 4 reports the synthesis and reactivity studies of a N-heterocyclic supported three-coordinate cobalt amide chloride, (IPr)CoCl{$N(SiMe_3)_2$}. Protonolysis and attempts at salt metathesis are detailed. It was found that the compound reacts via aminolysis with alkali metal anilides instead of salt metathesis.

Chapter 5 reports a crystallographic study of a cobalt-containing inverse crown ether, bearing a central oxo ligand. This compound was found as a by-product of other reactions on several occasions from our work in Chapter 4.

Chapter 6 reports the synthesis and characterization of an N-heterocyclic carbene iron tetracarbonyl compound, (IPr*)$Fe(CO)_4$. The structure of this compound is reported, and

compared against other related literature compounds. Preliminary hydrosilylation activity is also included.

1.1 References.

(1) Lewis, N. S.; Nocera, D. G. *Proc. Natl. Acad. Sci.* **2006**, *103*, 15729.

(2) Cook, T. R.; Dogutan, D. K.; Reece, S. Y.; Surendranath, Y.; Teets, T. S.; Nocera, D. G. *Chem. Rev.* **2010**, *110*, 6474.

(3) Administration, E. I. *Annual Energy Outlook*; U.S. Department of Energy: Washington, DC., 2017.

(4) Gea *Global Energy Assessment - Toward a Sustainable Future* Cambridge University Press, Cambridge, UK and New York, NY, USA and the International Institute for Applied Systems Analysis, Laxenburg, Austria, 2012.

(5) Collares-Pereira, M.; Rabl, A. *Sol. Energy* **1979**, *22*, 155.

(6) Goeppert, A.; Czaun, M.; Surya Prakash, G. K.; Olah, G. A. *Energ. Environ. Sci.* **2012**, *5*, 7833.

(7) Kumar, B.; Llorente, M.; Froehlich, J.; Dang, T.; Sathrum, A.; Kubiak, C. P. *Annu. Rev. Phys. Chem.* **2012**, *63*, 541.

(8) Koppenol, W. H.; Rush, J. D. *J. Phys. Chem.* **1987**, *91*, 4429.

(9) Blankenship, R. E. *Molecular Mechanisms of Photosynthesis*; 2nd ed.; Wiley Blackwell: Oxford, UK, 2014.

(10) Han, Z.; Eisenberg, R. *Acc. Chem. Res.* **2014**, *47*, 2537.

(11) Karkas, M. D.; Verho, O.; Johnston, E. V.; Akermark, B. *Chem. Rev.* **2014**, *114*, 11863.

(12) Windle, C. D.; Perutz, R. N. *Coord. Chem. Rev.* **2012**, *256*, 2562.

(13) Izumi, Y. *Coord. Chem. Rev.* **2013**, *257*, 171.

(14) Thoi, V. S.; Kornienko, N.; Margarit, C. G.; Yang, P.; Chang, C. J. *J. Am. Chem. Soc.* **2013**, *135*, 14413.

(15) Hagfeldt, A.; Boschloo, G.; Sun, L.; Kloo, L.; Pettersson, H. *Chem. Rev.* **2010**, *110*, 6595.

(16) Prier, C. K.; Rankic, D. A.; MacMillan, D. W. *Chem. Rev.* **2013**, *113*, 5322.

(17) Shaw, M. H.; Twilton, J.; MacMillan, D. W. *J. Org. Chem.* **2016**, *81*, 6898.

(18) Tucker, J. W.; Stephenson, C. R. J. *J. Org. Chem.* **2012**, *77*, 1617.

(19) Shaw, M. H.; Twilton, J.; MacMillan, D. W. *J. Org. Chem.* **2016**, *81*, 6898.

(20) Prier, C. K.; Rankic, D. A.; MacMillan, D. W. C. *Chem. Rev.* **2013**, *113*, 5322.

(21) Concepcion, J. J.; House, R. L.; Papanikolas, J. M.; Meyer, T. J. *Proc. Natl. Acad. Sci.* **2012**, *109*, 15560.

(22) Gray, H. B.; Maverick, A. W. *Science* **1981**, *214*, 1201.

(23) Skubi, K. L.; Blum, T. R.; Yoon, T. P. *Chem. Rev.* **2016**, *116*, 10035.

(24) Da Re, R. E.; Hopkins, M. D. *Coord. Chem. Rev.* **2005**, *249*, 1396.

(25) Manna, J.; Gilbert, T. M.; Dallinger, R. F.; Geib, S. J.; Hopkins, M. D. *J. Am. Chem. Soc.* **1992**, *114*, 5870.

(26) Lovaasen, B. M.; Lockard, J. V.; Cohen, B. W.; Yang, S.; Zhang, X.; Simpson, C. K.; Chen, L. X.; Hopkins, M. D. *Inorg. Chem.* **2012**, *51*, 5660.

(27) Haines, D. E.; O'Hanlon, D. C.; Manna, J.; Jones, M. K.; Shaner, S. E.; Sun, J.; Hopkins, M. D. *Inorg. Chem.* **2013**, *52*, 9650.

(28) Pellegrin, Y.; Odobel, F. *C. R. Chim.* **2016**.

(29) Morales-Verdejo, C. A.; Newsom, M. I.; Cohen, B. W.; Vibbert, H. B.; Hopkins, M. D. *Chem. Commun.* **2013**, *49*, 10566.

(30) Wilson, A. D.; Newell, R. H.; McNevin, M. J.; Muckerman, J. T.; Rakowski DuBois, M.; DuBois, D. L. *J. Am. Chem. Soc.* **2006**, *128*, 358.

(31) Shaw, W. J.; Helm, M. L.; DuBois, D. L. *Biochim. Biophys. Acta* **2013**, *1827*, 1123.

(32) DuBois, D. L. *Inorg. Chem.* **2014**, *53*, 3935.

(33) Bullock, R. M.; Helm, M. L. *Acc. Chem. Res.* **2015**, *48*, 2017.

(34) Helm, M. L.; Stewart, M. P.; Bullock, R. M.; DuBois, M. R.; DuBois, D. L. *Science* **2011**, *333*, 863.

(35) Fang, M.; Wiedner, E. S.; Dougherty, W. G.; Kassel, W. S.; Liu, T.; DuBois, D. L.; Bullock, R. M. *Organometallics* **2014**, *33*, 5820.

(36) Yang, J. Y.; Bullock, R. M.; Dougherty, W. G.; Kassel, W. S.; Twamley, B.; DuBois, D. L.; Rakowski DuBois, M. *Dalton Trans.* **2010**, *39*, 3001.

(37) Galan, B. R.; Schoffel, J.; Linehan, J. C.; Seu, C.; Appel, A. M.; Roberts, J. A.; Helm, M. L.; Kilgore, U. J.; Yang, J. Y.; DuBois, D. L.; Kubiak, C. P. *J. Am. Chem. Soc.* **2011**, *133*, 12767.

(38) Tronic, T. A.; Kaminsky, W.; Coggins, M. K.; Mayer, J. M. *Inorg. Chem.* **2012**, *51*, 10916.

(39) Weiss, C. J.; Das, P.; Miller, D. L.; Helm, M. L.; Appel, A. M. *ACS Catal.* **2014**, *4*, 2951.

(40) Lilio, A. M.; Reineke, M. H.; Moore, C. E.; Rheingold, A. L.; Takase, M. K.; Kubiak, C. P. *J. Am. Chem. Soc.* **2015**, *137*, 8251.

(41) King, K. A.; Spellane, P. J.; Watts, R. J. *J. Am. Chem. Soc.* **1985**, *107*, 1431.

(42) Flamigni, L.; Barbieri, A.; Sabatini, C.; Ventura, B.; Barigelletti, F. In *Photochemistry and Photophysics of Coordination Compounds II*; Balzani, V., Campagna, S., Eds.; Springer Berlin Heidelberg: Berlin, Heidelberg, 2007, p 143.

(43) Connelly, N. G.; Geiger, W. E. *Chem. Rev.* **1996**, *96*, 877.

(44) Sattler, W.; Henling, L. M.; Winkler, J. R.; Gray, H. B. *J. Am. Chem. Soc.* **2015**, *137*, 1198.

(45) Vibbert, H. B., Unpublished results.

(46) Hopkinson, M. N.; Richter, C.; Schedler, M.; Glorius, F. *Nature* **2014**, *510*, 485.

(47) Gusev, D. G. *Organometallics* **2009**, *28*, 6458.

CHAPTER 2

Brønsted Acid–Base Chemistry of Tungsten–Alkylidyne Complexes. Incorporation of Second-Coordination-Sphere Bases for Intramolecular Deprotonation of Hydrido Ligands

2.1 Introduction.

Photoredox reactions sensitized by transition-metal chromophores are of considerable importance because they can produce highly reactive, chemically valuable, and otherwise difficult to generate transient species. For example, photoredox reactions lie at the heart of molecular approaches to artificial photosynthesis,[1-7] wherein they produce reactive redox states of water-splitting and CO_2-reduction catalysts, and are finding increasing application to the generation of organic radicals useful in organic synthesis.[8-10] In these contexts, photoredox chromophores effect the transfer of redox equivalents between oxidative and reductive half reactions of an overall transformation. Optimally, the oxidative and reductive half reactions should either both catalytically produce useful products or one should be a closed regenerative cycle. A significant barrier to achieving this aim is that productive bond-making and bond-breaking steps often are slow relative to unproductive electron-transfer reactions that restore the chromophore ground state (viz., back electron transfer). A typical approach to circumventing this barrier is to use in one of the half reactions a sacrificial oxidant or reductant that decomposes rapidly following its electron-transfer reaction with the excited chromophore. This prevents back electron transfer, which facilitates the other half reaction, but carries the cost of the stoichiometric (noncatalytic) consumption of the sacrificial reagent.[11] The development of new photoredox chromophores that catalytically utilize renewable redox equivalents rather than conventional sacrificial reagents, therefore, is an important goal.

Tungsten–alkylidyne chromophores of the general form $W(\equiv CR)L_4X$ (W = W(IV); R =

aryl, L = neutral ligand, X = anionic ligand) hold the potential to participate in catalytic photoredox cycles without use of conventional sacrificial reagents. These d^2-configured chromophores possess rationally controllable ground-state redox potentials[12-14] and excited-state energies,[15,16] as necessary to enable tuning of the excited-state redox potential, in addition to the requisite long-lived luminescent excited states.[15] Further, there is evidence that suitably designed derivatives could participate in catalytic photoredox cycles in which reducing equivalents are extracted from H_2 rather than a nonrenewable sacrificial donor, via the sequence of reactions shown in Scheme 2.1. Specifically, it has been shown that one-electron oxidation of the d^2-configured complex $W(CPh)(dppe)_2Cl$ (**M** in Scheme 2.1; dppe= 1,2-bis(diphenylphosphino)ethane), which is a typical luminescent chromophore of this class, yields the stable d^1 radical $[W(CPh)(dppe)_2Cl]^+$ (**M**$^+$);[17] this is also the product from a photoinduced reduction of an acceptor (A) by excited $W(CPh)(dppe)_2Cl$ (**M***). The $[W(CPh)(dppe)_2Cl]^+$ ion, in turn, has been found to react with H_2 in dichloromethane solution at room temperature to provide the d^0 seven-coordinate tungsten–benzylidyne hydride compound $[WH(CPh)(dppe)_2Cl]^+$ (**MH**$^+$).[18] Subsequent treatment of **MH**$^+$ with base (NaO^tBu) in DMSO solution results in deprotonation of the hydride ligand, closing the cycle to give the original compound $W(CPh)(dppe)_2Cl$.[18] This sequence of reactions suggests that tungsten–alkylidyne photoredox chromophores could participate in photochemical reductions in which renewable H_2 regenerates the chromophore rather than conventional sacrificial reductants.

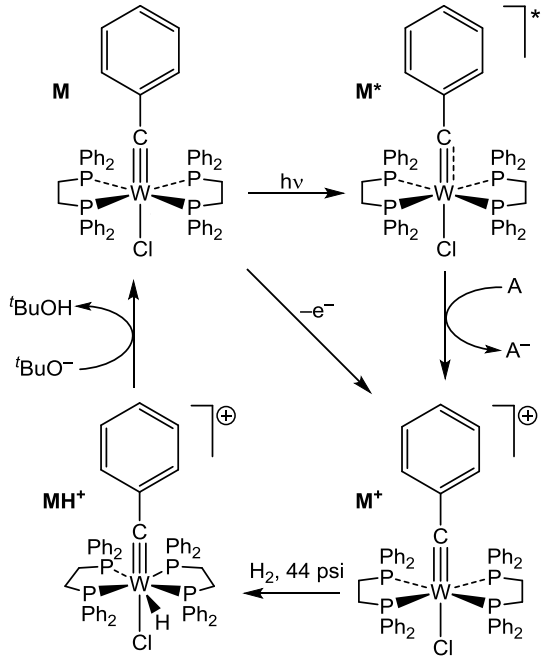

Scheme 2.1. Regeneration of a tungsten–alkylidyne photoreductant via H_2 oxidation.

Pioneering research by DuBois, Bullock, and coworkers into the development of hydrogenase-inspired transition-metal catalysts for proton reduction, H_2 oxidation, and activation of other small molecules, has resulted in the design of an extensive family of chelating phosphine ligands that contain structurally and thermodynamically tunable Brønsted amine bases in the second coordination sphere.[19-29] The presence of these bases improves catalytic activity by facilitating proton transfer to and from the metal center and through synergism with the metal in H–H bond-making and -breaking (Scheme 2.2). We wondered whether incorporation of ligands of this type into a tungsten–alkylidyne chromophore capable of the H_2-activation reactivity shown in Scheme 2.1 would provide similar benefits. Prerequisites to such activity are that the basicity of the pendant amine is sufficient to deprotonate a metal–hydride species such as $\mathbf{MH^+}$ (Scheme 2.1), and that the structure of the tether allows it to come within close contact of this proton.

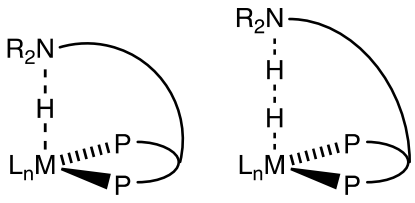

Scheme 2.2. Simplified representation of intramolecular H^+ transfer and H_2 activation/formation in a metal–phosphine complex containing a second-coordination-sphere amine.

We report here results of a study designed to probe these two points. First, the tungsten–benzylidyne hydride complex $[WH(CPh)(dmpe)_2Cl]^+$ (**1H**$^+$, Chart 1; dmpe = 1,2-bis(dimethylphosphino)ethane), which is analogous to **MH**$^+$ in Scheme 2.1, has been synthesized, structurally characterized in the solid state and solution, and its pK_a measured in THF. It is found that the pK_a of **1H**$^+$ is comparable to those of alkyl amines (e.g., potential second-sphere bases) and, further, that **1H**$^+$ is fluxional in solution through the postulated intermediacy of a tungsten–benzylidene complex whose structure increases the accessibility of the mobile H atom. Second, a tungsten–benzylidyne complex containing second- and outer-coordination-sphere amine bases, $W(CPh)(P_2NN)_2Cl$ (**2**, Chart 2.1; P_2NN = $N((CH_2)_3NMe_2)(CH_2PEt_2)_2$), has been synthesized, structurally characterized, and its acid–base chemistry investigated. It is found that the reaction between **2** and an acid competent to produce a tungsten–hydride derivative instead results in protonation of the pendant amine, and that the added proton undergoes intra- and inter-molecular exchange between ligands on the NMR time scale. This suggests that tungsten–alkylidyne hydride complexes formed via H_2 activation and would undergo intramolecular deprotonation of the hydrido ligand via P_2NN-like ligands.

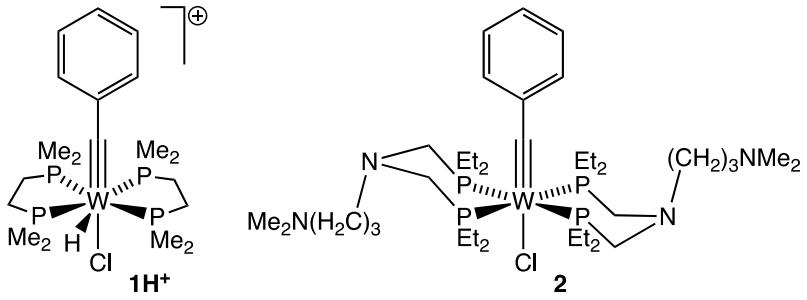

Chart 2.1. $[W(CPh)H(dmpe)_2Cl]^+$ (**1H**$^+$) and $W(CPh)(P_2NN)_2Cl$ (**2**).

2.2 Results and Discussion.

2.2.1. Synthesis, structure, and pK_a of $[WH(CPh)(dmpe)_2Cl]^+$ (1H$^+$). The research described in this section incorporates results reported by Michael Newsom, a former member of the Hopkins group.[30] Salts containing the tungsten–benzylidyne hydride ion $[WH(CPh)(dmpe)_2Cl]^+$ (**1H**$^+$) were prepared by protonation of $W(CPh)(dmpe)_2Cl$ (**1**), following a route similar to those used to synthesize other $[WH(CR)(R_2PCH_2CH_2PR_2)_2X]^+$-containing compounds.[18,31-34] Specifically, the reaction between **1** and HCl (1 equiv) in THF resulted in immediate precipitation of an off-white solid postulated to be **1H**[Cl].[30] Subsequent treatment of **1H**[Cl] with $Li[B(C_6F_5)_4]$ in acetonitrile resulted in salt metathesis to provided **1H**$[B(C_6F_5)_4]$ (82% yield), which has improved solubility in common polar organic solvents (Scheme 2.3). A ^{13}C-labeled isotopomer enriched at the benzylidyne α-carbon atom, $[WH(^{13}CPh)(dmpe)_2Cl][B(C_6F_5)_4]$ (**1H***$[B(C_6F_5)_4]$), was prepared in an analogous manner from $W(^{13}CPh)(dmpe)_2Cl$ (**1***). The formulation and purity of these compounds were established by multinuclear NMR spectroscopy, mass spectrometry, elemental analysis, and X-ray crystallography (see Section 2.4 Experimental Section for full details).

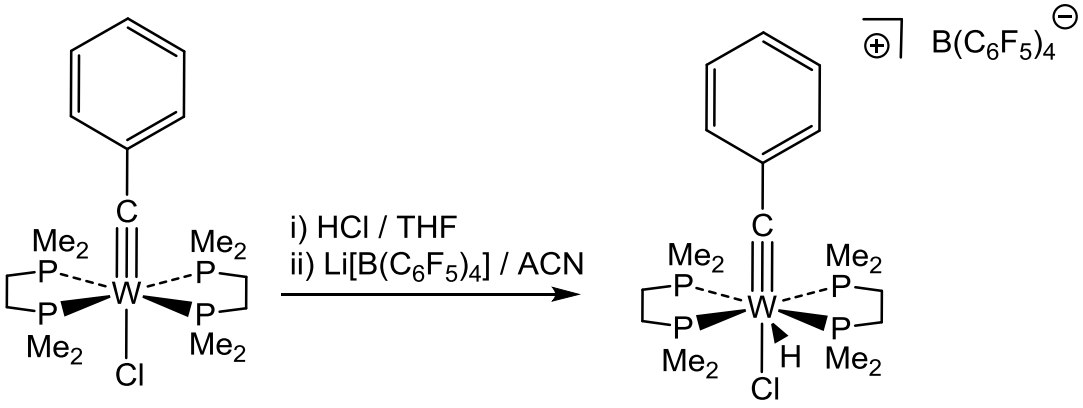

Scheme 2.3. Synthesis of **1H**[$B(C_6F_5)_4$].

The $\mathbf{1H}^+$ ion possesses a 7-coordinate, pentagonal-bipyramidal geometry about the tungsten center in the solid state, as determined by X-ray crystallography for **1H**[$B(C_6F_5)_4$] (Figure 2.1). The benzylidyne and chloride ligands are linearly disposed ($\angle$(C≡W–Cl) = 179.09(10)°) and occupy axial sites in the structure, and the four phosphorus nuclei and hydride ligand are arranged equatorially ($\angle(C{\equiv}W{-}P)_{avg}$ = 92.91[10]°, $\angle$(C≡W–H) = 92.8(11)°). The hydride ligand was located in the difference map (*d*(W–H) = 1.64(3) Å); it bisects the obtuse cleft between dmpe ligands. The WC bond length is typical of that for a tungsten–carbon triple bond (*d*(W≡C): $\mathbf{1H}^+$, 1.809(3); **1**,[12] 1.829(2) Å), consistent with the description of $\mathbf{1H}^+$ as a tungsten–benzylidyne complex. These structural features are qualitatively similar to those observed for other metal–alkylidyne hydride complexes that have been structurally characterized.[18,33-36] The bond lengths and angles found for $\mathbf{1H}^+$ are very close to those provided by a density functional theory geometry optimization of the ion in the gas phase (Table 2.4), indicating that this is the electronically preferred structure.

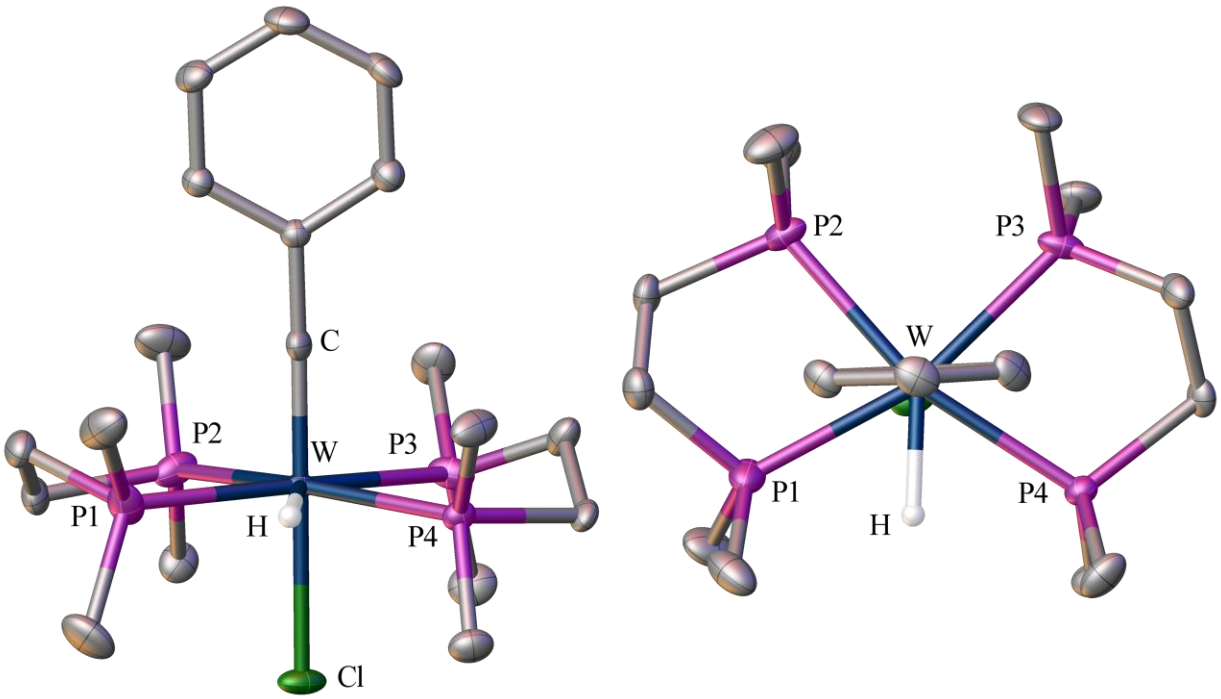

Figure 2.1. Structure of the $\mathbf{1H}^+$ ion in $\mathbf{1H}[B(C_6F_5)_4]\bullet 3(CH_3CN)$ (50% probability thermal ellipsoids). For clarity, H atoms other than the hydride ligand are omitted and only one orientation of the disordered dmpe CH_2CH_2 unit is shown. Select bond lengths (Å) and angles (°): W–C = 1.809(3), W–Cl = 2.5362(11), W–H = 1.64(3), $W–P(1,4)_{avg}$ = 2.4545[9], $W–P(2,3)_{avg}$ = 2.5600[9], P(1)–W–P(4) = 119.13(3), P(2)–W–P(3) = 86.45(3), $H–W–P(1,4)_{avg}$ = 59.6[11], C–W–Cl = 179.09(10), C–W–H = 92.8(11), $C–W–P_{avg}$ = 92.91[10].

The structure of $\mathbf{1H}^+$ is fluxional in solution at room temperature, as evidenced by marked changes to its ^{1}H- and ^{31}P-NMR spectra as a function of temperature. Newsom reported that at low temperature (190 K), the NMR spectra of $\mathbf{1H}[PF_6]$ in CD_2Cl_2 are consistent with the pentagonal-bipyramidal structure observed for $\mathbf{1H}^+$ in the crystal structure: the ^{31}P-NMR spectrum exhibits two complex multiplets (Figure 2.6), indicating the presence of two inequivalent pairs of phosphorus nuclei, and the ^{1}H NMR spectrum displays resonances for four corresponding inequivalent pairs of dmpe CH_3 groups (Figure 2.4).[30] The NMR spectra change significantly as the temperature is raised, and at room temperature are consistent with $\mathbf{1H}^+$ possessing a time-averaged structure of higher symmetry. Specifically, the two ^{31}P-NMR resonances broaden at ~240 K, coalesce at ~280 K, and become a broad single resonance at room

temperature (Figure 2.6), while the four ^{1}H-NMR resonances of the dmpe CH_3 groups evolve to become two resonances above 260 K (Figure 2.3). These observations indicate that the four phosphorus nuclei are symmetry-equivalent on the NMR time scale at room temperature. Consistent with this, the W–H ^{1}H-NMR resonance (Figure 2.3) and the W≡C ^{13}C-NMR resonance (Figure 2.5) appear as quintets at room temperature as a result of coupling to four equivalent ^{31}P centers.[37] Closely similar behavior has been observed in the variable-temperature NMR spectra of the related metal–alkylidyne hydride complexes $TaH(C^tBu)(dmpe)_2(ClAlMe_3)$,[35] $[WH(C^tBu)(dmpe)_2Cl]^+$,[32] $[WH(CH)(dmpe)_2Cl]^+$,[31] and $[WH(CPh)(dppe)_2Cl]^+$.[18] Schrock has interpreted these phenomena as arising from interconversion between 7-coordinate, pentagonal-bipyramidal structures via a 6-coordinate, pseudo-octahedral T-shaped metal–alkylidene structure (Scheme 2.4).[31,32,38] This hypothesis is supported by the independent synthesis of compositionally similar T-shaped metal-alkylidene complexes, e.g., $Ta(CH^tBu)(dmpe)_2Cl$.[35] The potential intermediacy of a 6-coordinate tungsten–benzylidene structure for **1H**$^+$ (Scheme 2.4) has design implications for related compounds with ligands bearing second-coordination-sphere Brønsted bases, as will be discussed later.

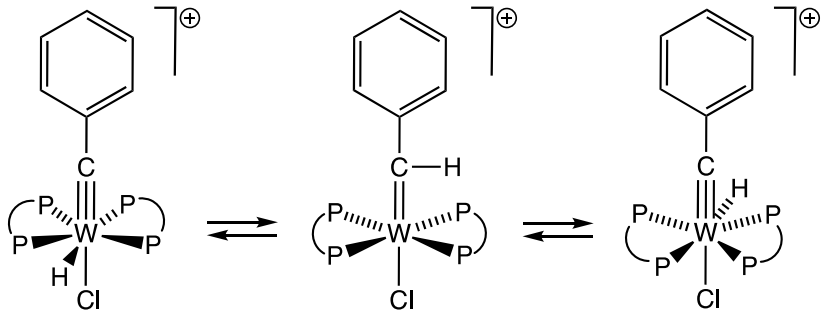

Scheme 2.4. Fluxional interconversion of 7-coordinate tungsten–benzylidyne hydride structures through a 6-coordinate T-shaped tungsten–benzylidene structure.

The pK_a of **1H**$^+$ in THF was measured by Newsom.[30] He found that that pyrrolidine (pyrr) was suitable for these experiments (Equation 2.1; pK_a(pyrrH$^+$) = 16.0 in THF).[39] Five

independent measurements provided pK_a(**1H**$^+$) = 16.8(1) in THF (Equation 2.2 and 2.3).[40,41] The acidities of other metal–alkylidyne hydride complexes have not been reported, so comparisons of the pK_a of **1H**$^+$ to those of related compounds are not possible, but more relevant to the present purpose is that its similarity to that of the alkyl ammonium pyrrH$^+$ suggests that incorporation of an alkyl amine base into the second-coordination-sphere could result in intramolecular of deprotonation of the hydride ligand.

$$\mathbf{1H}^+ + \text{pyrr} = \mathbf{1} + \text{pyrrH}^+ \tag{2.1}$$

$$K = \frac{[\mathbf{1}][\text{pyrrH}^+]}{[\mathbf{1H}^+][\text{pyrr}]} \tag{2.2}$$

$$\text{p}K_a(\mathbf{1H}^+) = \text{p}K_a(\text{pyrrH}^+) - \log(K) \tag{2.3}$$

2.2.2. Synthesis, characterization, structure, and properties of W(CPh)(P_2NN)$_2$Cl (2). To test the hypothesis that incorporating a pendant amine into the diphosphine ligands of a tungsten–alkylidyne hydride compound similar to **1H**$^+$ could result in intramolecular deprotonation, the complex W(CPh)(P_2NN)$_2$Cl (**2**, Chart 1; P_2NN = N((CH$_2$)$_3$NMe$_2$)(CH$_2$PEt$_2$)$_2$)[42] was synthesized. The P_2NN ligand was selected for three reasons. First, the presence of three alkyl groups on each phosphorus seemed likely to result in electron donation to tungsten similar to that provided by the dmpe ligands of **1H**$^+$, as required to endow the hypothetical hydride form of protonated **2** with a similar pK_a. Second, the P_2NN ligand contains both a second-coordination-sphere amine within the chelate backbone and an outer-sphere amine at the terminus of a flexible tether. The presence of two structurally distinct bases increases the probability of access to the proton. Third, the combined bases have a higher pK_a and were found in an iron H_2 oxidation catalyst to increase turnover frequency as compared to a single-base ligand.[42] Although the location of the hydride ligand in the equatorial plane hinders

its accessibility to a base appended to the backbone of a chelating phosphine ligand, fluxional passage of the H atom through a T-shaped tungsten–benzylidene structure (Scheme 2.4) positions it well for deprotonation (Scheme 2.5).

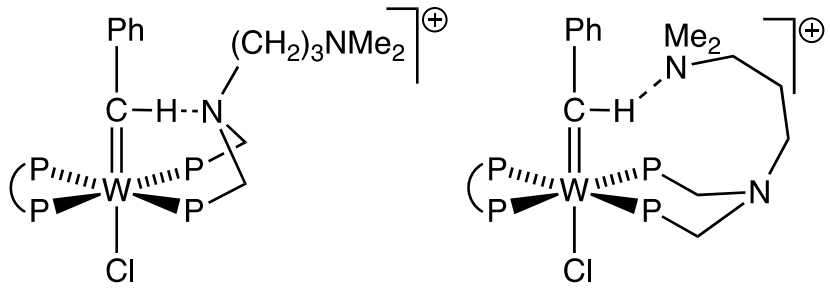

Scheme 2.5. Possible interactions between a benzylidene H atom and second- and outer-sphere amines.

Compound **2** was synthesized in 83% yield via a ligand-substitution reaction between W(CPh){P(OMe)$_3$}$_4$Cl[43] and P$_2$NN (2.1 equiv). The ^{1}H-, ^{13}C-, and ^{31}P-NMR spectra of **2** are consistent with its formulation as a pseudo-octahedral tungsten–benzylidyne complex; notable are the observation of the characteristic W≡C ^{13}C-NMR resonance at 250.3 ppm (cf. 252.3 for **1**),[13] a single ^{31}P-NMR resonance, and ^{1}H NMR signals that indicate the two P$_2$NN ligands are equivalent on the NMR time scale. The molecular structure of **2** provided by X-ray crystallography confirms this picture (Figure 2.2), exhibiting axial benzylidyne and chloride ligands and equatorial phosphine ligands. The two 6-member W(PCH$_2$NCH$_2$P) rings adopt different chair conformations in the solid state, consistent with the expectation from the NMR spectra that the barriers in solution to interconversion among conformations are low.

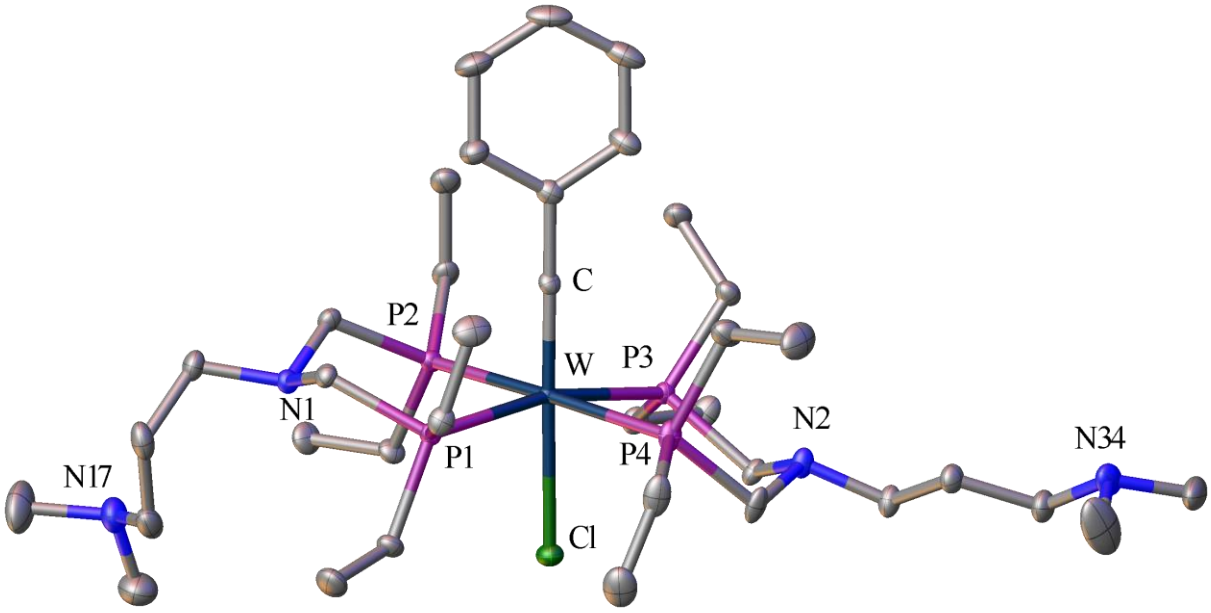

Figure 2.2. Structure of **2**·1/2(Et_2O) (50% probability ellipsoids). For clarity, H atoms, interstitial Et_2O, and disordered conformations are not shown. Select bond lengths (Å) and angles (°). W–C = 1.813(3), W–Cl = 2.5885(7), $W–P_{avg}$ = 2.4754[8], $P(1,3)–W–P(2,4)_{avg}$ = 83.91[3], $P(1,2)–W–P(3,4)_{avg}$ = 95.80[3], C–W–Cl = 178.33(9).

The molecular structure and electronic structure and properties of **2** are closely similar to those of **1**, suggesting that the pK_a of $\mathbf{1H}^+$ provides a reasonable estimate for that of the hypothetical tungsten–benzylidyne hydride form of protonated **2**. Specifically, the core bond lengths (W≡C, W–P, W–Cl) and bond angles (C–W–P, C–W–Cl) of **1**[12] and **2** are essentially identical (Δd < 0.04 Å, $\Delta\angle$ < 0.5°), with the single exception that the P–W–P angles of **2** differ slightly (by ~3°) from those of **1** owing to the different backbones of the chelating phosphine ligands (Table 2.2). The electrochemistry exhibited by **2** in THF is correspondingly close to that previously reported for **1**, with both possessing a reversible oxidation (by cyclic voltammetry) arising from the $(d_{xy})^2/(d_{xy})^1$ couple at oxidation potentials that are identical within experimental error ($E_{1/2}^{0/+}$, V vs. $FeCp_2^{0/+}$: **1**, –0.82 V;[13] **2**, −0.83 V, Figure 2.11). Similarly, the electronic-absorption spectra of the compounds exhibit only small differences from each other (Figure 2.12), displaying the characteristic $^1[d_{xy}\rightarrow\pi^*(WCPh)]$ band (**1**, 532 nm; **2**, 548 nm) and

$^1[\pi(WCPh)\rightarrow\pi^*(WCPh)]$ band (**1**, 338 nm; **2**, 336 nm) at similar wavelengths. Compound **2** also exhibits the $^3[d_{xy}\leftarrow\pi^*(WCPh)]$ photoluminescence typical of $W(CPh)L_4X$ chromophores (Figure 2.13). Given their similar molecular and electronic structures and properties, it is reasonable to assume that the pK_a of the hypothetical hydrido form of protonated **2**, $[WH(CPh)(P_2NN)_2Cl]^+$, is reasonably approximated by that measured for $\mathbf{1H}^+$.[44] That such a 7-coordinate structure is plausible is supported by a DFT calculation, which predicts a structure for $[WH(CPh)(P_2NN)_2Cl]^+$ that is qualitatively similar to that of $\mathbf{1H}^+$ (Figure 2.21 and Table 2.5).

2.2.3. Protonation of 2 and characterization of $\mathbf{2H}^+$. Compound **2** was protonated via its reaction in THF with the pyridinium ion (as present in $[HNC_5H_5][B(C_6H_3\text{-}3,5\text{-}(CF_3)_2)_4]$, denoted [pyH][$BAr^{F24}$]). Pyridinium (p$K_a$ = 7.8 in THF)[39] was used because it is expected to be capable of protonating **2** either at the tungsten center, which would produce a tungsten–hydride compound (cf. pK_a($\mathbf{1H}^+$) = 16.8), or at either of the alkyl amine moieties of the P_2NN ligand. The reaction between **2** and [pyH][BAr^{F24}] (1 equiv) results in the formation of a new compound, denoted **2H**[BAr^{F24}], as evidenced by changes to the electronic-absorption and ^{1}H- and ^{31}P-NMR spectra of the reaction mixture. The electronic-absorption spectrum of **2H**[BAr^{F24}] exhibits $^1[d_{xy}\rightarrow\pi^*(WCPh)]$ and $^1[\pi(WCPh)\rightarrow\pi^*(WCPh)]$ bands that are similar to but distinct from those of **2** (Figure 2.14; $d_{xy}\rightarrow\pi^*$: **2**, 543 nm; $\mathbf{2H}^+$, 533 nm; $\pi\rightarrow\pi^*$: **2**, 335 nm; $\mathbf{2H}^+$, 331 nm). The $^{31}P\{^1H\}$-NMR spectrum of $\mathbf{2H}^+$ exhibits a broad resonance at –8.1 ppm rather than the sharp singlet observed for **2** at –9.3 ppm (Figure 2.15), and its ^{1}H-NMR spectrum exhibits broad resonances that, in some instances, are shifted markedly from those of **2** (Figures 2.16 and 2.17, Table 2.3). Neither the ^{1}H-NMR nor ^{31}P-NMR spectra of the reaction mixture display signals due to unreacted **2**, and the ^{1}H-NMR spectrum exhibits signals for free pyridine that integrate to 1 equiv, indicating the complete conversion of reactants to products. The spectra were not

observed to change over the course of several days, suggesting that **2H**$^+$ is a stable product. The protonation of **2** is reversible; addition of 1.05 equiv KO^{t}Bu to the reaction mixture containing **2H**$^+$ completely restores the electronic-absorption spectrum and sharp ^{1}H- and ^{31}P-NMR spectra of **2** (Figures 2.15 and 2.16), and produces ^{1}H-NMR signals for HO^{t}Bu (Figure 2.17).

The spectroscopic data for **2H**$^+$ indicate that it is not a tungsten–benzylidyne hydride complex in solution, but rather that the site of protonation is one of the pendant amine groups of the P_2NN ligand. The fact that the $^1[d_{xy} \rightarrow \pi^*(WCPh)]$ and $^1[\pi(WCPh) \rightarrow \pi^*(WCPh)]$ bands of **2H**$^+$ are only slightly shifted from those of **2** (Figure 2.14) indicates that the electronic structure of **2H**$^+$ is very similar to that of **2**, which is inconsistent with the presence of a hydride ligand. By comparison, **1** and **1H**$^+$ exhibit markedly different electronic-absorption spectra (Figure 2.18), as expected for two complexes that possess substantially different molecular structures and formal electron configurations (**1**, d^2; **1H**$^+$, d^0). Although the ^{31}P-NMR spectrum of **2H**$^+$ at room temperature exhibits a single broad resonance, like that of tungsten–hydride complex **1H**$^+$, upon cooling to 185 K this resonance evolves in a manner similar to that of **2** to produce, in both cases, a broad doublet of doublets with similar chemical shifts for both compounds (**2H**$^+$: δ 5.2 and 8.3, Figure 2.19; **2**: δ 7.1 and 10.6, Figure 2.20). This indicates that the ligand coordination geometry about the tungsten center is the same in both **2** and **2H**$^+$.[45] These ^{31}P-NMR spectra differ substantially from that for hydrido complex **1H**$^+$ (Figure 2.6), which exhibits two strongly split resonances (δ 40.88 and 21.59) as a result of the marked asymmetry within the pentagonal-bipyramidal structure.

The site of protonation within the P_2NN ligand of **2H**$^+$ was established to be the pendant NMe_2 group. Comparison of the ^{1}H-NMR chemical shifts of corresponding resonances in **2** and **2H**$^+$ (Table 2.3) indicates that only two differ between compounds by more than 0.1 ppm: N<u>Me</u>$_2$

($\Delta\delta$ = 0.38 ppm) and CH_2NMe_2 ($\Delta\delta \geq 0.33$). The other references differ in chemical shift by less than 0.1 ppm, indicating they are unaffected by protonation. The ^{1}H-NMR resonance arising from the added proton ($\underline{H}NMe_2(CH_2)_3$) was not observed (nor was it reported to be observed at room temperature in the previously studied complex $[Cp^{C5F4}NFeH(P_2NNH)]^+$ bearing this ligand),[42] but was clearly identified in the ^{2}H-NMR spectrum of **2D**[BAr^{F24}] at 8.11 ppm.

Because protonation at one P_2NN ligand in $\mathbf{2H^+}$ renders it inequivalent with the second P_2NN ligand, the fact that only one set of ligand resonances are observed in the ^{1}H and $^{31}P\{^1H\}$ NMR spectra is consistent with rapid exchange of the added proton between ligands. The fact that all resonances in the ^{1}H-NMR spectrum of $\mathbf{2H^+}$ are broad, including those for the WC$\underline{Ph}$ and P$\underline{Et_2}$ groups that are remote from the $HNMe_2$ site but close to the basic tungsten center and α-carbon atom (W≡CPh), strongly suggests that intramolecular proton transfer between P_2NN ligands is operative, possibly via 6-coordinate T-shaped tungsten–benzylidene and/or 7-coordinate tungsten–benzylidyne hydride transients (Schemes 2.4 and 2.5). Attempts to probe this further by variable temperature ^{1}H-NMR spectroscopy were unsuccessful because highly complicated spectra emerge at lower temperatures. Complex low-temperature ^{1}H-NMR spectra are also observed for **2**, most likely as a result of conformational locking of the 6-member $W(PCH_2NCH_2P)$ rings.

2.3 Conclusions.

The aim of this study was to probe whether tungsten–alkylidyne hydride complexes bearing second-coordination-sphere Brønsted bases could undergo intramolecular deprotonation, which would facilitate the H_2-activation-enabled regeneration of tungsten–alkylidyne photoredox chromophores (Scheme 2.1). The collective results for $\mathbf{1H^+}$, **2**, and $\mathbf{2H^+}$ indicate that this is plausible. The typical 7-coordinate tungsten–benzylidyne hydride complex $\mathbf{1H^+}$ is known to

possess a pK_a compatible with deprotonation by amine bases, and a fluxionally accessible 6-coordinate tungsten–benzylidene structure that improves the structural accessibility of the acidic hydrogen atom (Schemes 2.4 and 2.5).[30] The compound **2**, which incorporates ligands with pendant second- and outer-coordination-sphere amines, possesses a molecular structure, electronic structure, and redox potential very similar to **1**, suggesting that the hypothetical hydride form of protonated **2** should have a pK_a similar to that of $\mathbf{1H}^+$. It also exhibits photoluminescence, showing that the pendant amines do not interfere with the photophysical properties essential to photoredox function. The facts that the site of protonation of **2** is at the pendant NMe_2 group rather than the tungsten center, and that intramolecular exchange of this proton between the two P2NN ligands is operative, indicates that this site is the thermodynamic product.

Tungsten alkylidyne catalysts are a powerful class of photoredox chromophores whose properties can by broadly tuned via ligand variation. The incorporation of second-coordination-sphere bases provides a second level of control by manipulating the acid–base chemistry of these compounds without perturbing the molecular and electronic structure. These bases may facilitate deprotonation of metal hydrides and the shuttling of protons to the molecular periphery, improving turnover during chromophore regeneration.

2.4 Experimental Section.

2.4.1 Synthesis and Characterization of New Compounds.

General procedures. All experiments were performed under a nitrogen atmosphere using standard Schlenk and glovebox techniques. Solvents used for syntheses were HPLC grade, and purified by passing them under nitrogen pressure through an anaerobic, stainless-steel system consisting of either two 4.5 in. × 24 in. (1 gal) columns of activated A2 alumina (CH_3CN, Et_2O,

CH_2Cl_2, and THF) or one column of activated A2 alumina and one column of activated BASF R3-11 catalyst (toluene and pentane).[46] C_6D_6, CD_2Cl_2, and CD_3CN were stored over activated 3Å molecular sieves and THF-d_8 was stored over Na/K (1:2) alloy, from which they were transferred under vacuum. W(CPh)(dmpe)$_2$Cl (**1**),[13] W(CPh)Cl$_3$(dme),[47] N((CH$_2$)$_3$NMe$_2$)(CH$_2$PEt$_2$)$_2$ (P_2NN),[42] and W(CPh){P(OMe)$_3$}$_4$Cl[43] were prepared according to standard procedures. Na[BAr^{F24}] ([BAr^{F24}]$^-$ = [B(3,5-C$_6$H$_3$(CF$_3$)$_2$)$_4$]$^-$) was washed with cold CH_2Cl_2 until colorless and then dried under vacuum at 100 °C for 48 h.[48] [N^{n}Bu$_4$][PF$_6$] (Fluka, electrochemical grade) was recrystallized 2–3× from MeOH and dried under vacuum at 100 °C for 12 h. All other reagents were obtained from commercial sources and used as received. ^{1}H-, ^{2}H-, ^{13}C{^{1}H}-, and ^{31}P{^{1}H}-NMR spectra were recorded with Bruker Avance II+ 500, DRX 500, or DRX 400 NMR spectrometers; measurements were made at room temperature unless noted otherwise. Chemical shifts were measured relative to solvent resonances (^{1}H, ^{2}H, and ^{13}C)[49] or to an external standard of 85% H_3PO_4 (^{31}P). Variable-temperature NMR spectra were measured after allowing samples to equilibrate at the temperature set point for at least 15 minutes. High-resolution mass spectrometry employed an Agilent 6224 Accurate-Mass TOF LC/MS; spectra were calibrated against a purine standard.

[WH(CPh)(dmpe)$_2$Cl][B(C$_6$F$_5$)$_4$] (1H[B(C$_6$F$_5$)$_4$]) and [WH(^{13}CPh)(dmpe)$_2$Cl][B(C$_6$F$_5$)$_4$] (1H*[B(C$_6$F$_5$)$_4$]). The following synthesis is adapted from that reported by Newsom,[30] and the originally reported characterization data are supplemented below by new data acquired from this sample. To a stirred, room temperature solution of **1** (0.0637 g, 0.101 mmol) in THF (5 mL) was added a solution of HCl in diethyl ether (0.122 mL, 1 M, 0.122 mmol). The pink solution became colorless immediately and an off-white precipitate formed. The volatile components were removed under vacuum and a solution of Li[B(C$_6$F$_5$)$_4$] (0.070 g, 0.101 mmol) in acetonitrile (15

mL) was added to the remaining solid with stirring. The mixture was allowed to stir overnight, during which time a gray precipitate formed. The solution was filtered through Celite, reduced to dryness under vacuum, and the remaining solid was extracted into dichloromethane (5 mL), providing a yellow solution. The solution was filtered through Celite and the filtrate then reduced to dryness under vacuum. Recrystallization of the crude product from a concentrated acetonitrile solution cooled to –30 °C provided 0.108 g of light-yellow, needle-shaped crystals (82% yield). The ^{13}C-labeled compound **1H***[$B(C_6F_5)_4$] was prepared analogously from **1***. ^{1}H NMR (400.13 MHz, CD_2Cl_2; Figure 2.3): δ 7.17 (m, 3H, *m*- and *p*-Ph), 6.83 (m, 2H, *o*-Ph), 2.12 (br m, 8H, PCH_2), 1.98 (d, 12H, J = 8.5 Hz, PCH_3), 1.80 (for **1H*$^+$**: d quin, 1H, $^2J_{HP}$ = 39.2 Hz, $^2J_{HC}$ = 6.5 Hz, WH), 1.77 (d, 12H, J = 8.5 Hz, PCH_3). ^{1}H NMR (500.13 MHz, THF-d_8): δ 7.13 (m, 3H, *m*- and *p*-Ph), 6.97 (m, 2H, *o*-Ph), 2.21 (d, 8H, J = 17.6 Hz, PCH_2), 2.02 (d, 12H, J = 8.5 Hz, PCH_3), 1.91 (quin, 1H, $^2J_{HP}$ = 39.0 Hz, WH), 1.79 (d, 12H, J = 8.5 Hz, PCH_3). ^{13}C{^{1}H} NMR (100.63 MHz, CD_2Cl_2; Figure 2.5): δ 263.50 (for **1H*$^+$**: quin with satellites, $^2J_{CP}$ = 12 Hz, $^1J_{CW}$ = 189 Hz, WC), 148.55 (br d, $^1J_{CF}$ = 237 Hz, C_6F_5), 138.63 (br d, $^1J_{CF}$ = 246 Hz, C_6F_5), 136.43 (br d, $^1J_{CF}$ = 252 Hz, C_6F_5), 130.84 (br, Ph), 128.60 (for **1H*$^+$**: d, $^2J_{CC}$ = 3 Hz, Ph), 128.44 (Ph), 29.58 (m, PCH_2), 19.87 (m, PCH_3), 14.18 (m, PCH_3); the *ipso*-Ph and *ipso*-C_6F_5 resonances were not observed. ^{13}C{^{1}H} NMR (125.78 MHz, THF-d_8): δ 262.57 (for **1H*$^+$**: quin with satellites, $^2J_{CP}$ = 12 Hz, $^1J_{CW}$ = 189 Hz, WC). ^{31}P{^{1}H} NMR (125.78 MHz, CD_2Cl_2): δ 30.0 (br). ^{31}P{^{1}H} NMR (125.78 MHz, THF-d_8): δ 28.0 (br). HR-MS (ESI+, CH_2Cl_2) *m*/*z* for $^{13}CC_{18}H_{38}P_4ClW^+$ (**1H*$^+$**): calcd, 610.1107; found, 610.1122 [M^+].

W(CPh)(P_2NN)$_2$Cl (2). *Route A:* To a solution of W(CPh){$P(OMe)_3$}$_4$Cl (0.200 g, 0.248 mmol) in toluene (20 mL) was added a solution of P_2NN (0.160 g, 0.521 mmol) in toluene (10 mL). The mixture was refluxed with stirring for 12 h. The reaction mixture gradually changed color from

yellow to red to violet. Removal of the volatile components under vacuum yielded a violet solid; this was extracted into diethyl ether (ca. 10 mL). The resulting solution was filtered through a pad of Celite, and the filtrate was reduced to dryness under vacuum. The solid was washed with cold acetonitrile and dried under vacuum to yield 0.190 g of pure product (83% yield). *Route B:* To a stirred, room-temperature solution of $W(CPh)Cl_3(dme)$ (0.232 g, 0.494 mmol) in THF (10 mL) was added a solution of P_2NN (0.318 g, 1.03 mmol) in THF (5 mL). The solution rapidly changed color from turquoise to dark yellow/brown and a yellow precipitate formed. After 15 min, Na/Hg amalgam (0.4% w/w, 1.236 mmol Na) was added to the suspension and the reaction mixture was stirred vigorously overnight. The reaction mixture gradually changed color from dark yellow/brown to olive green to dark red. The solution phase was decanted from the mercury and the volatile components were removed from it under vacuum to yield a sticky red solid. The solid was extracted into toluene (ca. 15 mL) and the solution was filtered through a pad of Celite. The volatile components of the filtrate were removed under vacuum and the remaining solid was dissolved in a minimum volume of pentane (ca. 4 mL), filtered through Celite, and cooled to –50 °C overnight to yield a violet microcrystalline solid. The product was washed with cold acetonitrile and dried under vacuum to yield 0.124 g of product. The pentane mother liquor was concentrated and cooled to –50 °C to provide two additional crops of product, yielding 0.211 g total (46% yield). Single crystals suitable for X-ray diffraction measurements were grown from a concentrated Et_2O solution cooled to –50 °C overnight. The compound is soluble in THF, diethyl ether, benzene, and sparingly soluble in pentane and acetonitrile. ^1H (500.13 MHz, C_6D_6; Figure 2.8): δ 7.39 (d, 2H, *J* = 8.0 Hz, *o*-Ph), 7.08 (t, 2H, *J* = 7.5 Hz, *m*-Ph), 6.99 (t, 1H, *J* = 7.2 Hz, *p*-Ph), 3.39 (d, 4H, *J* = 12.5 Hz, PCH_2N), 2.93 (d, 4H, *J* = 12.5 Hz, PCH_2N), 2.51 (t, 4H, *J* = 7.0 Hz, $NC\underline{H}_2CH_2CH_2NMe_2$), 2.29 (m, 4H, *J* = 7.5 Hz, $PC\underline{H}_2CH_3$), 2.26 (t overlapped with δ 2.29,

4H, *J* = 7.0 Hz, $NCH_2CH_2C\underline{H}_2NMe_2$), 2.20–2.00 (m overlapped with δ 2.14, 12H, *J* = 7.5 Hz, $PC\underline{H}_2CH_3$), 2.14 (s, 12H, NMe_2), 1.66 (quin, 4H, *J* = 7.0 Hz, $NCH_2C\underline{H}_2CH_2NMe_2$), 1.15 (br m, 12H, $PCH_2C\underline{H}_3$), 1.09 (br m, 12H, $PCH_2C\underline{H}_3$). $^{13}C\{^1H\}$ (125.78 MHz, C_6D_6; Figure 2.7): 250.31 (WC), 155.12 (*ipso*-Ph), 130.48 (*o*-, *m*-, or *p*-Ph), 127.60 (*o*-, *m*-, or *p*-Ph), 122.76 (*o*-, *m*-, or *p*-Ph), 62.94 ($N\underline{C}H_2CH_2CH_2NMe_2$), 57.88 (2 overlapping peaks, $NCH_2CH_2\underline{C}H_2NMe_2$ and PCH_2N; assigned via an HMQC spectrum, Figure 2.9), 45.67 (NMe_2), 27.64 ($P\underline{C}H_2CH_3$), 25.56 ($NCH_2\underline{C}H_2CH_2NMe_2$), 22.33 ($P\underline{C}H_2CH_3$), 9.81 ($PCH_2\underline{C}H_3$), 9.01 ($PCH_2\underline{C}H_3$). $^{31}P\{^1H\}$ NMR (202.45 MHz, C_6D_6): –6.91 (s with satellites, $^1J_{PW}$ = 262 Hz; Figure 2.10). ^1H NMR (500.13 MHz, THF-d_8): δ 7.08 (d, 2H, *J* = 7.5 Hz, *o*-Ph), 6.91 (overlapping m, 3H, *m*- and *p*-Ph), 3.29 (d, 4H, *J* = 12.5 Hz, PCH_2N), 2.91 (d, 4H, *J* = 12.5 Hz, PCH_2N), 2.55 (t, 4H, *J* = 7.0 Hz, $NC\underline{H}_2CH_2CH_2NMe_2$), 2.29 (t, 4H, *J* = 7.0 Hz, $NCH_2CH_2C\underline{H}_2NMe_2$), 2.16 (s, 12H, NMe_2), 2.20–1.93 (m overlapped with δ 2.16, 16H, $PC\underline{H}_2CH_3$), 1.69 (quin, 4H, *J* = 7.0 Hz, $NCH_2C\underline{H}_2CH_2NMe_2$), 1.12 (br m, 12H, $PCH_2C\underline{H}_3$), 1.06 (br m, 12H, $PCH_2C\underline{H}_3$). $^{13}C\{^1H\}$ NMR (100.63 MHz, THF-d_8): δ 250.39 (WC), 155.17 (*ipso*-Ph), 130.64 (*o*- ,*m*-, or *p*-Ph), 127.46 (*o*, *m*-, or *p*-Ph), 122.57 (*o*-, *m*-, or *p*-Ph), 63.16 ($N\underline{C}H_2CH_2CH_2NMe_2$), 58.20 ($PCH_2N$), 58.06 ($NCH_2CH_2\underline{C}H_2NMe_2$), 45.63 ($NMe_2$), 27.77 ($P\underline{C}H_2CH_3$), 25.72 ($NCH_2\underline{C}H_2CH_2NMe_2$), 22.34 ($P\underline{C}H_2CH_3$), 9.72 ($PCH_2\underline{C}H_3$), 8.86 ($PCH_2\underline{C}H_3$). $^{31}P\{^1H\}$ NMR (202.4 MHz, THF-d_8): δ –9.32 (s with satellites, $^1J_{WP}$ = 262 Hz). HR-MS (ESI+, CH_2Cl_2) *m/z* for $WP_4ClN_4C_{37}H_{77}^+$: calcd, 920.4364; found, 920.4345 $[M]^+$.

$[HNC_5H_5][BAr^{F24}]$ ([pyH][BAr^{F24}]) and $[DNC_5H_5][BAr^{F24}]$ ([pyD][BAr^{F24}]). This salt was prepared via the procedure described for [2,6-lutidinium][BAr^{F24}] and dried under vacuum at room temperature.[50] ^1H NMR (500.13 MHz, CD_2Cl_2): δ 12.08 (br s, 1H, NH), 8.72 (tt, overlapped with δ 8.70, 1H, *J* = 8.0 Hz and 1.2 Hz, *p*-NC_5H_5), 8.70 (d, 2H, *J* = 5.5 Hz, *o*-

NC_5H_5), 8.18 (br t, 2H, *J* = 7.0 Hz, *m*-NC_5H_5), 7.72 (br s, 8H, *o*-Ar BAr^{F24}), 7.56 (br s, 4H, *p*-Ar BAr^{F24}). The deuterium-labeled (d_1) compound [DNC_5H_5][BAr^{F24}] ([pyD][BAr^{F24}]) was prepared analogously. ^{2}H NMR (76.77 MHz, THF-h_8): δ 14.66 (br s, ND).

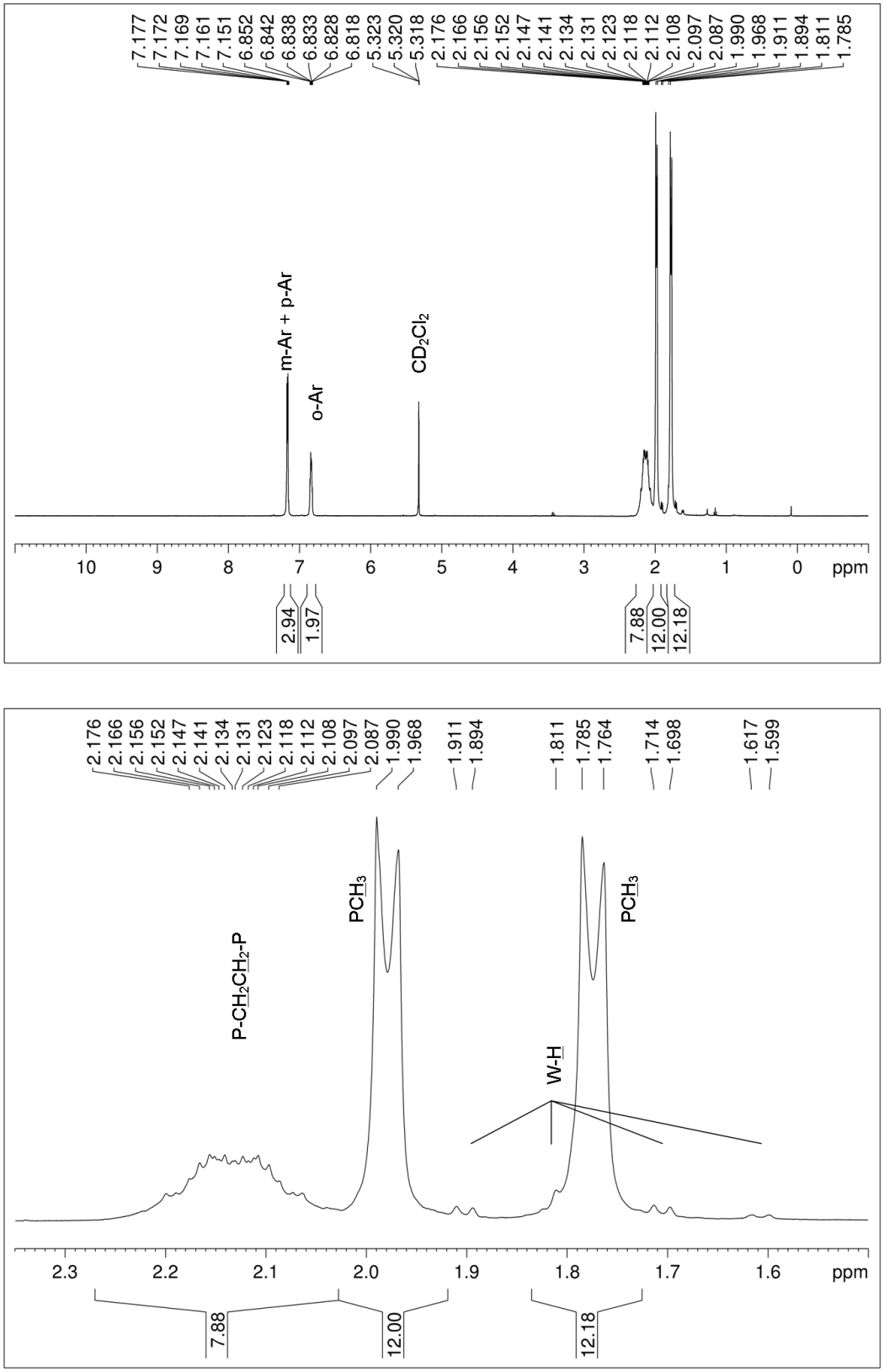

Figure 2.3. ^{1}H NMR spectrum (CD_2Cl_2) of [WH(^{13}CPh)(dmpe)$_2$Cl][B(C_6F_5)$_4$] (**1H***[B(C_6F_5)$_4$]) at room temperature. The bottom spectrum is an expansion of the top spectrum.

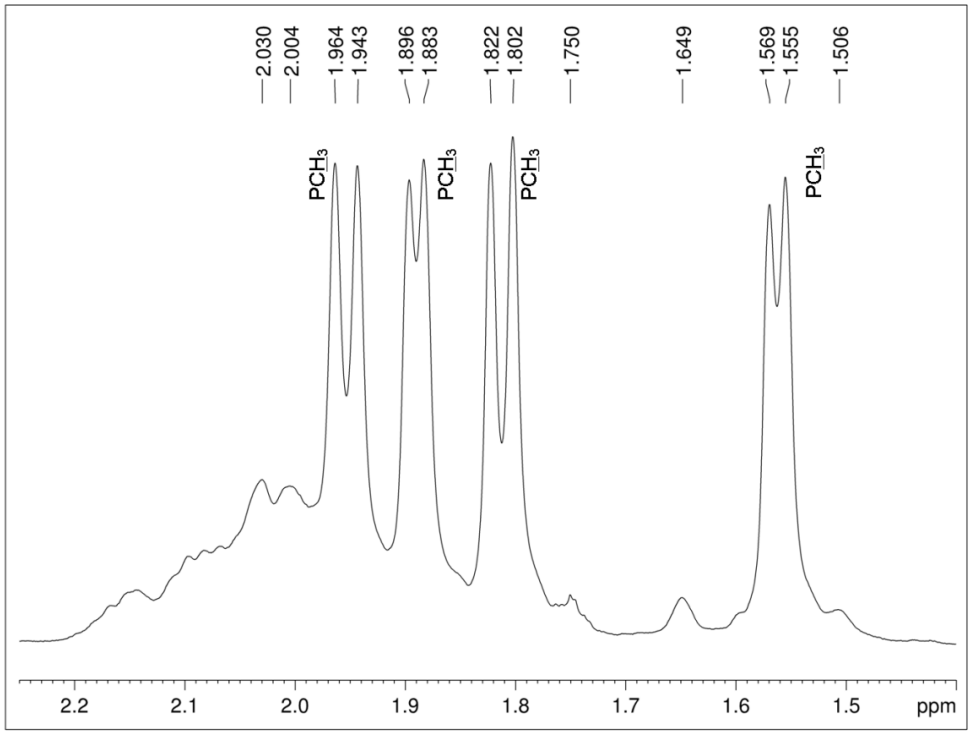

Figure 2.4. ^{1}H NMR spectrum (CD_2Cl_2) of [WH(CPh)(dmpe)$_2$Cl][B(C_6F_5)$_4$] (**1H**[B(C_6F_5)$_4$]) in the aliphatic and hydride region, T = 190.2 K. Figure adapted from data reported in ref 30. Compare with Figure 2.3.

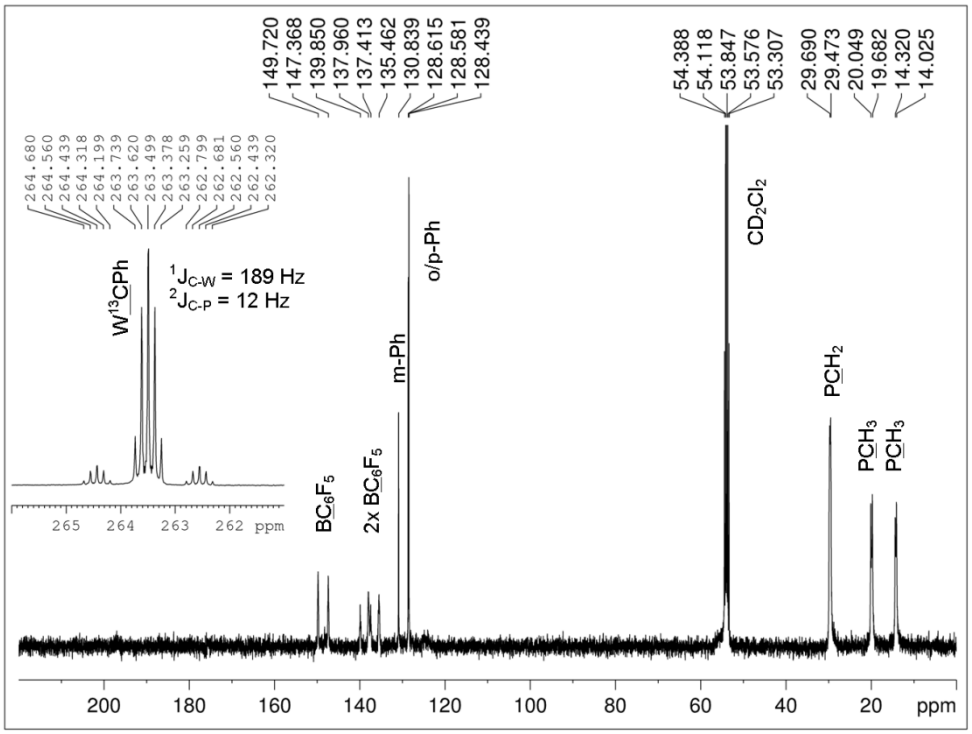

Figure 2.5. ^{13}C{^{1}H} NMR spectrum (CD_2Cl_2) of [WH(^{13}CPh)(dmpe)$_2$Cl][B(C_6F_5)$_4$] (**1H***[B(C_6F_5)$_4$]).

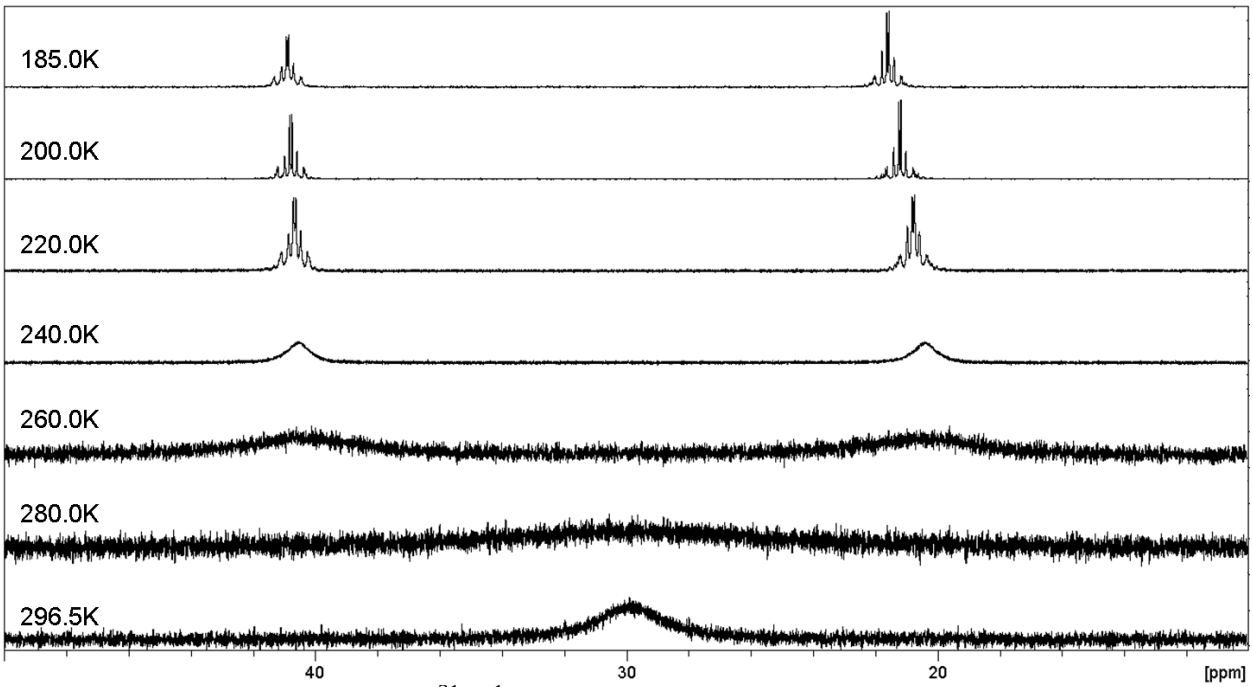

Figure 2.6. Variable-temperature $^{31}P\{^{1}H\}$ NMR spectra (CD_2Cl_2) of $[WH(CPh)(dmpe)_2Cl][PF_6]$ (**1H**$[PF_6]$). Figure adapted from data reported in ref 30.

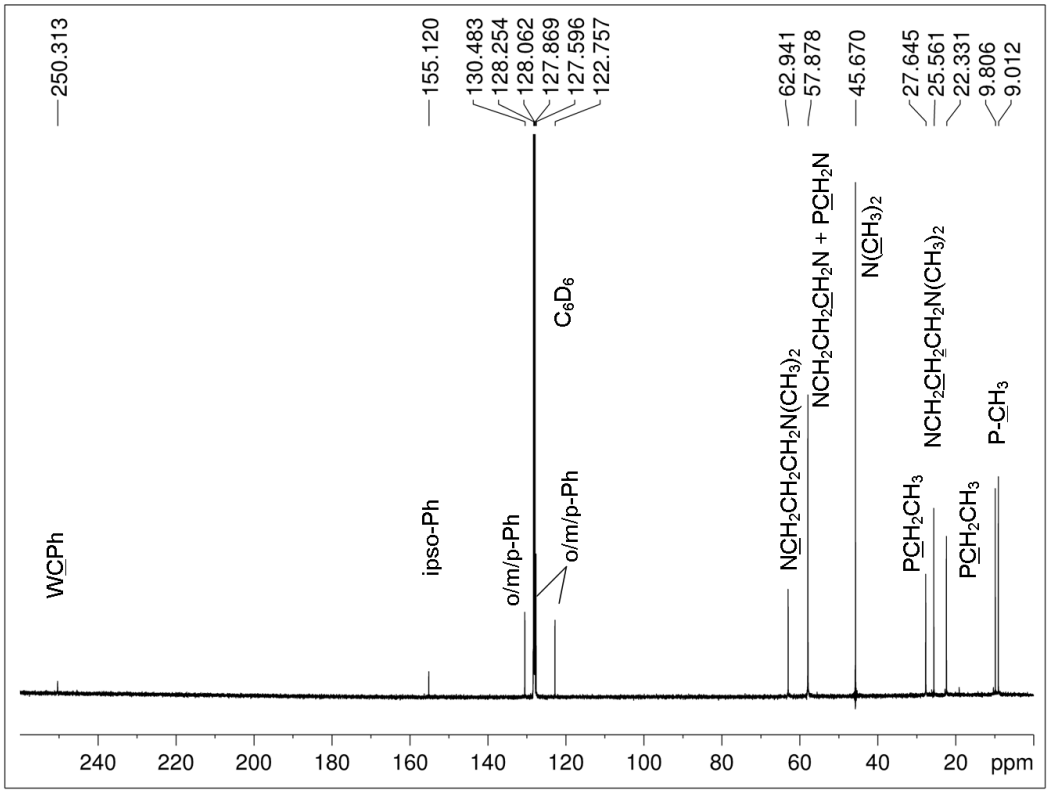

Figure 2.7. $^{13}C\{^{1}H\}$ NMR spectrum (C_6D_6) of $W(CPh)(P_2NN)_2Cl$ (**2**).

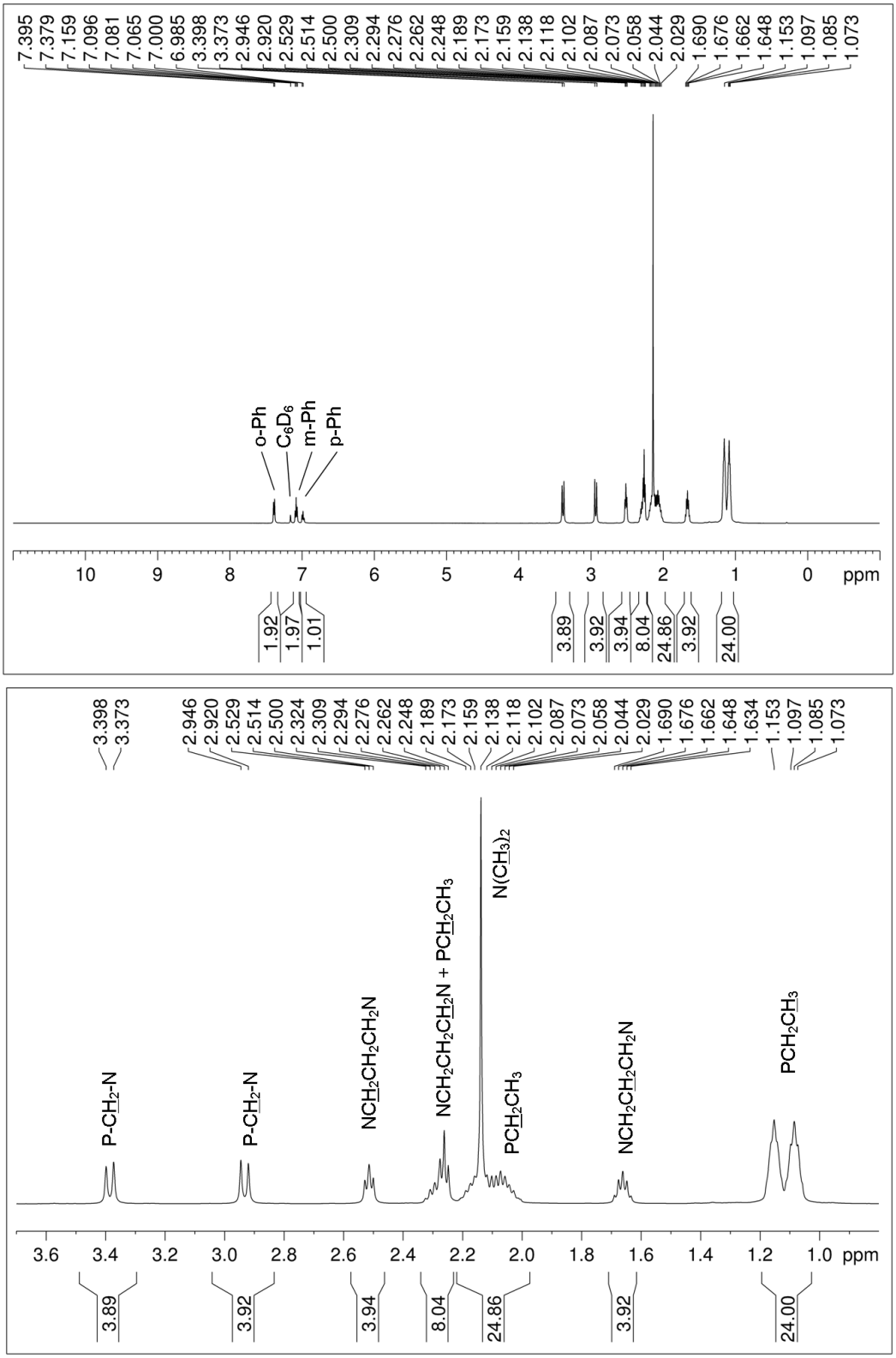

Figure 2.8. ^{1}H NMR spectrum (C_6D_6) of W(CPh)(P_2NN)$_2$Cl (**2**). The bottom spectrum is an expansion of the top spectrum.

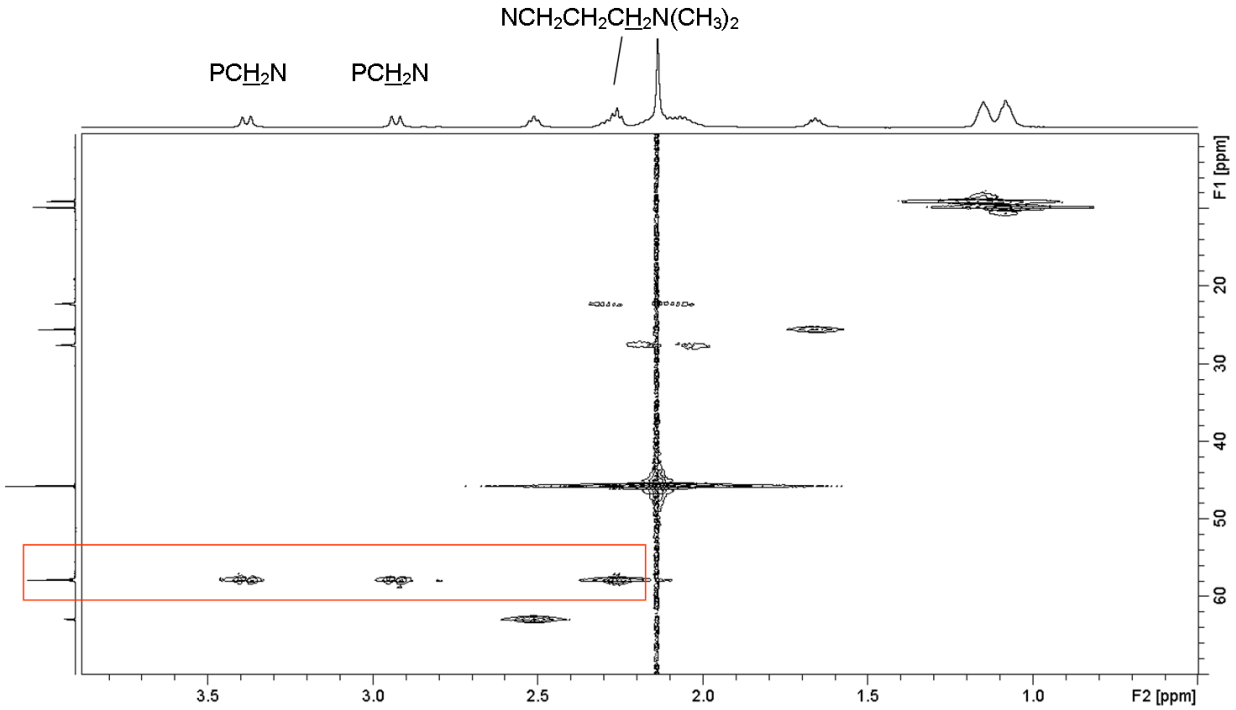

Figure 2.9. HMQC spectrum (C_6D_6) of W(CPh)($P_2NN)_2$Cl (**2**). The red box shows the overlap between the P$\underline{C}H_2N$ and $\underline{C}H_2NMe_2$ ^{13}C resonances.

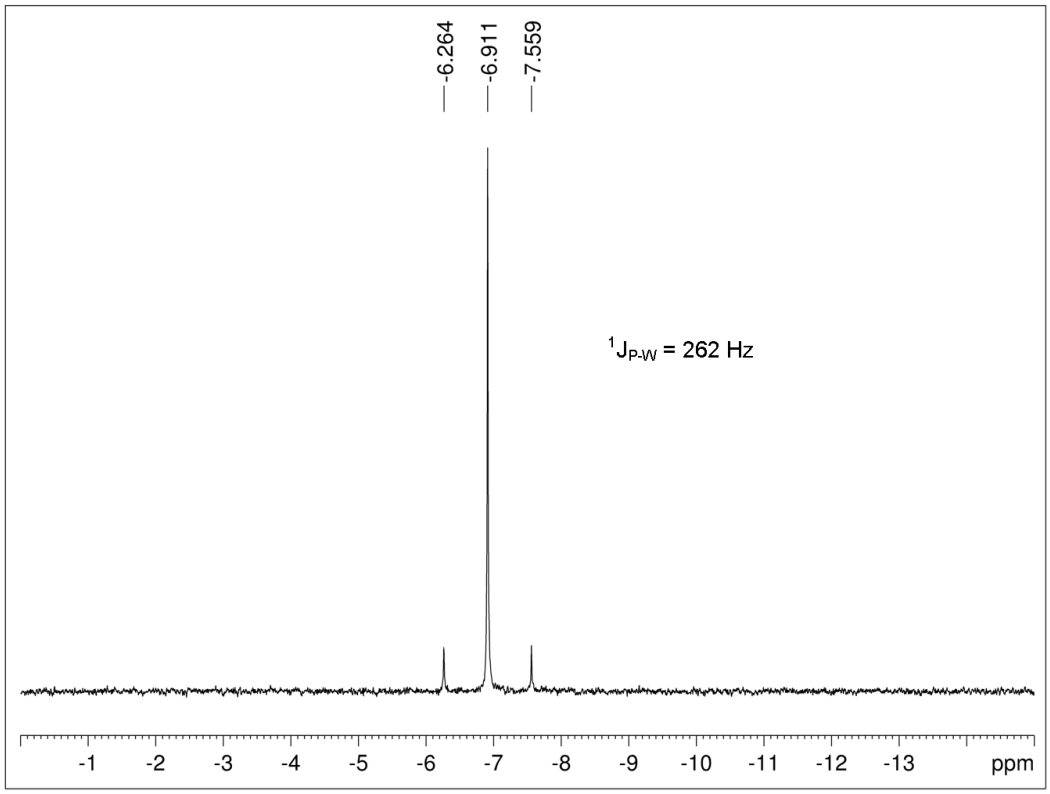

Figure 2.10. $^{31}P\{^1H\}$ NMR spectrum (C_6D_6) of W(CPh)($P_2NN)_2$Cl (**2**).

2.4.2. Single-Crystal X-ray Diffraction Studies.

General procedures. Under nitrogen, crystals were covered with Fluorolube, attached to the tip of a glass fiber, mounted in a stream of cold dry nitrogen at 100(2) K, and centered in the X-ray beam using a video camera. X-ray diffraction data were collected on a Bruker D8 VENTURE with PHOTON 100 CMOS detector system equipped with a microfocus molybdenum-target X-ray tube (λ = 0.71073 Å). Data were collected at 100(2) K using a routine of ϕ and ω scans to survey an entire hemisphere of reciprocal space and were indexed using the APEX3 program suite (Bruker AXS, version 2015.5–2). Data were corrected for absorption effects using the empirical and multiscan methods as implemented in SADABS (Bruker AXS, Version 2014/5) or TWINABS (Bruker AXS, Version 2012/1).[51] Space groups were determined based on systematic absences and intensity statistics. The structures were solved using Patterson or direct methods and refined by full-matrix least squares refinement on F^2 using the OLEX2 software package.[52] All non-hydrogen atoms were refined anisotropically and hydrogen atoms were placed in calculated positions, unless specified otherwise. Crystallographic data and details of the data collection and structure refinement are listed in Table 2.1.

Crystal structure of 1H[B(C_6F_5)$_4$]•3(CH_3CN). One interstitial acetonitrile molecule was found in the difference map and refined as normal. Two additional regions of linear residual electron density were discovered in the difference map, but refinement as acetonitrile molecules with disorder did not yield a suitable solution. The SQUEEZE[53] method as implemented in PLATON[54] was used to treat the disordered solvent, yielding solvent accessible voids at (0.000, 0.000, 0.000) of 93.7 Å^3 and 23 e^-, and (0.500, 0.000, 0.000) of 81.5 Å^3 and 24 e^-. The geometry, volume, and electrons in the voids are all consistent with two additional acetonitrile molecules.

The tungsten atom and chlorine atom were found to be disordered over two positions. The equivalent atoms were treated with an EADP restraint and allowed to refine freely to a ratio of 91.8:8.2. Electron density corresponding to lighter atoms of the minor component could not be discerned from the difference map. The hydride ligand was located in the difference map by temporarily cutting the data to $2\theta = 30°$ and allowed to refine freely on the full data set. Atoms C10–17 of the dmpe ligands were found to be disordered over two locations, treated as parts, and allowed to refine freely to a ratio of 73.4:26.6. Two sets of atoms from different parts located close in space (C13A/C13B and C17A/C17B) were treated with an EADP restraint. The P1–C10B–C11B–P backbone of one dmpe ligand from the minor component was treated with a RIGU restraint. Atom C11B was treated with an ISOR restraint to yield suitable thermal ellipsoids. Full tables of atomic coordinates, atomic displacement parameters, and bond metrics are given in Appendix II.1.

Crystal structure of 2•0.5(Et_2O). The interstitial ether molecule crystallized on an inversion center. The molecule was placed in Part –1, the occupancy was fixed to 0.50, and allowed to refine freely. A RIGU restraint was applied to the ether molecule for suitable refinement. One phosphine ethyl chain was disordered over two positions, treated as parts, and allowed to refine freely to a ratio of 53.4:46.6. A RIGU restraint was used on both parts of the disorder. The initial structure solution and refinements had an unsatisfactory goodness-of-fit, several non-positive definite atoms, and many $F_o > F_c$ suggesting possible twinning. The data reduction was revisited and the structure was refined as a three-component non-merohedral twinned crystal. The structure refined to a twin ratio of 43.34(9):28.71(7):27.95(6). Full tables of atomic coordinates, atomic displacement parameters, and bond metrics are given in Appendix II.2.

Table 2.1. Crystal Data and Structure Refinement Parameters for **1H[B(C_6F_5)$_4$]** and **2**.

Parameter	**1H[B(C_6F_5)$_4$]•3(CH_3CN)**	**2•0.5(Et_2O)**
Empirical formula	$C_{45}H_{41}BClF_{20}NP_4W$	$C_{39}H_{82}ClN_4O_{0.5}P_4W$
Formula weight	1329.78	958.26
Temperature (K)	100(2)	100(2)
Crystal system	monoclinic	triclinic
Space group	$P2_1/n$	P-1
***a* (Å)**	21.6011(11)	10.1671(7)
***b* (Å)**	8.3214(4)	11.6237(8)
***c* (Å)**	28.8908(14)	20.2729(14)
α (deg)	90	105.457(2)
β (deg)	90.8795(16)	96.009(2)
γ (deg)	90	90.452(2)
Volume (Å^3)	5192.5(4)	2294.9(3)
Z	4	2
ρ_{calc} (g/cm^3)	1.701	1.387
Abs coeff μ (mm^{-1})	2.505	2.746
***F*(000)**	2616	998
Crystal dimensions (mm^3)	0.17 × 0.16 × 0.07	0.317 × 0.278 × 0.194
Crystal habit	Colorless plate	Violet block
2Θ range for data collection (deg)	4.60 – 61.20	4.334 – 61.262
***h, k, l* ranges collected**	–30 ≤ h ≤ 30 –11 ≤ k ≤ 11 –41 ≤ l ≤ 41	–14 ≤ h ≤ 14 –16 ≤ k ≤ 16 0 ≤ l ≤ 29
Reflections collected	188724	211577
Independent reflections	15910 [R_{int}[a] = 0.0744]	14617 [R_{int}[a] = 0.0456]
Data / restraints / parameters	15910 / 29 / 740	14617 / 27 / 496
Goodness–of–fit on F^2 [d]	1.095	1.089
Final *R* indexes (*I* ≥ 2σ(*I*))	R_1[b] = 0.0377 wR_2[c] = 0.0687	R_1[b] = 0.0313 wR_2[c] = 0.0692
Final *R* indexes (all data)	R_1[b] = 0.0570 wR_2[c] = 0.0735	R_1[b] = 0.0349 wR_2[c] = 0.0713
Largest diff. peak/hole (e•Å^{-3})	0.918 / –0.742	2.186 / –1.202

[a] $R_{int} = \Sigma(|F_o^2 - \langle F_o^2 \rangle|) / \Sigma |F_o^2|$

[b] $R_1 = \Sigma ||F_o| - |F_c|| / \Sigma |F_o|$

[c] $wR_2 = \{\Sigma [w(F_o^2 - F_c^2)^2] / \Sigma [w(F_o^2)^2]\}^{1/2}$

[d] Goodness–of–fit = $[[w(F_o^2 - F_c^2)^2] / (N_{refl} - N_{params})^{1/2}$

Table 2.2. Core Bond Lengths (Å) and Bond Angles (°) of $W(CPh)(dmpe)_2Cl$ (**1**) and $W(CPh)(P_2NN)_2Cl$ (**2**).

	1[a]	**2**	Δ(**2**–**1**)
W≡C	1.829(2)	1.813(3)	–0.016
W–Cl	2.5834(5)	2.5885(7)	0.0051
$W–P_{avg}$	2.4368[6]	2.4754[8]	0.0386
$P–W–P_{intraligand,avg}$	80.775[19]	83.91[3]	3.13
$P–W–P_{interligand,avg}$	98.77[2]	95.80[3]	–2.97
C–W–Cl	178.38(6)	178.33(9)	–0.05
$C–W–P_{avg}$	93.60[6]	94.04[9]	0.44

[a] Ref[12] .

2.4.3. Electronic Spectroscopy, Photophysics, and Electrochemistry.

Electronic spectroscopic and photophysical measurements general procedures. Toluene used for electronic spectroscopy and photophysical measurements (Burdick & Jackson brand) was stored under vacuum over activated 3Å molecular sieves and then over Na/K (1:2) alloy, from which it was transferred under vacuum. Solution samples were prepared on a vacuum line in sealable cuvettes of path length 1 cm or 1 mm. The solvent was degassed with 5 freeze–pump–thaw cycles, transferred under vacuum into the cuvette, and sealed under purified nitrogen. Electronic-absorption spectra were recorded with a Cary 300 UV-visible spectrophotometer. The emission spectrum of **2** was recorded on a wavelength-calibrated PTI Quantmaster fluorimeter equipped with Peltier-cooled R928 photomultiplier-tube (PMT) and InGaAs array detectors. The emission monochrometer was wavelength-calibrated using the emission lines of an Ar lamp; wavelength accuracy is < 0.5 nm over the entire detection range. The excitation monochrometer was wavelength-calibrated using the calibrated emission monochrometer. The emission spectrum was collected using both detectors (PMT, $\lambda < 800$ nm; InGaAs, $\lambda > 700$ nm); the spectra were individually corrected for instrument response, intensity normalized in the overlapping wavelength region (700–800 nm), and merged into a single

spectrum. The emission lifetime of **2** was measured using a previously described pulsed-laser system.[55]

Electrochemical measurements. Cyclic voltammetry experiments were conducted at room temperature under a nitrogen atmosphere in a glovebox with a Bioanalytical Systems 100 B/W Electrochemical Workstation. A three-electrode configuration was utilized with Pt-disk working and auxiliary electrodes (area = 0.2 cm^2) and a Ag-wire quasi-reference electrode. Experiments were conducted in THF containing 0.1 M $[N^nBu_4][PF_6]$ as supporting electrolyte and 1.3 mM analyte. $[CoCp_2][PF_6]$ was added at the conclusion of the experiment as an internal reference; its potential relative to $FeCp_2$ was measured and found to be identical under our experimental conditions to the reported value ($E_{1/2}$ = –1.35 V vs $FeCp_2^{0/+}$).[56] Electrochemical data were analyzed using BAS 100W software (version 2.0).

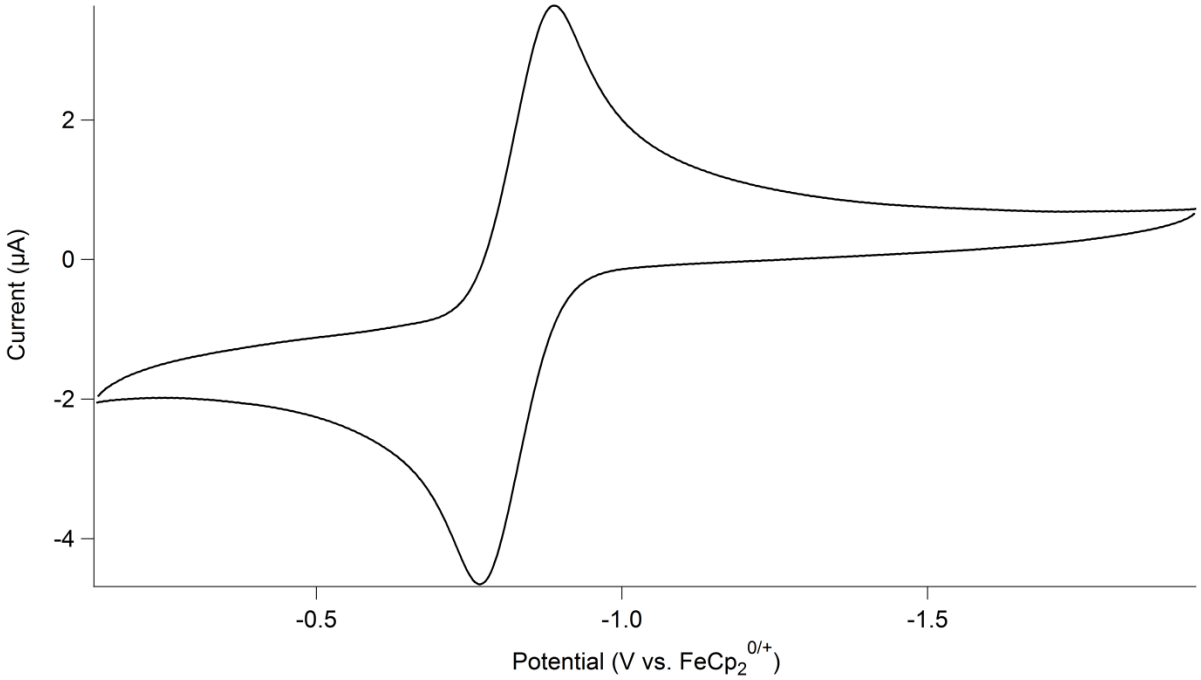

Figure 2.11. Cyclic voltammogram of $W(CPh)(P_2NN)_2Cl$ (**2**) in THF at room temperature (ν = 100 mV/s; 0.1 M $[N^nBu_4][[PF_6])$. $E_{1/2}$ = –0.83 V vs. $FeCp_2^{0/+}$.

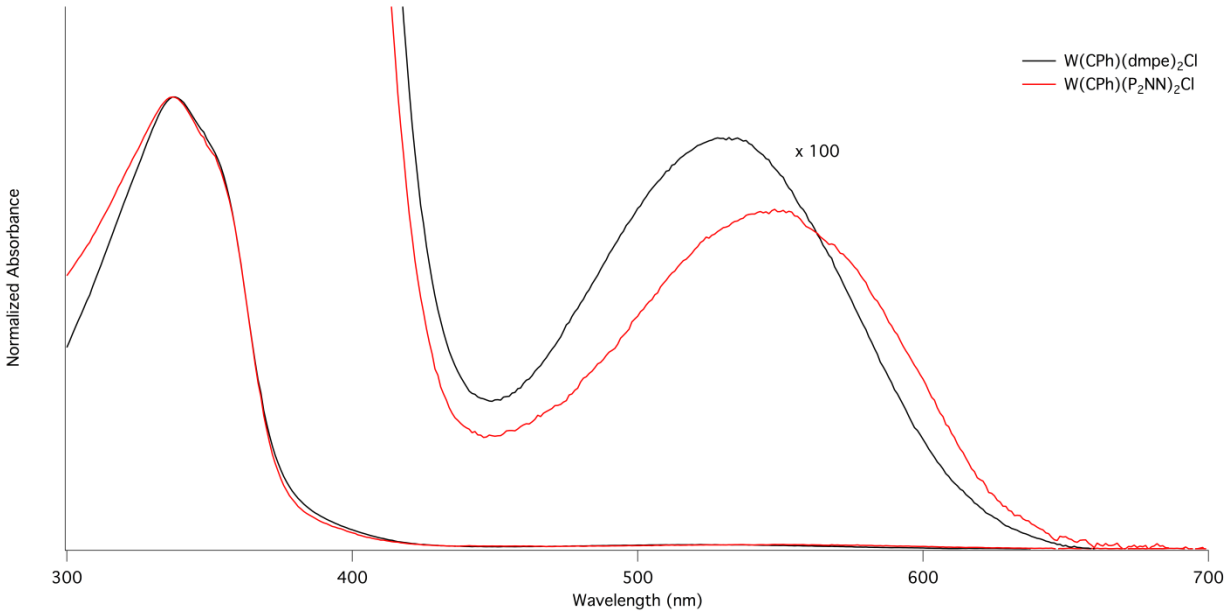

Figure 2.12. Electronic-absorption spectrum (toluene) overlay of W(CPh)(dmpe)$_2$Cl (**1**) and W(CPh)(P$_2$NN)$_2$Cl (**2**). **1**: λ_{max} = 338 nm, 532 nm. **2**: λ_{max} = 336 nm, 548 nm.

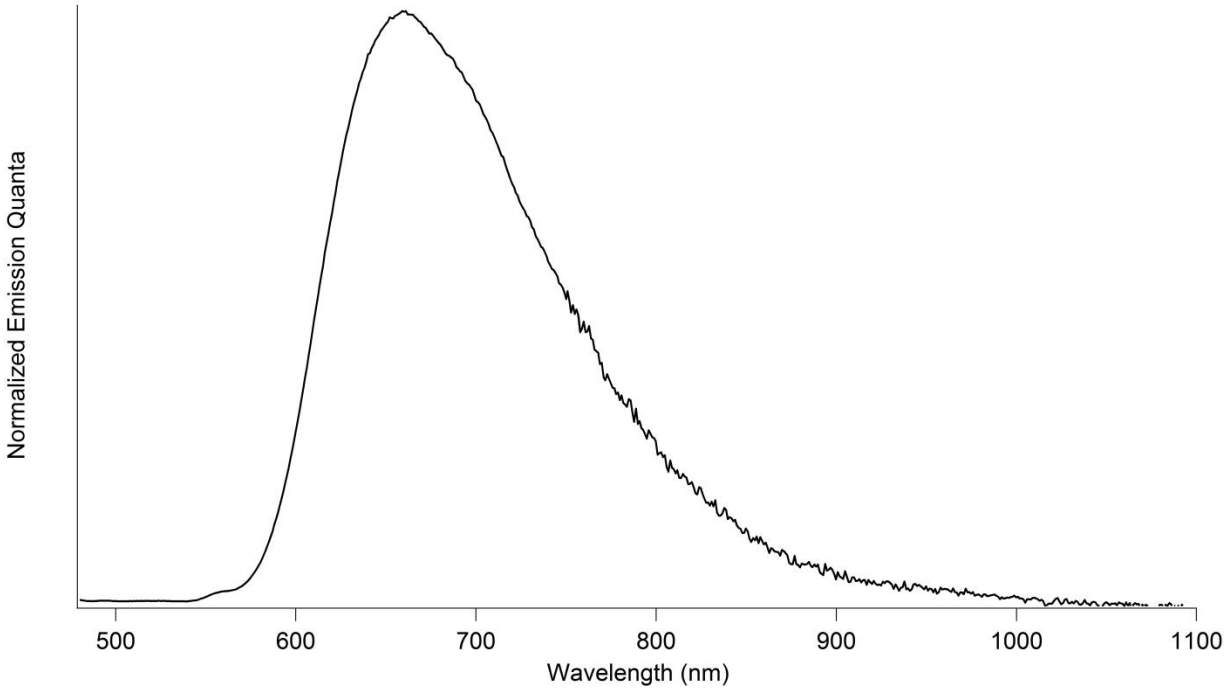

Figure 2.13. Emission spectrum (toluene) of W(CPh)(P$_2$NN)$_2$Cl (**2**): λ_{max} = 659 nm, τ = 125 ns.

2.4.4. Studies of the Protonation of W(CPh)(P$_2$NN)$_2$Cl (2).

General procedures. All experiments were performed under a nitrogen atmosphere using standard Schlenk and glovebox techniques and purified solvents, as described in Section 2.4.1.

NMR-scale reaction between 2 and [pyH][BAr^{F24}] to form 2H[BAr^{F24}]. In a typical NMR-scale reaction, a solution of **2** (0.0080 g, 0.00868 mmol, 1 equiv) in THF-d_8 (ca. 700 µL) was added to a vial containing [pyH][BAr^{F24}] (0.0080 g, 0.00848 mmol, 0.977 equiv), and the resulting solution was transferred to a J-Young NMR tube. The ^{1}H NMR spectrum of the reaction mixture exhibited resonances for pyridine but not for [pyH]$^+$, indicating that the latter had been consumed. The ^{1}H- and ^{31}P{^{1}H}-NMR spectra also exhibited resonances associated with protonated **2** (designated **2H**[BAr^{F24}]). ^{1}H NMR (500.13 MHz, THF-d_8; Figures 2.16 and 2.17): δ 7.79 (br s, 8H, *o*-Ar BAr^{F24}), 7.58 (br s, 4H, *p*-Ar BAr^{F24}), 7.11 and 6.92 (overlapping br s, 5H total, *o*-, *m*-, and *p*-Ph), 3.37 (v br, PC$\underline{H}_2$N), 2.88 (v br, PC$\underline{H}_2$N), 2.75 (br s, 4H, NC$\underline{H}_2$CH$_2$CH$_2$NMe$_2$ or NCH$_2$CH$_2$C$\underline{H}_2$NMe$_2$), 2.62 (br t, 4H, NC$\underline{H}_2$CH$_2$CH$_2$NMe$_2$ or NCH$_2$CH$_2$C$\underline{H}_2$NMe$_2$), 2.54 (br s, 12H, NMe$_2$), 2.19 (br, ~4H, PC$\underline{H}_2$CH$_3$), 1.98 (br, ~12H, PC$\underline{H}_2$CH$_3$), 1.84 (m, ~4H, NCH$_2$C$\underline{H}_2$CH$_2$NMe$_2$), 1.18 and 1.11 (overlapping br s, 24H, PCH$_2$C$\underline{H}_3$). The ^{1}H-NMR resonance associated with the added proton (N$\underline{H}$) was not detected; a sample of **2** protonated with [pyD][BAr^{F24}] exhibited identical ^{1}H and ^{31}P{^{1}H} NMR spectra to those above and a single resonance in the ^{2}H NMR spectrum (76.77 MHz, THF-h_8: δ 8.11, br s, N$\underline{D}$). ^{31}P{^{1}H} (202.4 MHz, THF-d_8; Figure 2.15): δ –8.1 (br). UV-Vis (THF, 23 °C; Figure 2.14): λ_{max} 331 nm, 533 nm.

NMR-scale reaction between 2H[BAr^{F24}] and KO^{t}Bu to form 2. To a solution of **2H**[BAr^{F24}] (0.0152 g, 0.00848 mmol, 1 equiv) in THF-d_8, prepared *in situ* as described above, was added a solution of KO^{t}Bu (97 µL, 91.9 mM in THF-d_8, 0.0089 mmol, 1.05 equiv). The ^{1}H-NMR spectrum of the reaction mixture exhibits only resonances attributable to [BAr^{F24}]$^-$, **2**, and HO^{t}Bu (Figure 2.16). The ^{31}P-NMR spectrum of the reaction mixture exhibits only the resonance for **2** (Figure 2.15).

Electronic-absorption spectroscopic monitoring of the acid-base interconversion of 2 and 2H[BAr^{F24}]. A solution of **2** (0.0070 g, 0.00760 mmol, 1 equiv) in 7.585 mL THF was prepared in a spectrophotometric cell containing both 1 cm and 1 mm pathlength cuvettes, and its electronic-absorption spectrum was recorded. To this solution was added via syringe a solution of [pyH][BAr^{F24}] (0.530 mL, 14.3 mM in THF, 0.00760 mmol, 1 equiv). The solution did not appear to change color following addition of the acid and thorough mixing. The absorption spectrum of the resulting product **2H**[BAr^{F24}] was recorded (Figure 2.16). To this solution was then added via syringe a solution of KO^{t}Bu (0.272 mL, 29.3 mM in THF, 0.00797 mmol, 1.05 equiv). After thorough mixing, the absorption spectrum of the sample was recorded (Figure 2.16). The final spectrum was essentially identical to that of the initial spectrum of **2**, indicating that the protonation to form **2H**$^{+}$ is reversible.

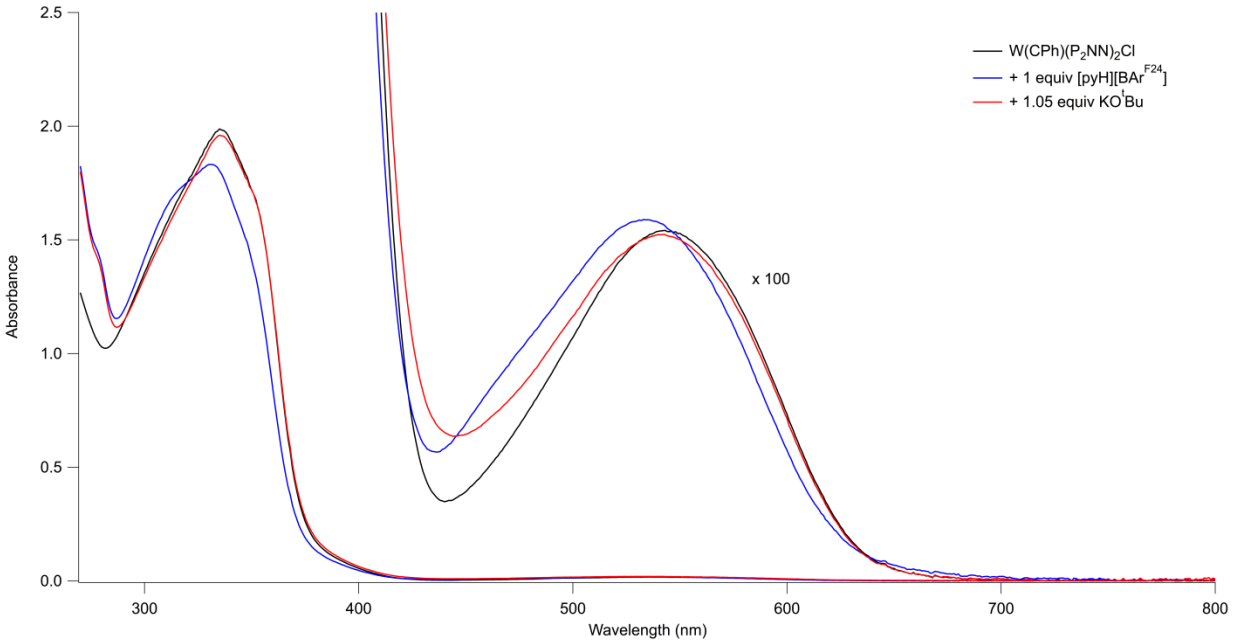

Figure 2.14. Electronic-absorption spectra (THF) of W(CPh)(P$_2$NN)$_2$Cl (**2**) and the in-situ reaction products formed from successive addition of: (1) [pyH][BAr^{F24}] (1 equiv), producing **2H**$^{+}$; (2) KO^{t}Bu (1.05 equiv), producing **2**. The absorbances of the reaction products have been adjusted to account for dilution of the sample that resulted from addition of the acid and base.

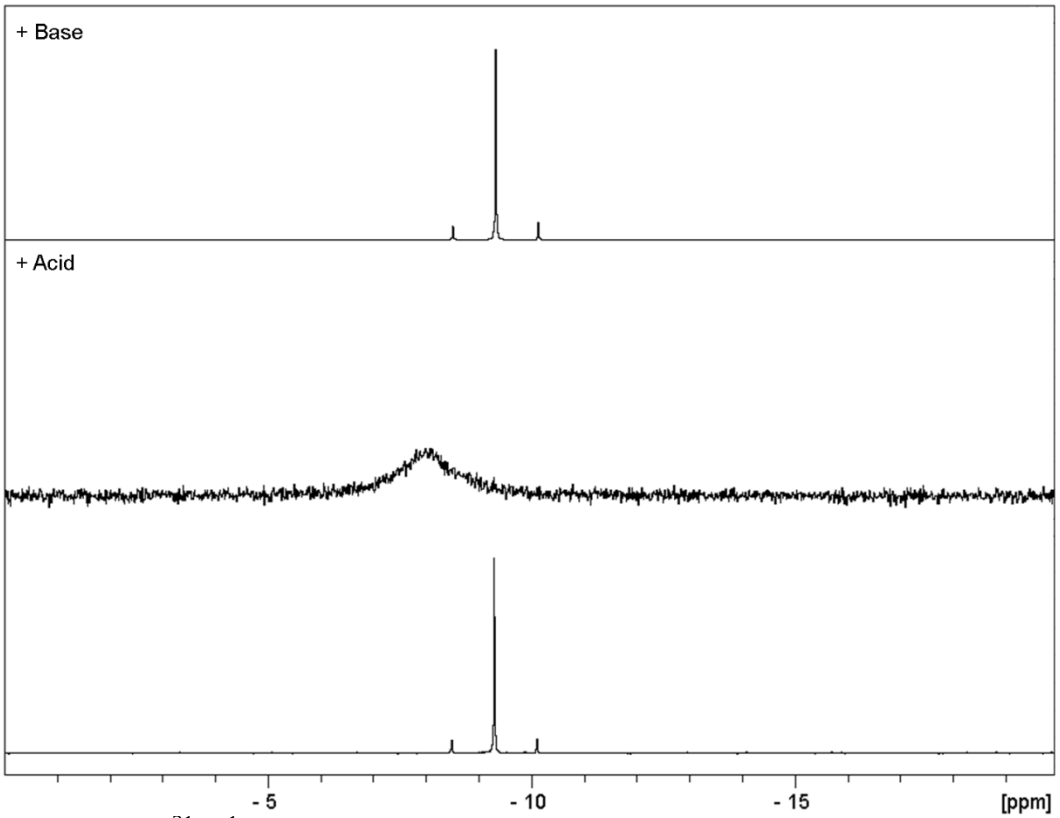

Figure 2.15. $^{31}P\{^{1}H\}$ NMR spectra (THF-d_8) of W(CPh)($P_2NN)_2$Cl (**2**) and the in-situ reaction products formed from successive addition of: (1) [pyH][BAr^{F24}] (1 equiv), producing $\mathbf{2H^+}$; (2) KO^{t}Bu (1.05 equiv), producing **2**.

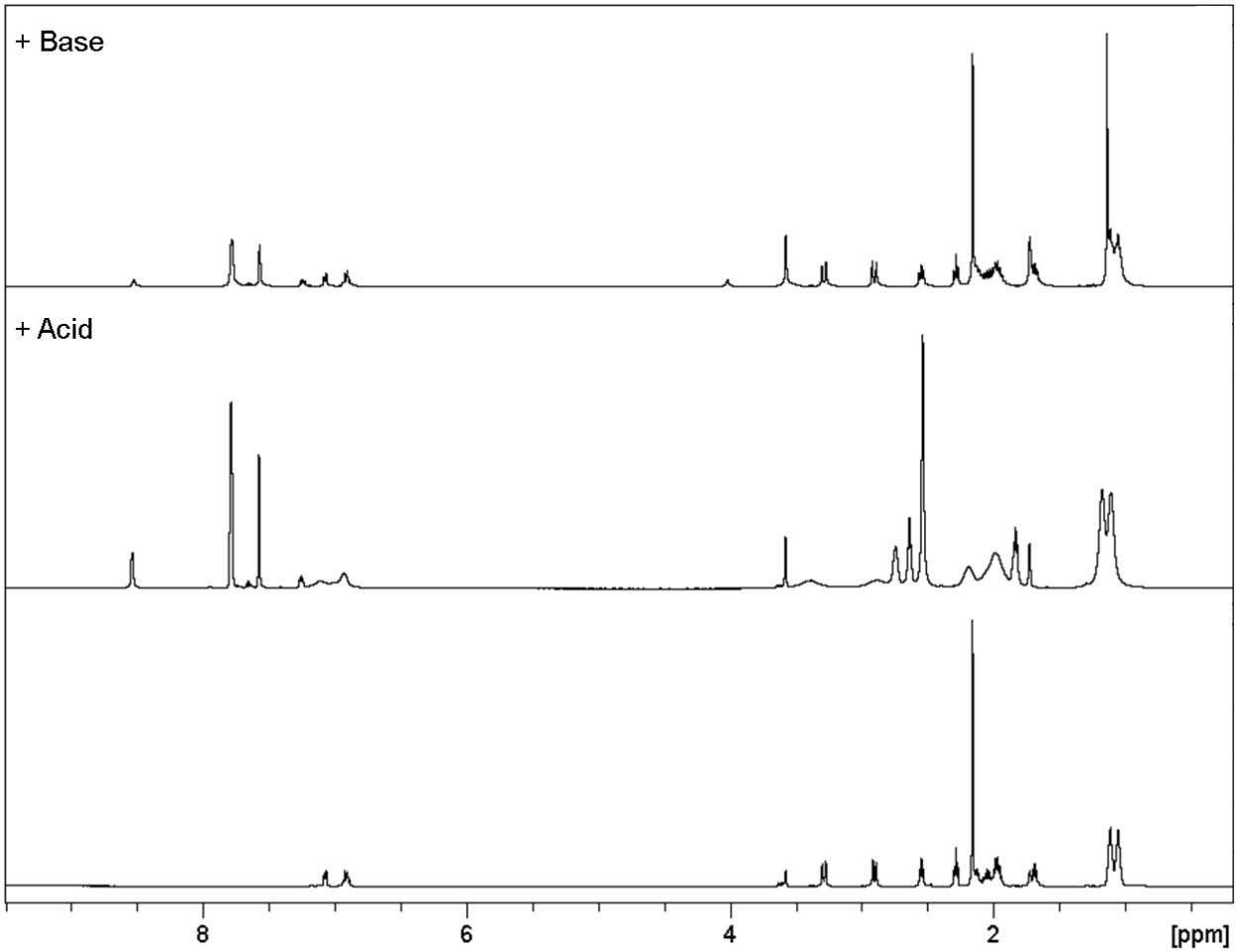

Figure 2.16. ^{1}H NMR spectra (THF-d_8) of W(CPh)(P_2NN)$_2$Cl (**2**) and the in-situ reaction products formed from successive addition of: (1) [pyH][BAr^{F24}] (1 equiv), producing **2H**$^+$ and pyridine; (2) KO^{t}Bu (1.05 equiv), producing **2** and HO^{t}Bu. Expansions of the spectrum of **2H**$^+$ are shown in Figure 2.17.

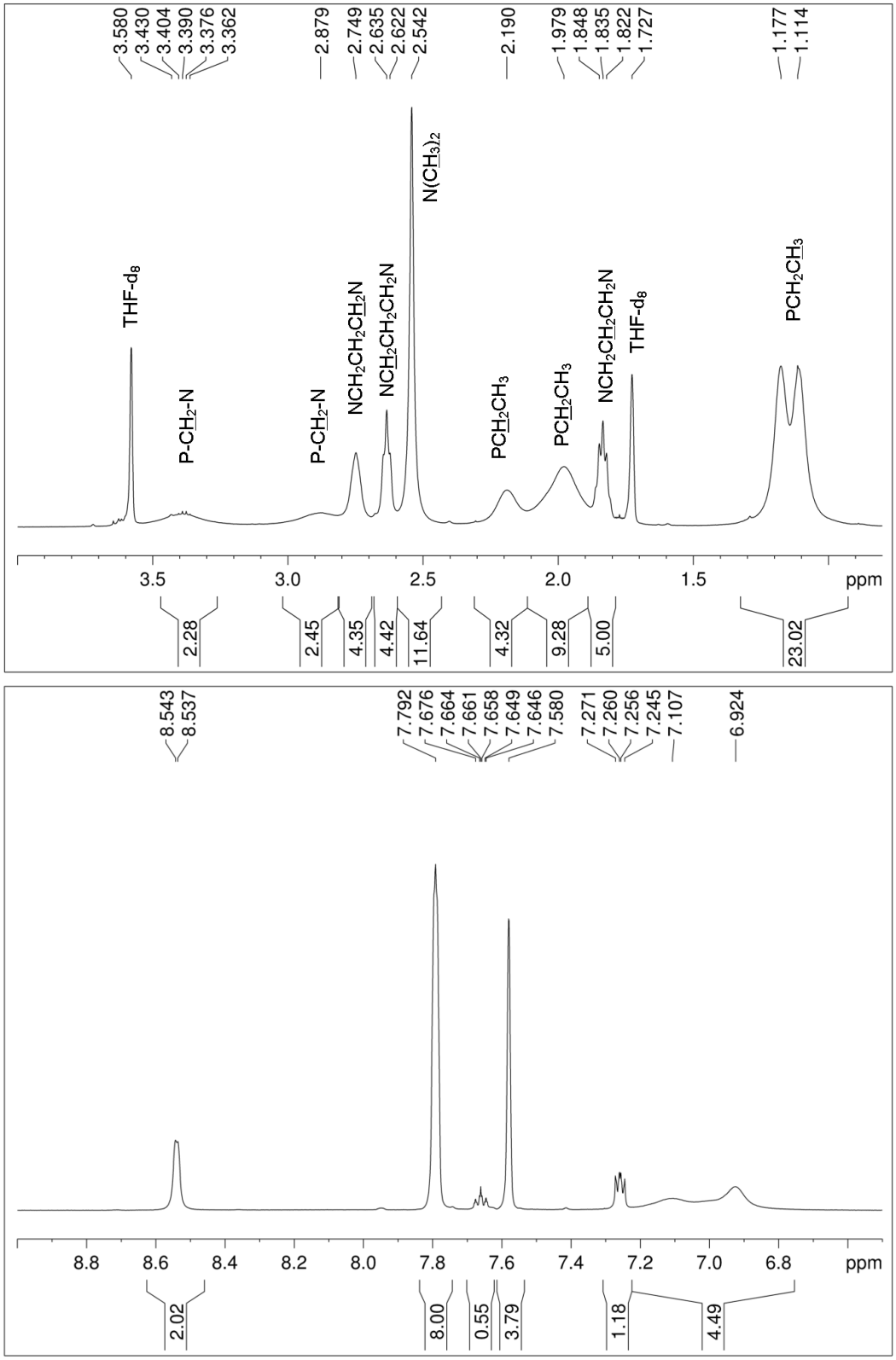

Figure 2.17. Expansions of the ^{1}H NMR spectrum (THF-d_8) of **2H**[BAr^{F24}]. For full spectrum and reaction details, see Figure 2.16 (middle).

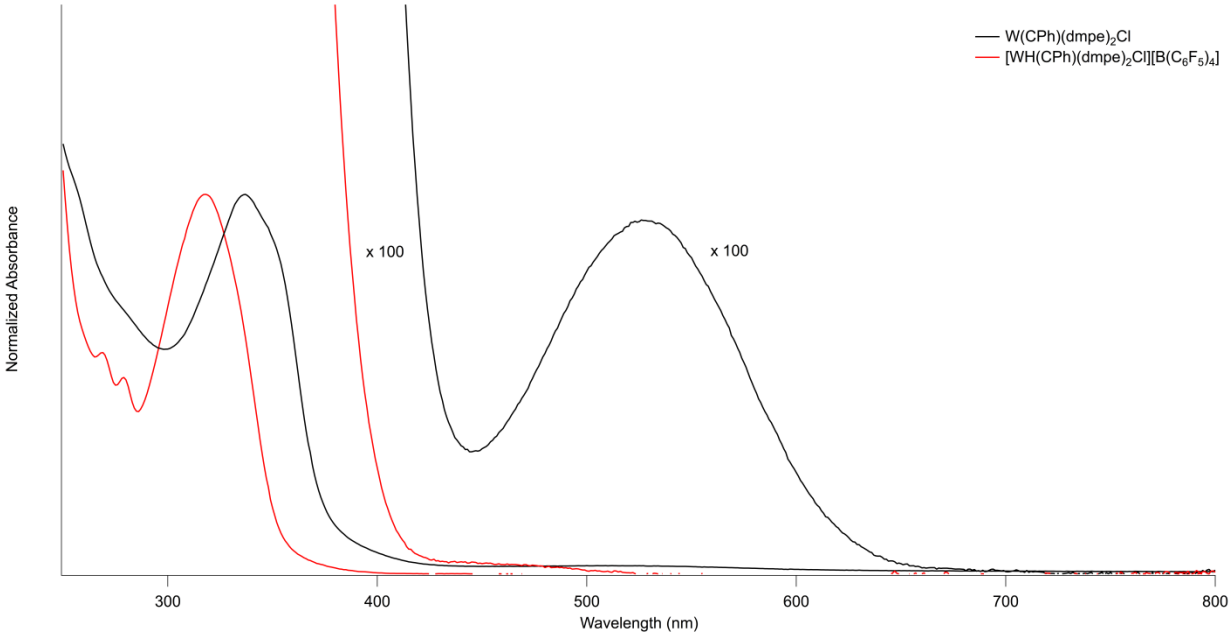

Figure 2.18. Electronic-absorption spectra (THF) of W(CPh)(dmpe)$_2$Cl (**1**) and [WH(CPh)(dmpe)$_2$Cl][B(C$_6$F$_5$)$_4$] (**1H**[B(C$_6$F$_5$)$_4$]). The spectrum of **1** was supplied by Hunter Vibbert of the Hopkins group.

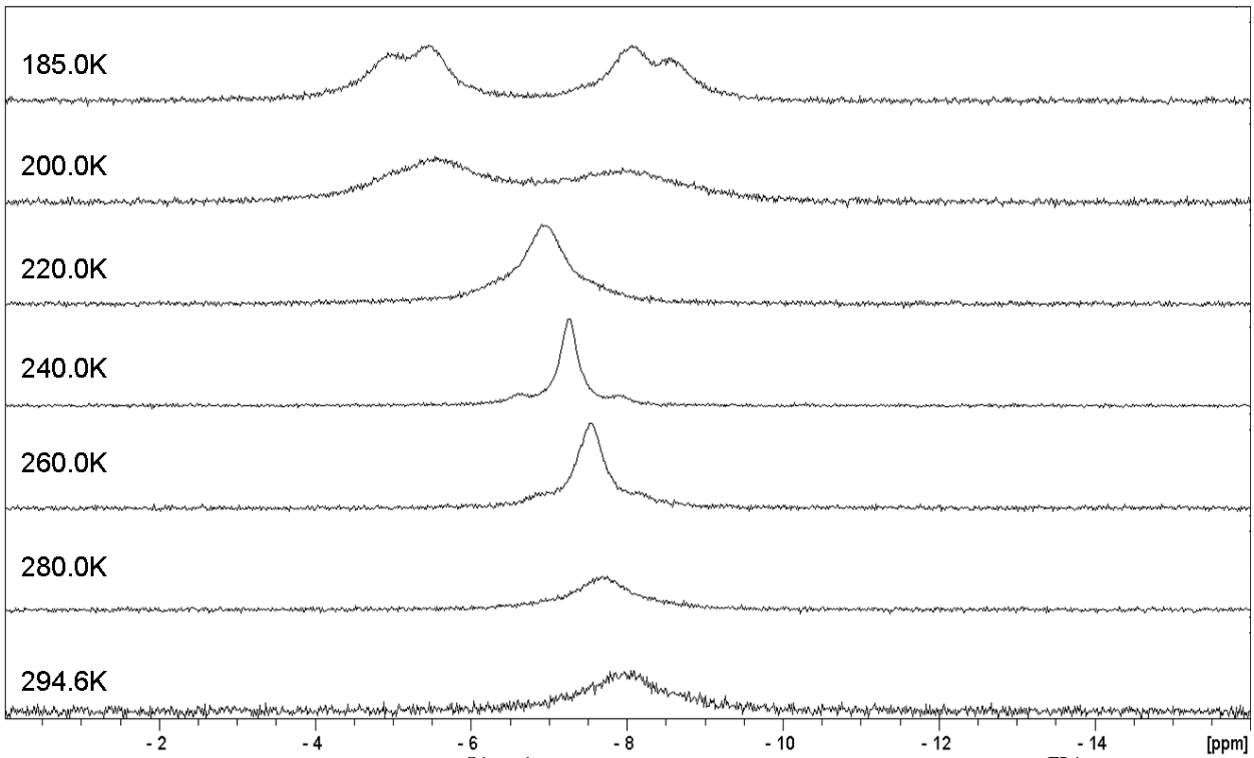

Figure 2.19. Variable-temperature ^{31}P{^{1}H} NMR spectra (THF-d$_8$) of **2H**[BAr^{F24}], formed in-situ from the reaction between W(CPh)(P$_2$NN)$_2$Cl (**2**) and [pyH][BAr^{F24}] (1 equiv).

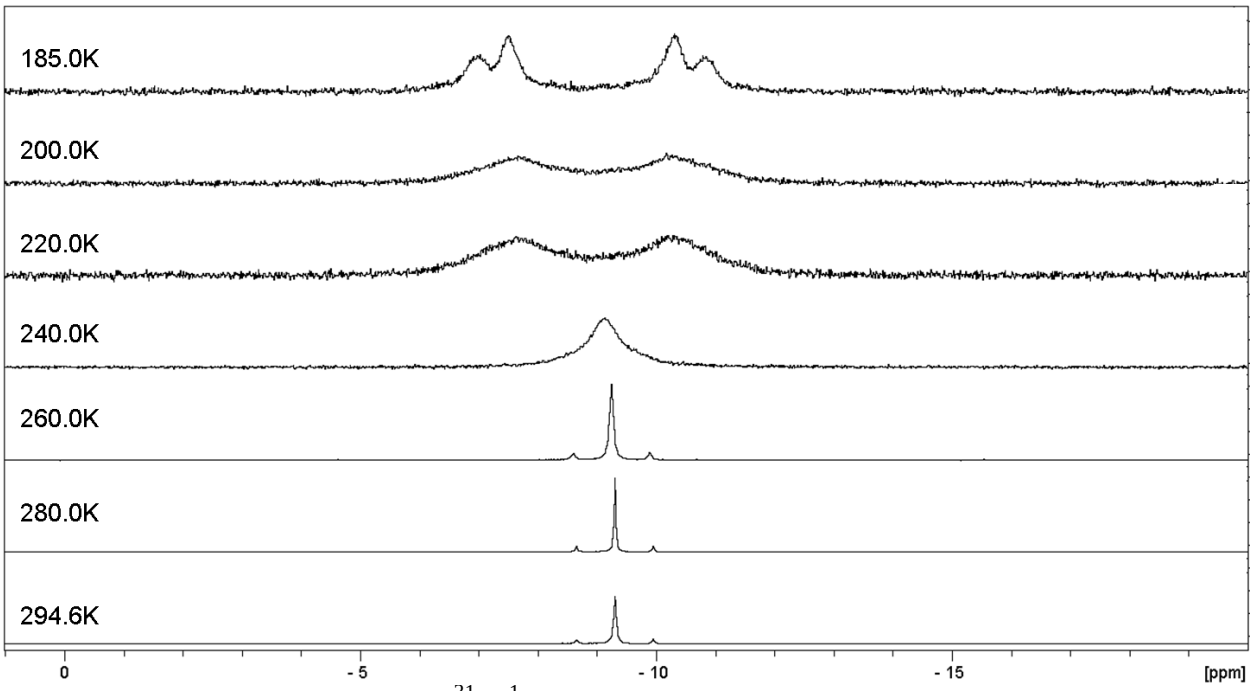

Figure 2.20. Variable-temperature $^{31}P\{^{1}H\}$ NMR (THF-d_8) of W(CPh)($P_2NN)_2$Cl (**2**).

Table 2.3. ^{1}H NMR Chemical Shifts for Corresponding Resonances of **2** and $\mathbf{2H^+}$.[a]

Assignment	**2**	$\mathbf{2H^+}$	$\lvert\Delta\delta\rvert$
CPh	7.08	7.11	0.03
	6.91	6.92	0.01
PCH_2N	3.29	3.37	0.08
	2.91	2.88	0.03
$NC\underline{H_2}CH_2CH_2NMe_2$	2.55	2.75 or <u>2.62</u>[b]	0.20 or <u>0.07</u>[b]
$NCH_2CH_2C\underline{H_2}NMe_2$	2.29	<u>2.75</u> or 2.62[b]	<u>0.46</u> or 0.33[b]
NMe_2	2.16	2.54	0.38
$NCH_2C\underline{H_2}CH_2NMe_2$	1.69	1.84	0.15
$PC\underline{H_2}CH_3$	2.20–1.93	2.19	≤0.05
	(overlap with 2.16)	1.98	
$PCH_2C\underline{H_3}$	1.12	1.18	0.06
	1.06	1.11	0.05

[a] THF-d_8 solution, room temperature. [b] Could not be unambiguously assigned; likely assignment underlined.

2.4.5. Density Functional Theory Calculations.

Methodology. Density functional theory (DFT) calculations of the geometries of $\mathbf{1H^+}$, and the hypothetical tungsten–hydrido form of protonated **2** in the gas phase were performed using Gaussian 09.[57] The calculations employed the B3P86 functional,[58-60] which benchmarking studies have shown provides accurate geometries for third row transition metal complexes.[61]

Prior DFT benchmarking studies of d^2 $W(CR)L_4X$ complexes demonstrated that calculations employing the LANL2DZ basis set and effective core potential for tungsten[62,63] and the DunningDZ basis set for other atoms[64,65] provided optimized gas-phase geometries that closely match experimental structures, and that triple-ζ-level basis sets offered little improvement.[13,17] To text whether this conclusion remained valid for tungsten–alkylidyne hydride complexes, two calculations were performed for **1H**$^+$; one using LANL2DZ/DunningDZ, and the second using the SDD basis set and effective core potential for tungsten[66] and the cc-pVTZ basis set for other atoms.[67] The geometries were optimized without symmetry constraints. Subsequent vibrational analyses demonstrated the absence of imaginary frequencies, confirming that the structures reside at potential surface minima. Selected experimental and calculated bond distances and angles are set out in Table 2.4 (**1H**$^+$). The SDD/cc-PVTZ calculation provided a closer match to the W–P and W–Cl bond distances than did the LANL2DZ/DunningDZ calculation; other distances and angles differ little between the two levels of theory. In view of the results, the structure of the hypothetical hydrido derivative of protonated **2** was calculated using SDD/cc-PVTZ basis sets. Select bond distances and angles are set out in Table 2.5 and the structure is depicted in Figure 2.21. The Cartesian coordinates for the optimized geometries are available as in Appendix II.

Table 2.4. Experimental and Calculated Bond Distances (Å) and Angles (deg) for [WH(CPh)(dmpe)$_2$Cl][B(C$_6$F$_5$)$_4$] (**1H**[B(C$_6$F$_5$)$_4$]) (X-Ray Crystallography) and **1H**$^+$ (DFT).

		DFT			
		A	**B**		
Nuclei	Exptl[a]	LANL2DZ + Dunning DZ[b]	SDD + cc-PVTZ[c]	Exptl – **A**	Exptl – **B**
W≡C1	1.809(3)	1.806	1.817	0.003	–0.008
C1–C2	1.446(4)	1.448	1.433	–0.002	0.013
W–P1	2.4466(9)	2.545	2.504	–0.098	–0.057
W–P2	2.5600(9)	2.596	2.572	–0.036	–0.012
W–P3	2.5599(9)	2.602	2.581	–0.042	–0.021
W–P4	2.4623(8)	2.543	2.504	–0.081	–0.042
W–Cl	2.5362(11)	2.597	2.574	–0.061	–0.038
W–H	1.64(3)	1.725	1.731	–0.085	–0.091
C1–W–Cl	179.09(10)	177.88	178.15	1.21	0.94
W–C1–C2	176.6(2)	178.99	179.12	–2.39	–2.52
P1–W–P3	163.04(3)	157.17	159.19	5.87	3.85
P2–W–P4	162.42(3)	160.64	162.64	1.78	–0.22
P1–W–P4	119.13(3)	121.13	119.25	–2.00	–0.12
P2–W–P3	86.45(3)	83.90	85.70	2.55	0.75
P1–W–H1	59.9(11)	60.7	59.6	–0.8	0.3
P4–W–H1	59.3(11)	60.7	59.7	–1.4	–0.4
C1–W–P1	90.19(10)	95.05	94.56	–4.86	–4.37
C1–W–P2	93.80(10)	92.52	92.13	1.28	1.67
C1–W–P3	94.47(10)	97.60	97.42	–3.13	–2.95
C1–W–P4	93.18(10)	93.38	92.80	–0.20	0.38
C1–W–P$_{min}$	90.19	92.52	92.13	–2.33	–1.94
C1–W–P$_{max}$	94.47	97.60	97.42	–3.13	–2.95
C1–W–H	88.1(11)	93.4	94.0	–5.3	–5.9

[a] Major component only. [b] LANL2DZ (W) + Dunning DZ (all other atoms). [c] SDD (W) + cc-PVTZ (all other atoms).

Table 2.5. Calculated Bond Distances (Å) and Angles (deg) for $[WH(CPh)(P_2NN)_2Cl]^+$ (DFT).

	DFT
Nuclei	SDD + cc-PVTZ[a]
W≡C1	1.813
C1–C2	1.433
W–P1	2.550
W–P2	2.635
W–P3	2.615
W–P4	2.526
W–Cl	2.574
W–H	1.712
C1–W–Cl	177.0
W–C1–C2	178.4
P1–W–P3	164.7
P2–W–P4	164.3
P1–W–P4	110.5
P2–W–P3	83.5
P1–W–H1	55.5
P4–W–H1	55.3
C1–W–P1	96.2
C1–W–P2	95.3
C1–W–P3	91.0
C1–W–P4	91.9
C1–W–P_{min}	91.0
C1–W–P_{max}	96.3
C1–W–H	92.9

[a] SDD (W) + cc-PVTZ (all other atoms).

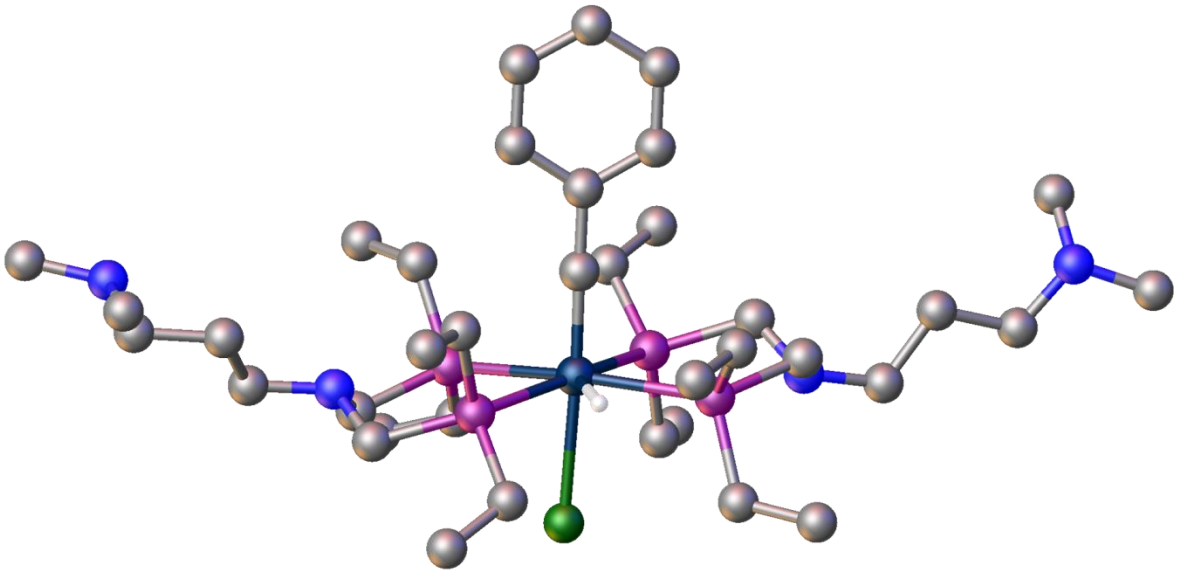

Figure 2.21. Calculated structure of the hypothetical $[WH(CPh)(P_2NN)_2Cl]^+$. Calculation performed in the gas phase at the B3BP86 level of theory. SDD basis set and effective core potentials on W atom, and cc-PVTZ on all other atoms. Hydrogen atoms except for W-H removed for clarity.

2.5 References.

(1) Karkas, M. D.; Verho, O.; Johnston, E. V.; Akermark, B. *Chem. Rev.* **2014**, *114*, 11863.

(2) Administration, E. I. *Annual Energy Outlook*; U.S. Department of Energy: Washington, DC., 2017.

(3) Concepcion, J. J.; House, R. L.; Papanikolas, J. M.; Meyer, T. J. *Proc. Natl. Acad. Sci.* **2012**, *109*, 15560.

(4) Collares-Pereira, M.; Rabl, A. *Sol. Energy* **1979**, *22*, 155.

(5) Han, Z.; Eisenberg, R. *Acc. Chem. Res.* **2014**, *47*, 2537.

(6) Windle, C. D.; Perutz, R. N. *Coord. Chem. Rev.* **2012**, *256*, 2562.

(7) Izumi, Y. *Coord. Chem. Rev.* **2013**, *257*, 171.

(8) Prier, C. K.; Rankic, D. A.; MacMillan, D. W. *Chem. Rev.* **2013**, *113*, 5322.

(9) Shaw, M. H.; Twilton, J.; MacMillan, D. W. *J. Org. Chem.* **2016**, *81*, 6898.

(10) Skubi, K. L.; Blum, T. R.; Yoon, T. P. *Chem. Rev.* **2016**, *116*, 10035.

(11) Pellegrin, Y.; Odobel, F. *C. R. Chim.* **2017**, *20*, 283.

(12) Rudshteyn, B.; Vibbert, H. B.; May, R.; Wasserman, E.; Warnke, I.; Hopkins, M. D.; Batista, V. S. *ACS Catal.* **2017**, *7*, 6134.

(13) Haines, D. E.; O'Hanlon, D. C.; Manna, J.; Jones, M. K.; Shaner, S. E.; Sun, J.; Hopkins, M. D. *Inorg. Chem.* **2013**, *52*, 9650.

(14) Pombeiro, A. J. L. *Eur. J. Inorg. Chem.* **2007**, 1473.

(15) Da Re, R. E.; Hopkins, M. D. *Coord. Chem. Rev.* **2005**, *249*, 1396.

(16) O'Hanlon, D. C.; Cohen, B. W.; Moravec, D. B.; Dallinger, R. F.; Hopkins, M. D. *J. Am. Chem. Soc.* **2014**, *136*, 3127.

(17) Lovaasen, B. M.; Lockard, J. V.; Cohen, B. W.; Yang, S.; Zhang, X.; Simpson, C. K.; Chen, L. X.; Hopkins, M. D. *Inorg. Chem.* **2012**, *51*, 5660.

(18) Morales-Verdejo, C. A.; Newsom, M. I.; Cohen, B. W.; Vibbert, H. B.; Hopkins, M. D. *Chem. Commun.* **2013**, *49*, 10566.

(19) Wilson, A. D.; Newell, R. H.; McNevin, M. J.; Muckerman, J. T.; Rakowski DuBois, M.; DuBois, D. L. *J. Am. Chem. Soc.* **2006**, *128*, 358.

(20) Shaw, W. J.; Helm, M. L.; DuBois, D. L. *Biochim. Biophys. Acta* **2013**, *1827*, 1123.

(21) DuBois, D. L. *Inorg. Chem.* **2014**, *53*, 3935.

(22) Bullock, R. M.; Helm, M. L. *Acc. Chem. Res.* **2015**, *48*, 2017.

(23) Helm, M. L.; Stewart, M. P.; Bullock, R. M.; DuBois, M. R.; DuBois, D. L. *Science* **2011**, *333*, 863.

(24) Fang, M.; Wiedner, E. S.; Dougherty, W. G.; Kassel, W. S.; Liu, T.; DuBois, D. L.; Bullock, R. M. *Organometallics* **2014**, *33*, 5820.

(25) Yang, J. Y.; Bullock, R. M.; Dougherty, W. G.; Kassel, W. S.; Twamley, B.; DuBois, D. L.; Rakowski DuBois, M. *Dalton Trans.* **2010**, *39*, 3001.

(26) Galan, B. R.; Schoffel, J.; Linehan, J. C.; Seu, C.; Appel, A. M.; Roberts, J. A.; Helm, M. L.; Kilgore, U. J.; Yang, J. Y.; DuBois, D. L.; Kubiak, C. P. *J. Am. Chem. Soc.* **2011**, *133*, 12767.

(27) Tronic, T. A.; Kaminsky, W.; Coggins, M. K.; Mayer, J. M. *Inorg. Chem.* **2012**, *51*, 10916.

(28) Weiss, C. J.; Das, P.; Miller, D. L.; Helm, M. L.; Appel, A. M. *ACS Catal.* **2014**, *4*, 2951.

(29) Lilio, A. M.; Reineke, M. H.; Moore, C. E.; Rheingold, A. L.; Takase, M. K.; Kubiak, C. P. *J. Am. Chem. Soc.* **2015**, *137*, 8251.

(30) Newsom, M. Structure and Reactivity of d^2, d^1, and d^0 Tungsten-Benzylidyne Compounds. Ph.D Thesis, The University of Chicago, December 2010.

(31) Holmes, S. J.; Schrock, R. R. *J. Am. Chem. Soc.* **1981**, *103*, 4599.

(32) Holmes, S. J.; Clark, D. N.; Turner, H. W.; Schrock, R. R. *J. Am. Chem. Soc.* **1982**, *104*, 6322.

(33) Ishii, Y.; Kawaguchi, M.; Hidai, M. *Chem. Lett.* **1995**, *24*, 983.

(34) Sun, J.; Shaner, S. E.; Jones, M. K.; O'Hanlon, D. C.; Mugridge, J. S.; Hopkins, M. D. *Inorg. Chem.* **2010**, *49*, 1687.

(35) Churchill, M. R.; Wasserman, H. J.; Turner, H. W.; Schrock, R. R. *J. Am. Chem. Soc.* **1982**, *104*, 1710.

(36) van der Eide, E. F.; Piers, W. E.; Romero, P. E.; Parvez, M.; McDonald, R. *Organometallics* **2004**, *23*, 314.

(37) The W-H resonance is obscured at low temperature due to overlap with the dmpe resonances.

(38) Wengrovius, J. H.; Schrock, R. R.; Churchill, M. R.; Wasserman, H. J. *J. Am. Chem. Soc.* **1982**, *104*, 1739.

(39) Garrido, G.; Koort, E.; Ràfols, C.; Bosch, E.; Rodima, T.; Leito, I.; Rosés, M. *J. Org. Chem.* **2006**, *71*, 9062.

(40) Abdur-Rashid, K.; Fong, T. P.; Greaves, B.; Gusev, D. G.; Hinman, J. G.; Landau, S. E.; Lough, A. J.; Morris, R. H. *J. Am. Chem. Soc.* **2000**, *122*, 9155.

(41) This pKa value for $\mathbf{1H^+}$ is referenced to the reported pK_a($HNEt_3^+$) = 14.9, which was measured via conductivity and potentiometric titration (Ref 39). Newsom (Ref 30) originally reported pK_a($\mathbf{1H^+}$) = 14.3(1), based on pK_a($HNEt_3^+$) = 12.5, which was determined relative to $HPCy(BPh)_4^+$ (Ref 40).

(42) Darmon, J. M.; Kumar, N.; Hulley, E. B.; Weiss, C. J.; Raugei, S.; Bullock, R. M.; Helm, M. L. *Chem. Sci.* **2015**, *6*, 2737.

(43) Mayr, A.; Dorries, A. M.; McDermott, G. A.; Van Engen, D. *Organometallics* **1986**, *5*, 1504.

(44) With the caveat that the smaller intraligand P-W-P angle could affect the pK_a due to increased steric pressure on the hydride ligand.

(45) Gea *Global Energy Assessment - Toward a Sustainable Future* Cambridge University Press, Cambridge, UK and New York, NY, USA and the International Institute for Applied Systems Analysis, Laxenburg, Austria, 2012.

(46) Pangborn, A. B.; Giardello, M. A.; Grubbs, R. H.; Rosen, R. K.; Timmers, F. J. *Organometallics* **1996**, *15*, 1518.

(47) Sun, J.; Simpson, C. K.; Hopkins, M. D.; Hock, A. S.; Schrock, R. R. In *Inorganic Syntheses: Volume 36*; John Wiley & Sons, Inc.: 2014, p 134.

(48) Yakelis, N. A.; Bergman, R. G. *Organometallics* **2005**, *24*, 3579.

(49) Fulmer, G. R.; Miller, A. J. M.; Sherden, N. H.; Gottlieb, H. E.; Nudelman, A.; Stoltz, B. M.; Bercaw, J. E.; Goldberg, K. I. *Organometallics* **2010**, *29*, 2176.

(50) Yandulov, D. V.; Schrock, R. R. *J. Am. Chem. Soc.* **2002**, *124*, 6252.

(51) Sheldrick, G. M., *TWINABS*, Version 2012/1. Bruker AXS, Inc., 2012.

(52) Dolomanov, O. V.; Bourhis, L. J.; Gildea, R. J.; Howard, J. A. K.; Puschmann, H. *J. Appl. Crystallogr.* **2009**, *42*, 339.

(53) Spek, A. *Acta Cryst. C* **2015**, *71*, 9.

(54) Spek, A. *Acta Cryst. D* **2009**, *65*, 148.

(55) La Porte, N. T.; Moravec, D. B.; Hopkins, M. D. *Proc. Natl. Acad. Sci.* **2014**, *111*, 9745.

(56) Bard, A. J.; Garcia, E.; Kukharenko, S.; Strelets, V. V. *Inorg. Chem.* **1993**, *32*, 3528.

(57) Frisch, M. J.; Trucks, G. W.; Schlegel, H. B.; Scuseria, G. E.; Robb, M. A.; Cheeseman, J. R.; Scalmani, G.; Barone, V.; Petersson, G. A.; Nakatsuji, H.; Li, X.; Caricato, M.; Marenich, A. V.; Bloino, J.; Janesko, B. G.; Gomperts, R.; Mennucci, B.; Hratchian, H. P.; Ortiz, J. V.; Izmaylov, A. F.; Sonnenberg, J. L.; Williams -Young, D.; Ding, F.; Lipparini, F.; Egidi, F.; Goings, J.; Peng, B.; Petrone, A.; Henderson, T.; Ranasinghe, D.; Zakrzewski, V. G.; Gao, J.; Rega, N.; Zheng, G.; Liang, W.; Hada, M.; Ehara, M.; Toyota, K.; Fukuda, R.; Hasegawa, J.; Ishida, M.; Nakajima, T.; Honda, Y.; Kitao, O.; Nakai, H.; Vreven, T.; Throssell, K.; Montgomery Jr., J. A.; Peralta, J. E.; Ogliaro, F.; Bearpark, M. J.; Heyd, J. J.; Brothers, E. N.; Kudin, K. N.; Staroverov, V. N.; Keith, T. A.; Kobayashi, R.; Normand, J.; Raghavachari, K.; Rendell, A. P.; Burant, J. C.; Iyengar, S. S.; Tomasi, J.; Cossi, M.; Millam, J. M.; Klene, M.; Adamo, C.; Cammi, R.; Ochterski, J. W.; Martin, R. L.; Morokuma, K.; Farkas, O.; Foresman, J. B.; Fox, D. J., *Gaussian 09, Revision A.02,* Wallingford, CT. 2016.

(58) Lee, C.; Yang, W.; Parr, R. G. *Phys. Rev. B* **1988**, *37*, 785.

(59) Becke, A. D. *J. Chem. Phys.* **1993**, *98*, 5648.

(60) Stephens, P. J.; Devlin, F. J.; Chabalowski, C. F.; Frisch, M. J. *J. Phys. Chem.* **1994**, *98*, 11623.

(61) Bühl, M.; Reimann, C.; Pantazis, D. A.; Bredow, T.; Neese, F. *J. Chem. Theory Comput.* **2008**, *4*, 1449.

(62) Hay, P. J.; Wadt, W. R. *J. Chem. Phys.* **1985**, *82*, 270.

(63) Hay, P. J.; Wadt, W. R. *J. Chem. Phys.* **1985**, *82*, 299.

(64) Dunning, T. H.; Hay, P. J. *Methods of Electronic Structure Theory*; Plenum Press: New York, 1977; Vol. 3.

(65) Dunning, T. H.; Hay, P. J. In *Methods of Electronic Structure Theory*; Schaefer III, H. F., Ed.; Springer US: Boston, MA, 1977; Vol. 3, p 1.

(66) Andrae, D.; Häußermann, U.; Dolg, M.; Stoll, H.; Preuß, H. *Theor. Chim. Acta* **1990**, *77*, 123.

(67) Kendall, R. A.; Dunning, T. H.; Harrison, R. J. *J. Chem. Phys.* **1992**, *96*, 6796.

CHAPTER 3

Tungsten–Alkylidyne Complexes Containing N-Heterocyclic Carbene Equatorial Ligands: A Computational Screening and Synthetic Investigation.

3.1 Introduction

Photosynthesis, the production of food and sugars from CO_2, H_2O, and sunlight in plants is driven by several photoredox processes.[1] The development of light-promoted redox reactions has been recognized as a technique to accomplish chemical transformations in more environmentally benign ways. The photochemical properties of and photoactivation of small molecules by transition metal chromophores has been the subject of investigation for decades,[2] but has recently garnered renewed interest.[3,4] Conventional photoreductants, such as $[Ru(bpy)_3]^{2+}$ and *fac*-$Ir(ppy)_3$, have excited-state oxidation potentials of −1.2 V and −2.1 V respectively (vs $Fc^{0/+}$ in ACN) rendering them efficient photoreductants.[5-7] These versatile photocatalysts have a wide scope of applications in organic chemistry.[4,5,8] By developing visible light photoreductants with even more negative oxidation potentials, a substrate scope with more breadth including less conventional substrates may become accessible. The strongest photoreductants to date in the literature, developed by Gray and co-workers, have potentials as high as −2.8 V.[9] Continuing this trend may allow for reactions typically preformed with reactive alkali metals to be carried out with homogeneous photoredox catalysts.

Tungsten alkylidyne compounds are powerful photoreduction catalysts. This class of compounds possesses a highly modular structure. The tunable structure provides a means by which synthetic manipulation can be used to modulate the electronic properties of the resulting compounds.[10] It has been previously shown the highest occupied molecular orbital (HOMO) and

primary redox orbital of tungsten–alkylidyne complexes of type $W(CR)L_4X$ is primarily of d_{xy} parentage, which has non-bonding symmetry with respect to the W≡C axis and π symmetry with the equatorial ligands.[11] Consistent with this, the ligands located around the equatorial plane have been shown to exhibit the strongest influence on the energy of the HOMO, with a less significant secondary influence from the axial ligands.[10] The lowest unoccupied molecular orbital (LUMO) is primarily of π*(W≡C) symmetry.[11] The axial X ligand and nature of the alkylidyne R group have the strongest influence on the energy of the LUMO. The HOMO and LUMO orbitals are orthogonal by symmetry, allowing relatively independent manipulation of the energy of each orbital by ligand or R group variation. The HOMO orbital has its primary influence on $E_{1/2}$ of the compound, while the LUMO orbital has its primary influence on E_{00}.

Density functional theory (DFT) and experiment have shown that the predicted energy of the HOMO of tungsten alkylidynes tracks close to linearly with the ground state oxidation potential.[10,12] Stronger sigma donating equatorial ligands will increase the electron density and thus raise the energy of the HOMO, resulting in stronger reductants. The use of ligands with stronger sigma donating capabilities than the prototypical PR_3 type phosphines would be necessary to accomplish this. N-heterocyclic carbenes (NHCs) are an attractive choice for this purpose.[13] NHC ligands are often stronger donors than their phosphine counterparts as evidenced by their respective Tolman parameters.[14] Additionally, both classes of ligands are sterically and electronically tunable. The use of NHC ligands in place of phosphines is predicted to yield a decrease in the oxidation potential providing more potent photoreductants.

The use of an NHC as a ligand in tungsten complexes has precedent but is not well explored. This class of ligands primarily finds use in stabilizing low oxidation state tungsten complexes. A majority of compounds are tungsten carbonyl species. There is a growing body of

work on interesting, application driven low oxidation state tungsten chemistry using NHC ligands.[15-17] For example, the electron deficient species [(IMes)W(Cp*)$(CO)_2$][$B(C_6F_5)_4$][15] has shown activity toward ketone hydrogenation. The chemistry of high valent tungsten NHC compounds remains under developed.[18,19] A few tungsten (VI) examples have been prepared containing both oxo and alkylidene moieties.[20-22]

We will report here initial design parameters and a computational screen of a variety of tungsten alkylidyne compounds containing NHC ligands, including predicted electronic structures and oxidation potentials. A description of the exploratory synthetic studies on preparing both mono- and poly-substituted NHC compounds will be detailed including a crystallographically characterized tris(NHC) compound, W(CPh){$P(OMe)_3$}$(tmiy)_3$(OR). The synthesis and properties of a mono-NHC compound, W(CPh)(ICy)$(PMe_3)_3Cl$, will be reported including NMR, electrochemistry, electronic spectroscopy, and a crystal structure.

3.2 Results and Discussion

3.2.1 Computational Studies

3.2.1.1 Goals of Screening Studies. Computational modeling provides a powerful tool for structure and property prediction for tungsten–benzylidyne compounds. Computational screening of complexes with different ligands by density functional theory was used to inform our experimental endeavors. All screening calculations were undertaken with the B3P86 functional, and utilized LANL2DZ basis set and core potentials on tungsten and DunningDZ basis sets on all other atoms. The functional has previously been shown to yield suitable results for third-row transition metals.[23] The basis sets have been previously benchmarked for the computation of electronic structures of tungsten–alkylidyne compounds.[10,12]

The structures and steric viability of compounds of interest were evaluated for derivatives with different degrees of NHC substitution and bonding motifs. The computations additionally provided electronic structure predictions from which electrochemical data could be estimated to evaluate our hypothesis that NHC-containing complexes would be stronger reductants than phosphine-containing complexes.

3.2.1.2 Structure Prediction. A variety of $W(CR)(NHC)_n(PR_3)_{4-n}Cl$ compounds were explored computationally (Tables 3.1 and 3.2). It was found for $W(CR)(NHC)_4Cl$ (n = 4) that NHC ligands with Me or Et N-alkyl chains (IMe, SIMe, tmiy, BzIMe, IEt) yielded sterically viable complexes (Table 3.1). The calculated structures of the select examples $W(CPh)(IMe)_4Cl$, $W(CPh)(tmiy)_4Cl$, and $W(CPh)(IEt)_4Cl$ are shown in Figure 3.1. For ligands with N-Me groups, the nature of the backbone of the ligand (saturated, unsaturated, methylated, and benzylated) was not found to affect the structure. Calculations showed the IiPr ligand, with a branched alkyl chain, was too bulky to form a $W(CR)(NHC)_4Cl$ compound. The IiPr calculation converged without the presence of a fourth equatorial ligand, instead distorting the geometry of the equatorial ligands and forming agostic $CH_3\cdots W$ interactions between the ligand alkyl groups and the metal center to occupy the fourth coordination site. The calculated structure of $W(CPh)(IiPr)_3Cl$ is shown in Figure 3.2. Thus, an N-ethyl group is the computed steric limit for $W(CR)(NHC)_4Cl$ structures.

Table 3.1. Ligands explored for $W(CR)(NHC)_4Cl$ structures. All except IiPr converged to reasonable geometries.

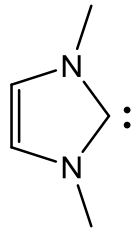	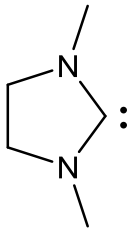	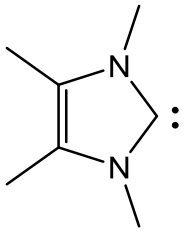	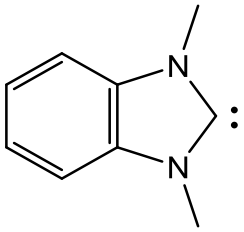	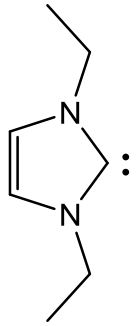	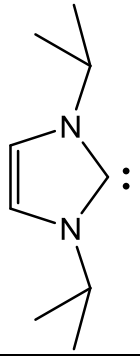
IMe	SIMe	tmiy	BzIMe	IEt	IiPr

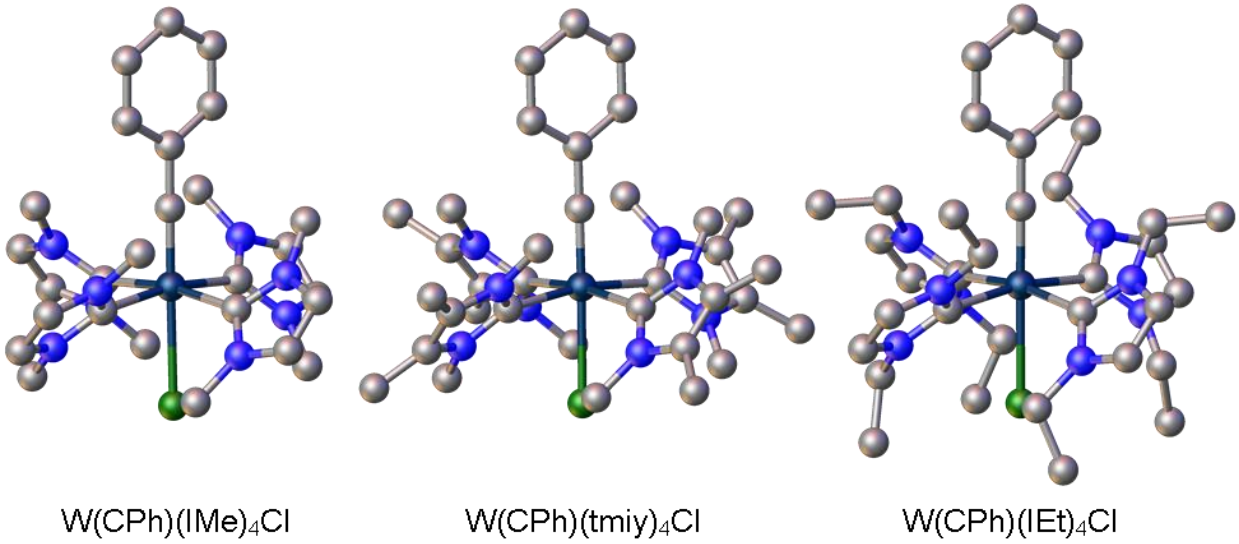

Figure 3.1. Computed structures of $W(CPh)(IMe)_4Cl$, $W(CPh)(tmiy)_4Cl$, and $W(CPh)(IEt)_4Cl$. Hydrogen atoms removed for clarity.

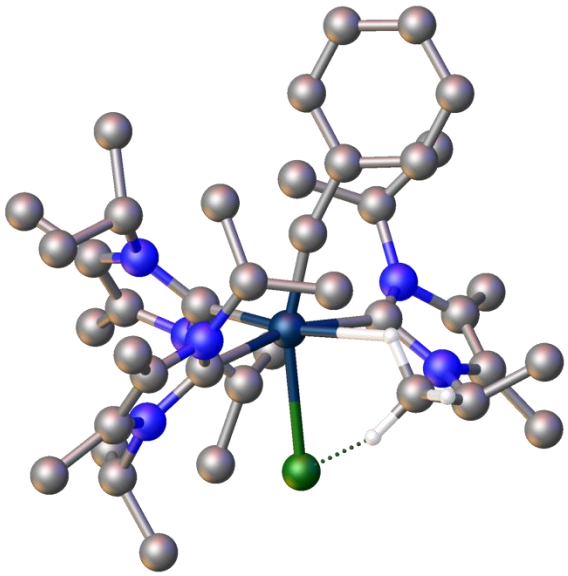

Figure 3.2. Computed structure of W(CPh)(IiPr)$_3$Cl. Hydrogen atoms, except those involved in agostic $CH_3\cdots W$ interactions, removed for clarity.

The ability of 6-coordinate metal complexes to support four NHC ligands with linear alkyl chains, but not four ligands with branched alkyl chains, is supported by experimental observations in the literature. For example, an isoelectronic (d^2) rhenium nitride, $ReNCl_2(PR_2Ph)_3$ (R = Me, Et), was found to react with 1,3-diethyl-4,5-dimethylimidazole-2-ylidene ($IEtMe_2$) or 1,3,4,5-tetramethylimidazole-2-ylidene (tmiy) to yield stable $[ReN(NHC)_4Cl]Cl$ salts.[24] The larger 1,3-diisopropyl-4,5-dimethylimidazol-2-ylidene ($IiPrMe_2$) failed to yield the analogous product, and is reported to lead to decomposition. Similar reactivity patterns are shown by the analogous phenylimido, $Re(NPh)Cl_3(PR_2Ph)_3$,[25] and oxo, $Re(O)Cl_3(PPh_3)$,[26] compounds. Only a rhenium dioxo core, bearing two short axial ligands, can accommodate four $IiPrMe_2$ ligands with elongation of the Re-C bond to form a $[Re(O)_2(IiPrMe_2)_4]^{2+}$ cation.[26] This cation was frequently encountered as the major decomposition product in the previous syntheses. Structural analysis and computations indicate that the longer chloride ligand provides steric repulsion with the $IiPrMe_2$ ligand to prevent stable

structures.[24] Similar trends are also seen in the Chatt-type molybdenum dinitrogen compounds, $Mo(N_2)_2(NHC)_4$.[27] Reduction of $MoCl_4(THF)_2$ with KC_8 in the presence of the same 1,3-dialkyl-4,5-dimethylimidazol-2-ylidine ligands (tmiy, $IEtMe_2$, $IiPrMe_2$) results in $Mo(N_2)_2(NHC)_4$ compounds for tmiy and $IEtMe_2$, but with $IiPrMe_2$ produces the tris(dinitrogen) complex fac-$Mo(N_2)_3(IiPrMe_2)_3$.[27] Under argon in the presence of excess ligand, fac-$Mo(N_2)_3(IiPrMe_2)_3$ exists in equilibrium with $Mo(N_2)_2(IiPrMe_2)_4$ but the latter compound cannot be isolated cleanly in the bulk due to contamination with either $Mo(N_2)_3(IiPrMe_2)_3$ or excess ligand, though it has been crystallographically characterized.[27]

Because the calculations for $W(CR)(NHC)_4Cl$ showed that ligands with R groups bulkier than Et were not sterically viable, calculations were conducted in which these bulkier ligands were incorporated into mixed $W(CR)(NHC)_n(PMe_3)_{4-n}Cl$ compounds with $n < 4$ (Table 3.2) to search for potentially viable combinations. For *trans*-$W(CR)(NHC)_2(PMe_3)_2Cl$ ($n = 2$), the NHC ligands ICy and IiPr formed reasonable structures (Figure 3.3). The NHC ligand IMes, with the bulky and less conformationally flexible N-mesityl group, did not converge to a reasonable $n = 2$ geometry. For $W(CR)(NHC)(PMe_3)_3Cl$ ($n = 1$), the NHC ligands ICy, IiPr, and IMes converged to reasonable structures (Figure 3.4). All three derivatives show a nonlinear distortion of the C≡W-Cl axis. The IMes compound additionally displays a π-π stacking geometry with the benzylidyne ligand. In addition to these combinations, the $n = 3$ compound $W(CR)(tmiy)_3\{P(OMe)_3\}Cl$ was calculated because of its relevance to an experimental result described below. This was found to converge to a reasonable structure.

Table 3.2. Computationally converged $W(CR)(NHC)_n(PR_3)_{4-n}Cl$ (n < 4) compounds and their coordination numbers.

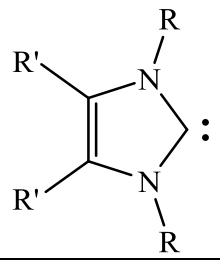	R R’ Ligand PR_3	Me Me Tmiy $P(OMe)_3$	iPr H IiPr PMe_3	Cy H ICy PMe_3	Mes H IMes PMe_3
$W(CR)(NHC)_n(PR_3)_{4-n}Cl$	n =	3	1, 2	1, 2	1

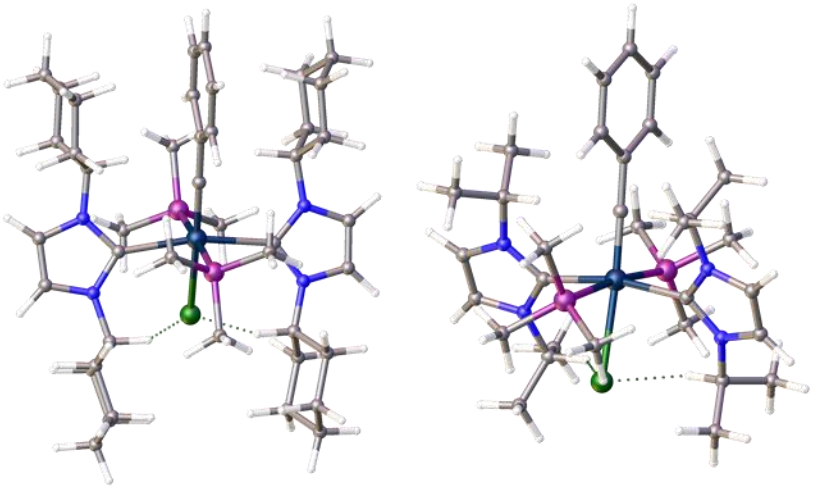

Figure 3.3. Computed structures for *trans*-$W(CR)(NHC)_2(PMe_3)_2Cl$ (n = 2) with the NHC ligands ICy (left) and IiPr (right).

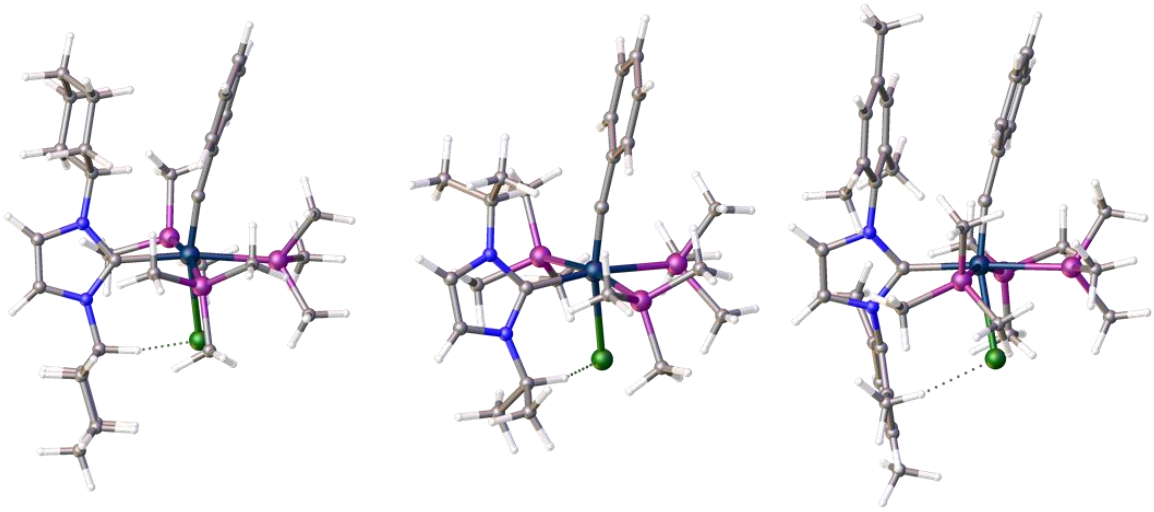

Figure 3.4. Computed structures for *trans*-W(CR)(NHC)(PMe_3)$_3$Cl (n = 3), for the NHC ligands ICy (left), IiPr (middle), and IMes (right).

The results of calculated structures above provide guidance as to the likely maximum coordination numbers for NHC ligands on a tungsten–alkylidyne compound. It is reasonable to expect that lower coordination numbers for each ligand would also be stable, as shown by the results for tmiy, IiPr, and ICy ligands. The substitution pattern may be able to be controlled by variation of reactant stoichiometry, synthetic precursors, and/or reaction conditions.

3.2.1.3 Calculated Electronic Structures and Oxidation Potentials. Electronic structure information for each hypothetical complex can also be gleaned from DFT calculations. Previous computational studies on W(CR)(PR_3)$_4$Cl compounds have shown that they generally have a HOMO primarily of non-bonding d_{xy} parentage and LUMO primarily of W≡C π^* parentage.[11,28] It has also been reported that the HOMO energy tracks linearly with the oxidation potential according to Eq 3.1, where the units for $E_{1/2}$ are V vs $FeCp_2^{0/+}$ and E(d_{xy}) is in V.[10] This correlation was established using calculations conducted with the same level of theory employed here.

$$E_{1/2} = -0.97\left(E\left(d_{xy}\right)\right) - 5.59 \quad (3.1)$$

In the present study, it was found through the calculations that $W(CR)(NHC)_n(PR_3)_{4-n}Cl$ compounds retain the same d_{xy} HOMO and π* LUMO as their phosphine analogs. As a representative example, the frontier orbitals for $W(CPh)(tmiy)_4Cl$ are shown in Figure 3.5. Other compounds were found to have similar orbitals. Some delocalization of the HOMO across the π system of the NHC ligands is observed.

NHC ligands were found to increase the energy of the HOMO, and consequently are predicted to decrease the oxidation potential, of the computed compounds. The calculated HOMO energies and predicted oxidation potentials of sterically viable complexes are collected in Table 3.3. $W(CPh)(tmiy)_4Cl$ possesses a HOMO energy of −3.160 eV, which predicts a ground state oxidation potential of −2.525 V vs $FeCp_2^{0/+}$ according to Eq 3.1. This value is significantly more negative than the observed oxidation potential of $W(CPh)(PMe_3)_4Cl$ (−0.85 V vs $FeCp_2^{0/+}$).[10] As expected, every additional ligand confers additional electron density to the metal center resulting in an additive effect to the predicted oxidation potential based on substitution.

Table 3.3. HOMO energies of computationally investigated $W(CR)(NHC)_n(PR_3)_{4-n}Cl$, and the calculated oxidation potential.

Ligand	IMe	tmiy	IEt	IiPr	IiPr	ICy	ICy	IMes
n =	4	4	4	2	1	2	1	1
HOMO (eV)	−3.473	−3.160	−3.441	−3.864	−4.152	−3.841	−4.135	−4.187
$E_{1/2}$ (pred.) (V vs $FeCp_2^{0/+}$)	−2.221	−2.525	−2.252	−1.842	−1.563	−1.809	−1.579	−1.529

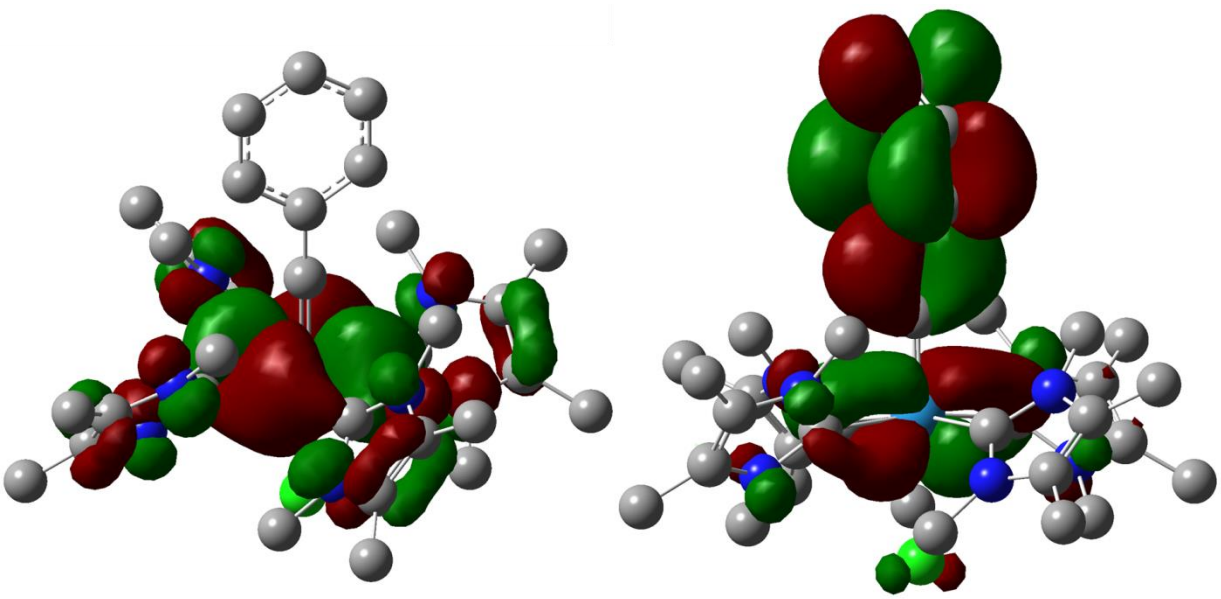

Figure 3.5. Calculated HOMO (left) and LUMO (right) of W(CPh)(tmiy)$_4$Cl.

The electronics of NHC ligands can be tuned by manipulation of the backbone of the ligand. This effect can be observed in Table 3.4 by a series of calculations showing the influence of the nature of the backbone on the HOMO energy for NHC ligands with identical N-Me groups. The HOMO energy, and thus oxidation potential, is shown to be tunable over a range of approximately 1 V. Electron donating methyl groups on the backbone increase the sigma donating strength of the ligands and decrease the oxidation potential. Electron delocalizing benzimidazole displays a considerably less negative oxidation potential.

Table 3.4. Electronic effects of a series of W(CPh)(NHC)$_4$Cl complexes with N-methyl NHC ligands bearing various backbone substitution motifs. Listed in order of most electron donating to most electron withdrawing.

Ligand	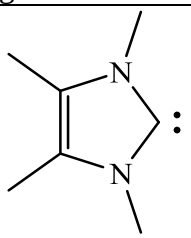 tmiy	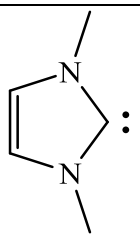 IMe	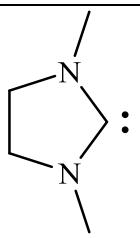 SIMe	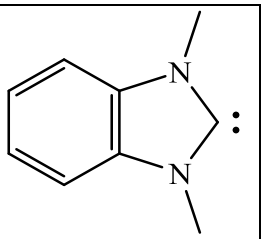 BzIMe
HOMO (eV)	−3.160	−3.473	−3.576	−4.141
$E_{1/2}$ (V vs $FeCp_2^{0/+}$, pred.)	−2.525	−2.221	−2.121	−1.573

In addition to our computational work on $W(CPh)(NHC)_4Cl$ compounds, the effects of mono- and disubstitution patterns in mixed $W(CR)(NHC)_n(PR_3)_{4-n}Cl$ species were also investigated. The mixed $W(CR)(NHC)_n(PR_3)_{4-n}Cl$ species retained the d_{xy} HOMO and π^* LUMO despite having a lower-symmetry equatorial ligand environment. For example, the frontier orbitals of both the mono- and disubstituted species $W(CPh)(ICy)(PMe_3)_3Cl$ and $W(CPh)(ICy)_2(PMe_3)_2Cl$, shown in Figure 3.6, retain a d_{xy} HOMO and π^* LUMO. These two compounds, $W(CPh)(ICy)(PMe_3)_3Cl$ and $W(CPh)(ICy)_2(PMe_3)_2Cl$, possess predicted HOMO energies of −4.135 and −3.841 eV, respectively. These values are consistent with the results for $W(CPh)(IMe)_4Cl$, for which each NHC ligand raises the HOMO energy by ca. 0.3 eV.

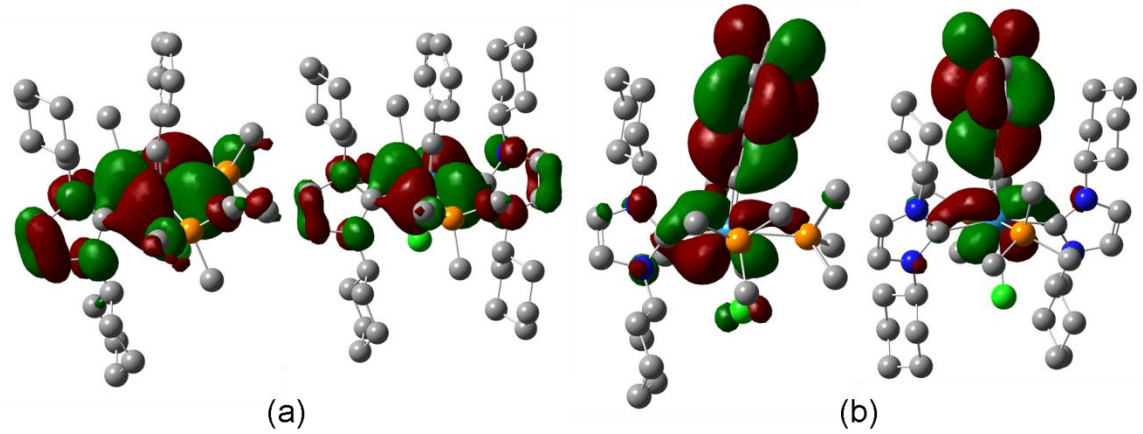

Figure 3.6. (a) HOMO for $W(CPh)(ICy)(PMe_3)_3Cl$ and $W(CPh)(ICy)_2(PMe_3)_2Cl$. (b) LUMO for $W(CPh)(ICy)(PMe_3)_3Cl$ and $W(CPh)(ICy)_2(PMe_3)_2Cl$.

3.2.2. Synthesis of $W(CPh)(NHC)_n(PR_3)_{4-n}Cl$ Complexes.

3.2.2.1 Synthetic targets and strategies. The screening calculations led us to choose the NHC ligand tmiy as the most promising candidate for $W(CPh)(NHC)_4Cl$ complexes and the ICy ligand as the most promising candidate for preparing mixed $W(CPh)(NHC)_n(PR_3)_{4-n}Cl$ complexes. Two primary synthetic strategies have been utilized to prepare d^2 tungsten–

benzylidyne complexes: a reductive pathway and a ligand substitution pathway. These are shown in Scheme 1. The reductive pathway proceeds by reacting $W(CPh)Cl_3(dme)$ in THF with the desired ligand (in excess) and subsequent two-electron reduction with Na/Hg amalgam.[29] This route has been applied to the synthesis of many $W(CPh)L_4X$ complexes. The reductive route is also well suited to thermally sensitive compounds as it proceeds at room temperature or below. The ligand substitution pathway involves reacting the incoming ligand of choice with a $W(CPh)(PR_3)_4X$ complex, typically at elevated temperature for an extended period of time. This approach has been applied most frequently with incoming chelating ligands. Examples include the synthesis of $W(CPh)(dppe)_2Cl$ via the reaction between $W(CPh)\{P(OMe)_3\}_4Cl$ and 2 equiv dppe in dichloromethane at reflux for 24 h,[30] and of $W(CH)(dmpe)_2Cl$ by the reaction between $W(CH)(PMe_3)_4Cl$ and 2 equiv dmpe at 110 °C in chlorobenzene in a sealed glass tube for 48 h.[31] This route is also amenable to partial substitutions. For example, the synthesis of $W(CPh)(dppe)\{P(OMe)_3\}_2Cl$ was accomplished by the reaction between $W(CPh)\{P(OMe)_3\}_4Cl$ and 1 equiv dppe in dichloromethane at reflux for 2 h.[30]

The targeted compound $W(CPh)(tmiy)_4Cl$ was approached synthetically using both the reductive and ligand substitution methods. The targeted mixed complexes $W(CPh)(ICy)_n(PMe_3)_{4-n}Cl$ (n = 1,2) were approached using the ligand substitution method, which seems well suited for mono and di-substitutions because the PMe_3 ligands already present stabilize transient coordinatively unsaturated species to prevent decomposition. This route also provides a convenient mechanism for reaction condition screening via $^{31}P\{^1H\}$ NMR. Tungsten has a 14% abundance S = ½ NMR active nuclei, ^{183}W, which shows ^1J coupling to ^{31}P allowing for identification of tungsten-containing products.

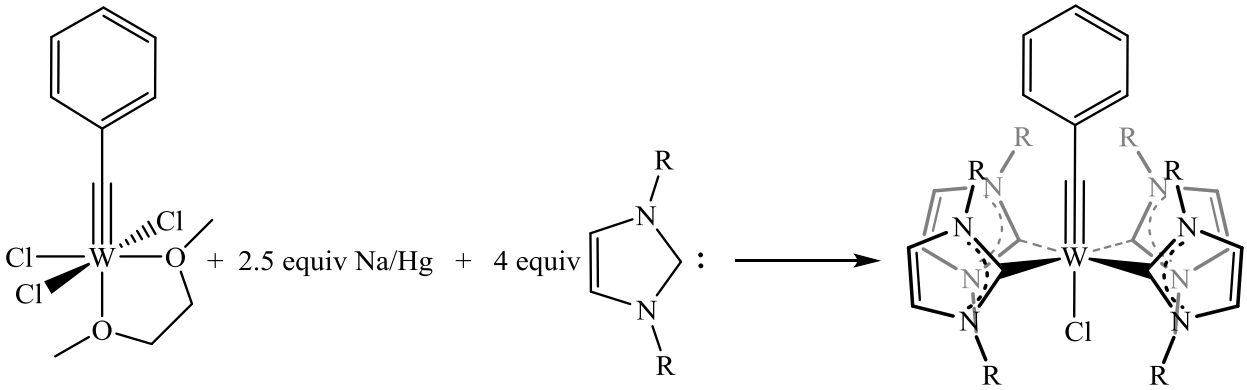

Reductive pathway

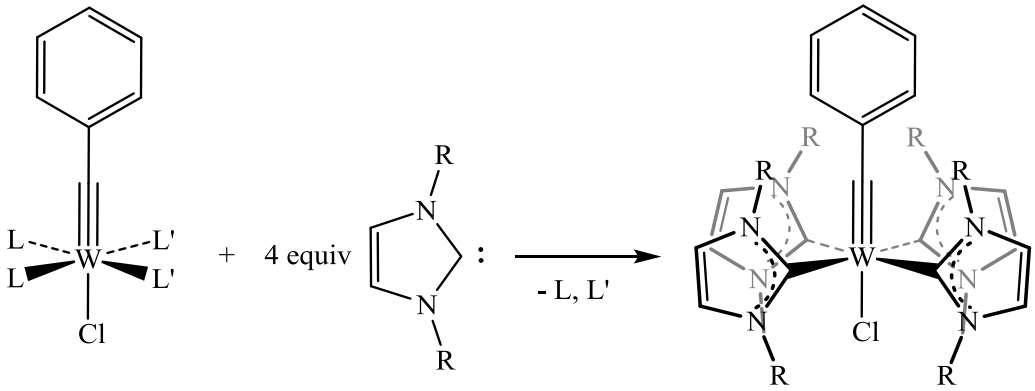

Ligand replacement pathway

Scheme 3.1. Synthetic pathways to tungsten alkylidyne compounds.

3.2.2.2 Attempted synthesis of W(CPh)(tmiy)$_4$Cl via the reductive pathway. The initial reaction of W(CPh)Cl$_3$(dme) with tmiy mirrored the reactivity of trimethylphosphine with the related synthetic precursor W(CR)(OPEt$_3$)Cl$_3$[32,33] by forming initial tmiy adducts postulated to be W(CPh)Cl$_3$(tmiy)$_2$ and [W(CPh)Cl$_2$(tmiy)$_3$]Cl (Scheme 3.2), as determined by ^{1}H-NMR and ESI-MS analysis of reaction mixtures (Figure 3.7). Two equiv of tmiy react with W(CPh)Cl$_3$(dme) in 1:1 Et$_2$O:THF, causing a color change from blue to green, with a trace of yellow precipitate, to form a compound postulated to be W(CPh)Cl$_3$(tmiy)$_2$ as a soluble green compound. The ^{1}H-NMR spectrum in C$_6$D$_6$ of an aliquot of this reaction mixture revealed two broad resonances consistent with a tmiy ligand at δ 1.47 (N-Me) and 3.83 (C-Me), which are shifted from those of free tmiy (δ 1.58 and 3.37, respectively). Numerous resonances in both the

aliphatic and aromatic region indicated that the sample had already begun to decompose and/or that the reaction directly produced side products, and prevented clear identification of the CPh resonances (Figure 3.7). The yellow precipitate was reminiscent of the product of reaction between $W(CR)(OPEt_3)Cl_3$ and 3.4 equiv PMe_3, which produced a yellow precipitate identified as $[W(CPh)(PMe_3)_3Cl_2]Cl$.[32,33] To probe whether the yellow precipitate here was of similar stoichiometry, 3.5 equiv of tmiy and $W(CPh)Cl_3(dme)$ were reacted in 1:1 THF:Et_2O, causing a color change from blue to green and production of a copious yellow precipitate. The yellow insoluble salt was formulated to be $[W(CPh)Cl_2(tmiy)_3]Cl$ based on ESI-MS , which showed a peak at *m/z* 715.23 with the correct isotope pattern. As both $W(CPh)Cl_3(tmiy)_2$ and $[W(CPh)Cl_2(tmiy)_3]Cl$ decompose into a red-brown intractable mixture within 90 min, attempts to isolate and purify them prior to subsequent two-electron reduction were not undertaken.

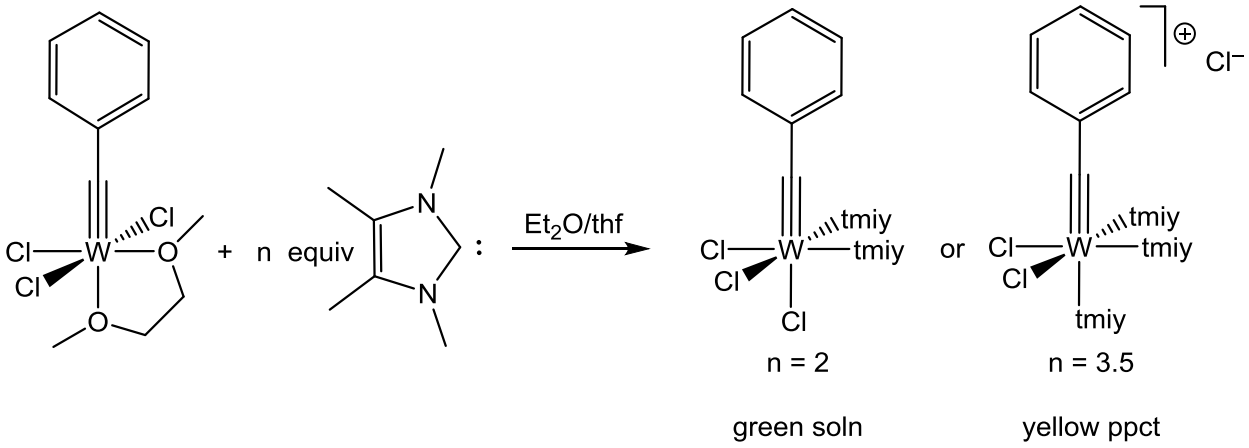

Scheme 3.2. Reactions of $W(CPh)Cl_3(dme)$ with tmiy ligand.

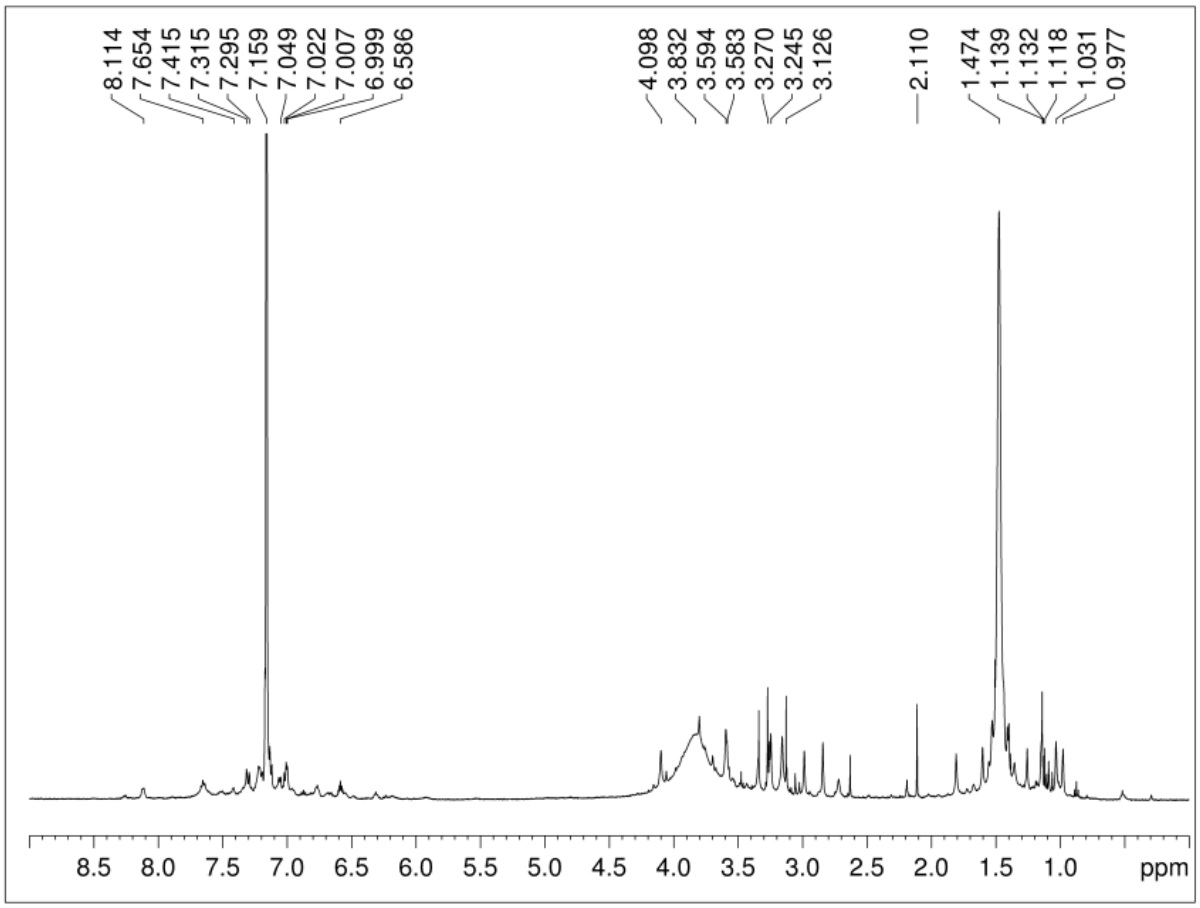

Figure 3.7. ^{1}H-NMR of the reaction of W(CPh)Cl_3(dme) with 2 equiv tmiy.

We next studied a one-pot reduction approach with the hope that two-electron reduction of in situ W(CPh)Cl_3(tmiy)$_2$ and/or [W(CPh)Cl_2(tmiy)$_3$]Cl would proceed rapidly and be completed before significant decomposition occurs. W(CPh)Cl_3(dme) was reacted with 4.1 equiv of tmiy in THF at room temperature causing a color change from blue to dark yellow-brown with a small amount of yellow precipitate consistent with the previous observations. The adduct and salt are much more soluble in pure THF than in a mixture of THF and Et_2O. Reduction at room temperature with 2.1 equiv Na/Hg results in a color change to brown and finally dark red. Upon workup, two fractions could be separated; a dark red material and a violet material. The violet material was found to be insoluble in aliphatic, aromatic, and ethereal solvents but could be

dissolved in polar solvents such as acetonitrile. This material lacked observable ^{1}H-NMR C<u>Ph</u> resonances, but did exhibit resonances attributable to the tmiy methyl groups (Figure 3.8, right). The red material contained several components, and over time produced more of the purple material; this indicated that the latter was probably a decomposition product. A clean sample of the red product could never be isolated. However, ESI-MS identified the primary product as $W(CPh)(tmiy)_4Cl$ (Figure 3.8, top). In view of the instability of the initially formed $W(CPh)(timy)_nCl_m$ adducts and the complex mixture of products formed upon two-electron reduction, the reductive route was not further studied.

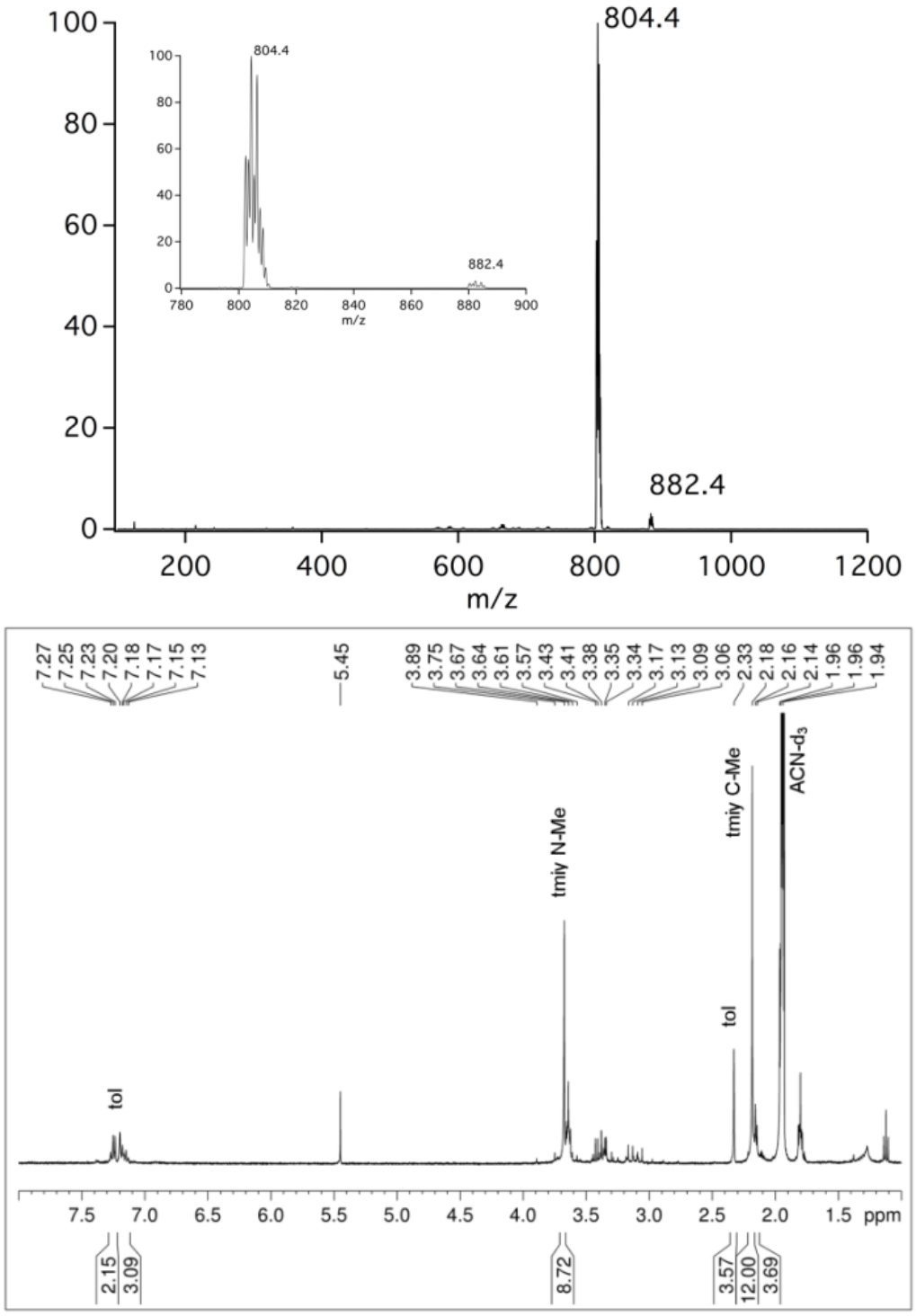

Figure 3.8. Top. ESI-MS of crude W(CPh)(tmiy)$_4$Cl formed via reduction pathway. Assigned *m/z* peaks: 882.4 [W(CPh)(tmiy)$_4$(TFA)]$^+$, 804.4 [W(CPh)(tmiy)$_4$Cl]$^+$. Bottom. ^{1}H-NMR of purple material in ACN-d$_3$.

3.2.2.3 Attempted Synthesis of W(CPh)(tmiy)$_4$Cl via Ligand Substitution. The ligand replacement pathway was also investigated in order to access our synthetic target of W(CPh)(tmiy)$_4$Cl. An NMR scale experiment was undertaken in order to monitor reaction progress and screen conditions. Upon mixing W(CPh){P(OMe)$_3$}$_4$Cl with 4.1 equiv of tmiy in C_6D_6 at room temperature, the color quickly changed from yellow to red-orange. Unlike other ligand substitution reactions involving W(CPh)(PR$_3$)$_4$Cl complexes, which require elevated temperatures, substitution with tmiy progressed at room temperature. Monitoring of the reaction mixture by ^{1}H and ^{31}P{^{1}H} NMR shows that within 20 min free P(OMe)$_3$ is generated, and new ^{31}P resonances begin to appear consistent with substitution intermediates including one singlet at δ 169.96 with ^{183}W-P satellites ($^1J_{W\text{-}P}$ = 444 Hz) (Figure 3.9, top). The singlet multiplicity would be consistent with either cis or trans W(CPh)(tmiy)$_2${P(OMe)$_3$}$_2$Cl or W(CPh)(tmiy)$_3${P(OMe)$_3$}Cl. After 2.5 h, approximately 33% of the starting material had been consumed as judged by the ratio of free P(OMe)$_3$ to W(CPh){P(OMe)$_3$}$_4$Cl. The earlier resonance at δ 169.96 was still present, but the intensity of the peak had remained relatively constant, indicating it may be an initial intermediate that reacts further. In addition, six singlet ^{31}P resonances appeared in the range of δ 167-182. Most are quite low in intensity, which prevented identification of tungsten satellites (Figure 3.9, top). The ^{1}H spectrum shows a number of new resonances, including new resonances in the aryl and tmiy regions. After 3 d, all of the free tmiy was consumed, as indicated by the ^{1}H spectrum, even though the W(CPh){P(OMe)$_3$}$_4$Cl was only ca. 60% consumed (Figure 3.9, bottom). The ^{1}H spectrum showed a large number of resonances suggesting that multiple products are formed. The ^{31}P{^{1}H} spectrum showed the same sets of intermediates as observed at 2.5 h, with one singlet resonance at δ 167.50 growing in intensity, with most others decreasing in intensity. This resonance had

^{183}W-P satellites ($^{1}J_{W\text{-}P}$ = 445 Hz), indicating it may be another intermediate. The resonance at δ 169.96 was observed at early time points, and the resonance at δ 167.50 was observed at late time points indicating that they may both be intermediates along the same reaction pathway.

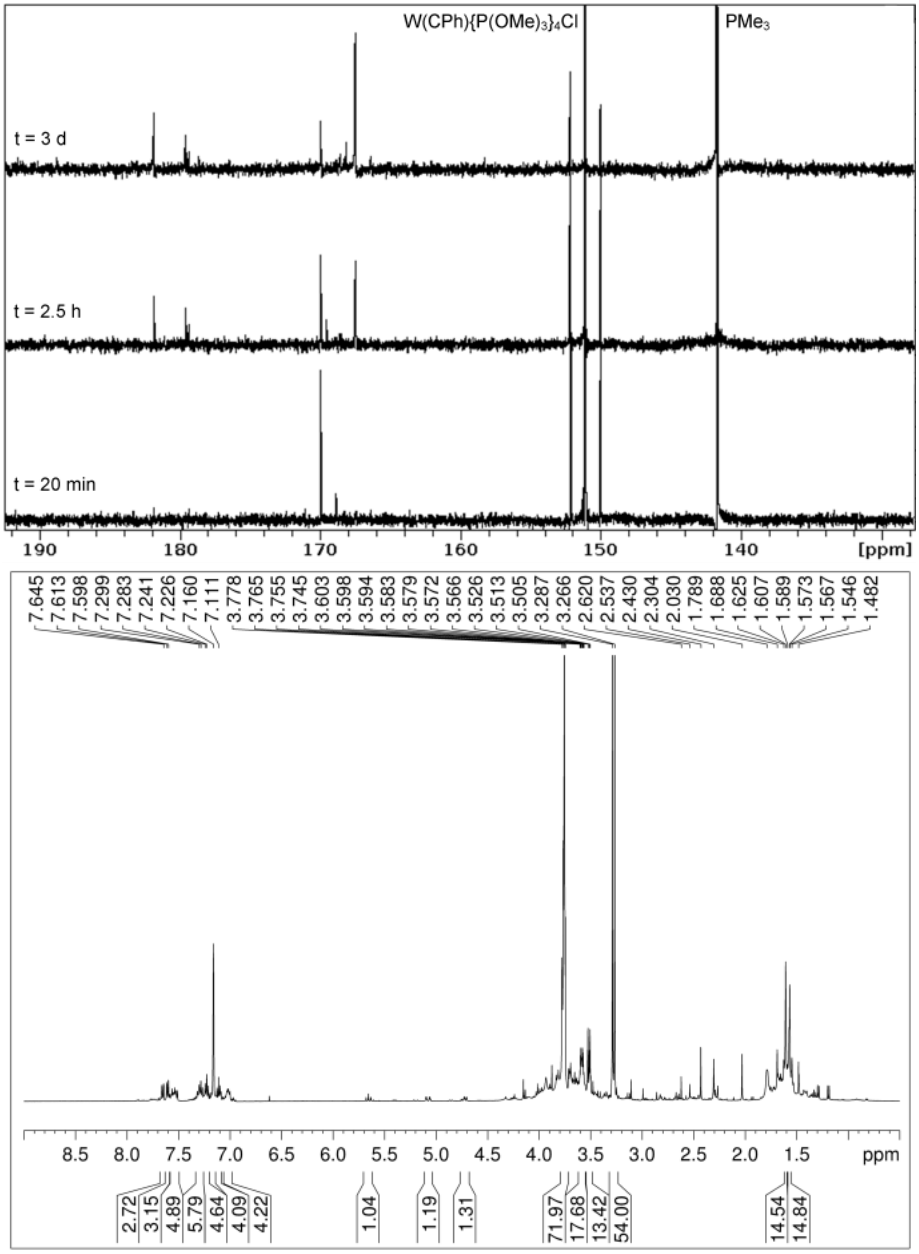

Figure 3.9. Top. Progression of the reaction of W(CPh){P(OMe)$_3$}$_4$Cl with 4.1 equiv tmiy by ^{31}P{^{1}H} NMR. All spectra scaled identically. Bottom. Final ^{1}H NMR of reaction mixture.

To identify some of the intermediates, W(CPh){P(OMe)$_3$}$_4$Cl was reacted with 2 equiv tmiy in C_6D_6, which cleanly generated the same $^{31}P\{^1H\}$ singlet resonance at δ 167.50 ($^1J_{W\text{-}P}$ = 447 Hz) after 1 day (Figure 3.10, bottom). The singlet $^{31}P\{^1H\}$ resonance, and ^1H NMR integrations were consistent with this product being W(CPh)(tmiy)$_2${P(OMe)$_3$}$_2$Cl.

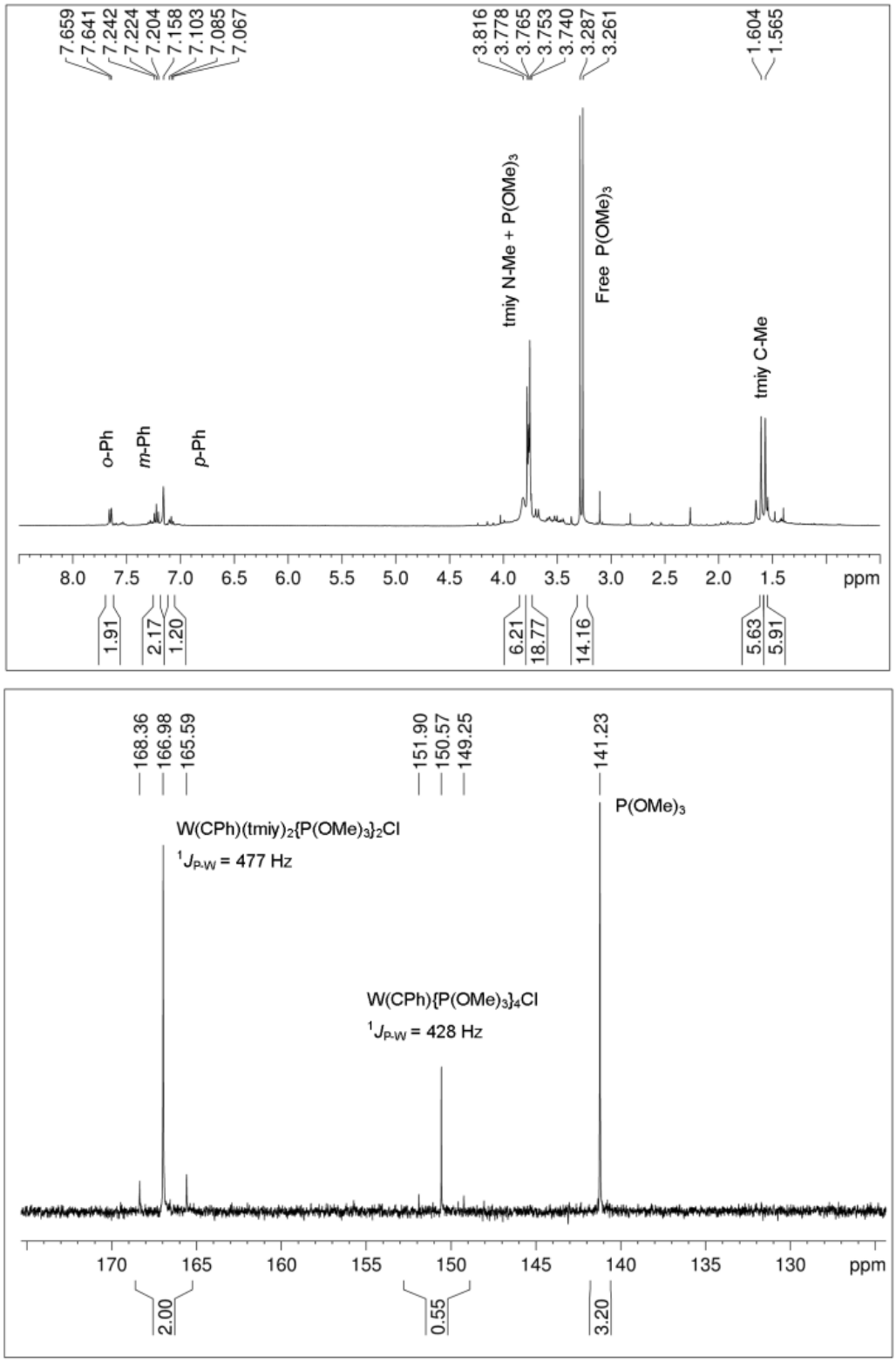

Figure 3.10. ^{1}H (top) and $^{31}P\{^{1}H\}$ (bottom) spectra of intentionally prepared $W(CPh)(tmiy)_2\{P(OMe)_3\}_2Cl$.

With the results of the NMR scale reaction in C_6D_6, small preparatory scale reactions in other solvents were screened to determine the optimal synthetic route to W(CPh)(tmiy)$_4$Cl. Ethereal solvents were selected for their ability to coordinate and stabilize open coordination sites in an attempt to reduce by-products and the complicated reaction mixture observed in C_6D_6. A trial preparatory scale reaction of W(CPh){P(OMe)$_3$}$_4$Cl with 4.5 equiv tmiy was carried out in THF at room temperature. Reaction progress was monitored via $^{31}P\{^1H\}$ NMR of aliquots spiked with C_6D_6. The reaction showed essentially complete consumption of the W(CPh){P(OMe)$_3$}$_4$Cl starting material after 14 h. The reaction in THF showed primarily free P(OMe)$_3$ via $^{31}P\{^1H\}$ NMR, along with small amounts of residual starting material and intermediates observed in the C_6D_6 reaction. Removal of the volatile components of the reaction mixture gave a dark red residue. Extraction with pentane and filtration through Celite yielded 64% crude yield of a red solid. The ^{1}H NMR spectrum again showed a complicated mixture, with the presence of some of the same products as observed before with C_6D_6 (Figure 3.11). Numerous aliphatic resonances, including several broad features were present. The aromatic region also had a broad mass of resonances. Dissolving the product in a minimal amount of Et_2O, layering with 2,2-dimethylbutane, and cooling to −35 °C for 3 d yielded purple plates suitable for X-ray diffraction.

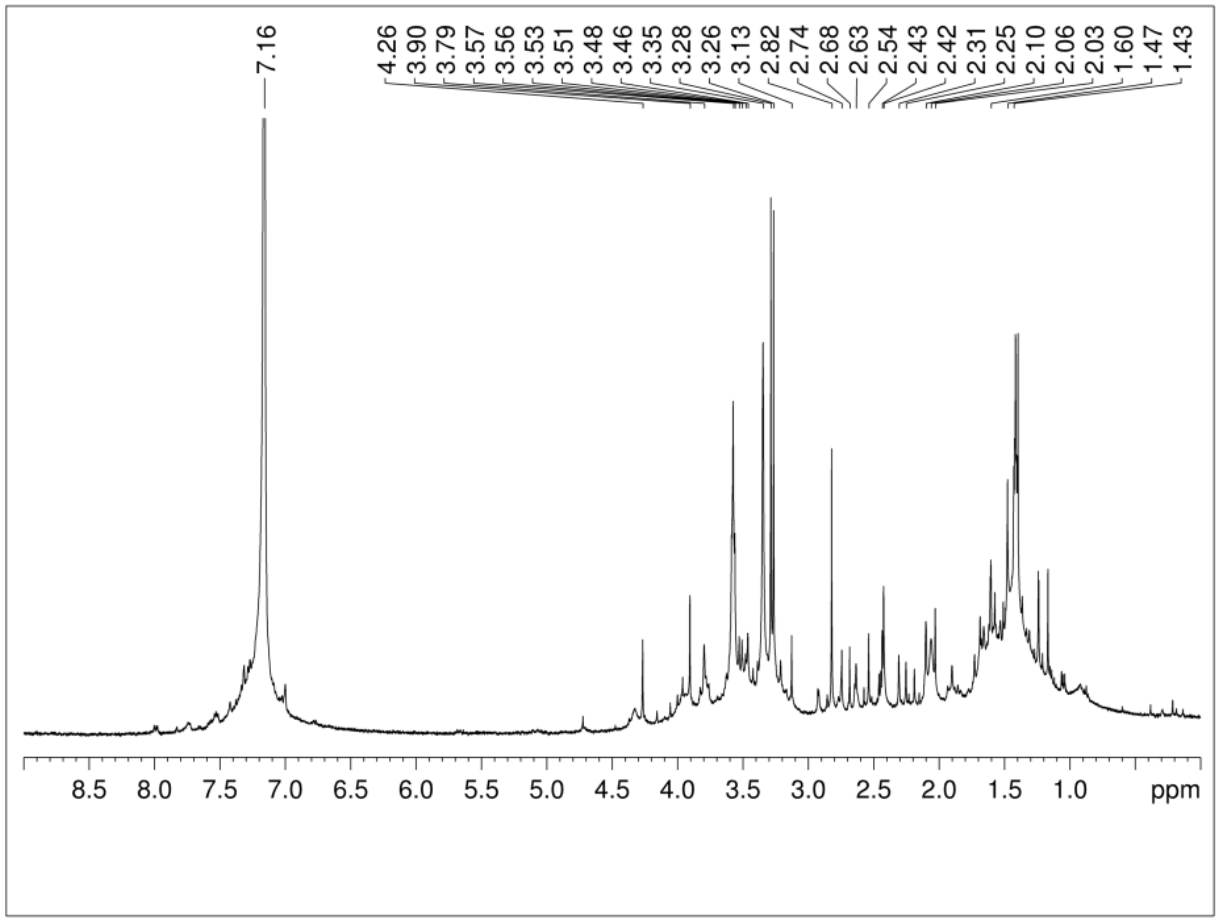

Figure 3.11. ^{1}H NMR of preparatory scale reaction of W(CPh){P(OMe)$_3$}$_4$Cl with 4.1 equiv tmiy in THF.

The single crystal X-ray structure results were unexpected. The structure was revealed to be a trisubstituted species, W(CPh)(tmiy)$_3${P(OMe)$_3$}(OBu) (Figure 3.12). The thermal ellipsoids of the carbon chain get progressively larger down the carbon chain. Due to the large ellipsoids, it is not possible to discern whether the chain is an n-butyl group or is unsaturated. We speculate that the alkoxide group originated from a ring-opened THF molecule at some point in the synthetic protocol of the complex or a reagent. One possibility is in the synthesis of tmiy, which is prepared by reduction of 1,3,4,5-tetramethylimidazole-2-thione with molten potassium in refluxing THF.[34] Despite the uncertainty about the nature of the OBu group, this structure shows that the target W(CPh)(tmiy)$_4$Cl or a close derivative is likely stable.

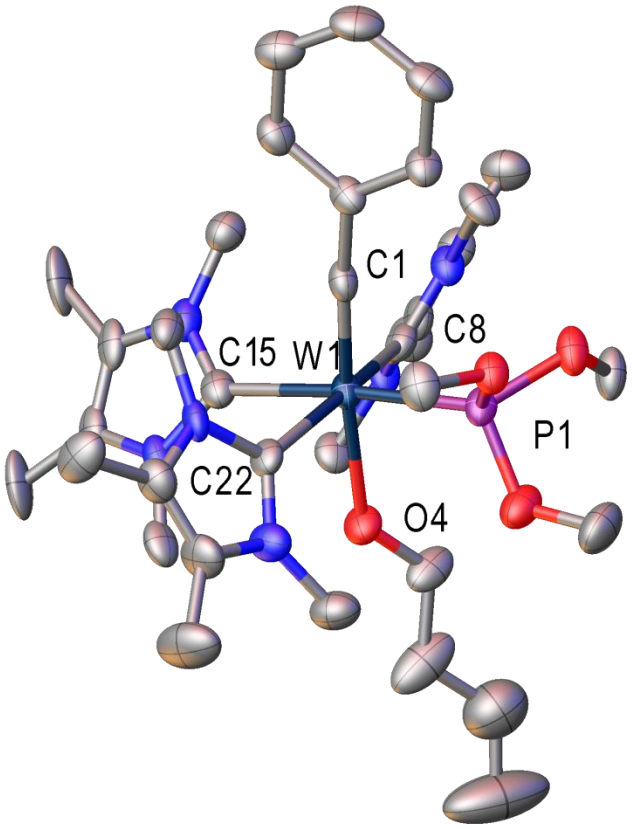

Figure 3.12. Structure of W(CPh)(tmiy)$_3${P(OMe)$_3$}(OBu)•Et$_2$O (50% probability thermal ellipsoids). For clarity, H atoms and solvent molecules are omitted for clarity. Select bond lengths and angles (Å, °): W–C1 = 1.813(10), W–P1 = 2.351(2), W–C8 = 2.228(10), W–C15 = 2.244(10), W–C22 = 2.228(10), W–O4 = 2.187(7), C1–W–O4 = 174.2(3), P1–W–C15 = 175.0(3), C8–W–C22 = 164.9(3).

This experiment was repeated with 6 equiv tmiy to try to eliminate all intermediates and form a single product. After stirring overnight at room temperature, an aliquot of the reaction was taken. The ^{31}P{^{1}H} NMR showed exclusively free P(OMe)$_3$. The ^{1}H NMR was again messy and difficult to interpret. Most telling, however, were ESI-MS results, which showed *m/z* peaks consistent with the formation of W(CPh)(tmiy)$_4$Cl (Figure 3.13). The two largest peaks were observed at 882.4 and 804.4, each with tungsten isotope splitting patterns, which are assigned to [W(CPh)(tmiy)$_4$(TFA)]$^+$ (TFA = 1,1,1-trifluoroacetate) and [W(CPh)(tmiy)$_4$Cl]$^+$ respectively. The trifluoroacetate axial ligand is likely formed from anion exchange with residual

trifluoroacetic acid present in the internal components of the instrument, which originates from the aqueous mobile phase used in other operations. Other tungsten containing *m/z* peaks are observed, but their identities could not be definitively assigned. Multiple attempts to crystallize the product of this reaction were not successful.

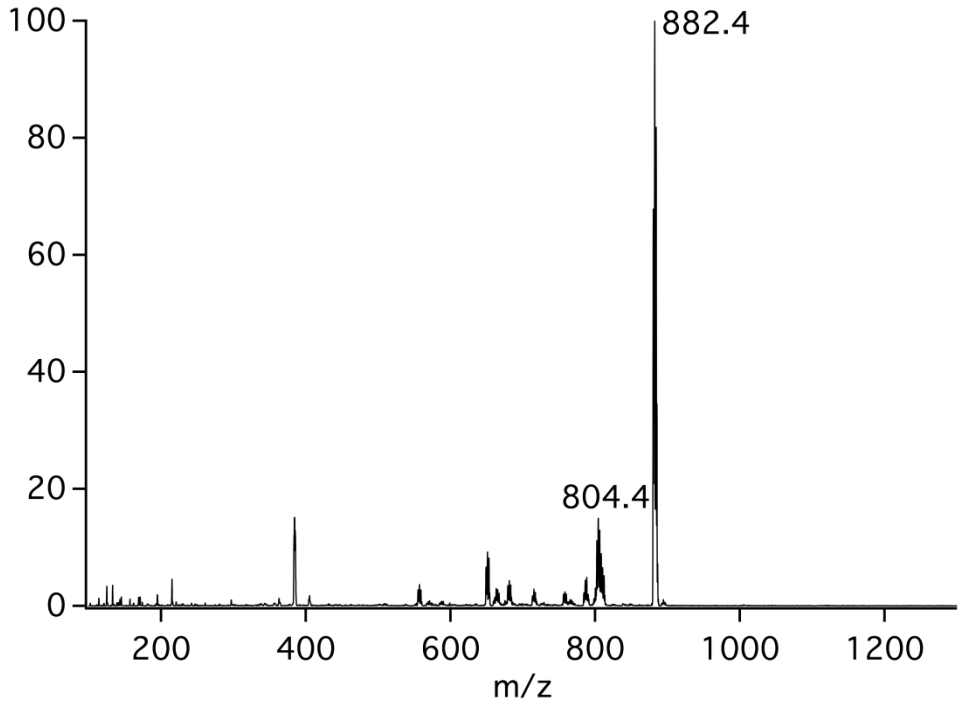

Figure 3.13. ESI-MS of reaction of W(CPh){P(OMe)$_3$}$_4$Cl with 6 equiv tmiy. Assigned *m/z* peaks: 882.4 [W(CPh)(tmiy)$_4$(TFA)]$^+$, 804.4 [W(CPh)(tmiy)$_4$Cl]$^+$.

Another starting material, W(CPh)(PMe$_3$)$_4$Cl, has also been utilized in the ligand substitution route. A test reaction between W(CPh)(PMe$_3$)$_4$Cl and 4.5 equiv tmiy in C_6D_6 was carried out to judge the viability of this route. The reaction with tmiy proceeds at room temperature, albeit slowly, as monitored by ^{31}P NMR spectroscopy. Over the course of 3 d nearly all the W(CPh)(PMe$_3$)$_4$Cl is consumed. The reaction slowly changed from purple to dark red. One singlet is initially observed after 1 h at δ −6.67 ($^1J_{P\text{-}W}$ = 296 Hz) as an intermediate during the reaction (W(CPh)(PMe$_3$)$_4$Cl δ −22.57, $^1J_{P\text{-}W}$ = 281 Hz). A second singlet at δ −20.80

containing ^{183}W-^{31}P coupling ($^{1}J_{P\text{-}W}$ = 277 Hz) is observed to have begun to form after 16 h. The ^{1}H NMR of this reaction mixture contains several resonances, but one major product is visible with integrations consistent with W(CPh)(tmiy)$_4$Cl (Figure 3.14). Broad resonances corresponding to a coordinated tmiy ligand grow in. Backbone C-methyl resonances are observed at δ 1.80 (free C-CH_3 = δ 1.58), and two N-methyl groups are observed at δ 3.75 and 3.93 (free N-CH_3 = δ 3.36). Aromatic resonances can be observed in the range of δ 7.19-7.42 (W(CPh)(PMe_3)$_4$Cl = δ 6.97-7.16). Toward the end of the reaction, all resonances began to get broader.

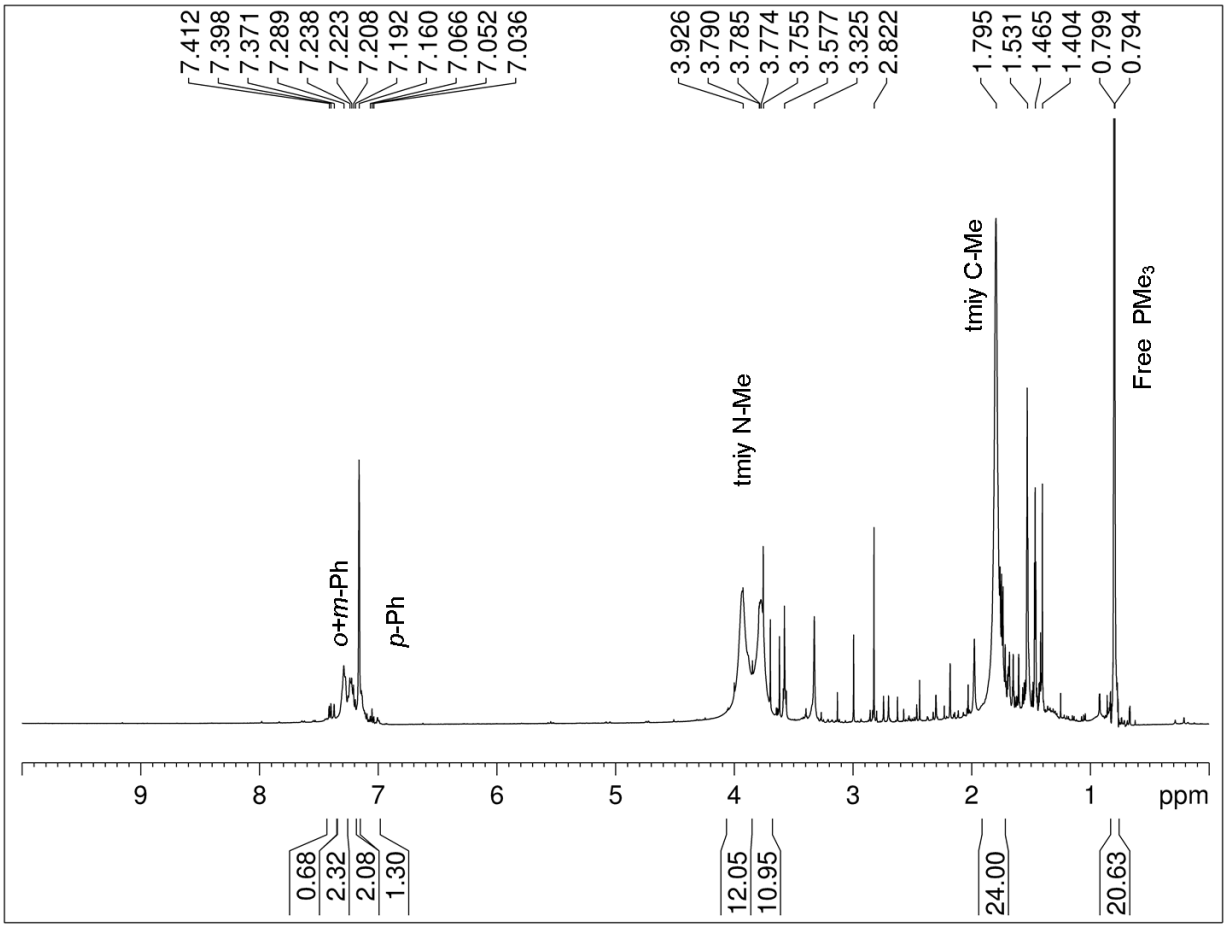

Figure 3.14. ^{1}H NMR spectrum from reaction of W(CPh)(PMe_3)$_4$Cl with 4.5 equiv tmiy.

The same reaction was screened with various conditions and solvents to determine the optimal synthetic route (Table 3.5). In all cases, the reaction mixture turns from purple to dark red. Ethereal solvents, while increasing the rate of reaction, also produced significantly more by-products. A reaction conducted in Et_2O provided the fastest reaction rate of all solvents tested.

Table 3.5. Trial reactions of $W(CPh)(PMe_3)_4Cl$ with 4.5 equiv tmiy with different solvents and conditions.

Trial	Solvent	Conditions	Outcome
1	C_6D_6	Room temperature in J. Young NMR tube, covered with foil.	Slow reaction, new products visible after 16 hr via ^{31}P NMR. Complete consumption after 3 d.
2	THF	Room temperature in sealed heavy wall glass bomb	Small amounts of intermediates similar to those from C_6D_6. Still required 3 d, and much messier ^1H NMR. Same products as trial 1.
3	THF	50 °C in J. Young NMR tube.	Total consumption within 2 h. Same major product as trial 1. Again, very messy ^1H NMR.
4	THF	50 °C under N_2, not sealed.	Total consumption of $W(CPh)(PMe_3)_4Cl$ within 2 h. Some purple solid in reaction flask. No product peaks, or extremely broad. Potential O_2/H_2O contamination.
5	C_6D_6	50 °C in J. Young NMR tube.	Total consumption of $W(CPh)(PMe_3)_4Cl$ within ca. 3 h. Two N-Me resonances merged into one broad resonance, but cleanest overall reaction.
6a	Et_2O	Room temperature J. Young NMR tube.	18% consumption of $W(CPh)(PMe_3)_4Cl$ within 1 h.
6b	Et_2O	Sample 6a 50 °C in J. Young NMR tube.	80% conversion in 30 min, 85% after 50 min. Some precipitate visible. Continued heating for 3 h total. Very broad product resonances after extended heating, and significant by products.

A preparatory scale reaction was done in Et_2O in a sealed heavy walled glass bomb, similar to trial 6b. A shorter reaction time was utilized to prevent the ^1H-NMR broadening observed at longer times and potential decomposition. $W(CPh)(PMe_3)_4Cl$ was reacted with 4.5

equiv tmiy in Et_2O for 80 min. The red product isolated contained significant amounts of by-products, but the NMR spectrum was not as broad as with the trial with extended heating. Several attempts to purify the product were carried out, but nothing proved successful. The product was found to decompose in acetonitrile and dichloromethane. Attempts to purify the compound by silica column resulted in all of the product sticking to the silica and no elution of product. Filtration through a plug of alumina decomposed the product. Drying the sample under a N_2 flow additionally resulted in decomposition. Attempts to grow crystals of the product were unsuccessful.

The evidence from these sets of experiments is promising for the formation of $W(CPh)(tmiy)_4Cl$. ESI-MS from the reaction of $W(CPh)\{P(OMe)_3\}_4Cl$ with tmiy shows peaks consistent with $W(CPh)(tmiy)_4Cl$. The crystal structure of $W(CPh)(tmiy)_3\{P(OMe)_3\}(OBu)$ also shows that $W(CPh)(tmiy)_4Cl$ or a close derivative is likely stable. The NMR evidence from the reaction with $W(CPh)(PMe_3)_4Cl$ also supports the formation of $W(CPh)(tmiy)_4Cl$. However, much work remains with respect to optimization of the reaction conditions and workup. The desired product of these reactions is found to be sensitive to a variety of conditions. The most promising reaction was found to be $W(CPh)(PMe_3)_4Cl$ with tmiy in aromatic solvents. Preparation of $W(CPh)(tmiy)_4Cl$ will likely require careful synthetic preparation and manipulation.

3.2.2.4 Synthesis and Characterization of $W(CPh)(ICy)(PMe_3)_3Cl$ via Ligand Substitution. Mono-NHC-substituted $W(CPh)(NHC)(PR_3)_3Cl$ species are predicted to be less reducing than $W(CPh)(NHC)_4Cl$ compounds, but, as a consequence, are probably also less reactive. Given the difficulties encountered above with attempts to synthesize $W(CPh)(tmiy)_4Cl$, but the encouragement offered by the crystal structure of $W(CPh)(tmiy)_3\{P(OMe)_3\}(OBu)$ that

mixed-ligand compounds may be stable, attention was turned to these targets. The ICy ligand appeared to be an ideal candidate based on computational screening. The flexible steric bulk was anticipated to provide a means to accommodate the other ligands. A trans-$W(CPh)(ICy)_2(PMe_3)_2Cl$ complex was computationally predicted to be viable, but it was predicted that over-substitution following formation of $W(CPh)(ICy)(PMe_3)_3Cl$ could be limited by maintaining relatively mild reaction conditions.

We found with the trial reactions for $W(CPh)(NHC)_4Cl$ that ethereal solvents result in a more rapid reaction, and heat additionally increases the reaction rate. The reactions of $W(CPh)(PMe_3)_4Cl$ and $W(CPh)\{P(OMe)_3\}_4Cl$ with 2.1 equiv ICy were screened in different ethereal solvents and at different conditions (Table 3.6). The reaction of $W(CPh)\{P(OMe)_3\}_4Cl$ with 2.1 equiv ICy in Et_2O showed multiple phosphorus and tungsten containing products by ^{31}P NMR, in addition to a phosphorus containing product that did not contain tungsten. The reaction of $W(CPh)(PMe_3)_4Cl$ with 2.1 equiv ICy in Et_2O produced primarily one product, with integrals and multiplicities indicative of a mono-substituted species. A small amount of phosphorus containing side products was noted. An identical reaction performed in 1,2-dimethoxyethane (dme) also produced only one product, with integrals and multiplicities indicative of $W(CPh)(ICy)(PMe_3)_3Cl$.

Table 3.6. Experimental conditions screened for the reaction of $W(CPh)(PR_3)_4Cl$ + 2.1 equiv ICy.

Trial	Solvent	Conditions	Outcome
1	Et_2O	$W(CPh)(PMe_3)_4Cl$ + 2.1 equiv ICy. Heated at 50 °C in J. Young NMR tube.	Turned green. $^{31}P\{^1H\}$ NMR indicated a doublet and triplet, consistent with mono-substitution.
2	Et_2O	$W(CPh)\{P(OMe)_3\}_4Cl$ + 2.1 equiv ICy. Heated at 50 °C in J. Young NMR tube.	Turned orange-red. $^{31}P\{^1H\}$ NMR indicated several products.
3	dme	$W(CPh)(PMe_3)_4Cl$ + 2.1 equiv ICy. Heated at 50 °C in J. Young NMR tube.	Turned green. Clean reaction and formation of single phosphorus product. Some precipitate, but otherwise good. ^1H NMR showed fairly clean product. Reaction complete after 4 h, but stable overnight at elevated temperature.
4	dme	$W(CPh)(PMe_3)_4Cl$ + 1 equiv ICy. Heated at 50 °C in sealed heavy wall glass bomb.	After 4 h, the $W(CPh)(PMe_3)_4Cl$ was about 66% consumed. Additional 0.5 equiv ICy added and heated for additional 4 h resulting in complete consumption of $W(CPh)(PMe_3)_4Cl$.

Through screening the series of reaction conditions described, it was found that the reaction of $W(CPh)(PMe_3)_4Cl$ with 1.5 equiv ICy in dimethoxyethane at 50 °C for 4 h in a sealed tube provided optimal conditions to provide the product $W(CPh)(ICy)(PMe_3)_3Cl$ as a green solid in 75% yield (Scheme 3.3). Samples of $W(CPh)(ICy)(PMe_3)_3Cl$ regularly have small amounts of unreacted $W(CPh)(PMe_3)_4Cl$ present, which has proven difficult to separate. Thus, the physical data presented here are preliminary.

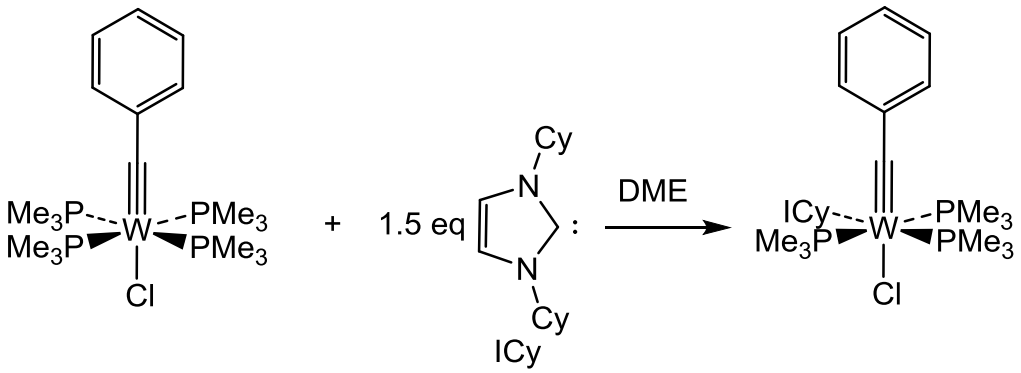

Scheme 3.3. Synthesis of W(CPh)(ICy)$(PMe_3)_3$Cl.

The ^{1}H NMR of W(CPh)(ICy)$(PMe_3)_3$Cl indicates that the ICy ligand does not rotate freely about the W-C_{NHC} bond (Figure 3.15). This results in inequivalent CH=CH backbone resonances and inequivalent cyclohexyl resonances. The PMe_3 group *trans* to the NHC ligand is observed as a virtually coupled doublet. The PMe_3 groups *cis* to the NHC ligand are observed as a virtually coupled triplet. Two $^{31}P\{^1H\}$ resonances are observed, as expected for two sets of inequivalent PMe_3 groups (Figure 3.16). The PMe_3 group *trans* to the NHC appears as a triplet with ^{183}W satellites ($^1J_{PW}$ = 263 Hz), and the two PMe_3 groups cis to the NHC appear as a doublet with ^{183}W satellites ($^1J_{PW}$ = 284 Hz). In addition to $^1J_{PW}$ coupling, the inequivalency of the two PMe_3 groups gives rise to $^3J_{PP}$ coupling of 12.5 Hz. NHC ligands have a strong trans influence, which accounts for the lower P-W coupling constant for that ligand.

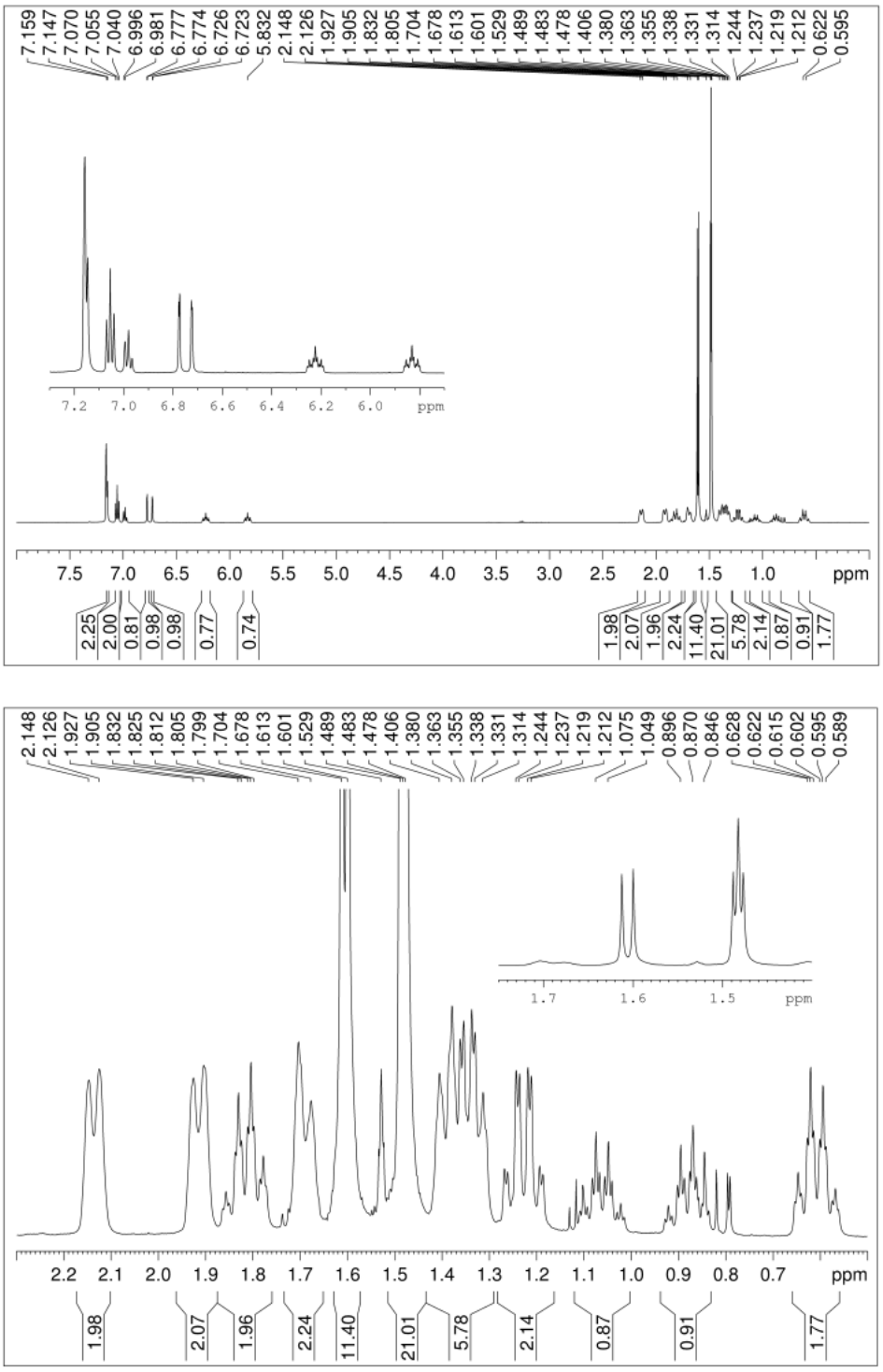

Figure 3.15. ^{1}H NMR of W(CPh)(ICy)(PMe_3)$_3$Cl. Top spectrum is the full width spectrum, and contains an inset of the alkene and aromatic region. Bottom spectrum is the aliphatic region, scaled for visibility of cyclohexyl resonances. Inset shows standard scale PMe_3 resonances.

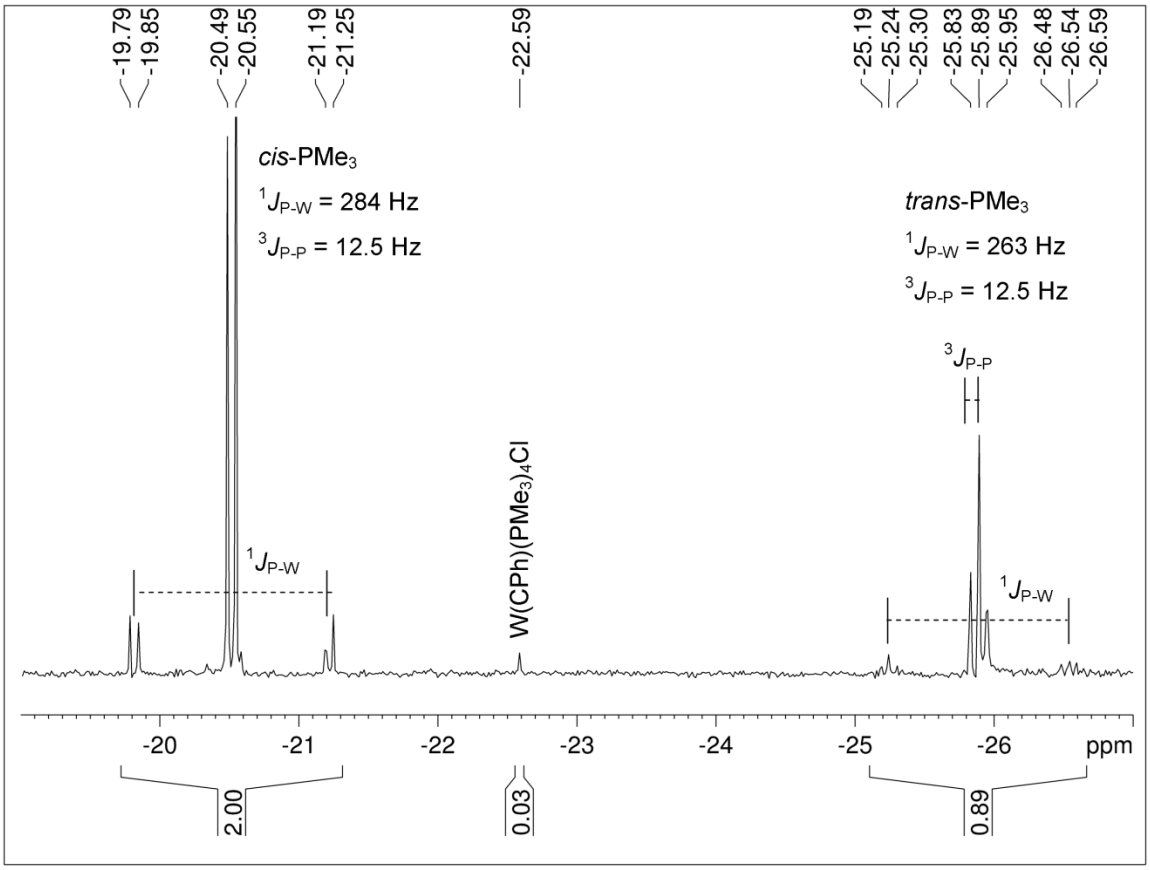

Figure 3.16. $^{31}P\{^{1}H\}$ NMR of W(CPh)(ICy)(PMe_3)$_3$Cl with couplings labeled.

Cooling a concentrated Et_2O solution of W(CPh)(ICy)(PMe_3)$_3$Cl to −50 °C overnight produced green blocks suitable for X-ray diffraction. W(CPh)(ICy)(PMe_3)$_3$Cl possesses an octahedral structure with axial benzylidyne and chloride ligands, and three equatorial PMe_3 and one ICy ligands. There are two unique molecules in the asymmetric unit with unique sets of bond lengths. The molecular structure and a space filling model of one of the unique molecules of W(CPh)(ICy)(PMe_3)$_3$Cl are shown in Figure 3.17.

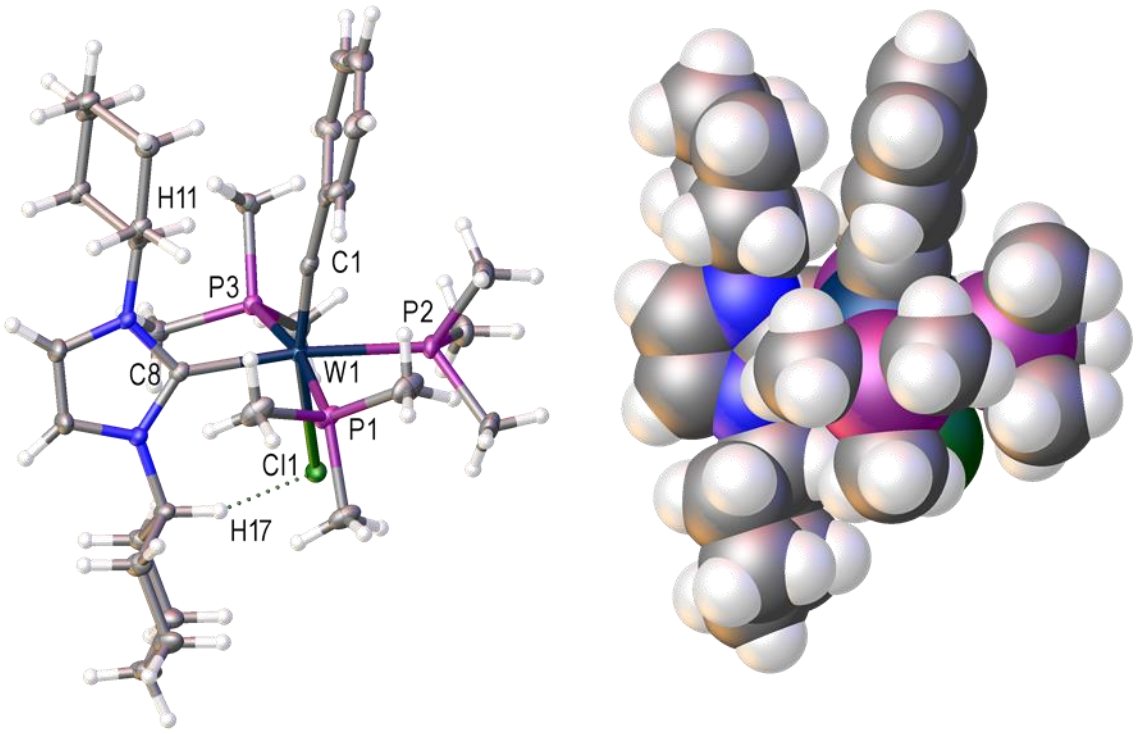

Figure 3.17. Structure of the W(CPh)(ICy)$(PMe_3)_3Cl$ (50% probability thermal ellipsoids). For clarity, only one unique molecule is shown. Bond lengths and angles are provided as part of Table 3.7.

The bonding metrics of W(CPh)(ICy)$(PMe_3)_3Cl$ compare favorably with both tungsten NHC compounds and tungsten alkylidyne compounds. The $W{\equiv}C_{avg}$ (1.817[2] Å) and $W\text{-}Cl_{avg}$ (2.6183[5] Å) bond lengths are typical of a tungsten alkylidyne structure. The cis- and trans-PMe_3 groups display no overall difference in W-P bonds lengths, with the cis-W-P bonds displaying an average length of 2.4619[9] Å, and the trans W-P bonds having an average length of 2.4660[6] Å. The two molecules display somewhat different $W\text{-}C_{NHC}$ bond lengths of 2.2386(19) Å and 2.282(2) Å for an average length of 2.260[2] Å. A tungsten(0) compound bearing the same $W\text{-}C_{NHC}$ ligand, $W(ICy)(CO)_5$, has a $W\text{-}C_{NHC}$ bond length of 2.282(3) Å.[35] The average $W{-}C_{NHC}$ distance in W(CPh)(ICy)$(PMe_3)_3Cl$, at 2.260[2] Å, falls slightly over the mean of reported $W{-}C_{NHC}$ distances (range 2.131–2.301 Å, mean 2.238 Å).[36,37] A majority of W(0)

carbonyl species reside on the longer end of this spectrum, however, while higher oxidation species tend to fall on the shorter end of the continuum. The shortest bonds are all found for electron deficient tungsten radicals bearing IMes ligands.[15,16] Comparison with compounds containing tungsten centers in the II-VI oxidation states bears a more striking difference (range 2.183–2.246 Å, mean 2.216 Å).[36,37] The complex described previously, $W(CPh)(tmiy)_3\{P(OMe)_3\}(OR)$, has an average W-$C_{NHC}$ bond of 2.233[9] Å. It is likely that steric interactions are a factor in the relatively long W-C_{NHC} distance in $W(CPh)(ICy)(PMe_3)_3Cl$.

$W(CPh)(ICy)(PMe_3)_3Cl$ crystallizes as a chain along the crystallographic C axis with alternating short (2.695 Å) and long (2.924 Å) Cl···HC NHC backbone interactions as shown in Figure 3.18 ($\Sigma r_{vdW} = 3.02$ Å).[38] In addition to the intermolecular interactions, $W(CPh)(ICy)(PMe_3)_3Cl$ also displays intramolecular interactions. The ICy ligand shows short contacts between the ipso proton of the cyclohexyl group and the chlorine (2.417 Å and 2.481 Å, Σr_{vdW} Cl,H = 3.02 Å, Figure 3.17).[38]

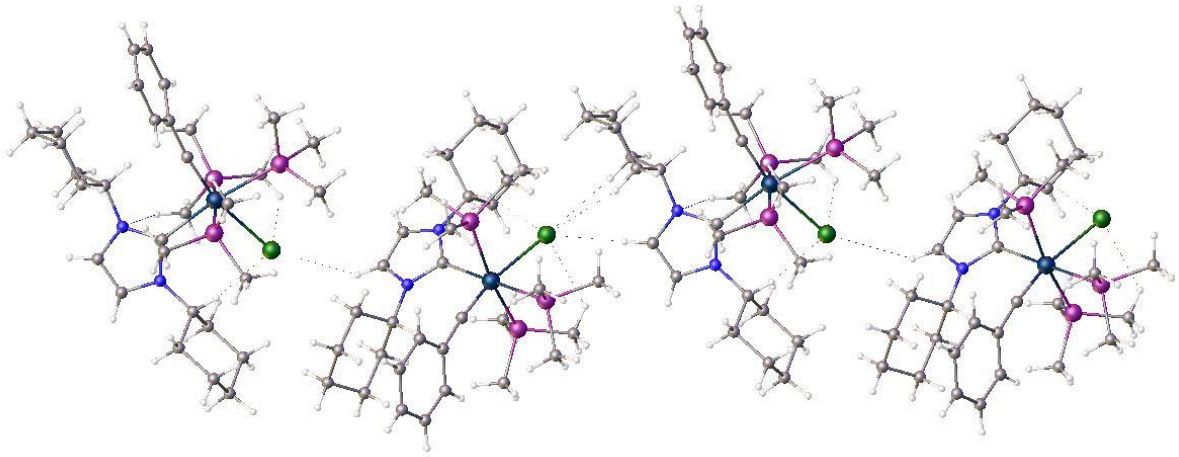

Figure 3.18. Intermolecular interactions of $W(CPh)(ICy)(PMe_3)_3Cl$ along the crystallographic C axis. Cl···HC NHC backbone: 2.695 Å, 2.924 Å.

The compound W(CPh)(ICy)(PMe_3)$_3$Cl maintains the electronic structure of the parent W(CPh)(PR_3)$_4$Cl compounds, but the ICy ligand significantly perturbs the electronic spectrum and electrochemistry. The preliminary UV-Vis spectrum of W(CPh)(ICy)(PMe_3)$_3$Cl displays a $d_{xy} \rightarrow \pi^*$ transition at 569 nm and $\pi \rightarrow \pi^*$ transition at 349 nm (Figure 3.19). These are quite red shifted relative to the transitions of W(CPh)(PMe_3)$_4$Cl of cf. 335 nm and 530 nm respectively. The electrochemistry of W(CPh)(ICy)(PMe_3)$_3$Cl shows two features; a reversible couple at -0.292 V and an irreversible couple at -0.912 V vs. $Fc^{0/+}$ as measured by differential pulse voltammetry (Figure 3.19).

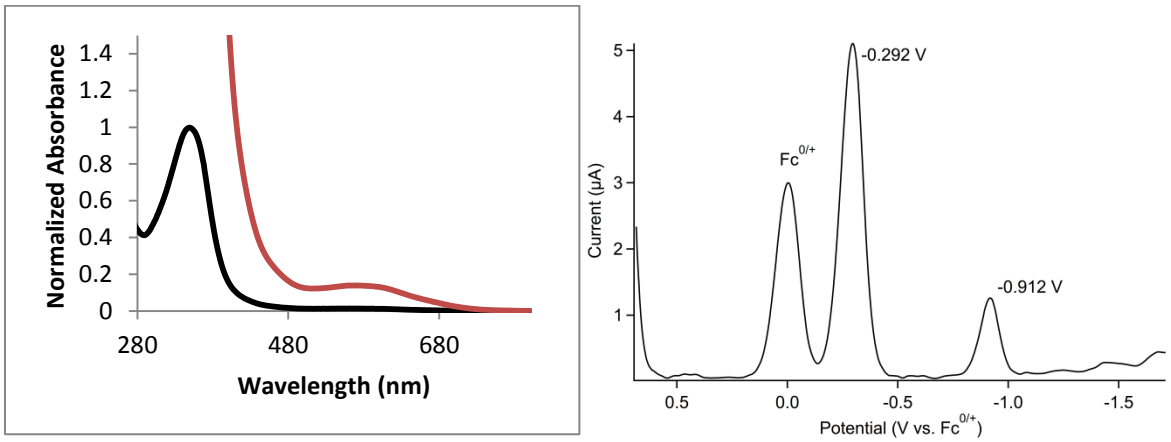

Figure 3.19. Left. Electronic–absorption spectrum of W(CPh)ICy(PMe_3)$_3$Cl (toluene). λ_{max} = 569 nm ($d_{xy} \rightarrow \pi^*$(WCPh)), 349 nm (π(WCPh)$\rightarrow\pi^*$(WCPh). Right. DPV of W(CPh)(ICy)(PMe_3)$_3$Cl.

Discrepancies were observed between the computed structure and crystal structure of W(CPh)(ICy)(PMe_3)$_3$Cl. Most notably, the benchmarked functional B3P86 and basis sets LANL2DZ/DunningDZ that perform well for many other tungsten–alkylidyne complexes predicted a W-C_{NHC} bond length that is much shorter than observed experimentally and W-P and W-Cl bond lengths that are much longer. Given the strong influence of the equatorial ligands on the energetics of the d_{xy} HOMO, and correlation with oxidation potential, this raises concerns with our computational predictions. A small benchmarking study was undertaken to see if the

computed structure could be improved (Table 3.7). Utilizing a basis set with additional polarization functions on light atoms (6-31G** vs. DunningDZ) gave a more suitable geometric agreement. Using triple-zeta functional with f orbital polarization for tungsten (LANL2TZ(f)) in combination with 6-31G** results in only marginally better agreement at considerably higher computational expense. A more thorough investigation of the experimental properties and computational modeling of tungsten alkylidyne complexes bearing N-heterocyclic carbene ligands would be required to validate a suitable computational model.

Table 3.7. Comparison of the X-ray crystal structure of W(CPh)(ICy)(PMe_3)$_3$Cl with computed structures at different levels of theory.

Functional Basis Set (W) Basis Set (C,H,N,P,Cl)	Experimental		B3P86 LANL2DZ DunningDZ	B3P86 SDD SDD	B3P86 LANL2DZ 6-31G**	B3P86 LANL2TZ(f) 6-31G**
	X-Ray 1	X-Ray 2				
W≡C	1.820(2)	1.814(2)	1.812	1.818	1.813	1.808
W-Cl	2.5984(5)	2.6381(5)	2.688	2.650	2.631	2.607
W-C_{NHC}	2.282(2)	2.2386(19)	2.177	2.265	2.256	2.251
W-P_{trans}	2.4573(6)	2.4746(5)	2.583	2.525	2.505	2.500
W-P_{cis}	2.4621(6)	2.4477(6)	2.549	2.474	2.466	2.463
W-P_{cis}	2.4810(5)	2.4804(5)	2.510	2.533	2.500	2.498
Carbyne-Ph	1.451(3)	1.447(3)	1.447	1.432	1.439	1.439
NHC H-Carbyne	2.253	2.343	2.215	2.220	2.204	2.200
NHC H-Cl	2.420	2.479	2.374	2.347	2.294	2.299
Angles						
C-W-Cl	166.98(3)	165.96(6)	165.10	166.10	167.90	168.00
Ph-C-W	173.83(16)	173.47(16)	172.40	173.00	173.70	173.90
P-W-P (trans)	166.888(18)	169.633(19)	169.40	169.80	168.80	169.10
P-W-NHC	176.65(5)	172.36(5)	172.50	172.30	174.40	174.60
C≡W-C_{NHC}-N torsion	16.89	23.14	22.20	20.90	22.30	22.40

3.3 Conclusions.

The experimental results on $W(CR)(NHC)_n(PR_3)_{4-n}Cl$ compounds bearing multiple small NHC ligands show some promising results. The reactive nature and apparent instability of the resulting species makes synthesis and characterization challenging. The formation of the desired compound $W(CPh)(tmiy)_4Cl$ is supported by ESI-MS and ^1H NMR. The results described indicate that these are synthetically viable targets, though future work will be needed to prepare and characterize these samples. The work with the large ligand, ICy, shows a mono-substituted species $W(CPh)(ICy)(PMe_3)_3Cl$ to be a stable compound. Future work will be required to complete the full characterization of this compound. Investigation into di-substitution with more forcing conditions will also need to be explored.

3.4 Experimental Section.

3.4.1 General procedures. All experiments were performed under a nitrogen atmosphere using standard Schlenk and glovebox techniques. Solvents used for syntheses were HPLC grade, and purified by passing them under nitrogen pressure through an anaerobic, stainless-steel system consisting of either two 4.5 in. × 24 in. (1 gal) columns of activated A2 alumina (CH_3CN, Et_2O, CH_2Cl_2, and THF) or one column of activated A2 alumina and one column of activated BASF R3-11 catalyst (toluene and pentane).[39] Anhydrous dimethoxyethane was purchased from Aldrich, and stored over activated 3 Å molecular sieves. C_6D_6, CD_2Cl_2, and CD_3CN were obtained from Cambridge Isotope Labs and stored over activated 3 Å molecular sieves. $W(CPh)Cl_3(dme)$,[29] $W(CPh)\{P(OMe)_3\}_4Cl$,[30] $W(CPh)(PMe_3)_4Cl$,[10] ICy,[40] and tmiy[34] were prepared according to standard procedures. $[N^nBu_4][PF_6]$ (Fluka, electrochemical grade) was recrystallized 2–3× from MeOH and dried under vacuum at 100 °C for 12 h. All other reagents

were obtained from commercial sources and used as received. ^{1}H-, ^{2}H-, ^{13}C{^{1}H}-, ^{13}C{^{1}H,^{31}P}-, and ^{31}P{^{1}H}-NMR spectra were recorded with Bruker Avance II+ 500, DRX 500, or DRX 400 NMR spectrometers; measurements were made at room temperature unless noted otherwise. Chemical shifts were measured relative to solvent resonances (^{1}H, ^{2}H, and ^{13}C)[41] or to an external standard of 85% H_3PO_4 (^{31}P). Electrospray Ionization mass spectrometry (ESI-MS) employed an Agilent 6130 LCMS.

W(CPh)(ICy)(PMe$_3$)$_3$Cl. Note: The following operation should be conducted behind a blast shield. In a 50 mL heavy walled glass bomb sealed with a Teflon Young's tap, W(CPh)(PMe$_3$)$_4$Cl (75 mg, 0.1224 mmol) and 1,3-bis(cyclohexyl)imidazol-2-ylidene (ICy, 28.4 mg, 0.1224 mmol, 1 equiv) in 10 mL DME were heated to 50 °C for 4 h, resulting in a color change from violet to brown and the formation of a small amount of off-white precipitate (found to be [ICyH]Cl). Reaction progress was monitored by ^{31}P{^{1}H}-NMR spectroscopy of aliquots spiked with C_6D_6. Noting that the W(CPh)(PMe$_3$)$_4$Cl was approximately 66% consumed, an additional charge of ICy was added (14.2 mg, 0.0612 mmol, additional 0.5 equiv, 1.5 equiv ICy total), the bomb resealed, and the mixture reheated to 50 °C for an additional 4 h. Upon completion of the reaction as judged by ^{31}P{^{1}H}-NMR, the reaction mixture was filtered through a fine frit to remove the precipitate. The volatiles were removed under vacuum and the dark residue extracted with 5 mL Et_2O, which was filtered through Celite to remove a red insoluble material. The volatiles were removed under vacuum to yield 66 mg of W(CPh)(ICy)(PMe$_3$)$_3$Cl as a green product, 75% yield. The product from this reaction contained a small amount of unreacted W(CPh)(PMe$_3$)$_4$Cl, which proved difficult to separate by chemical means. Single crystals suitable for X-ray diffraction were grown by cooling a concentrated solution of W(CPh)(ICy)(PMe$_3$)$_3$Cl in Et_2O to −50 °C.

^{1}H-NMR (500.13 MHz, C_6D_6): 7.15 (2H, o-Ph, overlaps with C_6D_6 resonance), 7.06 (t, 2H, m-Ph, $^{3}J_{HH}$ = 7.3 Hz), 6.98 (t, 1H, p-Ph, $^{3}J_{HH}$ = 7.3Hz) 6.78 (d, 1H, N-C<u>H</u>=C<u>H</u>=N, $^{3}J_{HH}$ = 1.9 Hz), 6.72 (d, 1H, N-C<u>H</u>=C<u>H</u>=N, $^{3}J_{HH}$ = 1.9 Hz) 6.22 (tt, 1H, N-CH, $^{3}J_{HH}$ = 12.0 Hz, 3.8 Hz), 5.83 (tt, 1H, N-CH, $^{3}J_{HH}$ = 11.7 Hz, 3.5 Hz), 2.14 (br d, 2H, $^{3}J_{HH}$ = 11.0 Hz), 1.92 (br d, 2H, $^{3}J_{HH}$ = 10.8 Hz), 1.82 (qt, 2H, J_{HH} = 13.2 Hz, 3.3 Hz), 1.69 (br d, 2H, $^{3}J_{HH}$ = 13.2 Hz), 1.61 (app d, 9H, $^{2}J_{HP}$ = 6.0 Hz, PMe_3 trans to NHC), 1.48 (app t, 18H, J = 2.8 Hz, 2 PMe_3 cis to NHC), 1.40-1.30 (2 overlapping multiplets, 6H total), 1.23 (qd, 2H, $^{3}J_{HH}$ = 12.5 Hz, 3.5 Hz), 1.06 (qt, 1H, $^{3}J_{HH}$ = 13.2 Hz, 3.8 Hz), 0.88 (qt, 1H, $^{3}J_{HH}$ = 13.0 Hz, 3.5 Hz), 0.61 (qt, 2H $^{3}J_{HH}$ = 13.2 Hz, 3.4 Hz). ^{31}P{^{1}H} (202.44 MHz, C_6D_6): −20.62 (d, 2P, $^{1}J_{PW}$ = 284 Hz, $^{2}J_{PP}$ = 12.5 Hz, PMe_3 cis to NHC), −25.89 (t, 1P, $^{1}J_{PW}$ = 263 Hz, $^{2}J_{PP}$ = 12.5 Hz, PMe_3 trans to NHC) DPV (vs. $Fc^{0/+}$, 0.1M NBu_4PF_6 in THF): −0.292 V (reversible), −0.912 V (irreversible) (See Figure 3.19).

3.5 References.

(1) Blankenship, R. E. *Molecular Mechanisms of Photosynthesis*; 2nd ed.; Wiley Blackwell: Oxford, UK, 2014.

(2) Gray, H. B.; Maverick, A. W. *Science* **1981**, *214*, 1201.

(3) Shaw, M. H.; Twilton, J.; MacMillan, D. W. *J. Org. Chem.* **2016**, *81*, 6898.

(4) Tucker, J. W.; Stephenson, C. R. J. *J. Org. Chem.* **2012**, *77*, 1617.

(5) Prier, C. K.; Rankic, D. A.; MacMillan, D. W. C. *Chem. Rev.* **2013**, *113*, 5322.

(6) King, K. A.; Spellane, P. J.; Watts, R. J. *J. Am. Chem. Soc.* **1985**, *107*, 1431.

(7) Flamigni, L.; Barbieri, A.; Sabatini, C.; Ventura, B.; Barigelletti, F. In *Photochemistry and Photophysics of Coordination Compounds II*; Balzani, V., Campagna, S., Eds.; Springer Berlin Heidelberg: Berlin, Heidelberg, 2007, p 143.

(8) Teegardin, K.; Day, J. I.; Chan, J.; Weaver, J. *Org. Process Res. Dev.* **2016**, *20*, 1156.

(9) Sattler, W.; Henling, L. M.; Winkler, J. R.; Gray, H. B. *J. Am. Chem. Soc.* **2015**, *137*, 1198.

(10) Haines, D. E.; O'Hanlon, D. C.; Manna, J.; Jones, M. K.; Shaner, S. E.; Sun, J.; Hopkins, M. D. *Inorg. Chem.* **2013**, *52*, 9650.

(11) Da Re, R. E.; Hopkins, M. D. *Coord. Chem. Rev.* **2005**, *249*, 1396.

(12) Lovaasen, B. M.; Lockard, J. V.; Cohen, B. W.; Yang, S.; Zhang, X.; Simpson, C. K.; Chen, L. X.; Hopkins, M. D. *Inorg. Chem.* **2012**, *51*, 5660.

(13) Hopkinson, M. N.; Richter, C.; Schedler, M.; Glorius, F. *Nature* **2014**, *510*, 485.

(14) Gusev, D. G. *Organometallics* **2009**, *28*, 6458.

(15) Dioumaev, V. K.; Szalda, D. J.; Hanson, J.; Franz, J. A.; Morris Bullock, R. *Chem. Commun.* **2003**, 1670.

(16) Roberts, J. A. S.; Franz, J. A.; van der Eide, E. F.; Walter, E. D.; Petersen, J. L.; DuBois, D. L.; Bullock, R. M. *J. Am. Chem. Soc.* **2011**, *133*, 14593.

(17) van der Eide, E. F.; Liu, T.; Camaioni, D. M.; Walter, E. D.; Bullock, R. M. *Organometallics* **2012**, *31*, 1775.

(18) Bellemin-Laponnaz, S.; Dagorne, S. *Chem. Rev.* **2014**, *114*, 8747.

(19) Wang, Z.; Jiang, L.; Mohamed, D. K. B.; Zhao, J.; Hor, T. S. A. *Coord. Chem. Rev.* **2015**, *293-294*, 292.

(20) Dodds, C. A.; Spicer, M. D.; Tuttle, T. *Organometallics* **2011**, *30*, 6262.

(21) Schowner, R.; Frey, W.; Buchmeiser, M. R. *J. Am. Chem. Soc.* **2015**, *137*, 6188.

(22) Herrmann, W. A.; Lobmaier, G. M.; Elison, M. *J. Organomet. Chem.* **1996**, *520*, 231.

(23) Bühl, M.; Reimann, C.; Pantazis, D. A.; Bredow, T.; Neese, F. *J. Chem. Theory Comput.* **2008**, *4*, 1449.

(24) Braband, H.; Oehlke, E.; Abram, U. *Z. Anorg. Allg. Chem.* **2006**, *632*, 1051.

(25) Braband, H.; Przyrembel, D.; Abram, U. *Z. Anorg. Allg. Chem.* **2006**, *632*, 779.

(26) Kückmann, T. I.; Abram, U. *Inorg. Chem.* **2004**, *43*, 7068.

(27) Ohki, Y.; Aoyagi, K.; Seino, H. *Organometallics* **2015**, *34*, 3414.

(28) Manna, J.; Gilbert, T. M.; Dallinger, R. F.; Geib, S. J.; Hopkins, M. D. *J. Am. Chem. Soc.* **1992**, *114*, 5870.

(29) Sun, J.; Simpson, C. K.; Hopkins, M. D.; Hock, A. S.; Schrock, R. R. In *Inorganic Syntheses: Volume 36*; John Wiley & Sons, Inc.: 2014, p 134.

(30) Mayr, A.; Dorries, A. M.; McDermott, G. A.; Van Engen, D. *Organometallics* **1986**, *5*, 1504.

(31) Holmes, S. J.; Clark, D. N.; Turner, H. W.; Schrock, R. R. *J. Am. Chem. Soc.* **1982**, *104*, 6322.

(32) Wengrovius, J. H.; Sancho, J.; Schrock, R. R. *J. Am. Chem. Soc.* **1981**, *103*, 3932.

(33) Schrock, R. R.; Clark, D. N.; Sancho, J.; Wengrovius, J. H.; Rocklage, S. M.; Pedersen, S. F. *Organometallics* **1982**, *1*, 1645.

(34) Kuhn, N.; Kratz, T. *Synthesis* **1993**, *1993*, 561.

(35) Herrmann, W. A.; Köcher, C.; Gooßen, L. J.; Artus, G. R. J. *Chem. Eur. J.* **1996**, *2*, 1627.

(36) Groom, C. R.; Bruno, I. J.; Lightfoot, M. P.; Ward, S. C. *Acta Cryst. B* **2016**, *72*, 171.

(37) Bruno, I. J.; Cole, J. C.; Edgington, P. R.; Kessler, M.; Macrae, C. F.; McCabe, P.; Pearson, J.; Taylor, R. *Acta Cryst. B* **2002**, *58*, 389.

(38) Alvarez, S. *Dalton Trans.* **2013**, *42*, 8617.

(39) Pangborn, A. B.; Giardello, M. A.; Grubbs, R. H.; Rosen, R. K.; Timmers, F. J. *Organometallics* **1996**, *15*, 1518.

(40) Ortega, N.; Richter, C.; Glorius, F. *Org. Lett.* **2013**, *15*, 1776.

(41) Fulmer, G. R.; Miller, A. J. M.; Sherden, N. H.; Gottlieb, H. E.; Nudelman, A.; Stoltz, B. M.; Bercaw, J. E.; Goldberg, K. I. *Organometallics* **2010**, *29*, 2176.

Chapter 4

Protonolysis and Amide Exchange Reactions of a Three-Coordinate Cobalt Amide Complex Supported by an N-Heterocyclic Carbene Ligand[1]

Presented in the next three chapters are the results of the work performed during the first three years of my graduate student career. Prior to my work in the laboratory of Prof. Michael Hopkins, I spent the three years in the laboratory of Prof. Gregory Hillhouse working on the subject of low-coordinate cobalt amide compounds. Prof. Hillhouse passed away in March of 2014. After this, I took on Prof. Hopkins as an advisor to complete my doctoral research.

4.1 Introduction.

Cobalt N-heterocyclic carbene (NHC) compounds have found increasing utility as catalysts for cross coupling,[2] alkyne trimerization,[3] alkene hydroarylation,[4] and other reactions.[5] Additionally, NHC-supported cobalt species have been shown to activate aryl C-H bonds for further functionalization.[6] While in most of these cases the active cobalt species is generated *in situ* and its structure is unknown, it is likely that low-coordinate cobalt complexes are involved in critical steps of these reactions. The preparation and characterization of such species is important to better understand the mechanisms and optimize the performance of these catalysts.

Several routes to three-coordinate NHC cobalt compounds have been reported (Scheme 4.1). Salt metathesis of metal halide sources with alkali reagents is the most common route to access these iron, cobalt, and nickel species. As a representative example, $\{IPrCoCl_2\}_2$ (IPr = 1,3-di(2,6-diisopropylphenyl)imidazolin-2-ylidene) reacts with four equiv of $Mg(CH_2SiMe_3)Br$ affording $IPrCo(CH_2SiMe_3)_2$ (Scheme 4.1, eq 1).[2g] Alternatively, displacement of weaker ligands or coordination of unsaturated fragments also allows for access to two and three-coordinate Fe, Co, and Ni species. This approach may be illustrated by the displacement of PPh_3

from $CoCl(PPh_3)_3$ by 1,3-bis(2,4,6-trimethylphenyl)imidazolin-2-ylidene (IMes) yielding $(IMes)_2CoCl$ (Scheme 4.1, eq 2).[7] Protonolysis of highly basic ligands offers another route to access low-coordinate species. The double amine elimination reaction of $\{Co(\mu\text{-}N(SiMe_3)_2)N(SiMe_3)_2\}_2$ with [NHC-H]Br imidazolium salts yields $(NHC)_2CoBr_2$ compounds.[8] However, it was recently discovered that by using bulky [NHC-H]Cl salts such as [IMesH]Cl or [SIMesH]Cl (SIMes = 1,3-di(2,4,6-trimethylphenyl)-4,5-dihydroimidazolin-2-ylidene), the posited intermediate three-coordinate mono-NHC species in this reaction, $(NHC)CoCl\{N(SiMe_3)_2\}$, could be isolated (Scheme 4.1, eq 3).[9] This route has the advantage that compounds of NHC ligands that are not stable as free carbenes may be efficiently synthesized. However, there are limitations to this route. To obtain the mixed chloride amide species, the steric environment of the NHC must be carefully selected to avoid over substitution or the formation of ionic salts.[9] The cobalt starting material for this preparation is additionally somewhat complicated to prepare, and does not store well.[9,10,11,12] An alternative route to these same complexes may be provided salt metathesis of a halide starting material. Here we describe the synthesis of the mixed (NHC)Co amide chloride species $IPrCoCl\{N(SiMe_3)_2\}$ (**1**), and its utility as a synthetic entry point to other low-coordinate cobalt species.

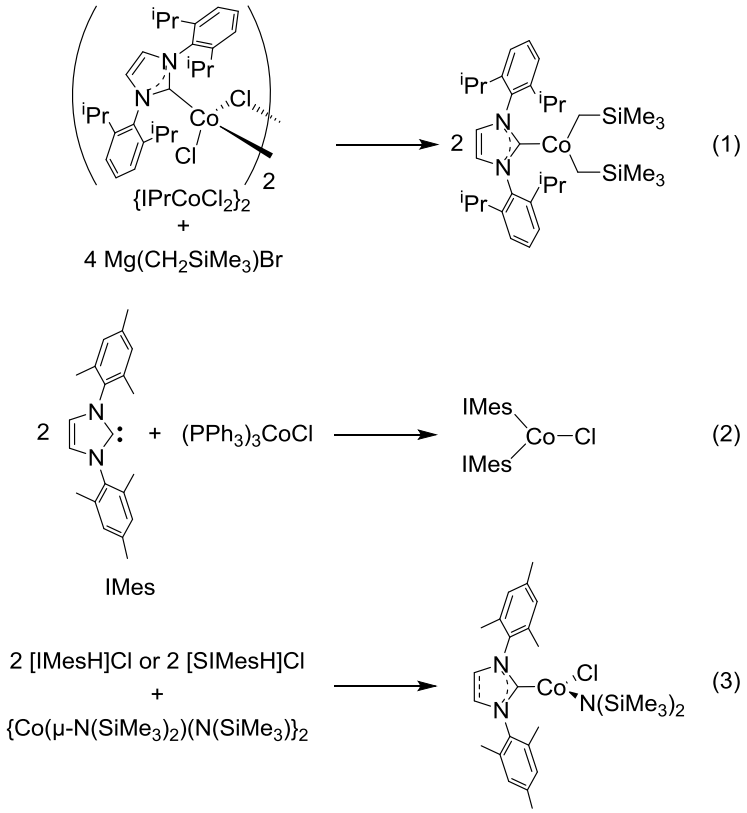

Scheme 4.1. Synthetic routes to NHC supported low-coordinate cobalt compounds.

4.2 Results and Discussion.

4.2.1 Synthesis and Characterization of IPrCoCl{N(SiMe$_3$)$_2$} (1). The amine elimination reaction of {Co(μ-N(SiMe$_3$)$_2$)N(SiMe$_3$)$_2$}$_2$ with two equiv of [IPrH]Cl affords IPrCoCl{N(SiMe$_3$)$_2$} (**1**, Scheme 4.2) as a bright-green air-sensitive solid in 60% isolated yield. In our hands however, this route proved to be problematic. The {Co(μ-N(SiMe$_3$)$_2$)N(SiMe$_3$)$_2$}$_2$ starting material is time-consuming to prepare, requiring distillation and subsequent recrystallization,[10,11,12,13] and the HN(SiMe$_3$)$_2$ coproduct from the reaction with [IPrH]Cl is difficult to remove. The method is viable, but to avoid these issues, we devised an alternative route to **1**, as shown in Scheme 4.2. The reaction of 1.98 equiv of NaN(SiMe$_3$)$_2$ with {IPrCoCl$_2$}$_2$[2f,1g] in Et$_2$O also affords **1** in 93% isolated yield. The use of slightly less than two

equiv of $NaN(SiMe_3)_2$ is important to avoid challenges associated with removal of this starting material from the final product. This route gave a better yield and cleaner product, and was more amenable to producing **1** on large scale, compared to the amine elimination route. Furthermore, $\{IPrCoCl_2\}_2$[2f,1g] is easier to prepare than $\{Co(\mu\text{-}N(SiMe_3)_2)N(SiMe_3)_2\}_2$.[10,11,12,13] Compound **1** is highly air-sensitive, changing from green to blue upon exposure to the atmosphere.

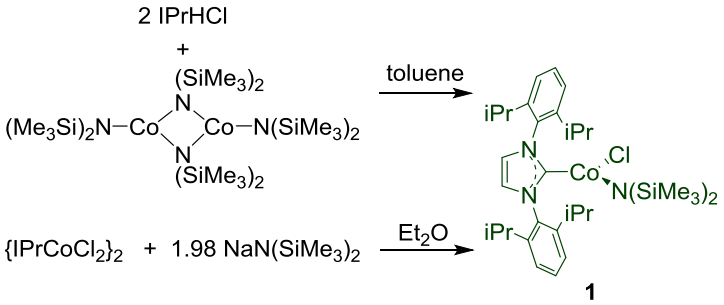

Scheme 4.2. Synthetic routes to compound **1**.

Crystals of **1** suitable for X-ray diffraction were obtained by crystallization from a 1/1 toluene/hexanes solution at −35 °C to afford **1** as bright green needles. The solid state structure of **1** is shown in Figure 4.1. The geometry around cobalt is trigonal planar, with the sum of the angles being 359.99(7)°. Steric interactions between the NHC and $–N(SiMe_3)_2$ ligands result in the C7–Co–N1 angle being opened to 133.78(7)°, with a concomitant contraction of the C7–Co–Cl1 and N1-Co-Cl1 bond angles. The plane of the NHC ring is almost perpendicular to the cobalt trigonal plane (angle between planes = 86.60(6)°). Layfield has noted that the torsion angle between the NHC plane and the cobalt trigonal plane in related $(NHC)Co\{N(SiMe_3)_2\}_2$ compounds can be correlated with the overall bulk of the combined ligands, with bulkier ligands favoring smaller torsion angles.[14] The presence of a nearly perpendicular torsion angle in **1** is consistent with this observation, as a chloride provides less steric strain as compared to a second $–N(SiMe_3)_2$ ligand. The amide group is nearly planar at nitrogen, the slight deviation from

planarity again being attributable to steric crowding with the NHC ligand. The Si1–N1–Si2 plane is nearly perpendicular to the cobalt trigonal plane (angle between planes = 88.44(4)°).

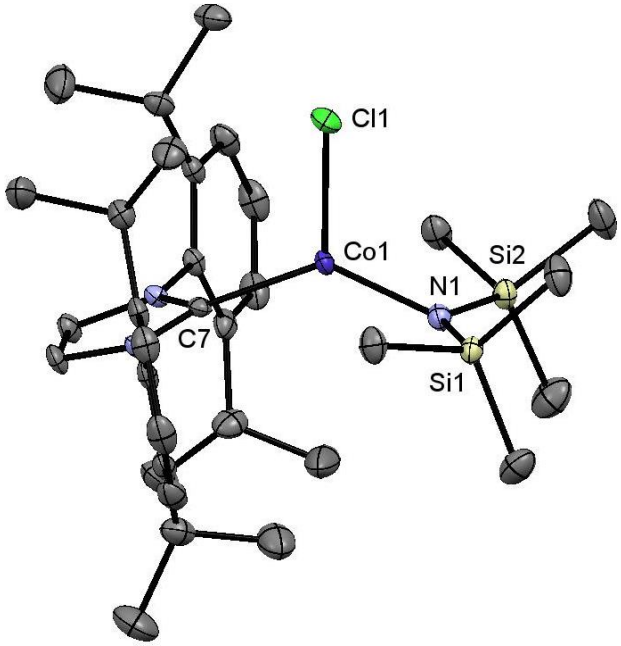

Figure 4.1. Molecular structure of IPrCoCl{N(SiMe$_3$)$_2$} (**1**). Hydrogen atoms are omitted. Selected metrical parameters (Å, deg): Co1–N1 1.9046(16), Co1–C7 2.055(2), Co1–Cl1 2.2324(6), N1–Co1–C7 133.78(7), N1–Co1–Cl1 112.94(5), C7–Co1–Cl1 113.27(5).

Compound **1** exhibits a solution magnetic moment of 5.0(1) *B.M.* as measured by the Evans method. This value is larger than the predicted spin-only moment for high-spin Co(II) in a trigonal planar environment (S = 3/2, 3.87 *B.M.*), but is comparable to values for similar compounds. For example, IMesCoCl{N(SiMe$_3$)$_2$},[9] SIMesCoCl{N(SiMe$_3$)$_2$},[9] IPrCo{N(SiMe$_3$)$_2$}$_2$,[13] and (nacnac)CoN(SiMe$_3$)$_2$[15] exhibit solution magnetic moments of 4.8, 4.9, 4.7, and 4.9 *B.M.* respectively. Other trigonal planar three-coordinate Co(II) complexes also exhibit μ_{eff} values in this range.[13,14] The higher-than-spin-only magnetic moments in these compounds have been attributed to large zero-field splitting and g-tensor anisotropy.[13,14] In accord with the paramagnetic nature of **1**, the ^{1}H-NMR spectrum is broad and contains

resonances in the range of δ 93 to −45, but this spectrum is assignable based on peak integrations.

4.2.2 Reaction of 1 with BHT-H to Generate IPrCoCl(BHT) (2). The reaction of **1** with 2,6-$^{t}Bu_2$-4-Me-phenol (BHT-H) in Et_2O produces IPrCoCl(BHT) (**2**), which was isolated by crystallization from Et_2O/Hexanes in 71% yield as an air-sensitive red powder (Scheme 4.3). Compound **2** can also be prepared in 65% yield as a red microcrystalline solid by the reaction of two equiv of Na[BHT] with $\{IPrCoCl_2\}_2$ in THF followed by crystallization from toluene. However, the product from this route was consistently contaminated with small amounts of impurities, one of which was identified by X-ray diffraction as the green salt $[IPrH][Co(BHT)_3]$ (See Appendix II.9).

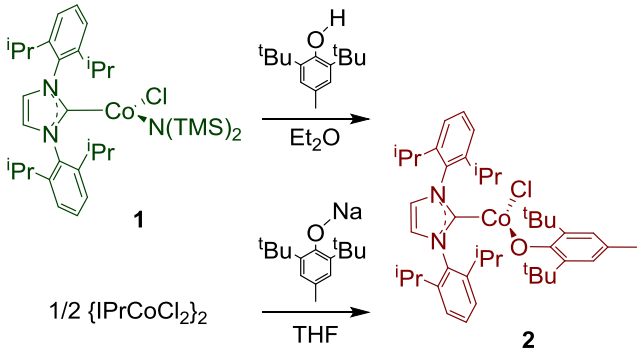

Scheme 4.3. Synthesis of compound **2**.

Slow diffusion of hexanes into a dilute Et_2O solution of **2** at −35 °C afforded X-ray quality block-shaped red crystals. The solid state structure of **2** (Figure 4.2) is similar to that of **1**. The geometry at cobalt is trigonal planar with a sum of angles at cobalt equal to 357.28(9)°. The plane of the NHC ligand is nearly perpendicular to the Cl–Co–O plane, however the cobalt center is displaced 0.23 Å out of the NHC plane toward the chloride as a result of steric crowding between ^{t}Bu groups of the phenoxide ligand and the isopropyl groups of the NHC ligand as illustrated in Fig 4.2b and 4.2c.

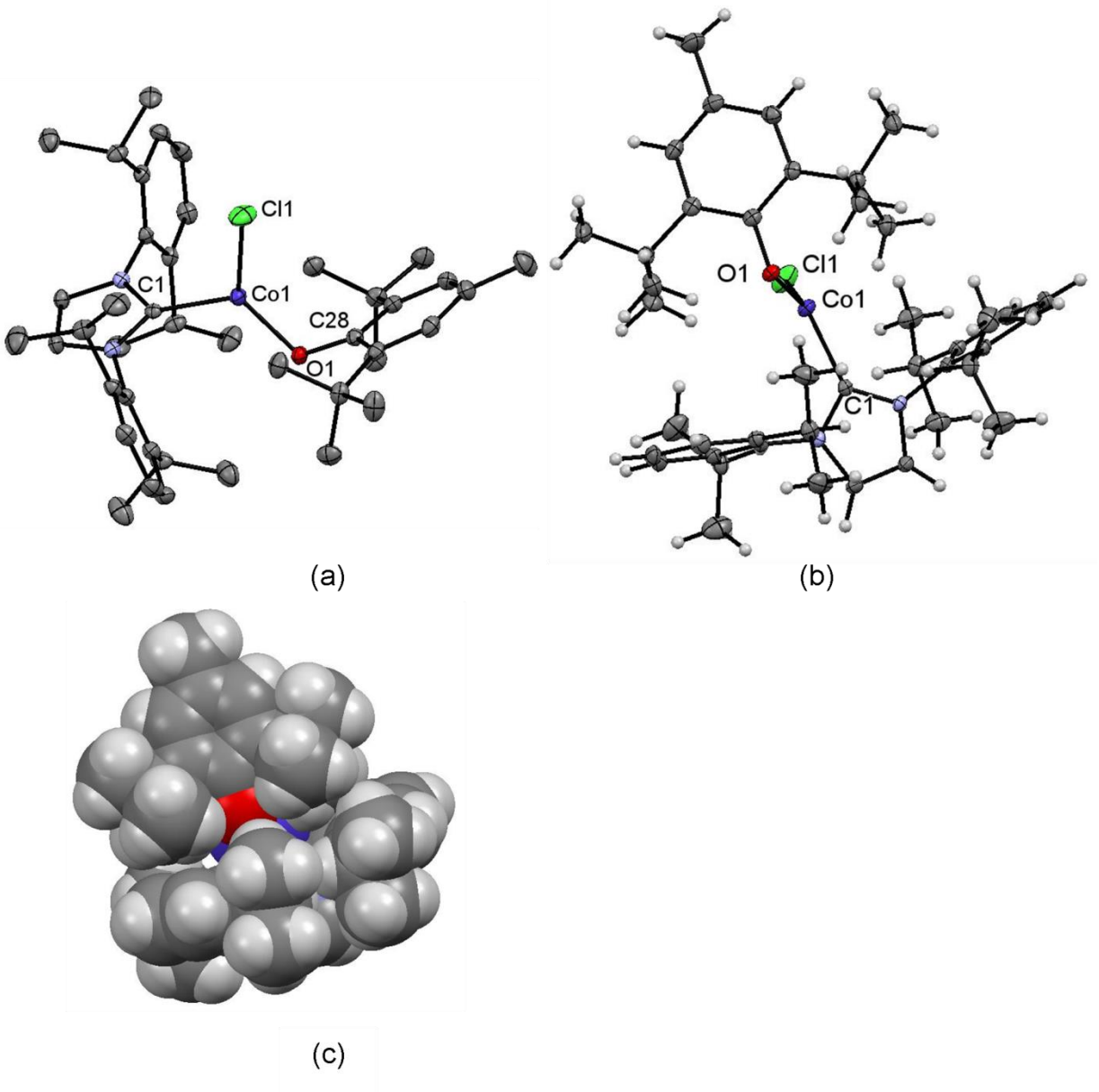

Figure 4.2. (a) Molecular structure of IPrCoCl(BHT) (**2**). Hydrogen atoms are omitted. Selected metrical parameters (Å, deg): Co1–C1 2.033(2), Co1–O1 1.8756(14), Co1–Cl1 2.2061(6), O1–Co1-C1 124.71(7), O1–Co1–Cl1 120.53(4), C1–Co1–Cl1 112.04(5). (b) Alternate view of **2** with Hydrogen atoms included. (c) Spacefilling view of **2** in same perspective as (b) illustrating the steric interactions between ^{i}Pr and ^{t}Bu groups.

Compound **2** exhibits a solution magnetic moment of 5.1(1) *B.M.* (Evans method). This value is similar that of **1** (5.1(1) *B.M*). All nine of the expected ^{1}H-NMR resonances for **2** are

observed in the range of δ 110 to −66 and can be assigned based on peak integration and comparison to the spectrum of **1**.

4.2.3. Generation of IPrCoCl(NH(DIPP)) (4) and Disproportionation to IPrCo(NH(DIPP))$_2$ (3) and {IPrCoCl$_2$}$_2$. The reaction of **1** with one equiv of 2,6-diisopropylaniline (NH_2DIPP) in C_6D_6 at room temperature over several days generates a mixture of {IPrCoCl$_2$}$_2$, IPrCo(NH(DIPP))$_2$ (**3**), and a species assigned as IPrCoCl(NH(DIPP)) (**4**) (Scheme 4.4). Compound **3** was prepared independently as described below. Interestingly, the reaction of **1** with one equiv of Li[NH(DIPP)] also generates the same mixture of {IPrCoCl$_2$}$_2$, **3**, and **4**, implying that the lithium amide reacts with **1** via net amide exchange, rather than the expected salt metathesis with the Co-Cl group (Scheme 4.4). Finally, the reaction of {IPrCoCl$_2$}$_2$ with two equiv of Li[NH(DIPP)] generates the same mixture of {IPrCoCl$_2$}$_2$, **3**, and **4** (Scheme 4.4). These results suggest that **4** is formed initially in these reactions and undergoes disproportionation to an equilibrium mixture of **4**, **3** and {IPrCoCl$_2$}$_2$. The reaction of {IPrCoCl$_2$}$_2$ with isolated **3** also generates a mixture of {IPrCoCl$_2$}$_2$, **3**, and **4**, confirming that these three species are in equilibrium in solution. The equilibrium in benzene favors {IPrCoCl$_2$}$_2$ and **3**. The addition of an additional equiv of Li[NH(DIPP)] to the equilibrium mixture of {IPrCoCl$_2$}$_2$, **3**, and **4** results in complete conversion to **3**.

The generation of the same mixture of mixture of {IPrCoCl$_2$}$_2$, **3**, and **4** via several different routes (Scheme 4.4), and the ability to convert this mixture entirely to **3** by adding Li[NH(DIPP)], support the assignment of **4** as the mixed anilide chloride complex, IPrCoCl(NH(DIPP)). An analogous compound with a less sterically encumbering NHC ligand, [SIMesCo(μ-Cl)(NH(DIPP))]$_2$ was recently reported and shown to adopt a dimeric structure with bridging chlorides in the solid state.[16]

The observed conversion of **1** to **4** and **3** via reaction with Li[NH(DIPP)] and NH_2DIPP has parallels in iron chemistry. The iron analogue of **1**, IPrFeCl{$N(SiMe_3)_2$}, also reacts with both either Li[NH(DIPP)] or NH_2DIPP to afford IPrFe(NH(DIPP))$_2$.[9] Similarly, (Cp')Fe{$N(SiMe_3)_2$} (Cp' = 1,2,4-^{t}Bu$_3$-C_5H_2) reacts with Li[NH(2,4,6-^{t}Bu$_3$-C_6H_2)] to yield an equilibrium mixture of (Cp')Fe{$N(SiMe_3)_2$} and (Cp')Fe{NH(2,4,6-^{t}Bu$_3$-C_6H_2)}. (Cp')Fe{$N(SiMe_3)_2$} also reacts with *p*-toluidine to yield [(Cp')Fe{NH(4-Me-C_6H_4)}]$_2$.[17] The pK_a of $HN(SiMe_3)_2$ is 26 in DMSO,[18] and 25.8 in THF.[19] A pK_a value for NH_2DIPP could not be located, but it may reasonably be approximated to be at least as large as that for NH_2Ph, which has a pK_a of 30.6 in DMSO.[20] The displacement $[N(SiMe_3)_2]^-$ by $[NH(DIPP)]^-$ in the cobalt and iron systems can be ascribed to the greater basicity and nucleophilicity of $[NH(DIPP)]^-$. While simple acid-base considerations predict that NH_2DIPP is not sufficiently acidic for the protonolysis of Co-$N(SiMe_3)_2$ or Fe-$N(SiMe_3)_2$ bonds, these compounds do not behave as simple salts due to the covalency in the M-$N(SiMe_3)_2$ bonds.

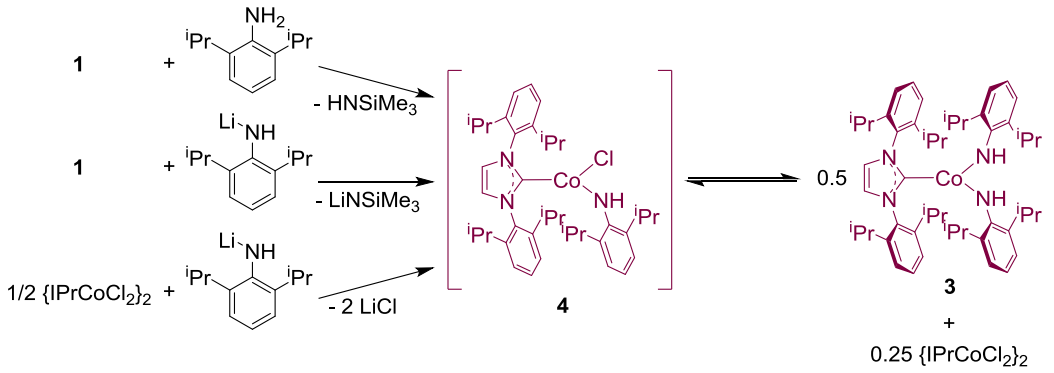

Scheme 4.4. Generation of IPrCoCl(NH(DIPP)) (**4**) and disproportionation to an equilibrium mixture of IPrCo(NH(DIPP))$_2$ (**3**) and {$IPrCoCl_2$}$_2$.

4.2.4. Synthesis and Characterization of IPrCo(NH(DIPP))$_2$ (3). Compound **3** can be prepared independently by the reaction of {$IPrCoCl_2$}$_2$ with four equiv of Li[NH(DIPP)] in THF. Removal of the solvent under vacuum and extraction into dichloromethane affords **3** as an air-

sensitive dark violet solid in 94% isolated yield (Scheme 4.5). Alternatively, reaction of **1** with two equiv of Li[NH(DIPP)] generates **3** as the only product (Scheme 4.5).

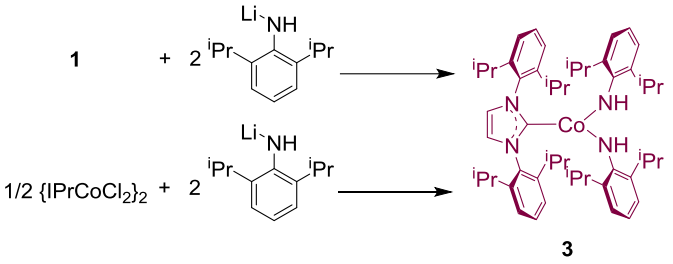

Scheme 4.5. Synthesis of (IPr)Co(NH(DIPP))$_2$ (**3**).

Single crystals of **3** were obtained from a concentrated pentane solution at −35 °C as dark violet needles. The solid state structure of **3** is shown in Figure 4.3. Like compounds **1** and **2**, **3** exhibits a trigonal-planar three-coordinate cobalt core. In contrast to **1** and **2** however, the NHC plane is nearly parallel to the N_{amide}–Co–N_{amide} plane (angle between planes 5.98(7)°). The reduction of the torsion angle from 90° with increasing steric demand is in agreement with Layfield's observations from (NHC)Co{N(SiMe$_3$)$_2$}$_2$ compounds.[14] This geometry accommodates the bulky anilides by minimizing steric interactions between the isopropyl methyl groups of the NHC and anilide ligands. The solid-state structure of **3** also exhibits short contacts between the cobalt center and two C*H*Me$_2$ methine hydrogens of the anilide ligand, rendering the cobalt center pseudo-trigonal bipyramidal (Co···H = 2.235(22) Å). The hydrogen atoms with close contacts were located in the difference map and refined isotropically. However, the FTIR spectrum of **3** did not display reduced-frequency C-H stretching bands that could be conclusively assigned to the agostic Co···H-C units. A related compound, (IMes'-NDIPP)Co(NH(DIPP)), has been prepared, and displays similar structural parameters, including a close Co···H contact.

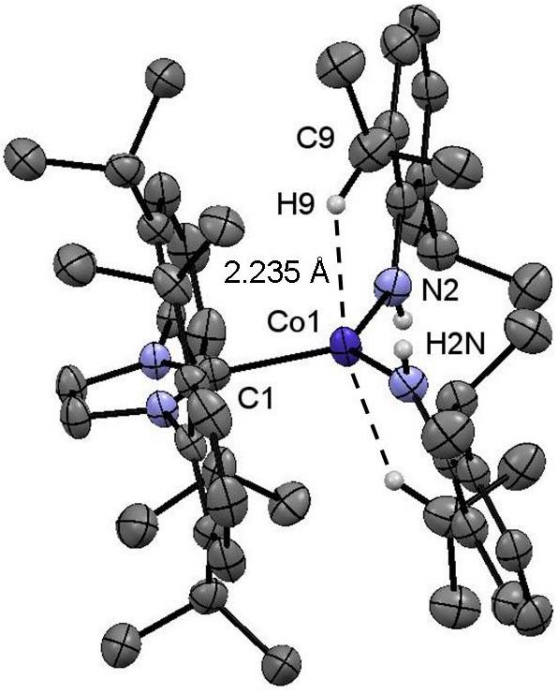

Figure 4.3. Molecular structure of IPrCo(NH(DIPP))$_2$ (**3**). Hydrogen atoms, except the N–H (H2N) and short-contact C*H*Me$_2$ (H9) hydrogens, are omitted. The structure contains half a unique molecule per asymmetric unit. The NHC ligand diisopropylphenyl group is disordered over two positions, only one of which is shown. Selected metrical parameters (Å, deg): Co1–C1 2.061(2), Co1–N2 1.8934(13), Co1···H9 2.235(22), C9–H9 1.00(2), N2–Co1–N2 126.15(8), N2–Co1–C1 116.93(4).

Compound **3** exhibits a solution magnetic moment of 4.5(1) *B.M.* as measured by the Evans method in CD_2Cl_2. The related compound, IPrCo(CH_2SiMe_3)$_2$ has the same ligand orientation around the cobalt center, but has a solution magnetic moment of 5.1 B.M.[2g] The low magnetic moment for **3** in comparison with other compounds in this chapter may result from the short Co···H contacts. Other high spin cobalt (II) species in pseudo-trigonal bipyramidal geometries have been shown to exhibit magnetic moments similar to that of **3**.[21]

Variable temperature dc magnetic susceptibility measurements were obtained on a solid sample of **3** to better probe the effect of the Co···H interactions. The μ_{eff} value determined by variable temperature SQUID magnetometry is relatively constant between 100 to 300 K,

indicating that there is no significant structural changes over this temperature range. The variable temperature magnetic susceptibility of **3** is shown in Figure 4.4 as χT vs T plot. The experimental data were simulated using JulX[22] using the spin Hamiltonian in eq 4.1:

$$H = D\left[\hat{S}_z^{\,2} - {}^{1}/_{3}\,(S(S+1)) + \tfrac{E}{D}\left(\hat{S}_x^{\,2} - \hat{S}_y^{\,2}\right)\right] + \mu_B \cdot \hat{S} \cdot g \cdot B \qquad (4.1)$$

Variables used to fit the data were the isotropic gyromagnetic ratio, g, and the axial zero field splitting parameter, D. Temperature independent paramagnetism (TIP), the rhombic zero field splitting parameter (E), intermolecular interactions (Weiss Temperature, Θ), and paramagnetic impurities were not considered in the fit. Output of fit can be found in Figure 4.14, Simulation (black line in plot) of the data at 1.0T provided g = 2.204(1), and $|D|$ = 42(1). At 300K, a χT value of 2.21 K emu mol^{-1} is observed. Using the relation in eq 4.2

$$\mu_{eff} = (7.997\chi T)^{1/2} \qquad (4.2)$$

we observe an effective magnetic moment of 4.21 *B.M.* at this temperature. Below 100K, we observe a deviation from Curie-Weiss behavior and a decrease of χT to 1.13 K emu mol^{-1} at 1.8K. At 300K, the solid state magnetic moment of **3** is noted to be somewhat lower than in solution, but still higher than a S=3/2 spin-only contribution. The small difference in the solid state and solution μ_{eff} values may reflect differences in the strength of the Co···H interactions resulting from packing forces or solvation.

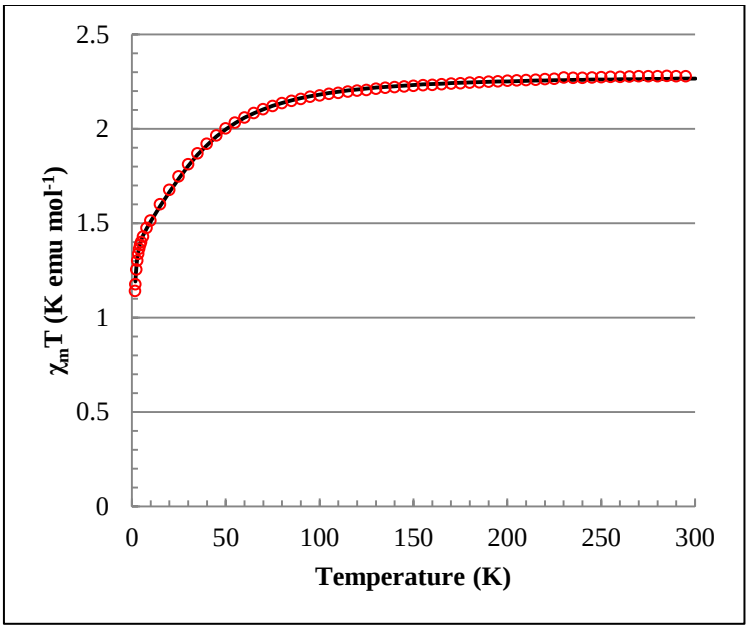

Figure 4.4. Variable temperature dc magnetic susceptibility of **3** collected under a field of 1.0 T. Red circles represent experimental data, while black line corresponds to fit, as described in the text.

Compound **3** is thermally stable up to 85 °C in solution for several days before eventually beginning to slowly plate out black solid. Compound **3** reacts readily with an excess of dry oxygen to form IPr=O, 2,6-diisopropylaniline, and bis(2,6-diisopropyl)azobenzene as established by ^{1}H-NMR and ESI-MS (See experimental section).

4.2.5. Synthesis and Structure of IPrCoCl(NHDMP) (5). To avoid the instability of **4** toward disproportionation, we utilized a more sterically encumbering anilide ligand. The reaction of two equiv of lithium 2,6-dimesitylanilide (Li[NHDMP]) with $\{IPrCoCl_2\}_2$ in diethyl ether at −35 °C and subsequent warming affords IPrCoCl(NHDMP) (**5**), which was isolated in 78% yield as a dark purple air-sensitive solid (Scheme 4.6). The reaction of **1** with one equiv of Li[NHDMP] gives the same product. Thus, as observed for the reaction of **1** with Li[NH(DIPP)], net amide exchange instead of salt metathesis is the favored pathway.

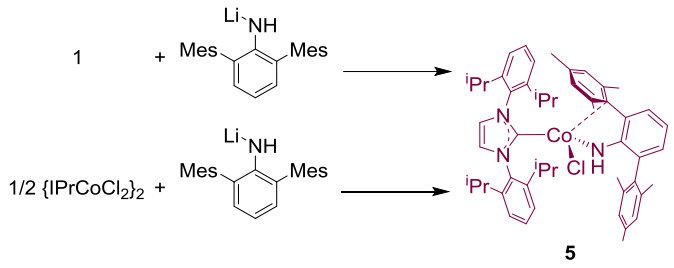

Scheme 4.6. Synthesis of (IPr)CoCl(NHDMP) (**5**).

Single crystals of **5** were obtained from a concentrated toluene solution at −35 °C as dark purple blocks. The solid state structure of **5** is shown in Figure 4.5. The cobalt center of **5** exhibits a distorted tetrahedral geometry due to a cobalt-arene interaction with a mesityl group of the anilide ligand, resulting in pyramidalization of the cobalt center. The cobalt–C_{ipso} distance (2.577(3) Å), is well within the sum of the van der Waals radii (4.17 Å),[23] but is longer than those observed in cobalt η^6-arene complexes (ca 2.15-2.20 Å).[24] Power observed a similar Co–arene interaction in the Co(II) aryl amide species {2,6-(2,6-^{i}Pr$_2$-Ph)$_2$-Ph}Co(NHDMP).[18f] The Co–C_{ispo} distance in that case (2.393 Å) is 0.184Å shorter than that in **5**, most likely due to the lower coordination number, and both distances are significantly longer than those in cobalt η^6-arene complexes. The pseudo-four-coordinate homoleptic cobalt (II) bisamide species Co(NHDMP)$_2$ and Co{NH-2,6-(2,4,6-^{i}Pr$_2$-Ph)$_2$-Ph}$_2$ also display short Co–arene contacts of 2.56 Å (avg) and 2.61 Å (avg) respectively, which are comparable to that of the pseudo-four-coordinate **5**.[25]

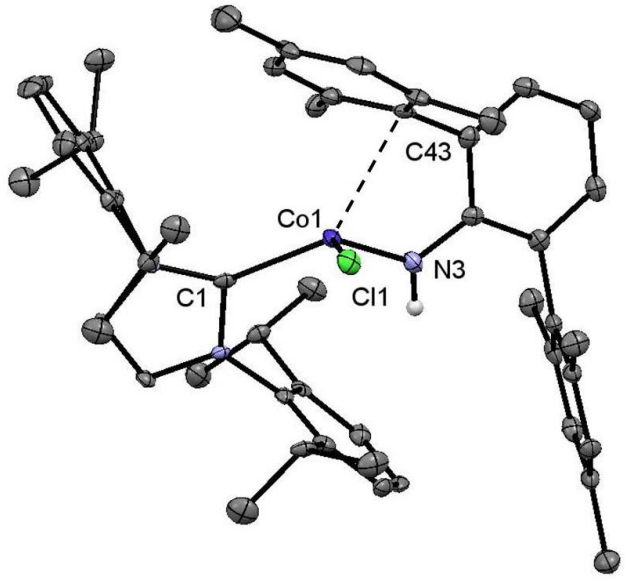

Figure 4.5. Molecular structure of IPrCoCl(NHDMP)•2(toluene) (**5**). Solvent and hydrogen atoms, except the amide N-H (H3N) hydrogen, are omitted. Selected metrical parameters (Å, deg): Co1–C1 2.070(4), Co1–N3 1.901(3), Co1–Cl1 2.2391(12), Co1–C43 2.577, N3–Co1–C1 116.85(17), N3–Co1–Cl1 118.61(11), C1–Co1–Cl1 105.82(12).

Compound **5** exhibits a solution magnetic moment of 3.7(1) *B.M.* as measured by the Evans method, which is close to the spin-only value for high-spin Co (II) in a tetrahedral environment. Thus the low magnetic moment compared to **1**, **2**, and **3** is likely a result of the pyramidalization of the cobalt center. Magnetic moments close to the spin-only value were observed in other pseudo-tetrahedral neutral NHC cobalt compounds such as (IMes'-NDipp)Co(NH(DIPP)) (3.9(1) *B.M.*,**Error! Bookmark not defined.** $(IMes)_2CoCl_2$ (3.9(1) *B.M.*),[1g] {PhB(^{t}BuIm)$_3$}CoCl (3.9(3) *B.M.*),[26] and {PhB(^{t}BuIm)$_3$}CoNH^{t}Bu (4.0(3) *B.M.*).[27]

4.3 Conclusions.

The three-coordinate (NHC)Co complex IPrCoCl{N(SiMe$_3$)$_2$} (**1**) is a useful starting material for the synthesis of other low-coordinate (NHC)Co species by protonolysis and displacement of the –N(SiMe$_3$)$_2$ group. The protonolysis reaction of **1** with 2,6-^{t}Bu$_2$-4-Me-phenol results in clean formation of a three coordinate species, IPrCoCl(BHT) (**2**). The reaction of **1** with 2,6-

diisopropylaniline or 1 equiv Li[NH(DIPP)] generates IPrCoCl(NH(DIPP)) (**4**), which is unstable toward disproportionation to an equilibrium mixture of **4**, IPrCo(NH(DIPP))$_2$ (**3**), and {IPrCoCl$_2$}$_2$. The reaction of **1** with 2 equiv Li[NH(DIPP)] yields **3** as the only product. The reaction of **1** with Li[NHDMP] yields a stabile mixed anilide chloride complex, IPrCoCl(NHDMP) (**5**), which displays short a contact between cobalt and a flanking aryl ipso-carbon of the terphenyl amide in the solid state, rendering the compound pseudo-tetrahedral. In contrast to the instability of **4**, the sterics of the bulkier anilide and possible additional stabilization afforded by arene coordination in **5** stabilize this species against disproportionation to {IPrCoCl$_2$}$_2$ and IPrCo(NHDMP)$_2$.

4.4 Experimental Section.

4.4.1 General Considerations. Unless noted otherwise, all operations were performed under a purified nitrogen atmosphere in a standard MBraun Lab Master 130 drybox or under an argon atmosphere using high-vacuum and Schlenk techniques. Hexanes, pentane, and toluene were dried by passage through activated alumina and Q-5 columns under nitrogen. Q-5 was activated by heating at 200 °C under a 5% H_2 in N_2 atmosphere. CH_2Cl_2 was dried by passage through two activated alumina columns under nitrogen. THF was distilled from a dark-purple THF solution of sodium benzophenone ketyl, and stored over 4 Å molecular sieves. Diethyl ether, benzene, and bis(trimethylsilyl)ether were stirred for 24 h over metallic sodium and filtered under nitrogen through a plug of activated alumina. CD_2Cl_2 and C_6D_6 were purchased from Cambridge Isotope Laboratory, degassed, dried over CaH_2, transferred under vacuum, and stored over 4 Å molecular sieves. Molecular sieves, alumina, silica, and Celite were dried under dynamic vacuum overnight at 180 °C. 2,6-Diisopropylaniline (NH_2DIPP) was distilled under vacuum and lithiated with n-BuLi at −35 °C in pentane. [IPrH]Cl,[28] {Co(μ-

$N(SiMe_3)_2)N(SiMe_3)_2\}_2$,[9-12] $\{IPrCoCl_2\}_2$,[1f,1g] Na[BHT],[29] and Li[NHDMP][30] were prepared by literature methods. Unless noted, all other chemicals were purchased from commercial sources and used without further purification.

All NMR spectra were recorded using a Bruker DRX-400 or DRX-500 spectrometer. ^{1}H-NMR spectra were referenced to solvent residual resonances at δ 7.16 for C_6D_6, and δ 5.32 for CD_2Cl_2 Solution magnetic susceptibilities were calculated using the Evans method using bis(trimethylsilyl)ether as an internal standard.[31] Elemental analyses were performed by Robertson Microlit Laboratories (Ledgewood, NJ). FTIR spectra were recorded using a Thermo Nicolet NEXUS 670 spectrometer. Mass spectra were recorded using an Agilent 6130 Quadrupole LC/MS with electrospray ionization.

IPrCoCl(N(SiMe$_3$)$_2$) (1). *Route A:* A suspension of $\{IPrCoCl_2\}_2$ (0.500 g, 0.482 mmol, 1 equiv) in 5 mL Et_2O was cooled to −35 °C and stirred. A solution of $NaN(SiMe_3)_2$ (173.0 mg, 0.955 mmol, 1.98 equiv) in 10 mL Et_2O was cooled to −35 °C and added dropwise to the stirred suspension of $\{IPrCoCl_2\}_2$. The mixture was allowed to warm to ambient temperature, resulting in dissolution of $\{IPrCoCl_2\}_2$ (<5 min) and a color change from blue to green. A white precipitate formed within ca. 15 min. The mixture was stirred overnight, filtered through a fine frit, and evaporated to dryness. The residue was extracted with toluene and filtered through celite. The solvent was evaporated under vacuum to yield 0.5720 g (93% yield) of **1** as a bright green solid. Crystals suitable for X-ray diffraction were obtained by cooling a saturated solution of **1** in 1:1 hexanes:toluene to −35 °C.

Route B: [IPrH]Cl (223.9 mg, 0.527 mmol, 2 equiv) was suspended in 5 mL toluene. $\{Co(\mu\text{-}N(SiMe_3)_2)N(SiMe_3)_2\}_2$ (200 mg, 0.263 mmol, 1 equiv) was dissolved in 3 mL toluene and added to the stirred suspension of [IPrH]Cl. The [IPrH]Cl rapidly dissolved, and the mixture

darkened from green to green-brown (ca. 10 min). After stirring overnight, the mixture was filtered through celite, and the solvent was removed under vacuum. Washing of the green-brown waxy solid with hexanes afforded 203.4 mg of **1** (60% yield). ^{1}H-NMR (C_6D_6): δ 93.5 (br s, 2H, C*H*=C*H*, NHC backbone), 72.4 (br s, 4H, *CH*Me_2), 18.3 (br s, 12H, CH*Me*$_2$), −2.3 (br s, 18H, $SiMe_3$), −29.0 (br s, 4H, m-Ar), −29.8 (br s, 2H, p-Ar), −43.4 (br s, 12H, CH*Me*$_2$). ^{1}H-NMR data shown in Figure 4.6. μ_{eff} = 5.0(1) *B.M.* (C_6D_6, Evans Method). Elemental analyses of multiple crystalline samples returned results consistently low in carbon. Representative elemental analysis for $C_{34}H_{54}N_3Si_2ClCo$: calcd. %C = 61.61, %H = 8.46, %N = 6.53; found: %C = 58.47, %H = 8.60, %N = 6.25.

IPrCoCl(BHT) (2). *Route A:* Separate solutions of compound **1** (359.1 mg, 0.558 mmol, 1 equiv) and BHT-H (129.1 mg, 0.586 mmol, 1.05 equiv) in 5 mL Et_2O were prepared. The solution of **1** was stirred, and the solution of BHT-H was added dropwise, resulting in a rapid color change from green to dark red. Some product begins to precipitate from the reaction mixture within ca. 30 min. The mixture was allowed to stir for 3 hr. The mixture was concentrated to 2 mL, 8 mL was hexanes added, and stored at −35 °C overnight resulting in the formation of a red solid. Filtration of the reaction mixture on a fine frit and washing of the red solid with 3x1 mL of cold hexanes yielded 307.6 mg of **2** (78.5% yield) as a red powder. Crystals suitable for X-ray diffraction were obtained by diffusion of hexanes into a dilute ether solution at −35 °C over the course of a week.

Route B: A solution of NaBHT (47.9 mg, 0.192 mmol, 2 equiv) in 3 mL THF was cooled to −35 °C. A solution of $\{IPrCoCl_2\}_2$ (100.0 mg, 0.096 mmol, 1 equiv) in 5 mL THF was cooled to −35 °C and stirred. The solution of NaBHT was added dropwise to the stirred solution of $\{IPrCoCl_2\}_2$, resulting in a color change from blue to brown and finally dark red (ca. 1 h). The

solution was allowed to warm to ambient temperature and stirred overnight. The reaction mixture was filtered through a fine frit to remove an off white solid, and the solvent was evaporated. The residue was extracted with 15 mL toluene and filtered through Celite. The filtrate was concentrated and stored in the freezer at −35 °C overnight to yield a red solid that was collected on a glass frit and washed with cold hexanes. Further concentration of the mother liquor yielded additional product. Total yield from 3 crops: 80.8 mg (65% yield). Note: This product was contaminated by small amounts of impurities, one of which was identified by single crystal X-ray diffraction as the green salt [IPrH][Co(BHT)$_3$]. See Appendix II.9. ^{1}H-NMR (C_6D_6): δ 110.6 (br s, 4H, C*H*Me$_2$), 93.4 (br s, 2H) and 88.4 (br s, 2H, C*H*=C*H* NHC backbone and phenoxide m-Ar), 61.1 (br s, 3H, phenoxide p-Me), 14.8 (br s, 12H, CH*Me*$_2$), −27.6 and −27.7 (2 overlapping broad resonances, 6H total, NHC m-Ar and p-Ar), −37.7 (br s, 12H, CH*Me*$_2$), −66.1 (br s, 18H, t-Bu). ^{1}H-NMR data shown in Figure 4.7. μ_{eff} = 5.1(1) *B.M.* (C_6D_6, Evans Method). Elemental Analysis for $C_{42}H_{59}N_2OClCo$: calcd. %C = 71.83, %H = 8.47, %N = 3.99; found: %C = 71.74, %H = 8.61, %N = 3.99.

IPrCo(NH(DIPP))$_2$ (3). A solution of {IPrCoCl$_2$}$_2$ (220.0 mg, 0.212 mmol, 1 equiv) in 6 mL THF was cooled to −35 °C and stirred. A solution of Li[NH(DIPP)] (155.5 mg, 0.848 mmol, 4 equiv) in 6 mL THF was cooled to −35 °C. The solution of Li[NH(DIPP)] was added dropwise to the stirred solution of {IPrCoCl$_2$}$_2$, and the mixture was allowed to warm to ambient temperature, resulting in a rapid color change from blue to dark violet. After stirring overnight, the solvent was removed, and the residue was extracted with 10 mL CH_2Cl_2. The CH_2Cl_2 solution was filtered through celite. Removal of the solvent under vacuum yielded 319.7 mg (94% yield) of **3** as a dark violet solid. Crystals suitable for X-ray diffraction were obtained by cooling a saturated solution of **3** in pentane.

*From **1**:* Li[NH(DIPP)] (57.0 mg, 0.311 mmol, 2 equiv) was dissolved in 3 mL THF and the solution was cooled to −35 °C. Compound **1** (100 mg, 0.155 mmol, 1 equiv) was dissolved in 5 mL THF and the solution was cooled to −35 °C. The solution of Li[NH(DIPP)] was added rapidly to the cold stirred solution of **1**. The color changed quickly from green to brown to dark violet. After stirring overnight, the reaction mixture was filtered through Celite, and the solvent was removed under vacuum. Extraction of the residue with dichloromethane and filtration through celite to remove a dark solid afforded a dark violet solution. The solution was concentrated, layered with bis(trimethylsilyl)ether, and cooled to −35 °C to afford 124.0 mg (46% yield) of **3** as a dark violet solid. ^{1}H-NMR (CD_2Cl_2): δ 57.2 (br s, 4H), 54.2 (br s, 2H), 27.5 (br s, 4H, C*H*Me$_2$), 6.5 (2 overlapping broad resonances 18H total, 12H CH*Me*$_2$ + 6H) 1.2 (br s, 6H), −5.8 and −6.2 (2 overlapping broad resonances, 6H total, m-Ar and p-Ar), −11.7 (br s, 12H, CH*Me*$_2$), −90.1 (br s, 2H, C*H*=C*H* NHC backbone). N-H resonances not observed. ^{1}H-NMR data in CD_2Cl_2 shown in Figure 4.8. ^{1}H-NMR (C_6D_6): δ 58.1 (br s, 4H), 54.0 (br s, 2H), 28.0 (br s, 4H), 6.5 (2 overlapping broad resonances 18H total, 12H + 6H), 1.2 (br s, 6H), −5.5 and −5.7 (2 overlapping broad resonances, 6H total), −11.7 (br s, 12H), −94.9 (br s, 2H). μ_{eff} = 4.5(1) *B.M.* (CD_2Cl_2, Evans Method). FTIR (KBr pellet) 3368 cm$^-$ (N-H stretch). C-H stretches associated with Co···H close contacts were not conclusively observed. Full spectrum in Figure 4.11. Elemental Analysis for $C_{51}H_{72}N_4Co$: calcd. %C = 76.56, %H = 9.07, %N = 7.00; found: %C = 76.32, %H = 9.32, %N = 6.81.

NMR data for IPrCoCl(NH(DIPP)) (4). ^{1}H-NMR (C_6D_6): δ 86.0, 58.8, 9.2, 6.3 4.7, −13.8, −16.9, −112.1.

Reaction of 1 with NH_2DIPP. *At ambient conditions*: 2,6-Diisopropylaniline (12.9 µL, 13.8 mg, 0.0777 mmol, 1 equiv) was added via micropipette to a solution of **1** (50 mg, 0.0777 mmol,

1 equiv) in 5 mL of toluene. The reaction was stirred for 3 d at ambient conditions over which time the color gradually turned from green to brown. A 1 mL aliquot was filtered through celite and the solvent removed under vacuum. An NMR sample was prepared in C_6D_6 which showed that a mixture of $\{IPrCoCl_2\}_2$, **3**, **4**, and unreacted starting materials was present (Figure 4.9).

At 70 °C: 2,6-Diisopropylaniline (3.1 μL, 2.9 mg, 0.0163 mmol, 1.05 equiv) was added via micropipette to a solution of **1** (10 mg, 0.0155 mmol, 1 equiv) in ca. 700 μL of d^8-toluene in a J-Young NMR tube. The tube was sealed, heated in an oil bath at 70 °C, and monitored by ^{1}H-NMR. After 36 h the reaction had essentially gone to completion and the ^{1}H-NMR spectrum displayed resonances for $\{IPrCoCl_2\}_2$, **3**, and **4**, as well $HN(SiMe_3)_2$. The color rapidly changed from green to brown and then gradually to deep violet during the course of the reaction. After completion, the volatile materials were vacuum transferred to a second J-Young NMR tube, and analyzed by ^{1}H-NMR which showed that only $HN(SiMe_3)_2$ and trace NH_2DIPP were present (Figure 4.10). ^{1}H-NMR data of **3** (d^8-toluene): δ 58.3, 55.9, 28.0, 6.5 (overlaps with **4**), 1.1, -4.7, -10.3, - 95.6. ^{1}H-NMR data of **4** (d^8-toluene): δ 86.0, 60.1 and 59.9 (two overlapping peaks), 9.2, 6.5 (overlaps with **3**), -14.2 and -14.3 (two overlapping peaks), -17.3, -107.0. ^{1}H-NMR data of **$\{IPrCoCl_2\}_2$** (d^8-toluene): δ 36.6, 16.1, 4.4, -0.0, -0.6, -1.4.

Reaction of 1 with 1 eqiv Li[NH(DIPP)]. A solution of **1** (50 mg, 0.0777 mmol, 1 equiv) in 5 mL of THF was cooled to -35 °C and stirred. A solution of Li[NH(DIPP)] (14.2 mg, 0.0777 mmol, 1 equiv) in 3 mL of THF was cooled to -35 °C, and added rapidly to the cold stirring solution of **1**. The color changed quickly from green to brown to dark violet. After stirring for 3 h, the reaction mixture was filtered through celite, and the solvent was removed under vacuum. ^{1}H-NMR analysis of a sample prepared in C_6D_6 showed that a mixture of $\{IPrCoCl_2\}_2$, **3**, and **4** was present.

Reaction of 3 with $\{IPrCoCl_2\}_2$. A solution of **1** (7.7 mg, 0.0096 mmol, 2 equiv) in 1 mL of C_6D_6 was added to solid $\{IPrCoCl_2\}_2$ (5.0 mg, 0.0048 mmol, 1 equiv), and the mixture was stirred overnight. The violet solution was filtered into an NMR tube. A small amount of **4** was generated and observed in the NMR spectrum, along with **3** and $\{IPrCoCl_2\}_2$.

Reaction of 3 with Oxygen. Compound **3** (5.0 mg, 0.00625 mmol) was added to an NMR tube with a J-Young tap, and dissolved in 700 μL of C_6D_6. The tube was attached to a high vacuum line, the solution was frozen, and the head space was evacuated. The headspace was refilled with an atmosphere of dry oxygen. The J-Young tap was closed, and the solution was allowed to thaw. The color rapidly changed from dark violet to brown, with concomitant disappearance of **3** from the NMR spectrum. The sample was left at room temperature overnight, and a dark solid deposited on the walls and bottom of the NMR tube. The sample was filtered on the bench top through a glass filter into a clean NMR tube. The ^{1}H-HMR spectrum contained only diamagnetic compounds, identified as IPr=O, NH_2DIPP, and bis(2,6-diisopropylphenyl)azobenzene. The identities of these products were confirmed by comparison of the ^{1}H-NMR data to NMR data of authentic samples, and by ESI-MS analysis.

IPrCoCl(NHDMP) (5). A suspension of $\{IPrCoCl_2\}_2$ (200 mg, 0.193 mmol, 1 equiv) in 4 mL Et_2O was cooled to −35 °C and stirred. A solution of Li[NHDMP] (128.1 mg 0.386 mmol, 2 equiv) in 8 mL Et_2O was cooled to −35 °C. The solution of Li[NHDMP] was added dropwise to the stirring suspension of $\{IPrCoCl_2\}_2$ and allowed to warm to ambient temperature, resulting in a color change from blue to dark purple. The reaction was allowed to stir overnight. The reaction mixture was filtered through a fine frit to remove a white solid, and the solvent was removed under vacuum. The resulting dark purple residue was extracted with pentane (ca. 40 mL) and filtered through Celite. Removal of the solvent under vacuum yielded 240 mg (77%

yield) of **5** as a dark purple solid. Crystals suitable for X-ray diffraction were obtained by cooling a concentrated toluene solution to −35 °C.

*From **1**:* **1** (10 mg, 0.015 mmol, 1 equiv) was dissolved in ca. 800 µL of C_6D_6, and added to solid Li[NHDMP] (5.2 mg, 0.015 mmol, 1 equiv) with stirring. The color changed quickly from green to brown to dark purple. The reaction was stirred overnight. The solution was filtered through a pipette filter containing celite into an NMR tube. The NMR spectrum showed the formation of **5** along with a -$N(SiMe_3)_2$ resonance at δ 0.12. The ^{1}H-NMR spectrum cannot be assigned with confidence, but characteristic resonances are reported. ^{1}H-NMR (C_6D_6): δ 50.6 (br s), 38.7(bs s), 6.8(br s), 5.7(br s), 3.5(br s), −1.8(br s), −5.3(br s), −10.3(br s), −17.8 (br s), −82.4(br s) ^{1}H-NMR data shown in Figures 4.12 and 4.13. μ_{eff} = 3.7(1) *B.M.* (C_6D_6, Evans Method). Elemental Analysis for $C_{34}H_{54}N_3ClCo$: %C = 75.49, %H = 7.70, %N = 5.18; found: %C = 75.15, %H = 7.36, %N = 5.02.

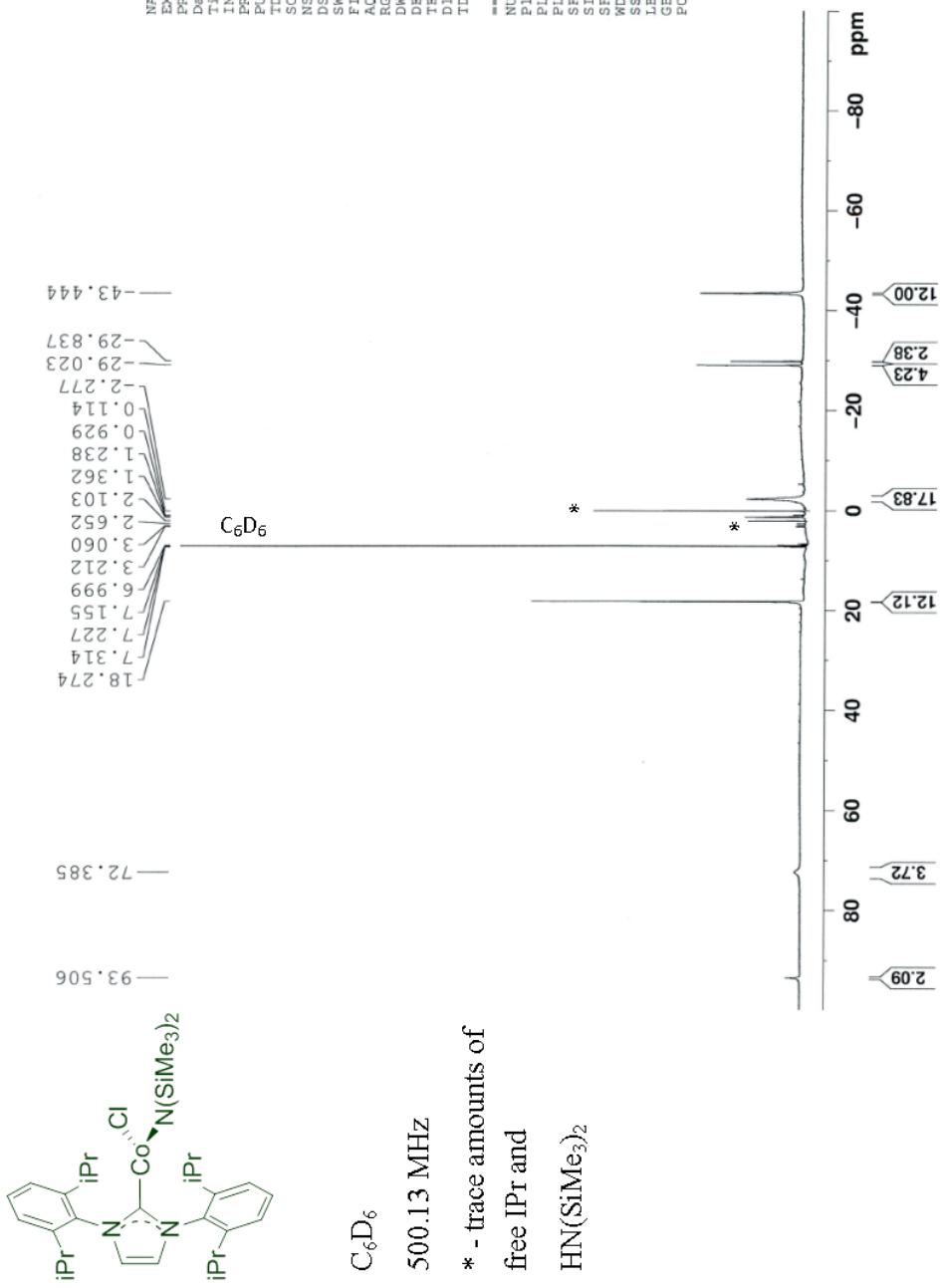

Figure 4.6. ^{1}H-NMR of IPrCoCl{N(SiMe$_3$)$_2$} (**1**).

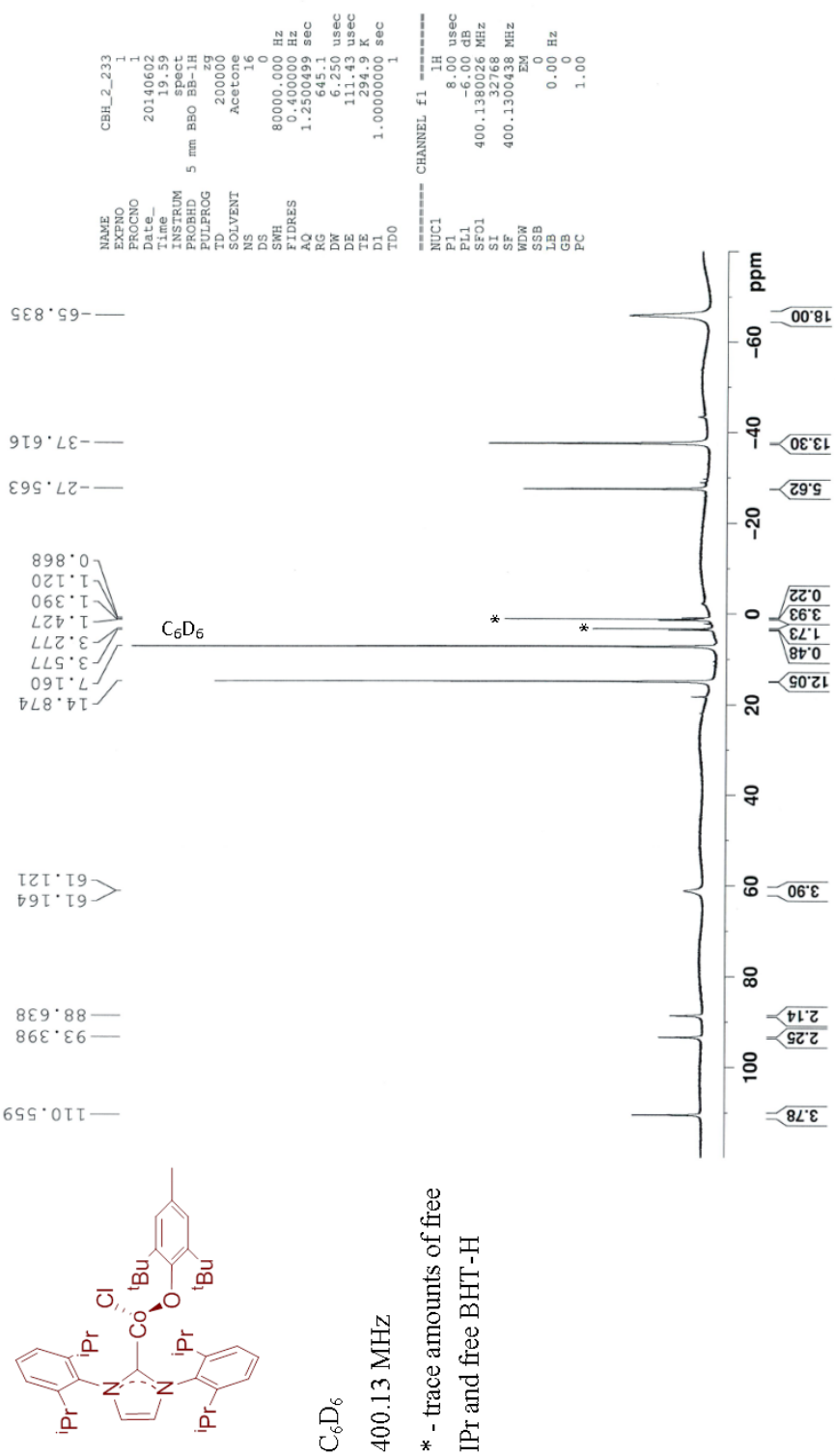

Figure 4.7. ^{1}H-NMR of IPrCoCl(BHT) (**2**).

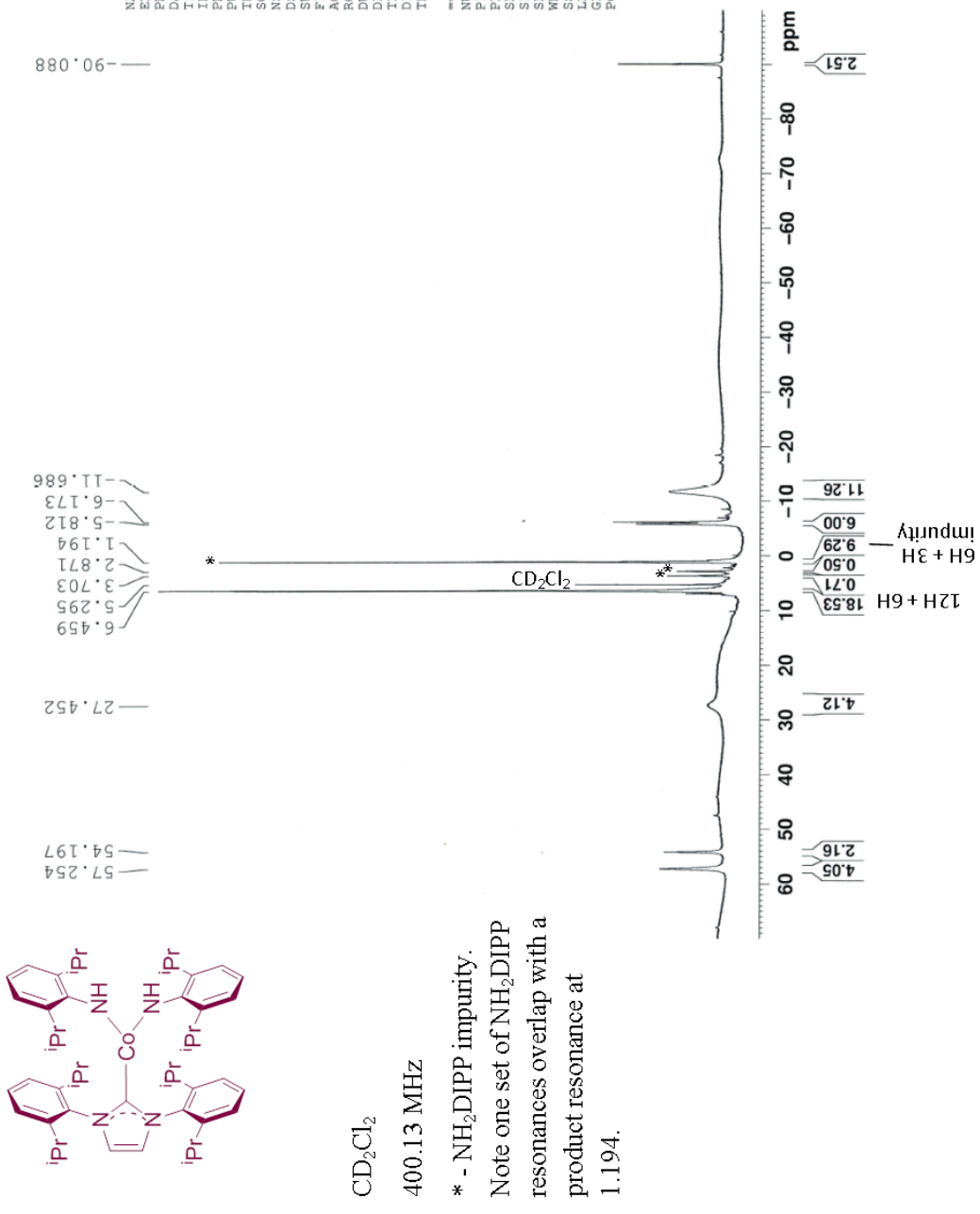

Figure 4.8. ^{1}H-NMR of IPrCo(NH(DIPP))$_2$ (**3**).

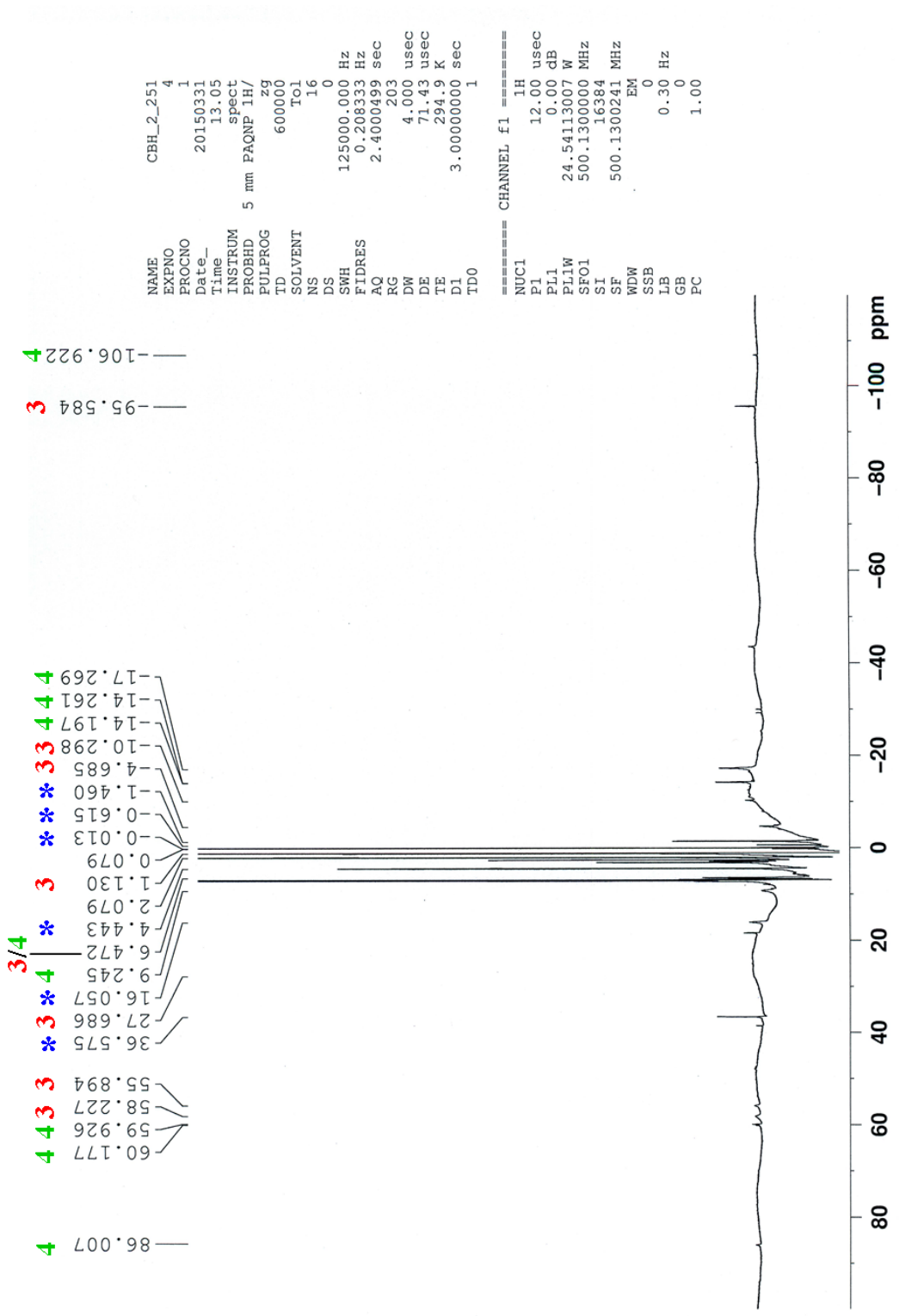

Figure 4.9. Reaction of **1** with NH_2DIPP.

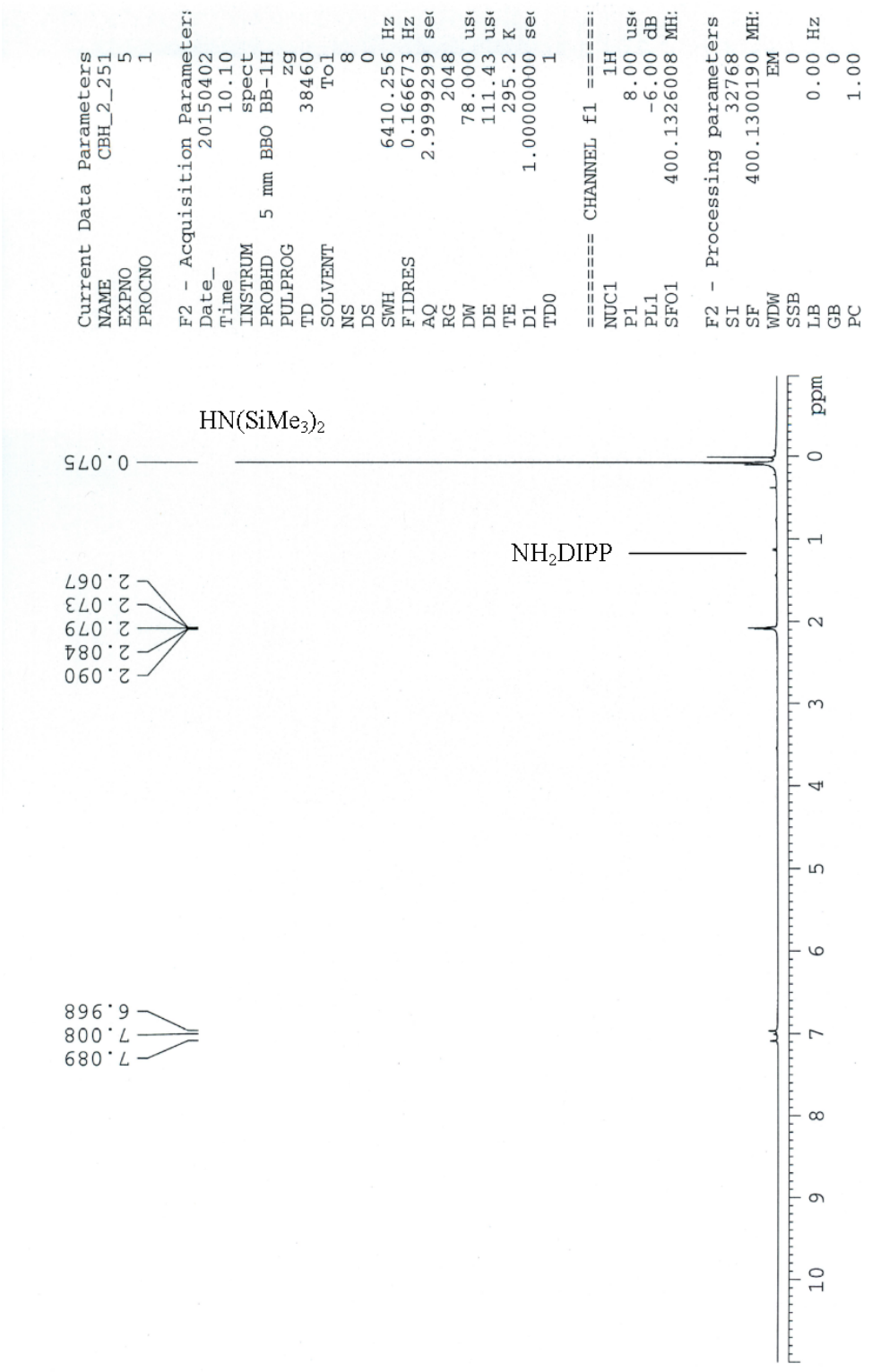

Volatiles after the reaction of **1** with NH_2DIPP.
$HN(SiMe_3)_2$ with trace of NH_2DIPP

Figure 4.10. Volatiles of reaction of **1** with NH_2DIPP.

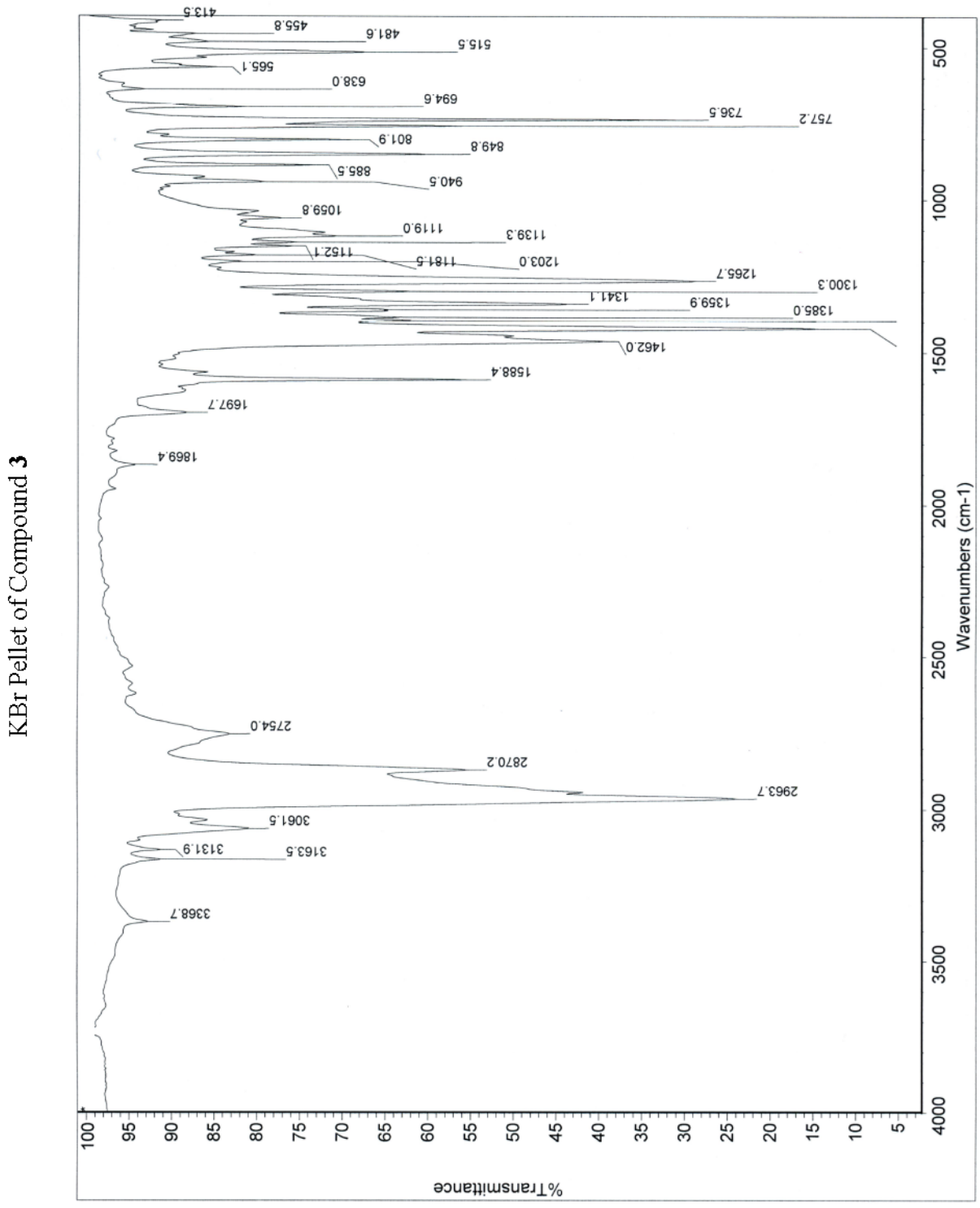

Figure 4.11. FTIR Spectrum of **3**.

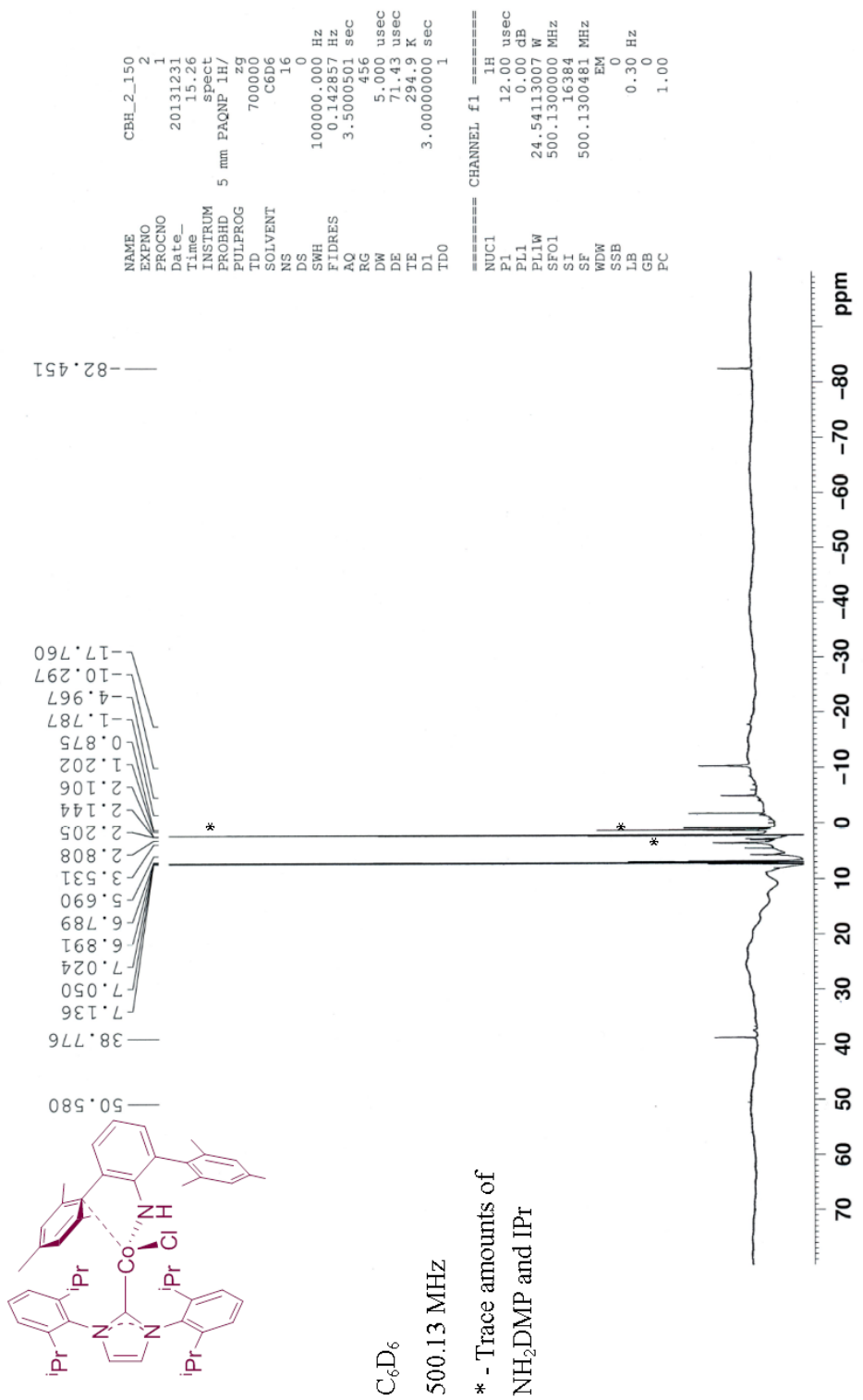

Figure 4.12. ^{1}H-NMR of IPrCoCl(NHDMP) (**5**).

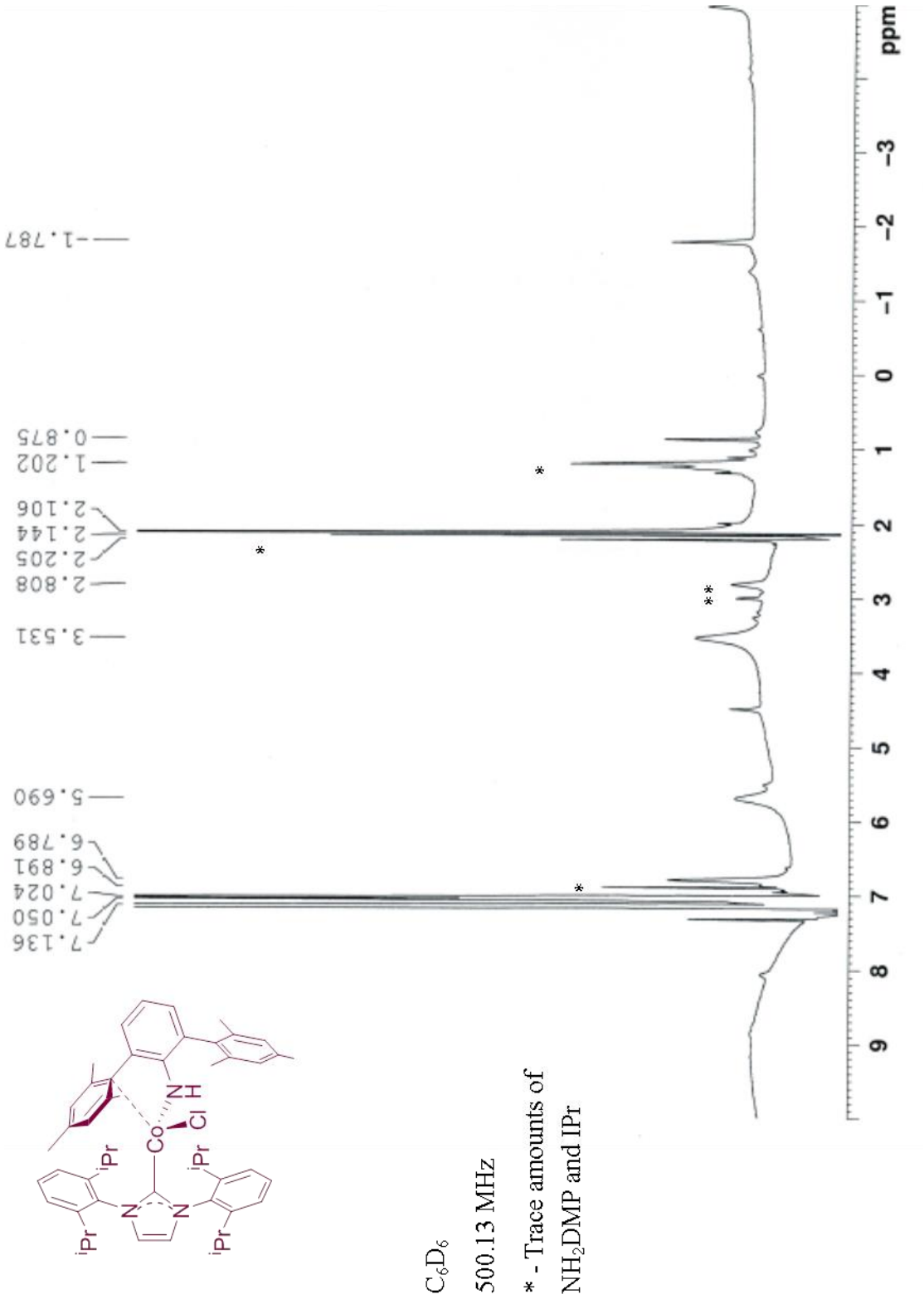

Figure 4.13. Diamagnetic region of NMR of IPrCoCl(NHDMP) (**5**).

4.4.2. Single Crystal X-ray Diffraction. Crystals were loaded onto a glass slide in the glovebox and covered with STP oil or fluorolube. Suitable crystals were selected using stereo and polarizing microscopes under oil blanketed with a stream of nitrogen, attached to the tip of a glass fiber, mounted in a stream of cold dry nitrogen at 100(2) K, and centered in the X-ray beam using a video camera. X-ray diffraction data were collected on a Bruker D8 VENTURE with PHOTON 100 CMOS detector system equipped with a microfocus Mo-target X-ray tube (λ = 0.71073 Å). All data were collected at 100(2) K using a routine of ϕ and ω scans to survey an entire sphere of reciprocal space and were indexed using the APEX2 program suits.[32] Data were corrected for absorption effects using the empirical and multi-scan methods as implemented in SADABS.[33] Space groups were determined based on systematic absences and intensity statistics. The structures were solved using Patterson or direct methods and refined by full-matrix least-squares refinement on F^2 using the Bruker SHELXTL (version 6.14) software package.[34] All non-hydrogen atoms were refined anisotropically and hydrogen atoms were placed in calculated positions, unless specified otherwise. Full tables of atomic coordinates, atomic displacement parameters, and bond metrics are given in Appendix II.5-9. Crystal structures are also available online.[35] All figures in text are drawn at 50% thermal ellipsoid probability level.

Compound 3. Crystallized with half a unique molecule per asymmetric unit. Short-contact C*H*Me2 (H9) hydrogen atoms were located in the difference map, and refined isotropically. The anilide N–H hydrogen atoms (H2N) were located in the difference map, restrained to a typical N–H bond distance (0.88 Å), and refined isotropically. The 2,6-diisopropylphenyl groups of the NHC ligand were disordered over two positions which converged to 55:45 occupancy. Full tables of atomic coordinates, atomic displacement parameters, and bond metrics are given in Appendix II.5.

Compound 5. Crystallized with two molecules of toluene per molecule of **5** in the asymmetric unit. The amide N–H hydrogen atom (H3N) was located in the difference map, restrained to a typical N–H bond distance (0.88 Å), and allowed to refine isotropically. The data was restricted to 0.95 Å due to a lack of high angle diffraction. This may be a result of crystallizing as thin plates or decomposition of the crystal during data collection. The solution included in CIF was solved in the Pbca space group (R1 = 4.99%, wR2 = 10.69%, GooF = 1.140). A suitable solution in the monoclinic space group P21/c with $\beta \approx 90°$ was able to be obtained, but resulted in poorer refinement parameters (R1 = 5.87%, wR2 = 12.93%, GooF = 1.214). Full tables of atomic coordinates, atomic displacement parameters, and bond metrics are given in Appendix II.7.

[IPrH][Co(BHT)$_3$]. Crystallized with three molecules of toluene and one half molecule of hexane per asymmetric unit. The identities of the solvent molecules could be determined, however they exhibited heavy disorder and very large thermal ellipsoids. This was treated by application of the program SQUEEZE[36] as implemented in Platon[37] using the "fab" file construct and ABIN command in XL. This construct allows the use of a solvent density distribution to be added to calculation of structure factors rather than modifying the observed intensities through the subtraction of a solvent contribution. SQUEEZE algorithm located a void, centered at (0, .002, -0.056), with a volume of 2794 Å^3 (ca. 32% of the unit cell volume) and an electron count of 581 e^-. The disordered solvent was expected to contain 700 e^- of electron density. This discrepancy may result from partial occupancy of some of the sites. Two isopropyl groups from the [IPrH] cation are disordered over two positions each. Full tables of atomic coordinates, atomic displacement parameters, and bond metrics are given in Appendix II.9.

4.4.3. Magnetic Measurements. Magnetic data were collected using a Quantum Design MPMS-XL SQUID magnetometer. Measurements for **3** were performed on a polycrystalline sample sealed in a polyethylene bag under a dinitrogen atmosphere. Dc susceptibility measurements were collected in the temperature range of 1.8 to 300 K under an applied dc field of 1.0 T. Dc susceptibility data were corrected for diamagnetic contributions from the sample holder and for the core diamagnetism of the sample. The core diamagnetism was estimated to be -769×10^{-6} emu/mol using Pascal's constants.[38] The experimental data were simulated using JulX. The output and fitting is shown in Figure 4.14.

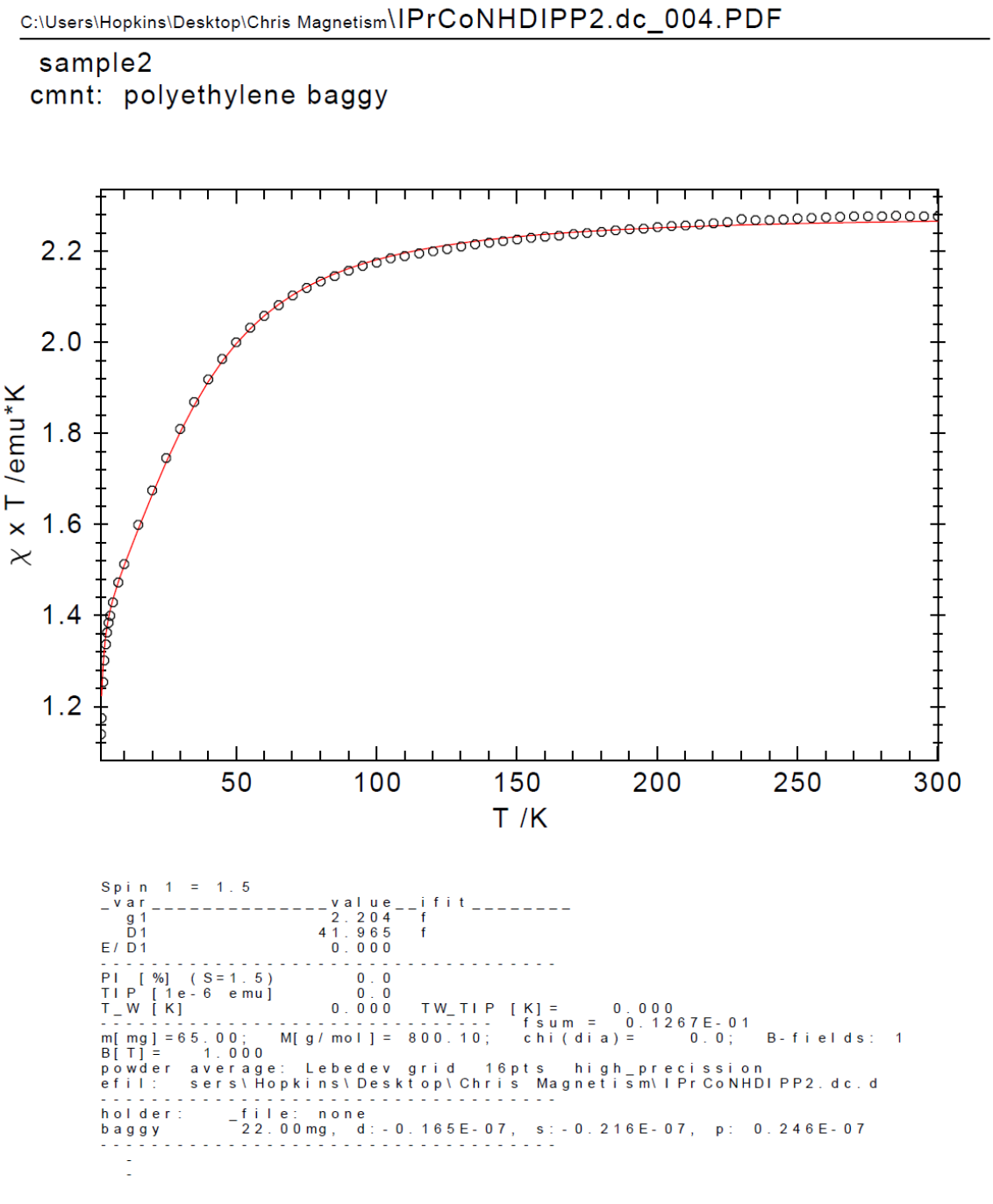

Figure 4.14. JulX Output for DC magnetic susceptibility of **3** and fit.

Note: After the submission of this manuscript, a publication reporting similar work, including the synthesis of **3** was published.[39]

4.5 References.

(1) The results described in this chapter have been published in the following: Hansen, C. B.; Jordan, R. F.; Hillhouse, G. L. *Inorg. Chem.* **2015**, *54*, 4603.

(2) (a) Hamaguchi, H.; Uemura, M.; Yasui, H.; Yorimitsu, H.; Oshima, K. *Chem. Lett.* **2008**, *37*, 1178. (b) Xi, Z.; Liu, B.; Lu, C.; Chen, W. *Dalton Trans*. **2009**, 7008. (c) Hatakeyama, T.; Hashimoto, S.; Ishizuka, K,; Nakamura, M. *J. Am. Chem. Soc.* **2009**, *131*, 11949. (d) Mo, Z.; Li, Y.; Lee, H. K.; Deng, L. *Organometallics* **2011**, *30*, 4687. (e) Song, W.; Ackermann, L. *Angew. Chem. Int. Ed.* **2012**, *51*, 8251. (f) Matsubara, K.; Sueyasu, T.; Esaki, M.; Kumamoto, A.; Nagao, S.; Yamamoto, H.; Koga, Y.; Kawata, S.; Matsumoto, T. *Eur. J. Inorg. Chem.* **2012**, 3079. (g) Przyojski, J. A; Arman, H. D.; Tonzetich, Z. J. *Organometallics* **2013**, *32*, 723. (h) Gao, K.; Yoshikai, N. *J. Am. Chem. Soc.* **2013**, *135*, 9279.

(3) (a) Saino, N.; Kogure, D.; Okamoto, S. *Org. Lett*. **2005**, *7*, 3065. (b) Geny, A.; Gaudrel, S.; Slowinski, F.; Amatore, M.; Chouraqui, G.; Malacria, M.; Aubert, C.; Gandon, V. *Adv. Synth. Catal.* **2009**, *351*, 271.

(4) (a) Gao, K. Yoshikai, N. *J. Am. Chem. Soc.* **2011**, *133*, 400. (b) Ding, Z.; Yoshikai, N. *Angew. Chem. Int. Ed.* **2013**, *52*, 8574. (c) Yamakawa, T.; Yoshikai, N. *Chem. Asian J.* **2014**, *9*, 1242.

(5) (a) Cesar, V.; Gade, L. H.; Bellemin-Laponnaz, S. Chapter 8 NHC–Cobalt, Rhodium and Iridium Complexes in Catalysis in *N-Heterocyclic Carbenes : From Laboratory Curiosities to Efficient Synthetic Tools*; Díez-González, S., Ed.; Royal Society of Chemistry: Cambridge, **2011**; 228. (b) Gibson, S. E.; Johnstone, C.; Loch, J. A.; Steed, J. W.; Stevenazzi, A. *Organometallics* **2003**, *22*, 5374. (c) Someya, H.; Ohmiya, H.; Yorimitsu, H.; Oshima, K. *Org. Lett.* **2007**, *99*, 1565. (d) Someya, H.; Ohmiya, H.; Yorimitsu, H.; Oshima, K. *Tetrahedron* **2007**, *63*, 8609. (e) Kobayashi, T.; Ohmiya, H.; Yorimitsu, H.; Oshima, K. *J. Am. Chem. Soc.* **2008**, *130*, 11276. (f) Park, S. R.; Findlay, N. J.; Garnier, J.; Zhou, S.; Spicer, M. D.; Murphy, J. A. *Tetrahedron* **2009**, *65*, 10756. (g) Gu, S.; Xu, D.; Chen, W. *Dalton Trans.* **2011**, *40*, 1576. (h) Yu, R. P., Darmon, J. M.; Milsmann, C.; Margulieux, G. W.; Sieber, S. C. E.; DeBeer, S.; Chirik, P. J. *J. Am. Chem. Soc.* **2013**, *135*, 13168.

(6) Gao, K.; Yoshikai, N. *Acc. Chem. Res.* **2014**, *47*, 1208.

(7) Mo, Z.; Chen, D.; Leng, X.; Deng, L.*Organometallics* **2012**, *31*, 7040.

(8) Danopoulos, A. A.; Wright, J. A.; Motherwell, W. B.; Ellwood, S. *Organometallics* **2004**, 23, 4807.

(9) Danopoulos, A. A.; Braunstein, P.; Stylianides, N.; Wesolek, M. *Organometallics* **2011**, *30*, 6514.

(10) Bürger, H.; Wannagat, U. *Monatsh. Chem*. **1963**, *94*, 1007.

(11) Andersen, R. A.; Faegri, K.; Green, J. C.; Haaland, A.; Lappert, M. F.; Leung, W. P.; Rypdal, K. *Inorg. Chem.***1988**, *27*, 1782.

(12) Murray, D.; Power, P. P. *Inorg. Chem.* **1984**, *23*, 4584.

(13) Bryan, A. M.; Long, G. J.; Grandjean, F.; Power, P. P. *Inorg. Chem.* **2013**, 52, 12152.

(14) Day, B. M.; Pal, K.; Pugh, T.; Tuck, J.; Layfield, R. A. *Inorg. Chem.*, **2014**, *53*, 10578.

(15) Panda, A.; Stender, M.; Wright, R. J.; Olmstead, M. M.; Klavins, P.; Power, P. P. *Inorg. Chem.* **2002**, *41*, 3909.

(16) Danopoulos, A. A.; Braunstein, P. *Dalton Trans.* **2013**, *42*, 7276.

(17) Walter, M. D.; White, P. S. *Inorg. Chem.* **2012**, *51*, 11860.

(18) Grimm, D. T.; Bartness, J. E. *J. Am. Chem. Soc.* **1992**, *114*, 1127.

(19) Fraser, R. R.; Mansour, T. S., Savard, S. *J. Org. Chem.* **1985**, *50*, 3232.

(20) Bordwell, F. G. *Acc. Chem. Res.* **1988**, *21*, 456.

(21) For representative examples see:
(a) Yeung, C-T.; Sham, K-C.; Lee, W-S.; Wong, W-T.; Wong, W-Y.; Kwong, H-L. *Inorg. Chim. Acta.* **2009**, *362*, 3267. (b) Champouret, Y. D. M.; Maréchal, J-D.; Chaggar, R. K.; Fawcett, J.; Singh, K.; Maseras, F.; Solan, G. A. *New J. Chem.* **2007,** *31*, 75. (c) Judge, J. S.; Feiff, W. M.; Intille, G. M.; Ballway, P.; Baker, W. A. *J. Inorg. Nucl. Chem.* **1967**, *29*, 1711. (d) Sacconi, L.; Bertini, I. *J. Am. Chem. Soc.* **1968**, *90*, 5443. (e) Tenza, K.; Hanton, M. J.; Slawin, A. M. Z. *Organometallics* **2009**, *28*, 4852. (f) Müller, G.; Klinga, M.; Leskelä, M.; Rieger, B. *Z. Anorg. Allg. Chem.* **2002**, *628*, 2839.

(22) Bill, E. JulX 1.4.1, A Program for the Simulation and Analysis of Magnetic Susceptibility Data; Max Plank Institute for Bioinorganic Chemistry: Mülheim an der Ruhr, 2008.

(23) Alvarez, S. *Dalton Trans*. **2013**, *42*, 8617.

(24) For select examples see:
Radonovich, L. J.; Klabunde, K. J.; Behrens, C. B.; McCollor, D. P.; Anderson, B. B. *Inorg. Chem*, **1980**, *19*, 1221. Dai, X.; Kapoor, P.; Warren, T. J. *J. Am. Chem. Soc.* **2004**, *126*, 4798. (c) Duga, T. R.; Sun, X.; Rybak-Akimova, E. V.; Olatunji-Oho, O.; Cundari, T. R.; Holland, P. L. *J. Am. Chem. Soc.* **2011**, *133*, 12418. (d) Lei, H.; Ellis, B. D.; Ni, C.; Granjean, F.; Long, G. J.; Power, P. P. *Inorg. Chem.* **2008**, *47*, 10205. (e) Nguyen, T.; Merrill, W. A.; Ni, C.; Lei, H.; Fettinger, J. C.; Ellis, B. D. Long, G. L.; Brynda, M.; Power, P. P. *Angew. Chem., Int. Ed.* **2008**, *47*, 9115. (f) Ni, C.; Fettinger, J. C.; Long, G. L.; Power, P. P. *Inorg. Chem.* **2009**, *48*, 2443. (g) Jones, C.; Schulten, C.; Rose, R. P.; Stasch, A.; Aldridge, S.; Woodul, W. D.; Murray, K. S.; Moubaraki, B.; Brynda, M.; La Macchia, G.; Gagliardi, L. *Angew. Chem., Int. Ed*. **2009**, *48*, 2406.

(25) Bryan, A. M.; Merrill, W. A.; Reiff, W. M.; Fettinger, J. C.; Power, P. P. *Inorg. Chem.* **2012**, *51*, 3366.

(26) Cowley, R. E.; Bontchev, R. P.; Duesler, E. N.; Smith, J. M. *Inorg. Chem.* **2006**, *24*, 9771.

(27) Cowley, R. E.; Bontchev, R. P.; Sorrell, J.; Sarracino, O.; Feng, Y.; Wang, H.; Smith, J. M. *J. Am. Chem. Soc.* **2007**, *129*, 2424.

(28) Jafarpour, L.; Stevens, E. D.; Nolan, S. P. *J. Organomet. Chem.* **2000,** *606*, 49.

(29) Healy, M. D.; Barron, A. R. *J. Organomet. Chem.* **1990**, *381*, 165.

(30) Gavenonis, J.; Tilley, T. D. *Organometallics* **2002**, *21*, 5549.

(31) Evans, D. F. *J. Chem. Soc.* **1959**, 2003.

(32) Bruker AXS, *APEX2*, version 2014.9-0, 2014, Madison, Wisconsin, USA.

(33) Bruker AXS, *SADABS*, version 2014/4, 2014, Madison, Wisconsin, USA.

(34) Sheldrick, G. M. *Acta Cryst.* **2008**, *A64*, 112.

(35) Hansen, C. B.; Jordan, R. F.; Hillhouse, G. L. *Inorg. Chem.* **2015**, *54*, 4603. http://pubs.acs.org/doi/suppl/10.1021/ic502670x

(36) van der Sluis, P.; Spek, A. L. *Acta Cryst.* **1990**, *A46*, 194.

(37) Spek, A. L. *Acta Cryst***. 2009**, *D65*, 148.

(38) Bain, G. A.; Berry, J. F. *J. Chem. Ed.* **2008**, *84*, 532.

(39) Massard, A.; Braunstein, P.; Danopolous, A. A.; Choua, S.; Rabu, P. *Organometallics*, **2015**, *34*, 2429.

CHAPTER 5

Crystal Structure of a New Inverse Crown Ether, μ^4-oxo-tetrakis(μ^2-bis(trimethylsilyl)amide)dicobalt(II)disodium(I), $[Co_2Na_2(\mu^2\text{-}N(SiMe_3)_2)_4](\mu^4\text{-}O)$[1]

5.1 Introduction.

The title compound, $[Co_2Na_2(\mu^2\text{-}N(SiMe_3)_2)_4](\mu^4\text{-}O)$ (**1**), represents a new entry into the class of inverse crown ethers (Scheme 5.1). Each cobalt center is formally in the +2 oxidation state. The structure contains one half of a unique molecule per asymmetric unit with the central μ^4-oxo ligand residing on an inversion center. In the crystal, bulky $SiMe_3$ substituents prevent additional interactions with cobalt; however, weak intermolecular $Na\cdots H_3C\text{-}Si$ interactions form an infinite chain along the crystallographic *b* axis.

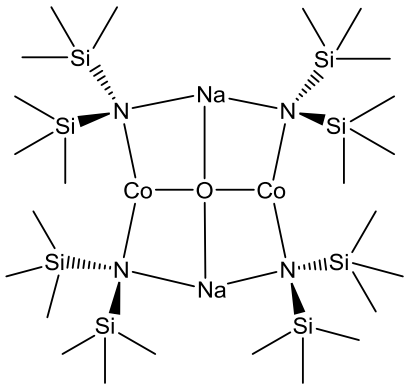

Scheme 5.1. Diagram of $Co_2Na_2(\mu^2\text{-}N(SiMe_3)_2)_4](\mu^4\text{-}O)$, (**1**).

Compounds that feature oxo-bridged cobalt clusters have been of great interest in recent years as active homogeneous[2] and heterogeneous[3] oxygen evolution catalysts. Bridging cobalt-oxo species also find applications in magnetic materials[4] and in hydrocarbon oxidation.[5] In the course of studies of low-coordinate cobalt compounds,[6] we isolated and structurally characterized a cobalt-containing tetrametallic cluster featuring a central μ^4-bridging oxo ligand, $[Co_2Na_2(\mu^2\text{-}N(SiMe_3)_2)_4](\mu^4\text{-}O)$ (**1**) as shown in Scheme 5.1. Compound **1** fits into the larger

class of "inverse crown ethers" illustrated in Scheme 5.2.[7] Compound (**1**) is the first cobalt based inverse crown ether. The majority of examples contain magnesium[8-11] or zinc[12] as M′, though there are manganese,[13,14] aluminum,[15] and ytterbium[16] complexes published as well.

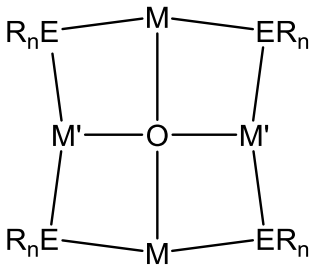

M = Li, Na, K
M' = Mg, Al, Zn, Yb, Mn
ER$_n$ = N(SiMe$_3$)$_2$, tmp, phenoxides
(tmp = 2,2,6,6-tetramethylpiperidine)

Scheme 5.2. General structure of "inverse crown ether" bonding motif.

5.2 Results and Discussion.

5.2.1 Structural Commentary. Crystals of (**1**) suitable for X-ray diffraction were obtained as reaction by-products via crystallization from toluene at −35 °C. Attempts at a rational synthesis of **1** were not successful. The molecular structure of compound (**1**) is shown in Figure 5.1. Relevant bond metrics are presented in Table 5.1. The asymmetric unit contains half of a unique molecule comprised of an oxygen atom located on an inversion center, one cobalt atom, one sodium atom, and two $[N(SiMe_3)_2]^-$ ligands with the remainder of the molecule being completed by inversion symmetry. All opposing M-O-M bonds are crystallographically imposed to 180°. The four bridging nitrogen atoms lie slightly out of plane from the four metal atoms, exhibiting a dihedral angle of 8.1 (2)° between their respective planes as shown in Figure 5.1b.

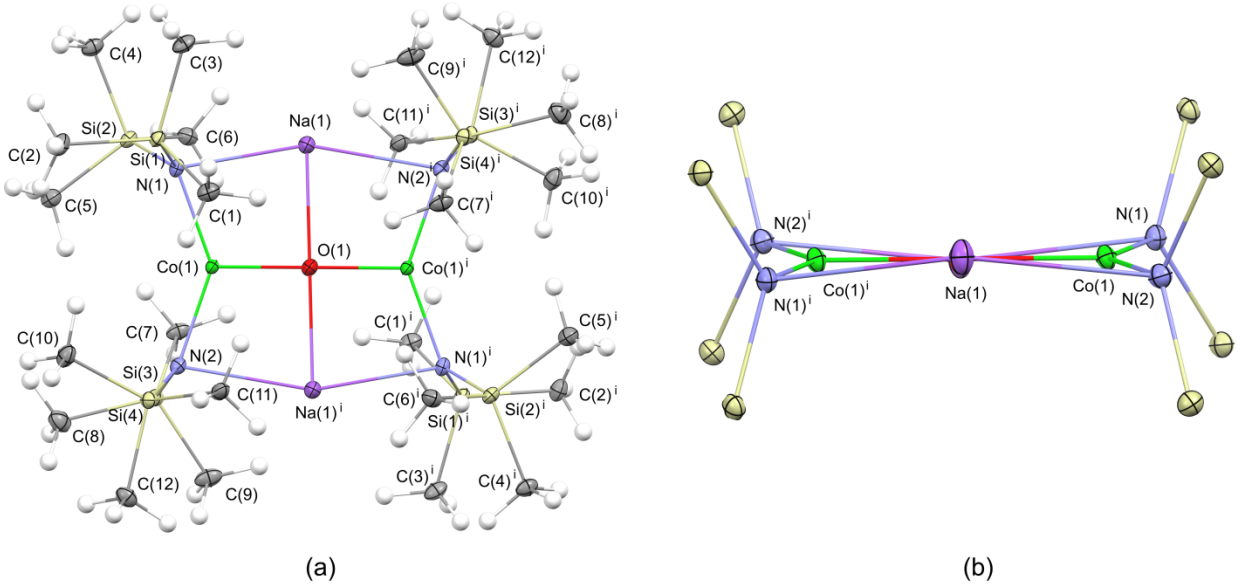

Figure 5.1. a) Molecular structure of **1** showing displacement ellipsoids at the 50% probability level. b) An alternate view of **1** down the Na-O-Na axis displaying ring offset. Hydrogen and carbon atoms truncated for clarity. [Symmetry code: (i) −x+1, −y+1, −z+1]

Table 5.1. Selected geometric parameters of compound **1**.

Bonds (Å)			
Co(1)−O(1)	1.8245(10)	Na(1)−O(1)	2.293(3)
Co(1)−N(1)	1.952(6)	Na(1)−N(1)	2.498(6)
Co(1)−N(2)	1.953(5)	Na(1)−N(2)	2.551(6)
Angles (°)			
Co(1)−O(1)−Co(1)	180	Na(1)−O(1)−Na(1)	180
N(1)−Co(1)−N(2)	141.5(2)	N(1)−Na(1)−N(2)	155.61(19)

The majority of cobalt bridging oxo compounds possess bent angles, so the oxygen atom in (**1**) is unusual in that it is linear. With a central oxo, by charge balance each cobalt center is formally Co(II). While the paramagnetic nature of (**1**) prevents NMR confirmation, it is unlikely that the central O-atom is actually a hydroxo ligand. The structurally related anionic compound $[Na_4(\mu^2\text{-}N(SiMe_3)_2)_4(\mu^4\text{-}OH)]^-$, which bears a central μ^4-OH, is noticeably pyramidalized, possessing Na−O−Na angles of 140.1(2)° and 142.4(2)°.[17] Additionally, the Co(1)−O(1) bond length of 1.8245(10) Å is significantly shorter than other structurally characterized complexes of

Co(II) bearing approximately linear bridging hydroxo ligands, which display bond lengths ranging from 1.975 (2) to 2.3766 (6) Å.[18-20]

Compound **1** is isostructural with magnesium,[8] manganese,[13] and zinc[12] containing analogues of the general formula $[M'_2Na_2(\mu^2\text{-}N(SiMe_3)_2)_4](\mu^4\text{-}O)$, all of which contain planar linear bridging oxo ligands. Among the four compounds, **1** has comparatively short bonds (Table 5.2). For instance, compound **1** displays the shortest M′−O and M′−N bond lengths, as well as the most acute N–M′–M bond angle. The short bond distances and acute bond angles may enhance the torsion of the metal plane from the nitrogen plane in **1**.

Table 5.2. Comparison of bond lengths and angles of isostructural $[M'_2Na_2(\mu^2\text{-}N(SiMe_3)_2)_4](\mu^4\text{-}O)$ compounds.

	Co[a]	Mn[13]	Mg[8]	Zn[12]
M′−O (Å)	1.8245(10)	1.9272(2)	1.8575(4)	1.8733(9)
M′−N (Å)	1.952 (6)	2.0909(12)	2.054(1)	1.986(2)
	1.953(5)	2.0884(12)	2.049(1)	1.983(2)
N−M′−N (°)	141.5(2)	147.42(5)	144.48(11)	141.58(9)

[a]This work.

5.2.2 Supramolecular Features. In the solid state, the steric bulk of the amide ligands prevents further intermolecular interactions of either the cobalt atoms or the oxo ligand, as can be observed in the space filling model of **1** presented in Figure 5.2. Some weak interactions can be noted for sodium however, which is consistent with the open site around sodium visible in Figure 5.2b. The sodium atoms and one Si-CH_3 group from each molecule coordinate to a neighboring Si-CH_3 group and sodium atom, respectively, forming an infinite chain along the crystallographic *b* axis, as illustrated in Figure 5.3. The two close Na···H contact distances of 2.961 Å and 2.886 Å fall within the range of previously structurally characterized literature examples of various molecules containing sodium bis(trimethylsilyl)amide moieties (2.55-3.0

Å).[13,21,22] This type of intermolecular interaction has been previously noted in the solid state for related potassium based inverse crown ethers bearing bridging peroxo ligands,[9] and in related sodium containing precursors.[13]

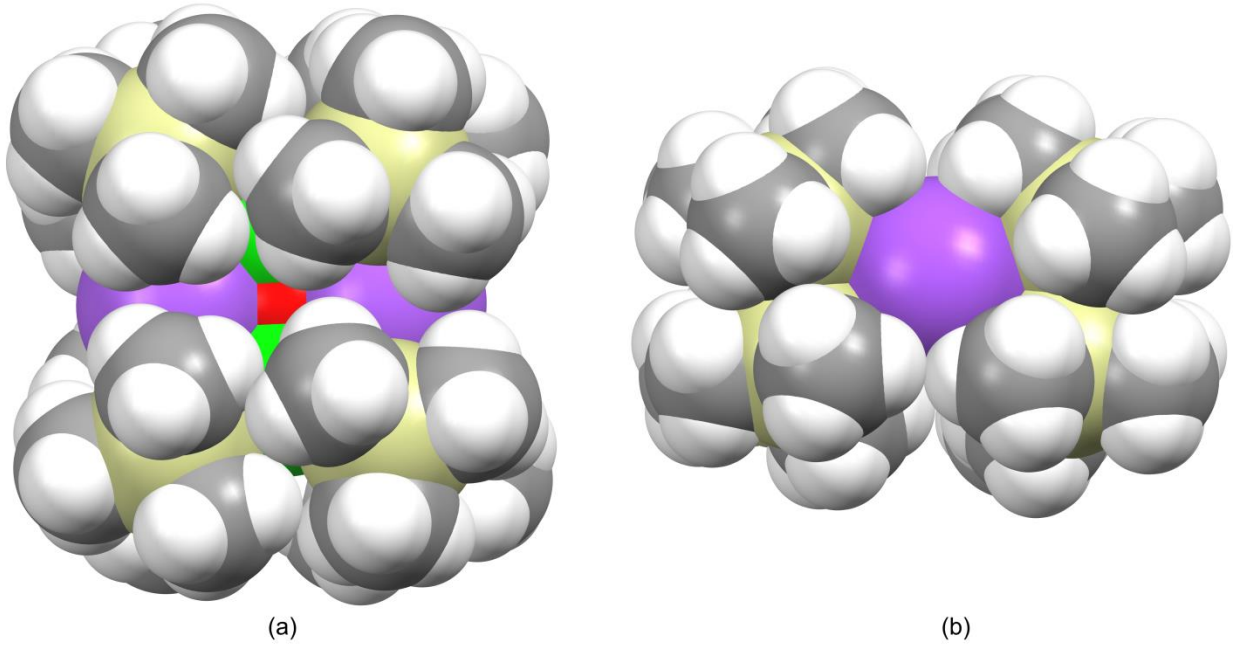

Figure 5.2. (a) Top view of a space filling model of **1**, showing the sterically shielded cobalt atoms. (b) Side on view, displaying the open pocket around sodium that allows for weak interactions. [Color scheme: cobalt (green), sodium (violet), silicon (yellow), oxygen (red), carbon (grey), hydrogen (white)].

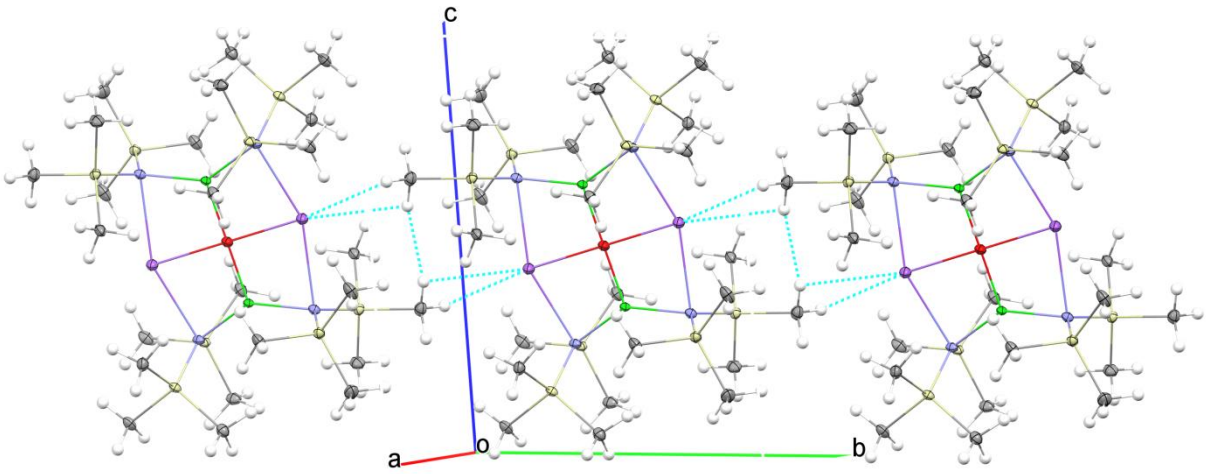

Figure 5.3. Packing diagram of **1**, showing Na···H contacts forming an infinite chain that extends along the *b* axis. [Symmetry code: −x+1, −y+1, −z+1]

5.2.3 Source of Oxygen. Compound **1** was obtained as single crystals on multiple occasions as a side product of two different reactions; however, attempts at a rational synthesis were not successful. It was observed as a byproduct of the reaction of $[(IPr)CoCl_2]_2$ with $NaN(SiMe_3)_2$ as well as during the attempted intentional preparation of $Na[Co\{N(SiMe_3)_2\}_3]$. These reactions used conditions and reagents that were nominally free of oxygen and water. Nonetheless, trace oxygen or water are the likely sources of the bridging oxo ligand. Adventitious water[16,17] and oxygen[9,11,13] have both been shown to be potential oxygen atom sources, and have been previously utilized to generate this type of structure. Additionally, fragmentation of tetrahydrofuran has also been identified as a potential oxygen atom source in one case.[14]

5.2.4 Database Survey. A search of the Cambridge Structural Database[23] reveals that structurally characterized oxo-centered inverse crown ethers are rare. The first examples were prepared from magnesium [CSD refcodes: EJEKEJ,[8] SUJQOD, SUJQUJ[10]]. Further examples focused on transition metal containing complexes [Zinc CSD refcodes: WOQTIF.[12] Manganese CSD refcodes: CIVRAB, CIVRIJ ,[13] WUVROV.[14] Aluminum CSD refcodes: BABMEY.[15] Ytterbium CSD refcodes: IMIBUC, IMICUJ.[16]].

5.3 Conclusions.

The compound $[Co_2Na_2(\mu^2\text{-}N(SiMe_3)_2)_4](\mu^4\text{-}O)$ (**1**) was isolated as a by-product of our experimental studies on low-coordinate cobalt amides and characterized via single crystal X-ray crystallography. Rational attempts to intentionally synthesize **1** were unsuccessful. Compound **1** represents a new entry into the rare class of oxo-centered inverse crown ethers, and the first containing cobalt. Compound **1** has the shortest M–O and M–N bonds of any characterized

examples from this class of compounds. Intermolecular Na···H_3C-Si interactions form an infinite chain along the crystallographic *b* axis in the solid state.

5.4 Experimental Section.

General Considerations. Unless noted otherwise, all operations were performed under a purified nitrogen atmosphere in a standard MBraun Lab Master 130 drybox or under an argon atmosphere using high-vacuum and Schlenk techniques. Toluene was dried by passage through a column of activated alumina and a column of Q-5 under nitrogen, and stored over molecular sieves.[24] Q-5 was activated by heating at 200 °C under a 5% H_2 in N_2 atmosphere. THF was distilled from a dark-purple THF solution of sodium benzophenone ketyl, and stored over 4Å molecular sieves. Molecular sieves and Celite were dried under dynamic vacuum overnight at 180 °C. $[(IPr)CoCl_2]_2$ was prepared according to a literature procedure.[25,26] Anhydrous $CoCl_2$ was initially dried in a 140 °C oven for 18 h, and then dried at 120 °C under dynamic vacuum for 24 h. All other chemicals were purchased from commercial sources and used without further purification.

Synthesis and Crystallization of 1. Method 1: In a glovebox $[(IPr)CoCl_2]_2$ [25,26] (IPr = 1,3-di(2,6-diisopropylphenyl)imidazolin-2-ylidene) (50 mg, 0.048 mmol, 1 equiv.) was dissolved in 3 mL toluene and cooled to −35 °C. A −35 °C solution of $NaN(SiMe_3)_2$ (Sigma-Aldrich, titrated to 0.844M in THF) (22.9 µL, 0.193 mmol, 4 equiv) was added dropwise to the solution of $[(IPr)CoCl_2]_2$ with stirring. The reaction mixture rapidly changed color from blue to turquoise to green and became turbid. The solution was allowed to warm to ambient temperature and stirred for 1 h. The reaction was filtered through Celite and the filtrate reduced to dryness under vacuum. The resulting green solid was dissolved in minimal toluene, passed through a

Pasteur pipette filter, and stored at −35 °C for several days. The resulting precipitate was primarily thin green plates of (IPr)CoCl($N(SiMe_3)_2$),[6] which was occasionally accompanied by a small number of dark green-blue blocks of compound **1**.

Method 2: While attempting to prepare a compound of the type Na[$Co\{N(SiMe_3)_2\}_3$], compound **1** was occasionally observed as a minor by-product during recrystallization attempts. In a typical reaction anhydrous $CoCl_2$ (100 mg, 0.77 mmol, 1 equiv) was suspended in 2 mL THF and cooled to −35 °C. $NaN(SiMe_3)_2$ (423.6 mg, 2.31 mmol, 3 equiv) was dissolved in 10 mL THF, cooled to −35 °C, then added to the stirred slurry of $CoCl_2$. The reaction mixture was allowed to warm to ambient temperature and stir overnight, over which time it slowly turned green and turbid. The reaction mixture was filtered through Celite and rinsed with additional THF until washings were colorless, leaving a white solid remaining on the Celite pad. The combined THF fractions were combined and concentrated under vacuum to a yield waxy green solid. The resulting solid was recrystallized from a solution in minimal toluene cooled to −35 °C. Compound **1** was occasionally observed as blue-green blocks.

Single Crystal X-ray Diffraction. Crystals were loaded onto a glass slide in the glovebox and covered with STP oil. Suitable crystals were selected using stereo and polarizing microscopes under oil blanketed with a stream of nitrogen, attached to the tip of a glass fiber, mounted in a stream of cold dry nitrogen at 100(2) K, and centered in the X-ray beam using a video camera. X-ray diffraction data were collected on a Bruker Smart Apex I system with Siemens Platform goniometer with a Charged Coupled Device (CCD) detector. Data were collected at 100(2) K using a routine of ϕ scans to survey an entire hemisphere of reciprocal space and were indexed using the APEX3 program suite.[27] Data were corrected for absorption effects using the multi-scan methods as implemented in TWINABS.[28] Space groups were

determined based on systematic absences and intensity statistics. The structures were solved using direct methods and refined by full-matrix least squares refinement on F^2 using the OLEX2 software package.[29] Crystal data, data collection, and structure refinement details are summarized in Table 5.3. All H atoms are placed at idealized positions for structure factor calculations. [C-H = 0.98 Å, U_{iso}(H) set to 1.5U_{eq}(C)]. The initial structure solution and refinements had a goodness-of-fit of about 0.88 and many $F_o > F_c$ suggesting possible twinning. The data reduction was revisited and the structure was refined as a two component non-merohedral twinned crystal. The second domain is rotated from the first domain by 3.3° about reciprocal axis [1 0 0.5] as determined by CELL_NOW.[30] The structure refined to a twin ratio ca. 88:12. Full tables of atomic coordinates, atomic displacement parameters, and bond metrics are given in Appendix II.10.

Table 5.3. Crystal data and structure refinement for compound **1**.

Identification code	final bridging oxo
Empirical formula	$C_{24}H_{72}Co_2N_4Na_2OSi_8$
Formula weight	821.41
Temperature/K	100(2)
Crystal system	triclinic
Space group	P-1
a/Å	8.8839(18)
b/Å	10.591(2)
c/Å	12.700(3)
α/°	96.75(4)
β/°	108.93(3)
γ/°	99.15(3)
Volume/Å^3	1097.4(5)
Z	1
ρ_{calc}g/cm^3	1.243
μ/mm^{-1}	1.017
F(000)	440.0
Crystal size/mm^3	0.3 × 0.24 × 0.2
Radiation	MoKα (λ = 0.71073)
2Θ range for data collection/°	3.448 to 52.97
Index ranges	$-11 \leq h \leq 10$ $-13 \leq k \leq 13$ $0 \leq l \leq 15$
Reflections collected	4421
Independent reflections	4421 [R_{int} = 0.0892, R_{sigma} = 0.1114]
Data/restraints/parameters	4421/0/200
Goodness-of-fit on F^2	1.025
Final R indexes [I>=2σ (I)]	R_1 = 0.0646, wR_2 = 0.1402
Final R indexes [all data]	R_1 = 0.0910, wR_2 = 0.1535
Largest diff. peak/hole / e Å^{-3}	1.07/-0.54

5.5 References.

(1) The results described in this chapter have been published in the following: Hansen, C. B.; Filatov, A. S.; Hillhouse, G. L. Acta Cryst. E 2016, 72, 780.

(2) Blakemore, J. D.; Crabtree, R. H.; Brudvig, G. W. *Chem. Rev.* **2015**, *115*, 12974.

(3) Karkas, M. D.; Verho, O.; Johnston, E. V.; Akermark, B. *Chem. Rev.* **2014**, *114*, 11863.

(4) Heering, C.; Boldog, I.; Vasylyeva, V.; Sanchiz, J.; Janiak, C. *CrystEngComm* **2013**, *15*, 9757.

(5) Sumner, C. E.; Steinmetz, G. R. *J. Am. Chem. Soc.* **1985**, *107*, 6124.

(6) Hansen, C. B.; Jordan, R. F.; Hillhouse, G. L. *Inorg. Chem.* **2015**, *54*, 4603.

(7) Mulvey, R. E. *Organometallics* **2006**, *25*, 1060.

(8) Kennedy, A. R.; MacLellan, J. G.; Mulvey, R. E. *Acta Cryst. C* **2003**, *59*, m302.

(9) R. Kennedy, A.; E. Mulvey, R.; A. Roberts, B.; B. Rowlings, R.; L. Raston, C. *Chem. Commun.* **1999**, 353.

(10) Kennedy, A. R.; Mulvey, R. E.; Rowlings, R. B. *J. Am. Chem. Soc.* **1998**, *120*, 7816.

(11) Kennedy, A. R.; Mulvey, R. E.; Rowlings, R. B. *Angew. Chem. Int. Ed.* **1998**, *37*, 3180.

(12) Forbes, G. C.; Kennedy, A. R.; Mulvey, R. E.; Rowlings, R. B.; Clegg, W.; Liddle, S. T.; Wilson, C. C. *Chem. Commun.* **2000**, 1759.

(13) Kennedy, A. R.; Klett, J.; Mulvey, R. E.; Newton, S.; Wright, D. S. *Chem. Commun.* **2008**, 308.

(14) Mulvey, R. E.; Blair, V. L.; Clegg, W.; Kennedy, A. R.; Klett, J.; Russo, L. *Nat. Chem.* **2010**, *2*, 588.

(15) Wu, J.; Pan, X.; Tang, N.; Lin, C.-C. *Inorg. Chem.* **2010**, *49*, 5362.

(16) Lu, X.-H.; Ma, M.-T.; Yao, Y.-M.; Zhang, Y.; Shen, Q. *Inorg. Chem. Commun.* **2010**, *13*, 1566.

(17) Clark, N. M.; Garcia-Alvarez, P.; Kennedy, A. R.; O'Hara, C. T.; Robertson, G. M. *Chem. Commun.* **2009**, 5835.

(18) Li, Z.-Y.; Dai, Y.; Zhang, H.; Zhu, J.; Zhang, J.-J.; Liu, S.-Q.; Duan, C.-Y. *Eur. J. Inorg. Chem.* **2014**, *2014*, 384.

(19) Reger, D. L.; Pascui, A. E.; Foley, E. A.; Smith, M. D.; Jezierska, J.; Ozarowski, A. *Inorg. Chem.* **2014**, *53*, 1975.

(20) Wendelstorf, C.; Krämer, R. *Angew. Chem. Int. Ed.* **1997**, *36*, 2791.

(21) Driess, M.; Pritzkow, H.; Skipinski, M.; Winkler, U. *Organometallics* **1997**, *16*, 5108.

(22) Sarazin, Y.; Coles, S. J.; Hughes, D. L.; Hursthouse, M. B.; Bochmann, M. *Eur. J. Inorg. Chem.* **2006**, *2006*, 3211.

(23) Groom, C. R.; Allen, F. H. *Angew. Chem. Int. Ed.* **2014**, *53*, 662.

(24) Pangborn, A. B.; Giardello, M. A.; Grubbs, R. H.; Rosen, R. K.; Timmers, F. J. *Organometallics* **1996**, *15*, 1518.

(25) Matsubara, K.; Sueyasu, T.; Esaki, M.; Kumamoto, A.; Nagao, S.; Yamamoto, H.; Koga, Y.; Kawata, S.; Matsumoto, T. *Eur. J. Inorg. Chem.* **2012**, *2012*, 3079.

(26) Przyojski, J. A.; Arman, H. D.; Tonzetich, Z. J. *Organometallics* **2013**, *32*, 723.

(27) Bruker, *APEX3*, 2015.5-2. Bruker AXS Inc., Madison, Wisconsin, USA. 2015.

(28) Bruker, *TWINABS*, Version 2012/1. Bruker AXS Inc., Madison, Wisconsin, USA. 2012.

(29) Dolomanov, O. V.; Bourhis, L. J.; Gildea, R. J.; Howard, J. A. K.; Puschmann, H. *J. Appl. Crystallogr.* **2009**, *42*, 339.

(30) Sheldrick, G. M., *CELL_NOW*, Version 2008/4. Georg-August-Universität Göttingen, Göttingen, Germany. 2008.

CHAPTER 6.

An Extremely Bulky N-Heterocyclic Carbene Iron Tetracarbonyl Catalyst for the Hydrosilylation of Aldehydes.

6.1 Introduction

N-Heterocyclic carbene (NHC) ligands have gained enormous popularity in transition-metal chemistry for their ability to form strong metal–ligand bonds, their broadly tunable steric profiles and electronic properties, and the wide range of metal coordination numbers they stablize.[1-4] One of the first examples of a transition metal NHC compound to be prepared was the iron carbonyl (IMe)Fe(CO)$_4$.[6] Compounds of the general form (NHC)Fe(CO)$_4$ have been shown to be efficient and low-cost catalysts for hydrosilylation[7,8] and hydroborylation[9] of carbonyl bonds, as well as for the dehydration of primary amides into nitriles (Scheme 6.1).[10] In these reactions, complexes with bulkier NHC ligands show better catalytic stability than those containing smaller supporting ligands. For example, the catalysts (IMes)Fe(CO)$_4$ and (IPr)Fe(CO)$_4$ show near quantitative conversion of benzaldehyde upon hydrosilylation with phenyl silane. Under identical conditions the less sterically encumbering compounds (IMe)Fe(CO)$_4$ and (IiPr)Fe(CO)$_4$ showed reduced activity compared to their IMes and IPr counterparts(see Chart 6.1 for relative sizes of ligands).[8]

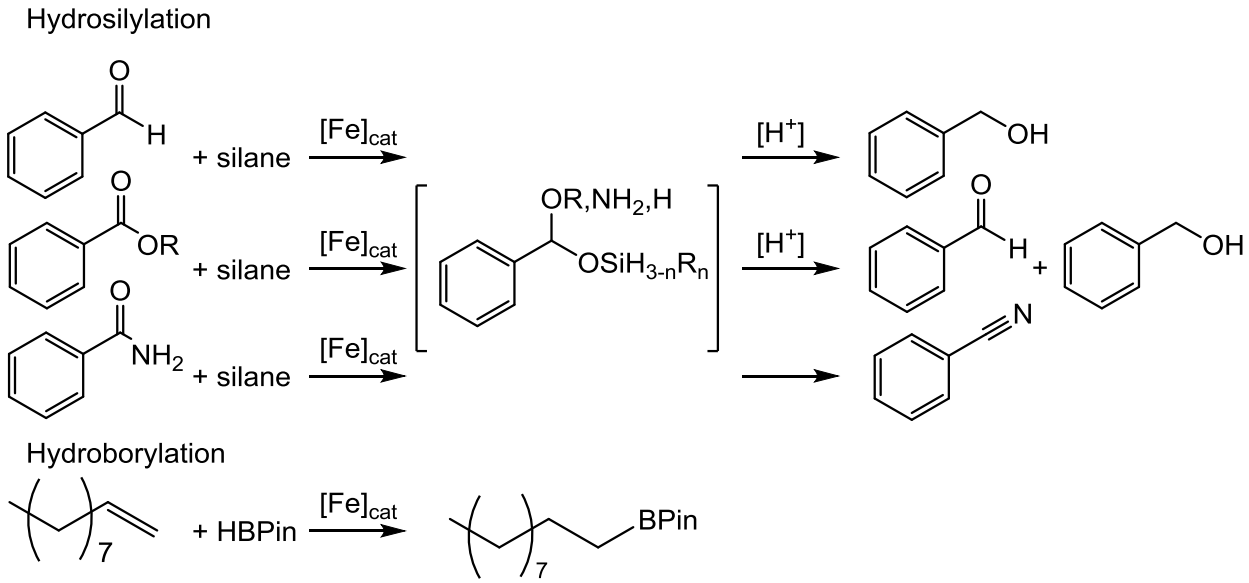

Scheme 6.1. Synthetic transformations carried out by $(NHC)Fe(CO)_4$ catalysts.

Bulky NHC supporting ligands have been used to stabilize low-coordinate species and to control reactivity.[11,12] In view of the prior results on the relationship between steric bulk and catalytic activity for $(NHC)Fe(CO)_4$ compounds, we wondered what influence even bulkier NHC ligands might have on the structure and reactivity of these complexes. The IPr* ligand was chosen here as it possesses an extremely bulky steric profile (Chart 6.1).[15] The aryl groups on this ligand are flexible; they can bend back to allow accommodate bulky ligands,[16] or encapsulate the metal site to sterically protect the metal center.[15,17] By utilizing a bulky ligand the selectivity may be improved by increasing reaction rates with smaller substrates and favoring activation of only a single bond in substrates bearing multiple reactive sites. The steric pressure provided may also alter the preferred synthetic pathway of a given transformation.[17] The steric bulk of the ligand can protect and stabilize coordinatively unsaturated active species. These factors are envisioned to provide a mechanism to improve the activity of first row transition metal catalysts.

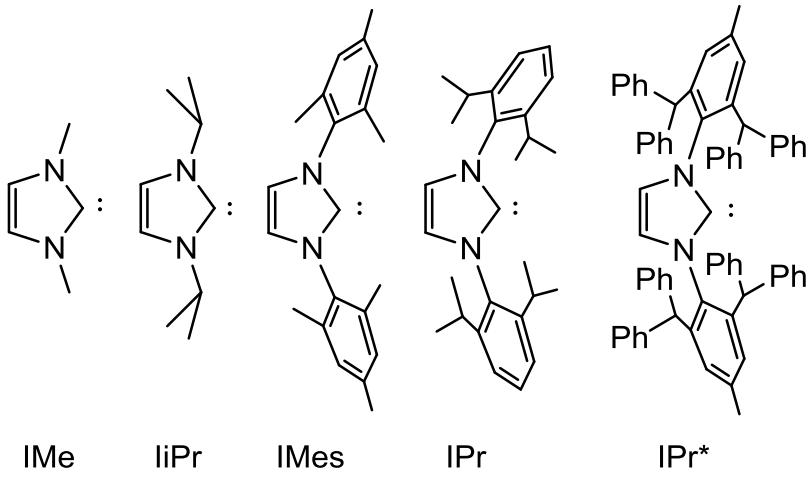

Chart 6.1. Ligands discussed in this chapter.

Here we report the preparation, characterization, and reactivity of a bulky N-heterocyclic carbene iron tetracarbonyl compound, (IPr*)Fe(CO)$_4$. Included is a single crystal structure and comparison to known structurally characterized analogues. It was found that, compared to these trigonal-bipyramidal compounds, the increased bulk of the NHC ligand leads to substantial geometric distortion. Preliminary reactivity studies on the hydrosilylation of benzaldehyde with phenylsilane were undertaken. (IPr*)Fe(CO)$_4$ was shown to be a competent catalyst at elevated temperatures, with a preference for formation of the doubly activated silyl ether PhHSi(OCH$_2$Ph)$_2$.

6.2 Results and Discussion.

6.2.1 Synthesis and characterization of (IPr*)Fe(CO)$_4$. Several routes exist to prepare compounds of the type (NHC)Fe(CO)$_4$, as shown in Scheme 6.2. The original preparation involved the reaction of an imidazolium salt with K[HFe(CO)$_4$], followed by sublimation of the product.[6] More typical methods involve photolysis of Fe(CO)$_5$ in the presence of the desired ligand.[10] A newer route has eliminated the necessity for photolysis by incorporating a catalytic amount of Fe(I) to labilize the iron precursor for ligand replacement.[7,10] Both of these routes

involve working with the toxic and volatile $Fe(CO)_5$ iron source. After the completion of this work a new high yielding method was developed by Royo to produce iron tetracarbonyl species by refluxing the NHC salt with $Fe_3(CO)_{12}$.[8]

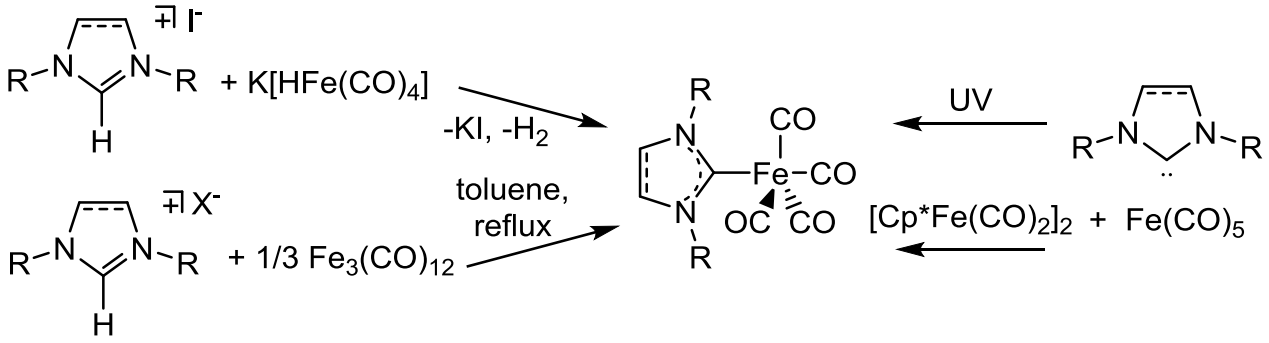

Scheme 6.2. Previously utilized routes to $(NHC)Fe(CO)_4$ species.

In order to avoid the direct use of $Fe(CO)_5$, we developed a method using $Fe_2(CO)_9$ as the iron source. In the presence of tetrahydrofuran, $Fe_2(CO)_9$ is known to dissociate into $(THF)Fe(CO)_4$, which can undergo facile ligand substitution.[19] This starting material has been used extensively to prepare $(diene)Fe(CO)_3$ species.[20] The reaction of $Fe_2(CO)_9$ with one-half equivalent IPr* per Fe in THF at room temperature overnight yields the desired compound, $(IPr^*)Fe(CO)_4$, in good yield (62% yield based on IPr*) and high purity as an off white diamagnetic solid (Scheme 6.3). The reaction was also found to work well in toluene, giving $(IPr^*)Fe(CO)_4$, in 85% yield (based on IPr*). The compound was characterized by ^1H NMR, FTIR, elemental analysis, and single crystal X-ray diffraction.

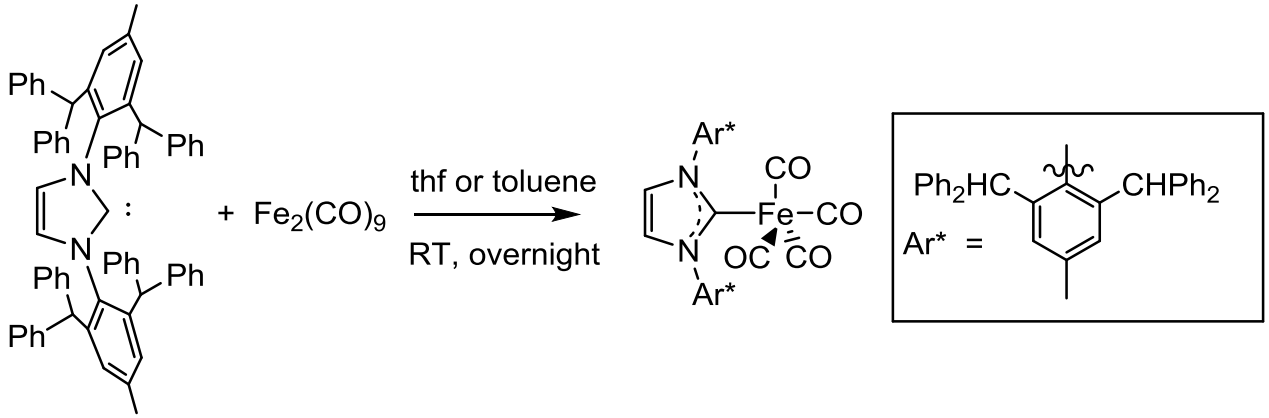

Scheme 6.3. Synthesis of (IPr*)$Fe(CO)_4$ from $Fe_2(CO)_9$.

The molecular structure of (IPr*)$Fe(CO)_4$ (**1**) in the solid state was determined via a single crystal X-ray diffraction study. The structure of **1** is shown in Figure 6.1, and bond distances and bond angles for this and related complexes are set out in Table 6.1. Compound **1** exhibits a 5-coordinate geometry about the iron center that is neither a classical square-pyramidal nor trigonal-bipyramidal structure. This contrasts with the bonding motif found for other structurally characterized (NHC)$Fe(CO)_4$ compounds, which can be described as trigonal bipyramidal (or approximately so) with the NHC residing in an axial position.

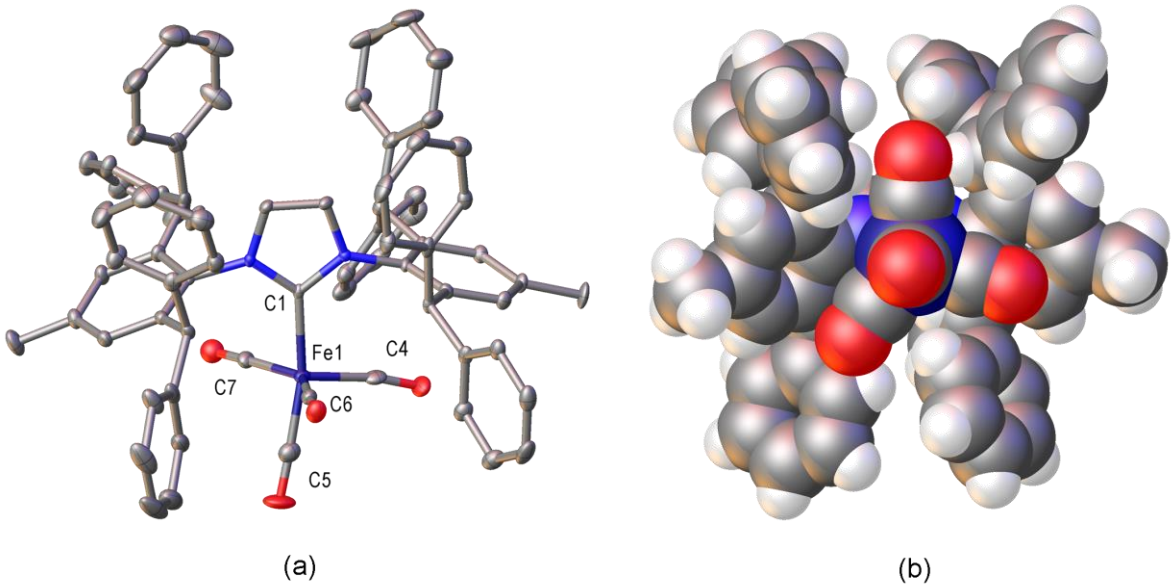

Figure 6.1. (a) Structure of (IPr*)Fe(CO)$_4$•(toluene) (50% probability thermal ellipsoids). For clarity, H atoms and solvent molecules are omitted. (b) Space filling model of (IPr*)Fe(CO)$_4$ displaying steric interactions responsible for distorted carbonyl groups. Select bond lengths and angles are given in Table 6.1.

Addison introduced a simple structural index factor, τ_5, to help illustrate and compare structural distortions in five-coordinate complexes that lie in the continuum between idealized trigonal bipyramidal and square pyramidal structures.[18] The value of the index factor is defined according to Equation 6.1

$$\tau_5 = (\alpha - \beta) / 60\ ^\circ \qquad (6.1)$$

where α and β are the two largest L-M-L angles in the molecule. For an idealized square pyramidal structure the two largest angles are 180˚, leading to $\tau_5 = 0$, whereas for idealized trigonal-bipyramidal structures the two largest angles are 180˚ and 120˚, leading to $\tau_5 = 1$. For previously reported (NHC)Fe(CO)$_4$ complexes (Table 6.1) a general trend is observed, wherein an increase in NHC ligand bulk results in an increased distortion about the metal away from a trigonal-bipyramidal structure. Compounds containing the IMes ($\tau_5 = 0.92$) and SIMes ($\tau_5 = 0.91$) ligands show near idealized trigonal bipyramidal geometries: the equatorial OC_{eq}–Fe–CO_{eq} angles are 120±1˚ and the axial C_{NHC}–Fe–CO_{ax} angle approaches linearity (~175˚). Increasing

the bulk of the aromatic group of the NHC from mesityl to 2,6-diisopropylphenyl, in (IPr)$Fe(CO)_4$, results in a distorted trigonal-bipyramidal geometry (τ_5 = 0.68), as manifested by a modest increase for one OC_{eq}–Fe–CO_{eq} angle (129˚), less regularity in the other two angles (117˚ and 113˚), and a less linear axial C_{NHC}–Fe–CO_{ax} arrangement (170˚). Extending this trend to the (IPr*)$Fe(CO)_4$ complex reported here results in a geometry that is formally closer to a square pyramidal geometry than trigonal-bipyramidal (τ_5 = 0.44), although it is not recognizably one or the other. One CO–Fe–CO angle is opened by strain to 140.03°, which is larger than observed for any of the other compounds, the nominal *trans* C_{NHC}–Fe–CO angle (166.58˚) is more bent than other examples, and the remaining OC–Fe–CO angles are smaller than any previously reported for this class of compounds (107˚, 112˚). Examination of the space filling model of **1** (Figure 6.1b) reveals steric crowding around the metal center from the NHC ligand near the expanded OC–Fe–CO angle.

Table 6.1. Select bond metrics for (IPr*)Fe(CO)$_4$ and other related NHC analogues. Additional structures for (IMes)Fe(CO)$_4$ and (IPr)Fe(CO)$_4$ have been published and match well with the presented data.[5]

Compound	(IPr*)Fe(CO)$_4$[a]	(IMes)Fe(CO)$_4$[8]	(SIMes)Fe(CO)$_4$[7]	(IPr)Fe(CO)$_4$[7]	(IMe)Fe(CO)$_4$[13]	Fe(CO)$_5$[14]
Fe-C_{NHC}	2.0090(19)	1.992(2)	2.007(2)	2.0041(14)	2.007(5)	
	1.788(2)	1.797(2)	1.785(3)	1.7868(18)	1.774(5)	1.8131(3)[d]
Fe-CO_{eq}	1.805(2)	1.807(2)	1.8048(9)[d]	1.8069(18)	1.785(6)	1.8098(5)
	1.791(2)	1.7971(19)	1.8048(9)[d]	1.8106(18)	1.808((5)	1.8131(3)[d]
Fe-CO_{ax}	1.780(2)	1.783(2)	1.782(3)	1.7727(17)	1.767(6)	1.8187(3)[d]
C_{NHC}-Fe-CO_{ax}	166.64(9)	175.36(8)	175.86(11)	170.64(7)	167.6(2)	178.818(17)
C_{NHC}-Fe-CO_{eq}	86.50(8)	84.41(8)	85.65(10)	84.09(7)	84.1(2)	90.222(12)[d]
	100.24(8)	95.10(8)	95.93(6)[d]	94.30(7)	88.8(2)	90.222(12)[d]
	89.75(8)	95.68(8)	95.93(6)[d]	98.49(6)	99.4(2)	89.409(9)
	107.80(16)	119.01(9)	118.97(6)[d]	129.93(8)	134.9[c]	117.122(18)
CO_{eq}-Fe-CO_{ex}	112.01(17)	120.41(9)	118.97(6)[d]	113.09(9)	108.6(3)	121.439(9)[d]
	140.03(17)	120.30(9)	121.46(11)	116.64(8)	116.5(3)	121.439(9)[d]
CO_{eq}-Fe-CO_{ax}	87.56(10)	91.06(9)	90.21(12)	88.13(8)	87.8(3)	90.395(11)[d]
	92.97(10)	86.34(9)	86.07(7)[d]	86.70(8)	90.3(3)	90.395(11)[d]
	87.07(10)	87.36(8)	86.07(7)[d]	89.64(7)	92.6(3)	89.409(9)
τ_5[b]	0.44	0.92	0.91	0.68	0.55	0.96

[a]This work. [b]$\tau_5 = (\alpha - \beta) / 60$ °; see Eq. 6.1.[18]; [c]no e.s.d. given; [d]related by symmetry

The iron carbene bond distance (Fe(1)-C(1) = 2.0090(19) Å) is consistent with other structurally characterized $(NHC)Fe(CO)_4$ compounds. The iron carbonyl bond distances also fall in line with known examples. The structure of $(IPr^*)Fe(CO)_4$ is symmetric in solution as judged by its NMR spectra The ^1H spectrum shows a symmetric ligand environment and free rotation of the C_{NHC}-Fe bond by the presence of one set of methyl resonances and eight sets of aromatic resonances. The ^{13}C spectrum shows one resonance for all carbonyl ligands.

6.2.2. Hydrosilylation Reactivity. $(NHC)Fe(CO)_4$ compounds have shown good activity as hydrosilylation catalysts. The mechanism for $(NHC)Fe(CO)_4$ catalyzed hydrosilylation is proposed to involve an initial dissociation of a carbonyl ligand to yield a coordinatively unsaturated species. This may be accomplished thermally or photolytically. The coordinatively unsaturated species then activates a Si-H bond to form an octahedral iron(II) silyl hydride. The unsaturated bond is then capable of inserting into either the Fe-H or Fe-Si bond, followed by reductive elimination to yield a silyl ether and regenerate the active coordinatively unsaturated species (Scheme 6.4).

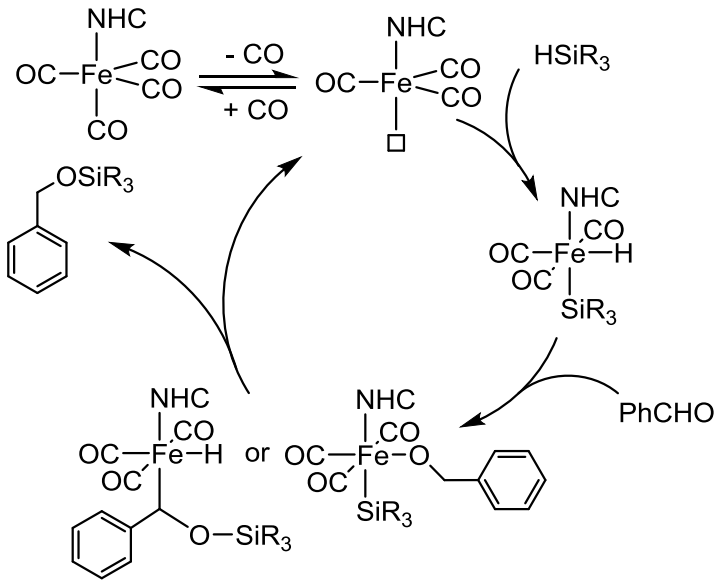

Scheme 6.4. Proposed mechanism for $(NHC)Fe(CO)_4$ catalyzed hydrosilylation of aldehydes.

In view of these results, we studied whether (IPr*)$Fe(CO)_4$ showed similar reactivity. Preliminary reactivity studies were performed between 1.1 equiv phenylsilane and 1 equiv benzaldehyde in C_6D_6 using 1 mol% of (IPr*)$Fe(CO)_4$. At 65 °C, it was observed that all of the benzaldehyde was consumed in 4 h giving a mixture of $PhHSi(OCH_2Ph)_2$ and $PhH_2Si(OCH_2Ph)$ as determined by ^{1}H-NMR in a *ca.* 2:1 ratio with significant amounts of residual $PhSiH_3$ (Scheme 6.5). The identities and ratios of the products were assigned based on diagnostic resonances of $PhHSi(OCH_2Ph)_2$ at δ 4.74 (s, 4H, $OC\underline{H_2}Ph$) and 5.34 (s, 1H, $Si\underline{H}$),[21] and $PhH_2Si(OCH_2Ph)$ at δ 4.85 (s, 2H, $OC\underline{H_2}Ph$).[22] At room temperature, the reaction was sluggish, showing <10% consumption of benzaldehyde after 23 h. Despite the larger ligand, the primary product was shown to be the doubly activated silyl ether, $PhHSi(OCH_2Ph)_2$ by a ratio of ca. 2:1. A comparison with other hydrosilylation results are given in Table 6.2. Further work will be required to establish optimal conditions, the silane and substrate scope, as well as probe the lower bound of catalyst loading.

Table 6.2. Preliminary hydrosilylation trials, and comparison with published literature examples.

Catalyst (mol % loading)	Reaction	Conditions	Consumption (%)[a]
IPr* (1)[b]	$(C_6H_5)CHO$ + 1.1 equiv $PhSiH_3$	C_6D_6, 4 h, 65 °C	>99
IPr* (1)[b]	$(C_6H_5)CHO$ + 1.1 equiv $PhSiH_3$	C_6D_6, 23 h, RT	<10
IMes (2)[c]	$((C_6H_5)CHO$ + 1.2 equiv $PhSiH_3$	THF, 4 h, RT	>99
IMes (2)[c]	$(C_6H_5)CHO$ + 1.1 equiv $PhSiH_3$	ACN, 24 h, RT	>99
IMes (2)[c]	$(C_6H_5)CHO$ + 1.2 equiv Ph_2SiH_2	THF, 24 h, RT	80
IMes (1)[c]	$(C_6H_5)CHO$ + 1.1 equiv $PhSiH_3$	THF, 4 h, RT	>99
IMes (0.5)[c]	$(C_6H_5)CHO$ + 1.1 equiv $PhSiH_3$	THF, 4 h, RT	60
IPr (1)[c]	$(C_6H_5)CHO$ + 1.1 equiv $PhSiH_3$	THF, 4 h, RT	90
IMe (1)[c]	$(C_6H_5)CHO$ + 1.1 equiv $PhSiH_3$	THF, 4 h, RT	45
IiPr (1)[c]	$(C_6H_5)CHO$ + 1.1 equiv $PhSiH_3$	THF, 4 h, RT	50
IMes (1)[c]	$(p\text{-}CF_3\text{-}C_6H_4)CHO$ + 1.1 equiv $PhSiH_3$	THF, 4 h, RT	83
IMes (1)[c]	$(p\text{-}NO_2\text{-}C_6H_4)CHO$ + 1.1 equiv $PhSiH_3$	THF, 4 h, RT	95
IMes (1)[c]	$(p\text{-}CN\text{-}C_6H_4)CHO$ + 1.1 equiv $PhSiH_3$	THF, 4 h, RT	91
IMes (1)[c]	$(p\text{-}Br\text{-}C_6H_4)CHO$ + 1.1 equiv $PhSiH_3$	THF, 4 h, RT	94
IMes (1)[c]	$(p\text{-}COMe\text{-}C_6H_4)CHO$ + 1.1 equiv $PhSiH_3$	THF, 4 h, RT	97

[a]As determined by NMR. [b]This work. [c]See ref.[8]

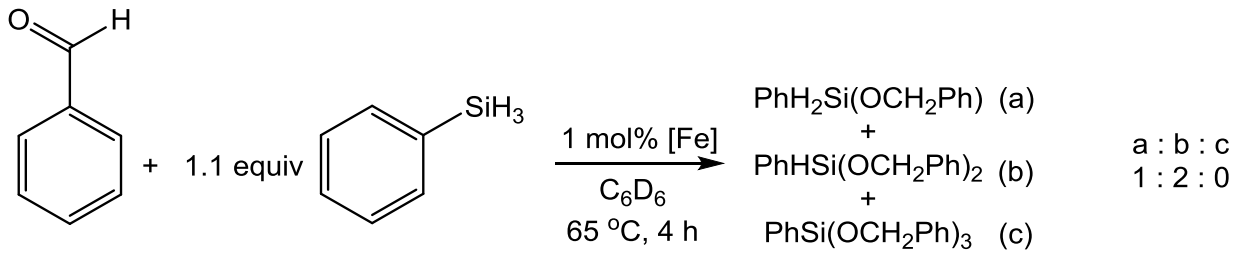

Scheme 6.5. Hydrosilylation of benzaldehyde with phenylsilane using 1 mol% (IPr*)$Fe(CO)_4$.

6.3 Conclusions

We reported here a new (NHC)$Fe(CO)_4$ compound using the bulky IPr* ligand. The solid state structure showed significant distortion from the typically found trigonal bipyramidal structure to one that was roughly half way across the trigonal-bipyramidal/square-pyramidal continuum. This compound extends the trend of distortion seen between analogous compounds with IMes and IPr ligands. NMR spectroscopy indicated that the compound possesses a symmetric solution structure. Preliminary reactivity studies have shown (IPr*)$Fe(CO)_4$ to be a competent hydrosilation catalyst, primarily forming the double activated species $PhHSi(OCH_2Ph)_2$.

6.4. Experimental Section.

6.4.1. General Considerations. Unless noted otherwise, all operations were performed under a purified nitrogen atmosphere in a standard MBraun Lab Master 130 drybox or under an argon atmosphere using high-vacuum and Schlenk techniques. Hexanes and toluene were dried by passage through activated alumina and Q-5 columns under nitrogen. Q-5 was activated by heating at 200 °C under a 5% H_2 in N_2 atmosphere. THF was distilled from a dark-purple THF solution of sodium benzophenone ketyl, and stored over 4Å molecular sieves. Diethyl ether was stirred for 24 h over metallic sodium and filtered under nitrogen through a plug of activated alumina. C_6D_6 was purchased from Cambridge Isotope Laboratory, degassed, dried over CaH_2,

transferred under vacuum, and stored over 4 Å molecular sieves. Molecular sieves, alumina, silica, and Celite were dried under dynamic vacuum overnight at 180 °C. Unless noted, chemicals were purchased from commercial sources and used without further purification. The IPr* ligand was prepared according to the literature.[15]

All NMR spectra were recorded using a Bruker DRX-400 or DRX-500 spectrometer. ^{1}H-NMR spectra were internally referenced to solvent δ 7.16 for C_6D_6. Elemental analyses were performed by Robertson Microlit Laboratories (Ledgewood, NJ). FTIR spectra were recorded using a Thermo Nicolet NEXUS 670 spectrometer.

(IPr*)Fe(CO)$_4$. To a stirred, room temperature suspension of $Fe_2(CO)_9$ (0.175 g, 0.481 mmol, 2.2 equiv Fe per NHC) in toluene (5 mL) was added a slurry of IPr* (0.400 g, 0.438 mmol) in toluene (5 mL). The reaction mixture was stirred overnight, during which time the orange crystals of $Fe_2(CO)_9$ dissolved and the solution became green. The solution was filtered through Celite to remove unreacted $Fe_2(CO)_9$, and the filtrate was reduced to dryness under vacuum. The resulting solid was washed sequentially with 2 x 5 mL hexanes and 2 x 5 mL diethyl ether to yield **(IPr*)Fe(CO)$_4$** as an off white solid in 85% yield. X-ray quality single crystals were grown from layering a dilute toluene solution of (IPr*)Fe(CO)$_4$ with hexanes and allowing to stand at room temperature for several days. ^{1}H NMR (400.13 MHz, C_6D_6): δ 7.54 (d, 8H, J = 7.6 Hz, Ph_{flank}), 7.17 (t, 8H, J = 7.6 Hz, Ph_{flank}), 7.02 (t, 8H, J = 7.6 Hz, Ph_{flank}), 6.86 (2 overlapping resonances m and s, 12 H total, Ph_{flank} + m-Ph_{main}), 6.78 (m, 8H, Ph_{flank}), 5.72 (s, 4H, C<u>H</u>Ph_2), 5.31 (s, 2H, backbone CH), 1.82 (s, 6H, p-CH_3). ^{13}C{^{1}H} NMR (500.13 MHz): δ 215.39 (CO), 190.03 (carbene), 143.51, 143.31, 143.29, 140.27, 136.95, 130.71, 130.52, 129.76, 128.40, 128.14, 126.87, 126.48, 125.47 (13 total aromatic + backbone CH), 51.77 (<u>C</u>HPh_2),

21.05 (*p*-Me). FTIR (Fluorolube mull, KBr plates): ν(CO) 2036, 1955, 1931, 1917 cm^{-1}. *Anal.* Calc. (found) for $C_{73}H_{56}N_2FeO_4$: C 81.10% (81.05%), H 5.22% (5.38%), N 2.59% (2.87%).

Hydrosilylation of benzaldehyde. In a typical experiment (IPr*)$Fe(CO)_4$ (10.8 mg, 1 mol%) was dissolved in 650 μL C_6D_6 and added to a J. Young NMR tube. Benzaldehyde (101.9 μL, 106 mg, 1.0 mmol) and phenylsilane (135.6 μL, 119 mg, 1.1 mmol, 1.1 equiv) were then added to the NMR tube. The NMR tube was sealed, and the reaction was monitored by ^1H NMR under the reaction conditions below. Progress of the reaction can be monitored by the following diagnostic resonances for each reagent and product. Benzaldehyde: δ 9.68 (s, 1H, C<u>H</u>O), phenylsilane: δ 4.19 (s with satellites, $^1J_{H\text{-}Si}$ = 160.1 Hz, 3H), $PhSiH(OCH_2Ph)_2$: δ 4.74 (s, 4H, OC<u>H</u>$_2$Ph) and 5.34 (s, 1H, Si<u>H</u>),[21] $PhSiH_2(OCH_2Ph)$: 4.85 (s, 2H, OC<u>H</u>$_2$Ph).[22] Consumption was monitored by disappearance of the aldehyde C(O)<u>H</u> of benzaldehyde, and generation of silylated species.

Table 6.3. Results of hydrosilylation trials.

Catalyst (mol % loading)	Reaction	Conditions	Conversion (%)[a]
IPr* (1)	$(C_6H_5)CHO$ + 1.1 equiv $PhSiH_3$	C_6D_6, 4 h, 65 °C	>99
IPr* (1)	$(C_6H_5)CHO$ + 1.1 equiv $PhSiH_3$	C_6D_6, 23 h, 23 h	10

[a]By NMR.

6.4.2. Single Crystal X-ray Diffraction. Crystals were loaded onto a glass slide in the glovebox and covered with STP oil. Suitable crystals were selected using stereo and polarizing microscopes under oil blanketed with a stream of nitrogen, attached to the tip of a glass fiber, mounted in a stream of cold dry nitrogen at 100(2) K, and centered in the X-ray beam using a video camera. X-ray diffraction data were collected on a Bruker D8 VENTURE with PHOTON 100 CMOS detector system equipped with a microfocus Mo-target X-ray tube (λ = 0.71073 Å). All data were collected at 100(2) K using a routine of ϕ and ω scans to survey an entire sphere of reciprocal space and were indexed using the APEX3 program suits.[23] Data were corrected for

absorption effects using the empirical and multi-scan methods as implemented in SADABS. Space groups were determined based on systematic absences and intensity statistics. The structures were solved using Patterson or direct methods and refined by full-matrix least-squares refinement on F^2 using the Bruker SHELXTL (version 6.14) software package. All non-hydrogen atoms were refined anisotropically and hydrogen atoms were placed in calculated positions, unless specified otherwise. Full tables of atomic coordinates, atomic displacement parameters, and bond metrics are given in Appendix II.11. All figures in text are drawn at 50% thermal ellipsoid probability level.

(IPr*)$Fe(CO)_4$ crystallized with one molecule of toluene per asymmetric unit. The toluene group was found to be disordered over two positions and treated as parts which converged to *ca.* 67:33 occupancy.

6.5 References.

(1) Peris, E. *Chem. Rev.* **2017**.

(2) Diez-Gonzalez, S. *N-Heterocyclic Carbenes*; 2 ed.; The Royal Society of Chemistry, 2017.

(3) Díez-González, S.; Marion, N.; Nolan, S. P. *Chem. Rev.* **2009**, *109*, 3612.

(4) Bellemin-Laponnaz, S.; Dagorne, S. *Chem. Rev.* **2014**, *114*, 8747.

(5) Hashimoto, T.; Hoshino, R.; Hatanaka, T.; Ohki, Y.; Tatsumi, K. *Organometallics* **2014**, *33*, 921.

(6) Öfele, K.; Kreiter, C. G. *Chem. Ber.* **1972**, *105*, 529.

(7) Li, H.; Misal Castro, L. C.; Zheng, J.; Roisnel, T.; Dorcet, V.; Sortais, J.-B.; Darcel, C. *Angew. Chem. Int. Ed.* **2013**, *52*, 8045.

(8) Warratz, S.; Postigo, L.; Royo, B. *Organometallics* **2013**, *32*, 893.

(9) Zheng, J.; Sortais, J.-B.; Darcel, C. *ChemCatChem* **2014**, *6*, 763.

(10) Elangovan, S.; Quintero-Duque, S.; Dorcet, V.; Roisnel, T.; Norel, L.; Darcel, C.; Sortais, J.-B. *Organometallics* **2015**, *34*, 4521.

(11) Power, P. P. *Chem. Rev.* **2012**, *112*, 3482.

(12) Roy, S.; Mondal, K. C.; Roesky, H. W. *Acc. Chem. Res.* **2016**, *49*, 357.

(13) Huttner, G.; Gartzke, W. *Chem. Ber.* **1972**, *105*, 2714.

(14) Farrugia, L. J.; Evans, C. *J. Phys. Chem. A* **2005**, *109*, 8834.

(15) Berthon-Gelloz, G.; Siegler, M. A.; Spek, A. L.; Tinant, B.; Reek, J. N. H.; Marko, I. E. *Dalton Trans.* **2010**, *39*, 1444.

(16) Laskowski, C. A.; Miller, A. J. M.; Hillhouse, G. L.; Cundari, T. R. *J. Am. Chem. Soc.* **2011**, *133*, 771.

(17) Gómez-Suárez, A.; Ramón, R. S.; Songis, O.; Slawin, A. M. Z.; Cazin, C. S. J.; Nolan, S. P. *Organometallics* **2011**, *30*, 5463.

(18) Addison, A. W.; Rao, T. N.; Reedijk, J.; van Rijn, J.; Verschoor, G. C. *J. Chem. Soc., Dalton Trans.* **1984**, 1349.

(19) Cotton, F. A.; Troup, J. M. *J. Am. Chem. Soc.* **1974**, *96*, 3438.

(20) Knölker, H.-J. *Chem. Rev.* **2000**, *100*, 2941.

(21) Yang, J.; Tilley, T. D. *Angew. Chem. Int. Ed.* **2010**, *49*, 10186.

(22) Yang, Z.; Zhong, M.; Ma, X.; De, S.; Anusha, C.; Parameswaran, P.; Roesky, H. W. *Angew. Chem. Int. Ed.* **2015**, *54*, 10225.

(23) Bruker, *APEX3*, Version 2015.5-2. Bruker AXS, Inc., 2015.

APPENDIX I.

Synthesis and Crystal Structure of a Bulky Cobalt Bis(anilide).

I.1 Introduction.

During the work described in Chapter 4 a homoleptic bis(anilide), Co(NHAr*)$_2$•2Toluene (NHAr* = 2,6-bis(benzhydryl)-4-methyl-anilide), was prepared and characterized crystallographically (Figure I.1). This compound was prepared by the experimental route described below. Attempts to prepare additional samples for full characterization were unsuccessful.

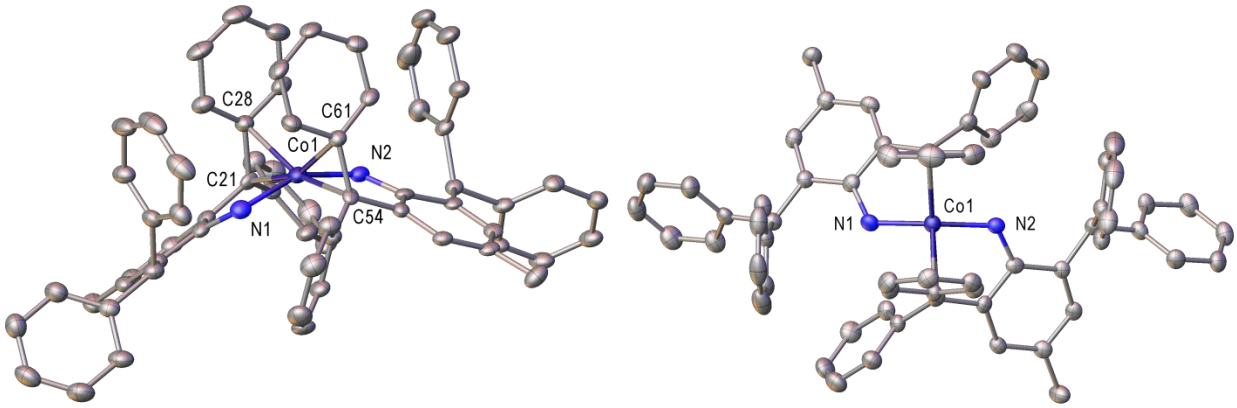

Figure I.1. Molecular structure of Co(NHAr*)$_2$•2(toluene) (50% probability ellipsoids). Hydrogen atoms and solvent molecules removed for clarity.

There is some uncertainty about the protonation status of the two trityl-like sites (C21 and C54) that exhibit close contacts with the cobalt center. Adding hydrogen atoms at calculated positions results in no essentially no change to the structure. The structure refines with almost identical metrics with (R1 = 7.48%, wR2 = 18.95%, GooF = 1.019) or without (R1 = 7.49%, wR2 = 18.80%, GooF = 1.014) the protons present (Table I.1). Placing the protons in calculated positions, and subsequently allowing them to refine freely does not result in a chemically reasonable geometry after final refinement.

I.2 Experimental Section

I.2.1 General Considerations. Unless noted otherwise, all operations were performed under a purified nitrogen atmosphere in a standard MBraun Lab Master 130 drybox or under an argon atmosphere using high-vacuum and Schlenk techniques. Toluene was dried by passage through activated alumina and Q-5 columns under nitrogen. Q-5 was activated by heating at 200 °C under a 5% H_2 in N_2 atmosphere. THF was distilled from a dark-purple THF solution of sodium benzophenone ketyl, and stored over 4Å molecular sieves. Celite was dried under dynamic vacuum overnight at 180 °C. Unless noted, chemicals were purchased from commercial sources and used without further purification. Anhydrous $CoCl_2$ was prepared by heating commercial $CoCl_2 \cdot 6H_2O$ under dynamic vacuum overnight at 150 °C. The NH_2Ar^* ligand was prepared according to the literature.[1]

$Co(NHAr^*)_2$. To a stirred, −40 °C solution of NH_2Ar^* (0.500 g, 1.139 mmol, 2 equiv) in a 1:1 mixture of THF:toluene (6 mL) was added a 1.60M solution of butyl lithium (0.705 mL, 1.170 mmol, 2.05 equiv) resulting in a color change from colorless to yellow to red, accompanied by a red precipitate near the end of addition. To this cooled slurry was added anhydrous $CoCl_2$ (0.074 g, 0.570 mmol, 1 equiv) as a solid. The reaction mixture was allowed to warm to room temperature and stirred overnight, during which time the reaction mixture became green. The volatiles were removed under vacuum and dried for several hours, and the dark colored residue was extracted with toluene (10 mL) to give a red-brown solution. The toluene solution was filtered through Celite, and residue washed with additional toluene (4x 5 mL) until nearly colorless. The toluene washings were combined, concentrated to ca. 10 mL, and cooled to −40 °C for several days to yield $Co(NHAr^*)_2 \cdot 2$(toluene) as red and green dichroic blocks.

I.2.2 Single Crystal X-ray Diffraction. Crystals were loaded onto a glass slide in the glovebox and covered with STP oil. Suitable crystals were selected using stereo and polarizing microscopes under oil blanketed with a stream of nitrogen, attached to the tip of a glass fiber, mounted in a stream of cold dry nitrogen at 100(2) K, and centered in the X-ray beam using a video camera. X-ray diffraction data were collected on a Bruker D8 VENTURE with PHOTON 100 CMOS detector system equipped with a microfocus Mo-target X-ray tube (λ = 0.71073 Å). All data were collected at 100(2) K using a routine of ϕ and ω scans to survey an entire sphere of reciprocal space and were indexed using the APEX3 program suits.[2] Data were corrected for absorption effects using the empirical and multi-scan methods as implemented in SADABS. Space groups were determined based on systematic absences and intensity statistics. The structures were solved using Patterson or direct methods and refined by full-matrix least-squares refinement on F^2 using the Bruker SHELXTL (version 6.14) software package. All non-hydrogen atoms were refined anisotropically and hydrogen atoms were placed in calculated positions, unless specified otherwise. Full tables of atomic coordinates, atomic displacement parameters, and bond metrics are given in Appendix II.12. All figures in text are drawn at 50% thermal ellipsoid probability level. Full tables of atomic coordinates, atomic displacement parameters, and bond metrics for refined structures with and without trityl-like protons are given in Appendices II.12 and II.13 respectively.

$Co(NHAr^*)_2$•2Toluene. Crystallized with two molecules of toluene per asymmetric unit, which were refined normally.

Table I.1 Crystal data and structure refinement for Co(NHAr*)$_2$•2(Toluene).

Identification code	With trityl-like protons	Without trityl-like protons
Empirical formula	$C_{80}H_{72}CoN_2$	$C_{80}H_{70}CoN_2$
Formula weight	1120.32	1118.31
Temperature/K	99.99	99.99
Crystal system	monoclinic	monoclinic
Space group	$P2_1/n$	$P2_1/n$
a/Å	14.414(2)	14.414(2)
b/Å	17.888(3)	17.888(3)
c/Å	23.482(4)	23.482(4)
α/°	90	90
β/°	101.148(4)	101.148(4)
γ/°	90	90
Volume/Å^3	5940.6(17)	5940.6(17)
Z	4	4
ρ_{calc}g/cm^3	1.253	1.250
μ/mm^{-1}	0.338	0.338
F(000)	2372.0	2364.0
Crystal size/mm^3	0.192 × 0.137 × 0.124	0.192 × 0.137 × 0.124
Radiation	MoKα (λ = 0.71073)	MoKα (λ = 0.71073)
2Θ range for data collection/°	4.31 to 53.012	4.31 to 53.012
Index ranges	$-17 \le h \le 17$ $-21 \le k \le 21$ $-29 \le l \le 28$	$-17 \le h \le 17$ $-21 \le k \le 21$ $-29 \le l \le 28$
Reflections collected	63559	63559
Independent reflections	11672 [R_{int} = 0.1181, R_{sigma} = 0.1332]	11672 [R_{int} = 0.1181, R_{sigma} = 0.1332]
Data/restraints/parameters	11672/0/752	11672/0/752
Goodness-of-fit on F^2	1.019	1.014
Final R indexes [I>=2σ (I)]	R_1 = 0.0748, wR_2 = 0.1523	R_1 = 0.0749, wR_2 = 0.1508
Final R indexes [all data]	R_1 = 0.1629, wR_2 = 0.1895	R_1 = 0.1628, wR_2 = 0.1880
Largest diff. peak/hole / e Å^{-3}	0.93/-1.20	1.16/-1.19

I.3 References

(1) Berthon-Gelloz, G.; Siegler, M. A.; Spek, A. L.; Tinant, B.; Reek, J. N. H.; Marko, I. E. *Dalton Trans.* **2010**, *39*, 1444.

(2) AXS, B., *APEX3*, Version 2015.5-2. Bruker AXS, Inc., 2015.

Appendix II. Single Crystal X-Ray Diffraction Tables.

II.1 Diffraction data for $[WH(CPh)(dmpe)_2Cl][B(C_6F_5)_4]$•ACN

Table II.1. Crystal data and structure refinement for $[WH(CPh)(dmpe)_2Cl][B(C_6F_5)_4]$.

Identification code	$[WH(CPh)(dmpe)_2Cl][B(C_6F_5)_4]$
Empirical formula	$C_{45}H_{41}BClF_{20}NP_4W$
Formula weight	1329.78
Temperature/K	100(2)
Crystal system	monoclinic
Space group	$P2_1/n$
a/Å	21.6011(11)
b/Å	8.3214(4)
c/Å	28.8908(14)
α/°	90
β/°	90.8795(16)
γ/°	90
Volume/Å^3	5192.5(4)
Z	4
ρ_{calc}g/cm^3	1.701
μ/mm^{-1}	2.505
F(000)	2616.0
Crystal size/mm^3	0.17 × 0.16 × 0.07
Radiation	MoKα (λ = 0.71073)
2Θ range for data collection/°	4.6 to 61.2
Index ranges	$-30 \leq h \leq 30$, $-11 \leq k \leq 11$, $-41 \leq l \leq 41$
Reflections collected	188724
Independent reflections	15910 [R_{int} = 0.0744, R_{sigma} = 0.0361]
Data/restraints/parameters	15910/12/719
Goodness-of-fit on F^2	1.096
Final R indexes [I>=2σ (I)]	R_1 = 0.0378, wR_2 = 0.0687
Final R indexes [all data]	R_1 = 0.0570, wR_2 = 0.0735
Largest diff. peak/hole / e Å^{-3}	0.92/-0.74

Table II.2. Fractional Atomic Coordinates ($\times 10^4$) and Equivalent Isotropic Displacement Parameters ($Å^2 \times 10^3$) for $[WH(CPh)(dmpe)_2Cl][B(C_6F_5)_4]$. U_{eq} is defined as 1/3 of of the trace of the orthogonalised U_{IJ} tensor.

Atom	***x***	***y***	***z***	**U(eq)**
W(1)	4753.4(2)	2436.4(3)	2521.7(2)	11.85(5)
Cl(1)	5536.5(5)	183.3(12)	2612.8(5)	26.0(2)
W(1X)	4931.0(12)	2913(3)	2531.3(6)	11.85(5)
Cl(1X)	5681(7)	561(18)	2658(6)	26.0(2)
P(1)	4292.0(5)	1061.7(11)	1852.0(3)	27.27(19)
P(2)	5426.2(4)	3377.1(11)	1852.1(3)	24.16(18)
P(3)	5489.0(4)	4033.7(10)	3050.7(3)	23.63(18)
P(4)	4392.1(4)	1762.5(10)	3302.2(3)	17.12(15)
C(1)	4203.9(14)	4063(4)	2452.1(10)	17.1(6)
C(2)	3736.2(13)	5292(3)	2393.7(10)	14.9(5)
C(3)	3537.9(14)	6239(4)	2764.7(11)	20.8(6)
C(4)	3078.8(15)	7368(4)	2707.7(11)	24.7(6)
C(5)	2800.3(14)	7597(4)	2277.5(12)	25.8(6)
C(6)	2992.9(15)	6704(4)	1902.5(12)	22.8(7)
C(7)	3453.8(14)	5566(4)	1956.9(10)	17.4(6)
C(8)	3455.8(19)	1111(5)	1805.4(14)	38.7(10)
C(9)	4475.9(19)	-1043(4)	1798.7(15)	38.8(10)
C(10A)	4475(2)	2018(6)	1305.2(15)	24.1(9)
C(11A)	5172(2)	2242(6)	1311.5(14)	23.0(9)
C(12A)	5351(3)	5409(6)	1677(2)	36.7(13)
C(13A)	6249(5)	2961(10)	1838(4)	24.8(16)
C(10B)	4781(7)	1618(17)	1323(4)	24.1(9)
C(11B)	5009(6)	3274(16)	1363(4)	23.0(9)
C(12B)	5581(9)	5723(18)	1914(6)	36.7(13)
C(13B)	6176(15)	2620(40)	1789(12)	24.8(16)
C(14A)	5678(7)	6140(15)	2828(5)	29(3)
C(15A)	6225(6)	3215(18)	3147(5)	29.7(10)
C(16A)	5133(6)	4411(15)	3558(4)	25(3)
C(17A)	4925(8)	2810(30)	3765(9)	19.3(12)
C(14B)	5289(2)	6104(6)	3158(2)	37.7(14)
C(15B)	6325(2)	4061(7)	3001.6(19)	29.7(10)
C(16B)	5425(2)	3148(6)	3654.1(16)	23.7(10)
C(17B)	4746(2)	2926(9)	3763(3)	19.3(12)
C(18)	3580.7(16)	2140(5)	3402.1(13)	30.9(8)
C(19)	4488.9(16)	-310(4)	3476.5(12)	25.8(7)
F(1)	1254.5(9)	4166(2)	5696.9(7)	29.8(5)
F(2)	1100(1)	6308(3)	6353.2(9)	41.5(6)

Table II.2. Continued.

F(3)	2008.6(10)	8447(2)	6579.8(7)	34.3(5)
F(4)	3105.9(10)	8292(3)	6131.9(8)	39.0(6)
F(5)	3308.3(9)	6037(3)	5499.6(7)	31.8(5)
F(6)	1564.8(9)	6022(3)	4766.6(7)	30.7(5)
F(7)	1758.4(12)	8382(3)	4161.8(7)	41.1(6)
F(8)	2876.4(13)	8736(3)	3759.6(7)	46.4(7)
F(9)	3796.4(12)	6593(3)	3959.1(8)	46.3(6)
F(10)	3636.6(10)	4307(2)	4565.5(8)	32.9(5)
F(11)	1965.8(9)	1379(2)	5760.6(6)	24.5(4)
F(12)	1076.9(10)	-790(2)	5615.8(7)	31.8(5)
F(13)	486(1)	-986(3)	4775.6(8)	34.8(5)
F(14)	809.9(13)	1063(3)	4090.9(8)	53.6(7)
F(15)	1680.5(11)	3229(3)	4219.5(7)	39.0(6)
F(16)	3212.4(10)	3137(3)	6024.7(7)	32.6(5)
F(17)	4095.4(11)	975(3)	6123.2(8)	44.1(6)
F(18)	4444.8(10)	-896(3)	5404.1(8)	40.7(6)
F(19)	3846.6(11)	-599(3)	4572.4(7)	34.9(5)
F(20)	2930.1(9)	1519(2)	4462.2(6)	25.2(4)
C(20)	2298.4(14)	4938(4)	5563.6(10)	17.8(6)
C(21)	1746.1(15)	5115(4)	5798.0(11)	20.3(6)
C(22)	1645.7(15)	6243(4)	6139.1(12)	24.2(7)
C(23)	2101.9(16)	7308(4)	6254.7(11)	23.4(6)
C(24)	2656.8(15)	7230(4)	6027.5(11)	22.5(7)
C(25)	2741.2(15)	6064(4)	5700.0(11)	20.9(6)
C(26)	2583.3(15)	4996(4)	4702.4(10)	19.5(6)
C(27)	2131.4(16)	6113(4)	4577.2(11)	23.5(7)
C(28)	2223.2(18)	7349(4)	4266.3(11)	29.2(7)
C(29)	2783(2)	7529(5)	4058.4(10)	33.5(8)
C(30)	3242.2(19)	6452(4)	4160.2(12)	29.9(8)
C(31)	3138.9(17)	5235(4)	4478.5(11)	24.9(7)
C(32)	1863.7(13)	2478(4)	5007.5(9)	18.2(5)
C(33)	1684.4(14)	1368(4)	5338.2(10)	18.7(6)
C(34)	1228.8(15)	223(4)	5272.8(11)	20.2(6)
C(35)	924.7(15)	134(4)	4851.6(13)	25.9(7)
C(36)	1086.6(17)	1173(5)	4510.7(12)	30.2(8)
C(37)	1545.5(16)	2294(4)	4588.1(11)	24.6(7)
C(38)	3025.4(13)	2486(4)	5230.0(9)	17.9(5)
C(39)	3348.7(15)	2258(4)	5645.3(11)	23.0(7)
C(40)	3814.4(16)	1146(4)	5707.1(12)	27.5(7)
C(41)	3990.7(16)	182(4)	5347.8(12)	26.1(7)
C(42)	3681.9(16)	334(4)	4928.9(12)	23.5(7)

Table II.2. Continued.

C(43)	3214.1(15)	1442(4)	4884(1)	19.5(6)
B(1)	2442.7(16)	3714(4)	5125.8(11)	17.0(6)
N(49)	7315.3(19)	-31(5)	2249.7(15)	56.5(11)
C(44)	7015.3(18)	-1380(5)	3023.8(14)	34.1(8)
C(45)	7187.0(19)	-615(5)	2592.0(16)	37.8(9)

Table II.3 Anisotropic Displacement Parameters ($Å^2 \times 10^3$) for $[WH(CPh)(dmpe)_2Cl][B(C_6F_5)_4]$. The Anisotropic displacement factor exponent takes the form: $-2\pi^2[h^2a^{*2}U_{11}+2hka^*b^*U_{12}+\ldots]$.

Atom	U_{11}	U_{22}	U_{33}	U_{23}	U_{13}	U_{12}
W(1)	11.36(8)	10.04(8)	14.21(5)	1.24(6)	1.95(4)	0.37(7)
Cl(1)	21.9(6)	19.9(6)	36.6(5)	8.9(4)	8.5(5)	9.6(4)
W(1X)	11.36(8)	10.04(8)	14.21(5)	1.24(6)	1.95(4)	0.37(7)
Cl(1X)	21.9(6)	19.9(6)	36.6(5)	8.9(4)	8.5(5)	9.6(4)
P(1)	39.9(5)	17.8(4)	24.3(4)	-1.2(3)	3.8(4)	-7.5(4)
P(2)	16.4(4)	27.9(4)	28.2(4)	12.5(4)	4.0(3)	0.9(3)
P(3)	14.6(4)	15.6(4)	40.6(5)	-2.8(4)	-0.3(3)	-2.8(3)
P(4)	17.0(4)	16.5(4)	17.9(4)	3.3(3)	1.2(3)	-0.5(3)
C(1)	20.0(15)	20.0(14)	11.5(13)	-1.1(11)	2.0(11)	1.1(12)
C(2)	13.5(13)	14.8(13)	16.4(13)	0.7(11)	0.7(11)	0(1)
C(3)	18.8(15)	22.2(15)	21.2(15)	-2.6(12)	-1.1(12)	0.2(12)
C(4)	23.2(15)	22.0(15)	28.9(15)	-11.0(14)	2.5(12)	4.6(14)
C(5)	19.7(14)	19.8(15)	37.9(17)	-2.0(15)	-1.9(12)	7.4(14)
C(6)	20.1(15)	22.0(16)	26.1(16)	0.6(13)	-8.2(13)	2.1(12)
C(7)	16.1(14)	17.1(14)	18.9(14)	-1.6(11)	-0.7(11)	-0.3(11)
C(8)	48(2)	23.2(18)	44(2)	0.5(16)	-20.1(19)	-5.1(17)
C(9)	41(2)	20.3(17)	55(3)	-14.5(17)	7.6(19)	-5.4(16)
C(10A)	25(3)	29(2)	18.3(18)	-2.2(16)	-3.8(19)	3.4(18)
C(11A)	26(2)	28(2)	14.3(16)	-3.1(16)	2.7(15)	2.9(17)
C(12A)	43(3)	21(2)	48(4)	11(2)	17(3)	2(2)
C(13A)	17(3)	33(4)	25(3)	3(3)	4(2)	-1(3)
C(10B)	25(3)	29(2)	18.3(18)	-2.2(16)	-3.8(19)	3.4(18)
C(11B)	26(2)	28(2)	14.3(16)	-3.1(16)	2.7(15)	2.9(17)
C(12B)	43(3)	21(2)	48(4)	11(2)	17(3)	2(2)
C(13B)	17(3)	33(4)	25(3)	3(3)	4(2)	-1(3)
C(14A)	37(8)	17(6)	34(7)	3(5)	-2(6)	-12(5)
C(15A)	16(2)	33(3)	41(3)	4(2)	0.5(19)	-5.8(19)
C(16A)	32(7)	21(6)	20(6)	4(5)	-8(5)	-5(5)
C(17A)	17(3)	26(2)	14.9(14)	-0.8(14)	-5(3)	5(3)
C(14B)	30(3)	15(2)	68(4)	1(2)	-5(3)	-2.6(19)
C(15B)	16(2)	33(3)	41(3)	4(2)	0.5(19)	-5.8(19)
C(16B)	18(2)	26(2)	27(2)	-8.7(18)	-1.6(17)	1.0(17)
C(17B)	17(3)	26(2)	14.9(14)	-0.8(14)	-5(3)	5(3)
C(18)	24.3(17)	38(2)	30.8(18)	11.8(15)	10.8(14)	9.5(14)
C(19)	24.0(17)	20.3(15)	33.0(18)	7.0(14)	2.0(14)	0.4(13)
F(1)	20.5(10)	26.2(10)	42.9(12)	-10.0(9)	8.9(9)	-5.7(8)
F(2)	33.8(12)	30.7(12)	61.0(15)	-19.6(11)	28.7(11)	-7.5(10)

Table II.3 Continued.

F(3)	42.4(13)	24(1)	36.8(12)	-14.2(9)	11.1(10)	-3.3(9)
F(4)	33.9(12)	37.6(13)	45.7(13)	-20.6(11)	5.7(10)	-14.9(10)
F(5)	23.4(10)	39.7(12)	32.7(11)	-13.2(10)	7.2(9)	-8.1(9)
F(6)	29.0(11)	33.0(11)	30.0(11)	8.0(9)	-4.2(9)	4.1(9)
F(7)	66.9(17)	26.8(11)	29.2(11)	4.7(9)	-16.3(11)	6.9(11)
F(8)	97(2)	20.8(11)	21.4(10)	5.9(9)	6.9(12)	-12.4(12)
F(9)	65.9(17)	29.9(12)	44.1(14)	-0.3(10)	34.9(12)	-14.6(11)
F(10)	30.5(11)	26.1(11)	42.7(13)	3.2(9)	18.1(10)	-2.9(9)
F(11)	32.5(11)	27.1(10)	13.9(8)	3.2(7)	-1.8(8)	-4.2(8)
F(12)	41.6(13)	25.1(10)	28.9(11)	5.5(9)	7.1(9)	-10.1(9)
F(13)	29.4(11)	31.7(11)	43.2(13)	-4.9(10)	-0.3(10)	-13.3(9)
F(14)	70.4(18)	53.3(16)	36.1(13)	9.9(12)	-34.2(13)	-26.8(14)
F(15)	59.6(15)	39.7(12)	17.3(10)	8.4(9)	-15(1)	-21.4(11)
F(16)	38.7(12)	40.8(12)	18.0(9)	-8.2(9)	-8.0(8)	15.2(10)
F(17)	43.5(14)	56.1(16)	32.0(12)	-7.4(11)	-20.2(10)	21.0(12)
F(18)	34.3(12)	38.7(13)	49.1(14)	-0.5(11)	-1.8(10)	19.5(10)
F(19)	45.6(13)	28.8(11)	30.6(11)	-8.2(9)	8.7(10)	7.9(10)
F(20)	33.4(11)	27.7(10)	14.5(8)	-1.7(8)	-1.0(8)	1.2(8)
C(20)	21.7(15)	17.6(14)	14.1(13)	3.6(11)	0.1(11)	1.6(11)
C(21)	19.0(15)	17.0(14)	24.9(16)	-0.4(12)	0.9(12)	-3.1(11)
C(22)	22.7(16)	18.4(15)	31.7(18)	-3.2(13)	8.5(14)	-1.0(12)
C(23)	32.0(17)	16.5(15)	21.8(14)	-2.5(12)	3.7(12)	1.3(13)
C(24)	24.0(15)	21.5(17)	22.0(14)	-2.2(12)	2.1(12)	-6.8(12)
C(25)	19.9(15)	23.0(15)	19.9(15)	-1.0(12)	1.2(12)	-1.5(12)
C(26)	27.1(16)	20.0(15)	11.5(13)	-2.7(11)	0.5(12)	-2.6(12)
C(27)	31.1(18)	24.2(16)	14.9(14)	1.5(12)	-4.0(13)	-2.4(14)
C(28)	50(2)	19.2(16)	18.6(14)	-1.4(14)	-8.7(14)	-0.1(16)
C(29)	69(3)	18.6(14)	13.3(13)	2.4(15)	4.7(14)	-12.0(19)
C(30)	47(2)	21.6(16)	21.9(16)	-2.6(13)	13.8(15)	-11.9(15)
C(31)	37.0(19)	19.1(15)	18.8(15)	-1.9(12)	8.2(14)	-4.8(14)
C(32)	18.2(13)	20.7(13)	15.6(12)	0.4(14)	0.6(10)	-0.2(13)
C(33)	19.8(15)	21.2(15)	15.1(13)	-2.8(11)	-0.4(11)	1.9(12)
C(34)	20.9(15)	18.8(14)	21.2(15)	0.4(12)	6.8(12)	-1.1(12)
C(35)	18.3(16)	24.5(16)	34.9(19)	-3.5(14)	-0.8(14)	-4.9(13)
C(36)	33.3(19)	30.2(18)	26.9(17)	0.0(15)	-12.2(15)	-6.2(15)
C(37)	32.7(17)	23.2(17)	17.6(13)	3.4(13)	-6.0(12)	-3.8(14)
C(38)	17.0(12)	20.6(13)	16.3(12)	0.2(14)	1.3(10)	-2.8(13)
C(39)	22.7(15)	27.0(18)	19.3(14)	-3.9(13)	-2.9(12)	3.1(13)
C(40)	27.1(18)	31.4(18)	23.7(16)	-1.1(14)	-9.9(14)	5.4(14)
C(41)	21.6(16)	24.4(16)	32.2(18)	0.9(14)	-1.5(14)	7.5(13)
C(42)	26.1(17)	19.8(15)	24.8(16)	-3.7(13)	5.9(13)	-0.9(13)

Table II.3 Continued.

C(43)	22.3(15)	19.7(14)	16.6(14)	0.6(12)	0.3(12)	-3.5(12)
B(1)	15.7(15)	21.9(16)	13.5(14)	-1.3(13)	2.8(12)	-3.2(13)
N(49)	53(2)	53(2)	64(3)	22(2)	20(2)	11(2)
C(44)	29.0(19)	31.6(19)	42(2)	3.3(17)	6.4(16)	-1.0(15)
C(45)	33(2)	28.7(19)	52(3)	3.9(18)	8.7(18)	8.7(16)

Table II.4 Bond Lengths for $[WH(CPh)(dmpe)_2Cl][B(C_6F_5)_4]$.

Atom	Atom	Length/Å	Atom	Atom	Length/Å
W(1)	Cl(1)	2.5362(11)	F(5)	C(25)	1.363(4)
W(1)	P(1)	2.4466(9)	F(6)	C(27)	1.350(4)
W(1)	P(2)	2.5600(9)	F(7)	C(28)	1.352(4)
W(1)	P(3)	2.5599(9)	F(8)	C(29)	1.342(4)
W(1)	P(4)	2.4623(8)	F(9)	C(30)	1.344(4)
W(1)	C(1)	1.809(3)	F(10)	C(31)	1.344(4)
W(1X)	Cl(1X)	2.564(16)	F(11)	C(33)	1.355(3)
W(1X)	P(1)	2.837(3)	F(12)	C(34)	1.345(4)
W(1X)	P(2)	2.282(2)	F(13)	C(35)	1.345(4)
W(1X)	P(3)	2.125(3)	F(14)	C(36)	1.347(4)
W(1X)	P(4)	2.704(2)	F(15)	C(37)	1.354(4)
W(1X)	C(1)	1.850(4)	F(16)	C(39)	1.354(4)
P(1)	C(8)	1.810(4)	F(17)	C(40)	1.346(4)
P(1)	C(9)	1.803(4)	F(18)	C(41)	1.337(4)
P(1)	C(10A)	1.818(5)	F(19)	C(42)	1.342(4)
P(1)	C(10B)	1.929(14)	F(20)	C(43)	1.358(3)
P(2)	C(11A)	1.899(4)	C(20)	C(21)	1.389(4)
P(2)	C(12A)	1.772(5)	C(20)	C(25)	1.392(4)
P(2)	C(13A)	1.812(11)	C(20)	B(1)	1.658(5)
P(2)	C(11B)	1.665(12)	C(21)	C(22)	1.381(4)
P(2)	C(12B)	1.988(15)	C(22)	C(23)	1.363(5)
P(2)	C(13B)	1.75(3)	C(23)	C(24)	1.377(5)
P(3)	C(14A)	1.914(12)	C(24)	C(25)	1.369(4)
P(3)	C(15A)	1.747(13)	C(26)	C(27)	1.392(5)
P(3)	C(16A)	1.694(13)	C(26)	C(31)	1.386(5)
P(3)	C(14B)	1.804(5)	C(26)	B(1)	1.655(5)
P(3)	C(15B)	1.813(5)	C(27)	C(28)	1.382(5)
P(3)	C(16B)	1.900(5)	C(28)	C(29)	1.367(5)
P(4)	C(17A)	1.95(2)	C(29)	C(30)	1.365(6)
P(4)	C(17B)	1.806(7)	C(30)	C(31)	1.389(5)
P(4)	C(18)	1.808(3)	C(32)	C(33)	1.389(4)
P(4)	C(19)	1.808(3)	C(32)	C(37)	1.392(4)
C(1)	C(2)	1.446(4)	C(32)	B(1)	1.651(5)
C(2)	C(3)	1.402(4)	C(33)	C(34)	1.380(4)
C(2)	C(7)	1.412(4)	C(34)	C(35)	1.376(5)
C(3)	C(4)	1.374(4)	C(35)	C(36)	1.361(5)
C(4)	C(5)	1.386(5)	C(36)	C(37)	1.377(5)
C(5)	C(6)	1.383(5)	C(38)	C(39)	1.392(4)
C(6)	C(7)	1.381(4)	C(38)	C(43)	1.390(4)

Table II.4 Continued

C(10A)	C(11A)	1.516(7)	C(38)	B(1)	1.645(5)
C(10B)	C(11B)	1.468(19)	C(39)	C(40)	1.377(5)
C(16A)	C(17A)	1.53(3)	C(40)	C(41)	1.370(5)
C(16B)	C(17B)	1.515(7)	C(41)	C(42)	1.379(5)
F(1)	C(21)	1.352(4)	C(42)	C(43)	1.372(5)
F(2)	C(22)	1.341(4)	N(49)	C(45)	1.140(5)
F(3)	C(23)	1.352(4)	C(44)	C(45)	1.454(6)
F(4)	C(24)	1.343(4)			

Table II.5 Bond Angles for [WH(CPh)(dmpe)$_2$Cl][B(C$_6$F$_5$)$_4$].

Atom	Atom	Atom	Angle/°	Atom	Atom	Atom	Angle/°
Cl(1)	W(1)	P(2)	85.35(3)	C(10A)	C(11A)	P(2)	110.2(3)
Cl(1)	W(1)	P(3)	85.12(3)	C(11B)	C(10B)	P(1)	110.4(9)
P(1)	W(1)	Cl(1)	89.96(4)	C(10B)	C(11B)	P(2)	107.0(9)
P(1)	W(1)	P(2)	76.96(3)	C(17A)	C(16A)	P(3)	108.4(12)
P(1)	W(1)	P(3)	163.04(3)	C(16A)	C(17A)	P(4)	107.1(14)
P(1)	W(1)	P(4)	119.13(3)	C(17B)	C(16B)	P(3)	108.8(4)
P(3)	W(1)	P(2)	86.45(3)	C(16B)	C(17B)	P(4)	108.2(4)
P(4)	W(1)	Cl(1)	87.53(3)	C(21)	C(20)	C(25)	112.5(3)
P(4)	W(1)	P(2)	162.42(3)	C(21)	C(20)	B(1)	127.6(3)
P(4)	W(1)	P(3)	76.94(3)	C(25)	C(20)	B(1)	119.6(3)
C(1)	W(1)	Cl(1)	179.09(10)	F(1)	C(21)	C(20)	120.7(3)
C(1)	W(1)	P(1)	90.19(10)	F(1)	C(21)	C(22)	114.8(3)
C(1)	W(1)	P(2)	93.80(10)	C(22)	C(21)	C(20)	124.4(3)
C(1)	W(1)	P(3)	94.47(10)	F(2)	C(22)	C(21)	120.4(3)
C(1)	W(1)	P(4)	93.18(9)	F(2)	C(22)	C(23)	119.9(3)
Cl(1X)	W(1X)	P(1)	89.1(4)	C(23)	C(22)	C(21)	119.7(3)
Cl(1X)	W(1X)	P(4)	83.8(4)	F(3)	C(23)	C(22)	120.7(3)
P(2)	W(1X)	Cl(1X)	87.0(4)	F(3)	C(23)	C(24)	120.3(3)
P(2)	W(1X)	P(1)	74.12(6)	C(22)	C(23)	C(24)	118.9(3)
P(2)	W(1X)	P(4)	168.95(11)	F(4)	C(24)	C(23)	119.5(3)
P(3)	W(1X)	Cl(1X)	83.3(4)	F(4)	C(24)	C(25)	121.2(3)
P(3)	W(1X)	P(1)	172.40(9)	C(25)	C(24)	C(23)	119.3(3)
P(3)	W(1X)	P(2)	105.35(13)	F(5)	C(25)	C(20)	119.2(3)
P(3)	W(1X)	P(4)	79.66(6)	F(5)	C(25)	C(24)	115.8(3)
P(4)	W(1X)	P(1)	99.58(10)	C(24)	C(25)	C(20)	125.1(3)
C(1)	W(1X)	Cl(1X)	161.1(4)	C(27)	C(26)	B(1)	119.1(3)
C(1)	W(1X)	P(1)	78.00(13)	C(31)	C(26)	C(27)	113.1(3)
C(1)	W(1X)	P(2)	102.38(12)	C(31)	C(26)	B(1)	127.4(3)
C(1)	W(1X)	P(3)	109.37(14)	F(6)	C(27)	C(26)	119.6(3)
C(1)	W(1X)	P(4)	84.81(12)	F(6)	C(27)	C(28)	116.4(3)
C(8)	P(1)	W(1)	116.23(14)	C(28)	C(27)	C(26)	124.0(3)
C(8)	P(1)	W(1X)	120.90(14)	F(7)	C(28)	C(27)	120.3(3)
C(8)	P(1)	C(10A)	99.0(2)	F(7)	C(28)	C(29)	119.4(3)
C(8)	P(1)	C(10B)	119.6(5)	C(29)	C(28)	C(27)	120.2(3)
C(9)	P(1)	W(1)	115.73(15)	F(8)	C(29)	C(28)	120.5(4)
C(9)	P(1)	W(1X)	118.76(15)	F(8)	C(29)	C(30)	121.0(3)
C(9)	P(1)	C(8)	103.70(18)	C(30)	C(29)	C(28)	118.6(3)
C(9)	P(1)	C(10A)	107.4(2)	F(9)	C(30)	C(29)	119.9(3)
C(9)	P(1)	C(10B)	92.4(5)	F(9)	C(30)	C(31)	120.2(4)

Table II.5 Continued.

C(10A)	P(1)	W(1)	113.02(15)	C(29)	C(30)	C(31)	119.9(3)
C(10B)	P(1)	W(1X)	98.7(4)	F(10)	C(31)	C(26)	121.7(3)
C(11A)	P(2)	W(1)	108.00(14)	F(10)	C(31)	C(30)	114.0(3)
C(12A)	P(2)	W(1)	117.21(19)	C(26)	C(31)	C(30)	124.2(3)
C(12A)	P(2)	C(11A)	102.4(3)	C(33)	C(32)	C(37)	112.7(3)
C(12A)	P(2)	C(13A)	105.2(3)	C(33)	C(32)	B(1)	119.4(2)
C(13A)	P(2)	W(1)	121.8(4)	C(37)	C(32)	B(1)	127.7(3)
C(13A)	P(2)	C(11A)	99.1(3)	F(11)	C(33)	C(32)	119.3(3)
C(11B)	P(2)	W(1X)	117.8(5)	F(11)	C(33)	C(34)	115.9(3)
C(11B)	P(2)	C(12B)	102.4(7)	C(34)	C(33)	C(32)	124.8(3)
C(11B)	P(2)	C(13B)	112.5(12)	F(12)	C(34)	C(33)	120.9(3)
C(12B)	P(2)	W(1X)	99.7(5)	F(12)	C(34)	C(35)	119.9(3)
C(13B)	P(2)	W(1X)	118.3(12)	C(35)	C(34)	C(33)	119.2(3)
C(13B)	P(2)	C(12B)	102.1(10)	F(13)	C(35)	C(34)	120.5(3)
C(14A)	P(3)	W(1)	114.1(4)	F(13)	C(35)	C(36)	120.7(3)
C(15A)	P(3)	W(1)	116.6(5)	C(36)	C(35)	C(34)	118.8(3)
C(15A)	P(3)	C(14A)	102.2(7)	F(14)	C(36)	C(35)	119.5(3)
C(16A)	P(3)	W(1)	109.1(4)	F(14)	C(36)	C(37)	120.1(3)
C(16A)	P(3)	C(14A)	102.9(6)	C(35)	C(36)	C(37)	120.4(3)
C(16A)	P(3)	C(15A)	111.0(7)	F(15)	C(37)	C(32)	120.8(3)
C(14B)	P(3)	W(1X)	113.94(19)	F(15)	C(37)	C(36)	115.1(3)
C(14B)	P(3)	C(15B)	104.0(2)	C(36)	C(37)	C(32)	124.1(3)
C(14B)	P(3)	C(16B)	101.0(3)	C(39)	C(38)	B(1)	127.9(3)
C(15B)	P(3)	W(1X)	120.31(19)	C(43)	C(38)	C(39)	112.7(3)
C(15B)	P(3)	C(16B)	99.4(2)	C(43)	C(38)	B(1)	119.2(2)
C(16B)	P(3)	W(1X)	115.42(16)	F(16)	C(39)	C(38)	120.8(3)
C(17A)	P(4)	W(1)	109.5(8)	F(16)	C(39)	C(40)	115.2(3)
C(17B)	P(4)	W(1X)	103.6(3)	C(40)	C(39)	C(38)	124.0(3)
C(17B)	P(4)	C(18)	100.9(2)	F(17)	C(40)	C(39)	120.4(3)
C(17B)	P(4)	C(19)	105.1(3)	F(17)	C(40)	C(41)	119.2(3)
C(18)	P(4)	W(1)	115.35(12)	C(41)	C(40)	C(39)	120.4(3)
C(18)	P(4)	W(1X)	120.03(12)	F(18)	C(41)	C(40)	120.8(3)
C(18)	P(4)	C(17A)	112.1(6)	F(18)	C(41)	C(42)	120.8(3)
C(18)	P(4)	C(19)	103.26(16)	C(40)	C(41)	C(42)	118.3(3)
C(19)	P(4)	W(1)	115.81(12)	F(19)	C(42)	C(41)	119.3(3)
C(19)	P(4)	W(1X)	121.19(13)	F(19)	C(42)	C(43)	121.3(3)
C(19)	P(4)	C(17A)	99.8(7)	C(43)	C(42)	C(41)	119.4(3)
C(2)	C(1)	W(1)	176.6(2)	F(20)	C(43)	C(38)	118.9(3)
C(2)	C(1)	W(1X)	166.1(3)	F(20)	C(43)	C(42)	116.0(3)
C(3)	C(2)	C(1)	122.0(3)	C(42)	C(43)	C(38)	125.1(3)
C(3)	C(2)	C(7)	117.4(3)	C(26)	B(1)	C(20)	101.9(2)

C(7)	C(2)	C(1)	120.7(3)
C(4)	C(3)	C(2)	121.4(3)
C(3)	C(4)	C(5)	120.3(3)
C(6)	C(5)	C(4)	119.8(3)
C(7)	C(6)	C(5)	120.3(3)
C(6)	C(7)	C(2)	120.9(3)
C(11A)	C(10A)	P(1)	105.8(3)

C(32)	B(1)	C(20)	113.0(2)
C(32)	B(1)	C(26)	113.3(2)
C(38)	B(1)	C(20)	113.2(2)
C(38)	B(1)	C(26)	112.8(2)
C(38)	B(1)	C(32)	103.1(2)
N(49)	C(45)	C(44)	178.9(5)

Table II.6 Torsion Angles for [WH(CPh)(dmpe)$_2$Cl][B(C$_6$F$_5$)$_4$].

A	B	C	D	Angle/°	A	B	C	D	Angle/°
W(1)	P(1)	C(10A)	C(11A)	50.3(3)	C(22)	C(23)	C(24)	C(25)	-1.5(5)
W(1)	P(2)	C(11A)	C(10A)	37.3(3)	C(23)	C(24)	C(25)	F(5)	-178.3(3)
W(1)	P(3)	C(16A)	C(17A)	55.7(10)	C(23)	C(24)	C(25)	C(20)	1.6(5)
W(1X)	P(2)	C(11B)	C(10B)	-62.7(10)	C(25)	C(20)	C(21)	F(1)	177.3(3)
W(1X)	P(3)	C(16B)	C(17B)	-46.8(4)	C(25)	C(20)	C(21)	C(22)	-1.8(5)
W(1X)	P(4)	C(17B)	C(16B)	-39.0(5)	C(25)	C(20)	B(1)	C(26)	-57.3(3)
W(1X)	C(1)	C(2)	C(3)	-76.0(10)	C(25)	C(20)	B(1)	C(32)	-179.2(3)
W(1X)	C(1)	C(2)	C(7)	104.9(10)	C(25)	C(20)	B(1)	C(38)	64.1(4)
Cl(1X)	W(1X)	C(1)	C(2)	174.6(15)	C(26)	C(27)	C(28)	F(7)	179.8(3)
P(1)	W(1X)	C(1)	C(2)	-137.5(10)	C(26)	C(27)	C(28)	C(29)	0.3(5)
P(1)	C(10A)	C(11A)	P(2)	-54.3(4)	C(27)	C(26)	C(31)	F(10)	177.9(3)
P(1)	C(10B)	C(11B)	P(2)	58.6(11)	C(27)	C(26)	C(31)	C(30)	-0.2(5)
P(2)	W(1X)	C(1)	C(2)	-67.0(10)	C(27)	C(26)	B(1)	C(20)	-58.1(3)
P(3)	W(1X)	C(1)	C(2)	44.4(10)	C(27)	C(26)	B(1)	C(32)	63.6(4)
P(3)	C(16A)	C(17A)	P(4)	-56.8(12)	C(27)	C(26)	B(1)	C(38)	-179.8(3)
P(3)	C(16B)	C(17B)	P(4)	53.7(5)	C(27)	C(28)	C(29)	F(8)	-179.4(3)
P(4)	W(1X)	C(1)	C(2)	121.5(10)	C(27)	C(28)	C(29)	C(30)	0.9(5)
C(1)	C(2)	C(3)	C(4)	-177.9(3)	C(28)	C(29)	C(30)	F(9)	179.6(3)
C(1)	C(2)	C(7)	C(6)	177.9(3)	C(28)	C(29)	C(30)	C(31)	-1.7(5)
C(2)	C(3)	C(4)	C(5)	-0.1(5)	C(29)	C(30)	C(31)	F(10)	-176.8(3)
C(3)	C(2)	C(7)	C(6)	-1.2(4)	C(29)	C(30)	C(31)	C(26)	1.4(5)
C(3)	C(4)	C(5)	C(6)	-1.1(5)	C(31)	C(26)	C(27)	F(6)	179.7(3)
C(4)	C(5)	C(6)	C(7)	1.1(5)	C(31)	C(26)	C(27)	C(28)	-0.7(5)
C(5)	C(6)	C(7)	C(2)	0.0(5)	C(31)	C(26)	B(1)	C(20)	114.1(3)
C(7)	C(2)	C(3)	C(4)	1.2(5)	C(31)	C(26)	B(1)	C(32)	-124.3(3)
C(8)	P(1)	C(10A)	C(11A)	173.9(3)	C(31)	C(26)	B(1)	C(38)	-7.7(4)
C(9)	P(1)	C(10A)	C(11A)	-78.6(3)	C(32)	C(33)	C(34)	F(12)	-178.8(3)
C(12A)	P(2)	C(11A)	C(10A)	-87.1(4)	C(32)	C(33)	C(34)	C(35)	0.6(5)
C(13A)	P(2)	C(11A)	C(10A)	165.1(4)	C(33)	C(32)	C(37)	F(15)	-177.1(3)
C(12B)	P(2)	C(11B)	C(10B)	-170.8(10)	C(33)	C(32)	C(37)	C(36)	2.1(5)
C(13B)	P(2)	C(11B)	C(10B)	80.2(14)	C(33)	C(32)	B(1)	C(20)	-62.9(4)
C(14A)	P(3)	C(16A)	C(17A)	177.2(10)	C(33)	C(32)	B(1)	C(26)	-178.2(3)
C(15A)	P(3)	C(16A)	C(17A)	-74.1(12)	C(33)	C(32)	B(1)	C(38)	59.6(3)
C(14B)	P(3)	C(16B)	C(17B)	76.6(4)	C(33)	C(34)	C(35)	F(13)	178.9(3)
C(15B)	P(3)	C(16B)	C(17B)	-177.0(4)	C(33)	C(34)	C(35)	C(36)	0.5(5)
C(18)	P(4)	C(17B)	C(16B)	-163.8(4)	C(34)	C(35)	C(36)	F(14)	177.5(3)
C(19)	P(4)	C(17B)	C(16B)	89.1(5)	C(34)	C(35)	C(36)	C(37)	-0.2(6)
F(1)	C(21)	C(22)	F(2)	2.0(5)	C(35)	C(36)	C(37)	F(15)	178.0(3)
F(1)	C(21)	C(22)	C(23)	-177.2(3)	C(35)	C(36)	C(37)	C(32)	-1.2(6)

Table II.6 Continued.

F(2)	C(22)	C(23)	F(3)	-0.8(5)	C(37)	C(32)	C(33)	F(11)	178.5(3)
F(2)	C(22)	C(23)	C(24)	-179.4(3)	C(37)	C(32)	C(33)	C(34)	-1.8(5)
F(3)	C(23)	C(24)	F(4)	0.2(5)	C(37)	C(32)	B(1)	C(20)	123.0(3)
F(3)	C(23)	C(24)	C(25)	179.9(3)	C(37)	C(32)	B(1)	C(26)	7.8(5)
F(4)	C(24)	C(25)	F(5)	1.5(5)	C(37)	C(32)	B(1)	C(38)	-114.4(3)
F(4)	C(24)	C(25)	C(20)	-178.6(3)	C(38)	C(39)	C(40)	F(17)	-178.5(3)
F(6)	C(27)	C(28)	F(7)	-0.6(5)	C(38)	C(39)	C(40)	C(41)	0.5(6)
F(6)	C(27)	C(28)	C(29)	-180.0(3)	C(39)	C(38)	C(43)	F(20)	179.1(3)
F(7)	C(28)	C(29)	F(8)	1.2(5)	C(39)	C(38)	C(43)	C(42)	-2.3(5)
F(7)	C(28)	C(29)	C(30)	-178.5(3)	C(39)	C(38)	B(1)	C(20)	7.5(5)
F(8)	C(29)	C(30)	F(9)	-0.1(5)	C(39)	C(38)	B(1)	C(26)	122.6(3)
F(8)	C(29)	C(30)	C(31)	178.6(3)	C(39)	C(38)	B(1)	C(32)	-114.9(3)
F(9)	C(30)	C(31)	F(10)	1.9(5)	C(39)	C(40)	C(41)	F(18)	179.6(3)
F(9)	C(30)	C(31)	C(26)	-179.9(3)	C(39)	C(40)	C(41)	C(42)	-1.3(6)
F(11)	C(33)	C(34)	F(12)	0.9(4)	C(40)	C(41)	C(42)	F(19)	-180.0(3)
F(11)	C(33)	C(34)	C(35)	-179.7(3)	C(40)	C(41)	C(42)	C(43)	0.3(5)
F(12)	C(34)	C(35)	F(13)	-1.6(5)	C(41)	C(42)	C(43)	F(20)	-179.7(3)
F(12)	C(34)	C(35)	C(36)	179.9(3)	C(41)	C(42)	C(43)	C(38)	1.6(5)
F(13)	C(35)	C(36)	F(14)	-0.9(6)	C(43)	C(38)	C(39)	F(16)	-177.9(3)
F(13)	C(35)	C(36)	C(37)	-178.6(3)	C(43)	C(38)	C(39)	C(40)	1.2(5)
F(14)	C(36)	C(37)	F(15)	0.3(5)	C(43)	C(38)	B(1)	C(20)	-177.2(3)
F(14)	C(36)	C(37)	C(32)	-178.9(3)	C(43)	C(38)	B(1)	C(26)	-62.1(4)
F(16)	C(39)	C(40)	F(17)	0.7(5)	C(43)	C(38)	B(1)	C(32)	60.5(3)
F(16)	C(39)	C(40)	C(41)	179.7(3)	B(1)	C(20)	C(21)	F(1)	4.0(5)
F(17)	C(40)	C(41)	F(18)	-1.4(6)	B(1)	C(20)	C(21)	C(22)	-175.2(3)
F(17)	C(40)	C(41)	C(42)	177.7(3)	B(1)	C(20)	C(25)	F(5)	-6.2(4)
F(18)	C(41)	C(42)	F(19)	-0.9(5)	B(1)	C(20)	C(25)	C(24)	173.9(3)
F(18)	C(41)	C(42)	C(43)	179.4(3)	B(1)	C(26)	C(27)	F(6)	-7.1(4)
F(19)	C(42)	C(43)	F(20)	0.6(5)	B(1)	C(26)	C(27)	C(28)	172.5(3)
F(19)	C(42)	C(43)	C(38)	-178.1(3)	B(1)	C(26)	C(31)	F(10)	5.3(5)
C(20)	C(21)	C(22)	F(2)	-178.8(3)	B(1)	C(26)	C(31)	C(30)	-172.7(3)
C(20)	C(21)	C(22)	C(23)	2.0(5)	B(1)	C(32)	C(33)	F(11)	3.6(4)
C(21)	C(20)	C(25)	F(5)	179.9(3)	B(1)	C(32)	C(33)	C(34)	-176.7(3)
C(21)	C(20)	C(25)	C(24)	0.0(5)	B(1)	C(32)	C(37)	F(15)	-2.7(5)
C(21)	C(20)	B(1)	C(26)	115.6(3)	B(1)	C(32)	C(37)	C(36)	176.5(3)
C(21)	C(20)	B(1)	C(32)	-6.3(4)	B(1)	C(38)	C(39)	F(16)	-2.3(5)
C(21)	C(20)	B(1)	C(38)	-123.0(3)	B(1)	C(38)	C(39)	C(40)	176.9(3)
C(21)	C(22)	C(23)	F(3)	178.4(3)	B(1)	C(38)	C(43)	F(20)	3.0(4)
C(21)	C(22)	C(23)	C(24)	-0.2(5)	B(1)	C(38)	C(43)	C(42)	-178.4(3)
C(22)	C(23)	C(24)	F(4)	178.7(3)					

Table II.7 Hydrogen Atom Coordinates (Å×10^4) and Isotropic Displacement Parameters (Å^2×10^3) for [WH(CPh)(dmpe)$_2$Cl][B(C$_6$F$_5$)$_4$].

Atom	***x***	***y***	***z***	**U(eq)**
H	4205(15)	1100(40)	2594(11)	14
H(3)	3724.95	6096.81	3061.61	25
H(4)	2951.73	7993.61	2964.36	30
H(5)	2477.99	8365.23	2240.22	31
H(6)	2807.37	6874.06	1606.29	27
H(7)	3582.47	4960.14	1696.86	21
H(8A)	3278.07	574.21	2074.42	58
H(8B)	3321.64	556.48	1521.98	58
H(8C)	3314.84	2230.34	1794.6	58
H(9A)	4925.99	-1175.84	1784.78	58
H(9B)	4283.27	-1470.98	1515.22	58
H(9C)	4318.35	-1625.25	2067.14	58
H(10A)	4344.83	1329.07	1041.87	29
H(10B)	4262.81	3067.77	1276.84	29
H(11A)	5296.97	2847.6	1033.18	28
H(11B)	5377.88	1179.23	1305	28
H(12A)	4912.15	5664.13	1625.99	55
H(12B)	5575.68	5575.7	1388.42	55
H(12C)	5523.34	6112.06	1918.32	55
H(13A)	6467.12	3661.7	2058.95	37
H(13B)	6402.22	3159.82	1525.68	37
H(13C)	6322.93	1834.86	1921.86	37
H(10C)	5136.49	870.93	1300.57	29
H(10D)	4526.25	1508.2	1036.61	29
H(11C)	4657.89	4035.91	1373.16	28
H(11D)	5268.66	3548.41	1094.89	28
H(12D)	5190.78	6273.33	1980.62	55
H(12E)	5749.37	6138.35	1625.19	55
H(12F)	5877.68	5912.69	2168.33	55
H(13D)	6418.39	2822.86	2072.71	37
H(13E)	6374.03	3143.31	1527.02	37
H(13F)	6155.19	1455.38	1733.56	37
H(14A)	5938.92	6055.01	2554.18	44
H(14B)	5899.24	6744.15	3070.01	44
H(14C)	5293.14	6700.67	2744.68	44
H(15A)	6184.53	2129.47	3274.24	44
H(15B)	6456.39	3891.43	3366.63	44
H(15C)	6446.02	3165.94	2853.57	44

Table II.7 Continued.

H(16A)	5422.79	4961.85	3774.26	29
H(16B)	4770.7	5117.79	3503.69	29
H(17A)	4694.88	2993.08	4053.47	23
H(17B)	5288.91	2123.26	3837.63	23
H(14D)	5324.52	6721.85	2870.94	57
H(14E)	5571.82	6550.39	3393.6	57
H(14F)	4863.06	6164.81	3268.23	57
H(15D)	6475.21	2965.18	2950.6	44
H(15E)	6510.13	4490.15	3287.48	44
H(15F)	6440.19	4742.21	2740.03	44
H(16C)	5641.16	2100.09	3669.07	28
H(16D)	5620.94	3877.97	3883.83	28
H(17C)	4540.36	3985.04	3786.94	23
H(17D)	4703.42	2358.37	4061.95	23
H(18A)	3492.67	3284.08	3355.41	46
H(18B)	3480.67	1837.39	3720.13	46
H(18C)	3329.1	1502.16	3184.84	46
H(19A)	4232.12	-1000.64	3276.87	39
H(19B)	4362.35	-435.6	3798.81	39
H(19C)	4924.55	-618.28	3448.32	39
H(A)	7134.24	-2516.33	3016.39	51
H(B)	6566.78	-1293.7	3063.26	51
H(C)	7229.26	-846.37	3282.86	51

Table II.8 Atomic Occupancy for [WH(CPh)(dmpe)$_2$Cl][B(C$_6$F$_5$)$_4$].

Atom	***Occupancy***	**Atom**	***Occupancy***	**Atom**	***Occupancy***
W(1)	0.9184(8)	Cl(1)	0.9184(8)	W(1X)	0.0816(8)
Cl(1X)	0.0816(8)	C(10A)	0.734(5)	H(10A)	0.734(5)
H(10B)	0.734(5)	C(11A)	0.734(5)	H(11A)	0.734(5)
H(11B)	0.734(5)	C(12A)	0.734(5)	H(12A)	0.734(5)
H(12B)	0.734(5)	H(12C)	0.734(5)	C(13A)	0.734(5)
H(13A)	0.734(5)	H(13B)	0.734(5)	H(13C)	0.734(5)
C(10B)	0.266(5)	H(10C)	0.266(5)	H(10D)	0.266(5)
C(11B)	0.266(5)	H(11C)	0.266(5)	H(11D)	0.266(5)
C(12B)	0.266(5)	H(12D)	0.266(5)	H(12E)	0.266(5)
H(12F)	0.266(5)	C(13B)	0.266(5)	H(13D)	0.266(5)
H(13E)	0.266(5)	H(13F)	0.266(5)	C(14A)	0.269(5)
H(14A)	0.269(5)	H(14B)	0.269(5)	H(14C)	0.269(5)
C(15A)	0.269(5)	H(15A)	0.269(5)	H(15B)	0.269(5)
H(15C)	0.269(5)	C(16A)	0.269(5)	H(16A)	0.269(5)
H(16B)	0.269(5)	C(17A)	0.269(5)	H(17A)	0.269(5)
H(17B)	0.269(5)	C(14B)	0.731(5)	H(14D)	0.731(5)
H(14E)	0.731(5)	H(14F)	0.731(5)	C(15B)	0.731(5)
H(15D)	0.731(5)	H(15E)	0.731(5)	H(15F)	0.731(5)
C(16B)	0.731(5)	H(16C)	0.731(5)	H(16D)	0.731(5)
C(17B)	0.731(5)	H(17C)	0.731(5)	H(17D)	0.731(5)

Table II.9 Solvent masks information for [WH(CPh)(dmpe)$_2$Cl][B(C$_6$F$_5$)$_4$].

Number	**X**	**Y**	**Z**	**Volume**	**Electron count**	**Content**
1	0.000	0.000	0.000	93.7	23.2	None
2	0.000	0.500	0.500	81.5	23.8	?
3	0.500	0.500	0.500	93.7	23.2	?
4	0.500	0.000	0.000	81.5	23.8	?

II.2 Diffraction data for [W(CPh)(P_2NN)$_2$Cl]• ½ Et_2O

Table II.10 Crystal data and structure refinement for W(CPh)(P_2NN)$_2$Cl.

Identification code	W(CPh)(P_2NN)$_2$Cl
Empirical formula	$C_{39}H_{82}ClN_4O_{0.5}P_4W$
Formula weight	958.26
Temperature/K	100(2)
Crystal system	triclinic
Space group	P-1
a/Å	10.1671(7)
b/Å	11.6237(8)
c/Å	20.2729(14)
α/°	105.457(2)
β/°	96.009(2)
γ/°	90.452(2)
Volume/Å^3	2294.9(3)
Z	2
ρ_{calc}g/cm^3	1.387
μ/mm^{-1}	2.746
F(000)	998.0
Crystal size/mm^3	0.317 × 0.278 × 0.194
Radiation	MoKα (λ = 0.71073)
2Θ range for data collection/°	4.334 to 61.262
Index ranges	$-14 \leq h \leq 14$, $-16 \leq k \leq 16$, $0 \leq l \leq 29$
Reflections collected	14617
Independent reflections	14617 [R_{int} = ?, R_{sigma} = 0.0313]
Data/restraints/parameters	14617/27/496
Goodness-of-fit on F^2	1.089
Final R indexes [I>=2σ (I)]	R_1 = 0.0313, wR_2 = 0.0693
Final R indexes [all data]	R_1 = 0.0349, wR_2 = 0.0713
Largest diff. peak/hole / e Å^{-3}	2.19/-1.20

Table II.11. Fractional Atomic Coordinates ($\times 10^4$) and Equivalent Isotropic Displacement Parameters ($Å^2 \times 10^3$) for $W(CPh)(P_2NN)_2Cl$. U_{eq} is defined as 1/3 of of the trace of the orthogonalised U_{IJ} tensor.

Atom	***x***	***y***	***z***	**U(eq)**
W(1)	5598.7(2)	6875.7(2)	3142.1(2)	9.84(3)
Cl(1)	5654.2(8)	9187.5(6)	3499.4(4)	18.21(13)
P(1)	6545.5(7)	6953.8(7)	2085.8(4)	11.83(13)
P(2)	3452.5(8)	6822.8(7)	2450.2(4)	11.94(14)
P(3)	4651.2(7)	7322.6(6)	4264.6(4)	11.44(13)
P(4)	7735.1(8)	7028.5(8)	3888.1(4)	17.10(15)
N(1)	4253(3)	6633(2)	1162.3(12)	13.6(5)
N(2)	6947(3)	7888(2)	5185.8(13)	16.5(5)
C(1)	5536(3)	5257(2)	2913.8(14)	12.6(5)
C(2)	5453(3)	3957(3)	2727.6(16)	16.1(5)
C(3)	5528(3)	3329(3)	3230.0(18)	21.9(6)
C(4)	5419(4)	2090(3)	3050(2)	28.5(8)
C(5)	5224(4)	1454(3)	2368(2)	29.7(8)
C(6)	5154(4)	2050(3)	1860(2)	28.4(8)
C(7)	5281(4)	3289(3)	2036.4(17)	21.6(6)
C(8)	8148(3)	6294(3)	1878.4(16)	17.6(6)
C(9)	8251(4)	5003(3)	1915(2)	27.6(7)
C(10)	6727(3)	8459(3)	1968.6(16)	17.2(6)
C(11)	7565(4)	8641(3)	1421.3(19)	27.2(7)
C(13)	5599(3)	6210(3)	1244.5(14)	14.5(5)
C(14)	3751(3)	6393(3)	426.6(15)	20.1(6)
C(15)	4366(4)	7217(3)	65.9(18)	26.6(8)
C(16)	4075(4)	8517(3)	354.3(19)	28.3(8)
N(17)	2674(4)	8763(3)	277.5(16)	30.3(7)
C(19)	2426(6)	9957(4)	682(2)	42.8(11)
C(20)	2182(6)	8635(5)	-441(2)	51.3(14)
C(21)	3374(3)	6075(3)	1523.0(15)	15.5(6)
C(22)	2762(3)	8279(3)	2435.2(16)	16.8(6)
C(23)	1610(4)	8292(3)	1888.6(18)	22.8(7)
C(24)	2001(3)	6012(3)	2618.7(16)	18.6(6)
C(25)	2045(3)	4649(3)	2404.9(18)	22.6(7)
C(26)	9350(3)	7390(4)	3641.0(18)	27.1(8)
C(27)	9449(4)	8628(4)	3519(2)	33.5(9)
C(28)	8027(15)	5537(14)	4083(8)	23(2)
C(29)	9333(8)	5380(7)	4473(4)	36(2)
C(28A)	8246(17)	5798(16)	4230(10)	25(3)
C(29A)	8827(8)	4782(7)	3744(5)	32(2)

Table II.11 Continued

C(30)	7885(3)	8139(3)	4736.1(15)	21.0(6)
C(31)	7423(3)	8450(3)	5915.1(15)	18.9(6)
C(32)	8616(3)	7867(3)	6185.4(16)	19.2(6)
C(33)	8872(4)	8348(3)	6964.1(17)	24.1(7)
N(34)	9918(3)	7755(3)	7275.7(16)	25.7(6)
C(35)	11204(5)	8031(6)	7096(3)	59.7(16)
C(36)	9929(5)	8098(4)	8021(2)	38.1(10)
C(37)	5643(3)	8328(3)	5016.6(14)	15.3(5)
C(38)	4340(3)	6071(3)	4624.2(15)	16.8(5)
C(39)	3237(3)	5187(3)	4218.2(17)	21.3(6)
C(40)	3102(3)	8144(3)	4342.1(15)	16.1(5)
C(41)	2456(3)	8341(3)	5012.3(17)	22.2(6)
O(2)	10068(12)	5030(7)	-90(4)	69(2)
C(12)	10889(15)	3210(9)	98(6)	89(5)
C(17)	10117(9)	4313(7)	379(3)	55(2)
C(18)	9364(9)	6092(6)	125(4)	56(2)
C(1A)	9378(17)	6784(9)	-412(6)	97(6)

Table II.12 Anisotropic Displacement Parameters ($Å^2 \times 10^3$) for W(CPh)(P_2NN)$_2$Cl. The Anisotropic displacement factor exponent takes the form: $-2\pi^2[h^2a^{*2}U_{11}+2hka^*b^*U_{12}+\ldots]$.

Atom	**U_{11}**	**U_{22}**	**U_{33}**	**U_{23}**	**U_{13}**	**U_{12}**
W(1)	7.93(5)	9.75(5)	11.75(5)	2.98(3)	0.41(3)	0.09(3)
Cl(1)	21.0(4)	13.6(3)	19.5(3)	3.7(2)	1.6(3)	-0.7(3)
P(1)	9.6(3)	13.4(3)	13.1(3)	4.5(3)	1.3(2)	0.5(3)
P(2)	8.6(3)	13.4(3)	14.1(3)	4.6(3)	0.0(2)	-0.1(3)
P(3)	8.8(3)	13.4(3)	12.0(3)	3.5(2)	0.8(2)	0.2(2)
P(4)	9.4(4)	26.5(4)	15.0(4)	5.3(3)	0.6(3)	3.1(3)
N(1)	11.7(12)	15.4(12)	14.1(11)	5.0(9)	0.2(9)	1.0(9)
N(2)	11.0(11)	24.3(13)	13.5(11)	4.3(10)	0.3(9)	1.8(10)
C(1)	11.0(12)	13.8(12)	13.9(12)	4.8(10)	1.4(9)	3.1(10)
C(2)	12.9(13)	16.5(13)	20.5(14)	6.5(11)	4.1(10)	1.8(11)
C(3)	23.6(17)	18.5(14)	27.7(16)	10.8(12)	8.8(13)	4.6(12)
C(4)	27.3(19)	19.7(16)	46(2)	18.3(15)	14.7(16)	5.9(14)
C(5)	24.8(19)	11.5(14)	53(2)	6.1(14)	12.0(17)	1.7(13)
C(6)	28(2)	17.2(16)	34.7(19)	-1.4(14)	1.9(15)	-3.9(14)
C(7)	23.7(17)	17.1(14)	22.3(15)	3.2(12)	1.4(12)	-0.4(12)
C(8)	12.1(13)	21.8(14)	18.2(14)	3.4(11)	3.1(10)	2.8(11)
C(9)	18.0(16)	22.9(16)	40(2)	5.3(14)	3.4(14)	6.6(13)
C(10)	15.6(14)	16.1(13)	21.6(14)	8.7(11)	1.2(11)	-2.6(11)
C(11)	30(2)	28.6(17)	27.4(17)	14.8(14)	4.0(14)	-8.0(15)
C(13)	16.3(14)	14.2(13)	12.1(12)	1.8(10)	1.4(10)	0.9(11)
C(14)	19.8(16)	24.7(16)	13.8(13)	3.4(12)	-1.8(11)	0.1(13)
C(15)	24.6(19)	40(2)	19.9(15)	16.2(14)	0.0(13)	2.8(16)
C(16)	28(2)	32.0(19)	28.1(18)	17.6(15)	-8.0(14)	-8.7(16)
N(17)	34(2)	33.4(17)	23.9(15)	11.8(13)	-5.3(13)	1.4(15)
C(19)	56(3)	28(2)	44(3)	11.6(18)	-2(2)	0(2)
C(20)	55(3)	61(3)	33(2)	12(2)	-16(2)	20(3)
C(21)	13.4(14)	16.5(14)	15.4(13)	3.4(11)	-1(1)	-2.8(11)
C(22)	15.2(15)	14.9(14)	21.5(15)	7.3(11)	0.7(11)	4.1(11)
C(23)	16.5(16)	25.7(17)	26.9(17)	10.5(13)	-3.5(12)	6.6(13)
C(24)	12.7(14)	22.7(15)	20.3(14)	6.6(12)	-0.6(11)	-6.1(12)
C(25)	19.0(16)	22.6(16)	26.6(16)	8.8(13)	0.0(12)	-5.7(13)
C(26)	10.5(14)	50(2)	20.5(16)	8.5(15)	2.1(11)	-0.1(14)
C(27)	20.3(18)	50(2)	33(2)	16.9(18)	3.7(15)	-7.2(16)
C(28)	18(4)	23(6)	30(7)	11(4)	-2(4)	-3(4)
C(29)	28(4)	33(4)	41(4)	9(3)	-14(3)	6(3)
C(28A)	21(7)	24(7)	32(7)	13(5)	-4(5)	4(5)
C(29A)	24(4)	32(4)	38(5)	8(3)	-5(3)	6(3)
C(30)	9.3(13)	37.3(18)	12.7(13)	1.7(12)	-2(1)	-4.2(12)

Table II.12 Continued.

C(31)	16.0(14)	25.8(16)	13.5(13)	3.8(12)	-0.7(11)	3.8(12)
C(32)	16.9(15)	22.2(16)	17.9(14)	6.4(12)	-3.4(11)	1.7(12)
C(33)	24.0(17)	27.8(17)	19.0(16)	7.5(13)	-6.7(12)	0.3(14)
N(34)	19.1(15)	31.8(16)	27.0(15)	13.9(12)	-9.8(11)	-5.1(12)
C(35)	19(2)	104(5)	70(4)	55(3)	-14(2)	-10(2)
C(36)	55(3)	29.3(19)	25.9(19)	9.6(15)	-19.8(18)	-3.6(19)
C(37)	12.4(13)	17.8(13)	12.7(12)	-0.4(10)	-0.1(10)	1(1)
C(38)	14.6(13)	19.0(13)	19.0(13)	8.9(11)	1.1(10)	-1.6(11)
C(39)	20.0(15)	20.8(15)	23.9(15)	9.1(12)	-1.2(12)	-6.1(12)
C(40)	8.8(12)	19.9(14)	18.5(13)	3.4(11)	1.3(10)	1.7(10)
C(41)	13.2(14)	28.3(16)	21.3(15)	-1.0(12)	4.9(11)	2.1(12)
O(2)	88(6)	70(4)	52(5)	11(3)	39(4)	-11(4)
C(12)	126(14)	84(7)	72(10)	24(7)	60(10)	10(7)
C(17)	45(6)	74(5)	40(5)	6(4)	11(4)	-21(4)
C(18)	54(6)	71(5)	36(5)	0(4)	5(4)	-19(4)
C(1A)	170(20)	64(7)	53(7)	6(6)	28(8)	-9(8)

Table II.13 Bond Lengths for $W(CPh)(P_2NN)_2Cl$.

Atom	Atom	Length/Å	Atom	Atom	Length/Å
W(1)	Cl(1)	2.5885(7)	C(3)	C(4)	1.389(4)
W(1)	P(1)	2.4606(7)	C(4)	C(5)	1.376(6)
W(1)	P(2)	2.4583(8)	C(5)	C(6)	1.382(6)
W(1)	P(3)	2.4926(7)	C(6)	C(7)	1.389(5)
W(1)	P(4)	2.4900(8)	C(8)	C(9)	1.525(5)
W(1)	C(1)	1.813(3)	C(10)	C(11)	1.524(4)
P(1)	C(8)	1.847(3)	C(14)	C(15)	1.518(5)
P(1)	C(10)	1.838(3)	C(15)	C(16)	1.511(6)
P(1)	C(13)	1.854(3)	C(16)	N(17)	1.456(5)
P(2)	C(21)	1.842(3)	N(17)	C(19)	1.451(5)
P(2)	C(22)	1.844(3)	N(17)	C(20)	1.458(5)
P(2)	C(24)	1.854(3)	C(22)	C(23)	1.529(5)
P(3)	C(37)	1.848(3)	C(24)	C(25)	1.529(5)
P(3)	C(38)	1.832(3)	C(26)	C(27)	1.528(6)
P(3)	C(40)	1.847(3)	C(28)	C(29)	1.510(17)
P(4)	C(26)	1.843(4)	C(28A)	C(29A)	1.49(2)
P(4)	C(28)	1.898(18)	C(31)	C(32)	1.517(4)
P(4)	C(28A)	1.81(2)	C(32)	C(33)	1.521(4)
P(4)	C(30)	1.845(3)	C(33)	N(34)	1.452(4)
N(1)	C(13)	1.466(4)	N(34)	C(35)	1.449(6)
N(1)	C(14)	1.476(4)	N(34)	C(36)	1.454(5)
N(1)	C(21)	1.462(4)	C(38)	C(39)	1.526(4)
N(2)	C(30)	1.464(4)	C(40)	C(41)	1.534(4)
N(2)	C(31)	1.476(4)	O(2)	C(17)	1.4195
N(2)	C(37)	1.466(4)	O(2)	C(18)	1.4198
C(1)	C(2)	1.457(4)	C(12)	C(17)	1.5179
C(2)	C(3)	1.399(4)	C(18)	C(1A)	1.5177
C(2)	C(7)	1.401(4)			

Table II.14. Bond Angles for $W(CPh)(P_2NN)_2Cl$.

Atom	Atom	Atom	Angle/°	Atom	Atom	Atom	Angle/°
P(1)	W(1)	Cl(1)	88.36(2)	C(21)	N(1)	C(13)	110.3(2)
P(1)	W(1)	P(3)	166.36(2)	C(21)	N(1)	C(14)	110.6(2)
P(1)	W(1)	P(4)	96.89(3)	C(30)	N(2)	C(31)	110.6(2)
P(2)	W(1)	Cl(1)	90.61(2)	C(30)	N(2)	C(37)	110.3(2)
P(2)	W(1)	P(1)	84.78(3)	C(37)	N(2)	C(31)	109.7(2)
P(2)	W(1)	P(3)	94.71(2)	C(2)	C(1)	W(1)	178.7(2)
P(2)	W(1)	P(4)	176.88(3)	C(3)	C(2)	C(1)	121.4(3)
P(3)	W(1)	Cl(1)	78.01(2)	C(3)	C(2)	C(7)	117.5(3)
P(4)	W(1)	Cl(1)	86.81(3)	C(7)	C(2)	C(1)	121.1(3)
P(4)	W(1)	P(3)	83.04(3)	C(4)	C(3)	C(2)	121.1(3)
C(1)	W(1)	Cl(1)	178.33(9)	C(5)	C(4)	C(3)	120.3(3)
C(1)	W(1)	P(1)	93.31(9)	C(4)	C(5)	C(6)	119.9(3)
C(1)	W(1)	P(2)	89.41(9)	C(5)	C(6)	C(7)	120.2(3)
C(1)	W(1)	P(3)	100.32(9)	C(6)	C(7)	C(2)	121.0(3)
C(1)	W(1)	P(4)	93.11(9)	C(9)	C(8)	P(1)	114.1(2)
C(8)	P(1)	W(1)	121.64(10)	C(11)	C(10)	P(1)	118.9(2)
C(8)	P(1)	C(13)	96.35(14)	N(1)	C(13)	P(1)	113.73(19)
C(10)	P(1)	W(1)	114.87(10)	N(1)	C(14)	C(15)	113.5(3)
C(10)	P(1)	C(8)	103.05(15)	C(16)	C(15)	C(14)	113.5(3)
C(10)	P(1)	C(13)	98.79(14)	N(17)	C(16)	C(15)	113.6(3)
C(13)	P(1)	W(1)	118.24(10)	C(16)	N(17)	C(20)	111.4(4)
C(21)	P(2)	W(1)	116.96(11)	C(19)	N(17)	C(16)	111.1(4)
C(21)	P(2)	C(22)	101.20(14)	C(19)	N(17)	C(20)	109.2(3)
C(21)	P(2)	C(24)	96.65(14)	N(1)	C(21)	P(2)	113.4(2)
C(22)	P(2)	W(1)	116.49(11)	C(23)	C(22)	P(2)	117.8(2)
C(22)	P(2)	C(24)	101.73(15)	C(25)	C(24)	P(2)	115.6(2)
C(24)	P(2)	W(1)	120.26(11)	C(27)	C(26)	P(4)	113.9(3)
C(37)	P(3)	W(1)	117.17(10)	C(29)	C(28)	P(4)	118.0(9)
C(38)	P(3)	W(1)	117.79(10)	C(29A)	C(28A)	P(4)	115.9(14)
C(38)	P(3)	C(37)	99.46(14)	N(2)	C(30)	P(4)	112.5(2)
C(38)	P(3)	C(40)	103.52(14)	N(2)	C(31)	C(32)	113.9(3)
C(40)	P(3)	W(1)	118.19(10)	C(31)	C(32)	C(33)	109.9(3)
C(40)	P(3)	C(37)	97.18(13)	N(34)	C(33)	C(32)	113.7(3)
C(26)	P(4)	W(1)	124.25(12)	C(33)	N(34)	C(36)	110.2(3)
C(26)	P(4)	C(28)	102.3(5)	C(35)	N(34)	C(33)	111.7(3)
C(26)	P(4)	C(30)	96.66(16)	C(35)	N(34)	C(36)	109.6(4)
C(28)	P(4)	W(1)	108.6(4)	N(2)	C(37)	P(3)	114.11(19)
C(28A)	P(4)	W(1)	120.0(5)	C(39)	C(38)	P(3)	114.8(2)
C(28A)	P(4)	C(26)	97.6(7)	C(41)	C(40)	P(3)	118.6(2)

Table II.14. Continued

C(28A)	P(4)	C(30)	94.6(6)	C(17)	O(2)	C(18)	113.5
C(30)	P(4)	W(1)	117.50(11)	O(2)	C(17)	C(12)	108.8
C(30)	P(4)	C(28)	105.2(5)	O(2)	C(18)	C(1A)	108.8
C(13)	N(1)	C(14)	110.8(2)				

Table II.15. Torsion Angles for W(CPh)(P_2NN)$_2$Cl.

A	B	C	D	Angle/°	A	B	C	D	Angle/°
W(1)	P(1)	C(8)	C(9)	51.2(3)	C(21)	P(2)	C(22)	C(23)	38.2(3)
W(1)	P(1)	C(10)	C(11)	167.0(2)	C(21)	P(2)	C(24)	C(25)	55.2(3)
W(1)	P(1)	C(13)	N(1)	56.4(2)	C(21)	N(1)	C(13)	P(1)	-79.4(3)
W(1)	P(2)	C(21)	N(1)	-61.4(2)	C(21)	N(1)	C(14)	C(15)	163.3(3)
W(1)	P(2)	C(22)	C(23)	166.2(2)	C(22)	P(2)	C(21)	N(1)	66.3(2)
W(1)	P(2)	C(24)	C(25)	-71.4(3)	C(22)	P(2)	C(24)	C(25)	158.1(2)
W(1)	P(3)	C(37)	N(2)	-60.2(2)	C(24)	P(2)	C(21)	N(1)	169.7(2)
W(1)	P(3)	C(38)	C(39)	-67.8(3)	C(24)	P(2)	C(22)	C(23)	-61.1(3)
W(1)	P(3)	C(40)	C(41)	175.5(2)	C(26)	P(4)	C(28)	C(29)	41.3(12)
W(1)	P(4)	C(26)	C(27)	62.6(3)	C(26)	P(4)	C(28A)	C(29A)	-58.2(10)
W(1)	P(4)	C(28)	C(29)	174.2(10)	C(26)	P(4)	C(30)	N(2)	-162.7(2)
W(1)	P(4)	C(28A)	C(29A)	78.9(12)	C(28)	P(4)	C(26)	C(27)	-174.5(5)
W(1)	P(4)	C(30)	N(2)	62.9(3)	C(28)	P(4)	C(30)	N(2)	-58.0(6)
N(1)	C(14)	C(15)	C(16)	-62.6(4)	C(28A)	P(4)	C(26)	C(27)	-162.9(6)
N(2)	C(31)	C(32)	C(33)	-169.4(3)	C(28A)	P(4)	C(30)	N(2)	-64.6(7)
C(1)	C(2)	C(3)	C(4)	178.6(3)	C(30)	P(4)	C(26)	C(27)	-67.3(3)
C(1)	C(2)	C(7)	C(6)	-177.6(3)	C(30)	P(4)	C(28)	C(29)	-59.2(12)
C(2)	C(3)	C(4)	C(5)	-0.5(6)	C(30)	P(4)	C(28A)	C(29A)	-155.6(9)
C(3)	C(2)	C(7)	C(6)	1.7(5)	C(30)	N(2)	C(31)	C(32)	-70.6(3)
C(3)	C(4)	C(5)	C(6)	0.9(6)	C(30)	N(2)	C(37)	P(3)	80.7(3)
C(4)	C(5)	C(6)	C(7)	0.0(6)	C(31)	N(2)	C(30)	P(4)	157.0(2)
C(5)	C(6)	C(7)	C(2)	-1.3(6)	C(31)	N(2)	C(37)	P(3)	-157.2(2)
C(7)	C(2)	C(3)	C(4)	-0.8(5)	C(31)	C(32)	C(33)	N(34)	174.3(3)
C(8)	P(1)	C(10)	C(11)	32.5(3)	C(32)	C(33)	N(34)	C(35)	68.9(5)
C(8)	P(1)	C(13)	N(1)	-172.4(2)	C(32)	C(33)	N(34)	C(36)	-169.0(3)
C(10)	P(1)	C(8)	C(9)	-178.3(2)	C(37)	P(3)	C(38)	C(39)	164.5(2)
C(10)	P(1)	C(13)	N(1)	-68.1(2)	C(37)	P(3)	C(40)	C(41)	-58.4(3)
C(13)	P(1)	C(8)	C(9)	-77.7(3)	C(37)	N(2)	C(30)	P(4)	-81.4(3)
C(13)	P(1)	C(10)	C(11)	-66.2(3)	C(37)	N(2)	C(31)	C(32)	167.5(3)
C(13)	N(1)	C(14)	C(15)	-74.0(3)	C(38)	P(3)	C(37)	N(2)	67.8(2)
C(13)	N(1)	C(21)	P(2)	82.7(3)	C(38)	P(3)	C(40)	C(41)	43.2(3)
C(14)	N(1)	C(13)	P(1)	157.7(2)	C(40)	P(3)	C(37)	N(2)	172.9(2)
C(14)	N(1)	C(21)	P(2)	-154.3(2)	C(40)	P(3)	C(38)	C(39)	64.7(3)
C(14)	C(15)	C(16)	N(17)	-62.8(4)	C(17)	O(2)	C(18)	C(1A)	179.9
C(15)	C(16)	N(17)	C(19)	168.3(3)	C(18)	O(2)	C(17)	C(12)	-180.0
C(15)	C(16)	N(17)	C(20)	-69.7(4)					

Table II.16. Hydrogen Atom Coordinates (Å×10^4) and Isotropic Displacement Parameters (Å^2×10^3) for W(CPh)(P_2NN)$_2$Cl.

Atom	***x***	***y***	***z***	**U(eq)**
H(3)	5655.53	3757.63	3702.91	26
H(4)	5479.99	1679.85	3398.57	34
H(5)	5137.68	606.83	2246.26	36
H(6)	5018.97	1611.23	1388.93	34
H(7)	5250.25	3688.41	1683.29	26
H(8A)	8291.63	6327.56	1408.24	21
H(8B)	8864	6784.98	2202.08	21
H(9A)	7657.28	4484.92	1539.52	41
H(9B)	7997.6	4940.86	2357.84	41
H(9C)	9163.79	4755.19	1871.22	41
H(10A)	5828.9	8732.12	1863.52	21
H(10B)	7103.57	8996.19	2415.92	21
H(11A)	7239.87	8093.68	974.9	41
H(11B)	8489.39	8480.64	1545.7	41
H(11C)	7504.06	9467.29	1391.11	41
H(13A)	6085.82	6344.62	871.68	17
H(13B)	5549.02	5339.23	1192.4	17
H(14A)	2779.7	6476.82	385.85	24
H(14B)	3928.11	5556.17	189.83	24
H(15A)	5336.62	7130.22	105.02	32
H(15B)	4031.35	6966.19	-429.53	32
H(16A)	4410.19	8767.1	849.56	34
H(16B)	4560.79	9002.93	118.89	34
H(19A)	2744.74	10044.3	1166.99	64
H(19B)	1473.05	10088.05	638.8	64
H(19C)	2891.38	10546.13	514.89	64
H(20A)	2700.09	9169.7	-624.39	77
H(20B)	1249.73	8841.84	-473.45	77
H(20C)	2267.08	7807.03	-708.49	77
H(21A)	3608.91	5230.89	1462.92	19
H(21B)	2452.62	6079.81	1310.01	19
H(22A)	2466.52	8643.98	2892.4	20
H(22B)	3488.01	8801.3	2375.11	20
H(23A)	1920.83	8068.36	1431.61	34
H(23B)	1259.58	9095.59	1975.94	34
H(23C)	909.92	7721.19	1908.02	34
H(24A)	1911.28	6276.62	3117.74	22
H(24B)	1197.15	6246.94	2373.41	22

Table II.16. Continued

H(25A)	1918.69	4358.59	1901.42	34
H(25B)	1340.52	4309.63	2598.32	34
H(25C)	2905.94	4406.4	2577.77	34
H(26A)	10050.34	7338.37	4008.84	33
H(26B)	9519.1	6783.04	3215.43	33
H(27A)	8648.19	8757.45	3237.38	50
H(27B)	10224.4	8682.15	3277.89	50
H(27C)	9536.46	9237.47	3961.75	50
H(28A)	7312.52	5384.56	4348.56	28
H(28B)	7931.18	4909.2	3639.62	28
H(29A)	10050.47	5411.42	4190.28	53
H(29B)	9316.58	4606.01	4579.34	53
H(29C)	9478.24	6021.32	4902.21	53
H(28C)	8906.16	6108.44	4635.35	30
H(28D)	7467.93	5486.13	4392.66	30
H(29D)	8199.53	4482.46	3329.69	48
H(29E)	9009.3	4140.12	3966.83	48
H(29F)	9652.54	5055.79	3614.9	48
H(30A)	8797.12	8146.61	4962.89	25
H(30B)	7729.44	8941.77	4669.25	25
H(31A)	6694.56	8417.08	6198.3	23
H(31B)	7654.93	9301.56	5970.61	23
H(32A)	9403.28	8035.67	5972.32	23
H(32B)	8454.85	6990.79	6061.12	23
H(33A)	9108.78	9212.01	7079.18	29
H(33B)	8044.83	8258.55	7166.61	29
H(35A)	11228.07	7713.52	6598.95	90
H(35B)	11890.87	7665.73	7342.35	90
H(35C)	11363.62	8898.53	7226.5	90
H(36A)	10144.83	8955.5	8200.63	57
H(36B)	10595.2	7648.88	8222.58	57
H(36C)	9055.04	7921.05	8140.64	57
H(37A)	5763.3	9115.24	4924.92	18
H(37B)	5141.59	8448.87	5421.49	18
H(38A)	5167.13	5633.47	4650.47	20
H(38B)	4113.35	6394.49	5100.18	20
H(39A)	3443.12	4865.4	3743.82	32
H(39B)	2397.72	5595.72	4216.09	32
H(39C)	3161.13	4531.85	4433.91	32
H(40A)	3280.16	8938.08	4270.57	19
H(40B)	2443.97	7713.91	3958.99	19

Table II.16. Continued.

H(41A)	1607.87	8721.73	4964.22	33
H(41B)	3040.88	8857.06	5392.87	33
H(41C)	2306.42	7569.94	5107.83	33
H(12A)	10524.84	2821.46	-377.1	134
H(12B)	10818.87	2653.72	382.14	134
H(12C)	11820.63	3442.85	108.55	134
H(17A)	9208.01	4075.06	437.56	66
H(17B)	10552.86	4771.04	834.25	66
H(18A)	9785.54	6584.39	575.39	68
H(18B)	8440.5	5889.38	178.15	68
H(1AA)	8878.71	6325.34	-843.27	146
H(1AB)	10294.26	6917.82	-492.02	146
H(1AC)	8971.36	7554.34	-248.02	146

Table II.17. Atomic Occupancy for W(CPh)(P_2NN)$_2$Cl.

Atom	***Occupancy***	**Atom**	***Occupancy***	**Atom**	***Occupancy***
C(28)	0.535(9)	H(28A)	0.535(9)	H(28B)	0.535(9)
C(29)	0.535(9)	H(29A)	0.535(9)	H(29B)	0.535(9)
H(29C)	0.535(9)	C(28A)	0.465(9)	H(28C)	0.465(9)
H(28D)	0.465(9)	C(29A)	0.465(9)	H(29D)	0.465(9)
H(29E)	0.465(9)	H(29F)	0.465(9)	O(2)	0.5
C(12)	0.5	H(12A)	0.5	H(12B)	0.5
H(12C)	0.5	C(17)	0.5	H(17A)	0.5
H(17B)	0.5	C(18)	0.5	H(18A)	0.5
H(18B)	0.5	C(1A)	0.5	H(1AA)	0.5
H(1AB)	0.5	H(1AC)	0.5		

II.3 Diffraction data for [W(CPh)(tmiy)$_3${P(OMe)$_3$OBu]•Et$_2$O.

Table II.18. Crystal data and structure refinement for W(CPh)(tmiy)$_3${P(OMe)$_3$}OBu

Identification code	W(CPh)(tmiy)$_3${P(OMe)$_3$}OBu
Empirical formula	$C_{39}H_{69}N_6O_5PW$
Formula weight	916.84
Temperature/K	100.01
Crystal system	monoclinic
Space group	$P2_1/n$
a/Å	11.404(2)
b/Å	27.321(6)
c/Å	15.696(3)
α/°	90
β/°	94.077(5)
γ/°	90
Volume/Å^3	4877.8(17)
Z	4
ρ_{calc}g/cm^3	1.2484
μ/mm^{-1}	2.442
F(000)	1894.4
Crystal size/mm^3	0.222 × 0.169 × 0.06
Radiation	Mo Kα (λ = 0.71073)
2Θ range for data collection/°	4.28 to 54.26
Index ranges	$-14 \leq h \leq 14$, $-34 \leq k \leq 34$, $-19 \leq l \leq 19$
Reflections collected	102701
Independent reflections	10714 [R_{int} = 0.0678, R_{sigma} = 0.0469]
Data/restraints/parameters	10714/0/475
Goodness-of-fit on F^2	1.075
Final R indexes [I>=2σ (I)]	R_1 = 0.0748, wR_2 = 0.1994
Final R indexes [all data]	R_1 = 0.0991, wR_2 = 0.2161
Largest diff. peak/hole / e Å^{-3}	4.09/-5.97

Table II.19.2 Fractional Atomic Coordinates ($\times 10^4$) and Equivalent Isotropic Displacement Parameters ($Å^2 \times 10^3$) for W(CPh)(tmiy)$_3${P(OMe)$_3$}OBu. U_{eq} is defined as 1/3 of of the trace of the orthogonalised U_{IJ} tensor.

Atom	***x***	***y***	***z***	**U(eq)**
W(1)	3668.7(3)	7353.95(15)	5330.4(2)	26.08(15)
P(1)	3852(2)	7043.8(10)	6728.9(16)	28.8(5)
O(3)	2727(6)	7001(3)	7303(4)	33.3(16)
O(1)	4582(6)	7326(3)	7530(5)	38.5(18)
O(4)	4817(6)	6772(3)	4920(5)	36.8(17)
O(2)	4420(7)	6500(3)	6832(5)	46(2)
N(4)	3621(7)	8054(4)	3660(5)	34(2)
N(1)	6163(6)	7847(3)	4840(5)	27.4(17)
N(3)	3562(7)	7316(3)	3217(5)	31.2(19)
N(2)	5517(7)	8227(3)	5905(5)	30.4(18)
N(6)	1094(7)	6985(3)	4596(5)	31.3(19)
N(5)	2170(8)	6347(3)	4871(6)	39(2)
C(16)	3668(8)	8061(5)	2801(7)	38.4(18)
C(17)	3648(8)	7599(5)	2495(7)	38.4(18)
C(22)	2206(8)	6845(4)	4918(7)	31(2)
C(25)	665(10)	7479(4)	4552(7)	37(2)
C(12)	6314(9)	7523(4)	4127(7)	36(2)
C(8)	5267(8)	7829(4)	5398(6)	31(2)
C(7)	1952(9)	8169(4)	7098(7)	34(2)
C(1)	2732(8)	7811(4)	5778(6)	30(2)
C(18)	3683(10)	8495(4)	4183(7)	39(2)
C(2)	2006(8)	8158(4)	6203(7)	32(2)
C(15)	3572(9)	7588(4)	3953(7)	33(2)
C(10)	6901(8)	8244(4)	5005(7)	34(2)
C(9)	6489(9)	8488(4)	5654(7)	35(2)
C(6)	1311(10)	8516(4)	7500(8)	42(3)
C(3)	1348(9)	8516(4)	5730(7)	36(2)
C(23)	415(9)	6583(4)	4353(8)	41(3)
C(11)	4824(9)	8386(5)	6592(7)	40(3)
C(31)	1621(9)	6852(5)	6912(7)	42(3)
C(19)	3442(9)	6787(5)	3184(7)	40(3)
C(14)	7943(10)	8337(5)	4506(8)	43(3)
C(32)	5785(10)	6573(5)	5235(8)	47(3)
C(29)	5830(9)	7359(5)	7460(7)	42(3)
C(24)	1078(10)	6189(5)	4516(9)	47(3)
C(26)	3092(11)	6010(5)	5156(9)	49(3)
C(4)	663(10)	8861(4)	6135(8)	44(3)

Table II.19. Continued.

C(20)	3705(11)	8532(6)	2286(7)	59(3)
C(5)	661(10)	8868(4)	7016(8)	46(3)
C(13)	6950(11)	8933(4)	6125(9)	46(3)
C(27)	-820(10)	6630(5)	4009(10)	54(3)
C(30)	4538(13)	6250(5)	7638(8)	57(4)
C(33)	6227(13)	6132(7)	4890(12)	81(6)
C(28)	823(13)	5657(5)	4351(13)	77(5)
O(5)	5910(20)	5110(6)	7724(12)	133(6)
C(34)	7263(18)	5929(8)	5249(15)	101(7)
C(35)	7740(30)	5510(8)	4970(20)	149(12)
C(37)	6450(30)	5110(15)	6930(18)	171(15)
C(36)	5300(40)	5030(12)	6290(20)	209(19)
C(38)	6680(30)	5232(13)	8340(20)	181(17)
C(39)	6060(40)	5292(13)	9180(20)	220(20)
C(21)	3612(11)	7426(6)	1628(7)	59(3)

Table II.20. Anisotropic Displacement Parameters ($Å^2 \times 10^3$) for $W(CPh)(tmiy)_3\{P(OMe)_3\}OBu$. The Anisotropic displacement factor exponent takes the form: $-2\pi^2[h^2a^{*2}U_{11}+2hka^*b^*U_{12}+\ldots]$.

Atom	**U_{11}**	**U_{22}**	**U_{33}**	**U_{12}**	**U_{13}**	**U_{23}**
W(1)	17.3(2)	40.3(3)	21.1(2)	2.68(17)	4.26(13)	-2.04(17)
P(1)	18.8(11)	44.5(15)	23.8(12)	4.6(10)	5.8(9)	2.0(11)
O(3)	22(3)	49(4)	29(4)	1(3)	4(3)	0(3)
O(1)	22(3)	68(5)	25(4)	1(3)	3(3)	0(4)
O(4)	24(4)	48(5)	39(4)	9(3)	3(3)	-2(3)
O(2)	43(5)	56(5)	41(4)	19(4)	10(4)	9(4)
N(4)	22(4)	54(6)	26(4)	5(4)	3(3)	1(4)
N(1)	17(4)	48(5)	18(4)	2(3)	8(3)	0(3)
N(3)	17(4)	54(5)	23(4)	0(4)	4(3)	-7(4)
N(2)	19(4)	46(5)	27(4)	3(3)	4(3)	-2(4)
N(6)	19(4)	53(6)	21(4)	1(4)	-3(3)	-6(4)
N(5)	24(4)	40(5)	51(6)	-1(4)	0(4)	-8(4)
C(16)	15(3)	73(5)	27(4)	3(3)	-3(3)	3(4)
C(17)	15(3)	73(5)	27(4)	3(3)	-3(3)	3(4)
C(22)	17(4)	44(6)	34(5)	8(4)	-1(4)	-2(4)
C(25)	32(6)	52(7)	26(5)	9(5)	3(4)	0(5)
C(12)	30(5)	51(6)	29(5)	5(5)	12(4)	-2(5)
C(8)	20(4)	43(6)	29(5)	9(4)	2(4)	6(4)
C(7)	24(5)	49(6)	29(5)	4(4)	7(4)	-2(5)
C(1)	21(5)	47(6)	22(5)	-2(4)	1(4)	-1(4)
C(18)	35(6)	44(6)	40(6)	5(5)	7(5)	4(5)
C(2)	17(4)	45(6)	33(5)	-1(4)	4(4)	-8(5)
C(15)	22(5)	45(6)	31(5)	6(4)	3(4)	-4(5)
C(10)	21(5)	51(7)	30(5)	1(4)	-5(4)	3(5)
C(9)	20(5)	47(6)	39(6)	1(4)	7(4)	6(5)
C(6)	37(6)	48(7)	41(6)	-4(5)	16(5)	-15(5)
C(3)	31(5)	47(6)	31(5)	-3(5)	7(4)	-4(5)
C(23)	28(5)	49(7)	44(6)	-9(5)	0(5)	-5(5)
C(11)	29(5)	59(7)	32(6)	-3(5)	11(4)	-16(5)
C(31)	22(5)	63(8)	41(6)	-7(5)	7(4)	0(6)
C(19)	29(5)	67(8)	23(5)	4(5)	7(4)	-10(5)
C(14)	29(5)	57(7)	44(7)	-1(5)	11(5)	1(6)
C(32)	38(6)	60(8)	45(7)	14(6)	24(5)	18(6)
C(29)	21(5)	74(8)	28(5)	1(5)	-1(4)	6(6)
C(24)	30(6)	49(7)	60(8)	-9(5)	-7(5)	-12(6)
C(26)	39(7)	41(7)	67(9)	4(5)	8(6)	-4(6)
C(4)	29(6)	42(6)	62(8)	0(5)	12(5)	-5(6)

Table II.20. Continued.

C(20)	39(5)	124(9)	12(3)	-17(5)	0(3)	5(4)
C(5)	40(6)	41(6)	62(8)	4(5)	23(6)	-12(6)
C(13)	38(6)	39(6)	62(8)	-5(5)	8(6)	-5(6)
C(27)	26(6)	54(8)	79(10)	-9(5)	-6(6)	9(7)
C(30)	59(8)	67(9)	46(7)	20(7)	8(6)	20(7)
C(33)	50(8)	95(12)	104(13)	29(8)	48(9)	58(10)
C(28)	45(8)	51(8)	131(16)	-9(7)	-10(9)	-24(9)
O(5)	200(20)	89(11)	114(13)	-9(12)	27(14)	-7(10)
C(34)	90(14)	93(15)	124(18)	12(12)	34(13)	29(13)
C(35)	170(30)	77(14)	210(30)	50(16)	110(20)	31(17)
C(37)	190(30)	230(40)	90(20)	30(30)	30(20)	-40(20)
C(36)	340(50)	130(30)	180(30)	-30(30)	160(40)	-10(30)
C(38)	210(40)	150(30)	170(30)	40(30)	-110(30)	-20(30)
C(39)	390(70)	150(30)	120(30)	-30(40)	-50(30)	10(20)
C(21)	39(5)	124(9)	12(3)	-17(5)	0(3)	5(4)

Table II.21. Bond Lengths for W(CPh)(tmiy)$_3${P(OMe)$_3$}OBu.

Atom	Atom	Length/Å	Atom	Atom	Length/Å
W(1)	P(1)	2.348(3)	N(6)	C(23)	1.382(14)
W(1)	O(4)	2.187(7)	N(5)	C(22)	1.363(14)
W(1)	C(22)	2.232(10)	N(5)	C(24)	1.396(14)
W(1)	C(8)	2.233(10)	N(5)	C(26)	1.445(15)
W(1)	C(1)	1.816(10)	C(16)	C(17)	1.350(17)
W(1)	C(15)	2.250(11)	C(16)	C(20)	1.522(19)
P(1)	O(3)	1.624(7)	C(17)	C(21)	1.438(16)
P(1)	O(1)	1.649(8)	C(7)	C(2)	1.411(14)
P(1)	O(2)	1.624(8)	C(7)	C(6)	1.379(15)
O(3)	C(31)	1.423(12)	C(1)	C(2)	1.452(14)
O(1)	C(29)	1.437(12)	C(2)	C(3)	1.412(15)
O(4)	C(32)	1.295(13)	C(10)	C(9)	1.331(15)
O(2)	C(30)	1.437(14)	C(10)	C(14)	1.490(14)
N(4)	C(16)	1.353(13)	C(9)	C(13)	1.498(16)
N(4)	C(18)	1.457(14)	C(6)	C(5)	1.404(18)
N(4)	C(15)	1.357(14)	C(3)	C(4)	1.404(15)
N(1)	C(12)	1.447(13)	C(23)	C(24)	1.329(17)
N(1)	C(8)	1.393(12)	C(23)	C(27)	1.478(15)
N(1)	C(10)	1.386(14)	C(32)	C(33)	1.43(2)
N(3)	C(17)	1.380(14)	C(24)	C(28)	1.501(18)
N(3)	C(15)	1.374(13)	C(4)	C(5)	1.383(18)
N(3)	C(19)	1.451(15)	C(33)	C(34)	1.39(2)
N(2)	C(8)	1.368(14)	O(5)	C(37)	1.43(3)
N(2)	C(9)	1.397(13)	O(5)	C(38)	1.31(3)
N(2)	C(11)	1.447(12)	C(34)	C(35)	1.35(3)
N(6)	C(22)	1.386(12)	C(37)	C(36)	1.61(5)
N(6)	C(25)	1.434(14)	C(38)	C(39)	1.55(5)

Table II.22 Bond Angles for W(CPh)(tmiy)$_3${P(OMe)$_3$}OBu.

Atom	Atom	Atom	Angle/°	Atom	Atom	Atom	Angle/°
O(4)	W(1)	P(1)	89.8(2)	C(17)	C(16)	N(4)	110.0(10)
C(22)	W(1)	P(1)	93.5(3)	C(20)	C(16)	N(4)	122.9(11)
C(22)	W(1)	O(4)	85.0(3)	C(20)	C(16)	C(17)	127.1(10)
C(8)	W(1)	P(1)	98.5(3)	C(16)	C(17)	N(3)	103.4(9)
C(8)	W(1)	O(4)	86.1(3)	C(21)	C(17)	N(3)	126.5(12)
C(8)	W(1)	C(22)	165.0(4)	C(21)	C(17)	C(16)	129.9(12)
C(1)	W(1)	P(1)	84.4(3)	N(6)	C(22)	W(1)	125.4(8)
C(1)	W(1)	O(4)	174.2(4)	N(5)	C(22)	W(1)	131.1(7)
C(1)	W(1)	C(22)	95.3(4)	N(5)	C(22)	N(6)	103.4(9)
C(1)	W(1)	C(8)	94.7(4)	N(1)	C(8)	W(1)	128.6(8)
C(15)	W(1)	P(1)	174.8(3)	N(2)	C(8)	W(1)	128.8(7)
C(15)	W(1)	O(4)	85.0(3)	N(2)	C(8)	N(1)	101.8(8)
C(15)	W(1)	C(22)	85.1(4)	C(6)	C(7)	C(2)	122.2(11)
C(15)	W(1)	C(8)	82.2(4)	C(2)	C(1)	W(1)	175.3(8)
C(15)	W(1)	C(1)	100.7(4)	C(1)	C(2)	C(7)	122.6(10)
O(3)	P(1)	W(1)	121.6(3)	C(3)	C(2)	C(7)	116.7(9)
O(1)	P(1)	W(1)	123.4(3)	C(3)	C(2)	C(1)	120.7(9)
O(1)	P(1)	O(3)	89.2(4)	N(4)	C(15)	W(1)	126.3(7)
O(2)	P(1)	W(1)	115.6(3)	N(3)	C(15)	W(1)	130.6(8)
O(2)	P(1)	O(3)	101.8(4)	N(3)	C(15)	N(4)	102.8(9)
O(2)	P(1)	O(1)	100.1(4)	C(9)	C(10)	N(1)	107.0(9)
C(31)	O(3)	P(1)	119.5(6)	C(14)	C(10)	N(1)	122.1(10)
C(29)	O(1)	P(1)	114.8(7)	C(14)	C(10)	C(9)	130.9(11)
C(32)	O(4)	W(1)	134.8(8)	C(10)	C(9)	N(2)	106.9(10)
C(30)	O(2)	P(1)	122.4(8)	C(13)	C(9)	N(2)	122.2(10)
C(18)	N(4)	C(16)	123.2(10)	C(13)	C(9)	C(10)	130.8(10)
C(15)	N(4)	C(16)	110.8(10)	C(5)	C(6)	C(7)	120.0(11)
C(15)	N(4)	C(18)	125.9(9)	C(4)	C(3)	C(2)	121.3(10)
C(8)	N(1)	C(12)	126.6(9)	C(24)	C(23)	N(6)	106.9(9)
C(10)	N(1)	C(12)	121.3(8)	C(27)	C(23)	N(6)	122.1(11)
C(10)	N(1)	C(8)	111.9(9)	C(27)	C(23)	C(24)	131.0(11)
C(15)	N(3)	C(17)	112.9(10)	C(33)	C(32)	O(4)	121.6(13)
C(19)	N(3)	C(17)	122.7(9)	C(23)	C(24)	N(5)	107.8(10)
C(19)	N(3)	C(15)	124.3(9)	C(28)	C(24)	N(5)	121.7(12)
C(9)	N(2)	C(8)	112.3(8)	C(28)	C(24)	C(23)	130.5(11)
C(11)	N(2)	C(8)	124.7(9)	C(5)	C(4)	C(3)	120.2(12)
C(11)	N(2)	C(9)	122.9(9)	C(4)	C(5)	C(6)	119.5(10)
C(25)	N(6)	C(22)	125.3(9)	C(34)	C(33)	C(32)	119.8(19)
C(23)	N(6)	C(22)	111.2(9)	C(38)	O(5)	C(37)	109(3)

Table II.22. Continued.

C(23)	N(6)	C(25)	123.5(9)	C(35)	C(34)	C(33)	124(3)
C(24)	N(5)	C(22)	110.7(9)	C(36)	C(37)	O(5)	99(3)
C(26)	N(5)	C(22)	127.0(9)	C(39)	C(38)	O(5)	109(3)
C(26)	N(5)	C(24)	122.3(10)				

Table II.23 Hydrogen Atom Coordinates (Å×10^4) and Isotropic Displacement Parameters (Å^2×10^3) for W(CPh)(tmiy)$_3${P(OMe)$_3$}OBu.

Atom	***x***	***y***	***z***	**U(eq)**
H(25a)	400(70)	7574(11)	5107(16)	55(4)
H(25b)	1300(20)	7699(6)	4400(50)	55(4)
H(25c)	10(50)	7501(8)	4120(40)	55(4)
H(12a)	6210(70)	7708(7)	3592(7)	54(4)
H(12b)	7100(30)	7380(20)	4180(30)	54(4)
H(12c)	5730(50)	7261(17)	4120(30)	54(4)
H(7)	2371(9)	7929(4)	7434(7)	41(3)
H(18a)	3510(70)	8413(7)	4768(14)	59(4)
H(18b)	4470(20)	8635(17)	4190(40)	59(4)
H(18c)	3110(50)	8735(12)	3950(30)	59(4)
H(6)	1309(10)	8518(4)	8105(8)	50(3)
H(3)	1368(9)	8524(4)	5127(7)	43(3)
H(11a)	4280(50)	8640(20)	6382(15)	60(4)
H(11b)	4380(60)	8107(8)	6800(40)	60(4)
H(11c)	5346(11)	8510(30)	7060(20)	60(4)
H(31a)	1350(40)	7095(16)	6480(40)	63(4)
H(31b)	1705(18)	6534(15)	6640(50)	63(4)
H(31c)	1050(20)	6830(30)	7348(11)	63(4)
H(19a)	3790(60)	6645(5)	3720(20)	59(4)
H(19b)	2608(10)	6700(5)	3110(50)	59(4)
H(19c)	3850(60)	6659(5)	2700(30)	59(4)
H(14a)	7683(12)	8390(30)	3904(12)	65(4)
H(14b)	8350(40)	8630(18)	4730(40)	65(4)
H(14c)	8480(40)	8055(14)	4560(40)	65(4)
H(29a)	6211(12)	7063(14)	7700(50)	62(4)
H(29b)	5990(10)	7390(30)	6857(8)	62(4)
H(29c)	6138(14)	7646(17)	7780(40)	62(4)
H(26a)	3710(40)	6186(8)	5500(50)	73(5)
H(26b)	2766(19)	5752(19)	5500(50)	73(5)
H(26c)	3430(50)	5860(30)	4659(9)	73(5)
H(4)	201(10)	9090(4)	5803(8)	53(3)
H(20a)	2910(20)	8670(20)	2220(60)	88(4)
H(20b)	4240(70)	8765(15)	2590(30)	88(4)
H(20c)	3980(80)	8461(8)	1720(20)	88(4)
H(5)	222(10)	9109(4)	7292(8)	56(4)
H(13a)	7620(50)	9066(19)	5840(30)	69(4)
H(13b)	6330(30)	9180(13)	6130(50)	69(4)
H(13c)	7210(70)	8843(8)	6714(18)	69(4)

Table II.23. Continued.

H(27a)	-1120(30)	6309(8)	3820(60)	80(5)
H(27b)	-1297(18)	6760(30)	4450(20)	80(5)
H(27c)	-864(15)	6860(30)	3520(40)	80(5)
H(30a)	5010(70)	6450(17)	8054(19)	86(5)
H(30b)	3758(13)	6190(30)	7840(30)	86(5)
H(30c)	4930(80)	5935(17)	7567(16)	86(5)
H(28a)	180(70)	5626(5)	3910(60)	115(8)
H(28b)	1530(40)	5497(11)	4160(80)	115(8)
H(28c)	600(100)	5502(11)	4880(20)	115(8)
H(35a)	7300(130)	5410(50)	4440(80)	224(18)
H(35b)	8560(60)	5570(20)	4860(150)	224(18)
H(35c)	7690(190)	5250(30)	5400(60)	224(18)
H(37a)	6850(30)	5426(15)	6826(18)	205(18)
H(37b)	7020(30)	4839(15)	6895(18)	205(18)
H(36a)	5530(40)	4970(130)	5720(50)	310(30)
H(36b)	4850(170)	4750(80)	6490(130)	310(30)
H(36c)	4810(160)	5330(50)	6290(180)	310(30)
H(38a)	7290(30)	4975(13)	8410(20)	220(20)
H(38b)	7070(30)	5543(13)	8200(20)	220(20)
H(21a)	4408(18)	7340(40)	1490(20)	88(4)
H(21b)	3100(70)	7140(20)	1566(17)	88(4)
H(21c)	3310(80)	7685(14)	1242(8)	88(4)
H(34a)	7875(18)	6184(8)	5222(15)	121(8)
H(34b)	7148(18)	5877(8)	5862(15)	121(8)
H(33a)	5605(13)	5880(7)	4914(12)	97(7)
H(33b)	6335(13)	6192(7)	4279(12)	97(7)
H(32a)	6410(10)	6823(5)	5208(8)	56(4)
H(32b)	5689(10)	6511(5)	5848(8)	56(4)
H(39a)	6640(40)	5384(13)	9640(20)	330(30)
H(39b)	5460(40)	5549(13)	9110(20)	330(30)
H(39c)	5690(40)	4983(13)	9320(20)	330(30)

II.4 Diffraction data for [W(CPh)(ICy)(PMe_3)$_4$Cl].

Table II.24. Crystal data and structure refinement for W(CPh)(ICy)(PMe_3)$_3$Cl.

Identification code	W(CPh)(ICy)(PMe_3)$_3$Cl
Empirical formula	$C_{31}H_{56}ClN_2P_3W$
Formula weight	768.98
Temperature/K	99.99
Crystal system	triclinic
Space group	P-1
a/Å	11.8310(7)
b/Å	16.6213(10)
c/Å	18.1739(11)
α/°	81.7520(10)
β/°	83.9550(10)
γ/°	79.3000(10)
Volume/Å^3	3464.0(4)
Z	4
ρ_{calc}g/cm^3	1.475
μ/mm^{-1}	3.573
F(000)	1568.0
Crystal size/mm^3	? × ? × ?
Radiation	MoKα (λ = 0.71073)
2Θ range for data collection/°	4.544 to 61.188
Index ranges	$-16 \leq h \leq 16$, $-23 \leq k \leq 23$, $-26 \leq l \leq 26$
Reflections collected	150196
Independent reflections	21293 [R_{int} = 0.0372, R_{sigma} = 0.0269]
Data/restraints/parameters	21293/330/716
Goodness-of-fit on F^2	1.059
Final R indexes [I>=2σ (I)]	R_1 = 0.0216, wR_2 = 0.0401
Final R indexes [all data]	R_1 = 0.0332, wR_2 = 0.0426
Largest diff. peak/hole / e Å^{-3}	0.87/-0.45

Table II.25. Fractional Atomic Coordinates ($\times 10^4$) and Equivalent Isotropic Displacement Parameters ($Å^2 \times 10^3$) for W(CPh)(ICy)(PMe_3)$_3$Cl. U_{eq} is defined as 1/3 of of the trace of the orthogonalised U_{IJ} tensor.

Atom	***x***	***y***	***z***	**U(eq)**
W(1)	1752.9(2)	2323.2(2)	3417.5(2)	11.06(2)
Cl(1)	3229.0(4)	1493.9(3)	2487.3(2)	17.57(9)
P(1)	2639.5(5)	3562.0(3)	3130.8(3)	18.81(10)
P(2)	784.2(4)	2657.3(3)	2242.2(3)	17.72(10)
P(3)	1211.4(4)	937.3(3)	3755.1(3)	13.64(9)
N(1)	2440.1(13)	1884.2(9)	5140.3(8)	13.8(3)
N(2)	3997.2(13)	1645.1(10)	4419.2(8)	15.3(3)
C(1)	506.5(16)	2921.0(11)	3875.1(9)	14.5(3)
C(2)	-542.4(16)	3418.3(11)	4158.6(9)	16.0(4)
C(3)	-1555.9(17)	3089.5(12)	4372.9(11)	21.5(4)
C(4)	-2561.8(18)	3567.4(13)	4643.4(12)	26.2(4)
C(5)	-2590.7(19)	4390.3(13)	4708.5(11)	26.4(5)
C(6)	-1602(2)	4726.4(13)	4507.1(11)	27.4(5)
C(7)	-594.9(18)	4254.2(12)	4244.2(11)	22.8(4)
C(8)	2829.7(16)	1936.3(11)	4391.0(9)	13.7(3)
C(9)	3334.9(16)	1576.0(12)	5592.8(10)	19.2(4)
C(10)	4295.4(17)	1418.1(12)	5146(1)	20.2(4)
C(11)	1262.3(15)	2161.8(11)	5470.3(9)	14.3(3)
C(12)	915.8(17)	1543.2(11)	6121.9(10)	17.7(4)
C(13)	-276.0(17)	1865.4(12)	6488.2(10)	19.9(4)
C(14)	-296.9(17)	2693.7(12)	6755.6(10)	20.0(4)
C(15)	10.4(17)	3323.3(12)	6104.9(10)	19.3(4)
C(16)	1186.8(16)	3015.0(11)	5715.5(10)	16.4(4)
C(17)	4884.3(16)	1581.9(12)	3788.9(10)	16.5(4)
C(18)	5336.0(16)	685.8(12)	3675.0(11)	19.9(4)
C(19)	6234.3(17)	629.3(13)	3007.6(11)	24.2(4)
C(20)	7219.7(18)	1071.6(15)	3100.1(12)	30.9(5)
C(21)	6774.7(18)	1961.8(14)	3229.7(12)	28.2(5)
C(22)	5873.3(17)	2019.4(13)	3895.9(11)	23.4(4)
C(23)	1794(2)	4536.2(12)	2731.8(12)	31.3(5)
C(24)	3110(2)	3925.5(14)	3934.9(12)	29.5(5)
C(25)	3945.7(19)	3529.0(13)	2490.8(11)	26.1(5)
C(26)	-531.0(19)	3430.7(14)	2263.5(12)	30.8(5)
C(27)	231.7(19)	1879.9(14)	1822.7(12)	28.7(5)
C(28)	1583(2)	3067.5(14)	1393.5(11)	28.4(5)
C(29)	-192.5(16)	906.3(12)	4268.1(11)	19.2(4)

Table II.25. Continued.

C(30)	2163.0(16)	196.3(11)	4369.8(10)	18.4(4)
C(31)	1134.5(19)	262.5(12)	3054.6(11)	24.8(4)
W(2)	4231.1(2)	2785.4(2)	8209.0(2)	11.76(2)
Cl(2)	2996.2(4)	2165.3(3)	7408.2(2)	18.11(9)
P(4)	5631.0(4)	1550.0(3)	7896.6(3)	15.10(9)
P(5)	4792.0(4)	3579.3(3)	7022.7(3)	17.62(10)
P(6)	2513.4(4)	3821.9(3)	8473.8(3)	18.81(10)
N(3)	4290.8(14)	1820.4(9)	9910.5(8)	15.9(3)
N(4)	2791.6(14)	1563.8(9)	9479.7(8)	16.4(3)
C(32)	5215.8(15)	3328.7(11)	8565.0(9)	14.5(3)
C(33)	6057.6(16)	3774.6(11)	8768.2(10)	16.4(4)
C(34)	5740.7(19)	4537.9(12)	9048.5(11)	24.0(4)
C(35)	6555(2)	4927.5(13)	9281.9(12)	29.0(5)
C(36)	7708.5(19)	4576.9(13)	9245.9(11)	26.2(5)
C(37)	8047.2(18)	3835.4(13)	8961.8(11)	25.2(4)
C(38)	7240.9(17)	3444.8(12)	8723.7(11)	21.5(4)
C(39)	3707.2(16)	1985.8(11)	9272.7(9)	14.3(3)
C(40)	3757.6(18)	1336.3(12)	10473.9(11)	23.2(4)
C(41)	2837.7(18)	1166.7(13)	10201.6(10)	23.2(4)
C(42)	5327.9(16)	2126.5(11)	10053.7(10)	16.2(4)
C(43)	4993.5(18)	2770.5(12)	10594.5(11)	22.9(4)
C(44)	6038.1(18)	3091.2(13)	10789.3(11)	25.5(4)
C(45)	6956(2)	2381.4(14)	11076.8(12)	30.6(5)
C(46)	7297.8(18)	1769.9(14)	10514.9(13)	30.3(5)
C(47)	6253.6(18)	1423.2(12)	10350.8(11)	24.5(4)
C(48)	1880.7(16)	1462.5(12)	9023.2(10)	17.3(4)
C(49)	689.2(19)	1580.1(17)	9447.8(13)	35.2(6)
C(50)	-224.8(19)	1476.8(17)	8944.5(14)	38.7(6)
C(51)	32.8(19)	626.2(15)	8696.4(13)	32.4(5)
C(52)	1220.3(18)	482.3(14)	8287.4(12)	28.3(5)
C(53)	2147.8(18)	615.3(13)	8758.1(12)	25.3(4)
C(54)	7132.0(17)	1489.0(13)	8076.8(12)	26.6(5)
C(55)	5392(2)	550.4(12)	8384.1(13)	30.0(5)
C(56)	5813.5(19)	1282.6(14)	6941.6(11)	27.4(5)
C(57)	6346.7(17)	3501.4(14)	6776.6(11)	26.6(5)
C(58)	4309.4(19)	3419.9(14)	6136.9(11)	27.1(5)
C(59)	4439(2)	4710.6(13)	6924.7(13)	29.4(5)
C(60A)	2688(6)	4843(4)	8678(3)	25.7(10)
C(60B)	2647(12)	4889(9)	8429(5)	25.7(10)
C(61A)	1447(5)	4124(3)	7744(3)	31.8(11)
C(61B)	1298(9)	3871(6)	7995(6)	31.8(11)

Table II.25. Continued.

C(62A)	1493(5)	3597(3)	9285(4)	46.4(16)
C(62B)	1965(9)	3697(7)	9464(7)	46.4(16)

Table II.26. Anisotropic Displacement Parameters ($Å^2 \times 10^3$) for W(CPh)(ICy)(PMe_3)$_3$Cl. The Anisotropic displacement factor exponent takes the form: $-2\pi^2[h^2a^{*2}U_{11}+2hka^*b^*U_{12}+\ldots]$.

Atom	U_{11}	U_{22}	U_{33}	U_{23}	U_{13}	U_{12}
W(1)	14.58(4)	9.50(3)	9.20(3)	-1.42(2)	-0.19(3)	-2.64(3)
Cl(1)	17.4(2)	21.9(2)	13.48(19)	-6.51(17)	-0.94(16)	-0.54(17)
P(1)	27.0(3)	14.2(2)	15.9(2)	-2.81(18)	5.44(19)	-8.7(2)
P(2)	20.6(3)	18.1(2)	12.7(2)	-0.04(18)	-3.32(18)	0.52(19)
P(3)	16.4(2)	10.9(2)	14.2(2)	-2.14(17)	-1.55(17)	-3.59(17)
N(1)	15.4(8)	16.7(8)	10.1(7)	-3.7(6)	0.2(6)	-3.9(6)
N(2)	14.6(8)	20.3(8)	11.3(7)	-3.2(6)	-0.8(6)	-3.4(6)
C(1)	20.5(9)	12.3(8)	11.1(8)	-0.1(6)	-1.0(7)	-5.1(7)
C(2)	21.5(10)	15.5(9)	9.9(8)	-1.0(7)	-2.6(7)	-0.3(7)
C(3)	22(1)	19.8(10)	24(1)	-9.8(8)	-2.0(8)	-1.5(8)
C(4)	18.4(10)	31.1(12)	30.1(11)	-12.1(9)	-1.5(8)	-0.5(9)
C(5)	25.9(11)	25.5(11)	23.8(10)	-7.7(8)	-1.2(8)	8.9(9)
C(6)	39.5(13)	14.9(10)	23.8(10)	-2.7(8)	5.6(9)	1.7(9)
C(7)	28.8(11)	15.6(9)	22.5(10)	-2.4(8)	5.2(8)	-4.0(8)
C(8)	18.3(9)	12.2(8)	11.5(8)	-3.5(6)	0.9(7)	-4.8(7)
C(9)	20.3(10)	25.3(10)	12.1(8)	-3.3(7)	-3.5(7)	-2.7(8)
C(10)	17.9(10)	27.5(11)	14.9(9)	-3.0(8)	-4.6(7)	-1.4(8)
C(11)	16.3(9)	16.4(9)	11.3(8)	-2.8(7)	-0.5(7)	-5.2(7)
C(12)	23.9(10)	15.4(9)	14.7(8)	-2.4(7)	2.0(7)	-7.4(8)
C(13)	22.1(10)	23.2(10)	16.4(9)	-3.6(7)	3.2(7)	-11.2(8)
C(14)	19.1(10)	24.8(10)	16.9(9)	-6.5(8)	4.5(7)	-6.1(8)
C(15)	21.7(10)	18.5(9)	18.4(9)	-6.0(7)	0.9(7)	-3.4(8)
C(16)	20.2(9)	15.9(9)	14.5(8)	-3.5(7)	0.7(7)	-7.2(7)
C(17)	14.7(9)	22.6(10)	13.1(8)	-5.3(7)	1.1(7)	-4.4(7)
C(18)	14.9(9)	24.7(10)	20.8(9)	-6.8(8)	-0.4(7)	-2.5(8)
C(19)	17.6(10)	32.0(11)	23.9(10)	-12.1(9)	2.1(8)	-2.6(8)
C(20)	16.4(10)	50.5(15)	28.6(11)	-15.9(10)	4.0(8)	-8.1(10)
C(21)	20.1(10)	44.9(14)	24.5(10)	-10.8(10)	2.3(8)	-15.5(10)
C(22)	22(1)	32.3(11)	19.9(9)	-9.9(8)	-0.1(8)	-10.7(9)
C(23)	45.2(14)	15.5(10)	29.4(11)	1.1(8)	8.6(10)	-4.9(9)
C(24)	42.2(14)	27.9(11)	24.3(11)	-9.6(9)	7.0(9)	-21.6(10)
C(25)	32.0(12)	24.3(11)	23.7(10)	-6.1(8)	9.8(9)	-13.9(9)
C(26)	31.9(12)	31.3(12)	23.7(11)	-0.9(9)	-7.0(9)	9(1)
C(27)	31.8(12)	33.3(12)	22.9(10)	-5.2(9)	-11.4(9)	-4.2(10)
C(28)	37.6(13)	29.4(12)	15.3(9)	4.6(8)	-2.8(9)	-3.7(10)
C(29)	16.4(9)	16.5(9)	25.5(10)	-1.5(8)	-1.6(8)	-6.3(7)
C(30)	19.2(10)	14.2(9)	20.5(9)	-0.3(7)	0.2(7)	-2.1(7)
C(31)	37.7(12)	16.6(10)	23.3(10)	-6.4(8)	-4.1(9)	-9.0(9)

Table II.26. Continued.

W(2)	13.63(4)	11.70(4)	9.47(3)	-0.92(3)	-2.28(3)	-0.54(3)
Cl(2)	19.2(2)	23.2(2)	13.47(19)	-2.86(17)	-3.20(16)	-6.30(18)
P(4)	14.5(2)	16.2(2)	14.6(2)	-5.31(18)	-1.53(17)	-0.13(18)
P(5)	19.5(2)	20.6(2)	13.7(2)	1.66(18)	-4.02(18)	-7.3(2)
P(6)	18.9(2)	14.5(2)	20.9(2)	-1.33(19)	-2.00(19)	2.07(19)
N(3)	20.8(8)	14.1(7)	12.6(7)	-0.8(6)	-3.4(6)	-2.5(6)
N(4)	19.1(8)	17.9(8)	12.0(7)	-0.9(6)	-1.2(6)	-3.6(6)
C(32)	16.9(9)	12.0(8)	12.9(8)	-1.1(6)	-1.8(7)	1.8(7)
C(33)	21.8(10)	15.0(9)	12.2(8)	1.5(7)	-3.0(7)	-4.4(7)
C(34)	26.2(11)	18(1)	28.5(11)	-5.2(8)	-7.4(9)	-1.0(8)
C(35)	41.1(13)	15.3(10)	33.2(12)	-7.5(9)	-9.3(10)	-4.6(9)
C(36)	34.7(12)	24.1(11)	24.4(10)	-0.6(8)	-7.7(9)	-15.8(9)
C(37)	21.9(11)	27.7(11)	27.4(11)	-3.9(9)	-3.4(8)	-7.0(9)
C(38)	23.7(10)	20.9(10)	21.3(10)	-6.4(8)	-1.4(8)	-4.7(8)
C(39)	17.1(9)	11.1(8)	12.9(8)	-2.6(6)	-1.0(7)	3.1(7)
C(40)	33.2(12)	23.6(10)	13.0(9)	3.1(7)	-5.1(8)	-8.0(9)
C(41)	31.6(11)	24(1)	14.7(9)	2.3(8)	-1.8(8)	-10.5(9)
C(42)	18.4(9)	15.8(9)	14.2(8)	-1.9(7)	-3.6(7)	-1.3(7)
C(43)	25.1(11)	19.2(10)	25.3(10)	-8.8(8)	-1.0(8)	-2.0(8)
C(44)	28.0(11)	29.4(11)	22.8(10)	-9.8(9)	-1.0(8)	-9.9(9)
C(45)	32.2(12)	41.8(13)	21(1)	0.3(9)	-9.4(9)	-14(1)
C(46)	21.8(11)	34.2(12)	32.0(12)	1(1)	-10.8(9)	3.1(9)
C(47)	27.7(11)	20.8(10)	22.5(10)	-1.8(8)	-8.3(8)	4.6(8)
C(48)	16.7(9)	20.9(10)	13.7(8)	-0.8(7)	-1.9(7)	-2.6(7)
C(49)	21.5(11)	55.4(16)	31.6(12)	-22.3(11)	3.1(9)	-4.3(11)
C(50)	15.5(11)	64.3(17)	39.2(13)	-24.7(12)	3.2(9)	-3.2(11)
C(51)	25.7(12)	47.2(14)	28.3(11)	-2.9(10)	-5.4(9)	-15.7(10)
C(52)	24.7(11)	30.4(12)	32.6(12)	-11.4(9)	-8.1(9)	-2.8(9)
C(53)	21.3(10)	23.6(11)	32.6(11)	-8.3(9)	-8.1(9)	-1.2(8)
C(54)	17.6(10)	29.8(11)	34.8(12)	-17.7(9)	-5.8(9)	2.4(8)
C(55)	32.1(12)	17.1(10)	36.3(12)	-4.7(9)	8(1)	2.6(9)
C(56)	32.0(12)	30.6(12)	20(1)	-13.1(9)	-3.3(9)	2.0(9)
C(57)	21.8(11)	36.8(12)	21.3(10)	1.6(9)	0.9(8)	-10.7(9)
C(58)	35.5(12)	33.8(12)	15.2(9)	3.7(8)	-6.1(8)	-17.1(10)
C(59)	34.3(13)	23.1(11)	31.4(12)	5.3(9)	-3.7(10)	-12.8(9)
C(60A)	26.5(14)	24.0(15)	29(3)	-14(3)	-12(3)	3.6(11)
C(60B)	26.5(14)	24.0(15)	29(3)	-14(3)	-12(3)	3.6(11)
C(61A)	29(2)	19(3)	48(4)	-7.2(19)	-22(2)	6.9(19)
C(61B)	29(2)	19(3)	48(4)	-7.2(19)	-22(2)	6.9(19)
C(62A)	34(3)	30(2)	58(4)	6.4(19)	28(3)	12(2)
C(62B)	34(3)	30(2)	58(4)	6.4(19)	28(3)	12(2)

Table II.27. Bond Lengths for W(CPh)(ICy)(PMe_3)$_3$Cl.

Atom	Atom	Length/Å	Atom	Atom	Length/Å
W(1)	Cl(1)	2.6383(4)	W(2)	P(5)	2.4572(5)
W(1)	P(1)	2.4475(5)	W(2)	P(6)	2.4621(5)
W(1)	P(2)	2.4745(5)	W(2)	C(32)	1.8189(18)
W(1)	P(3)	2.4804(5)	W(2)	C(39)	2.2812(18)
W(1)	C(1)	1.8133(18)	P(4)	C(54)	1.821(2)
W(1)	C(8)	2.2384(17)	P(4)	C(55)	1.823(2)
P(1)	C(23)	1.834(2)	P(4)	C(56)	1.8340(19)
P(1)	C(24)	1.833(2)	P(5)	C(57)	1.832(2)
P(1)	C(25)	1.831(2)	P(5)	C(58)	1.8329(19)
P(2)	C(26)	1.826(2)	P(5)	C(59)	1.836(2)
P(2)	C(27)	1.838(2)	P(6)	C(60A)	1.841(7)
P(2)	C(28)	1.835(2)	P(6)	C(60B)	1.799(14)
P(3)	C(29)	1.8228(19)	P(6)	C(61A)	1.878(5)
P(3)	C(30)	1.8406(19)	P(6)	C(61B)	1.741(10)
P(3)	C(31)	1.8327(18)	P(6)	C(62A)	1.846(6)
N(1)	C(8)	1.387(2)	P(6)	C(62B)	1.844(11)
N(1)	C(9)	1.386(2)	N(3)	C(39)	1.379(2)
N(1)	C(11)	1.476(2)	N(3)	C(40)	1.382(2)
N(2)	C(8)	1.380(2)	N(3)	C(42)	1.473(2)
N(2)	C(10)	1.385(2)	N(4)	C(39)	1.388(2)
N(2)	C(17)	1.471(2)	N(4)	C(41)	1.383(2)
C(1)	C(2)	1.447(3)	N(4)	C(48)	1.474(2)
C(2)	C(3)	1.404(3)	C(32)	C(33)	1.452(2)
C(2)	C(7)	1.409(3)	C(33)	C(34)	1.406(3)
C(3)	C(4)	1.388(3)	C(33)	C(38)	1.404(3)
C(4)	C(5)	1.384(3)	C(34)	C(35)	1.387(3)
C(5)	C(6)	1.381(3)	C(35)	C(36)	1.380(3)
C(6)	C(7)	1.380(3)	C(36)	C(37)	1.379(3)
C(9)	C(10)	1.333(3)	C(37)	C(38)	1.384(3)
C(11)	C(12)	1.527(2)	C(40)	C(41)	1.333(3)
C(11)	C(16)	1.531(2)	C(42)	C(43)	1.527(2)
C(12)	C(13)	1.530(3)	C(42)	C(47)	1.525(3)
C(13)	C(14)	1.520(3)	C(43)	C(44)	1.526(3)
C(14)	C(15)	1.524(3)	C(44)	C(45)	1.521(3)
C(15)	C(16)	1.527(3)	C(45)	C(46)	1.516(3)
C(17)	C(18)	1.522(3)	C(46)	C(47)	1.529(3)
C(17)	C(22)	1.530(3)	C(48)	C(49)	1.527(3)
C(18)	C(19)	1.528(3)	C(48)	C(53)	1.520(3)
C(19)	C(20)	1.524(3)	C(49)	C(50)	1.536(3)

Table II.27. Continued.

C(20)	C(21)	1.519(3)	C(50)	C(51)	1.513(3)
C(21)	C(22)	1.528(3)	C(51)	C(52)	1.513(3)
W(2)	Cl(2)	2.5984(4)	C(52)	C(53)	1.525(3)
W(2)	P(4)	2.4810(5)			

Table II.28. Bond Angles for W(CPh)(ICy)(PMe_3)$_3$Cl.

Atom	Atom	Atom	Angle/°	Atom	Atom	Atom	Angle/°
P(1)	W(1)	Cl(1)	93.595(16)	P(5)	W(2)	P(6)	93.267(18)
P(1)	W(1)	P(2)	91.145(17)	P(6)	W(2)	Cl(2)	88.018(16)
P(1)	W(1)	P(3)	169.630(17)	P(6)	W(2)	P(4)	166.882(17)
P(2)	W(1)	Cl(1)	77.471(15)	C(32)	W(2)	Cl(2)	166.96(6)
P(2)	W(1)	P(3)	95.673(16)	C(32)	W(2)	P(4)	98.66(6)
P(3)	W(1)	Cl(1)	80.321(15)	C(32)	W(2)	P(5)	82.41(6)
C(1)	W(1)	Cl(1)	165.96(5)	C(32)	W(2)	P(6)	94.17(6)
C(1)	W(1)	P(1)	89.49(6)	C(32)	W(2)	C(39)	100.29(7)
C(1)	W(1)	P(2)	88.78(6)	C(39)	W(2)	Cl(2)	92.61(5)
C(1)	W(1)	P(3)	98.44(6)	C(39)	W(2)	P(4)	86.50(4)
C(1)	W(1)	C(8)	98.83(7)	C(39)	W(2)	P(5)	176.65(4)
C(8)	W(1)	Cl(1)	94.95(5)	C(39)	W(2)	P(6)	88.53(4)
C(8)	W(1)	P(1)	88.45(5)	C(54)	P(4)	W(2)	117.95(7)
C(8)	W(1)	P(2)	172.37(5)	C(54)	P(4)	C(55)	99.02(11)
C(8)	W(1)	P(3)	83.76(4)	C(54)	P(4)	C(56)	100.41(10)
C(23)	P(1)	W(1)	119.86(8)	C(55)	P(4)	W(2)	117.41(7)
C(24)	P(1)	W(1)	115.26(7)	C(55)	P(4)	C(56)	98.16(10)
C(24)	P(1)	C(23)	98.61(11)	C(56)	P(4)	W(2)	119.90(7)
C(25)	P(1)	W(1)	118.55(7)	C(57)	P(5)	W(2)	115.75(7)
C(25)	P(1)	C(23)	99.89(10)	C(57)	P(5)	C(58)	100.49(10)
C(25)	P(1)	C(24)	101.13(10)	C(57)	P(5)	C(59)	97.05(10)
C(26)	P(2)	W(1)	115.36(7)	C(58)	P(5)	W(2)	121.66(7)
C(26)	P(2)	C(27)	98.24(10)	C(58)	P(5)	C(59)	98.51(10)
C(26)	P(2)	C(28)	101.17(10)	C(59)	P(5)	W(2)	118.96(8)
C(27)	P(2)	W(1)	122.47(7)	C(60A)	P(6)	W(2)	119.8(2)
C(28)	P(2)	W(1)	118.76(7)	C(60A)	P(6)	C(61A)	100.9(2)
C(28)	P(2)	C(27)	96.64(10)	C(60A)	P(6)	C(62A)	96.9(3)
C(29)	P(3)	W(1)	116.09(6)	C(60B)	P(6)	W(2)	119.8(5)
C(29)	P(3)	C(30)	101.24(9)	C(60B)	P(6)	C(62B)	95.9(5)
C(29)	P(3)	C(31)	99.61(9)	C(61A)	P(6)	W(2)	117.34(18)
C(30)	P(3)	W(1)	115.79(6)	C(61B)	P(6)	W(2)	118.7(4)
C(31)	P(3)	W(1)	122.39(7)	C(61B)	P(6)	C(60B)	103.0(5)
C(31)	P(3)	C(30)	98.06(9)	C(61B)	P(6)	C(62B)	103.9(4)
C(8)	N(1)	C(11)	127.84(15)	C(62A)	P(6)	W(2)	119.48(17)
C(9)	N(1)	C(8)	111.51(15)	C(62A)	P(6)	C(61A)	98.2(2)
C(9)	N(1)	C(11)	120.51(14)	C(62B)	P(6)	W(2)	112.1(3)
C(8)	N(2)	C(10)	111.77(15)	C(39)	N(3)	C(40)	112.34(16)
C(8)	N(2)	C(17)	127.58(15)	C(39)	N(3)	C(42)	128.14(15)
C(10)	N(2)	C(17)	120.63(15)	C(40)	N(3)	C(42)	119.43(15)

Table II.28. Continued.

C(2)	C(1)	W(1)	173.48(14)	C(39)	N(4)	C(48)	128.49(15)
C(3)	C(2)	C(1)	121.72(16)	C(41)	N(4)	C(39)	111.64(15)
C(3)	C(2)	C(7)	116.53(17)	C(41)	N(4)	C(48)	119.77(16)
C(7)	C(2)	C(1)	121.74(17)	C(33)	C(32)	W(2)	173.89(14)
C(4)	C(3)	C(2)	121.67(18)	C(34)	C(33)	C(32)	122.54(17)
C(5)	C(4)	C(3)	120.4(2)	C(38)	C(33)	C(32)	121.26(16)
C(6)	C(5)	C(4)	119.05(19)	C(38)	C(33)	C(34)	116.15(17)
C(7)	C(6)	C(5)	120.99(19)	C(35)	C(34)	C(33)	121.5(2)
C(6)	C(7)	C(2)	121.36(19)	C(36)	C(35)	C(34)	120.89(19)
N(1)	C(8)	W(1)	126.85(13)	C(37)	C(36)	C(35)	118.94(18)
N(2)	C(8)	W(1)	130.81(12)	C(36)	C(37)	C(38)	120.5(2)
N(2)	C(8)	N(1)	102.23(14)	C(37)	C(38)	C(33)	122.01(18)
C(10)	C(9)	N(1)	107.22(16)	N(3)	C(39)	W(2)	125.05(13)
C(9)	C(10)	N(2)	107.25(16)	N(3)	C(39)	N(4)	101.75(15)
N(1)	C(11)	C(12)	111.55(15)	N(4)	C(39)	W(2)	133.19(12)
N(1)	C(11)	C(16)	109.44(14)	C(41)	C(40)	N(3)	106.85(17)
C(12)	C(11)	C(16)	111.05(14)	C(40)	C(41)	N(4)	107.40(18)
C(11)	C(12)	C(13)	110.86(15)	N(3)	C(42)	C(43)	109.46(15)
C(14)	C(13)	C(12)	110.85(15)	N(3)	C(42)	C(47)	111.47(15)
C(13)	C(14)	C(15)	110.38(15)	C(47)	C(42)	C(43)	111.19(15)
C(14)	C(15)	C(16)	110.70(16)	C(44)	C(43)	C(42)	112.16(16)
C(15)	C(16)	C(11)	112.55(15)	C(45)	C(44)	C(43)	110.81(17)
N(2)	C(17)	C(18)	111.33(15)	C(46)	C(45)	C(44)	110.65(16)
N(2)	C(17)	C(22)	110.97(14)	C(45)	C(46)	C(47)	110.96(18)
C(18)	C(17)	C(22)	110.81(16)	C(42)	C(47)	C(46)	109.76(17)
C(17)	C(18)	C(19)	110.82(17)	N(4)	C(48)	C(49)	112.03(15)
C(20)	C(19)	C(18)	110.90(16)	N(4)	C(48)	C(53)	110.21(15)
C(21)	C(20)	C(19)	111.33(17)	C(53)	C(48)	C(49)	109.75(17)
C(20)	C(21)	C(22)	111.55(18)	C(48)	C(49)	C(50)	109.78(17)
C(21)	C(22)	C(17)	110.26(15)	C(51)	C(50)	C(49)	110.6(2)
P(4)	W(2)	Cl(2)	80.096(15)	C(50)	C(51)	C(52)	110.31(18)
P(5)	W(2)	Cl(2)	84.638(15)	C(51)	C(52)	C(53)	111.60(18)
P(5)	W(2)	P(4)	91.141(17)	C(48)	C(53)	C(52)	111.92(17)

Table II.29. Torsion Angles for W(CPh)(ICy)(PMe_3)$_3$Cl.

A	B	C	D	Angle/°	A	B	C	D	Angle/°
N(1)	C(9)	C(10)	N(2)	1.2(2)	N(3)	C(40)	C(41)	N(4)	-1.5(2)
N(1)	C(11)	C(12)	C(13)	176.45(14)	N(3)	C(42)	C(43)	C(44)	177.92(16)
N(1)	C(11)	C(16)	C(15)	-176.66(14)	N(3)	C(42)	C(47)	C(46)	-178.22(16)
N(2)	C(17)	C(18)	C(19)	178.61(15)	N(4)	C(48)	C(49)	C(50)	179.42(19)
N(2)	C(17)	C(22)	C(21)	-178.92(17)	N(4)	C(48)	C(53)	C(52)	179.59(17)
C(1)	C(2)	C(3)	C(4)	-179.88(18)	C(32)	C(33)	C(34)	C(35)	175.96(19)
C(1)	C(2)	C(7)	C(6)	179.27(18)	C(32)	C(33)	C(38)	C(37)	-175.62(18)
C(2)	C(3)	C(4)	C(5)	0.1(3)	C(33)	C(34)	C(35)	C(36)	0.1(3)
C(3)	C(2)	C(7)	C(6)	-1.6(3)	C(34)	C(33)	C(38)	C(37)	1.8(3)
C(3)	C(4)	C(5)	C(6)	-0.6(3)	C(34)	C(35)	C(36)	C(37)	1.0(3)
C(4)	C(5)	C(6)	C(7)	0.0(3)	C(35)	C(36)	C(37)	C(38)	-0.7(3)
C(5)	C(6)	C(7)	C(2)	1.2(3)	C(36)	C(37)	C(38)	C(33)	-0.8(3)
C(7)	C(2)	C(3)	C(4)	1.0(3)	C(38)	C(33)	C(34)	C(35)	-1.4(3)
C(8)	N(1)	C(9)	C(10)	-0.8(2)	C(39)	N(3)	C(40)	C(41)	1.4(2)
C(8)	N(1)	C(11)	C(12)	139.11(17)	C(39)	N(3)	C(42)	C(43)	107.1(2)
C(8)	N(1)	C(11)	C(16)	-97.59(19)	C(39)	N(3)	C(42)	C(47)	-129.50(19)
C(8)	N(2)	C(10)	C(9)	-1.3(2)	C(39)	N(4)	C(41)	C(40)	1.2(2)
C(8)	N(2)	C(17)	C(18)	-109.9(2)	C(39)	N(4)	C(48)	C(49)	-136.6(2)
C(8)	N(2)	C(17)	C(22)	126.13(19)	C(39)	N(4)	C(48)	C(53)	100.9(2)
C(9)	N(1)	C(8)	W(1)	176.41(12)	C(40)	N(3)	C(39)	W(2)	178.34(13)
C(9)	N(1)	C(8)	N(2)	-0.02(19)	C(40)	N(3)	C(39)	N(4)	-0.66(19)
C(9)	N(1)	C(11)	C(12)	-45.6(2)	C(40)	N(3)	C(42)	C(43)	-69.4(2)
C(9)	N(1)	C(11)	C(16)	77.7(2)	C(40)	N(3)	C(42)	C(47)	54.0(2)
C(10)	N(2)	C(8)	W(1)	-175.41(13)	C(41)	N(4)	C(39)	W(2)	-179.19(14)
C(10)	N(2)	C(8)	N(1)	0.81(19)	C(41)	N(4)	C(39)	N(3)	-0.30(19)
C(10)	N(2)	C(17)	C(18)	71.8(2)	C(41)	N(4)	C(48)	C(49)	47.5(2)
C(10)	N(2)	C(17)	C(22)	-52.1(2)	C(41)	N(4)	C(48)	C(53)	-75.0(2)
C(11)	N(1)	C(8)	W(1)	-8.0(2)	C(42)	N(3)	C(39)	W(2)	1.7(2)
C(11)	N(1)	C(8)	N(2)	175.61(15)	C(42)	N(3)	C(39)	N(4)	-177.35(16)
C(11)	N(1)	C(9)	C(10)	-176.78(16)	C(42)	N(3)	C(40)	C(41)	178.41(17)
C(11)	C(12)	C(13)	C(14)	-57.6(2)	C(42)	C(43)	C(44)	C(45)	-53.9(2)
C(12)	C(11)	C(16)	C(15)	-53.1(2)	C(43)	C(42)	C(47)	C(46)	-55.8(2)
C(12)	C(13)	C(14)	C(15)	58.9(2)	C(43)	C(44)	C(45)	C(46)	55.9(2)
C(13)	C(14)	C(15)	C(16)	-56.8(2)	C(44)	C(45)	C(46)	C(47)	-58.8(2)
C(14)	C(15)	C(16)	C(11)	54.4(2)	C(45)	C(46)	C(47)	C(42)	58.5(2)
C(16)	C(11)	C(12)	C(13)	54.07(19)	C(47)	C(42)	C(43)	C(44)	54.3(2)
C(17)	N(2)	C(8)	W(1)	6.2(3)	C(48)	N(4)	C(39)	W(2)	4.7(3)
C(17)	N(2)	C(8)	N(1)	-177.60(16)	C(48)	N(4)	C(39)	N(3)	-176.42(16)
C(17)	N(2)	C(10)	C(9)	177.20(16)	C(48)	N(4)	C(41)	C(40)	177.67(17)

Table II.29. Continued.

C(17)	C(18)	C(19)	C(20)	56.3(2)	C(48)	C(49)	C(50)	C(51)	59.7(3)
C(18)	C(17)	C(22)	C(21)	56.9(2)	C(49)	C(48)	C(53)	C(52)	55.8(2)
C(18)	C(19)	C(20)	C(21)	-55.2(2)	C(49)	C(50)	C(51)	C(52)	-58.0(3)
C(19)	C(20)	C(21)	C(22)	55.4(2)	C(50)	C(51)	C(52)	C(53)	55.3(3)
C(20)	C(21)	C(22)	C(17)	-55.9(2)	C(51)	C(52)	C(53)	C(48)	-54.8(3)
C(22)	C(17)	C(18)	C(19)	-57.4(2)	C(53)	C(48)	C(49)	C(50)	-57.8(3)

Table II.30. Hydrogen Atom Coordinates (Å×10^4) and Isotropic Displacement Parameters (Å^2×10^3) for W(CPh)(ICy)(PMe_3)$_3$Cl.

Atom	***x***	***y***	***z***	**U(eq)**
H(3)	-1553	2526	4332	26
H(4)	-3234	3328	4785	31
H(5)	-3281	4719	4889	32
H(6)	-1616	5291	4550	33
H(7)	77	4498	4118	27
H(9)	3275	1493	6123	23
H(10)	5045	1192	5298	24
H(11)	713	2212	5077	17
H(12A)	1494	1444	6496	21
H(12B)	904	1012	5940	21
H(13A)	-862	1926	6125	24
H(13B)	-473	1462	6917	24
H(14A)	262	2629	7138	24
H(14B)	-1075	2893	6987	24
H(15A)	26	3853	6290	23
H(15B)	-586	3423	5743	23
H(16A)	1792	2990	6059	20
H(16B)	1338	3414	5272	20
H(17)	4518	1866	3328	20
H(18A)	4686	420	3591	24
H(18B)	5687	387	4130	24
H(19A)	6545	42	2959	29
H(19B)	5864	881	2546	29
H(20A)	7647	779	3528	37
H(20B)	7762	1059	2647	37
H(21A)	6428	2271	2777	34
H(21B)	7428	2221	3319	34
H(22A)	5567	2607	3947	28
H(22B)	6237	1761	4358	28
H(23A)	1617	4486	2227	47
H(23B)	2239	4982	2710	47
H(23C)	1073	4662	3045	47
H(24A)	2439	4081	4282	44
H(24B)	3484	4406	3765	44
H(24C)	3658	3484	4188	44
H(25A)	4592	3171	2733	39
H(25B)	4123	4087	2359	39
H(25C)	3821	3311	2038	39

Table II.30. Continued.

H(26A)	-1103	3231	2642	46
H(26B)	-842	3530	1773	46
H(26C)	-354	3946	2387	46
H(27A)	867	1432	1716	43
H(27B)	-108	2136	1358	43
H(27C)	-359	1657	2171	43
H(28A)	1869	3558	1486	43
H(28B)	1070	3217	987	43
H(28C)	2236	2647	1254	43
H(29A)	-216	1138	4737	29
H(29B)	-317	333	4377	29
H(29C)	-799	1231	3967	29
H(30A)	2948	109	4127	28
H(30B)	1880	-330	4467	28
H(30C)	2168	415	4842	28
H(31A)	396	430	2830	37
H(31B)	1198	-310	3293	37
H(31C)	1768	306	2666	37
H(34)	4952	4792	9079	29
H(35)	6315	5443	9469	35
H(36)	8261	4842	9414	31
H(37)	8840	3591	8929	30
H(38)	7496	2938	8524	26
H(40)	4000	1158	10962	28
H(41)	2311	834	10456	28
H(42)	5649	2400	9571	19
H(43A)	4440	3239	10368	28
H(43B)	4603	2523	11058	28
H(44A)	6365	3409	10341	31
H(44B)	5794	3467	11175	31
H(45A)	7644	2600	11172	37
H(45B)	6656	2098	11554	37
H(46A)	7892	1312	10713	36
H(46B)	7635	2047	10047	36
H(47A)	6492	1032	9977	29
H(47B)	5939	1120	10813	29
H(48)	1867	1889	8575	21
H(49A)	507	2138	9608	42
H(49B)	685	1168	9899	42
H(50A)	-997	1559	9220	46
H(50B)	-235	1900	8502	46

Table II.30. Continued.

H(51A)	-554	574	8364	39
H(51B)	-5	203	9137	39
H(52A)	1227	865	7817	34
H(52B)	1396	-89	8158	34
H(53A)	2210	185	9196	30
H(53B)	2901	556	8459	30
H(54A)	7445	1945	7771	40
H(54B)	7581	962	7951	40
H(54C)	7178	1527	8606	40
H(55A)	5359	562	8924	45
H(55B)	6027	120	8237	45
H(55C)	4662	432	8254	45
H(56A)	5061	1245	6782	41
H(56B)	6330	750	6926	41
H(56C)	6147	1710	6606	41
H(57A)	6708	3667	7179	40
H(57B)	6481	3865	6314	40
H(57C)	6683	2930	6706	40
H(58A)	4529	2836	6066	41
H(58B)	4672	3758	5726	41
H(58C)	3469	3580	6145	41
H(59A)	3599	4883	6952	44
H(59B)	4777	4940	6442	44
H(59C)	4752	4913	7328	44
H(60A)	3059	4781	9145	39
H(60B)	1929	5195	8728	39
H(60C)	3168	5097	8271	39
H(60D)	3389	4925	8605	39
H(60E)	2018	5169	8746	39
H(60F)	2607	5154	7913	39
H(61A)	1796	4426	7302	48
H(61B)	757	4477	7942	48
H(61C)	1231	3626	7608	48
H(61D)	1499	3983	7458	48
H(61E)	692	4315	8152	48
H(61F)	1019	3344	8106	48
H(62A)	1102	3152	9200	70
H(62B)	919	4094	9354	70
H(62C)	1915	3426	9733	70
H(62D)	1738	3153	9595	70
H(62E)	1294	4128	9547	70

Table II.30. Continued.

H(62F)	2571	3743	9776	70

Table II.31. Atomic Occupancy for W(CPh)(ICy)(PMe_3)$_3$Cl.

Atom	***Occupancy***	**Atom**	***Occupancy***	**Atom**	***Occupancy***
C(60A)	0.630(7)	H(60A)	0.630(7)	H(60B)	0.630(7)
H(60C)	0.630(7)	C(60B)	0.370(7)	H(60D)	0.370(7)
H(60E)	0.370(7)	H(60F)	0.370(7)	C(61A)	0.630(7)
H(61A)	0.630(7)	H(61B)	0.630(7)	H(61C)	0.630(7)
C(61B)	0.370(7)	H(61D)	0.370(7)	H(61E)	0.370(7)
H(61F)	0.370(7)	C(62A)	0.630(7)	H(62A)	0.630(7)
H(62B)	0.630(7)	H(62C)	0.630(7)	C(62B)	0.370(7)
H(62D)	0.370(7)	H(62E)	0.370(7)	H(62F)	0.370(7)

II.5 Diffraction data for (IPr)CoCl{N(SiMe$_3$)$_2$}

Table II.32. Crystal data and structure refinement for (IPr)CoCl{N(SiMe$_3$)$_2$}.

Identification code	(IPr)CoCl{N(SiMe3)2}
Empirical formula	$C_{33}H_{54}ClCoN_3Si_2$
Formula weight	643.35
Temperature/K	100(2)
Crystal system	monoclinic
Space group	$P2_1/c$
a/Å	10.7820(5)
b/Å	17.8049(7)
c/Å	19.6609(9)
α/°	90
β/°	101.804(2)
γ/°	90
Volume/Å^3	3694.5(3)
Z	4
ρ_{calc}g/cm^3	1.157
μ/mm^{-1}	0.626
F(000)	1380.0
Crystal size/mm^3	0.181 × 0.132 × 0.073
Radiation	MoKα (λ = 0.71073)
2Θ range for data collection/°	4.232 to 50.696
Index ranges	$-12 \leq h \leq 12$, $-20 \leq k \leq 21$, $-23 \leq l \leq 23$
Reflections collected	79031
Independent reflections	6747 [R_{int} = 0.0708, R_{sigma} = 0.0304]
Data/restraints/parameters	6747/0/375
Goodness-of-fit on F^2	0.847
Final R indexes [I>=2σ (I)]	R_1 = 0.0316, wR_2 = 0.0981
Final R indexes [all data]	R_1 = 0.0481, wR_2 = 0.1113
Largest diff. peak/hole / e Å^{-3}	0.38/-0.20

Table II.33. Fractional Atomic Coordinates ($\times 10^4$) and Equivalent Isotropic Displacement Parameters ($Å^2 \times 10^3$) for (IPr)CoCl{$N(SiMe_3)_2$}. U_{eq} is defined as 1/3 of of the trace of the orthogonalised U_{IJ} tensor.

Atom	***x***	***y***	***z***	**U(eq)**
Co(1)	3548.1(2)	2029.7(2)	2323.3(2)	13.11(10)
Cl(1)	5116.0(5)	2871.0(3)	2481.4(3)	24.66(15)
Si(1)	1451.5(5)	2770.5(3)	1276.3(3)	15.62(15)
Si(2)	1386.6(5)	2781.6(3)	2836.3(3)	17.75(15)
N(1)	1911.3(15)	2479.6(9)	2119.8(9)	16.2(4)
N(2)	4553.3(15)	527.5(9)	3009.0(8)	12.3(4)
N(3)	4448.2(15)	473.7(9)	1915.6(8)	13.3(4)
C(1)	1526(2)	3812.3(12)	1172.4(13)	28.0(5)
C(2)	-194(2)	2473.8(15)	870.2(13)	30.7(6)
C(3)	2555(2)	2366.9(13)	755.9(11)	23.2(5)
C(4)	2521(2)	2460.7(13)	3632.4(11)	24.7(5)
C(5)	-232(2)	2418.9(16)	2861.3(14)	36.5(6)
C(6)	1316(3)	3831.2(13)	2911.9(13)	32.5(6)
C(7)	4178.4(18)	938.0(11)	2418(1)	12.4(4)
C(8)	5027.4(19)	-167.5(11)	2873.8(11)	17.1(4)
C(9)	4963.9(19)	-199.1(11)	2187.9(11)	17.0(4)
C(10)	4194.5(19)	621.9(11)	1179.4(10)	14.9(4)
C(11)	3106(2)	300.7(11)	775.6(11)	18.3(5)
C(12)	2898(2)	424.4(12)	64.8(11)	24.6(5)
C(13)	3750(2)	833.6(12)	-224.8(11)	24.7(5)
C(14)	4815(2)	1144.3(12)	187.7(11)	21.6(5)
C(15)	5063.5(19)	1048.8(11)	910.0(11)	16.4(4)
C(16)	6223.4(19)	1391.9(11)	1370.9(11)	17.6(5)
C(17)	7374(2)	871.6(13)	1450.0(13)	31.7(6)
C(18)	6539(2)	2164.7(13)	1119.5(13)	26.8(5)
C(19)	2157(2)	-135.4(12)	1099.9(12)	24.5(5)
C(20)	1613(3)	-819.0(14)	670.9(15)	43.3(7)
C(21)	1102(2)	373.1(14)	1230.5(15)	39.0(7)
C(22)	4417.0(18)	736.0(11)	3698.4(10)	13.2(4)
C(23)	3362.4(19)	463.1(11)	3928.2(11)	18.5(5)
C(24)	3296(2)	612.6(12)	4613.5(12)	24.2(5)
C(25)	4223(2)	1023.9(13)	5036.3(12)	25.7(5)
C(26)	5242(2)	1305.0(12)	4788.1(11)	22.3(5)
C(27)	5371.9(19)	1162.5(11)	4111.7(10)	15.8(4)
C(28)	6509.4(19)	1448.9(12)	3845.0(11)	18.9(5)
C(29)	7611(2)	893.7(14)	4012.2(14)	34.5(6)
C(30)	6925(2)	2231.5(13)	4116.7(13)	27.4(5)

Table II.33. Continued.

C(31)	2304(2)	39.2(12)	3449.9(12)	25.1(5)
C(32)	2307(3)	-792.4(13)	3621.9(14)	38.0(7)
C(33)	1011(3)	374.2(16)	3472(2)	67.1(12)

Table II.34. Anisotropic Displacement Parameters ($Å^2 \times 10^3$) for (IPr)CoCl{$N(SiMe_3)_2$}. The Anisotropic displacement factor exponent takes the form: $-2\pi^2[h^2a^{*2}U_{11}+2hka^*b^*U_{12}+\ldots]$.

Atom	**U_{11}**	**U_{22}**	**U_{33}**	**U_{23}**	**U_{13}**	**U_{12}**
Co(1)	15.35(16)	7.86(16)	15.89(17)	0.2(1)	2.66(12)	1.55(10)
Cl(1)	23.0(3)	12.4(3)	37.6(3)	-1.9(2)	3.8(2)	-4.2(2)
Si(1)	14.5(3)	14.4(3)	18.3(3)	2.0(2)	4.2(2)	2.7(2)
Si(2)	19.1(3)	17.3(3)	17.2(3)	-1.1(2)	4.5(2)	4.0(2)
N(1)	17.1(9)	13.1(9)	18.6(9)	0.1(7)	4.3(7)	2.0(7)
N(2)	15.4(8)	9.6(8)	11.9(9)	-0.5(7)	2.5(7)	-1.3(7)
N(3)	16.9(8)	9.7(8)	12.3(9)	-1.0(7)	0.8(7)	-0.5(7)
C(1)	34.4(13)	20.2(12)	32.7(14)	5.9(10)	14.6(11)	7.1(10)
C(2)	21.7(12)	41.6(15)	26.6(13)	0.6(11)	-0.4(10)	1.5(11)
C(3)	27.9(12)	22.5(12)	21.2(12)	1.9(9)	9.4(10)	5.8(10)
C(4)	32.3(13)	22.4(12)	17.9(12)	-1.1(9)	1.3(10)	5.5(10)
C(5)	26.5(13)	52.6(18)	32.6(15)	0.2(13)	11.0(11)	1.8(12)
C(6)	45.3(15)	21.0(13)	28.6(13)	-4.6(10)	0.9(11)	12.7(11)
C(7)	12.7(10)	9.8(10)	14.2(10)	-0.5(8)	1.6(8)	-2.9(8)
C(8)	22.3(11)	10.6(10)	17.3(11)	2.6(8)	1.5(9)	3.1(8)
C(9)	23.8(11)	8(1)	19.2(11)	-0.4(8)	4.3(9)	4.3(8)
C(10)	21.5(10)	10.7(10)	12.2(10)	1.0(8)	2.8(8)	5.1(8)
C(11)	23.2(11)	12.6(10)	17.3(11)	-1.4(8)	0.1(9)	4.2(9)
C(12)	30.1(12)	19.5(11)	20.2(12)	-4.2(9)	-4.3(10)	3.6(10)
C(13)	38.1(13)	23.1(12)	12.1(11)	0.2(9)	3.2(10)	9.4(10)
C(14)	30.0(12)	19.6(11)	17.1(11)	3.6(9)	9.1(10)	5.6(9)
C(15)	21.9(11)	10.6(10)	17.6(11)	0.0(8)	6.1(9)	5.2(8)
C(16)	20.9(11)	16.1(11)	16.7(11)	0.4(8)	5.9(9)	0.4(9)
C(17)	27.4(13)	22.7(12)	39.8(15)	-4.4(11)	-5.2(11)	3.8(10)
C(18)	23.8(12)	23.8(12)	34.5(14)	7.2(10)	10.0(11)	-3.1(10)
C(19)	27.1(12)	20.6(12)	22.7(12)	0.9(9)	-2(1)	-5.2(10)
C(20)	53.9(17)	23.2(14)	52.4(18)	-6.7(13)	9.8(14)	-12.7(12)
C(21)	33.3(14)	27.9(14)	59.3(19)	-2.9(13)	17.9(13)	-6.2(11)
C(22)	18.7(10)	11(1)	10.1(10)	2.2(8)	3.4(8)	2.0(8)
C(23)	19.0(11)	12.1(10)	25.3(12)	5.8(9)	6.5(9)	2.8(8)
C(24)	29.1(12)	19.5(12)	28.7(13)	6.3(10)	17(1)	2.6(10)
C(25)	42.0(14)	22.6(12)	15.6(11)	2.9(9)	13(1)	7.8(10)
C(26)	31.5(12)	19.0(11)	15.3(11)	-3.1(9)	2.0(9)	2.4(10)
C(27)	21.1(11)	10.7(10)	15.7(11)	0.2(8)	3.7(9)	2.8(8)
C(28)	21.9(11)	18.5(11)	15.6(11)	-3.2(9)	2.3(9)	-3.1(9)
C(29)	26.4(13)	28.4(13)	51.7(17)	1.2(12)	14.6(12)	4.8(11)
C(30)	26.5(13)	24.5(12)	30.7(14)	-5.7(10)	4.5(11)	-9.8(10)
C(31)	21.7(12)	23.6(12)	29.7(13)	7.5(10)	4.3(10)	-5.2(10)

Table II.34. Continued.

C(32)	43.1(16)	18.9(12)	45.7(16)	-2.7(11)	-5.9(13)	-2.6(11)
C(33)	23.6(14)	25.4(15)	144(4)	-10.0(19)	-2.8(18)	-2.7(12)

Table II.35. Bond Lengths for (IPr)CoCl{$N(SiMe_3)_2$}.

Atom	Atom	Length/Å	Atom	Atom	Length/Å
Co(1)	N(1)	1.9046(17)	C(11)	C(19)	1.524(3)
Co(1)	C(7)	2.0549(19)	C(12)	C(13)	1.384(3)
Co(1)	Cl(1)	2.2324(6)	C(13)	C(14)	1.379(3)
Si(1)	N(1)	1.7111(17)	C(14)	C(15)	1.401(3)
Si(1)	C(3)	1.865(2)	C(15)	C(16)	1.515(3)
Si(1)	C(2)	1.866(2)	C(16)	C(18)	1.524(3)
Si(1)	C(1)	1.870(2)	C(16)	C(17)	1.530(3)
Si(2)	N(1)	1.7086(18)	C(19)	C(21)	1.517(3)
Si(2)	C(4)	1.868(2)	C(19)	C(20)	1.528(3)
Si(2)	C(5)	1.871(2)	C(22)	C(23)	1.394(3)
Si(2)	C(6)	1.877(2)	C(22)	C(27)	1.398(3)
N(2)	C(7)	1.362(2)	C(23)	C(24)	1.390(3)
N(2)	C(8)	1.385(3)	C(23)	C(31)	1.522(3)
N(2)	C(22)	1.441(2)	C(24)	C(25)	1.373(3)
N(3)	C(7)	1.364(2)	C(25)	C(26)	1.384(3)
N(3)	C(9)	1.382(2)	C(26)	C(27)	1.389(3)
N(3)	C(10)	1.442(2)	C(27)	C(28)	1.517(3)
C(8)	C(9)	1.337(3)	C(28)	C(30)	1.526(3)
C(10)	C(15)	1.392(3)	C(28)	C(29)	1.528(3)
C(10)	C(11)	1.398(3)	C(31)	C(32)	1.519(3)
C(11)	C(12)	1.387(3)	C(31)	C(33)	1.526(3)

Table II.36. Bond Angles for (IPr)CoCl{$N(SiMe_3)_2$}.

Atom	Atom	Atom	Angle/°	Atom	Atom	Atom	Angle/°
N(1)	Co(1)	C(7)	133.78(7)	C(12)	C(11)	C(19)	121.23(19)
N(1)	Co(1)	Cl(1)	112.94(5)	C(10)	C(11)	C(19)	121.89(19)
C(7)	Co(1)	Cl(1)	113.27(5)	C(13)	C(12)	C(11)	120.9(2)
N(1)	Si(1)	C(3)	108.92(9)	C(14)	C(13)	C(12)	120.8(2)
N(1)	Si(1)	C(2)	112.99(10)	C(13)	C(14)	C(15)	120.8(2)
C(3)	Si(1)	C(2)	108.27(11)	C(10)	C(15)	C(14)	116.59(19)
N(1)	Si(1)	C(1)	113.32(10)	C(10)	C(15)	C(16)	122.01(18)
C(3)	Si(1)	C(1)	105.99(11)	C(14)	C(15)	C(16)	121.40(19)
C(2)	Si(1)	C(1)	107.01(11)	C(15)	C(16)	C(18)	112.47(18)
N(1)	Si(2)	C(4)	108.92(10)	C(15)	C(16)	C(17)	111.68(17)
N(1)	Si(2)	C(5)	112.40(10)	C(18)	C(16)	C(17)	110.44(18)
C(4)	Si(2)	C(5)	109.07(11)	C(21)	C(19)	C(11)	110.96(18)
N(1)	Si(2)	C(6)	113.85(11)	C(21)	C(19)	C(20)	110.6(2)
C(4)	Si(2)	C(6)	105.57(11)	C(11)	C(19)	C(20)	112.9(2)
C(5)	Si(2)	C(6)	106.74(13)	C(23)	C(22)	C(27)	123.60(19)
Si(2)	N(1)	Si(1)	128.65(10)	C(23)	C(22)	N(2)	117.51(17)
Si(2)	N(1)	Co(1)	114.08(9)	C(27)	C(22)	N(2)	118.80(17)
Si(1)	N(1)	Co(1)	113.78(9)	C(24)	C(23)	C(22)	117.06(19)
C(7)	N(2)	C(8)	111.86(16)	C(24)	C(23)	C(31)	120.88(19)
C(7)	N(2)	C(22)	126.47(16)	C(22)	C(23)	C(31)	122.04(19)
C(8)	N(2)	C(22)	121.54(16)	C(25)	C(24)	C(23)	120.9(2)
C(7)	N(3)	C(9)	111.93(16)	C(24)	C(25)	C(26)	120.8(2)
C(7)	N(3)	C(10)	126.26(16)	C(25)	C(26)	C(27)	121.0(2)
C(9)	N(3)	C(10)	121.76(16)	C(26)	C(27)	C(22)	116.70(19)
N(2)	C(7)	N(3)	102.85(16)	C(26)	C(27)	C(28)	121.09(19)
N(2)	C(7)	Co(1)	128.29(14)	C(22)	C(27)	C(28)	122.20(18)
N(3)	C(7)	Co(1)	128.55(14)	C(27)	C(28)	C(30)	112.72(18)
C(9)	C(8)	N(2)	106.63(17)	C(27)	C(28)	C(29)	110.85(18)
C(8)	C(9)	N(3)	106.72(17)	C(30)	C(28)	C(29)	110.81(19)
C(15)	C(10)	C(11)	124.03(19)	C(32)	C(31)	C(23)	112.27(18)
C(15)	C(10)	N(3)	118.53(17)	C(32)	C(31)	C(33)	109.6(2)
C(11)	C(10)	N(3)	117.40(18)	C(23)	C(31)	C(33)	111.3(2)
C(12)	C(11)	C(10)	116.8(2)				

Table II.37. Torsion Angles for (IPr)CoCl{$N(SiMe_3)_2$}.

A	B	C	D	Angle/°	A	B	C	D	Angle/°
C(4)	Si(2)	N(1)	Si(1)	-164.68(13)	C(11)	C(10)	C(15)	C(16)	179.35(19)
C(5)	Si(2)	N(1)	Si(1)	74.34(16)	N(3)	C(10)	C(15)	C(16)	-3.2(3)
C(6)	Si(2)	N(1)	Si(1)	-47.19(17)	C(13)	C(14)	C(15)	C(10)	0.7(3)
C(4)	Si(2)	N(1)	Co(1)	-7.32(13)	C(13)	C(14)	C(15)	C(16)	-179.49(19)
C(5)	Si(2)	N(1)	Co(1)	-128.30(12)	C(10)	C(15)	C(16)	C(18)	-143.0(2)
C(6)	Si(2)	N(1)	Co(1)	110.18(12)	C(14)	C(15)	C(16)	C(18)	37.2(3)
C(3)	Si(1)	N(1)	Si(2)	169.83(12)	C(10)	C(15)	C(16)	C(17)	92.1(2)
C(2)	Si(1)	N(1)	Si(2)	-69.81(16)	C(14)	C(15)	C(16)	C(17)	-87.6(2)
C(1)	Si(1)	N(1)	Si(2)	52.12(16)	C(12)	C(11)	C(19)	C(21)	-84.1(3)
C(3)	Si(1)	N(1)	Co(1)	12.40(13)	C(10)	C(11)	C(19)	C(21)	93.1(2)
C(2)	Si(1)	N(1)	Co(1)	132.77(11)	C(12)	C(11)	C(19)	C(20)	40.8(3)
C(1)	Si(1)	N(1)	Co(1)	-105.30(11)	C(10)	C(11)	C(19)	C(20)	-142.1(2)
C(8)	N(2)	C(7)	N(3)	-0.5(2)	C(7)	N(2)	C(22)	C(23)	95.6(2)
C(22)	N(2)	C(7)	N(3)	-176.30(16)	C(8)	N(2)	C(22)	C(23)	-79.8(2)
C(8)	N(2)	C(7)	Co(1)	-174.48(14)	C(7)	N(2)	C(22)	C(27)	-87.8(2)
C(22)	N(2)	C(7)	Co(1)	9.7(3)	C(8)	N(2)	C(22)	C(27)	96.8(2)
C(9)	N(3)	C(7)	N(2)	0.3(2)	C(27)	C(22)	C(23)	C(24)	-1.9(3)
C(10)	N(3)	C(7)	N(2)	177.62(17)	N(2)	C(22)	C(23)	C(24)	174.57(17)
C(9)	N(3)	C(7)	Co(1)	174.28(14)	C(27)	C(22)	C(23)	C(31)	176.38(19)
C(10)	N(3)	C(7)	Co(1)	-8.4(3)	N(2)	C(22)	C(23)	C(31)	-7.2(3)
C(7)	N(2)	C(8)	C(9)	0.5(2)	C(22)	C(23)	C(24)	C(25)	1.2(3)
C(22)	N(2)	C(8)	C(9)	176.54(17)	C(31)	C(23)	C(24)	C(25)	-177.07(19)
N(2)	C(8)	C(9)	N(3)	-0.3(2)	C(23)	C(24)	C(25)	C(26)	0.5(3)
C(7)	N(3)	C(9)	C(8)	0.0(2)	C(24)	C(25)	C(26)	C(27)	-1.7(3)
C(10)	N(3)	C(9)	C(8)	-177.47(18)	C(25)	C(26)	C(27)	C(22)	1.0(3)
C(7)	N(3)	C(10)	C(15)	83.7(2)	C(25)	C(26)	C(27)	C(28)	-178.0(2)
C(9)	N(3)	C(10)	C(15)	-99.3(2)	C(23)	C(22)	C(27)	C(26)	0.8(3)
C(7)	N(3)	C(10)	C(11)	-98.7(2)	N(2)	C(22)	C(27)	C(26)	-175.63(17)
C(9)	N(3)	C(10)	C(11)	78.4(2)	C(23)	C(22)	C(27)	C(28)	179.83(19)
C(15)	C(10)	C(11)	C(12)	-0.2(3)	N(2)	C(22)	C(27)	C(28)	3.4(3)
N(3)	C(10)	C(11)	C(12)	-177.67(18)	C(26)	C(27)	C(28)	C(30)	-38.1(3)
C(15)	C(10)	C(11)	C(19)	-177.48(19)	C(22)	C(27)	C(28)	C(30)	142.8(2)
N(3)	C(10)	C(11)	C(19)	5.0(3)	C(26)	C(27)	C(28)	C(29)	86.7(2)
C(10)	C(11)	C(12)	C(13)	1.4(3)	C(22)	C(27)	C(28)	C(29)	-92.3(2)
C(19)	C(11)	C(12)	C(13)	178.7(2)	C(24)	C(23)	C(31)	C(32)	-73.5(3)
C(11)	C(12)	C(13)	C(14)	-1.5(3)	C(22)	C(23)	C(31)	C(32)	108.3(2)
C(12)	C(13)	C(14)	C(15)	0.4(3)	C(24)	C(23)	C(31)	C(33)	49.7(3)
C(11)	C(10)	C(15)	C(14)	-0.9(3)	C(22)	C(23)	C(31)	C(33)	-128.5(2)
N(3)	C(10)	C(15)	C(14)	176.61(17)					

Table II.38. Hydrogen Atom Coordinates (Å×10^4) and Isotropic Displacement Parameters (Å^2×10^3) for (IPr)CoCl{N(SiMe$_3$)$_2$}.

Atom	***x***	***y***	***z***	**U(eq)**
H(2)	878	4051	1384	42
H(1)	1374	3938	677	42
H(3)	2366	3994	1402	42
H(4)	-276	1930	923	46
H(5)	-370	2602	375	46
H(6)	-798	2733	1099	46
H(7)	3430	2492	977	35
H(8)	2360	2577	285	35
H(9)	2456	1820	732	35
H(10)	2561	1911	3637	37
H(11)	2232	2637	4046	37
H(12)	3364	2666	3632	37
H(15)	-855	2653	2488	55
H(14)	-440	2541	3311	55
H(13)	-251	1873	2797	55
H(16)	2121	4049	2852	49
H(17)	1164	3966	3371	49
H(18)	625	4027	2552	49
H(37)	5337	-548	3204	21
H(36)	5223	-605	1936	20
H(28)	2159	225	-227	30
H(27)	3600	901	-714	30
H(19)	5386	1426	-20	26
H(20)	6028	1458	1843	21
H(22)	7170	386	1634	48
H(21)	8092	1098	1771	48
H(23)	7596	797	996	48
H(24)	6841	2112	684	40
H(26)	7202	2398	1472	40
H(25)	5779	2480	1041	40
H(35)	2620	-324	1562	29
H(30)	1083	-1108	926	65
H(29)	2307	-1136	584	65
H(31)	1098	-652	227	65
H(32)	1466	790	1532	58
H(34)	525	86	1457	58
H(33)	633	572	787	58
H(47)	2600	428	4792	29

Table II.38. Continued.

H(46)	4164	1117	5504	31
H(45)	5862	1600	5085	27
H(44)	6254	1484	3328	23
H(38)	7884	846	4517	52
H(40)	8319	1077	3815	52
H(39)	7337	403	3811	52
H(42)	6191	2568	4038	41
H(41)	7563	2425	3871	41
H(43)	7289	2204	4615	41
H(48)	2442	90	2964	30
H(51)	3127	-1011	3590	57
H(50)	1631	-1045	3292	57
H(49)	2163	-858	4095	57
H(52)	374	168	3089	101
H(53)	1045	921	3424	101
H(54)	782	248	3916	101

II.6 Diffraction data for (IPr)CoCl(OBHT)

Table II.39. Crystal data and structure refinement for (IPr)CoCl(OBHT).

Identification code	(IPr)CoCl(OBHT)
Empirical formula	$C_{42}H_{59}ClCoN_2O$
Formula weight	702.29
Temperature/K	100(2)
Crystal system	monoclinic
Space group	$P2_1/n$
a/Å	10.1555(6)
b/Å	20.2913(11)
c/Å	19.5144(11)
α/°	90
β/°	100.3857(19)
γ/°	90
Volume/Å^3	3955.4(4)
Z	4
ρ_{calc}g/cm^3	1.179
μ/mm^{-1}	0.534
F(000)	1508.0
Crystal size/mm^3	0.249 × 0.180 × 0.151
Radiation	MoKα (λ = 0.71073)
2Θ range for data collection/°	4.014 to 55.236
Index ranges	$-13 \leq h \leq 13$, $-26 \leq k \leq 26$, $-25 \leq l \leq 25$
Reflections collected	99354
Independent reflections	9193 [R_{int} = 0.0804, R_{sigma} = 0.0413]
Data/restraints/parameters	9193/0/439
Goodness-of-fit on F^2	0.894
Final R indexes [I>=2σ (I)]	R_1 = 0.0459, wR_2 = 0.1205
Final R indexes [all data]	R_1 = 0.0690, wR_2 = 0.1378
Largest diff. peak/hole / e Å^{-3}	0.90/-0.45

\

Table II.40. Fractional Atomic Coordinates ($\times 10^4$) and Equivalent Isotropic Displacement Parameters ($Å^2 \times 10^3$) for (IPr)CoCl(OBHT). U_{eq} is defined as 1/3 of of the trace of the orthogonalised U_{IJ} tensor.

Atom	***x***	***y***	***z***	**U(eq)**
Co(1)	1110.3(3)	2420.6(2)	2515.1(2)	16.0(1)
Cl(1)	-1023.9(5)	2144.3(3)	2359.0(3)	32.89(16)
O(1)	1642.4(13)	3294.8(7)	2718.2(7)	16.5(3)
N(1)	2585.2(15)	1130.6(8)	2280.4(8)	12.8(3)
N(2)	2937.6(15)	1417.1(8)	3351.1(9)	14.0(3)
C(1)	2333.2(18)	1623.6(9)	2712.6(10)	12.9(4)
C(2)	3334.8(19)	631.5(10)	2649.2(10)	16.6(4)
C(3)	3561(2)	814.4(10)	3319.8(11)	17.9(4)
C(4)	3062.4(19)	1808.9(9)	3974.9(10)	15.0(4)
C(5)	4087(2)	2279.6(10)	4088.9(11)	17.3(4)
C(6)	4193(2)	2653.8(10)	4693.2(12)	21.4(4)
C(7)	3347(2)	2548.2(10)	5165.1(12)	22.7(5)
C(8)	2369(2)	2066.5(10)	5045.0(11)	20.0(4)
C(9)	2189.9(19)	1686.4(10)	4441.7(10)	17.0(4)
C(10)	5070(2)	2368.0(11)	3591.3(11)	20.3(4)
C(11)	5044(2)	3064.8(12)	3301.2(13)	32.3(5)
C(12)	6491(2)	2177.2(13)	3937.3(14)	33.4(6)
C(13)	1124(2)	1155.7(11)	4313.3(11)	21.5(4)
C(14)	-237(2)	1407.5(13)	4427.1(15)	35.1(6)
C(15)	1563(3)	557.8(12)	4772.8(16)	37.9(6)
C(16)	2232.7(19)	1133.1(9)	1529.5(10)	14.0(4)
C(17)	3147.3(19)	1416.8(9)	1152.2(10)	15.5(4)
C(18)	2860(2)	1349.3(10)	431.9(11)	20.4(4)
C(19)	1721(2)	1023.4(11)	105.4(11)	21.9(4)
C(20)	813(2)	777.0(11)	491.2(11)	21.5(4)
C(21)	1046.5(19)	826.4(9)	1213.9(10)	15.6(4)
C(22)	4410(2)	1762.1(10)	1514.3(11)	19.6(4)
C(23)	4825(2)	2336.0(12)	1093.9(14)	30.1(5)
C(24)	5570(2)	1279.0(12)	1673.9(15)	35.2(6)
C(25)	63(2)	542.2(10)	1639.3(11)	19.2(4)
C(26)	344(2)	-189.1(11)	1789.1(13)	27.7(5)
C(27)	-1391(2)	635.1(11)	1279.7(13)	26.2(5)
C(28)	749.5(19)	3774.1(10)	2494.2(11)	16.6(4)
C(29)	489(2)	3961.6(9)	1780.2(11)	17.2(4)
C(30)	-543(2)	4408.8(10)	1561.0(11)	20.7(4)
C(31)	-1294(2)	4689.5(10)	2014.6(12)	22.6(5)
C(32)	-944(2)	4537.4(10)	2717.2(12)	20.3(4)

Table II.40. Continued.

C(33)	71(2)	4095.7(10)	2977.7(11)	18.1(4)
C(34)	1359(2)	3705.9(10)	1269.2(11)	20.3(4)
C(35)	1368(2)	2943.3(10)	1234.9(12)	23.3(5)
C(36)	863(2)	3953.8(11)	523.9(11)	26.6(5)
C(37)	2799(2)	3955.3(11)	1499.7(12)	23.9(5)
C(38)	451(2)	3965.9(10)	3765.3(11)	18.8(4)
C(39)	160(2)	3251.2(11)	3944.1(12)	26.4(5)
C(40)	1940(2)	4118.3(12)	4020.0(12)	25.5(5)
C(41)	-333(3)	4412.2(12)	4184.1(12)	29.4(5)
C(42)	-2415(2)	5163.5(13)	1752.9(14)	34.1(6)

Table II.41. Anisotropic Displacement Parameters ($Å^2 \times 10^3$) for (IPr)CoCl(OBHT). The Anisotropic displacement factor exponent takes the form: $-2\pi^2[h^2a^{*2}U_{11}+2hka^*b^*U_{12}+\ldots]$.

Atom	U_{11}	U_{22}	U_{33}	U_{23}	U_{13}	U_{12}
Co(1)	13.58(15)	13.97(15)	20.56(17)	-1.17(10)	3.33(11)	1.97(10)
Cl(1)	15.6(3)	31.2(3)	52.1(4)	-10.3(3)	6.6(2)	-3.3(2)
O(1)	16.3(7)	13.6(7)	19.5(7)	-1.1(5)	3.4(6)	1.8(5)
N(1)	10.9(7)	13.9(8)	14.5(8)	-0.4(6)	4.5(6)	0.4(6)
N(2)	13.0(7)	14.0(8)	15.3(8)	-1.3(6)	3.4(6)	-0.3(6)
C(1)	10.6(8)	14.9(9)	13.7(10)	0.1(7)	3.7(7)	-2.2(7)
C(2)	17.2(9)	15.3(9)	17.9(10)	0.5(7)	4.9(8)	3.3(7)
C(3)	17.0(9)	16.0(9)	20.5(11)	1.7(8)	2.6(8)	4.6(8)
C(4)	15.1(9)	16.7(9)	13(1)	-1.0(7)	2.0(7)	2.9(7)
C(5)	15.9(9)	18.5(10)	17.2(10)	0.8(8)	2.4(8)	1.3(7)
C(6)	20.2(10)	20(1)	22.3(12)	-4.0(8)	-0.5(9)	-1.6(8)
C(7)	24.1(11)	25.1(11)	17.8(11)	-7.8(8)	1.0(9)	4.7(9)
C(8)	19.4(10)	25.1(11)	16.3(10)	-1.6(8)	5.4(8)	5.7(8)
C(9)	15.3(9)	18.9(10)	16.7(10)	-0.6(8)	2.5(8)	3.3(8)
C(10)	16.9(10)	24.8(11)	19.7(11)	-1.0(8)	4.8(8)	-3.6(8)
C(11)	28.2(12)	35.7(13)	33.0(14)	12.2(11)	5.7(10)	0.9(10)
C(12)	21.6(12)	44.8(15)	35.7(14)	12.9(11)	10.1(10)	6.8(10)
C(13)	20.2(10)	25.6(11)	20.5(11)	-2.0(8)	8.5(8)	-4.2(8)
C(14)	17.2(11)	36.0(14)	52.7(17)	-4.7(12)	8.1(11)	-1.4(10)
C(15)	33.0(13)	27.2(13)	54.9(17)	9.1(12)	11.9(12)	-2.1(10)
C(16)	14.9(9)	13.5(9)	13.7(10)	-0.5(7)	3.4(7)	2.4(7)
C(17)	15.3(9)	15.0(9)	17.6(10)	0.0(7)	6.7(8)	2.3(7)
C(18)	19.1(10)	23.7(11)	20.1(11)	2.5(8)	8.4(8)	3.3(8)
C(19)	24.7(11)	27.8(11)	12.9(10)	-2.3(8)	2.2(8)	6.1(9)
C(20)	16.4(10)	24.7(11)	21.3(11)	-3.1(8)	-2.2(8)	2.3(8)
C(21)	13.2(9)	15.3(9)	19(1)	-0.4(7)	4.3(8)	1.7(7)
C(22)	17.4(10)	21.8(10)	21.1(11)	-2.5(8)	7.5(8)	-4.8(8)
C(23)	28.3(12)	27.3(12)	38.8(14)	1.8(10)	16.7(11)	-5.5(10)
C(24)	16.9(11)	30.9(13)	54.4(17)	4.7(12)	-2.1(11)	-4.2(9)
C(25)	15.6(9)	20.3(10)	23.0(11)	-2.2(8)	6.4(8)	-3.1(8)
C(26)	23.0(11)	24.9(11)	36.0(14)	7.2(10)	7.4(10)	0.2(9)
C(27)	15.3(10)	26.5(11)	37.2(14)	3.6(10)	5.7(9)	-2.8(8)
C(28)	15.3(9)	14.8(9)	19.8(11)	0.0(8)	3.3(8)	-0.8(7)
C(29)	18.2(10)	15.2(9)	18.3(11)	-2.3(8)	3.3(8)	-2.1(7)
C(30)	22.2(11)	19.3(10)	18.8(11)	-0.8(8)	-0.9(8)	-0.6(8)
C(31)	20(1)	19.6(10)	26.7(12)	-0.1(8)	0.3(9)	2.9(8)
C(32)	18.9(10)	16.9(10)	26.8(12)	-2.7(8)	8.8(8)	1.0(8)
C(33)	17.4(10)	15.6(9)	21.9(11)	-0.3(8)	5.5(8)	-2.7(7)

C(34)	23(1)	21.3(10)	17.3(11)	-1.4(8)	5.4(8)	-0.1(8)
C(35)	26.4(11)	22.3(11)	21.3(11)	-4.5(8)	4.2(9)	0.7(9)
C(36)	35.8(13)	25.6(11)	18.4(12)	-3.1(9)	5.1(10)	-0.8(9)
C(37)	25.0(11)	24.4(11)	24.2(12)	-1.7(9)	10.0(9)	-1.0(9)
C(38)	21.6(10)	18.5(10)	18.5(11)	1.4(8)	9.3(8)	1.9(8)
C(39)	33.1(12)	22.1(11)	26.2(12)	5.1(9)	11.3(10)	0.0(9)
C(40)	27.7(12)	30.3(12)	18.5(11)	-2.4(9)	4.4(9)	-2.9(9)
C(41)	42.0(14)	26.4(12)	24.5(12)	3.3(9)	19.0(11)	8.6(10)
C(42)	30.3(13)	36.1(14)	33.7(14)	-0.3(11)	-0.1(11)	14.5(11)

Table II.42. Bond Lengths for (IPr)CoCl(OBHT).

Atom	**Atom**	**Length/Å**	**Atom**	**Atom**	**Length/Å**
Co(1)	O(1)	1.8756(14)	C(17)	C(18)	1.390(3)
Co(1)	C(1)	2.0331(19)	C(17)	C(22)	1.519(3)
Co(1)	Cl(1)	2.2061(6)	C(18)	C(19)	1.384(3)
O(1)	C(28)	1.348(2)	C(19)	C(20)	1.385(3)
N(1)	C(1)	1.362(2)	C(20)	C(21)	1.391(3)
N(1)	C(2)	1.388(2)	C(21)	C(25)	1.523(3)
N(1)	C(16)	1.444(3)	C(22)	C(24)	1.521(3)
N(2)	C(1)	1.352(2)	C(22)	C(23)	1.527(3)
N(2)	C(3)	1.384(2)	C(25)	C(27)	1.528(3)
N(2)	C(4)	1.440(2)	C(25)	C(26)	1.529(3)
C(2)	C(3)	1.340(3)	C(28)	C(29)	1.422(3)
C(4)	C(5)	1.400(3)	C(28)	C(33)	1.423(3)
C(4)	C(9)	1.403(3)	C(29)	C(30)	1.394(3)
C(5)	C(6)	1.390(3)	C(29)	C(34)	1.537(3)
C(5)	C(10)	1.524(3)	C(30)	C(31)	1.390(3)
C(6)	C(7)	1.384(3)	C(31)	C(32)	1.388(3)
C(7)	C(8)	1.384(3)	C(31)	C(42)	1.508(3)
C(8)	C(9)	1.392(3)	C(32)	C(33)	1.391(3)
C(9)	C(13)	1.516(3)	C(33)	C(38)	1.538(3)
C(10)	C(11)	1.521(3)	C(34)	C(36)	1.536(3)
C(10)	C(12)	1.528(3)	C(34)	C(37)	1.536(3)
C(13)	C(14)	1.526(3)	C(34)	C(35)	1.549(3)
C(13)	C(15)	1.527(3)	C(38)	C(39)	1.533(3)
C(16)	C(21)	1.397(3)	C(38)	C(41)	1.535(3)
C(16)	C(17)	1.408(3)	C(38)	C(40)	1.536(3)

Table II.43. Bond Angles for (IPr)CoCl(OBHT).

Atom	Atom	Atom	Angle/°
O(1)	Co(1)	C(1)	124.71(7)
O(1)	Co(1)	Cl(1)	120.53(4)
C(1)	Co(1)	Cl(1)	112.04(5)
C(28)	O(1)	Co(1)	117.56(12)
C(1)	N(1)	C(2)	111.20(16)
C(1)	N(1)	C(16)	125.85(16)
C(2)	N(1)	C(16)	122.77(16)
C(1)	N(2)	C(3)	111.62(16)
C(1)	N(2)	C(4)	124.33(16)
C(3)	N(2)	C(4)	123.64(17)
N(2)	C(1)	N(1)	103.78(16)
N(2)	C(1)	Co(1)	125.54(14)
N(1)	C(1)	Co(1)	130.05(14)
C(3)	C(2)	N(1)	106.62(17)
C(2)	C(3)	N(2)	106.78(17)
C(5)	C(4)	C(9)	123.77(18)
C(5)	C(4)	N(2)	117.42(17)
C(9)	C(4)	N(2)	118.78(17)
C(6)	C(5)	C(4)	116.67(19)
C(6)	C(5)	C(10)	121.12(19)
C(4)	C(5)	C(10)	122.18(18)
C(7)	C(6)	C(5)	121.2(2)
C(8)	C(7)	C(6)	120.6(2)
C(7)	C(8)	C(9)	121.0(2)
C(8)	C(9)	C(4)	116.73(18)
C(8)	C(9)	C(13)	120.93(18)
C(4)	C(9)	C(13)	122.32(18)
C(11)	C(10)	C(5)	112.14(18)
C(11)	C(10)	C(12)	110.58(19)
C(5)	C(10)	C(12)	111.32(18)
C(9)	C(13)	C(14)	112.11(18)
C(9)	C(13)	C(15)	110.07(18)
C(14)	C(13)	C(15)	110.9(2)
C(21)	C(16)	C(17)	123.32(18)
C(21)	C(16)	N(1)	118.84(17)
C(17)	C(16)	N(1)	117.76(17)
C(18)	C(17)	C(16)	116.77(18)
C(18)	C(17)	C(22)	121.45(18)
C(16)	C(17)	C(22)	121.75(18)
C(19)	C(18)	C(17)	121.23(19)
C(18)	C(19)	C(20)	120.35(19)
C(19)	C(20)	C(21)	121.12(19)
C(20)	C(21)	C(16)	117.08(18)
C(20)	C(21)	C(25)	121.12(18)
C(16)	C(21)	C(25)	121.79(18)
C(17)	C(22)	C(24)	110.85(18)
C(17)	C(22)	C(23)	113.16(18)
C(24)	C(22)	C(23)	108.84(18)
C(21)	C(25)	C(27)	112.18(18)
C(21)	C(25)	C(26)	110.71(17)
C(27)	C(25)	C(26)	109.83(17)
O(1)	C(28)	C(29)	120.41(17)
O(1)	C(28)	C(33)	119.59(18)
C(29)	C(28)	C(33)	120.00(18)
C(30)	C(29)	C(28)	118.12(18)
C(30)	C(29)	C(34)	120.60(19)
C(28)	C(29)	C(34)	121.21(18)
C(31)	C(30)	C(29)	122.7(2)
C(32)	C(31)	C(30)	117.75(19)
C(32)	C(31)	C(42)	121.3(2)
C(30)	C(31)	C(42)	120.9(2)
C(31)	C(32)	C(33)	123.04(19)
C(32)	C(33)	C(28)	117.94(19)
C(32)	C(33)	C(38)	120.73(18)
C(28)	C(33)	C(38)	121.32(17)
C(36)	C(34)	C(37)	107.56(17)
C(36)	C(34)	C(29)	112.04(18)
C(37)	C(34)	C(29)	109.09(17)
C(36)	C(34)	C(35)	106.85(17)
C(37)	C(34)	C(35)	109.20(18)
C(29)	C(34)	C(35)	111.97(17)
C(39)	C(38)	C(41)	107.29(17)
C(39)	C(38)	C(40)	109.63(18)
C(41)	C(38)	C(40)	106.48(18)
C(39)	C(38)	C(33)	111.44(18)
C(41)	C(38)	C(33)	111.75(17)
C(40)	C(38)	C(33)	110.09(16)

Table II.44. Hydrogen Atom Coordinates (Å×10^4) and Isotropic Displacement Parameters (Å^2×10^3) for (IPr)CoCl(OBHT).

Atom	***x***	***y***	***z***	**U(eq)**
H(2)	3630	237	2463	20
H(3)	4055	576	3700	21
H(6)	4857	2988	4784	26
H(7)	3440	2809	5575	27
H(8)	1810	1994	5379	24
H(10)	4791	2062	3189	24
H(11A)	4127	3178	3081	48
H(11B)	5632	3090	2955	48
H(11C)	5356	3375	3681	48
H(12A)	6794	2469	4334	50
H(12B)	7092	2220	3599	50
H(12C)	6497	1720	4100	50
H(13)	1029	1013	3816	26
H(14A)	-173	1546	4913	53
H(14B)	-902	1055	4322	53
H(14C)	-508	1784	4119	53
H(15A)	2451	414	4703	57
H(15B)	919	199	4648	57
H(15C)	1601	677	5263	57
H(18)	3456	1530	159	24
H(19)	1561	968	-386	26
H(20)	17	571	258	26
H(22)	4234	1941	1967	24
H(23A)	5157	2165	687	45
H(23B)	5533	2590	1386	45
H(23C)	4050	2622	939	45
H(24A)	5322	914	1953	53
H(24B)	6357	1505	1934	53
H(24C)	5780	1107	1237	53
H(25)	191	780	2095	23
H(26A)	-299	-363	2062	42
H(26B)	1255	-242	2053	42
H(26C)	255	-431	1348	42
H(27A)	-1554	1102	1166	39
H(27B)	-1990	490	1592	39
H(27C)	-1563	373	851	39
H(30)	-742	4526	1082	25
H(32)	-1419	4745	3035	24

Table II.44. Continued.

H(35A)	2029	2770	1621	35
H(35B)	1602	2803	792	35
H(35C)	478	2774	1270	35
H(36A)	-38	3781	352	40
H(36B)	1472	3802	221	40
H(36C)	837	4437	523	40
H(37A)	2803	4438	1501	36
H(37B)	3359	3794	1175	36
H(37C)	3154	3793	1969	36
H(39A)	-783	3150	3765	40
H(39B)	347	3193	4451	40
H(39C)	730	2954	3730	40
H(40A)	2182	4014	4517	38
H(40B)	2106	4587	3948	38
H(40C)	2483	3851	3758	38
H(41A)	-1289	4308	4065	44
H(41B)	-190	4874	4072	44
H(41C)	-20	4339	4683	44
H(42A)	-2385	5285	1270	51
H(42B)	-2314	5560	2044	51
H(42C)	-3276	4953	1774	51

II.7 Diffraction data for (IPr)Co(NHDIPP)$_2$

Table II.45. Crystal data and structure refinement for (IPr)Co(NHDIPP)$_2$.

Identification code	(IPr)Co(NHDIPP)$_2$
Empirical formula	$C_{51}H_{72}CoN_4$
Formula weight	800.05
Temperature/K	100(2)
Crystal system	monoclinic
Space group	C2/c
a/Å	21.5951(8)
b/Å	9.2309(3)
c/Å	24.4704(8)
α/°	90
β/°	112.3443(11)
γ/°	90
Volume/Å^3	4511.7(3)
Z	4
ρ_{calc}g/cm^3	1.178
μ/mm^{-1}	0.418
F(000)	1732.0
Crystal size/mm^3	0.230 × 0.133 × 0.091
Radiation	MoKα (λ = 0.71073)
2Θ range for data collection/°	4.292 to 53.63
Index ranges	$-27 \leq h \leq 26$, $-11 \leq k \leq 11$, $-31 \leq l \leq 31$
Reflections collected	34372
Independent reflections	4813 [R_{int} = 0.0317, R_{sigma} = 0.0232]
Data/restraints/parameters	4813/32/403
Goodness-of-fit on F^2	1.031
Final R indexes [I>=2σ (I)]	R_1 = 0.0364, wR_2 = 0.0863
Final R indexes [all data]	R_1 = 0.0514, wR_2 = 0.0932
Largest diff. peak/hole / e Å^{-3}	0.30/-0.25

Table II.46. Fractional Atomic Coordinates ($\times 10^4$) and Equivalent Isotropic Displacement Parameters ($Å^2 \times 10^3$) for (IPr)Co(NHDIPP)$_2$. U_{eq} is defined as 1/3 of of the trace of the orthogonalised U_{IJ} tensor.

Atom	***x***	***y***	***z***	**U(eq)**
Co(1)	5000	8730.4(3)	7500	28.8(1)
N(2)	5449.7(7)	9656.2(15)	8234.3(6)	32.9(3)
C(1)	5000	6498(2)	7500	27.3(5)
C(2)	4853.7(8)	4147.0(16)	7206.8(6)	32.9(4)
C(3)	6099.2(8)	10082.0(16)	8566.0(6)	30.2(3)
C(4)	6581.8(9)	10157.9(17)	8307.0(7)	35.4(4)
C(5)	7231.5(9)	10588(2)	8648.1(8)	41.2(4)
C(6)	7424.5(9)	10934.1(19)	9238.8(8)	41.2(4)
C(7)	6958.0(9)	10861.4(17)	9494.3(7)	35.2(4)
C(8)	6300.1(8)	10450.3(16)	9176.9(6)	30.5(3)
C(9)	6398.2(10)	9827(2)	7655.7(8)	45.0(5)
C(10)	6099.7(10)	11153(2)	7282.5(8)	49.5(5)
C(11A)	7036(4)	9612(15)	7480(3)	47(2)
C(11B)	6919(3)	8924(14)	7532(3)	50.0(18)
C(12)	5793.9(8)	10445.5(19)	9464.1(7)	36.3(4)
C(13)	6097.7(10)	10224(2)	10134.8(7)	50.9(5)
C(14)	5374.4(10)	11828(2)	9312.4(8)	47.5(5)
N(1)	4763.9(6)	5580.3(13)	7028.8(5)	27.0(3)
C(15A)	4406(3)	5953(13)	6433(4)	23.8(15)
C(16A)	3709(3)	5996(7)	6180(2)	27.9(12)
C(17A)	3409(2)	6181(6)	5572(2)	40.1(12)
C(18A)	3789(4)	6404(8)	5242(3)	44.8(18)
C(19A)	4475(3)	6405(5)	5495(2)	42.3(11)
C(20A)	4806(3)	6205(7)	6111(3)	28.2(12)
C(21A)	3288(2)	5713(6)	6537(2)	35.4(11)
C(22A)	3053(3)	4138(8)	6476(4)	49.0(15)
C(23A)	2660(2)	6666(5)	6351(3)	61.0(12)
C(24A)	5571(3)	6205(6)	6389(2)	34.1(13)
C(25A)	5860(3)	4693(7)	6446(3)	55.4(17)
C(26A)	5881(2)	7212(7)	6074(3)	40.9(13)
C(15B)	4571(4)	5955(17)	6374(4)	22.6(19)
C(16B)	3889(4)	6112(9)	6062(3)	27.4(14)
C(17B)	3681(4)	6333(8)	5457(3)	41(2)
C(18B)	4142(5)	6302(7)	5191(3)	53.3(18)
C(19B)	4811(4)	6126(8)	5512(3)	53.0(17)
C(20B)	5048(3)	5927(9)	6124(3)	33.9(17)
C(21B)	3388(3)	6086(6)	6351(3)	33.5(14)

Table II.46. Continued.

C(22B)	3223(5)	4542(10)	6483(6)	56(2)
C(23B)	2730(2)	6879(6)	5997(2)	55.8(14)
C(24B)	5780(4)	5667(10)	6484(3)	57(3)
C(25B)	6063(4)	4383(8)	6286(4)	70(2)
C(26B)	6236(5)	6902(11)	6614(6)	61(3)
C(26C)	6130(7)	7095(17)	6247(8)	43(4)

Table II.47. Anisotropic Displacement Parameters ($Å^2 \times 10^3$) for (IPr)Co(NHDIPP)$_2$. The Anisotropic displacement factor exponent takes the form: $-2\pi^2[h^2a^{*2}U_{11}+2hka^*b^*U_{12}+\ldots]$.

Atom	**U_{11}**	**U_{22}**	**U_{33}**	**U_{23}**	**U_{13}**	**U_{12}**
Co(1)	37.11(18)	23.18(16)	15.77(14)	0	-1.59(12)	0
N(2)	34.2(8)	34.8(7)	20.8(6)	-4.4(5)	0.5(6)	2.7(6)
C(1)	27.8(11)	27.9(11)	17.8(9)	0	-0.9(8)	0
C(2)	44.6(9)	23.3(7)	22.8(7)	-2.4(6)	3.9(7)	-0.6(7)
C(3)	36.4(9)	23.9(7)	21.1(7)	-0.8(6)	0.6(7)	3.2(6)
C(4)	42.6(10)	31.6(8)	24.8(8)	-2.3(6)	4.6(7)	3.1(7)
C(5)	45.2(10)	40.4(10)	37.2(9)	-5.2(8)	14.5(8)	-3.8(8)
C(6)	38.5(9)	39.0(9)	36.2(9)	-7.8(7)	3.2(8)	-7.5(7)
C(7)	42.0(9)	31.4(8)	21.6(7)	-2.7(6)	0.2(7)	-1.1(7)
C(8)	37.3(9)	25.4(8)	19.9(7)	-0.1(6)	1.0(6)	3.1(6)
C(9)	43.7(10)	58.9(12)	27.5(9)	-6.5(8)	8.0(8)	8.3(9)
C(10)	49.8(11)	60.0(12)	30.1(9)	4.8(8)	5.5(8)	-11.9(9)
C(11A)	47(3)	62(5)	31(2)	-8(3)	13(2)	6(3)
C(11B)	46(3)	64(5)	39(2)	-10(3)	13.7(19)	-7(3)
C(12)	40.1(9)	40.9(9)	20.0(7)	-3.2(7)	2.6(7)	-1.1(7)
C(13)	54.7(12)	68.6(13)	22.2(8)	-0.3(8)	6.5(8)	-4.4(10)
C(14)	50.9(11)	52.7(11)	34.2(9)	-7.6(8)	10.9(8)	10.0(9)
N(1)	32.7(7)	23.8(6)	16.2(6)	0.5(5)	-0.1(5)	-1.3(5)
C(15A)	36(4)	21.2(18)	14(2)	0.2(15)	9(2)	-6(3)
C(16A)	29(3)	31(2)	17(2)	-3.6(18)	1.1(18)	3(2)
C(17A)	48(3)	32(2)	23(2)	0.4(15)	-5.7(19)	-3(2)
C(18A)	60(4)	42(2)	16(3)	6(3)	-3(3)	2(3)
C(19A)	67(4)	41(2)	15(2)	0.0(16)	11(3)	-12(2)
C(20A)	32(3)	29(2)	20.1(19)	-1.2(15)	6(2)	-4(2)
C(21A)	29(2)	38(3)	31(2)	-4.9(18)	1.4(17)	2.5(19)
C(22A)	46(4)	40(3)	60(3)	0(3)	19(3)	6(3)
C(23A)	38(2)	39(2)	97(4)	-8(3)	16(3)	1.7(16)
C(24A)	46(4)	34(2)	20(2)	3.6(16)	10(2)	-10(2)
C(25A)	47(3)	46(4)	72(4)	13(3)	22(2)	-2(3)
C(26A)	45(3)	48(3)	33(3)	5(2)	19(3)	-6(3)
C(15B)	26(4)	31(3)	9(3)	1(2)	4(3)	-11(3)
C(16B)	35(3)	23(2)	21(3)	-4.0(19)	7(2)	0(2)
C(17B)	56(5)	33(3)	18(4)	5(3)	-5(4)	-5(3)
C(18B)	96(6)	45(3)	11(2)	-4(2)	12(4)	5(4)
C(19B)	84(5)	54(4)	28(3)	-5(2)	28(3)	-17(4)
C(20B)	40(4)	46(4)	21(3)	-5(2)	18(3)	-10(3)
C(21B)	30(3)	29(3)	28(3)	-1(2)	-3(2)	-1(2)
C(22B)	31(4)	55(7)	81(4)	-3(4)	19(3)	-7(3)

Table II.47. Continued.

C(23B)	31(2)	43(3)	65(3)	-11(3)	-14(2)	6(2)
C(24B)	41(4)	103(9)	34(4)	-8(5)	21(3)	-18(5)
C(25B)	68(5)	32(3)	89(5)	-1(3)	7(4)	-11(3)
C(26B)	39(6)	47(6)	79(8)	-41(6)	1(7)	6(5)
C(26C)	33(8)	29(5)	58(12)	7(7)	8(8)	3(6)

Table II.48. Bond Lengths for (IPr)Co(NHDIPP)$_2$.

Atom	Atom	Length/Å	Atom	Atom	Length/Å
Co(1)	N(2)	1.8909(13)	C(16A)	C(17A)	1.390(7)
Co(1)	N(2)[1]	1.8910(13)	C(16A)	C(21A)	1.503(6)
Co(1)	C(1)	2.061(2)	C(17A)	C(18A)	1.368(8)
N(2)	C(3)	1.384(2)	C(18A)	C(19A)	1.370(9)
C(1)	N(1)	1.3639(17)	C(19A)	C(20A)	1.413(7)
C(1)	N(1)[1]	1.3640(17)	C(20A)	C(24A)	1.529(6)
C(2)	C(2)[1]	1.330(3)	C(21A)	C(22A)	1.528(7)
C(2)	N(1)	1.3834(19)	C(21A)	C(23A)	1.533(6)
C(3)	C(4)	1.413(2)	C(24A)	C(25A)	1.513(6)
C(3)	C(8)	1.430(2)	C(24A)	C(26A)	1.516(8)
C(4)	C(5)	1.390(2)	C(15B)	C(20B)	1.384(8)
C(4)	C(9)	1.520(2)	C(15B)	C(16B)	1.386(10)
C(5)	C(6)	1.381(2)	C(16B)	C(17B)	1.389(8)
C(6)	C(7)	1.375(3)	C(16B)	C(21B)	1.501(7)
C(7)	C(8)	1.388(2)	C(17B)	C(18B)	1.381(10)
C(8)	C(12)	1.508(2)	C(18B)	C(19B)	1.368(9)
C(9)	C(10)	1.516(3)	C(19B)	C(20B)	1.398(8)
C(9)	C(11B)	1.519(6)	C(20B)	C(24B)	1.508(8)
C(9)	C(11A)	1.605(8)	C(21B)	C(22B)	1.533(8)
C(12)	C(14)	1.527(3)	C(21B)	C(23B)	1.540(7)
C(12)	C(13)	1.532(2)	C(24B)	C(26B)	1.460(10)
N(1)	C(15A)	1.409(9)	C(24B)	C(25B)	1.495(8)
N(1)	C(15B)	1.534(10)	C(24B)	C(26C)	1.725(19)
C(15A)	C(16A)	1.393(8)	C(26B)	C(26C)	0.86(2)
C(15A)	C(20A)	1.394(7)			

[1]1-X,+Y,3/2-Z

Table II.49. Bond Angles for (IPr)Co(NHDIPP)$_2$.

Atom	Atom	Atom	Angle/°	Atom	Atom	Atom	Angle/°
N(2)	Co(1)	N(2)[1]	126.26(9)	C(17A)	C(16A)	C(21A)	120.3(4)
N(2)	Co(1)	C(1)	116.87(4)	C(15A)	C(16A)	C(21A)	121.8(5)
N(2)[1]	Co(1)	C(1)	116.87(4)	C(18A)	C(17A)	C(16A)	120.8(5)
C(3)	N(2)	Co(1)	136.53(12)	C(17A)	C(18A)	C(19A)	121.3(5)
N(1)	C(1)	N(1)[1]	103.21(17)	C(18A)	C(19A)	C(20A)	120.3(5)
N(1)	C(1)	Co(1)	128.40(8)	C(15A)	C(20A)	C(19A)	116.9(6)
N(1)[1]	C(1)	Co(1)	128.40(8)	C(15A)	C(20A)	C(24A)	123.1(5)
C(2)[1]	C(2)	N(1)	106.98(8)	C(19A)	C(20A)	C(24A)	119.9(6)
N(2)	C(3)	C(4)	120.47(14)	C(16A)	C(21A)	C(22A)	111.1(5)
N(2)	C(3)	C(8)	121.18(15)	C(16A)	C(21A)	C(23A)	113.0(4)
C(4)	C(3)	C(8)	118.35(14)	C(22A)	C(21A)	C(23A)	107.1(5)
C(5)	C(4)	C(3)	119.55(15)	C(25A)	C(24A)	C(26A)	111.6(6)
C(5)	C(4)	C(9)	119.24(16)	C(25A)	C(24A)	C(20A)	112.3(5)
C(3)	C(4)	C(9)	121.18(15)	C(26A)	C(24A)	C(20A)	112.6(4)
C(6)	C(5)	C(4)	121.91(17)	C(20B)	C(15B)	C(16B)	125.0(7)
C(7)	C(6)	C(5)	118.89(16)	C(20B)	C(15B)	N(1)	120.3(7)
C(6)	C(7)	C(8)	122.01(15)	C(16B)	C(15B)	N(1)	114.1(5)
C(7)	C(8)	C(3)	119.28(15)	C(15B)	C(16B)	C(17B)	116.6(6)
C(7)	C(8)	C(12)	120.61(14)	C(15B)	C(16B)	C(21B)	123.0(6)
C(3)	C(8)	C(12)	120.07(14)	C(17B)	C(16B)	C(21B)	120.4(7)
C(10)	C(9)	C(11B)	120.0(5)	C(18B)	C(17B)	C(16B)	120.0(6)
C(10)	C(9)	C(4)	110.55(16)	C(19B)	C(18B)	C(17B)	121.7(5)
C(11B)	C(9)	C(4)	113.6(3)	C(18B)	C(19B)	C(20B)	120.5(6)
C(10)	C(9)	C(11A)	98.6(5)	C(15B)	C(20B)	C(19B)	116.1(7)
C(4)	C(9)	C(11A)	113.4(2)	C(15B)	C(20B)	C(24B)	122.4(7)
C(8)	C(12)	C(14)	110.63(14)	C(19B)	C(20B)	C(24B)	121.5(6)
C(8)	C(12)	C(13)	114.12(14)	C(16B)	C(21B)	C(22B)	112.4(7)
C(14)	C(12)	C(13)	110.17(15)	C(16B)	C(21B)	C(23B)	113.8(6)
C(1)	N(1)	C(2)	111.42(12)	C(22B)	C(21B)	C(23B)	108.8(6)
C(1)	N(1)	C(15A)	127.2(5)	C(26B)	C(24B)	C(25B)	111.4(6)
C(2)	N(1)	C(15A)	121.0(5)	C(26B)	C(24B)	C(20B)	118.2(8)
C(1)	N(1)	C(15B)	127.5(6)	C(25B)	C(24B)	C(20B)	113.8(6)
C(2)	N(1)	C(15B)	119.7(6)	C(26B)	C(24B)	C(26C)	29.7(6)
C(16A)	C(15A)	C(20A)	122.8(7)	C(25B)	C(24B)	C(26C)	102.2(8)
C(16A)	C(15A)	N(1)	122.8(6)	C(20B)	C(24B)	C(26C)	100.2(7)
C(20A)	C(15A)	N(1)	114.3(5)	C(26C)	C(26B)	C(24B)	92.5(13)
C(17A)	C(16A)	C(15A)	117.6(6)	C(26B)	C(26C)	C(24B)	57.7(13)

[1]1-X,+Y,3/2-Z

Table II.50. Hydrogen Atom Coordinates (Å×10^4) and Isotropic Displacement Parameters (Å^2×10^3) for (IPr)Co(NHDIPP)$_2$.

Atom	***x***	***y***	***z***	**U(eq)**
H(2N)	5218(9)	9700(20)	8431(8)	35(5)
H(2)	4730	3320	6958	39
H(5)	7552	10646	8470	49
H(6)	7872	11218	9465	49
H(7)	7090	11100	9901	42
H(9)	6042(10)	9060(20)	7533(9)	49(6)
H(10A)	5709	11480	7359	74
H(10B)	5963	10907	6863	74
H(10C)	6434	11928	7384	74
H(11A)	7306	10498	7571	71
H(11B)	6885	9404	7056	71
H(11C)	7307	8802	7705	71
H(11D)	7323	9504	7610	75
H(11E)	6739	8616	7118	75
H(11F)	7029	8069	7789	75
H(12)	5483	9616	9292	44
H(13A)	6379	9354	10228	76
H(13B)	5738	10109	10283	76
H(13C)	6371	11068	10323	76
H(14A)	5663	12666	9480	71
H(14B)	5026	11773	9477	71
H(14C)	5165	11934	8882	71
H(17A)	2935	6153	5383	48
H(18A)	3573	6561	4829	54
H(19A)	4728	6541	5256	51
H(21A)	3565	5908	6962	43
H(22A)	2768	3940	6063	73
H(22B)	2798	3970	6726	73
H(22C)	3443	3494	6599	73
H(23A)	2789	7688	6366	91
H(23B)	2429	6505	6621	91
H(23C)	2360	6416	5948	91
H(24A)	5700	6589	6799	41
H(25A)	5754	4280	6052	83
H(25B)	5666	4084	6668	83
H(25C)	6347	4736	6656	83
H(26A)	5791	6842	5676	61
H(26B)	6366	7265	6296	61

Table II.50. Continued.

H(26C)	5686	8181	6047	61
H(17B)	3222	6506	5226	50
H(18B)	3990	6406	4775	64
H(19B)	5118	6138	5318	64
H(21B)	3596	6597	6738	40
H(22D)	3074	3968	6119	84
H(22E)	2866	4574	6638	84
H(22F)	3623	4098	6777	84
H(23D)	2506	6396	5616	84
H(23E)	2827	7886	5931	84
H(23F)	2436	6860	6219	84
H(24B)	5789	5372	6880	69
H(25D)	5795	3523	6282	104
H(25E)	6527	4226	6559	104
H(25F)	6052	4558	5888	104
H(26D)	6581	6797	7012	92
H(26E)	5985	7798	6593	92
H(26F)	6449	6940	6324	92
H(26G)	6583	6778	6495	64
H(26H)	5981	7839	6456	64
H(26I)	6131	7497	5877	64

Table II.51. Atomic Occupancy for (IPr)Co(NHDIPP)$_2$.

Atom	***Occupancy***	**Atom**	***Occupancy***	**Atom**	***Occupancy***
C(11A)	0.48(2)	H(11A)	0.48(2)	H(11B)	0.48(2)
H(11C)	0.48(2)	C(11B)	0.52(2)	H(11D)	0.52(2)
H(11E)	0.52(2)	H(11F)	0.52(2)	C(15A)	0.55
C(16A)	0.55	C(17A)	0.55	H(17A)	0.55
C(18A)	0.55	H(18A)	0.55	C(19A)	0.55
H(19A)	0.55	C(20A)	0.55	C(21A)	0.55
H(21A)	0.55	C(22A)	0.55	H(22A)	0.55
H(22B)	0.55	H(22C)	0.55	C(23A)	0.55
H(23A)	0.55	H(23B)	0.55	H(23C)	0.55
C(24A)	0.55	H(24A)	0.55	C(25A)	0.55
H(25A)	0.55	H(25B)	0.55	H(25C)	0.55
C(26A)	0.55	H(26A)	0.55	H(26B)	0.55
H(26C)	0.55	C(15B)	0.45	C(16B)	0.45
C(17B)	0.45	H(17B)	0.45	C(18B)	0.45
H(18B)	0.45	C(19B)	0.45	H(19B)	0.45
C(20B)	0.45	C(21B)	0.45	H(21B)	0.45
C(22B)	0.45	H(22D)	0.45	H(22E)	0.45
H(22F)	0.45	C(23B)	0.45	H(23D)	0.45
H(23E)	0.45	H(23F)	0.45	C(24B)	0.45
H(24B)	0.45	C(25B)	0.45	H(25D)	0.45
H(25E)	0.45	H(25F)	0.45	C(26B)	0.225
H(26D)	0.225	H(26E)	0.225	H(26F)	0.225
C(26C)	0.225	H(26G)	0.225	H(26H)	0.225
H(26I)	0.225				

II.8 Diffraction data for (IPr)CoCl(NHDMP)•2Tol

Table II.52. Crystal data and structure refinement for (IPr)CoCl(NHDMP).

Identification code	(IPr)CoCl(NHDMP)
Empirical formula	$C_{65}H_{78}ClCoN_3$
Formula weight	995.68
Temperature/K	100(2)
Crystal system	orthorhombic
Space group	Pbca
a/Å	10.0070(7)
b/Å	28.2641(19)
c/Å	39.221(3)
α/°	90
β/°	90
γ/°	90
Volume/Å^3	11093.2(14)
Z	8
ρ_{calc}g/cm^3	1.192
μ/mm^{-1}	0.400
F(000)	4264.0
Crystal size/mm^3	0.227 × 0.113 × 0.047
Radiation	MoKα (λ = 0.71073)
2Θ range for data collection/°	4.154 to 44.058
Index ranges	$-10 \leq h \leq 10$, $-29 \leq k \leq 29$, $-41 \leq l \leq 41$
Reflections collected	146951
Independent reflections	6813 [R_{int} = 0.1444, R_{sigma} = 0.0407]
Data/restraints/parameters	6813/1/654
Goodness-of-fit on F^2	1.172
Final R indexes [I>=2σ (I)]	R_1 = 0.0499, wR_2 = 0.0988
Final R indexes [all data]	R_1 = 0.0735, wR_2 = 0.1069
Largest diff. peak/hole / e Å^{-3}	0.39/-0.29

Table II.53. Fractional Atomic Coordinates ($\times 10^4$) and Equivalent Isotropic Displacement Parameters ($Å^2 \times 10^3$) for (IPr)CoCl(NHDMP). U_{eq} is defined as 1/3 of of the trace of the orthogonalised U_{IJ} tensor.

Atom	***x***	***y***	***z***	**U(eq)**
Co(1)	2694.4(5)	9998.2(2)	1168.4(2)	12.27(14)
Cl(1)	4650.2(9)	10356.6(4)	1270.0(3)	18.3(2)
N(1)	718(3)	10399.2(11)	1652.5(7)	9.1(7)
N(2)	714(3)	10892.3(11)	1243.5(8)	10.6(8)
N(3)	2491(3)	9351.5(11)	1297.3(8)	15.0(8)
C(1)	1234(4)	10464.0(13)	1334.0(9)	10.4(9)
C(2)	-98(4)	10770.1(14)	1752.9(10)	12.0(9)
C(3)	-90(4)	11078.7(14)	1497.2(10)	13.9(9)
C(4)	925(4)	9986.7(14)	1863.5(9)	10.5(9)
C(5)	2026(4)	9975.6(14)	2081.9(9)	12.1(9)
C(6)	2145(4)	9584.1(14)	2291.9(9)	14.4(9)
C(7)	1203(4)	9229.5(14)	2286.1(10)	15.3(10)
C(8)	141(4)	9245.6(14)	2063.2(10)	15.2(10)
C(9)	-20(4)	9625.7(13)	1841.8(9)	10.3(9)
C(10)	3032(4)	10378.9(14)	2095.8(10)	14.7(10)
C(11)	4447(4)	10210.0(16)	2175.9(11)	24.9(11)
C(12)	2600(4)	10754.1(15)	2355.2(10)	24.8(11)
C(13)	-1176(4)	9644.2(14)	1589.5(10)	13.4(9)
C(14)	-1379(4)	9174.1(15)	1407.1(11)	21.5(10)
C(15)	-2470(4)	9798.9(15)	1762.3(10)	22.1(10)
C(16)	938(4)	11173.2(13)	938.1(9)	9.6(9)
C(17)	-27(4)	11162.3(13)	681(1)	12.4(9)
C(18)	108(4)	11491.0(14)	417.9(10)	18.1(10)
C(19)	1126(4)	11817.6(14)	419.2(10)	19.4(10)
C(20)	2072(4)	11816.5(14)	675.2(10)	18(1)
C(21)	2020(4)	11491.1(13)	940.7(10)	11.9(9)
C(22)	-1191(4)	10817.3(14)	687.6(10)	15.4(10)
C(23)	-1576(4)	10632.3(15)	332.1(10)	21.4(10)
C(24)	-2437(4)	11034.8(16)	854.7(11)	25.3(11)
C(25)	3082(4)	11478.5(14)	1216.2(10)	14.8(10)
C(26)	4458(4)	11598.6(15)	1077.5(11)	23.3(11)
C(27)	2732(4)	11801.2(15)	1514.7(10)	22.9(10)
C(28)	2822(4)	8964.6(13)	1109.1(9)	12.6(9)
C(29)	3120(4)	9033.9(14)	755.8(10)	15.1(10)
C(30)	3410(4)	8653.3(14)	549.3(10)	16.6(10)
C(31)	3457(4)	8198.9(14)	670.8(10)	16.6(10)
C(32)	3221(4)	8126.8(14)	1017(1)	17.3(10)

Table II.53. Continued.

C(33)	2910(4)	8496.7(13)	1235.8(10)	13.0(9)
C(34)	3203(4)	9528.2(14)	620.8(9)	14.2(10)
C(35)	4465(4)	9727.7(14)	556.9(10)	17(1)
C(36)	4543(4)	10163.8(14)	401.4(10)	19.3(10)
C(37)	3412(4)	10422.8(14)	315.8(10)	17.3(10)
C(38)	2178(4)	10232.3(14)	391.1(10)	18.6(10)
C(39)	2036(4)	9783.9(14)	538.6(10)	15.5(10)
C(40)	5720(4)	9487.4(15)	678.9(11)	24.6(11)
C(41)	670(4)	9565.4(15)	582.7(11)	20.3(10)
C(42)	3534(5)	10907.4(15)	159.6(11)	29.3(12)
C(43)	2802(4)	8393.8(13)	1610.7(9)	13.1(9)
C(44)	3849(4)	8531.5(13)	1828.5(10)	13.4(10)
C(45)	3785(4)	8409.7(13)	2172.3(10)	14.5(10)
C(46)	2716(4)	8160.8(13)	2308.1(10)	16.1(10)
C(47)	1702(4)	8027.4(14)	2089(1)	16.6(10)
C(48)	1710(4)	8141.4(13)	1742.2(10)	15(1)
C(49)	5052(4)	8790.1(15)	1694.3(11)	20.2(10)
C(50)	545(4)	8001.7(15)	1520.8(11)	20.3(10)
C(51)	2654(4)	8052.7(14)	2683.6(10)	22.1(10)
C(52)	6630(5)	2897.1(16)	574.8(11)	29.0(12)
C(53)	7225(4)	2490.8(16)	457.2(10)	27.1(11)
C(54)	6507(5)	2155.3(17)	273.0(11)	30.7(12)
C(55)	5174(5)	2227.3(16)	203.8(11)	28.8(12)
C(56)	4557(5)	2633.9(16)	321.9(11)	29.6(12)
C(57)	5270(4)	2961.7(17)	507.3(11)	27.2(11)
C(59)	9318(4)	2052.4(15)	2039.9(11)	23.5(11)
C(60)	9686(5)	2346.4(15)	1773.4(12)	27.1(12)
C(61)	8855(5)	2413.7(16)	1496.3(12)	28.8(12)
C(62)	7631(5)	2189.0(15)	1482.9(12)	30.5(12)
C(63)	7248(4)	1897.6(15)	1748.4(11)	25.7(11)
C(64)	8080(4)	1831.6(15)	2023.0(11)	24.2(11)
C(65)	10240(5)	1975.3(17)	2338.9(12)	37.7(13)
C(58)	7398(5)	3255.6(17)	776.1(13)	46.5(14)

Table II.54. Anisotropic Displacement Parameters ($Å^2 \times 10^3$) for (IPr)CoCl(NHDMP). The Anisotropic displacement factor exponent takes the form: $-2\pi^2[h^2a^{*2}U_{11}+2hka^*b^*U_{12}+\ldots]$.

Atom	**U_{11}**	**U_{22}**	**U_{33}**	**U_{23}**	**U_{13}**	**U_{12}**
Co(1)	10.9(3)	13.9(3)	12.0(3)	0.0(2)	2.3(2)	1.7(3)
Cl(1)	11.4(5)	22.4(6)	21.1(6)	-1.6(5)	1.0(5)	-0.1(4)
N(1)	7.9(17)	12.4(18)	6.9(18)	0.2(14)	-1.6(14)	1.8(15)
N(2)	8.4(17)	14.4(19)	8.8(19)	0.9(15)	2.5(15)	0.3(14)
N(3)	15.9(19)	17(2)	12(2)	-3.8(17)	2.2(17)	2.0(15)
C(1)	8(2)	17(2)	6(2)	0.2(18)	-1.1(18)	-3.0(18)
C(2)	11(2)	16(2)	9(2)	-1(2)	3.0(19)	0.4(19)
C(3)	13(2)	13(2)	16(2)	-2(2)	2.8(19)	3.8(18)
C(4)	11(2)	11(2)	10(2)	1.4(19)	6.0(17)	0.9(19)
C(5)	12(2)	16(2)	8(2)	-3.2(19)	3.3(17)	-0.5(19)
C(6)	12(2)	21(2)	10(2)	0.3(19)	-1.7(18)	6(2)
C(7)	20(2)	18(2)	8(2)	3.6(18)	5(2)	6(2)
C(8)	13(2)	15(2)	17(2)	-0.6(19)	4(2)	-0.6(18)
C(9)	8(2)	14(2)	9(2)	-0.8(18)	5.7(17)	2.4(18)
C(10)	11(2)	24(2)	10(2)	1.3(18)	-2.0(18)	-3.1(19)
C(11)	13(2)	40(3)	22(3)	4(2)	-3(2)	-3(2)
C(12)	21(2)	28(3)	26(3)	-5(2)	-3(2)	-7(2)
C(13)	10(2)	18(2)	13(2)	1.9(18)	-2.5(18)	-4.2(18)
C(14)	16(2)	28(3)	21(3)	-6(2)	1(2)	-2(2)
C(15)	15(2)	30(3)	21(2)	-4(2)	-5(2)	3(2)
C(16)	10(2)	10(2)	9(2)	1.3(17)	6.0(18)	4.2(18)
C(17)	10(2)	17(2)	11(2)	-0.5(19)	3.0(19)	5.5(18)
C(18)	14(2)	29(3)	12(2)	3(2)	-5.1(19)	5(2)
C(19)	21(3)	20(2)	17(2)	11(2)	2(2)	-1(2)
C(20)	16(2)	15(2)	23(2)	3(2)	3(2)	-2.5(19)
C(21)	7(2)	15(2)	13(2)	-0.3(18)	2.6(18)	1.1(18)
C(22)	13(2)	20(2)	13(2)	3.0(19)	-0.8(19)	-2.4(19)
C(23)	12(2)	33(3)	19(2)	1(2)	-2.8(19)	-4(2)
C(24)	12(2)	37(3)	27(3)	1(2)	5(2)	-2(2)
C(25)	13(2)	17(2)	14(2)	3.7(19)	-1.2(19)	-0.6(18)
C(26)	15(2)	30(3)	25(3)	-2(2)	-1(2)	-3(2)
C(27)	17(2)	30(3)	22(2)	-3(2)	0(2)	-5(2)
C(28)	8(2)	20(2)	10(2)	-1.7(19)	-2.2(18)	-0.3(18)
C(29)	12(2)	17(2)	17(2)	-0.9(19)	-3.4(19)	0.8(18)
C(30)	14(2)	24(3)	12(2)	-2(2)	0.6(19)	-0.9(19)
C(31)	17(2)	19(3)	13(2)	-7(2)	-0.2(19)	0.9(19)
C(32)	14(2)	14(2)	24(3)	-1(2)	-1(2)	1.7(19)
C(33)	10(2)	13(2)	16(2)	-1.1(18)	-0.9(18)	-0.6(18)

Table II.54. Continued.

C(34)	18(2)	20(2)	5(2)	-3.7(18)	2.1(18)	1.7(19)
C(35)	19(2)	22(3)	10(2)	-1.2(19)	6.1(19)	-1(2)
C(36)	17(2)	28(3)	12(2)	-3(2)	6.4(19)	-5(2)
C(37)	24(3)	18(2)	10(2)	-2.0(19)	8(2)	-3(2)
C(38)	23(3)	23(2)	10(2)	0.6(19)	1(2)	8(2)
C(39)	15(2)	22(2)	9(2)	-3.3(19)	3.0(19)	2.3(19)
C(40)	16(2)	32(3)	26(3)	-4(2)	0(2)	1(2)
C(41)	17(2)	27(3)	17(2)	4(2)	-0.1(19)	6(2)
C(42)	41(3)	26(3)	21(3)	3(2)	6(2)	-3(2)
C(43)	16(2)	10(2)	13(2)	-1.2(17)	3.0(19)	3.1(19)
C(44)	15(2)	11(2)	14(2)	-0.9(18)	0.2(19)	0.8(18)
C(45)	15(2)	15(2)	14(2)	-2.2(19)	-5.2(19)	1.6(19)
C(46)	18(2)	12(2)	19(2)	1.9(18)	4(2)	3.6(19)
C(47)	11(2)	15(2)	23(3)	0.2(19)	6(2)	0.1(18)
C(48)	14(2)	11(2)	20(3)	-4.2(19)	3(2)	3.2(19)
C(49)	13(2)	26(3)	22(2)	1(2)	1(2)	-4(2)
C(50)	14(2)	22(3)	25(3)	-1(2)	0(2)	-1.1(19)
C(51)	24(2)	22(2)	21(2)	3.5(19)	4(2)	0(2)
C(52)	38(3)	28(3)	21(3)	0(2)	3(2)	1(2)
C(53)	22(3)	36(3)	24(2)	3(2)	0(2)	5(2)
C(54)	37(3)	30(3)	25(3)	4(2)	8(2)	5(2)
C(55)	41(3)	27(3)	18(3)	4(2)	3(2)	-9(2)
C(56)	24(3)	39(3)	26(3)	11(2)	5(2)	-4(2)
C(57)	23(3)	36(3)	22(3)	8(2)	10(2)	9(2)
C(59)	19(3)	18(3)	33(3)	-11(2)	0(2)	8(2)
C(60)	21(3)	16(3)	44(3)	-10(2)	6(3)	1(2)
C(61)	26(3)	29(3)	31(3)	3(2)	8(2)	4(2)
C(62)	28(3)	31(3)	33(3)	-3(2)	-1(2)	11(2)
C(63)	12(2)	32(3)	34(3)	-7(2)	4(2)	0(2)
C(64)	27(3)	23(3)	22(3)	0(2)	8(2)	7(2)
C(65)	37(3)	39(3)	37(3)	-13(2)	-12(3)	7(2)
C(58)	49(4)	40(3)	50(3)	-9(3)	1(3)	-5(3)

Table II.55. Bond Lengths for (IPr)CoCl(NHDMP).

Atom	Atom	Length/Å	Atom	Atom	Length/Å
Co(1)	N(3)	1.907(3)	C(29)	C(34)	1.496(5)
Co(1)	C(1)	2.071(4)	C(30)	C(31)	1.371(6)
Co(1)	Cl(1)	2.2395(11)	C(31)	C(32)	1.393(6)
N(1)	C(1)	1.364(5)	C(32)	C(33)	1.388(5)
N(1)	C(2)	1.386(5)	C(33)	C(43)	1.503(5)
N(1)	C(4)	1.445(5)	C(34)	C(35)	1.406(6)
N(2)	C(1)	1.365(5)	C(34)	C(39)	1.411(5)
N(2)	C(3)	1.384(5)	C(35)	C(36)	1.378(6)
N(2)	C(16)	1.454(5)	C(35)	C(40)	1.506(6)
N(3)	C(28)	1.360(5)	C(36)	C(37)	1.390(6)
C(2)	C(3)	1.329(5)	C(37)	C(38)	1.379(6)
C(4)	C(9)	1.394(5)	C(37)	C(42)	1.505(6)
C(4)	C(5)	1.396(5)	C(38)	C(39)	1.401(5)
C(5)	C(6)	1.385(5)	C(39)	C(41)	1.510(6)
C(5)	C(10)	1.521(5)	C(43)	C(48)	1.403(5)
C(6)	C(7)	1.376(5)	C(43)	C(44)	1.407(5)
C(7)	C(8)	1.377(5)	C(44)	C(45)	1.393(5)
C(8)	C(9)	1.391(5)	C(44)	C(49)	1.504(5)
C(9)	C(13)	1.524(5)	C(45)	C(46)	1.386(5)
C(10)	C(11)	1.527(5)	C(46)	C(47)	1.382(6)
C(10)	C(12)	1.532(5)	C(46)	C(51)	1.505(5)
C(13)	C(14)	1.523(5)	C(47)	C(48)	1.398(6)
C(13)	C(15)	1.525(5)	C(48)	C(50)	1.506(5)
C(16)	C(17)	1.397(5)	C(52)	C(53)	1.373(6)
C(16)	C(21)	1.407(5)	C(52)	C(57)	1.399(6)
C(17)	C(18)	1.395(5)	C(52)	C(58)	1.497(6)
C(17)	C(22)	1.519(5)	C(53)	C(54)	1.392(6)
C(18)	C(19)	1.375(6)	C(54)	C(55)	1.376(6)
C(19)	C(20)	1.380(6)	C(55)	C(56)	1.384(6)
C(20)	C(21)	1.390(5)	C(56)	C(57)	1.377(6)
C(21)	C(25)	1.516(5)	C(59)	C(60)	1.385(6)
C(22)	C(24)	1.537(6)	C(59)	C(64)	1.389(6)
C(22)	C(23)	1.538(5)	C(59)	C(65)	1.508(6)
C(25)	C(26)	1.519(6)	C(60)	C(61)	1.382(6)
C(25)	C(27)	1.525(5)	C(61)	C(62)	1.380(6)
C(28)	C(33)	1.416(5)	C(62)	C(63)	1.382(6)
C(28)	C(29)	1.431(5)	C(63)	C(64)	1.374(6)
C(29)	C(30)	1.378(5)			

Table II.56. Bond Angles for (IPr)CoCl(NHDMP).

Atom	Atom	Atom	Angle/°	Atom	Atom	Atom	Angle/°
N(3)	Co(1)	C(1)	116.80(15)	C(30)	C(29)	C(28)	120.4(4)
N(3)	Co(1)	Cl(1)	118.65(11)	C(30)	C(29)	C(34)	120.6(4)
C(1)	Co(1)	Cl(1)	105.86(11)	C(28)	C(29)	C(34)	118.8(3)
C(1)	N(1)	C(2)	112.4(3)	C(31)	C(30)	C(29)	122.3(4)
C(1)	N(1)	C(4)	125.4(3)	C(30)	C(31)	C(32)	118.0(4)
C(2)	N(1)	C(4)	122.1(3)	C(33)	C(32)	C(31)	122.0(4)
C(1)	N(2)	C(3)	111.9(3)	C(32)	C(33)	C(28)	120.0(4)
C(1)	N(2)	C(16)	129.8(3)	C(32)	C(33)	C(43)	118.4(3)
C(3)	N(2)	C(16)	118.3(3)	C(28)	C(33)	C(43)	121.3(3)
C(28)	N(3)	Co(1)	126.9(3)	C(35)	C(34)	C(39)	119.9(4)
N(1)	C(1)	N(2)	102.3(3)	C(35)	C(34)	C(29)	119.2(4)
N(1)	C(1)	Co(1)	118.0(3)	C(39)	C(34)	C(29)	120.9(4)
N(2)	C(1)	Co(1)	138.7(3)	C(36)	C(35)	C(34)	119.2(4)
C(3)	C(2)	N(1)	106.2(3)	C(36)	C(35)	C(40)	119.8(4)
C(2)	C(3)	N(2)	107.2(3)	C(34)	C(35)	C(40)	120.8(4)
C(9)	C(4)	C(5)	123.8(4)	C(35)	C(36)	C(37)	122.2(4)
C(9)	C(4)	N(1)	117.3(3)	C(38)	C(37)	C(36)	118.2(4)
C(5)	C(4)	N(1)	118.9(3)	C(38)	C(37)	C(42)	121.0(4)
C(6)	C(5)	C(4)	116.8(4)	C(36)	C(37)	C(42)	120.7(4)
C(6)	C(5)	C(10)	121.4(3)	C(37)	C(38)	C(39)	122.2(4)
C(4)	C(5)	C(10)	121.8(3)	C(38)	C(39)	C(34)	118.3(4)
C(7)	C(6)	C(5)	120.9(4)	C(38)	C(39)	C(41)	120.6(4)
C(6)	C(7)	C(8)	121.0(4)	C(34)	C(39)	C(41)	120.9(4)
C(7)	C(8)	C(9)	120.7(4)	C(48)	C(43)	C(44)	119.8(4)
C(8)	C(9)	C(4)	116.7(3)	C(48)	C(43)	C(33)	120.9(4)
C(8)	C(9)	C(13)	121.3(3)	C(44)	C(43)	C(33)	119.2(3)
C(4)	C(9)	C(13)	122.0(3)	C(45)	C(44)	C(43)	119.0(4)
C(5)	C(10)	C(11)	112.7(3)	C(45)	C(44)	C(49)	119.7(4)
C(5)	C(10)	C(12)	110.9(3)	C(43)	C(44)	C(49)	121.2(3)
C(11)	C(10)	C(12)	109.9(3)	C(46)	C(45)	C(44)	122.2(4)
C(14)	C(13)	C(9)	112.1(3)	C(47)	C(46)	C(45)	117.7(4)
C(14)	C(13)	C(15)	110.2(3)	C(47)	C(46)	C(51)	121.5(4)
C(9)	C(13)	C(15)	111.5(3)	C(45)	C(46)	C(51)	120.7(4)
C(17)	C(16)	C(21)	123.5(3)	C(46)	C(47)	C(48)	122.6(4)
C(17)	C(16)	N(2)	118.4(3)	C(47)	C(48)	C(43)	118.6(4)
C(21)	C(16)	N(2)	117.5(3)	C(47)	C(48)	C(50)	119.8(4)
C(18)	C(17)	C(16)	116.9(4)	C(43)	C(48)	C(50)	121.6(4)
C(18)	C(17)	C(22)	120.9(3)	C(53)	C(52)	C(57)	117.8(4)
C(16)	C(17)	C(22)	122.1(3)	C(53)	C(52)	C(58)	121.4(4)

Table II. 56. Continued.

C(19)	C(18)	C(17)	121.1(4)	C(57)	C(52)	C(58)	120.8(4)
C(18)	C(19)	C(20)	120.6(4)	C(52)	C(53)	C(54)	121.4(4)
C(19)	C(20)	C(21)	121.4(4)	C(55)	C(54)	C(53)	120.1(4)
C(20)	C(21)	C(16)	116.5(4)	C(54)	C(55)	C(56)	119.3(4)
C(20)	C(21)	C(25)	121.6(3)	C(57)	C(56)	C(55)	120.3(4)
C(16)	C(21)	C(25)	122.0(3)	C(56)	C(57)	C(52)	121.1(4)
C(17)	C(22)	C(24)	111.9(3)	C(60)	C(59)	C(64)	118.1(4)
C(17)	C(22)	C(23)	113.2(3)	C(60)	C(59)	C(65)	120.7(4)
C(24)	C(22)	C(23)	108.7(3)	C(64)	C(59)	C(65)	121.2(4)
C(21)	C(25)	C(26)	112.0(3)	C(61)	C(60)	C(59)	121.1(4)
C(21)	C(25)	C(27)	111.9(3)	C(62)	C(61)	C(60)	120.0(4)
C(26)	C(25)	C(27)	110.5(3)	C(61)	C(62)	C(63)	119.5(4)
N(3)	C(28)	C(33)	125.1(3)	C(64)	C(63)	C(62)	120.2(4)
N(3)	C(28)	C(29)	117.8(3)	C(63)	C(64)	C(59)	121.1(4)
C(33)	C(28)	C(29)	117.1(3)				

Table II.57. Hydrogen Atom Coordinates (Å×10^4) and Isotropic Displacement Parameters (Å^2×10^3) for (IPr)CoCl(NHDMP).

Atom	***x***	***y***	***z***	**U(eq)**
H(3N)	2240(40)	9290(15)	1502(6)	29(14)
H(2)	-530(40)	10767(13)	1961(10)	14
H(3)	-550	11373	1490	17
H(6)	2888	9560	2442	17
H(7)	1287	8970	2438	18
H(8)	-489	8994	2061	18
H(10)	3049	10532	1866	18
H(11A)	4489	10101	2413	37
H(11B)	5076	10472	2143	37
H(11C)	4684	9949	2023	37
H(12A)	1710	10872	2296	37
H(12B)	3240	11017	2352	37
H(12C)	2576	10614	2584	37
H(13)	-951	9887	1413	16
H(14A)	-534	9073	1304	32
H(14B)	-2056	9212	1229	32
H(14C)	-1678	8935	1571	32
H(15A)	-2723	9565	1935	33
H(15B)	-3181	9824	1591	33
H(15C)	-2337	10107	1871	33
H(18)	-514	11489	235	22
H(19)	1178	12046	242	23
H(20)	2773	12043	670	22
H(22)	-916	10539	828	18
H(23A)	-1981	10889	200	32
H(23B)	-2216	10372	356	32
H(23C)	-773	10518	215	32
H(24A)	-2229	11124	1090	38
H(24B)	-3164	10803	854	38
H(24C)	-2712	11316	727	38
H(25)	3121	11147	1306	18
H(26A)	4486	11934	1014	35
H(26B)	4641	11404	876	35
H(26C)	5133	11535	1253	35
H(27A)	3452	11791	1684	34
H(27B)	1896	11694	1620	34
H(27C)	2623	12126	1432	34
H(30)	3583	8708	314	20

Table II.57. Continued.

H(31)	3645	7941	523	20
H(32)	3274	7815	1106	21
H(36)	5399	10292	351	23
H(38)	1399	10411	341	22
H(40A)	6494	9622	561	37
H(40B)	5665	9148	631	37
H(40C)	5818	9536	925	37
H(41A)	-17	9798	523	30
H(41B)	552	9468	821	30
H(41C)	588	9289	434	30
H(42A)	2712	10983	35	44
H(42B)	4294	10912	2	44
H(42C)	3676	11142	340	44
H(45)	4497	8500	2319	17
H(47)	972	7851	2177	20
H(49A)	4775	9097	1601	30
H(49B)	5474	8602	1514	30
H(49C)	5692	8840	1880	30
H(50A)	-106	7825	1657	31
H(50B)	862	7803	1333	31
H(50C)	120	8287	1429	31
H(51A)	1719	8046	2758	33
H(51B)	3136	8298	2811	33
H(51C)	3067	7744	2727	33
H(53)	8145	2438	502	32
H(54)	6937	1876	195	37
H(55)	4683	2000	76	35
H(56)	3638	2687	275	35
H(57)	4830	3236	591	33
H(60)	10523	2504	1781	33
H(61)	9126	2615	1315	35
H(62)	7057	2234	1293	37
H(63)	6406	1742	1741	31
H(64)	7803	1631	2204	29
H(65A)	10621	1656	2327	57
H(65B)	9736	2010	2552	57
H(65C)	10961	2210	2332	57
H(58A)	8357	3214	734	70
H(58B)	7214	3213	1020	70
H(58C)	7127	3574	707	70

II.9 Diffraction data for [IPrH][Co(OBHT)$_3$].

Table II.58. Crystal data and structure refinement for [IPrH][Co(OBHT)$_3$].

Identification code	[IPrH][Co(OBHT)$_3$]
Empirical formula	$C_{72}H_{106}CoN_2O_3$
Formula weight	1106.51
Temperature/K	100(2)
Crystal system	monoclinic
Space group	$P2_1/c$
a/Å	14.9597(6)
b/Å	39.0620(16)
c/Å	16.4401(7)
α/°	90
β/°	115.1810(10)
γ/°	90
Volume/Å^3	8693.9(6)
Z	4
ρ_{calc}g/cm^3	0.845
μ/mm^{-1}	0.232
F(000)	2412.0
Crystal size/mm^3	0.269 × 0.255 × 0.190
Radiation	MoKα (λ = 0.71073)
2Θ range for data collection/°	4.156 to 50.254
Index ranges	$-17 \leq h \leq 16$, $-46 \leq k \leq 46$, $-19 \leq l \leq 19$
Reflections collected	170294
Independent reflections	15502 [R_{int} = 0.0657, R_{sigma} = 0.0298]
Data/restraints/parameters	15502/24/780
Goodness-of-fit on F^2	1.028
Final R indexes [I>=2σ (I)]	R_1 = 0.0586, wR_2 = 0.1491
Final R indexes [all data]	R_1 = 0.0785, wR_2 = 0.1623
Largest diff. peak/hole / e Å^{-3}	0.30/-0.40

Table II.59. Fractional Atomic Coordinates ($\times 10^4$) and Equivalent Isotropic Displacement Parameters ($Å^2 \times 10^3$) for [IPrH][Co(OBHT)$_3$]. U_{eq} is defined as 1/3 of of the trace of the orthogonalised U_{IJ} tensor.

Atom	***x***	***y***	***z***	**U(eq)**
Co(1)	4553.0(2)	3835.0(2)	5303.7(2)	30.8(1)
N(1)	2638.9(16)	3555.1(6)	8082.9(14)	34.6(5)
N(2)	3839.6(17)	3699.1(6)	9332.8(14)	35.5(5)
O(1)	3251.3(13)	3911.7(5)	4534.7(12)	36.6(4)
O(2)	4828.5(13)	3828.1(4)	6529.3(12)	34.9(4)
O(3)	5510.9(14)	3732.6(5)	4934.3(13)	41.6(5)
C(1)	-532(3)	3862.7(12)	1620(3)	101.5(18)
C(2)	493(2)	3864.2(9)	2384(2)	58.0(9)
C(3)	770(2)	3632.4(8)	3078(2)	52.5(8)
C(4)	1697.6(19)	3630.7(7)	3801.0(19)	36.8(6)
C(5)	2381.6(18)	3887.9(7)	3832.9(18)	32.9(6)
C(6)	2107.7(19)	4131.7(7)	3123.4(18)	36.3(6)
C(7)	1176(2)	4110.2(8)	2417(2)	48.1(7)
C(8)	2818(2)	4415.3(7)	3120.9(19)	39.9(6)
C(9)	3190(3)	4629.7(8)	3989(2)	53.9(8)
C(10)	3696(2)	4253.0(8)	3017(2)	44.3(7)
C(11)	2333(2)	4666.6(8)	2337(2)	56.4(8)
C(12)	1938(2)	3369.2(7)	4560.9(18)	39.4(6)
C(13)	1107(2)	3105.6(8)	4359(2)	49.8(8)
C(14)	2082(3)	3553.2(9)	5427(2)	58.9(9)
C(15)	2865(2)	3163.3(8)	4710(2)	48.2(7)
C(16)	6964(3)	4195.4(12)	10199(2)	80.9(13)
C(17)	6441(2)	4104.8(10)	9210(2)	54.9(8)
C(18)	6524(2)	3782.2(9)	8897(2)	54.3(8)
C(19)	6003(2)	3680.5(8)	8003(2)	43.7(7)
C(20)	5374.5(19)	3924.6(7)	7377.0(18)	35.2(6)
C(21)	5299.5(19)	4261.5(7)	7680.7(18)	36.6(6)
C(22)	5843(2)	4336.5(8)	8589(2)	46.9(7)
C(23)	6121(3)	3313.5(8)	7708(2)	54.6(8)
C(24)	6614(3)	3328.7(10)	7062(2)	67(1)
C(25)	6807(3)	3093.5(10)	8510(3)	76.4(12)
C(26)	5119(3)	3129.2(8)	7290(2)	58.5(9)
C(27)	4654.0(19)	4540.2(7)	7046.0(19)	36.5(6)
C(28)	4676(2)	4875.8(8)	7534(2)	49.4(8)
C(29)	3566(2)	4428.7(7)	6578(2)	41.7(7)
C(30)	5056(2)	4626.5(7)	6354(2)	42.6(7)
C(31)	8412(3)	3458.6(16)	3675(3)	102.4(18)

Table II.59. Continued.

C(32)	7659(2)	3527.4(10)	4038(2)	54.4(9)
C(33)	7683(2)	3823.4(8)	4499.1(18)	42.3(7)
C(34)	6988.3(18)	3899.9(6)	4821.6(17)	31.7(6)
C(35)	6200.0(18)	3666.0(6)	4646.5(16)	29.1(5)
C(36)	6157(2)	3358.9(7)	4175.0(18)	37.3(6)
C(37)	6895(2)	3301.0(9)	3889(2)	53.1(8)
C(38)	7058(2)	4235.3(7)	5328(2)	44.2(7)
C(39)	7961(2)	4452.1(9)	5436(3)	73.5(12)
C(40)	6149(2)	4460.8(7)	4809(2)	54.1(9)
C(41)	7172(2)	4162.5(9)	6287(2)	55.7(9)
C(42)	5300(2)	3103.6(8)	3944(2)	56.6(9)
C(43)	4319(2)	3278.8(8)	3328(2)	51.5(8)
C(44)	5253(3)	2967.4(9)	4804(3)	74.5(12)
C(45)	5425(3)	2789.2(11)	3429(4)	108(2)
C(46)	-192(2)	3290.9(9)	6220(2)	50.3(8)
C(47)	516(2)	3036.5(8)	6566.6(19)	46.2(7)
C(48)	1476(2)	3115.3(7)	7188.7(18)	39.8(6)
C(49)	1654.7(19)	3459.6(7)	7437.1(17)	36.2(6)
C(50)	968(2)	3722.4(8)	7090.8(19)	43.6(7)
C(51)	31(2)	3626.3(9)	6475(2)	50.7(8)
C(52A)	2267(7)	2851.0(18)	7520(5)	46.1(9)
C(53A)	2235(12)	2650(3)	8313(8)	98(4)
C(54A)	2301(9)	2594(3)	6829(5)	73(3)
C(52B)	2274(7)	2836(2)	7621(8)	46.1(9)
C(53B)	1827(9)	2503(3)	7788(13)	74(4)
C(54B)	2730(11)	2763(4)	6957(9)	70(4)
C(55)	1208(2)	4096.8(8)	7344(2)	49.2(7)
C(56)	1034(2)	4316.3(9)	6529(2)	58.9(9)
C(57)	634(4)	4232.4(9)	7849(3)	74.9(12)
C(58)	2918(2)	3582.6(6)	8964.9(17)	34.5(6)
C(59)	3404(2)	3659.6(7)	7888.9(18)	38.9(6)
C(60)	4152(2)	3750.7(7)	8667.2(18)	40.4(6)
C(61)	4412(2)	3779.1(7)	10277.0(17)	38.6(6)
C(62)	5066(3)	3533.1(9)	10819(2)	60.6(10)
C(63)	5597(3)	3618.6(11)	11719(2)	71.7(12)
C(64)	5484(2)	3930.1(9)	12048(2)	56.6(9)
C(65)	4835(2)	4166.0(8)	11489.4(19)	43.8(7)
C(66)	4279(2)	4096.8(7)	10580.7(18)	37.2(6)
C(67)	3574(3)	4363.2(7)	9963(2)	47.8(7)
C(68)	2821(3)	4480.7(11)	10292(3)	75.1(11)
C(69)	4175(3)	4673.6(9)	9884(3)	73.7(11)

Table II.59. Continued.

C(70A)	5372(11)	3238(4)	10375(11)	60(2)
C(71A)	4624(11)	2968(3)	10403(10)	91(6)
C(72A)	6477(13)	3143(6)	10884(10)	89(6)
C(70B)	5064(8)	3154(3)	10498(7)	60(2)
C(71B)	4653(15)	2866(3)	10882(13)	179(7)
C(72B)	6150(8)	3054(4)	10753(12)	117(5)

Table II.60. Anisotropic Displacement Parameters ($Å^2 \times 10^3$) for [IPrH][Co(OBHT)$_3$]. The Anisotropic displacement factor exponent takes the form: $-2\pi^2[h^2a^{*2}U_{11}+2hka^*b^*U_{12}+\ldots]$.

Atom	**U_{11}**	**U_{22}**	**U_{33}**	**U_{23}**	**U_{13}**	**U_{12}**
Co(1)	28.48(19)	28.50(18)	36.2(2)	-3.65(14)	14.56(15)	-1.40(14)
N(1)	34.2(12)	37.4(12)	25.6(11)	1.3(9)	6.4(9)	-1(1)
N(2)	38.6(13)	37.1(12)	26.6(11)	-1.6(9)	9.9(10)	0.7(10)
O(1)	28(1)	42.7(11)	36.6(10)	-5.9(8)	11.3(8)	-6.0(8)
O(2)	35.9(10)	32.9(9)	34(1)	0.1(8)	13.1(8)	3.8(8)
O(3)	34.4(10)	46.2(11)	50.2(12)	-7.1(9)	23.8(9)	-1.1(8)
C(1)	48(2)	101(3)	102(3)	45(3)	-20(2)	-26(2)
C(2)	32.0(16)	62(2)	59(2)	12.8(16)	-0.5(15)	-9.2(15)
C(3)	31.3(16)	55.9(19)	59(2)	5.1(16)	8.7(15)	-13.1(14)
C(4)	27.7(14)	39.5(15)	42.4(15)	-3.9(12)	14.0(12)	-3.6(11)
C(5)	25.1(13)	37.7(14)	38.0(14)	-7.6(11)	15.4(12)	-1.6(11)
C(6)	31.7(14)	36.3(14)	43.1(15)	-1.9(12)	18.0(13)	-1.0(11)
C(7)	36.0(16)	48.6(18)	50.6(18)	10.7(14)	9.4(14)	-1.1(13)
C(8)	33.3(14)	38.2(15)	47.6(16)	1.0(12)	16.6(13)	-2.7(12)
C(9)	60(2)	34.7(16)	67(2)	-7.6(14)	27.1(18)	-7.2(14)
C(10)	33.9(15)	50.3(17)	52.7(18)	2.5(14)	22.3(14)	-5.1(13)
C(11)	45.4(18)	47.5(18)	77(2)	13.7(16)	26.3(17)	-3.1(14)
C(12)	31.9(14)	45.5(16)	37.9(15)	-7.0(12)	11.9(12)	-9.8(12)
C(13)	40.4(17)	52.7(18)	52.8(19)	1.8(14)	16.4(15)	-12.5(14)
C(14)	75(2)	64(2)	49.9(19)	-12.1(16)	38.2(18)	-23.7(18)
C(15)	37.5(16)	42.3(16)	56.1(19)	4.1(14)	11.4(14)	-5.8(13)
C(16)	48(2)	115(3)	47(2)	-21(2)	-10.8(17)	1(2)
C(17)	31.7(16)	77(2)	42.2(17)	-11.7(16)	2.6(14)	-3.5(15)
C(18)	31.3(16)	73(2)	44.6(18)	8.1(16)	2.3(14)	8.8(15)
C(19)	30.8(14)	51.3(17)	44.5(16)	2.6(13)	11.6(13)	6.5(13)
C(20)	24.6(13)	41.3(15)	36.4(15)	1.1(11)	9.7(12)	2.6(11)
C(21)	24.4(13)	41.4(15)	42.4(15)	-5.8(12)	12.7(12)	-5.5(11)
C(22)	28.4(14)	55.4(18)	48.3(18)	-13.9(14)	8.1(13)	-6.9(13)
C(23)	58(2)	52.6(19)	48.2(18)	14.4(15)	17.9(16)	25.3(16)
C(24)	67(2)	70(2)	66(2)	18.6(18)	30.2(19)	38.3(19)
C(25)	79(3)	72(3)	68(2)	28(2)	20(2)	37(2)
C(26)	76(2)	36.3(17)	56(2)	2.8(14)	21.4(18)	6.5(16)
C(27)	30.0(14)	35.9(14)	44.1(16)	-8.4(12)	16.1(12)	-0.5(11)
C(28)	48.7(18)	43.6(17)	56.9(19)	-16.3(14)	23.4(16)	-3.0(14)
C(29)	31.5(15)	42.4(16)	48.7(17)	-3.8(13)	14.5(13)	5.0(12)
C(30)	43.0(16)	32.8(14)	55.5(18)	-2.5(13)	24.4(14)	2.9(12)
C(31)	45(2)	199(6)	67(3)	-39(3)	27(2)	12(3)
C(32)	27.8(15)	95(3)	35.5(16)	-9.7(16)	9.1(13)	10.4(16)

Table II.60. Continued.

C(33)	26.8(14)	61.9(19)	36.0(15)	6.8(14)	11.4(12)	0.5(13)
C(34)	24.3(13)	31.2(13)	33.2(14)	6.8(10)	6.3(11)	5(1)
C(35)	25.5(13)	30.9(13)	31.3(13)	4.3(10)	12.4(11)	5.9(10)
C(36)	32.3(14)	35.1(14)	36.9(15)	-4.4(11)	7.6(12)	6.9(11)
C(37)	37.9(17)	65(2)	45.0(18)	-21.0(15)	6.5(14)	16.6(15)
C(38)	27.9(14)	32.7(15)	59.2(19)	-1.2(13)	6.3(13)	1.9(11)
C(39)	37.4(18)	43.3(19)	118(3)	2(2)	12(2)	-5.3(15)
C(40)	38.8(17)	27.1(14)	79(2)	-0.9(14)	7.9(16)	4.7(12)
C(41)	41.2(17)	54.9(19)	55(2)	-25.6(16)	5.3(15)	7.3(15)
C(42)	43.4(18)	33.8(16)	79(2)	-18.3(16)	12.6(17)	0.1(13)
C(43)	34.6(16)	51.1(18)	60(2)	-15.5(15)	12.1(15)	-7.0(14)
C(44)	50(2)	39.6(18)	115(3)	26(2)	17(2)	-8.0(15)
C(45)	62(3)	57(2)	170(5)	-66(3)	16(3)	-1(2)
C(46)	32.9(16)	64(2)	40.7(17)	-1.8(15)	3.0(13)	-2.3(14)
C(47)	41.9(17)	47.1(17)	37.2(16)	0.9(13)	4.8(13)	-6.3(14)
C(48)	38.4(15)	43.0(16)	30.1(14)	6.4(12)	7.0(12)	-1.1(12)
C(49)	32.1(14)	45.5(16)	25.2(13)	3.2(11)	6.5(11)	-1.4(12)
C(50)	37.4(16)	51.1(17)	33.4(15)	0.9(13)	6.5(13)	6.1(13)
C(51)	40.3(17)	55.6(19)	43.6(17)	-1.5(14)	5.8(14)	6.4(14)
C(52A)	44.5(17)	38.7(17)	37(2)	6.4(14)	-0.3(16)	-1.4(13)
C(53A)	151(11)	64(6)	91(7)	39(6)	62(8)	45(7)
C(54A)	72(6)	70(6)	62(4)	-1(4)	14(4)	28(5)
C(52B)	44.5(17)	38.7(17)	37(2)	6.4(14)	-0.3(16)	-1.4(13)
C(53B)	77(7)	47(6)	105(10)	23(6)	45(7)	9(5)
C(54B)	64(8)	62(8)	81(8)	25(6)	29(6)	24(6)
C(55)	41.3(17)	47.5(17)	45.8(17)	0.1(14)	6.1(14)	8.2(14)
C(56)	43.6(18)	68(2)	65(2)	8.9(17)	22.2(17)	-3.5(16)
C(57)	119(4)	48(2)	72(2)	-2.6(18)	55(3)	10(2)
C(58)	37.0(15)	33.7(14)	27.9(13)	0.9(11)	9.0(12)	0.8(11)
C(59)	38.7(15)	47.1(16)	30.6(14)	0.7(12)	14.7(12)	-2.4(13)
C(60)	35.4(15)	51.1(17)	34.1(15)	-2.8(12)	14.2(13)	-3.8(13)
C(61)	35.7(15)	49.9(17)	25.2(13)	-6.8(12)	8.3(12)	-1.4(12)
C(62)	57(2)	73(2)	34.2(16)	-11.0(15)	2.8(15)	26.1(18)
C(63)	66(2)	89(3)	34.1(17)	-12.9(17)	-4.4(16)	33(2)
C(64)	50.9(19)	76(2)	31.7(16)	-12.8(15)	6.4(15)	1.6(17)
C(65)	50.8(18)	43.9(16)	37.7(16)	-12.0(13)	19.8(14)	-10.9(14)
C(66)	41.5(15)	36.9(15)	34.6(14)	-2.3(11)	17.5(13)	-9.0(12)
C(67)	70(2)	33.4(15)	38.4(16)	-0.4(12)	21.6(15)	-2.9(14)
C(68)	66(2)	76(3)	85(3)	29(2)	34(2)	18(2)
C(69)	113(3)	44.3(19)	83(3)	8.9(18)	61(3)	-5(2)
C(70A)	73(6)	67(6)	32(3)	1(3)	13(3)	33(5)

Table II.60. Continued.

C(71A)	114(9)	21(5)	74(9)	-10(5)	-21(7)	20(5)
C(72A)	94(8)	107(14)	33(5)	-2(7)	-4(7)	76(9)
C(70B)	73(6)	67(6)	32(3)	1(3)	13(3)	33(5)
C(71B)	339(19)	74(8)	227(16)	-70(9)	221(16)	-84(10)
C(72B)	87(7)	91(8)	147(13)	-42(7)	24(8)	35(6)

Table II.61. Bond Lengths for [IPrH][Co(OBHT)$_3$].

Atom	Atom	Length/Å	Atom	Atom	Length/Å
Co(1)	O(3)	1.8229(18)	C(32)	C(37)	1.383(5)
Co(1)	O(1)	1.8399(18)	C(33)	C(34)	1.386(4)
Co(1)	O(2)	1.8771(18)	C(34)	C(35)	1.421(4)
N(1)	C(58)	1.332(3)	C(34)	C(38)	1.532(4)
N(1)	C(59)	1.375(4)	C(35)	C(36)	1.415(4)
N(1)	C(49)	1.450(3)	C(36)	C(37)	1.389(4)
N(2)	C(58)	1.328(3)	C(36)	C(42)	1.539(4)
N(2)	C(60)	1.375(3)	C(38)	C(40)	1.538(4)
N(2)	C(61)	1.452(3)	C(38)	C(41)	1.538(5)
O(1)	C(5)	1.325(3)	C(38)	C(39)	1.540(4)
O(2)	C(20)	1.335(3)	C(42)	C(44)	1.541(5)
O(3)	C(35)	1.330(3)	C(42)	C(43)	1.544(4)
C(1)	C(2)	1.513(5)	C(42)	C(45)	1.547(5)
C(2)	C(3)	1.376(5)	C(46)	C(51)	1.373(5)
C(2)	C(7)	1.386(4)	C(46)	C(47)	1.386(4)
C(3)	C(4)	1.391(4)	C(47)	C(48)	1.397(4)
C(4)	C(5)	1.419(4)	C(48)	C(49)	1.398(4)
C(4)	C(12)	1.533(4)	C(48)	C(52A)	1.489(8)
C(5)	C(6)	1.424(4)	C(48)	C(52B)	1.550(5)
C(6)	C(7)	1.386(4)	C(49)	C(50)	1.391(4)
C(6)	C(8)	1.536(4)	C(50)	C(51)	1.386(4)
C(8)	C(10)	1.531(4)	C(50)	C(55)	1.521(4)
C(8)	C(11)	1.535(4)	C(52A)	C(54A)	1.533(5)
C(8)	C(9)	1.541(4)	C(52A)	C(53A)	1.541(5)
C(12)	C(14)	1.527(4)	C(52B)	C(53B)	1.539(5)
C(12)	C(15)	1.529(4)	C(52B)	C(54B)	1.540(5)
C(12)	C(13)	1.538(4)	C(55)	C(56)	1.518(4)
C(16)	C(17)	1.517(4)	C(55)	C(57)	1.521(5)
C(17)	C(22)	1.373(5)	C(59)	C(60)	1.341(4)
C(17)	C(18)	1.387(5)	C(61)	C(66)	1.383(4)
C(18)	C(19)	1.396(4)	C(61)	C(62)	1.390(4)
C(19)	C(20)	1.425(4)	C(62)	C(63)	1.390(4)
C(19)	C(23)	1.547(4)	C(62)	C(70A)	1.536(18)
C(20)	C(21)	1.429(4)	C(62)	C(70B)	1.573(11)
C(21)	C(22)	1.394(4)	C(63)	C(64)	1.371(5)
C(21)	C(27)	1.533(4)	C(64)	C(65)	1.369(5)
C(23)	C(24)	1.532(5)	C(65)	C(66)	1.392(4)
C(23)	C(26)	1.536(5)	C(66)	C(67)	1.522(4)
C(23)	C(25)	1.542(4)	C(67)	C(68)	1.515(5)

Table II.61. Continued.

C(27)	C(28)	1.530(4)	C(67)	C(69)	1.547(5)
C(27)	C(30)	1.534(4)	C(70A)	C(72A)	1.547(5)
C(27)	C(29)	1.538(4)	C(70A)	C(71A)	1.553(5)
C(31)	C(32)	1.505(5)	C(70B)	C(71B)	1.542(5)
C(32)	C(33)	1.375(5)	C(70B)	C(72B)	1.545(5)

Table II.62. Bond Angles for [IPrH][Co(OBHT)$_3$].

Atom	Atom	Atom	Angle/°	Atom	Atom	Atom	Angle/°
O(3)	Co(1)	O(1)	123.99(9)	C(35)	C(34)	C(38)	121.2(2)
O(3)	Co(1)	O(2)	120.65(8)	O(3)	C(35)	C(36)	120.0(2)
O(1)	Co(1)	O(2)	115.13(8)	O(3)	C(35)	C(34)	120.3(2)
C(58)	N(1)	C(59)	108.8(2)	C(36)	C(35)	C(34)	119.7(2)
C(58)	N(1)	C(49)	124.6(2)	C(37)	C(36)	C(35)	117.8(3)
C(59)	N(1)	C(49)	126.4(2)	C(37)	C(36)	C(42)	120.6(3)
C(58)	N(2)	C(60)	109.0(2)	C(35)	C(36)	C(42)	121.5(2)
C(58)	N(2)	C(61)	125.9(2)	C(32)	C(37)	C(36)	123.5(3)
C(60)	N(2)	C(61)	125.0(2)	C(34)	C(38)	C(40)	110.4(2)
C(5)	O(1)	Co(1)	161.28(17)	C(34)	C(38)	C(41)	110.5(2)
C(20)	O(2)	Co(1)	150.89(17)	C(40)	C(38)	C(41)	111.2(3)
C(35)	O(3)	Co(1)	178.19(19)	C(34)	C(38)	C(39)	112.7(3)
C(3)	C(2)	C(7)	117.8(3)	C(40)	C(38)	C(39)	105.9(2)
C(3)	C(2)	C(1)	121.8(3)	C(41)	C(38)	C(39)	105.9(3)
C(7)	C(2)	C(1)	120.3(3)	C(36)	C(42)	C(44)	110.9(3)
C(2)	C(3)	C(4)	123.4(3)	C(36)	C(42)	C(43)	109.5(3)
C(3)	C(4)	C(5)	118.0(3)	C(44)	C(42)	C(43)	110.7(3)
C(3)	C(4)	C(12)	120.2(2)	C(36)	C(42)	C(45)	111.6(3)
C(5)	C(4)	C(12)	121.7(2)	C(44)	C(42)	C(45)	106.9(4)
O(1)	C(5)	C(4)	120.5(2)	C(43)	C(42)	C(45)	107.2(3)
O(1)	C(5)	C(6)	120.0(2)	C(51)	C(46)	C(47)	120.9(3)
C(4)	C(5)	C(6)	119.4(2)	C(46)	C(47)	C(48)	120.7(3)
C(7)	C(6)	C(5)	118.8(2)	C(47)	C(48)	C(49)	115.8(3)
C(7)	C(6)	C(8)	119.4(2)	C(47)	C(48)	C(52A)	121.6(4)
C(5)	C(6)	C(8)	121.7(2)	C(49)	C(48)	C(52A)	122.5(4)
C(6)	C(7)	C(2)	122.4(3)	C(47)	C(48)	C(52B)	122.1(5)
C(10)	C(8)	C(11)	107.1(2)	C(49)	C(48)	C(52B)	122.0(5)
C(10)	C(8)	C(6)	109.2(2)	C(50)	C(49)	C(48)	125.0(3)
C(11)	C(8)	C(6)	112.5(2)	C(50)	C(49)	N(1)	116.9(2)
C(10)	C(8)	C(9)	109.8(2)	C(48)	C(49)	N(1)	118.0(2)
C(11)	C(8)	C(9)	106.6(3)	C(51)	C(50)	C(49)	116.1(3)
C(6)	C(8)	C(9)	111.5(2)	C(51)	C(50)	C(55)	120.5(3)
C(14)	C(12)	C(15)	109.9(3)	C(49)	C(50)	C(55)	123.4(3)
C(14)	C(12)	C(4)	109.7(2)	C(46)	C(51)	C(50)	121.4(3)
C(15)	C(12)	C(4)	111.3(2)	C(48)	C(52A)	C(54A)	117.1(6)
C(14)	C(12)	C(13)	107.2(2)	C(48)	C(52A)	C(53A)	110.9(6)
C(15)	C(12)	C(13)	106.1(2)	C(54A)	C(52A)	C(53A)	108.4(7)
C(4)	C(12)	C(13)	112.5(2)	C(53B)	C(52B)	C(54B)	109.1(8)
C(22)	C(17)	C(18)	117.1(3)	C(53B)	C(52B)	C(48)	111.6(7)

Table II.62. Continued.

C(22)	C(17)	C(16)	121.3(3)
C(18)	C(17)	C(16)	121.6(3)
C(17)	C(18)	C(19)	123.5(3)
C(18)	C(19)	C(20)	118.1(3)
C(18)	C(19)	C(23)	120.4(3)
C(20)	C(19)	C(23)	121.5(3)
O(2)	C(20)	C(19)	119.2(2)
O(2)	C(20)	C(21)	121.4(2)
C(19)	C(20)	C(21)	119.3(2)
C(22)	C(21)	C(20)	118.1(3)
C(22)	C(21)	C(27)	119.4(2)
C(20)	C(21)	C(27)	122.5(2)
C(17)	C(22)	C(21)	123.8(3)
C(24)	C(23)	C(26)	111.9(3)
C(24)	C(23)	C(25)	105.8(3)
C(26)	C(23)	C(25)	106.8(3)
C(24)	C(23)	C(19)	109.5(3)
C(26)	C(23)	C(19)	110.8(3)
C(25)	C(23)	C(19)	111.8(3)
C(28)	C(27)	C(21)	112.6(2)
C(28)	C(27)	C(30)	105.8(2)
C(21)	C(27)	C(30)	109.2(2)
C(28)	C(27)	C(29)	106.7(2)
C(21)	C(27)	C(29)	111.4(2)
C(30)	C(27)	C(29)	110.9(2)
C(33)	C(32)	C(37)	117.4(3)
C(33)	C(32)	C(31)	121.4(4)
C(37)	C(32)	C(31)	121.2(3)
C(32)	C(33)	C(34)	123.0(3)
C(33)	C(34)	C(35)	118.5(2)
C(33)	C(34)	C(38)	120.3(2)
C(54B)	C(52B)	C(48)	107.0(7)
C(56)	C(55)	C(57)	111.2(3)
C(56)	C(55)	C(50)	111.7(3)
C(57)	C(55)	C(50)	111.2(3)
N(2)	C(58)	N(1)	107.9(2)
C(60)	C(59)	N(1)	107.2(2)
C(59)	C(60)	N(2)	107.0(2)
C(66)	C(61)	C(62)	124.0(3)
C(66)	C(61)	N(2)	118.0(2)
C(62)	C(61)	N(2)	118.1(2)
C(61)	C(62)	C(63)	116.4(3)
C(61)	C(62)	C(70A)	119.0(6)
C(63)	C(62)	C(70A)	122.4(6)
C(61)	C(62)	C(70B)	122.4(4)
C(63)	C(62)	C(70B)	120.2(4)
C(64)	C(63)	C(62)	121.5(3)
C(65)	C(64)	C(63)	120.3(3)
C(64)	C(65)	C(66)	121.2(3)
C(61)	C(66)	C(65)	116.7(3)
C(61)	C(66)	C(67)	122.5(2)
C(65)	C(66)	C(67)	120.8(3)
C(68)	C(67)	C(66)	112.2(3)
C(68)	C(67)	C(69)	109.8(3)
C(66)	C(67)	C(69)	109.2(3)
C(62)	C(70A)	C(72A)	112.9(12)
C(62)	C(70A)	C(71A)	97.6(9)
C(72A)	C(70A)	C(71A)	116.1(14)
C(71B)	C(70B)	C(72B)	105.1(11)
C(71B)	C(70B)	C(62)	119.6(8)
C(72B)	C(70B)	C(62)	107.2(9)

Table II.63. Hydrogen Atom Coordinates (Å×10^4) and Isotropic Displacement Parameters (Å^2×10^3) for [IPrH][Co(OBHT)$_3$].

Atom	***x***	***y***	***z***	**U(eq)**
H(1A)	-597	3667	1225	152
H(1B)	-638	4076	1276	152
H(1C)	-1024	3844	1864	152
H(3)	303	3465	3063	63
H(7)	999	4270	1937	58
H(9A)	3483	4478	4512	81
H(9B)	2635	4755	4016	81
H(9C)	3689	4793	3993	81
H(10A)	3456	4124	2452	66
H(10B)	4043	4098	3522	66
H(10C)	4148	4433	3011	66
H(11A)	2809	4844	2370	85
H(11B)	1758	4773	2374	85
H(11C)	2120	4543	1767	85
H(13A)	500	3224	4288	75
H(13B)	1299	2942	4858	75
H(13C)	993	2983	3804	75
H(14A)	2622	3719	5587	88
H(14B)	2243	3385	5913	88
H(14C)	1472	3673	5338	88
H(15A)	2776	3052	4147	72
H(15B)	2976	2989	5172	72
H(15C)	3436	3317	4906	72
H(16A)	6481	4205	10456	121
H(16B)	7286	4419	10267	121
H(16C)	7462	4021	10514	121
H(18)	6957	3622	9312	65
H(22)	5797	4561	8789	56
H(24A)	6197	3460	6526	100
H(24B)	6701	3096	6886	100
H(24C)	7260	3440	7360	100
H(25A)	6856	2863	8299	115
H(25B)	6536	3080	8957	115
H(25C)	7465	3198	8783	115
H(26A)	4658	3262	6776	88
H(26B)	4854	3108	7739	88
H(26C)	5207	2901	7087	88
H(28A)	4417	4837	7983	74

Table II.63. Continued.

H(28B)	4267	5047	7099	74
H(28C)	5358	4959	7834	74
H(29A)	3512	4220	6228	63
H(29B)	3174	4611	6176	63
H(29C)	3318	4383	7032	63
H(30A)	5739	4707	6665	64
H(30B)	4648	4806	5950	64
H(30C)	5037	4421	6004	64
H(31A)	8978	3612	3966	154
H(31B)	8114	3498	3025	154
H(31C)	8635	3220	3799	154
H(33)	8200	3983	4601	51
H(37)	6872	3095	3574	64
H(39A)	8567	4323	5781	110
H(39B)	7965	4665	5755	110
H(39C)	7926	4507	4842	110
H(40A)	6120	4516	4217	81
H(40B)	6200	4673	5145	81
H(40C)	5549	4337	4734	81
H(41A)	6579	4046	6259	84
H(41B)	7261	4379	6614	84
H(41C)	7750	4016	6598	84
H(43A)	4188	3468	3652	77
H(43B)	3779	3112	3151	77
H(43C)	4367	3367	2790	77
H(44A)	5862	2843	5166	112
H(44B)	4687	2813	4641	112
H(44C)	5178	3160	5153	112
H(45A)	5361	2861	2836	162
H(45B)	4914	2620	3358	162
H(45C)	6079	2688	3768	162
H(46)	-842	3232	5800	60
H(47)	347	2806	6379	55
H(51)	-466	3796	6224	61
H(52A)	2911	2977	7761	55
H(53A)	2225	2810	8767	147
H(53B)	2821	2503	8580	147
H(53C)	1639	2508	8096	147
H(54A)	1719	2445	6628	110
H(54B)	2900	2454	7104	110
H(54C)	2305	2718	6312	110

Table II.63. Continued.

H(52B)	2797	2922	8202	55
H(53D)	1356	2408	7212	111
H(53E)	1485	2552	8168	111
H(53F)	2355	2336	8090	111
H(54D)	3165	2563	7162	105
H(54E)	3113	2962	6928	105
H(54F)	2202	2717	6360	105
H(55)	1926	4111	7759	59
H(56A)	326	4321	6129	88
H(56B)	1396	4220	6206	88
H(56C)	1267	4550	6724	88
H(57A)	781	4476	7981	112
H(57B)	826	4106	8413	112
H(57C)	-76	4203	7478	112
H(58)	2528	3529	9276	41
H(59)	3403	3666	7311	47
H(60)	4779	3835	8744	48
H(63)	6049	3458	12115	86
H(64)	5857	3983	12665	68
H(65)	4762	4381	11726	53
H(67)	3215	4260	9352	57
H(68A)	2457	4282	10359	113
H(68B)	2358	4641	9857	113
H(68C)	3160	4595	10875	113
H(69A)	3728	4838	9453	110
H(69B)	4665	4596	9677	110
H(69C)	4512	4783	10474	110
H(70A)	5217	3298	9737	73
H(71A)	4688	2946	11019	136
H(71B)	4760	2746	10200	136
H(71C)	3951	3040	10006	136
H(72A)	6884	3330	10827	133
H(72B)	6611	2934	10626	133
H(72C)	6638	3105	11520	133
H(70B)	4700	3149	9828	73
H(71D)	4875	2643	10760	268
H(71E)	3929	2874	10599	268
H(71F)	4893	2896	11533	268
H(72D)	6504	3034	11408	175
H(72E)	6463	3230	10538	175
H(72F)	6171	2834	10476	175

Table II.64. Atomic Occupancy for [IPrH][Co(OBHT)$_3$].

Atom	***Occupancy***	**Atom**	***Occupancy***	**Atom**	***Occupancy***
C(52A)	0.571(17)	H(52A)	0.571(17)	C(53A)	0.571(17)
H(53A)	0.571(17)	H(53B)	0.571(17)	H(53C)	0.571(17)
C(54A)	0.571(17)	H(54A)	0.571(17)	H(54B)	0.571(17)
H(54C)	0.571(17)	C(52B)	0.429(17)	H(52B)	0.429(17)
C(53B)	0.429(17)	H(53D)	0.429(17)	H(53E)	0.429(17)
H(53F)	0.429(17)	C(54B)	0.429(17)	H(54D)	0.429(17)
H(54E)	0.429(17)	H(54F)	0.429(17)	C(70A)	0.399(13)
H(70A)	0.399(13)	C(71A)	0.399(13)	H(71A)	0.399(13)
H(71B)	0.399(13)	H(71C)	0.399(13)	C(72A)	0.399(13)
H(72A)	0.399(13)	H(72B)	0.399(13)	H(72C)	0.399(13)
C(70B)	0.601(13)	H(70B)	0.601(13)	C(71B)	0.601(13)
H(71D)	0.601(13)	H(71E)	0.601(13)	H(71F)	0.601(13)
C(72B)	0.601(13)	H(72D)	0.601(13)	H(72E)	0.601(13)
H(72F)	0.601(13)				

II.10 Diffraction data for $[Co_2Na_2(\mu^2\text{-}N(SiMe_3)_2)_4](\mu^4\text{-}O)$.

Table II.65. Crystal data and structure refinement for $[Co_2Na_2(\mu^2\text{-}N(SiMe_3)_2)_4](\mu^4\text{-}O)$.

Identification code	$[Co_2Na_2(\mu^2\text{-}N(SiMe_3)_2)_4](\mu^4\text{-}O)$.
Empirical formula	$C_{24}H_{72}Co_2N_4Na_2OSi_8$
Formula weight	821.41
Temperature/K	100
Crystal system	triclinic
Space group	P-1
a/Å	8.8839(18)
b/Å	10.591(2)
c/Å	12.700(3)
α/°	96.75(4)
β/°	108.93(3)
γ/°	99.15(3)
Volume/Å^3	1097.4(5)
Z	1
ρ_{calc}g/cm^3	1.243
μ/mm^{-1}	1.017
F(000)	440.0
Crystal size/mm^3	0.3 × 0.24 × 0.2
Radiation	MoKα (λ = 0.71073)
2Θ range for data collection/°	3.448 to 52.97
Index ranges	$-11 \leq h \leq 10$, $-13 \leq k \leq 13$, $0 \leq l \leq 15$
Reflections collected	4421
Independent reflections	4421 [R_{int} = 0.0892, R_{sigma} = 0.1114]
Data/restraints/parameters	4421/0/200
Goodness-of-fit on F^2	1.025
Final R indexes [I>=2σ (I)]	R_1 = 0.0646, wR_2 = 0.1402
Final R indexes [all data]	R_1 = 0.0910, wR_2 = 0.1535
Largest diff. peak/hole / e Å^{-3}	1.07/-0.54

Table II.66. Fractional Atomic Coordinates ($\times 10^4$) and Equivalent Isotropic Displacement Parameters ($Å^2 \times 10^3$) for $[Co_2Na_2(\mu^2\text{-}N(SiMe_3)_2)_4](\mu^4\text{-}O)$. U_{eq} is defined as 1/3 of of the trace of the orthogonalised U_{IJ} tensor.

Atom	***x***	***y***	***z***	**U(eq)**
Co(1)	6123.9(8)	4820.8(7)	6453.0(5)	13.7(2)
Si(1)	4065.6(17)	2514.4(14)	7065.5(12)	17.4(3)
Si(2)	7131.5(17)	2135.7(14)	6609.9(12)	16.7(3)
Si(3)	9436.5(16)	6855.0(14)	7489.6(11)	16.5(3)
Si(4)	6806.1(16)	7099.4(14)	8453.8(11)	16.5(3)
Na(1)	4185(2)	2767.9(19)	4418.7(16)	22.2(5)
O(1)	5000	5000	5000	18.7(11)
N(1)	5621(5)	2967(4)	6570(3)	16.5(9)
N(2)	7424(5)	6528(4)	7365(3)	16.2(9)
C(1)	3045(6)	3891(5)	7230(4)	24.8(13)
C(2)	4707(7)	1928(6)	8440(5)	31.2(14)
C(3)	2418(6)	1205(5)	6018(5)	30.0(14)
C(4)	6502(7)	351(5)	6561(5)	25.5(13)
C(5)	8974(6)	2721(6)	7914(4)	27.2(14)
C(6)	7720(6)	2294(5)	5334(4)	23.3(13)
C(7)	9702(6)	5853(5)	6277(4)	23.9(13)
C(8)	10834(6)	6525(5)	8841(4)	24.9(13)
C(9)	10216(6)	8588(5)	7425(5)	24.8(13)
C(10)	6827(6)	5923(5)	9438(4)	24.2(13)
C(11)	4724(6)	7420(5)	7848(4)	23.7(13)
C(12)	8079(6)	8685(5)	9344(4)	23.2(13)

Table II.67. Anisotropic Displacement Parameters ($Å^2 \times 10^3$) for $[Co_2Na_2(\mu^2\text{-}N(SiMe_3)_2)_4](\mu^4\text{-}O)$. The Anisotropic displacement factor exponent takes the form: $-2\pi^2[h^2a^{*2}U_{11}+2hka^*b^*U_{12}+\ldots]$.

Atom	**U_{11}**	**U_{22}**	**U_{33}**	**U_{23}**	**U_{13}**	**U_{12}**
Co(1)	13.7(4)	13.2(4)	11.1(4)	0.3(3)	1.4(3)	2.2(3)
Si(1)	18.9(8)	16.7(8)	17.7(8)	3.0(6)	7.7(6)	3.6(6)
Si(2)	14.9(7)	16.5(8)	17.7(8)	3.2(6)	4.1(6)	3.7(6)
Si(3)	14.2(7)	18.0(8)	13.7(7)	0.7(6)	1.5(6)	2.1(6)
Si(4)	15.3(7)	17.0(8)	14.0(7)	-1.4(6)	3.4(6)	0.7(6)
Na(1)	26.8(12)	17.6(12)	17.1(11)	2.7(9)	1.8(9)	3.0(9)
O(1)	22(3)	17(3)	14(3)	1(2)	3(2)	2(2)
N(1)	15(2)	17(2)	15(2)	0.6(18)	4.4(18)	1.4(18)
N(2)	15(2)	20(3)	12(2)	1.6(18)	2.5(17)	3.6(19)
C(1)	24(3)	20(3)	28(3)	-4(2)	12(2)	2(2)
C(2)	44(4)	28(4)	30(3)	10(3)	20(3)	11(3)
C(3)	28(3)	24(3)	38(4)	-7(3)	17(3)	2(3)
C(4)	28(3)	23(3)	30(3)	8(2)	13(3)	11(3)
C(5)	23(3)	32(4)	22(3)	1(2)	2(2)	9(3)
C(6)	25(3)	18(3)	21(3)	-2(2)	2(2)	6(2)
C(7)	21(3)	22(3)	27(3)	0(2)	9(2)	3(2)
C(8)	21(3)	31(4)	19(3)	2(2)	3(2)	6(3)
C(9)	18(3)	25(3)	27(3)	-4(2)	8(2)	-3(2)
C(10)	24(3)	22(3)	23(3)	0(2)	6(2)	2(2)
C(11)	27(3)	18(3)	27(3)	5(2)	9(2)	5(2)
C(12)	24(3)	22(3)	23(3)	-3(2)	12(2)	2(2)

Table II.68. Bond Lengths for $[Co_2Na_2(\mu^2\text{-}N(SiMe_3)_2)_4](\mu^4\text{-}O)$.

Atom	Atom	Length/Å	Atom	Atom	Length/Å
Co(1)	Na(1)[1]	2.918(2)	Si(3)	C(9)	1.877(6)
Co(1)	O(1)	1.8398(9)	Si(4)	Na(1)[1]	3.490(3)
Co(1)	N(1)	1.977(4)	Si(4)	N(2)	1.727(4)
Co(1)	N(2)	1.980(4)	Si(4)	C(10)	1.863(6)
Si(1)	N(1)	1.721(4)	Si(4)	C(11)	1.862(5)
Si(1)	C(1)	1.861(5)	Si(4)	C(12)	1.870(5)
Si(1)	C(2)	1.865(6)	Na(1)	Co(1)[1]	2.918(2)
Si(1)	C(3)	1.869(5)	Na(1)	Si(3)[1]	3.458(3)
Si(2)	N(1)	1.709(4)	Na(1)	Si(4)[1]	3.490(3)
Si(2)	C(4)	1.872(6)	Na(1)	O(1)	2.314(2)
Si(2)	C(5)	1.866(5)	Na(1)	N(1)	2.579(4)
Si(2)	C(6)	1.874(5)	Na(1)	N(2)[1]	2.523(4)
Si(3)	Na(1)[1]	3.458(3)	O(1)	Co(1)[1]	1.8399(9)
Si(3)	N(2)	1.717(4)	O(1)	Na(1)[1]	2.314(2)
Si(3)	C(7)	1.867(5)	N(2)	Na(1)[1]	2.523(4)
Si(3)	C(8)	1.872(5)			

[1]1-X,1-Y,1-Z

Table II.69. Bond Angles for $[Co_2Na_2(\mu^2\text{-}N(SiMe_3)_2)_4](\mu^4\text{-}O)$.

Atom	Atom	Atom	Angle/°	Atom	Atom	Atom	Angle/°
O(1)	Co(1)	Na(1)[1]	52.46(5)	C(11)	Si(4)	C(12)	104.8(2)
O(1)	Co(1)	N(1)	108.39(12)	C(12)	Si(4)	Na(1)[1]	110.76(19)
O(1)	Co(1)	N(2)	110.26(13)	Co(1)[1]	Na(1)	Si(3)[1]	58.20(6)
N(1)	Co(1)	Na(1)[1]	159.62(12)	Co(1)[1]	Na(1)	Si(4)[1]	57.47(6)
N(1)	Co(1)	N(2)	141.35(17)	Si(3)[1]	Na(1)	Si(4)[1]	51.16(5)
N(2)	Co(1)	Na(1)[1]	58.31(12)	O(1)	Na(1)	Co(1)[1]	39.08(4)
N(1)	Si(1)	C(1)	110.5(2)	O(1)	Na(1)	Si(3)[1]	90.23(8)
N(1)	Si(1)	C(2)	114.4(2)	O(1)	Na(1)	Si(4)[1]	94.36(8)
N(1)	Si(1)	C(3)	111.2(2)	O(1)	Na(1)	N(1)	78.30(12)
C(1)	Si(1)	C(2)	108.3(2)	O(1)	Na(1)	N(2)[1]	80.67(12)
C(1)	Si(1)	C(3)	104.4(2)	N(1)	Na(1)	Co(1)[1]	117.16(12)
C(2)	Si(1)	C(3)	107.5(3)	N(1)	Na(1)	Si(3)[1]	139.95(12)
N(1)	Si(2)	C(4)	113.5(2)	N(1)	Na(1)	Si(4)[1]	165.71(12)
N(1)	Si(2)	C(5)	113.1(2)	N(2)[1]	Na(1)	Co(1)[1]	41.89(10)
N(1)	Si(2)	C(6)	108.9(2)	N(2)[1]	Na(1)	Si(3)[1]	28.21(10)
C(4)	Si(2)	C(6)	106.2(2)	N(2)[1]	Na(1)	Si(4)[1]	27.90(9)
C(5)	Si(2)	C(4)	105.5(3)	N(2)[1]	Na(1)	N(1)	155.82(15)
C(5)	Si(2)	C(6)	109.2(3)	Co(1)	O(1)	Co(1)[1]	180.0
N(2)	Si(3)	Na(1)[1]	43.99(14)	Co(1)	O(1)	Na(1)[1]	88.46(7)
N(2)	Si(3)	C(7)	109.4(2)	Co(1)	O(1)	Na(1)	91.54(7)
N(2)	Si(3)	C(8)	113.4(2)	Co(1)[1]	O(1)	Na(1)[1]	91.54(7)
N(2)	Si(3)	C(9)	113.5(2)	Co(1)[1]	O(1)	Na(1)	88.46(7)
C(7)	Si(3)	Na(1)[1]	86.99(17)	Na(1)	O(1)	Na(1)[1]	180.00(3)
C(7)	Si(3)	C(8)	108.6(2)	Co(1)	N(1)	Na(1)	81.02(15)
C(7)	Si(3)	C(9)	105.5(3)	Si(1)	N(1)	Co(1)	116.1(2)
C(8)	Si(3)	Na(1)[1]	157.06(18)	Si(1)	N(1)	Na(1)	104.36(18)
C(8)	Si(3)	C(9)	106.0(3)	Si(2)	N(1)	Co(1)	115.7(2)
C(9)	Si(3)	Na(1)[1]	84.84(18)	Si(2)	N(1)	Si(1)	124.7(3)
N(2)	Si(4)	Na(1)[1]	43.12(14)	Si(2)	N(1)	Na(1)	101.38(18)
N(2)	Si(4)	C(10)	111.6(2)	Co(1)	N(2)	Na(1)[1]	79.79(14)
N(2)	Si(4)	C(11)	109.2(2)	Si(3)	N(2)	Co(1)	115.9(2)
N(2)	Si(4)	C(12)	114.5(2)	Si(3)	N(2)	Si(4)	121.2(2)
C(10)	Si(4)	Na(1)[1]	141.68(18)	Si(3)	N(2)	Na(1)[1]	107.8(2)
C(10)	Si(4)	C(12)	106.4(2)	Si(4)	N(2)	Co(1)	114.6(2)
C(11)	Si(4)	Na(1)[1]	69.07(18)	Si(4)	N(2)	Na(1)[1]	108.98(19)
C(11)	Si(4)	C(10)	110.1(2)				

[1]1-X,1-Y,1-Z

Table II.70. Torsion Angles for $[Co_2Na_2(\mu^2\text{-}N(SiMe_3)_2)_4](\mu^4\text{-}O)$.

A	B	C	D	Angle/°	A	B	C	D	Angle/°
Na(1)[1]	Co(1)	O(1)	Na(1)	179.999(0)	C(5)	Si(2)	N(1)	Na(1)	151.5(2)
Na(1)[1]	Si(3)	N(2)	Co(1)	87.1(2)	C(6)	Si(2)	N(1)	Co(1)	-55.6(3)
Na(1)[1]	Si(3)	N(2)	Si(4)	-126.4(4)	C(6)	Si(2)	N(1)	Si(1)	146.4(3)
Na(1)[1]	Si(4)	N(2)	Co(1)	-87.2(2)	C(6)	Si(2)	N(1)	Na(1)	29.8(2)
Na(1)[1]	Si(4)	N(2)	Si(3)	125.9(4)	C(7)	Si(3)	N(2)	Co(1)	23.4(3)
N(1)	Co(1)	O(1)	Na(1)[1]	172.03(13)	C(7)	Si(3)	N(2)	Si(4)	170.0(3)
N(1)	Co(1)	O(1)	Na(1)	-7.97(13)	C(7)	Si(3)	N(2)	Na(1)[1]	-63.6(3)
N(2)	Co(1)	O(1)	Na(1)	171.82(13)	C(8)	Si(3)	N(2)	Co(1)	-98.0(3)
N(2)	Co(1)	O(1)	Na(1)[1]	-8.18(13)	C(8)	Si(3)	N(2)	Si(4)	48.5(4)
C(1)	Si(1)	N(1)	Co(1)	6.4(3)	C(8)	Si(3)	N(2)	Na(1)[1]	174.9(2)
C(1)	Si(1)	N(1)	Si(2)	164.3(3)	C(9)	Si(3)	N(2)	Co(1)	140.9(2)
C(1)	Si(1)	N(1)	Na(1)	-80.6(2)	C(9)	Si(3)	N(2)	Si(4)	-72.6(3)
C(2)	Si(1)	N(1)	Co(1)	-116.1(3)	C(9)	Si(3)	N(2)	Na(1)[1]	53.8(3)
C(2)	Si(1)	N(1)	Si(2)	41.8(4)	C(10)	Si(4)	N(2)	Co(1)	57.1(3)
C(2)	Si(1)	N(1)	Na(1)	157.0(2)	C(10)	Si(4)	N(2)	Si(3)	-89.8(3)
C(3)	Si(1)	N(1)	Co(1)	121.8(3)	C(10)	Si(4)	N(2)	Na(1)[1]	144.3(2)
C(3)	Si(1)	N(1)	Si(2)	-80.3(3)	C(11)	Si(4)	N(2)	Co(1)	-64.8(3)
C(3)	Si(1)	N(1)	Na(1)	34.9(3)	C(11)	Si(4)	N(2)	Si(3)	148.2(3)
C(4)	Si(2)	N(1)	Co(1)	-173.7(2)	C(11)	Si(4)	N(2)	Na(1)[1]	22.4(3)
C(4)	Si(2)	N(1)	Si(1)	28.3(4)	C(12)	Si(4)	N(2)	Co(1)	178.0(2)
C(4)	Si(2)	N(1)	Na(1)	-88.3(2)	C(12)	Si(4)	N(2)	Si(3)	31.1(4)
C(5)	Si(2)	N(1)	Co(1)	66.1(3)	C(12)	Si(4)	N(2)	Na(1)[1]	-94.8(3)
C(5)	Si(2)	N(1)	Si(1)	-92.0(3)					

[1]1-X,1-Y,1-Z

Table II.71. Hydrogen Atom Coordinates (Å×10^4) and Isotropic Displacement Parameters (Å^2×10^3) for $[Co_2Na_2(\mu^2\text{-}N(SiMe_3)_2)_4](\mu^4\text{-}O)$.

Atom	***x***	***y***	***z***	**U(eq)**
H(1A)	2812	4278	6546	37
H(1B)	3762	4550	7884	37
H(1C)	2026	3571	7348	37
H(2A)	5074	1113	8336	47
H(2B)	3784	1780	8705	47
H(2C)	5600	2583	9001	47
H(3A)	1989	1514	5304	45
H(3B)	1540	979	6315	45
H(3C)	2861	435	5886	45
H(4A)	6269	212	7247	38
H(4B)	7383	-80	6517	38
H(4C)	5523	-14	5895	38
H(5A)	9424	3638	7950	41
H(5B)	9791	2206	7893	41
H(5C)	8674	2625	8582	41
H(6A)	6872	1745	4663	35
H(6B)	8754	2018	5441	35
H(6C)	7843	3203	5232	35
H(7A)	9660	4953	6399	36
H(7B)	10758	6205	6222	36
H(7C)	8830	5874	5574	36
H(8A)	11074	7271	9448	37
H(8B)	11849	6385	8744	37
H(8C)	10310	5747	9038	37
H(9A)	9589	8788	6697	37
H(9B)	11367	8712	7503	37
H(9C)	10100	9168	8041	37
H(10A)	6380	5039	9000	36
H(10B)	6165	6131	9893	36
H(10C)	7949	5982	9939	36
H(11A)	4780	8203	7508	36
H(11B)	4269	7550	8450	36
H(11C)	4027	6677	7267	36
H(12A)	9202	8588	9700	35
H(12B)	7642	8948	9933	35
H(12C)	8060	9350	8868	35

II.11 Diffraction data for (IPr*)Fe(CO)$_4$•2Tol.

Table II.72. Crystal data and structure refinement for (IPr*)Fe(CO)$_4$.

Identification code	(IPr*)Fe(CO)4
Empirical formula	$C_{80}H_{64}FeN_2O_4$
Formula weight	1173.18
Temperature/K	100.01
Crystal system	monoclinic
Space group	$P2_1/c$
a/Å	10.3803(3)
b/Å	22.9244(7)
c/Å	26.5430(8)
α/°	90
β/°	97.7310(10)
γ/°	90
Volume/Å^3	6258.8(3)
Z	4
ρ_{calc}g/cm^3	1.245
μ/mm^{-1}	0.295
F(000)	2464.0
Crystal size/mm^3	0.233 × 0.152 × 0.129
Radiation	MoKα (λ = 0.71073)
2Θ range for data collection/°	4.34 to 51.506
Index ranges	-12 ≤ h ≤ 12, -28 ≤ k ≤ 27, -32 ≤ l ≤ 32
Reflections collected	111061
Independent reflections	11967 [R_{int} = 0.0505, R_{sigma} = 0.0266]
Data/restraints/parameters	11967/90/840
Goodness-of-fit on F^2	1.044
Final R indexes [I>=2σ (I)]	R_1 = 0.0449, wR_2 = 0.1014
Final R indexes [all data]	R_1 = 0.0595, wR_2 = 0.1081
Largest diff. peak/hole / e Å^{-3}	0.45/-0.52

Table II.73. Fractional Atomic Coordinates ($\times 10^4$) and Equivalent Isotropic Displacement Parameters ($Å^2 \times 10^3$) for (IPr*)Fe(CO)$_4$. U_{eq} is defined as 1/3 of of the trace of the orthogonalised U_{IJ} tensor.

Atom	*x*	*y*	*z*	U(eq)
Fe(1)	5452.8(3)	6646.0(2)	3376.9(2)	15.52(8)
O(1)	2681.3(15)	6747.7(9)	3456.7(7)	42.5(5)
O(2)	4771.4(15)	7044.2(8)	2322.4(6)	34.2(4)
O(3)	5907.4(16)	7059.9(7)	4432.3(6)	27.1(4)
O(4)	5270.9(15)	5369.4(7)	3444.7(6)	28.2(4)
N(1)	8374.6(15)	6441.3(7)	3515.1(6)	10.2(3)
N(2)	7929.1(15)	7301.5(7)	3223.4(6)	12.1(3)
C(1)	7349.0(18)	6792.1(8)	3346.1(7)	10.9(4)
C(2)	9555.1(18)	6724.0(8)	3503.6(7)	12.8(4)
C(3)	9277.0(18)	7260.9(8)	3325.9(7)	14.0(4)
C(4)	5446.1(19)	5859.4(10)	3406.1(8)	20.2(4)
C(5)	3761(2)	6695.9(10)	3421.7(8)	25.8(5)
C(6)	5744.1(19)	6915.6(9)	4014.2(8)	19.7(4)
C(7)	5075.8(19)	6911.6(10)	2739.7(8)	21.7(5)
C(8)	8275.1(18)	5825.1(8)	3616.5(7)	11.8(4)
C(9)	8249.0(18)	5435.0(8)	3212.8(7)	12.7(4)
C(10)	8120.7(19)	4844.6(8)	3311.2(7)	15.6(4)
C(11)	8036.9(19)	4637.7(9)	3797.7(7)	16.7(4)
C(12)	8125.5(19)	5037.6(9)	4195.5(7)	16.3(4)
C(13)	8250.9(18)	5631.2(8)	4115.0(7)	13.3(4)
C(14)	7858(2)	3996.4(9)	3893.5(8)	24.3(5)
C(15)	8476.2(19)	6061.8(8)	4556.3(7)	14.6(4)
C(16)	9917(2)	6220.4(8)	4666.7(7)	16.0(4)
C(17)	10273(2)	6777.4(9)	4845.0(8)	21.4(5)
C(18)	11569(2)	6949.8(10)	4910.7(9)	29.5(5)
C(19)	12527(2)	6570.8(11)	4803.8(8)	29.9(5)
C(20)	12191(2)	6013.6(10)	4638.6(8)	25.8(5)
C(21)	10895(2)	5839.2(9)	4570.3(7)	19.8(4)
C(22)	7861(2)	5862.7(8)	5018.4(7)	16.6(4)
C(23)	8567(2)	5795.3(9)	5494.8(8)	20.0(4)
C(24)	7948(2)	5641.1(9)	5910.2(8)	26.3(5)
C(25)	6626(2)	5551.9(10)	5851.7(9)	29.0(5)
C(26)	5906(2)	5611.8(10)	5376.5(9)	27.4(5)
C(27)	6524(2)	5766.8(9)	4963.9(8)	22.2(5)
C(28)	8474.5(19)	5637.6(8)	2685.3(7)	14.8(4)
C(29)	7542(2)	5354.3(9)	2264.4(7)	16.1(4)
C(30)	7890(2)	4870.5(10)	1997.4(8)	25.5(5)

Table II.73. Continued.

C(31)	7031(3)	4630.6(11)	1606.3(9)	33.9(6)
C(32)	5826(2)	4876.7(11)	1473.4(8)	33.1(6)
C(33)	5454(2)	5347.5(11)	1740.1(8)	29.8(5)
C(34)	6305(2)	5583.1(10)	2138.7(8)	22.2(5)
C(35)	9904(2)	5570.7(9)	2612.7(8)	18.9(4)
C(36)	10845(2)	5390.8(11)	3000.7(9)	29.5(5)
C(37)	12144(2)	5358.0(13)	2927.9(10)	39.4(6)
C(38)	12519(3)	5502.9(14)	2468.4(10)	43.9(7)
C(39)	11598(3)	5687.4(14)	2080.8(10)	43.1(7)
C(40)	10302(2)	5721.5(11)	2151.3(8)	31.3(6)
C(41)	7241.6(18)	7796.1(8)	2973.2(7)	13.6(4)
C(42)	7174.1(19)	7853.9(8)	2444.2(7)	16.5(4)
C(43)	6407(2)	8298.5(9)	2210.9(8)	19.5(4)
C(44)	5747(2)	8686.5(9)	2484.3(8)	19.4(4)
C(45)	5918(2)	8643.0(9)	3010.3(8)	18.2(4)
C(46)	6681.4(18)	8206.9(8)	3262.7(7)	14.8(4)
C(47)	4893(2)	9154.2(10)	2220.8(9)	30.1(5)
C(48)	7048(2)	8230.2(9)	3835.7(7)	17.4(4)
C(49)	8338(2)	8544.9(9)	3960.8(7)	19.7(4)
C(50)	8623(2)	9051.9(10)	3706.3(9)	28.4(5)
C(51)	9770(3)	9347.8(11)	3850.4(9)	36.6(6)
C(52)	10654(2)	9146.4(12)	4247.3(9)	35.0(6)
C(53)	10393(2)	8639.5(11)	4496.9(9)	29.1(5)
C(54)	9245(2)	8344.4(10)	4353.7(8)	23.7(5)
C(55)	5992(2)	8482.4(9)	4122.9(8)	23.6(5)
C(56)	4729(2)	8264.7(11)	4024.1(9)	31.1(5)
C(57)	3770(3)	8443.9(13)	4303.5(10)	41.2(7)
C(58)	4055(3)	8854.4(14)	4679.9(10)	46.6(8)
C(59)	5281(3)	9085.4(13)	4776.3(9)	44.2(7)
C(60)	6258(3)	8897.9(11)	4498.1(8)	32.4(6)
C(61)	8001(2)	7467.8(9)	2144.9(7)	18.4(4)
C(62)	9413(2)	7672.5(10)	2212.7(7)	22.3(5)
C(63)	9805(2)	8224.8(10)	2370.5(9)	31.9(6)
C(64)	11128(3)	8362.9(12)	2451.0(11)	42.2(7)
C(65)	12047(3)	7957.3(14)	2371.9(10)	45.1(7)
C(66)	11659(3)	7409.7(15)	2208.3(11)	50.8(8)
C(67)	10357(2)	7268.8(13)	2130.1(10)	39.4(6)
C(68)	7471(2)	7394.7(9)	1586.4(7)	18.9(4)
C(69)	6756(2)	6903.7(10)	1428.3(8)	29.2(5)
C(70)	6261(3)	6824.3(11)	921.8(9)	37.7(6)
C(71)	6456(2)	7242.6(11)	563.6(9)	32.7(6)

Table II.73. Continued.

C(72)	7177(2)	7731.2(10)	716.5(8)	26.9(5)
C(73)	7693(2)	7804.9(9)	1221.0(8)	22.4(5)
C(113)	2387(5)	5966(4)	778.0(19)	64.0(19)
C(112)	1176(7)	5699(2)	688(2)	52.0(18)
C(111)	57(4)	6019(2)	728(3)	41.1(19)
C(116)	150(5)	6606(2)	858(3)	45(2)
C(115)	1362(7)	6873(2)	949(2)	61(2)
C(114)	2480(5)	6553(4)	908.7(18)	67(2)
C(110)	-1234(4)	5720.2(19)	620.4(16)	48.3(12)
C(121)	2163(15)	6831(5)	923(4)	38(2)
C(126)	2569(13)	6263(6)	845(5)	34(3)
C(122)	831(15)	6946(7)	878(5)	46(3)
C(125)	1655(17)	5827(6)	717(6)	46(3)
C(123)	-29(16)	6500(9)	784(8)	54(4)
C(124)	309(18)	5943(9)	693(9)	56(4)
C(120)	3130(10)	7330(5)	1037(4)	62(3)

Table II.74. Anisotropic Displacement Parameters ($Å^2 \times 10^3$) for (IPr*)Fe(CO)$_4$. The Anisotropic displacement factor exponent takes the form: $-2\pi^2[h^2a^{*2}U_{11}+2hka^*b^*U_{12}+\ldots]$.

Atom	U_{11}	U_{22}	U_{33}	U_{23}	U_{13}	U_{12}
Fe(1)	11.86(14)	18.71(15)	16.31(15)	1.57(12)	3.06(11)	-0.60(12)
O(1)	15.0(9)	68.4(14)	46.1(11)	4.4(10)	11.0(7)	2.2(8)
O(2)	24.3(9)	54.0(11)	22.9(9)	12.4(8)	-2.5(7)	-3.1(8)
O(3)	36.2(9)	27.2(8)	19.0(8)	-0.3(7)	7.6(7)	1.1(7)
O(4)	23.7(8)	18.7(8)	42(1)	0.8(7)	3.6(7)	-6.7(7)
N(1)	12.1(8)	10.2(7)	8.5(7)	0.7(6)	1.7(6)	-0.8(6)
N(2)	14.0(8)	11.2(8)	11.3(8)	2.0(6)	2.5(6)	1.5(6)
C(1)	15.0(9)	11.0(9)	7.0(8)	0.1(7)	2.3(7)	0.1(7)
C(2)	11.6(9)	15.8(10)	10.8(9)	1.2(7)	1.2(7)	-0.6(8)
C(3)	13.0(9)	15.6(10)	13.6(9)	0.4(8)	2.9(7)	-2.7(8)
C(4)	12.7(10)	28.5(12)	19.1(10)	-0.3(9)	1.5(8)	-2.6(9)
C(5)	23.1(12)	32.0(13)	22.6(11)	2(1)	3.7(9)	-2.1(10)
C(6)	16.5(10)	20.6(11)	23.2(12)	4.7(9)	7.1(8)	0.4(8)
C(7)	11.8(10)	27.7(12)	25.4(12)	3.0(9)	2.2(8)	-1.1(9)
C(8)	12.0(9)	9.1(9)	14.1(9)	2.3(7)	0.5(7)	-0.5(7)
C(9)	13.2(9)	13.9(9)	10.8(9)	0.6(7)	0.8(7)	-0.4(8)
C(10)	19.1(10)	14.6(10)	12.8(9)	-2.7(8)	0.7(8)	-1.1(8)
C(11)	20.2(10)	13.7(10)	15.6(10)	1.7(8)	0.3(8)	-0.7(8)
C(12)	21.9(10)	16.1(10)	10.8(9)	4.0(8)	2.0(8)	0.0(8)
C(13)	13.9(9)	14.3(9)	11.6(9)	-0.2(8)	1.2(7)	0.9(8)
C(14)	41.8(14)	12.9(10)	17.4(11)	2.5(8)	0.5(9)	-4.5(9)
C(15)	21.4(10)	11.9(9)	10.5(9)	1.2(7)	2.1(8)	2.9(8)
C(16)	25.9(11)	14.8(10)	6.8(9)	2.7(7)	0.9(8)	-0.8(8)
C(17)	31.6(12)	14.1(10)	18(1)	0.6(8)	1.2(9)	-2.3(9)
C(18)	40.8(14)	21.6(12)	24.8(12)	2.7(10)	-0.7(10)	-12.4(11)
C(19)	26.5(12)	39.8(14)	22.6(12)	6.2(10)	0.0(9)	-11.9(11)
C(20)	23.2(11)	35.4(13)	18.5(11)	3.3(10)	1.8(9)	4(1)
C(21)	26.8(11)	18.7(10)	13.4(10)	1.0(8)	0.8(8)	1.0(9)
C(22)	27.0(11)	10.2(9)	13.3(10)	-1.4(8)	5.6(8)	2.1(8)
C(23)	28.9(12)	14.1(10)	17.5(10)	0.7(8)	4.6(9)	3.8(9)
C(24)	46.4(14)	20.9(11)	12.2(10)	3.0(9)	5.9(9)	4.9(10)
C(25)	46.2(15)	22.6(12)	22.2(12)	2.1(9)	19.3(11)	-1.8(10)
C(26)	30.3(12)	25.3(12)	29.1(12)	-1.6(10)	13.3(10)	-3.7(10)
C(27)	29.1(12)	21.6(11)	16.3(10)	-0.1(9)	4.4(9)	-0.3(9)
C(28)	21.7(10)	12.2(9)	10.9(9)	-0.1(8)	3.2(8)	-0.9(8)
C(29)	22.8(10)	16.3(10)	9.4(9)	2.2(8)	2.8(8)	-4.7(8)
C(30)	31.2(12)	24.8(12)	21.7(11)	-6.0(9)	8.1(9)	-6.2(10)
C(31)	45.5(15)	34.2(14)	23.6(12)	-11.9(10)	9.9(11)	-15.8(12)

Table II.74. Continued.

C(32)	42.3(15)	44.0(15)	12.4(10)	-3.2(10)	1.1(10)	-26.4(12)
C(33)	23.6(12)	44.4(15)	20.3(11)	10.7(11)	-1.6(9)	-9.1(11)
C(34)	27.5(12)	24.4(11)	15(1)	4.2(9)	3.7(9)	-2.7(9)
C(35)	23.6(11)	18.4(10)	15.2(10)	-0.8(8)	4.8(8)	-6.0(9)
C(36)	27.8(12)	36.7(14)	25.3(12)	9.2(10)	8.7(10)	-0.6(10)
C(37)	25.0(13)	55.8(17)	38.4(15)	13.4(13)	7.5(11)	1.8(12)
C(38)	24.6(13)	72(2)	37.7(15)	5.0(14)	14.1(11)	-4.9(13)
C(39)	35.1(14)	72(2)	24.6(13)	5.3(13)	13.3(11)	-16.6(14)
C(40)	30.8(13)	45.8(15)	17.0(11)	3.7(10)	2.4(9)	-11.1(11)
C(41)	12.2(9)	10.6(9)	18(1)	3.8(8)	1.5(7)	-0.5(7)
C(42)	20.6(10)	14(1)	15.3(10)	1.0(8)	3.5(8)	1.1(8)
C(43)	26.0(11)	19.2(10)	12.9(10)	3.3(8)	1.4(8)	2.8(9)
C(44)	21.1(11)	16.6(10)	20.1(10)	3.7(8)	0.9(8)	4.4(8)
C(45)	21.4(11)	14.9(10)	19.2(10)	0.5(8)	6.1(8)	4.3(8)
C(46)	14.6(9)	15.1(10)	14.9(10)	1.9(8)	3.2(8)	0.3(8)
C(47)	36.5(13)	30.3(13)	22.2(12)	5.2(10)	-0.2(10)	17.3(11)
C(48)	22.8(11)	15.3(10)	15(1)	3.5(8)	6.1(8)	5.4(8)
C(49)	26.6(11)	20.1(10)	13(1)	-2.2(8)	4.3(8)	2.5(9)
C(50)	33.6(13)	28.7(12)	21.3(11)	6.7(10)	-2.4(10)	-4.7(10)
C(51)	40.6(15)	36.1(14)	31.8(13)	9.7(11)	0.5(11)	-12.7(12)
C(52)	30.4(13)	43.9(15)	29.5(13)	-0.9(11)	0.1(10)	-9.2(11)
C(53)	26.9(12)	38.2(14)	21.2(11)	1.2(10)	-0.3(9)	4(1)
C(54)	28.8(12)	24.7(11)	17.9(10)	1.9(9)	3.9(9)	3.5(10)
C(55)	33.3(12)	23.7(11)	15.3(10)	8.3(9)	8.9(9)	11.7(10)
C(56)	30.2(13)	34.1(14)	31.5(13)	12.0(11)	12.9(10)	12.3(11)
C(57)	36.6(14)	52.9(17)	37.2(15)	18.7(13)	16.5(12)	18.4(13)
C(58)	45.3(17)	73(2)	25.2(13)	17.2(14)	16.5(12)	35.3(15)
C(59)	62.2(19)	54.4(17)	16.6(12)	2.9(12)	6.9(12)	33.9(15)
C(60)	42.8(15)	36.8(14)	17.9(11)	2.9(10)	5.9(10)	20.1(11)
C(61)	28.9(11)	14.1(10)	13.4(10)	5.2(8)	6.8(8)	5.8(8)
C(62)	28.5(12)	28.1(12)	11.1(10)	5.2(9)	5.5(8)	6.2(10)
C(63)	32.3(13)	26.5(13)	39.5(14)	11.7(11)	14.0(11)	0.7(10)
C(64)	45.4(16)	35.8(14)	47.0(16)	12.5(13)	12.2(13)	-11.1(13)
C(65)	24.8(13)	73(2)	38.2(15)	9.9(15)	5.4(11)	3.6(14)
C(66)	29.6(14)	75(2)	46.2(17)	-18.4(16)	-2.0(12)	17.3(15)
C(67)	32.5(14)	48.9(16)	34.3(14)	-14.2(12)	-4.5(11)	14.2(12)
C(68)	26.6(11)	17.2(10)	14.3(10)	1.3(8)	7.7(8)	4.6(9)
C(69)	46.9(15)	22.1(11)	21.0(11)	1.9(9)	13.1(10)	-9.0(11)
C(70)	52.5(17)	34.6(14)	27.0(13)	-6.6(11)	9.0(12)	-20.2(12)
C(71)	42.6(14)	40.2(14)	15.1(11)	-1(1)	2.9(10)	-6.2(12)
C(72)	40.2(14)	25.4(12)	16.1(11)	6.3(9)	7.2(10)	0.5(10)

Table II.74. Continued.

C(73)	31.8(12)	16.3(10)	19.3(11)	2.5(8)	4.4(9)	-0.2(9)
C(113)	58(4)	112(6)	26(3)	25(4)	16(3)	15(4)
C(112)	58(4)	73(4)	28(3)	18(3)	19(3)	20(3)
C(111)	53(3)	57(4)	14(3)	7(2)	7(2)	12(2)
C(116)	60(4)	58(4)	19(3)	0(3)	14(3)	4(3)
C(115)	64(4)	89(5)	32(3)	5(3)	13(4)	-10(4)
C(114)	54(4)	114(7)	36(3)	17(5)	17(3)	-4(4)
C(110)	60(3)	44(2)	38(2)	1.3(19)	-5(2)	11(2)
C(121)	55(6)	43(5)	16(4)	11(4)	8(4)	23(4)
C(126)	47(5)	38(5)	19(5)	7(4)	10(4)	16(4)
C(122)	50(6)	58(5)	30(6)	11(4)	5(5)	20(4)
C(125)	61(7)	39(5)	37(6)	10(4)	7(6)	5(4)
C(123)	62(6)	66(7)	35(9)	8(5)	9(5)	10(5)
C(124)	64(7)	61(7)	44(10)	10(5)	8(6)	8(5)
C(120)	66(6)	67(6)	52(6)	10(4)	8(4)	17(4)

Table II.75. Bond Lengths for (IPr*)$Fe(CO)_4$.

Atom	Atom	Length/Å	Atom	Atom	Length/Å
Fe(1)	C(1)	2.0090(19)	C(39)	C(40)	1.385(4)
Fe(1)	C(4)	1.805(2)	C(41)	C(42)	1.403(3)
Fe(1)	C(5)	1.780(2)	C(41)	C(46)	1.391(3)
Fe(1)	C(6)	1.788(2)	C(42)	C(43)	1.387(3)
Fe(1)	C(7)	1.791(2)	C(42)	C(61)	1.528(3)
O(1)	C(5)	1.143(3)	C(43)	C(44)	1.386(3)
O(2)	C(7)	1.151(3)	C(44)	C(45)	1.387(3)
O(3)	C(6)	1.149(3)	C(44)	C(47)	1.503(3)
O(4)	C(4)	1.145(3)	C(45)	C(46)	1.391(3)
N(1)	C(1)	1.361(2)	C(46)	C(48)	1.519(3)
N(1)	C(2)	1.390(2)	C(48)	C(49)	1.517(3)
N(1)	C(8)	1.444(2)	C(48)	C(55)	1.531(3)
N(2)	C(1)	1.373(2)	C(49)	C(50)	1.396(3)
N(2)	C(3)	1.392(2)	C(49)	C(54)	1.386(3)
N(2)	C(41)	1.452(2)	C(50)	C(51)	1.379(3)
C(2)	C(3)	1.336(3)	C(51)	C(52)	1.380(3)
C(8)	C(9)	1.393(3)	C(52)	C(53)	1.383(3)
C(8)	C(13)	1.399(3)	C(53)	C(54)	1.378(3)
C(9)	C(10)	1.388(3)	C(55)	C(56)	1.394(3)
C(9)	C(28)	1.523(3)	C(55)	C(60)	1.379(3)
C(10)	C(11)	1.389(3)	C(56)	C(57)	1.382(3)
C(11)	C(12)	1.392(3)	C(57)	C(58)	1.375(4)
C(11)	C(14)	1.507(3)	C(58)	C(59)	1.371(4)
C(12)	C(13)	1.386(3)	C(59)	C(60)	1.400(3)
C(13)	C(15)	1.525(3)	C(61)	C(62)	1.526(3)
C(15)	C(16)	1.528(3)	C(61)	C(68)	1.519(3)
C(15)	C(22)	1.527(3)	C(62)	C(63)	1.378(3)
C(16)	C(17)	1.394(3)	C(62)	C(67)	1.387(3)
C(16)	C(21)	1.389(3)	C(63)	C(64)	1.397(4)
C(17)	C(18)	1.391(3)	C(64)	C(65)	1.368(4)
C(18)	C(19)	1.379(4)	C(65)	C(66)	1.371(4)
C(19)	C(20)	1.380(3)	C(66)	C(67)	1.377(4)
C(20)	C(21)	1.392(3)	C(68)	C(69)	1.382(3)
C(22)	C(23)	1.383(3)	C(68)	C(73)	1.392(3)
C(22)	C(27)	1.393(3)	C(69)	C(70)	1.385(3)
C(23)	C(24)	1.394(3)	C(70)	C(71)	1.384(3)
C(24)	C(25)	1.375(3)	C(71)	C(72)	1.377(3)
C(25)	C(26)	1.384(3)	C(72)	C(73)	1.384(3)
C(26)	C(27)	1.388(3)	C(113)	C(112)	1.3900

Table II.75. Continued.

C(28)	C(29)	1.522(3)	C(113)	C(114)	1.3900
C(28)	C(35)	1.529(3)	C(112)	C(111)	1.3900
C(29)	C(30)	1.390(3)	C(111)	C(116)	1.3900
C(29)	C(34)	1.386(3)	C(111)	C(110)	1.499(6)
C(30)	C(31)	1.388(3)	C(116)	C(115)	1.3900
C(31)	C(32)	1.374(4)	C(115)	C(114)	1.3900
C(32)	C(33)	1.374(4)	C(121)	C(126)	1.392(15)
C(33)	C(34)	1.393(3)	C(121)	C(122)	1.398(16)
C(35)	C(36)	1.384(3)	C(121)	C(120)	1.526(18)
C(35)	C(40)	1.388(3)	C(126)	C(125)	1.388(19)
C(36)	C(37)	1.390(3)	C(122)	C(123)	1.36(2)
C(37)	C(38)	1.370(4)	C(125)	C(124)	1.42(2)
C(38)	C(39)	1.373(4)	C(123)	C(124)	1.354(19)

Table II.76. Bond Angles for (IPr*)Fe(CO)$_4$.

Atom	Atom	Atom	Angle/°	Atom	Atom	Atom	Angle/°
C(4)	Fe(1)	C(1)	100.24(8)	C(38)	C(37)	C(36)	120.5(2)
C(5)	Fe(1)	C(1)	166.64(9)	C(37)	C(38)	C(39)	119.3(2)
C(5)	Fe(1)	C(4)	92.97(10)	C(38)	C(39)	C(40)	120.4(2)
C(5)	Fe(1)	C(6)	87.56(10)	C(39)	C(40)	C(35)	121.0(2)
C(5)	Fe(1)	C(7)	87.07(10)	C(42)	C(41)	N(2)	119.14(17)
C(6)	Fe(1)	C(1)	86.50(8)	C(46)	C(41)	N(2)	119.48(17)
C(6)	Fe(1)	C(4)	107.81(9)	C(46)	C(41)	C(42)	121.37(17)
C(6)	Fe(1)	C(7)	139.79(10)	C(41)	C(42)	C(61)	120.64(17)
C(7)	Fe(1)	C(1)	89.75(8)	C(43)	C(42)	C(41)	117.70(18)
C(7)	Fe(1)	C(4)	112.24(10)	C(43)	C(42)	C(61)	121.50(17)
C(1)	N(1)	C(2)	111.71(15)	C(44)	C(43)	C(42)	122.16(19)
C(1)	N(1)	C(8)	124.54(15)	C(43)	C(44)	C(45)	118.39(18)
C(2)	N(1)	C(8)	123.05(15)	C(43)	C(44)	C(47)	121.09(19)
C(1)	N(2)	C(3)	110.98(15)	C(45)	C(44)	C(47)	120.49(19)
C(1)	N(2)	C(41)	124.64(15)	C(44)	C(45)	C(46)	121.61(18)
C(3)	N(2)	C(41)	124.11(15)	C(41)	C(46)	C(48)	120.65(17)
N(1)	C(1)	Fe(1)	127.96(13)	C(45)	C(46)	C(41)	118.30(18)
N(1)	C(1)	N(2)	103.43(15)	C(45)	C(46)	C(48)	120.49(17)
N(2)	C(1)	Fe(1)	127.93(13)	C(46)	C(48)	C(55)	114.33(17)
C(3)	C(2)	N(1)	106.74(16)	C(49)	C(48)	C(46)	109.32(16)
C(2)	C(3)	N(2)	107.12(16)	C(49)	C(48)	C(55)	112.43(17)
O(4)	C(4)	Fe(1)	170.32(18)	C(50)	C(49)	C(48)	121.91(19)
O(1)	C(5)	Fe(1)	177.6(2)	C(54)	C(49)	C(48)	119.79(19)
O(3)	C(6)	Fe(1)	176.23(19)	C(54)	C(49)	C(50)	118.2(2)
O(2)	C(7)	Fe(1)	174.6(2)	C(51)	C(50)	C(49)	120.5(2)
C(9)	C(8)	N(1)	118.61(16)	C(50)	C(51)	C(52)	120.5(2)
C(9)	C(8)	C(13)	121.51(17)	C(51)	C(52)	C(53)	119.6(2)
C(13)	C(8)	N(1)	119.85(16)	C(54)	C(53)	C(52)	119.9(2)
C(8)	C(9)	C(28)	121.47(17)	C(53)	C(54)	C(49)	121.3(2)
C(10)	C(9)	C(8)	118.26(17)	C(56)	C(55)	C(48)	119.3(2)
C(10)	C(9)	C(28)	120.05(17)	C(60)	C(55)	C(48)	122.2(2)
C(9)	C(10)	C(11)	121.83(18)	C(60)	C(55)	C(56)	118.4(2)
C(10)	C(11)	C(12)	118.30(18)	C(57)	C(56)	C(55)	121.3(3)
C(10)	C(11)	C(14)	120.94(18)	C(58)	C(57)	C(56)	119.6(3)
C(12)	C(11)	C(14)	120.75(18)	C(59)	C(58)	C(57)	120.2(2)
C(13)	C(12)	C(11)	121.84(18)	C(58)	C(59)	C(60)	120.2(3)
C(8)	C(13)	C(15)	120.01(17)	C(55)	C(60)	C(59)	120.3(3)
C(12)	C(13)	C(8)	118.13(17)	C(62)	C(61)	C(42)	110.99(17)
C(12)	C(13)	C(15)	121.65(17)	C(68)	C(61)	C(42)	114.60(17)

Table II.76. Continued.

C(13)	C(15)	C(16)	110.26(16)	C(68)	C(61)	C(62)	111.38(16)
C(13)	C(15)	C(22)	112.70(16)	C(63)	C(62)	C(61)	124.0(2)
C(22)	C(15)	C(16)	114.91(16)	C(63)	C(62)	C(67)	118.3(2)
C(17)	C(16)	C(15)	119.39(18)	C(67)	C(62)	C(61)	117.6(2)
C(21)	C(16)	C(15)	122.37(18)	C(62)	C(63)	C(64)	119.9(2)
C(21)	C(16)	C(17)	118.15(19)	C(65)	C(64)	C(63)	120.9(3)
C(18)	C(17)	C(16)	120.7(2)	C(64)	C(65)	C(66)	119.3(3)
C(19)	C(18)	C(17)	120.5(2)	C(65)	C(66)	C(67)	120.2(3)
C(18)	C(19)	C(20)	119.3(2)	C(66)	C(67)	C(62)	121.3(3)
C(19)	C(20)	C(21)	120.4(2)	C(69)	C(68)	C(61)	119.68(18)
C(16)	C(21)	C(20)	120.9(2)	C(69)	C(68)	C(73)	118.09(19)
C(23)	C(22)	C(15)	122.70(19)	C(73)	C(68)	C(61)	122.23(19)
C(23)	C(22)	C(27)	118.43(19)	C(68)	C(69)	C(70)	121.1(2)
C(27)	C(22)	C(15)	118.83(18)	C(71)	C(70)	C(69)	120.4(2)
C(22)	C(23)	C(24)	120.5(2)	C(72)	C(71)	C(70)	119.0(2)
C(25)	C(24)	C(23)	120.5(2)	C(71)	C(72)	C(73)	120.6(2)
C(24)	C(25)	C(26)	119.8(2)	C(72)	C(73)	C(68)	120.8(2)
C(25)	C(26)	C(27)	119.6(2)	C(112)	C(113)	C(114)	120.0
C(26)	C(27)	C(22)	121.2(2)	C(113)	C(112)	C(111)	120.0
C(9)	C(28)	C(35)	110.92(16)	C(112)	C(111)	C(110)	118.6(5)
C(29)	C(28)	C(9)	112.56(16)	C(116)	C(111)	C(112)	120.0
C(29)	C(28)	C(35)	113.37(16)	C(116)	C(111)	C(110)	121.4(5)
C(30)	C(29)	C(28)	122.12(19)	C(111)	C(116)	C(115)	120.0
C(34)	C(29)	C(28)	119.51(18)	C(116)	C(115)	C(114)	120.0
C(34)	C(29)	C(30)	118.37(19)	C(115)	C(114)	C(113)	120.0
C(31)	C(30)	C(29)	120.8(2)	C(126)	C(121)	C(122)	118.7(15)
C(32)	C(31)	C(30)	120.0(2)	C(126)	C(121)	C(120)	121.8(15)
C(31)	C(32)	C(33)	120.0(2)	C(122)	C(121)	C(120)	119.4(13)
C(32)	C(33)	C(34)	120.2(2)	C(125)	C(126)	C(121)	119.9(13)
C(29)	C(34)	C(33)	120.6(2)	C(123)	C(122)	C(121)	119.4(13)
C(36)	C(35)	C(28)	122.40(18)	C(126)	C(125)	C(124)	120.9(11)
C(36)	C(35)	C(40)	117.8(2)	C(124)	C(123)	C(122)	124.3(15)
C(40)	C(35)	C(28)	119.70(19)	C(123)	C(124)	C(125)	116.6(14)
C(35)	C(36)	C(37)	120.9(2)				

Table II.77. Torsion Angles for (IPr*)Fe(CO)$_4$.

A	B	C	D	Angle/°	A	B	C	D	Angle/°
N(1)	C(2)	C(3)	N(2)	-0.8(2)	C(37)	C(38)	C(39)	C(40)	-0.6(5)
N(1)	C(8)	C(9)	C(10)	-178.42(17)	C(38)	C(39)	C(40)	C(35)	0.0(4)
N(1)	C(8)	C(9)	C(28)	6.9(3)	C(40)	C(35)	C(36)	C(37)	-0.5(4)
N(1)	C(8)	C(13)	C(12)	178.59(17)	C(41)	N(2)	C(1)	Fe(1)	-15.8(3)
N(1)	C(8)	C(13)	C(15)	-6.6(3)	C(41)	N(2)	C(1)	N(1)	173.16(16)
N(2)	C(41)	C(42)	C(43)	173.93(18)	C(41)	N(2)	C(3)	C(2)	-173.09(17)
N(2)	C(41)	C(42)	C(61)	-10.6(3)	C(41)	C(42)	C(43)	C(44)	1.6(3)
N(2)	C(41)	C(46)	C(45)	-173.56(17)	C(41)	C(42)	C(61)	C(62)	-76.4(2)
N(2)	C(41)	C(46)	C(48)	15.0(3)	C(41)	C(42)	C(61)	C(68)	156.40(18)
C(1)	N(1)	C(2)	C(3)	0.1(2)	C(41)	C(46)	C(48)	C(49)	79.5(2)
C(1)	N(1)	C(8)	C(9)	83.7(2)	C(41)	C(46)	C(48)	C(55)	-153.47(18)
C(1)	N(1)	C(8)	C(13)	-98.4(2)	C(42)	C(41)	C(46)	C(45)	7.4(3)
C(1)	N(2)	C(3)	C(2)	1.2(2)	C(42)	C(41)	C(46)	C(48)	-163.99(18)
C(1)	N(2)	C(41)	C(42)	-96.1(2)	C(42)	C(43)	C(44)	C(45)	3.3(3)
C(1)	N(2)	C(41)	C(46)	84.9(2)	C(42)	C(43)	C(44)	C(47)	-178.3(2)
C(2)	N(1)	C(1)	Fe(1)	-170.46(13)	C(42)	C(61)	C(62)	C(63)	-20.3(3)
C(2)	N(1)	C(1)	N(2)	0.62(19)	C(42)	C(61)	C(62)	C(67)	156.95(19)
C(2)	N(1)	C(8)	C(9)	-85.9(2)	C(42)	C(61)	C(68)	C(69)	-97.8(2)
C(2)	N(1)	C(8)	C(13)	92.0(2)	C(42)	C(61)	C(68)	C(73)	83.0(2)
C(3)	N(2)	C(1)	Fe(1)	169.99(13)	C(43)	C(42)	C(61)	C(62)	98.9(2)
C(3)	N(2)	C(1)	N(1)	-1.10(19)	C(43)	C(42)	C(61)	C(68)	-28.3(3)
C(3)	N(2)	C(41)	C(42)	77.4(2)	C(43)	C(44)	C(45)	C(46)	-2.9(3)
C(3)	N(2)	C(41)	C(46)	-101.6(2)	C(44)	C(45)	C(46)	C(41)	-2.3(3)
C(8)	N(1)	C(1)	Fe(1)	18.9(3)	C(44)	C(45)	C(46)	C(48)	169.13(19)
C(8)	N(1)	C(1)	N(2)	-170.00(15)	C(45)	C(46)	C(48)	C(49)	-91.7(2)
C(8)	N(1)	C(2)	C(3)	170.86(16)	C(45)	C(46)	C(48)	C(55)	35.3(3)
C(8)	C(9)	C(10)	C(11)	-0.9(3)	C(46)	C(41)	C(42)	C(43)	-7.1(3)
C(8)	C(9)	C(28)	C(29)	-137.74(18)	C(46)	C(41)	C(42)	C(61)	168.43(18)
C(8)	C(9)	C(28)	C(35)	94.0(2)	C(46)	C(48)	C(49)	C(50)	42.6(3)
C(8)	C(13)	C(15)	C(16)	-75.1(2)	C(46)	C(48)	C(49)	C(54)	-140.41(19)
C(8)	C(13)	C(15)	C(22)	155.03(17)	C(46)	C(48)	C(55)	C(56)	50.5(3)
C(9)	C(8)	C(13)	C(12)	-3.6(3)	C(46)	C(48)	C(55)	C(60)	-133.1(2)
C(9)	C(8)	C(13)	C(15)	171.21(17)	C(47)	C(44)	C(45)	C(46)	178.7(2)
C(9)	C(10)	C(11)	C(12)	-2.0(3)	C(48)	C(49)	C(50)	C(51)	175.9(2)
C(9)	C(10)	C(11)	C(14)	178.19(19)	C(48)	C(49)	C(54)	C(53)	-176.1(2)
C(9)	C(28)	C(29)	C(30)	-97.7(2)	C(48)	C(55)	C(56)	C(57)	174.5(2)
C(9)	C(28)	C(29)	C(34)	82.5(2)	C(48)	C(55)	C(60)	C(59)	-175.3(2)
C(9)	C(28)	C(35)	C(36)	-4.6(3)	C(49)	C(48)	C(55)	C(56)	175.88(19)
C(9)	C(28)	C(35)	C(40)	178.72(19)	C(49)	C(48)	C(55)	C(60)	-7.7(3)

Table II.77. Continued.

C(10)	C(9)	C(28)	C(29)	47.7(2)	C(49)	C(50)	C(51)	C(52)	0.2(4)
C(10)	C(9)	C(28)	C(35)	-80.5(2)	C(50)	C(49)	C(54)	C(53)	0.9(3)
C(10)	C(11)	C(12)	C(13)	2.1(3)	C(50)	C(51)	C(52)	C(53)	0.9(4)
C(11)	C(12)	C(13)	C(8)	0.6(3)	C(51)	C(52)	C(53)	C(54)	-1.0(4)
C(11)	C(12)	C(13)	C(15)	-174.12(18)	C(52)	C(53)	C(54)	C(49)	0.1(4)
C(12)	C(13)	C(15)	C(16)	99.5(2)	C(54)	C(49)	C(50)	C(51)	-1.1(3)
C(12)	C(13)	C(15)	C(22)	-30.4(3)	C(55)	C(48)	C(49)	C(50)	-85.5(2)
C(13)	C(8)	C(9)	C(10)	3.7(3)	C(55)	C(48)	C(49)	C(54)	91.5(2)
C(13)	C(8)	C(9)	C(28)	-170.90(17)	C(55)	C(56)	C(57)	C(58)	1.4(4)
C(13)	C(15)	C(16)	C(17)	147.52(18)	C(56)	C(55)	C(60)	C(59)	1.1(3)
C(13)	C(15)	C(16)	C(21)	-28.9(2)	C(56)	C(57)	C(58)	C(59)	0.2(4)
C(13)	C(15)	C(22)	C(23)	123.6(2)	C(57)	C(58)	C(59)	C(60)	-1.1(4)
C(13)	C(15)	C(22)	C(27)	-59.0(2)	C(58)	C(59)	C(60)	C(55)	0.4(4)
C(14)	C(11)	C(12)	C(13)	-178.0(2)	C(60)	C(55)	C(56)	C(57)	-2.0(3)
C(15)	C(16)	C(17)	C(18)	-174.88(18)	C(61)	C(42)	C(43)	C(44)	-173.9(2)
C(15)	C(16)	C(21)	C(20)	175.02(18)	C(61)	C(62)	C(63)	C(64)	176.2(2)
C(15)	C(22)	C(23)	C(24)	176.72(18)	C(61)	C(62)	C(67)	C(66)	-176.6(2)
C(15)	C(22)	C(27)	C(26)	-177.00(19)	C(61)	C(68)	C(69)	C(70)	-180.0(2)
C(16)	C(15)	C(22)	C(23)	-3.9(3)	C(61)	C(68)	C(73)	C(72)	-178.8(2)
C(16)	C(15)	C(22)	C(27)	173.50(18)	C(62)	C(61)	C(68)	C(69)	135.2(2)
C(16)	C(17)	C(18)	C(19)	-0.5(3)	C(62)	C(61)	C(68)	C(73)	-44.0(3)
C(17)	C(16)	C(21)	C(20)	-1.5(3)	C(62)	C(63)	C(64)	C(65)	0.5(4)
C(17)	C(18)	C(19)	C(20)	-1.1(3)	C(63)	C(62)	C(67)	C(66)	0.7(4)
C(18)	C(19)	C(20)	C(21)	1.3(3)	C(63)	C(64)	C(65)	C(66)	0.4(4)
C(19)	C(20)	C(21)	C(16)	0.0(3)	C(64)	C(65)	C(66)	C(67)	-0.7(4)
C(21)	C(16)	C(17)	C(18)	1.7(3)	C(65)	C(66)	C(67)	C(62)	0.1(4)
C(22)	C(15)	C(16)	C(17)	-83.8(2)	C(67)	C(62)	C(63)	C(64)	-1.0(3)
C(22)	C(15)	C(16)	C(21)	99.7(2)	C(68)	C(61)	C(62)	C(63)	108.7(2)
C(22)	C(23)	C(24)	C(25)	0.2(3)	C(68)	C(61)	C(62)	C(67)	-74.1(2)
C(23)	C(22)	C(27)	C(26)	0.5(3)	C(68)	C(69)	C(70)	C(71)	-1.1(4)
C(23)	C(24)	C(25)	C(26)	0.4(3)	C(69)	C(68)	C(73)	C(72)	2.0(3)
C(24)	C(25)	C(26)	C(27)	-0.6(3)	C(69)	C(70)	C(71)	C(72)	1.6(4)
C(25)	C(26)	C(27)	C(22)	0.1(3)	C(70)	C(71)	C(72)	C(73)	-0.3(4)
C(27)	C(22)	C(23)	C(24)	-0.7(3)	C(71)	C(72)	C(73)	C(68)	-1.5(4)
C(28)	C(9)	C(10)	C(11)	173.83(18)	C(73)	C(68)	C(69)	C(70)	-0.7(4)
C(28)	C(29)	C(30)	C(31)	-178.3(2)	C(113)	C(112)	C(111)	C(116)	0.0
C(28)	C(29)	C(34)	C(33)	177.15(18)	C(113)	C(112)	C(111)	C(110)	179.1(6)
C(28)	C(35)	C(36)	C(37)	-177.3(2)	C(112)	C(113)	C(114)	C(115)	0.0
C(28)	C(35)	C(40)	C(39)	177.4(2)	C(112)	C(111)	C(116)	C(115)	0.0
C(29)	C(28)	C(35)	C(36)	-132.4(2)	C(111)	C(116)	C(115)	C(114)	0.0
C(29)	C(28)	C(35)	C(40)	50.9(3)	C(116)	C(115)	C(114)	C(113)	0.0

Table II.77. Continued.

C(29)	C(30)	C(31)	C(32)	1.0(3)	C(114)	C(113)	C(112)	C(111)	0.0
C(30)	C(29)	C(34)	C(33)	-2.7(3)	C(110)	C(111)	C(116)	C(115)	-179.1(6)
C(30)	C(31)	C(32)	C(33)	-2.4(4)	C(121)	C(126)	C(125)	C(124)	-3.9(19)
C(31)	C(32)	C(33)	C(34)	1.2(3)	C(121)	C(122)	C(123)	C(124)	-5(2)
C(32)	C(33)	C(34)	C(29)	1.3(3)	C(126)	C(121)	C(122)	C(123)	3.0(19)
C(34)	C(29)	C(30)	C(31)	1.5(3)	C(126)	C(125)	C(124)	C(123)	2.3(18)
C(35)	C(28)	C(29)	C(30)	29.3(3)	C(122)	C(121)	C(126)	C(125)	1(2)
C(35)	C(28)	C(29)	C(34)	-150.55(18)	C(122)	C(123)	C(124)	C(125)	2.0(19)
C(35)	C(36)	C(37)	C(38)	-0.1(4)	C(120)	C(121)	C(126)	C(125)	-176.8(11)
C(36)	C(35)	C(40)	C(39)	0.6(4)	C(120)	C(121)	C(122)	C(123)	-179.0(12)
C(36)	C(37)	C(38)	C(39)	0.7(5)					

Table II.78. Hydrogen Atom Coordinates (Å×10^4) and Isotropic Displacement Parameters (Å^2×10^3) for (IPr*)Fe(CO)$_4$.

Atom	*x*	*y*	*z*	U(eq)
H(2)	10397	6566	3603	15
H(3)	9885	7559	3278	17
H(10)	8089	4575	3038	19
H(12)	8099	4900	4532	20
H(14A)	6928	3906	3860	36
H(14B)	8267	3898	4238	36
H(14C)	8264	3768	3645	36
H(15)	8013	6428	4434	18
H(17)	9623	7042	4922	26
H(18)	11796	7332	5030	35
H(19)	13410	6692	4843	36
H(20)	12848	5747	4571	31
H(21)	10676	5454	4456	24
H(23)	9482	5854	5539	24
H(24)	8443	5597	6236	32
H(25)	6209	5450	6137	35
H(26)	4994	5547	5333	33
H(27)	6026	5808	4638	27
H(28)	8283	6065	2669	18
H(30)	8727	4702	2084	31
H(31)	7276	4296	1430	41
H(32)	5251	4721	1197	40
H(33)	4614	5513	1652	36
H(34)	6034	5903	2326	27
H(36)	10600	5288	3321	35
H(37)	12777	5234	3199	47
H(38)	13406	5476	2418	53
H(39)	11852	5792	1762	52
H(40)	9677	5850	1880	38
H(43)	6332	8338	1852	23
H(45)	5503	8918	3203	22
H(47A)	4031	8992	2104	45
H(47B)	5280	9300	1928	45
H(47C)	4811	9475	2458	45
H(48)	7194	7818	3954	21
H(50)	8024	9194	3432	34
H(51)	9953	9693	3675	44
H(52)	11438	9355	4348	42

Table II.78. Continued.

H(53)	11003	8495	4767	35
H(54)	9073	7997	4528	28
H(56)	4524	7987	3759	37
H(57)	2919	8285	4236	49
H(58)	3399	8978	4874	56
H(59)	5469	9374	5033	53
H(60)	7108	9058	4568	39
H(61)	8003	7070	2301	22
H(63)	9177	8511	2425	38
H(64)	11393	8744	2562	51
H(65)	12944	8054	2430	54
H(66)	12289	7127	2149	61
H(67)	10101	6887	2017	47
H(69)	6602	6616	1671	35
H(70)	5785	6481	820	45
H(71)	6098	7193	218	39
H(72)	7321	8020	474	32
H(73)	8206	8140	1319	27
H(113)	3152	5747	751	77
H(112)	1112	5298	598	62
H(116)	-614	6825	886	54
H(115)	1426	7274	1038	73
H(114)	3309	6735	971	80
H(11A)	-1200	5426	355	73
H(11B)	-1908	6008	505	73
H(11C)	-1440	5531	931	73
H(126)	3470	6173	880	41
H(122)	529	7333	913	55
H(125)	1937	5446	644	55
H(123)	-926	6584	781	65
H(124)	-324	5645	618	68
H(12A)	3700	7249	1355	92
H(12B)	2656	7694	1072	92
H(12C)	3655	7368	759	92

Table II.79. Atomic Occupancy for (IPr*)$Fe(CO)_4$.

Atom	*Occupancy*	Atom	*Occupancy*	Atom	*Occupancy*
C(113)	0.673(6)	H(113)	0.673(6)	C(112)	0.673(6)
H(112)	0.673(6)	C(111)	0.673(6)	C(116)	0.673(6)
H(116)	0.673(6)	C(115)	0.673(6)	H(115)	0.673(6)
C(114)	0.673(6)	H(114)	0.673(6)	C(110)	0.673(6)
H(11A)	0.673(6)	H(11B)	0.673(6)	H(11C)	0.673(6)
C(121)	0.327(6)	C(126)	0.327(6)	H(126)	0.327(6)
C(122)	0.327(6)	H(122)	0.327(6)	C(125)	0.327(6)
H(125)	0.327(6)	C(123)	0.327(6)	H(123)	0.327(6)
C(124)	0.327(6)	H(124)	0.327(6)	C(120)	0.327(6)
H(12A)	0.327(6)	H(12B)	0.327(6)	H(12C)	0.327(6)

II.12 Diffraction data for $Co(NHAr^*)_2$•2Tol w/ trityl protons.

Table II.80. Crystal data and structure refinement for $Co(NHAr^*)_2$•2Tol w/ trityl protons.

Identification code	mo_Hans13_0m
Empirical formula	$C_{80}H_{72}CoN_2$
Formula weight	1120.32
Temperature/K	99.99
Crystal system	monoclinic
Space group	$P2_1/n$
a/Å	14.414(2)
b/Å	17.888(3)
c/Å	23.482(4)
α/°	90
β/°	101.148(4)
γ/°	90
Volume/$Å^3$	5940.6(17)
Z	4
$\rho_{calc}g/cm^3$	1.253
μ/mm^{-1}	0.338
F(000)	2372.0
Crystal size/mm^3	0.192 × 0.137 × 0.124
Radiation	MoKα (λ = 0.71073)
2Θ range for data collection/°	4.31 to 53.012
Index ranges	$-17 \leq h \leq 17$, $-21 \leq k \leq 21$, $-29 \leq l \leq 28$
Reflections collected	63559
Independent reflections	11672 [R_{int} = 0.1181, R_{sigma} = 0.1332]
Data/restraints/parameters	11672/0/752
Goodness-of-fit on F^2	1.019
Final R indexes [I>=2σ (I)]	R_1 = 0.0748, wR_2 = 0.1523
Final R indexes [all data]	R_1 = 0.1629, wR_2 = 0.1895
Largest diff. peak/hole / e $Å^{-3}$	0.93/-1.20

Table II.81. Fractional Atomic Coordinates ($\times 10^4$) and Equivalent Isotropic Displacement Parameters ($Å^2 \times 10^3$) for $Co(NHAr^*)_2 \bullet 2Tol$ w/ trityl protons. U_{eq} is defined as 1/3 of of the trace of the orthogonalised U_{IJ} tensor.

Atom	***x***	***y***	***z***	**U(eq)**
Co(1)	2023.4(4)	6783.0(3)	903.5(2)	22.88(17)
N(1)	2046(2)	7815.1(18)	918.4(14)	25.3(8)
N(2)	2489(2)	5864.5(18)	733.9(13)	22.0(8)
C(1)	2721(3)	8176(2)	1299.1(16)	22.7(9)
C(2)	3328(3)	7696(2)	1676.5(17)	24.1(9)
C(3)	4137(3)	8001(2)	2022.5(17)	25.1(10)
C(4)	4315(3)	8755(2)	2034.6(17)	25.2(9)
C(5)	3662(3)	9228(2)	1683.0(17)	25.3(9)
C(6)	2873(3)	8959(2)	1315.9(16)	22.9(9)
C(7)	5175(3)	9075(2)	2427.6(18)	29.5(10)
C(8)	2190(3)	9445(2)	901.4(17)	25.3(10)
C(9)	1162(3)	9326(2)	965.7(18)	26.5(10)
C(10)	922(3)	9222(2)	1504.4(19)	32.1(10)
C(11)	-10(3)	9094(2)	1550(2)	43.2(13)
C(12)	-703(3)	9067(3)	1057(3)	49.6(14)
C(13)	-476(3)	9169(3)	518(2)	46.4(13)
C(14)	461(3)	9300(2)	476(2)	33.8(11)
C(15)	2427(3)	10270(2)	915.6(17)	24.3(9)
C(16)	2745(3)	10598(3)	453.0(19)	34.0(11)
C(17)	2934(3)	11355(3)	454(2)	41.3(12)
C(18)	2819(3)	11802(3)	915(2)	39.3(12)
C(19)	2507(3)	11481(3)	1377(2)	37.8(11)
C(20)	2310(3)	10723(3)	1374.9(19)	34.6(11)
C(21)	3067(3)	6897(2)	1670.2(15)	20.9(9)
C(22)	3899(3)	6373(2)	1828.4(17)	24.4(9)
C(23)	4149(3)	6091(2)	2379.9(18)	29.5(10)
C(24)	4933(3)	5634(3)	2536(2)	36.6(11)
C(25)	5475(3)	5449(2)	2133(2)	35.5(11)
C(26)	5244(3)	5736(3)	1584(2)	35.6(11)
C(27)	4466(3)	6203(2)	1430.5(18)	29.3(10)
C(28)	2208(3)	6667(2)	1891.7(17)	24.1(9)
C(29)	1998(3)	5904(2)	1949.1(16)	28.1(10)
C(30)	1205(3)	5682(3)	2153.4(18)	36.1(11)
C(31)	596(3)	6213(3)	2308.2(19)	42.7(13)
C(32)	791(3)	6960(3)	2262.2(19)	38.4(12)
C(33)	1579(3)	7194(3)	2055.1(17)	30.2(10)
C(34)	2393(3)	5653(2)	176.6(16)	21.0(9)

Table II.81. Continued.

C(35)	2838(2)	5013(2)	-18.9(16)	20.1(9)
C(36)	2771(2)	4930(2)	-608.2(17)	22.7(9)
C(37)	2274(3)	5424(2)	-1019.2(17)	24.0(9)
C(38)	1830(3)	6030(2)	-822.8(17)	21.8(9)
C(39)	1856(3)	6138(2)	-231.5(17)	21.0(9)
C(40)	2209(3)	5271(3)	-1655.6(17)	32.7(11)
C(41)	3425(3)	4526(2)	436.0(16)	22.0(9)
C(42)	2861(3)	4185(2)	861.0(17)	23.9(9)
C(43)	3304(3)	4052(2)	1426.6(19)	34.3(11)
C(44)	2806(4)	3752(3)	1824(2)	49.3(14)
C(45)	1857(4)	3597(3)	1661(2)	46.2(13)
C(46)	1411(3)	3733(3)	1104(2)	39.9(12)
C(47)	1908(3)	4020(2)	701.1(19)	28.8(10)
C(48)	3999(3)	3924(2)	201.5(17)	23.9(9)
C(49)	3584(3)	3305(2)	-97.7(17)	27.8(10)
C(50)	4126(3)	2765(2)	-295.8(18)	30.1(10)
C(51)	5103(3)	2827(2)	-179.5(19)	32.9(11)
C(52)	5524(3)	3439(2)	114.9(19)	33.9(11)
C(53)	4977(3)	3986(2)	299.8(18)	26.7(10)
C(54)	1365(2)	6766(2)	1.8(16)	20.6(9)
C(55)	1309(3)	7474(2)	-339.3(16)	22.4(9)
C(56)	2147(3)	7841(2)	-396.8(17)	26.4(10)
C(57)	2134(3)	8489(2)	-706.3(18)	32.9(11)
C(58)	1286(3)	8797(3)	-981.2(19)	35.7(11)
C(59)	452(3)	8440(3)	-939.7(19)	37.0(11)
C(60)	459(3)	7786(2)	-621.3(17)	30.2(10)
C(61)	583(3)	6589(2)	318.8(16)	21.5(9)
C(62)	69(3)	7161(2)	530.7(17)	27.8(10)
C(63)	-635(3)	6995(3)	838.6(18)	30.9(10)
C(64)	-837(3)	6266(2)	951.8(17)	29.5(10)
C(65)	-349(3)	5691(2)	744.1(17)	28.4(10)
C(66)	346(3)	5850(2)	433.1(16)	24.9(9)
C(75)	-1712(3)	7780(3)	2223(2)	42.6(12)
C(72)	6522(3)	9417(3)	1296(2)	49.1(14)
C(67)	5678(3)	9718(3)	1012.5(19)	38.0(11)
C(68)	5454(3)	10435(3)	1157(2)	41.5(12)
C(71)	7119(3)	9815(3)	1710(2)	49.8(14)
C(74)	-1640(3)	7869(3)	2810(2)	41.3(12)
C(76)	-2506(4)	7475(3)	1880(3)	59.0(16)
C(69)	6056(4)	10844(3)	1567(2)	43.5(12)
C(70)	6900(4)	10532(3)	1849(2)	46.7(13)

Table II.81. Continued.

C(73)	5006(3)	9263(3)	573(2)	53.0(14)
C(80)	-776(4)	8194(3)	3181(3)	72.1(18)
C(79)	-2401(5)	7637(3)	3049(3)	64.4(18)
C(78)	-3191(5)	7352(4)	2717(4)	84(3)
C(77)	-3247(4)	7276(3)	2129(4)	80(2)

Table II.82. Anisotropic Displacement Parameters ($Å^2 \times 10^3$) for $Co(NHAr^*)_2 \bullet 2Tol$ w/ trityl protons. The Anisotropic displacement factor exponent takes the form: $-2\pi^2[h^2a^{*2}U_{11}+2hka^*b^*U_{12}+\ldots]$.

Atom	**U_{11}**	**U_{22}**	**U_{33}**	**U_{23}**	**U_{13}**	**U_{12}**
Co(1)	17.6(3)	26.0(3)	26.6(3)	-0.5(3)	8.0(2)	-0.3(2)
N(1)	16.6(18)	31(2)	28(2)	1.7(16)	3.6(14)	2.0(15)
N(2)	17.7(18)	27(2)	22(2)	1.4(15)	6.1(13)	-1.5(14)
C(1)	16(2)	29(3)	26(2)	-4.3(19)	10.0(16)	0.0(17)
C(2)	21(2)	29(3)	26(2)	-4.0(18)	11.1(17)	0.1(17)
C(3)	15(2)	34(3)	27(2)	2.4(19)	6.8(17)	1.8(17)
C(4)	20(2)	29(3)	30(2)	-0.8(19)	11.4(17)	-0.8(17)
C(5)	22(2)	25(3)	32(3)	-3.0(19)	13.5(18)	-2.6(17)
C(6)	19(2)	25(3)	26(2)	0.9(18)	9.1(17)	-1.6(17)
C(7)	18(2)	34(3)	37(3)	-3(2)	5.4(18)	-2.1(18)
C(8)	21(2)	29(3)	27(2)	1.9(18)	7.9(17)	-1.7(17)
C(9)	24(2)	19(2)	37(3)	2.0(19)	9.4(19)	-1.0(17)
C(10)	28(3)	27(3)	45(3)	3(2)	16(2)	0.6(19)
C(11)	41(3)	28(3)	70(4)	-2(2)	35(3)	-2(2)
C(12)	27(3)	28(3)	99(5)	-3(3)	26(3)	0(2)
C(13)	27(3)	32(3)	77(4)	5(3)	2(2)	1(2)
C(14)	29(3)	26(3)	46(3)	0(2)	6(2)	1.0(19)
C(15)	17(2)	26(3)	30(3)	3.9(19)	4.0(17)	2.7(17)
C(16)	26(3)	35(3)	44(3)	7(2)	14(2)	-2.1(19)
C(17)	38(3)	40(3)	49(3)	11(2)	16(2)	-4(2)
C(18)	33(3)	26(3)	59(3)	7(2)	10(2)	-3(2)
C(19)	38(3)	33(3)	41(3)	-5(2)	6(2)	0(2)
C(20)	33(3)	30(3)	43(3)	2(2)	12(2)	-2(2)
C(21)	18(2)	32(3)	12(2)	-1.2(17)	1.9(15)	0.2(17)
C(22)	18(2)	27(3)	29(3)	-2.3(19)	7.4(17)	-4.8(17)
C(23)	25(2)	34(3)	30(3)	3(2)	5.7(18)	5.8(19)
C(24)	31(3)	40(3)	37(3)	8(2)	2(2)	3(2)
C(25)	20(2)	35(3)	50(3)	-2(2)	2(2)	10.0(19)
C(26)	15(2)	49(3)	43(3)	-12(2)	8.1(19)	2(2)
C(27)	22(2)	38(3)	31(3)	-2(2)	11.9(18)	-2.9(19)
C(28)	21(2)	25(3)	28(2)	-0.5(18)	9.4(17)	-1.3(17)
C(29)	24(2)	38(3)	23(2)	-2.8(19)	8.4(17)	-1.3(19)
C(30)	33(3)	44(3)	34(3)	1(2)	11(2)	-14(2)
C(31)	24(3)	69(4)	39(3)	5(3)	15(2)	-4(2)
C(32)	28(3)	55(4)	37(3)	4(2)	19(2)	7(2)
C(33)	27(2)	34(3)	32(3)	5(2)	12.7(19)	3.2(19)
C(34)	16(2)	27(3)	22(2)	2.5(18)	7.8(16)	-6.2(16)
C(35)	12(2)	24(2)	26(2)	0.4(18)	9.5(16)	-2.5(16)

Table II.82. Continued.

C(36)	12(2)	26(3)	32(3)	-1.7(19)	8.0(17)	-1.4(16)
C(37)	14(2)	32(3)	27(2)	1.4(19)	9.6(17)	-2.1(17)
C(38)	16(2)	25(2)	26(2)	3.9(18)	7.7(16)	-0.8(16)
C(39)	17(2)	21(2)	27(2)	-2.7(18)	8.3(16)	-4.2(16)
C(40)	27(2)	46(3)	27(3)	1(2)	9.0(18)	10(2)
C(41)	16(2)	24(2)	27(2)	-1.5(18)	7.3(17)	-0.3(16)
C(42)	23(2)	25(3)	27(3)	0.1(18)	12.5(18)	4.0(17)
C(43)	40(3)	31(3)	33(3)	0(2)	9(2)	2(2)
C(44)	80(4)	39(3)	34(3)	6(2)	23(3)	9(3)
C(45)	67(4)	32(3)	52(4)	2(2)	42(3)	-1(3)
C(46)	43(3)	38(3)	48(3)	-2(2)	31(2)	0(2)
C(47)	30(3)	26(3)	35(3)	0.2(19)	16.4(19)	0.2(18)
C(48)	17(2)	28(3)	29(2)	5.1(19)	10.7(17)	2.9(17)
C(49)	18(2)	32(3)	35(3)	0(2)	8.7(18)	-2.7(18)
C(50)	31(3)	24(3)	37(3)	2(2)	14(2)	-0.4(19)
C(51)	31(3)	29(3)	44(3)	6(2)	21(2)	4(2)
C(52)	24(2)	34(3)	48(3)	8(2)	18(2)	2.1(19)
C(53)	18(2)	24(3)	40(3)	3.2(19)	11.4(18)	-1.5(17)
C(54)	10(2)	25(2)	26(2)	-6.9(18)	3.0(15)	-3.5(16)
C(55)	20(2)	23(2)	26(2)	-0.7(18)	8.5(17)	1.7(17)
C(56)	21(2)	29(3)	33(3)	0(2)	13.0(18)	2.3(18)
C(57)	31(3)	38(3)	35(3)	4(2)	18(2)	-6(2)
C(58)	41(3)	31(3)	36(3)	10(2)	11(2)	2(2)
C(59)	29(3)	44(3)	38(3)	7(2)	7(2)	10(2)
C(60)	24(2)	35(3)	32(3)	3(2)	7.0(19)	0.0(18)
C(61)	17(2)	23(3)	25(2)	-0.5(17)	6.6(16)	1.0(16)
C(62)	23(2)	27(3)	35(3)	-1.7(19)	8.9(18)	-4.7(18)
C(63)	24(2)	38(3)	35(3)	-7(2)	14.8(19)	3.7(19)
C(64)	18(2)	40(3)	33(3)	-3(2)	13.3(18)	-3.9(19)
C(65)	21(2)	32(3)	33(3)	2(2)	7.5(18)	-5.3(18)
C(66)	16(2)	33(3)	27(2)	-5.0(19)	6.9(17)	0.0(17)
C(75)	28(3)	52(3)	51(3)	3(3)	17(2)	2(2)
C(72)	39(3)	62(4)	50(3)	-10(3)	17(3)	3(3)
C(67)	32(3)	47(3)	39(3)	-6(2)	17(2)	-3(2)
C(68)	34(3)	48(3)	46(3)	1(2)	18(2)	-2(2)
C(71)	36(3)	72(4)	43(3)	4(3)	13(2)	0(3)
C(74)	41(3)	37(3)	44(3)	1(2)	6(2)	9(2)
C(76)	41(3)	62(4)	68(4)	-14(3)	-5(3)	13(3)
C(69)	50(3)	38(3)	48(3)	0(2)	26(3)	-11(2)
C(70)	46(3)	60(4)	38(3)	0(3)	18(2)	-19(3)
C(73)	46(3)	59(4)	58(4)	-15(3)	18(3)	0(3)

Table II.82. Continued.

C(80)	76(4)	69(4)	62(4)	-17(3)	-10(3)	0(3)
C(79)	71(5)	58(4)	79(4)	31(3)	50(4)	32(3)
C(78)	39(4)	63(5)	165(8)	55(5)	55(5)	15(3)
C(77)	32(4)	42(4)	157(7)	6(4)	-6(4)	-3(3)

Table II.83. Bond Lengths for Co(NHAr*)$_2$•2Tol w/ trityl protons.

Atom	Atom	Length/Å	Atom	Atom	Length/Å
Co(1)	N(1)	1.847(3)	C(35)	C(41)	1.505(5)
Co(1)	N(2)	1.847(3)	C(36)	C(37)	1.400(5)
Co(1)	C(21)	2.121(4)	C(37)	C(38)	1.382(5)
Co(1)	C(28)	2.293(4)	C(37)	C(40)	1.504(5)
Co(1)	C(54)	2.147(4)	C(38)	C(39)	1.395(5)
Co(1)	C(61)	2.284(4)	C(39)	C(54)	1.488(5)
N(1)	C(1)	1.351(5)	C(41)	C(42)	1.531(5)
N(2)	C(34)	1.343(5)	C(41)	C(48)	1.524(5)
C(1)	C(2)	1.410(5)	C(42)	C(43)	1.378(6)
C(1)	C(6)	1.417(5)	C(42)	C(47)	1.385(5)
C(2)	C(3)	1.397(5)	C(43)	C(44)	1.390(6)
C(2)	C(21)	1.476(6)	C(44)	C(45)	1.375(7)
C(3)	C(4)	1.373(6)	C(45)	C(46)	1.363(7)
C(4)	C(5)	1.408(5)	C(46)	C(47)	1.391(6)
C(4)	C(7)	1.508(5)	C(48)	C(49)	1.384(5)
C(5)	C(6)	1.375(5)	C(48)	C(53)	1.388(5)
C(6)	C(8)	1.518(5)	C(49)	C(50)	1.379(6)
C(8)	C(9)	1.533(5)	C(50)	C(51)	1.386(6)
C(8)	C(15)	1.513(6)	C(51)	C(52)	1.371(6)
C(9)	C(10)	1.387(6)	C(52)	C(53)	1.379(6)
C(9)	C(14)	1.377(6)	C(54)	C(55)	1.492(5)
C(10)	C(11)	1.388(6)	C(54)	C(61)	1.499(5)
C(11)	C(12)	1.375(7)	C(55)	C(56)	1.404(5)
C(12)	C(13)	1.380(7)	C(55)	C(60)	1.393(5)
C(13)	C(14)	1.393(6)	C(56)	C(57)	1.366(6)
C(15)	C(16)	1.389(5)	C(57)	C(58)	1.382(6)
C(15)	C(20)	1.386(6)	C(58)	C(59)	1.381(6)
C(16)	C(17)	1.381(6)	C(59)	C(60)	1.388(6)
C(17)	C(18)	1.382(6)	C(61)	C(62)	1.410(5)
C(18)	C(19)	1.377(6)	C(61)	C(66)	1.405(5)
C(19)	C(20)	1.384(6)	C(62)	C(63)	1.387(5)
C(21)	C(22)	1.511(5)	C(63)	C(64)	1.373(6)
C(21)	C(28)	1.491(5)	C(64)	C(65)	1.387(6)
C(22)	C(23)	1.372(5)	C(65)	C(66)	1.378(5)
C(22)	C(27)	1.389(5)	C(75)	C(74)	1.371(6)
C(23)	C(24)	1.385(6)	C(75)	C(76)	1.379(7)
C(24)	C(25)	1.379(6)	C(72)	C(67)	1.378(6)
C(25)	C(26)	1.368(6)	C(72)	C(71)	1.368(7)
C(26)	C(27)	1.389(6)	C(67)	C(68)	1.381(6)
C(28)	C(29)	1.410(6)	C(67)	C(73)	1.510(6)

Table II.83. Continued.

C(28)	C(33)	1.412(5)	C(68)	C(69)	1.377(6)
C(29)	C(30)	1.381(6)	C(71)	C(70)	1.375(7)
C(30)	C(31)	1.388(6)	C(74)	C(80)	1.492(7)
C(31)	C(32)	1.375(6)	C(74)	C(79)	1.388(7)
C(32)	C(33)	1.384(6)	C(76)	C(77)	1.360(9)
C(34)	C(35)	1.430(5)	C(69)	C(70)	1.385(7)
C(34)	C(39)	1.408(5)	C(79)	C(78)	1.349(9)
C(35)	C(36)	1.377(5)	C(78)	C(77)	1.375(10)

Table II.84. Bond Angles for Co(NHAr*)$_2$•2Tol w/ trityl protons.

Atom	Atom	Atom	Angle/°	Atom	Atom	Atom	Angle/°
N(1)	Co(1)	N(2)	152.56(13)	N(2)	C(34)	C(35)	124.8(4)
N(1)	Co(1)	C(21)	83.13(15)	N(2)	C(34)	C(39)	115.4(4)
N(1)	Co(1)	C(28)	94.20(14)	C(39)	C(34)	C(35)	119.7(3)
N(1)	Co(1)	C(54)	92.05(14)	C(34)	C(35)	C(41)	117.4(3)
N(1)	Co(1)	C(61)	100.02(14)	C(36)	C(35)	C(34)	117.5(3)
N(2)	Co(1)	C(21)	92.37(14)	C(36)	C(35)	C(41)	124.8(3)
N(2)	Co(1)	C(28)	99.30(14)	C(35)	C(36)	C(37)	123.4(4)
N(2)	Co(1)	C(54)	83.36(14)	C(36)	C(37)	C(40)	119.7(4)
N(2)	Co(1)	C(61)	93.50(14)	C(38)	C(37)	C(36)	118.3(4)
C(21)	Co(1)	C(28)	39.23(13)	C(38)	C(37)	C(40)	122.0(4)
C(21)	Co(1)	C(54)	160.79(14)	C(37)	C(38)	C(39)	121.1(4)
C(21)	Co(1)	C(61)	159.78(14)	C(34)	C(39)	C(54)	116.9(3)
C(54)	Co(1)	C(28)	159.96(13)	C(38)	C(39)	C(34)	119.8(4)
C(54)	Co(1)	C(61)	39.41(13)	C(38)	C(39)	C(54)	123.3(4)
C(61)	Co(1)	C(28)	120.60(13)	C(35)	C(41)	C(42)	113.4(3)
C(1)	N(1)	Co(1)	119.9(3)	C(35)	C(41)	C(48)	115.0(3)
C(34)	N(2)	Co(1)	119.2(3)	C(48)	C(41)	C(42)	110.3(3)
N(1)	C(1)	C(2)	113.9(4)	C(43)	C(42)	C(41)	119.5(4)
N(1)	C(1)	C(6)	125.3(4)	C(43)	C(42)	C(47)	118.3(4)
C(2)	C(1)	C(6)	120.7(4)	C(47)	C(42)	C(41)	122.2(4)
C(1)	C(2)	C(21)	117.2(3)	C(42)	C(43)	C(44)	120.7(4)
C(3)	C(2)	C(1)	118.4(4)	C(45)	C(44)	C(43)	120.3(5)
C(3)	C(2)	C(21)	124.5(4)	C(46)	C(45)	C(44)	119.5(4)
C(4)	C(3)	C(2)	121.8(4)	C(45)	C(46)	C(47)	120.6(4)
C(3)	C(4)	C(5)	118.5(4)	C(42)	C(47)	C(46)	120.6(4)
C(3)	C(4)	C(7)	120.9(4)	C(49)	C(48)	C(41)	122.5(3)
C(5)	C(4)	C(7)	120.6(4)	C(49)	C(48)	C(53)	118.3(4)
C(6)	C(5)	C(4)	122.4(4)	C(53)	C(48)	C(41)	119.2(4)
C(1)	C(6)	C(8)	118.1(3)	C(50)	C(49)	C(48)	121.0(4)
C(5)	C(6)	C(1)	118.0(4)	C(49)	C(50)	C(51)	119.8(4)
C(5)	C(6)	C(8)	123.8(4)	C(52)	C(51)	C(50)	119.8(4)
C(6)	C(8)	C(9)	112.1(3)	C(51)	C(52)	C(53)	120.1(4)
C(15)	C(8)	C(6)	115.4(3)	C(52)	C(53)	C(48)	121.0(4)
C(15)	C(8)	C(9)	110.6(3)	C(39)	C(54)	Co(1)	102.9(2)
C(10)	C(9)	C(8)	121.6(4)	C(39)	C(54)	C(55)	115.0(3)
C(14)	C(9)	C(8)	119.3(4)	C(39)	C(54)	C(61)	118.7(3)
C(14)	C(9)	C(10)	119.0(4)	C(55)	C(54)	Co(1)	119.0(3)
C(9)	C(10)	C(11)	120.6(4)	C(55)	C(54)	C(61)	118.6(3)
C(12)	C(11)	C(10)	119.8(5)	C(61)	C(54)	Co(1)	75.2(2)
C(11)	C(12)	C(13)	120.4(5)	C(56)	C(55)	C(54)	119.4(3)

Table II.84. Continued.

C(12)	C(13)	C(14)	119.4(5)	C(60)	C(55)	C(54)	123.1(3)
C(9)	C(14)	C(13)	120.8(4)	C(60)	C(55)	C(56)	117.5(4)
C(16)	C(15)	C(8)	120.2(4)	C(57)	C(56)	C(55)	121.6(4)
C(20)	C(15)	C(8)	121.8(4)	C(56)	C(57)	C(58)	120.4(4)
C(20)	C(15)	C(16)	118.0(4)	C(59)	C(58)	C(57)	119.1(4)
C(17)	C(16)	C(15)	120.6(4)	C(58)	C(59)	C(60)	120.9(4)
C(16)	C(17)	C(18)	121.0(4)	C(59)	C(60)	C(55)	120.5(4)
C(19)	C(18)	C(17)	118.8(4)	C(54)	C(61)	Co(1)	65.36(19)
C(18)	C(19)	C(20)	120.4(4)	C(62)	C(61)	Co(1)	99.0(3)
C(19)	C(20)	C(15)	121.3(4)	C(62)	C(61)	C(54)	121.3(3)
C(2)	C(21)	Co(1)	103.8(2)	C(66)	C(61)	Co(1)	104.8(2)
C(2)	C(21)	C(22)	114.2(3)	C(66)	C(61)	C(54)	121.8(3)
C(2)	C(21)	C(28)	119.4(3)	C(66)	C(61)	C(62)	116.9(3)
C(22)	C(21)	Co(1)	123.2(3)	C(63)	C(62)	C(61)	121.0(4)
C(28)	C(21)	Co(1)	76.6(2)	C(64)	C(63)	C(62)	120.6(4)
C(28)	C(21)	C(22)	114.5(3)	C(63)	C(64)	C(65)	119.7(4)
C(23)	C(22)	C(21)	120.8(3)	C(66)	C(65)	C(64)	120.2(4)
C(23)	C(22)	C(27)	118.2(4)	C(65)	C(66)	C(61)	121.6(4)
C(27)	C(22)	C(21)	120.8(4)	C(74)	C(75)	C(76)	121.8(5)
C(22)	C(23)	C(24)	121.3(4)	C(71)	C(72)	C(67)	121.0(5)
C(25)	C(24)	C(23)	120.0(4)	C(72)	C(67)	C(68)	118.1(5)
C(26)	C(25)	C(24)	119.3(4)	C(72)	C(67)	C(73)	120.6(5)
C(25)	C(26)	C(27)	120.5(4)	C(68)	C(67)	C(73)	121.2(4)
C(22)	C(27)	C(26)	120.5(4)	C(69)	C(68)	C(67)	121.3(5)
C(21)	C(28)	Co(1)	64.15(19)	C(72)	C(71)	C(70)	120.9(5)
C(29)	C(28)	Co(1)	101.5(3)	C(75)	C(74)	C(80)	121.6(5)
C(29)	C(28)	C(21)	120.6(3)	C(75)	C(74)	C(79)	117.3(5)
C(29)	C(28)	C(33)	117.3(4)	C(79)	C(74)	C(80)	121.2(5)
C(33)	C(28)	Co(1)	105.0(3)	C(77)	C(76)	C(75)	119.0(6)
C(33)	C(28)	C(21)	122.0(4)	C(68)	C(69)	C(70)	119.8(5)
C(30)	C(29)	C(28)	121.2(4)	C(71)	C(70)	C(69)	118.9(5)
C(29)	C(30)	C(31)	120.2(4)	C(78)	C(79)	C(74)	121.6(6)
C(32)	C(31)	C(30)	119.7(4)	C(79)	C(78)	C(77)	119.8(6)
C(31)	C(32)	C(33)	121.0(4)	C(76)	C(77)	C(78)	120.4(6)
C(32)	C(33)	C(28)	120.5(4)				

Table II.85. Torsion Angles for Co(NHAr*)$_2$•2Tol w/ trityl protons.

A	B	C	D	Angle/°	A	B	C	D	Angle/°
Co(1)	N(1)	C(1)	C(2)	-3.1(4)	C(29)	C(28)	C(33)	C(32)	0.0(6)
Co(1)	N(1)	C(1)	C(6)	173.4(3)	C(29)	C(30)	C(31)	C(32)	-0.6(7)
Co(1)	N(2)	C(34)	C(35)	170.3(3)	C(30)	C(31)	C(32)	C(33)	1.0(7)
Co(1)	N(2)	C(34)	C(39)	-5.6(4)	C(31)	C(32)	C(33)	C(28)	-0.7(7)
Co(1)	C(21)	C(22)	C(23)	-134.0(3)	C(33)	C(28)	C(29)	C(30)	0.4(6)
Co(1)	C(21)	C(22)	C(27)	50.3(5)	C(34)	C(35)	C(36)	C(37)	-1.7(5)
Co(1)	C(21)	C(28)	C(29)	88.3(3)	C(34)	C(35)	C(41)	C(42)	60.5(4)
Co(1)	C(21)	C(28)	C(33)	-92.1(4)	C(34)	C(35)	C(41)	C(48)	-171.2(3)
Co(1)	C(28)	C(29)	C(30)	-113.3(4)	C(34)	C(39)	C(54)	Co(1)	14.1(4)
Co(1)	C(28)	C(33)	C(32)	111.7(4)	C(34)	C(39)	C(54)	C(55)	145.1(3)
Co(1)	C(54)	C(55)	C(56)	60.5(4)	C(34)	C(39)	C(54)	C(61)	-65.9(5)
Co(1)	C(54)	C(55)	C(60)	-121.2(4)	C(35)	C(34)	C(39)	C(38)	-5.6(5)
Co(1)	C(54)	C(61)	C(62)	85.6(3)	C(35)	C(34)	C(39)	C(54)	176.4(3)
Co(1)	C(54)	C(61)	C(66)	-92.6(3)	C(35)	C(36)	C(37)	C(38)	0.3(6)
Co(1)	C(61)	C(62)	C(63)	-111.5(4)	C(35)	C(36)	C(37)	C(40)	-177.7(4)
Co(1)	C(61)	C(66)	C(65)	107.6(4)	C(35)	C(41)	C(42)	C(43)	-148.4(4)
N(1)	Co(1)	N(2)	C(34)	-70.5(4)	C(35)	C(41)	C(42)	C(47)	30.0(5)
N(1)	C(1)	C(2)	C(3)	169.9(3)	C(35)	C(41)	C(48)	C(49)	-70.7(5)
N(1)	C(1)	C(2)	C(21)	-9.1(5)	C(35)	C(41)	C(48)	C(53)	110.7(4)
N(1)	C(1)	C(6)	C(5)	-172.1(3)	C(36)	C(35)	C(41)	C(42)	-126.0(4)
N(1)	C(1)	C(6)	C(8)	4.2(6)	C(36)	C(35)	C(41)	C(48)	2.3(5)
N(2)	Co(1)	N(1)	C(1)	-72.6(4)	C(36)	C(37)	C(38)	C(39)	-1.4(5)
N(2)	C(34)	C(35)	C(36)	-171.4(3)	C(37)	C(38)	C(39)	C(34)	4.1(6)
N(2)	C(34)	C(35)	C(41)	2.6(5)	C(37)	C(38)	C(39)	C(54)	-178.0(3)
N(2)	C(34)	C(39)	C(38)	170.6(3)	C(38)	C(39)	C(54)	Co(1)	-163.9(3)
N(2)	C(34)	C(39)	C(54)	-7.5(5)	C(38)	C(39)	C(54)	C(55)	-32.9(5)
C(1)	C(2)	C(3)	C(4)	4.9(6)	C(38)	C(39)	C(54)	C(61)	116.1(4)
C(1)	C(2)	C(21)	Co(1)	14.5(4)	C(39)	C(34)	C(35)	C(36)	4.3(5)
C(1)	C(2)	C(21)	C(22)	151.3(3)	C(39)	C(34)	C(35)	C(41)	178.3(3)
C(1)	C(2)	C(21)	C(28)	-67.8(5)	C(39)	C(54)	C(55)	C(56)	-62.1(5)
C(1)	C(6)	C(8)	C(9)	55.8(5)	C(39)	C(54)	C(55)	C(60)	116.1(4)
C(1)	C(6)	C(8)	C(15)	-176.3(3)	C(39)	C(54)	C(61)	Co(1)	96.8(3)
C(2)	C(1)	C(6)	C(5)	4.2(5)	C(39)	C(54)	C(61)	C(62)	-177.6(4)
C(2)	C(1)	C(6)	C(8)	-179.5(3)	C(39)	C(54)	C(61)	C(66)	4.2(5)
C(2)	C(3)	C(4)	C(5)	-0.5(6)	C(40)	C(37)	C(38)	C(39)	176.4(4)
C(2)	C(3)	C(4)	C(7)	177.8(3)	C(41)	C(35)	C(36)	C(37)	-175.2(3)
C(2)	C(21)	C(22)	C(23)	98.5(4)	C(41)	C(42)	C(43)	C(44)	179.1(4)
C(2)	C(21)	C(22)	C(27)	-77.2(5)	C(41)	C(42)	C(47)	C(46)	-177.8(4)
C(2)	C(21)	C(28)	Co(1)	98.5(3)	C(41)	C(48)	C(49)	C(50)	-179.0(4)
C(2)	C(21)	C(28)	C(29)	-173.2(4)	C(41)	C(48)	C(53)	C(52)	177.4(4)

Table II.85. Continued.

C(2)	C(21)	C(28)	C(33)	6.4(6)	C(42)	C(41)	C(48)	C(49)	59.0(5)
C(3)	C(2)	C(21)	Co(1)	-164.5(3)	C(42)	C(41)	C(48)	C(53)	-119.6(4)
C(3)	C(2)	C(21)	C(22)	-27.6(5)	C(42)	C(43)	C(44)	C(45)	-1.3(7)
C(3)	C(2)	C(21)	C(28)	113.3(4)	C(43)	C(42)	C(47)	C(46)	0.6(6)
C(3)	C(4)	C(5)	C(6)	-2.1(6)	C(43)	C(44)	C(45)	C(46)	0.7(7)
C(4)	C(5)	C(6)	C(1)	0.3(6)	C(44)	C(45)	C(46)	C(47)	0.5(7)
C(4)	C(5)	C(6)	C(8)	-175.7(4)	C(45)	C(46)	C(47)	C(42)	-1.2(7)
C(5)	C(6)	C(8)	C(9)	-128.2(4)	C(47)	C(42)	C(43)	C(44)	0.6(6)
C(5)	C(6)	C(8)	C(15)	-0.3(5)	C(48)	C(41)	C(42)	C(43)	81.0(4)
C(6)	C(1)	C(2)	C(3)	-6.7(5)	C(48)	C(41)	C(42)	C(47)	-100.6(4)
C(6)	C(1)	C(2)	C(21)	174.3(3)	C(48)	C(49)	C(50)	C(51)	2.1(6)
C(6)	C(8)	C(9)	C(10)	38.8(5)	C(49)	C(48)	C(53)	C(52)	-1.3(6)
C(6)	C(8)	C(9)	C(14)	-139.2(4)	C(49)	C(50)	C(51)	C(52)	-2.2(6)
C(6)	C(8)	C(15)	C(16)	109.3(4)	C(50)	C(51)	C(52)	C(53)	0.7(6)
C(6)	C(8)	C(15)	C(20)	-72.8(5)	C(51)	C(52)	C(53)	C(48)	1.1(6)
C(7)	C(4)	C(5)	C(6)	179.5(4)	C(53)	C(48)	C(49)	C(50)	-0.3(6)
C(8)	C(9)	C(10)	C(11)	-178.2(4)	C(54)	Co(1)	N(1)	C(1)	-152.1(3)
C(8)	C(9)	C(14)	C(13)	178.0(4)	C(54)	Co(1)	N(2)	C(34)	11.1(3)
C(8)	C(15)	C(16)	C(17)	177.8(4)	C(54)	C(55)	C(56)	C(57)	179.8(4)
C(8)	C(15)	C(20)	C(19)	-178.4(4)	C(54)	C(55)	C(60)	C(59)	-179.0(4)
C(9)	C(8)	C(15)	C(16)	-122.1(4)	C(54)	C(61)	C(62)	C(63)	-178.1(4)
C(9)	C(8)	C(15)	C(20)	55.8(5)	C(54)	C(61)	C(66)	C(65)	177.5(4)
C(9)	C(10)	C(11)	C(12)	0.3(6)	C(55)	C(54)	C(61)	Co(1)	-115.3(3)
C(10)	C(9)	C(14)	C(13)	-0.1(6)	C(55)	C(54)	C(61)	C(62)	-29.7(5)
C(10)	C(11)	C(12)	C(13)	-0.2(7)	C(55)	C(54)	C(61)	C(66)	152.1(4)
C(11)	C(12)	C(13)	C(14)	0.0(7)	C(55)	C(56)	C(57)	C(58)	-1.0(6)
C(12)	C(13)	C(14)	C(9)	0.1(7)	C(56)	C(55)	C(60)	C(59)	-0.7(6)
C(14)	C(9)	C(10)	C(11)	-0.2(6)	C(56)	C(57)	C(58)	C(59)	-0.1(7)
C(15)	C(8)	C(9)	C(10)	-91.6(4)	C(57)	C(58)	C(59)	C(60)	0.8(7)
C(15)	C(8)	C(9)	C(14)	90.4(4)	C(58)	C(59)	C(60)	C(55)	-0.3(6)
C(15)	C(16)	C(17)	C(18)	0.5(7)	C(60)	C(55)	C(56)	C(57)	1.4(6)
C(16)	C(15)	C(20)	C(19)	-0.4(6)	C(61)	Co(1)	N(1)	C(1)	169.0(3)
C(16)	C(17)	C(18)	C(19)	-0.3(7)	C(61)	Co(1)	N(2)	C(34)	49.3(3)
C(17)	C(18)	C(19)	C(20)	-0.3(7)	C(61)	C(54)	C(55)	C(56)	148.8(4)
C(18)	C(19)	C(20)	C(15)	0.7(7)	C(61)	C(54)	C(55)	C(60)	-32.9(5)
C(20)	C(15)	C(16)	C(17)	-0.2(6)	C(61)	C(62)	C(63)	C(64)	1.0(6)
C(21)	Co(1)	N(1)	C(1)	9.2(3)	C(62)	C(61)	C(66)	C(65)	-0.8(6)
C(21)	Co(1)	N(2)	C(34)	-150.1(3)	C(62)	C(63)	C(64)	C(65)	-1.6(6)
C(21)	C(2)	C(3)	C(4)	-176.2(4)	C(63)	C(64)	C(65)	C(66)	1.0(6)
C(21)	C(22)	C(23)	C(24)	-177.3(4)	C(64)	C(65)	C(66)	C(61)	0.2(6)
C(21)	C(22)	C(27)	C(26)	178.2(4)	C(66)	C(61)	C(62)	C(63)	0.2(6)

Table II.85. Continued.

C(21)	C(28)	C(29)	C(30)	-180.0(4)	C(75)	C(74)	C(79)	C(78)	-1.6(8)
C(21)	C(28)	C(33)	C(32)	-179.6(4)	C(75)	C(76)	C(77)	C(78)	-2.4(9)
C(22)	C(21)	C(28)	Co(1)	-120.7(3)	C(72)	C(67)	C(68)	C(69)	0.6(7)
C(22)	C(21)	C(28)	C(29)	-32.3(5)	C(72)	C(71)	C(70)	C(69)	0.7(7)
C(22)	C(21)	C(28)	C(33)	147.2(4)	C(67)	C(72)	C(71)	C(70)	-1.0(7)
C(22)	C(23)	C(24)	C(25)	-0.6(7)	C(67)	C(68)	C(69)	C(70)	-0.8(7)
C(23)	C(22)	C(27)	C(26)	2.4(6)	C(68)	C(69)	C(70)	C(71)	0.1(7)
C(23)	C(24)	C(25)	C(26)	1.8(7)	C(71)	C(72)	C(67)	C(68)	0.3(7)
C(24)	C(25)	C(26)	C(27)	-0.8(7)	C(71)	C(72)	C(67)	C(73)	-177.6(5)
C(25)	C(26)	C(27)	C(22)	-1.3(6)	C(74)	C(75)	C(76)	C(77)	1.7(8)
C(27)	C(22)	C(23)	C(24)	-1.4(6)	C(74)	C(79)	C(78)	C(77)	1.0(9)
C(28)	Co(1)	N(1)	C(1)	46.9(3)	C(76)	C(75)	C(74)	C(80)	179.5(5)
C(28)	Co(1)	N(2)	C(34)	171.0(3)	C(76)	C(75)	C(74)	C(79)	0.2(7)
C(28)	C(21)	C(22)	C(23)	-44.3(5)	C(73)	C(67)	C(68)	C(69)	178.5(4)
C(28)	C(21)	C(22)	C(27)	140.0(4)	C(80)	C(74)	C(79)	C(78)	179.1(5)
C(28)	C(29)	C(30)	C(31)	-0.1(6)	C(79)	C(78)	C(77)	C(76)	1.1(9)

Table II.86. Hydrogen Atom Coordinates (Å×10^4) and Isotropic Displacement Parameters (Å^2×10^3) for Co(NHAr*)$_2$•2Tol w/ trityl protons.

Atom	***x***	***y***	***z***	**U(eq)**
H(1)	1618	8071	678	30
H(2)	2770	5569	1015	26
H(3)	4577	7677	2256	30
H(5)	3771	9752	1700	30
H(7A)	5058	9109	2824	44
H(7B)	5306	9574	2291	44
H(7C)	5720	8749	2423	44
H(8)	2226	9269	502	30
H(10)	1400	9237	1845	39
H(11)	-170	9025	1921	52
H(12)	-1341	8977	1088	59
H(13)	-956	9151	178	56
H(14)	618	9371	105	41
H(16)	2834	10300	133	41
H(17)	3146	11572	132	50
H(18)	2952	12322	914	47
H(19)	2428	11780	1698	45
H(20)	2089	10511	1695	41
H(21)	2866	6801	1245	25
H(23)	3777	6211	2660	35
H(24)	5098	5449	2922	44
H(25)	6003	5125	2236	43
H(26)	5620	5616	1306	43
H(27)	4320	6408	1050	35
H(29)	2410	5535	1845	34
H(30)	1075	5165	2188	43
H(31)	48	6060	2445	51
H(32)	378	7322	2374	46
H(33)	1698	7713	2023	36
H(36)	3079	4514	-743	27
H(38)	1501	6377	-1095	26
H(40A)	1614	5012	-1809	49
H(40B)	2742	4957	-1710	49
H(40C)	2229	5745	-1862	49
H(41)	3898	4867	673	26
H(43)	3956	4166	1546	41
H(44)	3123	3654	2211	59
H(45)	1516	3398	1934	55
H(46)	754	3631	990	48

Table II.86. Continued.

H(47)	1591	4103	313	35
H(49)	2916	3251	-167	33
H(50)	3831	2351	-512	36
H(51)	5480	2448	-303	40
H(52)	6193	3485	192	41
H(53)	5274	4412	497	32
H(54)	1869	6910	339	25
H(56)	2738	7634	-216	32
H(57)	2712	8730	-733	40
H(58)	1277	9248	-1196	43
H(59)	-133	8645	-1131	44
H(60)	-122	7549	-596	36
H(62)	206	7669	461	33
H(63)	-980	7389	972	37
H(64)	-1308	6156	1172	35
H(65)	-494	5186	816	34
H(66)	672	5450	293	30
H(75)	-1201	7933	2049	51
H(72)	6692	8925	1202	59
H(68)	4873	10650	968	50
H(71)	7693	9594	1904	60
H(76)	-2535	7406	1476	71
H(69)	5893	11339	1657	52
H(70)	7320	10809	2134	56
H(73A)	5344	9066	280	80
H(73B)	4483	9581	383	80
H(73C)	4756	8847	769	80
H(80A)	-422	7798	3417	108
H(80B)	-960	8577	3435	108
H(80C)	-377	8419	2933	108
H(79)	-2365	7680	3456	77
H(78)	-3706	7204	2889	101
H(77)	-3808	7083	1894	96

II.13. Diffraction data for Co(NHAr*)$_2$•2Tol w/o trityl protons.

Table II.87. Crystal data and structure refinement for Co(NHAr*)$_2$•2Tol w/o trityl protons.

Identification code	mo_Hans13_0m no H
Empirical formula	$C_{80}H_{70}CoN_2$
Formula weight	1118.31
Temperature/K	99.99
Crystal system	monoclinic
Space group	$P2_1/n$
a/Å	14.414(2)
b/Å	17.888(3)
c/Å	23.482(4)
α/°	90
β/°	101.148(4)
γ/°	90
Volume/Å^3	5940.6(17)
Z	4
ρ_{calc}g/cm^3	1.250
μ/mm^{-1}	0.338
F(000)	2364.0
Crystal size/mm^3	0.192 × 0.137 × 0.124
Radiation	MoKα (λ = 0.71073)
2Θ range for data collection/°	4.31 to 53.012
Index ranges	$-17 \leq h \leq 17$, $-21 \leq k \leq 21$, $-29 \leq l \leq 28$
Reflections collected	63559
Independent reflections	11672 [R_{int} = 0.1181, R_{sigma} = 0.1332]
Data/restraints/parameters	11672/0/752
Goodness-of-fit on F^2	1.014
Final R indexes [I>=2σ (I)]	R_1 = 0.0749, wR_2 = 0.1508
Final R indexes [all data]	R_1 = 0.1628, wR_2 = 0.1880
Largest diff. peak/hole / e Å^{-3}	1.16/-1.19

Table II.88. Fractional Atomic Coordinates ($\times 10^4$) and Equivalent Isotropic Displacement Parameters ($Å^2 \times 10^3$) for $Co(NHAr^*)_2$•2Tol w/o trityl protons.. U_{eq} is defined as 1/3 of of the trace of the orthogonalised U_{IJ} tensor.

Atom	***x***	***y***	***z***	**U(eq)**
Co(1)	2023.5(4)	6782.9(3)	903.6(2)	22.96(17)
N(1)	2047(2)	7814.5(18)	918.5(14)	25.3(8)
N(2)	2489(2)	5864.6(18)	733.8(13)	21.9(8)
C(1)	2721(3)	8176(2)	1298.6(16)	22.5(9)
C(2)	3328(3)	7695(2)	1676.7(16)	24.2(9)
C(3)	4138(3)	8001(2)	2022.5(16)	24.9(10)
C(4)	4315(3)	8755(2)	2034.9(17)	25.1(9)
C(5)	3662(3)	9228(2)	1682.8(17)	25.1(9)
C(6)	2873(3)	8957(2)	1315.6(16)	22.9(9)
C(7)	5174(3)	9075(2)	2427.6(18)	29.5(10)
C(8)	2190(3)	9446(2)	901.5(17)	25.1(10)
C(9)	1163(3)	9326(2)	966.4(18)	26.5(10)
C(10)	922(3)	9222(2)	1504.9(19)	32(1)
C(11)	-11(3)	9094(2)	1550(2)	43.2(13)
C(12)	-703(3)	9067(3)	1057(3)	49.1(14)
C(13)	-477(3)	9169(3)	518(2)	46.5(13)
C(14)	459(3)	9300(2)	475(2)	33.7(11)
C(15)	2428(3)	10270(2)	915.3(17)	24.3(9)
C(16)	2745(3)	10599(2)	453.5(19)	33.8(11)
C(17)	2934(3)	11355(3)	454(2)	41.0(12)
C(18)	2820(3)	11802(3)	915(2)	39.1(11)
C(19)	2508(3)	11481(3)	1377(2)	37.4(11)
C(20)	2309(3)	10725(2)	1374.5(19)	34.8(11)
C(21)	3066(2)	6897(2)	1664.6(15)	21.0(9)
C(22)	3898(3)	6372(2)	1828.0(17)	24.1(9)
C(23)	4149(3)	6091(2)	2379.8(18)	29.4(10)
C(24)	4932(3)	5634(2)	2536(2)	36.8(11)
C(25)	5474(3)	5448(2)	2133(2)	35.3(11)
C(26)	5244(3)	5736(3)	1585(2)	35.6(11)
C(27)	4466(3)	6203(2)	1430.4(18)	29.3(10)
C(28)	2208(3)	6667(2)	1892.3(16)	23.9(9)
C(29)	1998(3)	5904(2)	1949.2(16)	28.2(10)
C(30)	1205(3)	5682(3)	2153.6(18)	36.0(11)
C(31)	596(3)	6213(3)	2308.1(19)	42.5(12)
C(32)	791(3)	6961(3)	2262.2(18)	38.2(12)
C(33)	1579(3)	7193(2)	2055.3(17)	30(1)
C(34)	2392(2)	5652(2)	176.6(16)	21.0(9)

Table II.88. Continued.

C(35)	2837(2)	5014(2)	-18.8(16)	20.1(9)
C(36)	2771(2)	4929(2)	-608.3(16)	22.8(9)
C(37)	2275(3)	5424(2)	-1018.9(17)	23.8(9)
C(38)	1830(2)	6030(2)	-823.0(16)	21.8(9)
C(39)	1856(3)	6139(2)	-231.5(16)	21.1(9)
C(40)	2208(3)	5273(3)	-1655.5(17)	32.8(11)
C(41)	3425(3)	4526(2)	436.0(16)	22.1(9)
C(42)	2861(3)	4185(2)	861.3(17)	23.8(9)
C(43)	3303(3)	4051(2)	1426.9(18)	34.1(11)
C(44)	2805(4)	3753(3)	1824(2)	49.3(14)
C(45)	1856(4)	3597(3)	1661(2)	46.3(13)
C(46)	1410(3)	3733(2)	1104(2)	39.8(12)
C(47)	1909(3)	4019(2)	700.8(18)	28.9(10)
C(48)	3999(3)	3925(2)	201.6(16)	23.8(9)
C(49)	3584(3)	3305(2)	-97.9(17)	27.9(10)
C(50)	4127(3)	2765(2)	-295.4(18)	29.8(10)
C(51)	5103(3)	2827(2)	-179.5(19)	33.1(11)
C(52)	5524(3)	3439(2)	114.8(19)	33.8(11)
C(53)	4977(3)	3987(2)	299.8(17)	26.6(10)
C(54)	1372(2)	6768(2)	6.8(16)	20.8(9)
C(55)	1310(3)	7473(2)	-339.1(16)	22.4(9)
C(56)	2147(3)	7842(2)	-397.1(17)	26.3(10)
C(57)	2135(3)	8489(2)	-706.3(18)	32.7(11)
C(58)	1286(3)	8797(2)	-981.1(19)	35.7(11)
C(59)	453(3)	8441(3)	-939.6(19)	36.8(11)
C(60)	459(3)	7786(2)	-621.7(17)	30.3(10)
C(61)	581(3)	6589(2)	318.5(16)	21.5(9)
C(62)	68(3)	7161(2)	530.7(17)	27.8(10)
C(63)	-634(3)	6996(2)	838.8(18)	30.8(10)
C(64)	-837(3)	6266(2)	951.8(17)	29.5(10)
C(65)	-349(3)	5691(2)	744.5(17)	28.5(10)
C(66)	346(3)	5851(2)	433.0(16)	24.9(9)
C(75)	-1711(3)	7780(3)	2224(2)	42.5(12)
C(72)	6523(3)	9416(3)	1296(2)	48.9(13)
C(67)	5678(3)	9719(3)	1012.1(19)	38.1(11)
C(68)	5454(3)	10436(3)	1156(2)	41.6(12)
C(71)	7120(3)	9817(3)	1710(2)	49.8(14)
C(74)	-1641(3)	7869(3)	2810(2)	41.3(12)
C(76)	-2507(4)	7476(3)	1880(3)	59.2(15)
C(69)	6056(3)	10845(3)	1567(2)	43.5(12)
C(70)	6900(4)	10533(3)	1849(2)	46.6(13)

Table II.88. Continued.

C(73)	5008(3)	9261(3)	573(2)	53.0(14)
C(80)	-774(4)	8194(3)	3181(3)	73.1(18)
C(79)	-2402(5)	7636(3)	3049(3)	64.1(18)
C(78)	-3191(5)	7350(4)	2715(4)	85(3)
C(77)	-3249(4)	7276(3)	2128(4)	79(2)

Table II.89 Anisotropic Displacement Parameters ($Å^2 \times 10^3$) for $Co(NHAr^*)_2$•2Tol w/o trityl protons.. The Anisotropic displacement factor exponent takes the form: $-2\pi^2[h^2a^{*2}U_{11}+2hka^*b^*U_{12}+\ldots]$.

Atom	**U_{11}**	**U_{22}**	**U_{33}**	**U_{23}**	**U_{13}**	**U_{12}**
Co(1)	17.7(3)	25.9(3)	26.8(3)	-0.6(3)	8.2(2)	-0.3(2)
N(1)	16.6(18)	32(2)	27(2)	1.6(16)	3.4(14)	2.2(15)
N(2)	17.4(18)	28(2)	22(2)	1.4(15)	5.7(13)	-1.5(14)
C(1)	16(2)	29(3)	25(2)	-4.2(19)	9.2(16)	-0.1(17)
C(2)	20(2)	30(3)	25(2)	-4.4(18)	10.7(17)	0.2(17)
C(3)	15(2)	34(3)	27(2)	2.4(18)	6.8(17)	2.0(17)
C(4)	20(2)	29(3)	29(2)	-0.6(19)	11.3(17)	-1.1(17)
C(5)	22(2)	25(2)	31(3)	-2.8(19)	13.2(18)	-2.7(17)
C(6)	19(2)	25(3)	26(2)	0.9(18)	9.1(17)	-1.4(16)
C(7)	18(2)	34(3)	37(3)	-3(2)	5.2(18)	-2.1(18)
C(8)	21(2)	30(3)	25(2)	1.7(18)	7.1(17)	-1.5(17)
C(9)	24(2)	20(2)	37(3)	2.4(19)	9.6(19)	-1.2(17)
C(10)	27(3)	28(3)	45(3)	3(2)	15(2)	0.3(18)
C(11)	41(3)	28(3)	71(4)	-2(2)	35(3)	-2(2)
C(12)	27(3)	28(3)	98(5)	-2(3)	26(3)	0(2)
C(13)	27(3)	32(3)	78(4)	6(3)	2(2)	1(2)
C(14)	28(3)	27(3)	46(3)	1(2)	6(2)	0.9(19)
C(15)	17(2)	26(3)	31(3)	3.8(19)	4.1(17)	2.3(17)
C(16)	27(2)	34(3)	44(3)	7(2)	14(2)	-2.0(19)
C(17)	38(3)	40(3)	48(3)	11(2)	16(2)	-4(2)
C(18)	33(3)	25(3)	59(3)	7(2)	9(2)	-3(2)
C(19)	38(3)	33(3)	41(3)	-5(2)	6(2)	0(2)
C(20)	33(3)	29(3)	44(3)	3(2)	13(2)	-2(2)
C(21)	16(2)	28(3)	19(2)	0.4(17)	3.9(15)	0.7(16)
C(22)	18(2)	27(3)	28(3)	-2.2(19)	6.9(17)	-4.9(17)
C(23)	24(2)	34(3)	30(3)	2(2)	5.6(18)	5.8(18)
C(24)	31(3)	41(3)	36(3)	9(2)	1(2)	3(2)
C(25)	19(2)	35(3)	49(3)	-2(2)	2(2)	9.7(18)
C(26)	15(2)	50(3)	43(3)	-12(2)	7.8(19)	1(2)
C(27)	22(2)	38(3)	31(3)	-2(2)	12.1(18)	-2.7(19)
C(28)	22(2)	26(3)	25(2)	-0.2(18)	8.6(17)	-1.2(17)
C(29)	24(2)	38(3)	23(2)	-2.8(19)	8.4(17)	-1.6(19)
C(30)	32(3)	44(3)	33(3)	2(2)	11(2)	-14(2)
C(31)	25(3)	68(4)	38(3)	5(2)	15(2)	-4(2)
C(32)	28(3)	55(4)	36(3)	4(2)	18(2)	7(2)
C(33)	27(2)	34(3)	32(3)	5(2)	12.5(18)	3.2(19)
C(34)	15(2)	28(2)	22(2)	2.7(18)	7.8(16)	-6.3(16)
C(35)	12(2)	25(2)	26(2)	0.5(18)	9.5(16)	-2.5(16)

Table II.89. Continued.

C(36)	12(2)	27(3)	31(3)	-1.8(19)	7.7(16)	-1.6(16)
C(37)	14(2)	33(3)	27(2)	1.1(19)	9.5(17)	-2.1(17)
C(38)	16(2)	25(2)	26(2)	4.1(18)	7.3(16)	-0.9(16)
C(39)	16(2)	22(2)	27(2)	-2.5(18)	7.9(16)	-4.4(16)
C(40)	27(2)	46(3)	27(3)	1(2)	9.3(18)	10(2)
C(41)	16(2)	24(2)	27(2)	-1.4(18)	7.0(16)	-0.7(16)
C(42)	22(2)	25(3)	27(2)	-0.3(18)	12.0(17)	3.6(17)
C(43)	39(3)	31(3)	33(3)	0(2)	9(2)	2(2)
C(44)	80(4)	39(3)	33(3)	6(2)	21(3)	9(3)
C(45)	67(4)	32(3)	52(4)	2(2)	42(3)	-1(3)
C(46)	42(3)	37(3)	49(3)	-1(2)	31(2)	-1(2)
C(47)	30(3)	26(3)	35(3)	0.3(19)	15.9(19)	0.5(18)
C(48)	17(2)	28(3)	29(2)	5.0(19)	10.3(17)	2.8(17)
C(49)	18(2)	33(3)	34(3)	0(2)	8.6(17)	-2.5(18)
C(50)	31(3)	24(3)	37(3)	1.6(19)	13.4(19)	-0.4(18)
C(51)	32(3)	29(3)	44(3)	7(2)	21(2)	5(2)
C(52)	24(2)	34(3)	47(3)	8(2)	17(2)	2.5(19)
C(53)	18(2)	24(3)	40(3)	3.4(19)	11.3(18)	-1.5(17)
C(54)	12(2)	22(2)	30(2)	-4.2(18)	8.2(16)	-2.4(16)
C(55)	20(2)	23(2)	26(2)	-1.3(18)	8.5(17)	1.7(16)
C(56)	21(2)	29(3)	33(3)	0(2)	12.8(18)	2.5(17)
C(57)	31(3)	38(3)	34(3)	3(2)	18(2)	-7(2)
C(58)	41(3)	31(3)	36(3)	10(2)	12(2)	2(2)
C(59)	29(3)	45(3)	37(3)	7(2)	6(2)	10(2)
C(60)	23(2)	35(3)	33(3)	3(2)	6.8(18)	-0.2(18)
C(61)	17(2)	24(2)	24(2)	-0.6(17)	6.1(16)	0.7(16)
C(62)	23(2)	27(3)	35(3)	-1.8(19)	8.9(18)	-4.6(18)
C(63)	24(2)	38(3)	34(3)	-7(2)	14.1(19)	3.3(19)
C(64)	18(2)	41(3)	32(3)	-3(2)	12.7(18)	-3.6(19)
C(65)	21(2)	33(3)	33(3)	2(2)	7.3(18)	-5.3(18)
C(66)	15(2)	33(3)	27(2)	-5.0(19)	6.8(16)	-0.1(17)
C(75)	29(3)	51(3)	51(3)	3(3)	16(2)	2(2)
C(72)	39(3)	61(4)	50(3)	-9(3)	16(2)	4(2)
C(67)	33(3)	47(3)	39(3)	-5(2)	17(2)	-3(2)
C(68)	35(3)	48(3)	47(3)	2(2)	18(2)	-2(2)
C(71)	35(3)	74(4)	42(3)	4(3)	12(2)	0(3)
C(74)	42(3)	37(3)	44(3)	0(2)	6(2)	9(2)
C(76)	42(3)	61(4)	68(4)	-14(3)	-5(3)	13(3)
C(69)	50(3)	38(3)	49(3)	0(2)	26(3)	-11(2)
C(70)	45(3)	60(4)	38(3)	0(3)	18(2)	-19(3)
C(73)	45(3)	59(4)	58(4)	-14(3)	18(3)	0(3)

Table II.89. Continued.

C(80)	77(4)	70(4)	62(4)	-16(3)	-10(3)	1(3)
C(79)	71(5)	58(4)	78(4)	31(3)	50(4)	31(3)
C(78)	39(4)	63(5)	167(8)	55(5)	55(5)	15(3)
C(77)	32(4)	42(4)	154(7)	6(4)	-5(4)	-3(3)

Table II.90. Bond Lengths for Co(NHAr*)$_2$•2Tol w/o trityl protons**.**

Atom	Atom	Length/Å	Atom	Atom	Length/Å
Co(1)	N(1)	1.846(3)	C(35)	C(41)	1.506(5)
Co(1)	N(2)	1.847(3)	C(36)	C(37)	1.400(5)
Co(1)	C(21)	2.110(4)	C(37)	C(38)	1.382(5)
Co(1)	C(28)	2.295(4)	C(37)	C(40)	1.504(5)
Co(1)	C(54)	2.134(4)	C(38)	C(39)	1.396(5)
Co(1)	C(61)	2.286(4)	C(39)	C(54)	1.489(5)
N(1)	C(1)	1.351(5)	C(41)	C(42)	1.531(5)
N(2)	C(34)	1.344(5)	C(41)	C(48)	1.523(5)
C(1)	C(2)	1.413(5)	C(42)	C(43)	1.378(5)
C(1)	C(6)	1.414(5)	C(42)	C(47)	1.384(5)
C(2)	C(3)	1.398(5)	C(43)	C(44)	1.388(6)
C(2)	C(21)	1.476(5)	C(44)	C(45)	1.376(7)
C(3)	C(4)	1.372(6)	C(45)	C(46)	1.363(7)
C(4)	C(5)	1.410(5)	C(46)	C(47)	1.393(6)
C(4)	C(7)	1.507(5)	C(48)	C(49)	1.386(5)
C(5)	C(6)	1.376(5)	C(48)	C(53)	1.389(5)
C(6)	C(8)	1.520(5)	C(49)	C(50)	1.378(5)
C(8)	C(9)	1.532(5)	C(50)	C(51)	1.385(6)
C(8)	C(15)	1.511(5)	C(51)	C(52)	1.371(6)
C(9)	C(10)	1.387(6)	C(52)	C(53)	1.379(6)
C(9)	C(14)	1.381(6)	C(54)	C(55)	1.494(5)
C(10)	C(11)	1.388(6)	C(54)	C(61)	1.503(5)
C(11)	C(12)	1.376(7)	C(55)	C(56)	1.404(5)
C(12)	C(13)	1.380(7)	C(55)	C(60)	1.395(5)
C(13)	C(14)	1.392(6)	C(56)	C(57)	1.364(6)
C(15)	C(16)	1.388(5)	C(57)	C(58)	1.383(6)
C(15)	C(20)	1.388(6)	C(58)	C(59)	1.380(6)
C(16)	C(17)	1.379(6)	C(59)	C(60)	1.387(6)
C(17)	C(18)	1.382(6)	C(61)	C(62)	1.409(5)
C(18)	C(19)	1.377(6)	C(61)	C(66)	1.403(5)
C(19)	C(20)	1.382(6)	C(62)	C(63)	1.385(5)
C(21)	C(22)	1.513(5)	C(63)	C(64)	1.375(6)
C(21)	C(28)	1.496(5)	C(64)	C(65)	1.385(6)
C(22)	C(23)	1.372(5)	C(65)	C(66)	1.380(5)
C(22)	C(27)	1.389(5)	C(75)	C(74)	1.369(6)
C(23)	C(24)	1.384(5)	C(75)	C(76)	1.381(7)
C(24)	C(25)	1.381(6)	C(72)	C(67)	1.381(6)
C(25)	C(26)	1.366(6)	C(72)	C(71)	1.371(7)
C(26)	C(27)	1.389(6)	C(67)	C(68)	1.381(6)
C(28)	C(29)	1.410(6)	C(67)	C(73)	1.510(6)

Table II.90. Continued.

C(28)	C(33)	1.412(5)	C(68)	C(69)	1.377(6)
C(29)	C(30)	1.381(5)	C(71)	C(70)	1.374(7)
C(30)	C(31)	1.388(6)	C(74)	C(80)	1.496(7)
C(31)	C(32)	1.375(6)	C(74)	C(79)	1.388(7)
C(32)	C(33)	1.382(6)	C(76)	C(77)	1.360(9)
C(34)	C(35)	1.429(5)	C(69)	C(70)	1.385(7)
C(34)	C(39)	1.410(5)	C(79)	C(78)	1.350(9)
C(35)	C(36)	1.377(5)	C(78)	C(77)	1.372(10)

Table II.91. Bond Angles for Co(NHAr*)$_2$•2Tol w/o trityl protons.

Atom	Atom	Atom	Angle/°	Atom	Atom	Atom	Angle/°
N(1)	Co(1)	N(2)	152.55(13)	N(2)	C(34)	C(35)	124.8(3)
N(1)	Co(1)	C(21)	83.12(15)	N(2)	C(34)	C(39)	115.3(4)
N(1)	Co(1)	C(28)	94.19(14)	C(39)	C(34)	C(35)	119.8(3)
N(1)	Co(1)	C(54)	91.96(14)	C(34)	C(35)	C(41)	117.4(3)
N(1)	Co(1)	C(61)	100.02(14)	C(36)	C(35)	C(34)	117.5(3)
N(2)	Co(1)	C(21)	92.28(14)	C(36)	C(35)	C(41)	124.7(3)
N(2)	Co(1)	C(28)	99.32(14)	C(35)	C(36)	C(37)	123.3(4)
N(2)	Co(1)	C(54)	83.39(14)	C(36)	C(37)	C(40)	119.8(4)
N(2)	Co(1)	C(61)	93.51(13)	C(38)	C(37)	C(36)	118.4(4)
C(21)	Co(1)	C(28)	39.42(13)	C(38)	C(37)	C(40)	121.8(4)
C(21)	Co(1)	C(54)	160.47(14)	C(37)	C(38)	C(39)	121.1(4)
C(21)	Co(1)	C(61)	159.94(14)	C(34)	C(39)	C(54)	116.5(3)
C(54)	Co(1)	C(28)	160.10(13)	C(38)	C(39)	C(34)	119.7(4)
C(54)	Co(1)	C(61)	39.57(13)	C(38)	C(39)	C(54)	123.8(3)
C(61)	Co(1)	C(28)	120.58(13)	C(35)	C(41)	C(42)	113.4(3)
C(1)	N(1)	Co(1)	120.0(3)	C(35)	C(41)	C(48)	115.0(3)
C(34)	N(2)	Co(1)	119.2(3)	C(48)	C(41)	C(42)	110.3(3)
N(1)	C(1)	C(2)	113.7(4)	C(43)	C(42)	C(41)	119.6(3)
N(1)	C(1)	C(6)	125.5(4)	C(43)	C(42)	C(47)	118.3(4)
C(2)	C(1)	C(6)	120.7(4)	C(47)	C(42)	C(41)	122.1(4)
C(1)	C(2)	C(21)	116.9(3)	C(42)	C(43)	C(44)	120.7(4)
C(3)	C(2)	C(1)	118.2(4)	C(45)	C(44)	C(43)	120.4(5)
C(3)	C(2)	C(21)	124.9(4)	C(46)	C(45)	C(44)	119.4(4)
C(4)	C(3)	C(2)	121.9(4)	C(45)	C(46)	C(47)	120.5(4)
C(3)	C(4)	C(5)	118.6(4)	C(42)	C(47)	C(46)	120.6(4)
C(3)	C(4)	C(7)	120.9(4)	C(49)	C(48)	C(41)	122.5(3)
C(5)	C(4)	C(7)	120.5(4)	C(49)	C(48)	C(53)	118.2(4)
C(6)	C(5)	C(4)	122.2(4)	C(53)	C(48)	C(41)	119.3(4)
C(1)	C(6)	C(8)	118.2(3)	C(50)	C(49)	C(48)	120.9(4)
C(5)	C(6)	C(1)	118.1(4)	C(49)	C(50)	C(51)	119.9(4)
C(5)	C(6)	C(8)	123.6(4)	C(52)	C(51)	C(50)	119.8(4)
C(6)	C(8)	C(9)	112.0(3)	C(51)	C(52)	C(53)	120.1(4)
C(15)	C(8)	C(6)	115.5(3)	C(52)	C(53)	C(48)	121.0(4)
C(15)	C(8)	C(9)	110.7(3)	C(39)	C(54)	Co(1)	103.4(2)
C(10)	C(9)	C(8)	121.8(4)	C(39)	C(54)	C(55)	114.6(3)
C(14)	C(9)	C(8)	119.3(4)	C(39)	C(54)	C(61)	118.4(3)
C(14)	C(9)	C(10)	118.9(4)	C(55)	C(54)	Co(1)	119.6(3)
C(9)	C(10)	C(11)	120.6(4)	C(55)	C(54)	C(61)	118.3(3)
C(12)	C(11)	C(10)	119.8(5)	C(61)	C(54)	Co(1)	75.7(2)
C(11)	C(12)	C(13)	120.4(5)	C(56)	C(55)	C(54)	119.2(3)

Table II.91. Continued.

C(12)	C(13)	C(14)	119.5(5)	C(60)	C(55)	C(54)	123.5(3)
C(9)	C(14)	C(13)	120.8(4)	C(60)	C(55)	C(56)	117.3(4)
C(16)	C(15)	C(8)	120.3(4)	C(57)	C(56)	C(55)	121.8(4)
C(16)	C(15)	C(20)	117.8(4)	C(56)	C(57)	C(58)	120.4(4)
C(20)	C(15)	C(8)	121.8(4)	C(59)	C(58)	C(57)	119.1(4)
C(17)	C(16)	C(15)	120.7(4)	C(58)	C(59)	C(60)	120.9(4)
C(16)	C(17)	C(18)	120.9(4)	C(59)	C(60)	C(55)	120.5(4)
C(19)	C(18)	C(17)	118.9(4)	C(54)	C(61)	Co(1)	64.75(19)
C(18)	C(19)	C(20)	120.2(4)	C(62)	C(61)	Co(1)	99.0(2)
C(19)	C(20)	C(15)	121.4(4)	C(62)	C(61)	C(54)	121.1(3)
C(2)	C(21)	Co(1)	104.3(2)	C(66)	C(61)	Co(1)	104.7(2)
C(2)	C(21)	C(22)	114.0(3)	C(66)	C(61)	C(54)	121.9(3)
C(2)	C(21)	C(28)	119.1(3)	C(66)	C(61)	C(62)	117.0(3)
C(22)	C(21)	Co(1)	123.7(3)	C(63)	C(62)	C(61)	121.1(4)
C(28)	C(21)	Co(1)	77.0(2)	C(64)	C(63)	C(62)	120.5(4)
C(28)	C(21)	C(22)	114.1(3)	C(63)	C(64)	C(65)	119.7(4)
C(23)	C(22)	C(21)	121.2(3)	C(66)	C(65)	C(64)	120.2(4)
C(23)	C(22)	C(27)	118.2(4)	C(65)	C(66)	C(61)	121.6(4)
C(27)	C(22)	C(21)	120.4(4)	C(74)	C(75)	C(76)	121.7(5)
C(22)	C(23)	C(24)	121.4(4)	C(71)	C(72)	C(67)	120.8(5)
C(25)	C(24)	C(23)	120.0(4)	C(72)	C(67)	C(73)	120.3(5)
C(26)	C(25)	C(24)	119.2(4)	C(68)	C(67)	C(72)	118.2(5)
C(25)	C(26)	C(27)	120.7(4)	C(68)	C(67)	C(73)	121.5(4)
C(22)	C(27)	C(26)	120.4(4)	C(69)	C(68)	C(67)	121.3(5)
C(21)	C(28)	Co(1)	63.63(19)	C(72)	C(71)	C(70)	120.9(5)
C(29)	C(28)	Co(1)	101.4(3)	C(75)	C(74)	C(80)	121.4(5)
C(29)	C(28)	C(21)	120.5(3)	C(75)	C(74)	C(79)	117.4(5)
C(29)	C(28)	C(33)	117.3(4)	C(79)	C(74)	C(80)	121.2(5)
C(33)	C(28)	Co(1)	105.0(3)	C(77)	C(76)	C(75)	119.1(6)
C(33)	C(28)	C(21)	122.2(4)	C(68)	C(69)	C(70)	119.8(5)
C(30)	C(29)	C(28)	121.3(4)	C(71)	C(70)	C(69)	118.9(5)
C(29)	C(30)	C(31)	120.1(4)	C(78)	C(79)	C(74)	121.5(6)
C(32)	C(31)	C(30)	119.7(4)	C(79)	C(78)	C(77)	120.0(6)
C(31)	C(32)	C(33)	121.0(4)	C(76)	C(77)	C(78)	120.3(6)
C(32)	C(33)	C(28)	120.6(4)				

Table II.92 Torsion Angles for Co(NHAr*)$_2$•2Tol w/o trityl protons.

A	B	C	D	Angle/°	A	B	C	D	Angle/°
Co(1)	N(1)	C(1)	C(2)	-3.1(4)	C(29)	C(28)	C(33)	C(32)	0.1(6)
Co(1)	N(1)	C(1)	C(6)	173.4(3)	C(29)	C(30)	C(31)	C(32)	-0.6(7)
Co(1)	N(2)	C(34)	C(35)	170.3(3)	C(30)	C(31)	C(32)	C(33)	1.0(7)
Co(1)	N(2)	C(34)	C(39)	-5.5(4)	C(31)	C(32)	C(33)	C(28)	-0.8(6)
Co(1)	C(21)	C(22)	C(23)	-133.7(3)	C(33)	C(28)	C(29)	C(30)	0.3(6)
Co(1)	C(21)	C(22)	C(27)	50.6(5)	C(34)	C(35)	C(36)	C(37)	-1.6(5)
Co(1)	C(21)	C(28)	C(29)	88.0(3)	C(34)	C(35)	C(41)	C(42)	60.5(4)
Co(1)	C(21)	C(28)	C(33)	-91.7(4)	C(34)	C(35)	C(41)	C(48)	-171.3(3)
Co(1)	C(28)	C(29)	C(30)	-113.4(4)	C(34)	C(39)	C(54)	Co(1)	13.8(4)
Co(1)	C(28)	C(33)	C(32)	111.8(4)	C(34)	C(39)	C(54)	C(55)	145.7(3)
Co(1)	C(54)	C(55)	C(56)	60.5(4)	C(34)	C(39)	C(54)	C(61)	-67.0(4)
Co(1)	C(54)	C(55)	C(60)	-120.7(4)	C(35)	C(34)	C(39)	C(38)	-5.5(5)
Co(1)	C(54)	C(61)	C(62)	85.2(3)	C(35)	C(34)	C(39)	C(54)	176.8(3)
Co(1)	C(54)	C(61)	C(66)	-92.1(3)	C(35)	C(36)	C(37)	C(38)	0.2(6)
Co(1)	C(61)	C(62)	C(63)	-111.5(4)	C(35)	C(36)	C(37)	C(40)	-177.7(3)
Co(1)	C(61)	C(66)	C(65)	107.6(4)	C(35)	C(41)	C(42)	C(43)	-148.4(4)
N(1)	Co(1)	N(2)	C(34)	-70.6(4)	C(35)	C(41)	C(42)	C(47)	30.1(5)
N(1)	C(1)	C(2)	C(3)	169.9(3)	C(35)	C(41)	C(48)	C(49)	-70.7(5)
N(1)	C(1)	C(2)	C(21)	-8.7(5)	C(35)	C(41)	C(48)	C(53)	110.7(4)
N(1)	C(1)	C(6)	C(5)	-172.1(3)	C(36)	C(35)	C(41)	C(42)	-126.0(4)
N(1)	C(1)	C(6)	C(8)	4.3(6)	C(36)	C(35)	C(41)	C(48)	2.3(5)
N(2)	Co(1)	N(1)	C(1)	-72.6(4)	C(36)	C(37)	C(38)	C(39)	-1.4(5)
N(2)	C(34)	C(35)	C(36)	-171.3(3)	C(37)	C(38)	C(39)	C(34)	4.1(5)
N(2)	C(34)	C(35)	C(41)	2.7(5)	C(37)	C(38)	C(39)	C(54)	-178.4(3)
N(2)	C(34)	C(39)	C(38)	170.5(3)	C(38)	C(39)	C(54)	Co(1)	-163.8(3)
N(2)	C(34)	C(39)	C(54)	-7.2(5)	C(38)	C(39)	C(54)	C(55)	-31.9(5)
C(1)	C(2)	C(3)	C(4)	5.0(6)	C(38)	C(39)	C(54)	C(61)	115.4(4)
C(1)	C(2)	C(21)	Co(1)	14.0(4)	C(39)	C(34)	C(35)	C(36)	4.3(5)
C(1)	C(2)	C(21)	C(22)	151.8(3)	C(39)	C(34)	C(35)	C(41)	178.3(3)
C(1)	C(2)	C(21)	C(28)	-68.8(5)	C(39)	C(54)	C(55)	C(56)	-63.2(5)
C(1)	C(6)	C(8)	C(9)	55.7(5)	C(39)	C(54)	C(55)	C(60)	115.6(4)
C(1)	C(6)	C(8)	C(15)	-176.3(3)	C(39)	C(54)	C(61)	Co(1)	97.7(3)
C(2)	C(1)	C(6)	C(5)	4.2(5)	C(39)	C(54)	C(61)	C(62)	-177.1(4)
C(2)	C(1)	C(6)	C(8)	-179.5(3)	C(39)	C(54)	C(61)	C(66)	5.6(5)
C(2)	C(3)	C(4)	C(5)	-0.7(6)	C(40)	C(37)	C(38)	C(39)	176.4(3)
C(2)	C(3)	C(4)	C(7)	177.7(3)	C(41)	C(35)	C(36)	C(37)	-175.1(3)
C(2)	C(21)	C(22)	C(23)	97.8(4)	C(41)	C(42)	C(43)	C(44)	179.0(4)
C(2)	C(21)	C(22)	C(27)	-77.9(5)	C(41)	C(42)	C(47)	C(46)	-177.7(4)
C(2)	C(21)	C(28)	Co(1)	99.3(3)	C(41)	C(48)	C(49)	C(50)	-178.9(4)
C(2)	C(21)	C(28)	C(29)	-172.7(3)	C(41)	C(48)	C(53)	C(52)	177.4(4)

Table II.92. Continued.

C(2)	C(21)	C(28)	C(33)	7.6(5)	C(42)	C(41)	C(48)	C(49)	59.1(5)
C(3)	C(2)	C(21)	Co(1)	-164.4(3)	C(42)	C(41)	C(48)	C(53)	-119.5(4)
C(3)	C(2)	C(21)	C(22)	-26.7(5)	C(42)	C(43)	C(44)	C(45)	-1.1(7)
C(3)	C(2)	C(21)	C(28)	112.7(4)	C(43)	C(42)	C(47)	C(46)	0.8(6)
C(3)	C(4)	C(5)	C(6)	-2.1(6)	C(43)	C(44)	C(45)	C(46)	0.6(7)
C(4)	C(5)	C(6)	C(1)	0.4(6)	C(44)	C(45)	C(46)	C(47)	0.6(7)
C(4)	C(5)	C(6)	C(8)	-175.8(3)	C(45)	C(46)	C(47)	C(42)	-1.3(6)
C(5)	C(6)	C(8)	C(9)	-128.1(4)	C(47)	C(42)	C(43)	C(44)	0.4(6)
C(5)	C(6)	C(8)	C(15)	-0.1(5)	C(48)	C(41)	C(42)	C(43)	81.0(4)
C(6)	C(1)	C(2)	C(3)	-6.8(5)	C(48)	C(41)	C(42)	C(47)	-100.5(4)
C(6)	C(1)	C(2)	C(21)	174.7(3)	C(48)	C(49)	C(50)	C(51)	2.0(6)
C(6)	C(8)	C(9)	C(10)	38.9(5)	C(49)	C(48)	C(53)	C(52)	-1.3(6)
C(6)	C(8)	C(9)	C(14)	-139.1(4)	C(49)	C(50)	C(51)	C(52)	-2.2(6)
C(6)	C(8)	C(15)	C(16)	109.2(4)	C(50)	C(51)	C(52)	C(53)	0.6(6)
C(6)	C(8)	C(15)	C(20)	-73.0(5)	C(51)	C(52)	C(53)	C(48)	1.1(6)
C(7)	C(4)	C(5)	C(6)	179.5(3)	C(53)	C(48)	C(49)	C(50)	-0.3(6)
C(8)	C(9)	C(10)	C(11)	-178.2(4)	C(54)	Co(1)	N(1)	C(1)	-152.0(3)
C(8)	C(9)	C(14)	C(13)	178.1(4)	C(54)	Co(1)	N(2)	C(34)	10.9(3)
C(8)	C(15)	C(16)	C(17)	177.8(4)	C(54)	C(55)	C(56)	C(57)	-179.8(4)
C(8)	C(15)	C(20)	C(19)	-178.5(4)	C(54)	C(55)	C(60)	C(59)	-179.5(4)
C(9)	C(8)	C(15)	C(16)	-122.2(4)	C(54)	C(61)	C(62)	C(63)	-177.3(4)
C(9)	C(8)	C(15)	C(20)	55.7(5)	C(54)	C(61)	C(66)	C(65)	176.7(4)
C(9)	C(10)	C(11)	C(12)	0.3(6)	C(55)	C(54)	C(61)	Co(1)	-116.3(3)
C(10)	C(9)	C(14)	C(13)	0.0(6)	C(55)	C(54)	C(61)	C(62)	-31.1(5)
C(10)	C(11)	C(12)	C(13)	-0.3(7)	C(55)	C(54)	C(61)	C(66)	151.7(4)
C(11)	C(12)	C(13)	C(14)	0.1(7)	C(55)	C(56)	C(57)	C(58)	-0.9(6)
C(12)	C(13)	C(14)	C(9)	0.0(7)	C(56)	C(55)	C(60)	C(59)	-0.7(6)
C(14)	C(9)	C(10)	C(11)	-0.1(6)	C(56)	C(57)	C(58)	C(59)	-0.2(7)
C(15)	C(8)	C(9)	C(10)	-91.6(4)	C(57)	C(58)	C(59)	C(60)	0.8(7)
C(15)	C(8)	C(9)	C(14)	90.4(4)	C(58)	C(59)	C(60)	C(55)	-0.3(6)
C(15)	C(16)	C(17)	C(18)	0.6(7)	C(60)	C(55)	C(56)	C(57)	1.3(6)
C(16)	C(15)	C(20)	C(19)	-0.5(6)	C(61)	Co(1)	N(1)	C(1)	169.0(3)
C(16)	C(17)	C(18)	C(19)	-0.3(7)	C(61)	Co(1)	N(2)	C(34)	49.2(3)
C(17)	C(18)	C(19)	C(20)	-0.3(6)	C(61)	C(54)	C(55)	C(56)	149.5(4)
C(18)	C(19)	C(20)	C(15)	0.8(6)	C(61)	C(54)	C(55)	C(60)	-31.7(5)
C(20)	C(15)	C(16)	C(17)	-0.1(6)	C(61)	C(62)	C(63)	C(64)	1.0(6)
C(21)	Co(1)	N(1)	C(1)	9.0(3)	C(62)	C(61)	C(66)	C(65)	-0.6(6)
C(21)	Co(1)	N(2)	C(34)	-150.0(3)	C(62)	C(63)	C(64)	C(65)	-1.5(6)
C(21)	C(2)	C(3)	C(4)	-176.5(3)	C(63)	C(64)	C(65)	C(66)	0.9(6)
C(21)	C(22)	C(23)	C(24)	-177.5(4)	C(64)	C(65)	C(66)	C(61)	0.2(6)
C(21)	C(22)	C(27)	C(26)	178.4(4)	C(66)	C(61)	C(62)	C(63)	0.1(6)

Table II.92. Continued.

C(21)	C(28)	C(29)	C(30)	-179.4(4)	C(75)	C(74)	C(79)	C(78)	-1.6(8)
C(21)	C(28)	C(33)	C(32)	179.8(4)	C(75)	C(76)	C(77)	C(78)	-2.4(9)
C(22)	C(21)	C(28)	Co(1)	-121.3(3)	C(72)	C(67)	C(68)	C(69)	0.6(7)
C(22)	C(21)	C(28)	C(29)	-33.4(5)	C(72)	C(71)	C(70)	C(69)	0.6(7)
C(22)	C(21)	C(28)	C(33)	147.0(4)	C(67)	C(72)	C(71)	C(70)	-0.9(7)
C(22)	C(23)	C(24)	C(25)	-0.5(7)	C(67)	C(68)	C(69)	C(70)	-0.8(7)
C(23)	C(22)	C(27)	C(26)	2.6(6)	C(68)	C(69)	C(70)	C(71)	0.2(7)
C(23)	C(24)	C(25)	C(26)	1.8(7)	C(71)	C(72)	C(67)	C(68)	0.2(7)
C(24)	C(25)	C(26)	C(27)	-0.8(7)	C(71)	C(72)	C(67)	C(73)	-177.7(4)
C(25)	C(26)	C(27)	C(22)	-1.4(6)	C(74)	C(75)	C(76)	C(77)	1.6(8)
C(27)	C(22)	C(23)	C(24)	-1.7(6)	C(74)	C(79)	C(78)	C(77)	0.8(9)
C(28)	Co(1)	N(1)	C(1)	47.0(3)	C(76)	C(75)	C(74)	C(80)	179.5(5)
C(28)	Co(1)	N(2)	C(34)	171.0(3)	C(76)	C(75)	C(74)	C(79)	0.4(7)
C(28)	C(21)	C(22)	C(23)	-43.6(5)	C(73)	C(67)	C(68)	C(69)	178.5(4)
C(28)	C(21)	C(22)	C(27)	140.7(4)	C(80)	C(74)	C(79)	C(78)	179.3(5)
C(28)	C(29)	C(30)	C(31)	0.0(6)	C(79)	C(78)	C(77)	C(76)	1.3(9)

Table II.93. Hydrogen Atom Coordinates (Å×10^4) and Isotropic Displacement Parameters (Å^2×10^3) for Co(NHAr*)$_2$•2Tol w/o trityl protons.

Atom	***x***	***y***	***z***	**U(eq)**
H(1)	1618	8070	678	30
H(2)	2770	5570	1015	26
H(3)	4579	7677	2255	30
H(5)	3770	9753	1700	30
H(7A)	5057	9109	2824	44
H(7B)	5305	9574	2291	44
H(7C)	5720	8749	2423	44
H(8)	2225	9270	502	30
H(10)	1399	9238	1846	38
H(11)	-170	9025	1921	52
H(12)	-1341	8977	1088	59
H(13)	-957	9151	178	56
H(14)	616	9371	104	40
H(16)	2834	10301	134	41
H(17)	3146	11572	132	49
H(18)	2954	12322	914	47
H(19)	2429	11780	1699	45
H(20)	2087	10513	1694	42
H(23)	3778	6212	2660	35
H(24)	5096	5448	2922	44
H(25)	6002	5123	2235	42
H(26)	5619	5616	1307	43
H(27)	4322	6409	1050	35
H(29)	2409	5536	1845	34
H(30)	1075	5166	2188	43
H(31)	47	6061	2445	51
H(32)	379	7323	2374	46
H(33)	1697	7713	2022	36
H(36)	3079	4514	-743	27
H(38)	1502	6377	-1095	26
H(40A)	1609	5020	-1810	49
H(40B)	2736	4953	-1710	49
H(40C)	2237	5747	-1861	49
H(41)	3898	4867	673	27
H(43)	3956	4164	1547	41
H(44)	3122	3655	2210	59
H(45)	1515	3398	1934	56
H(46)	753	3632	990	48
H(47)	1592	4101	312	35

Table II.93. Continued.

H(49)	2916	3251	-168	33
H(50)	3832	2351	-511	36
H(51)	5479	2448	-304	40
H(52)	6193	3485	191	41
H(53)	5274	4412	497	32
H(56)	2738	7635	-216	32
H(57)	2713	8728	-733	39
H(58)	1277	9248	-1195	43
H(59)	-132	8646	-1131	44
H(60)	-122	7550	-596	36
H(62)	206	7668	461	33
H(63)	-978	7390	973	37
H(64)	-1309	6156	1171	35
H(65)	-494	5186	817	34
H(66)	673	5451	293	30
H(75)	-1199	7932	2050	51
H(72)	6692	8924	1202	59
H(68)	4872	10651	968	50
H(71)	7694	9596	1904	60
H(76)	-2536	7407	1476	71
H(69)	5893	11340	1657	52
H(70)	7320	10809	2134	56
H(73A)	5344	9071	278	80
H(73B)	4479	9576	386	80
H(73C)	4766	8841	768	80
H(80A)	-404	7794	3403	110
H(80B)	-959	8559	3450	110
H(80C)	-392	8442	2934	110
H(79)	-2367	7679	3456	77
H(78)	-3706	7201	2887	102
H(77)	-3809	7084	1893	95